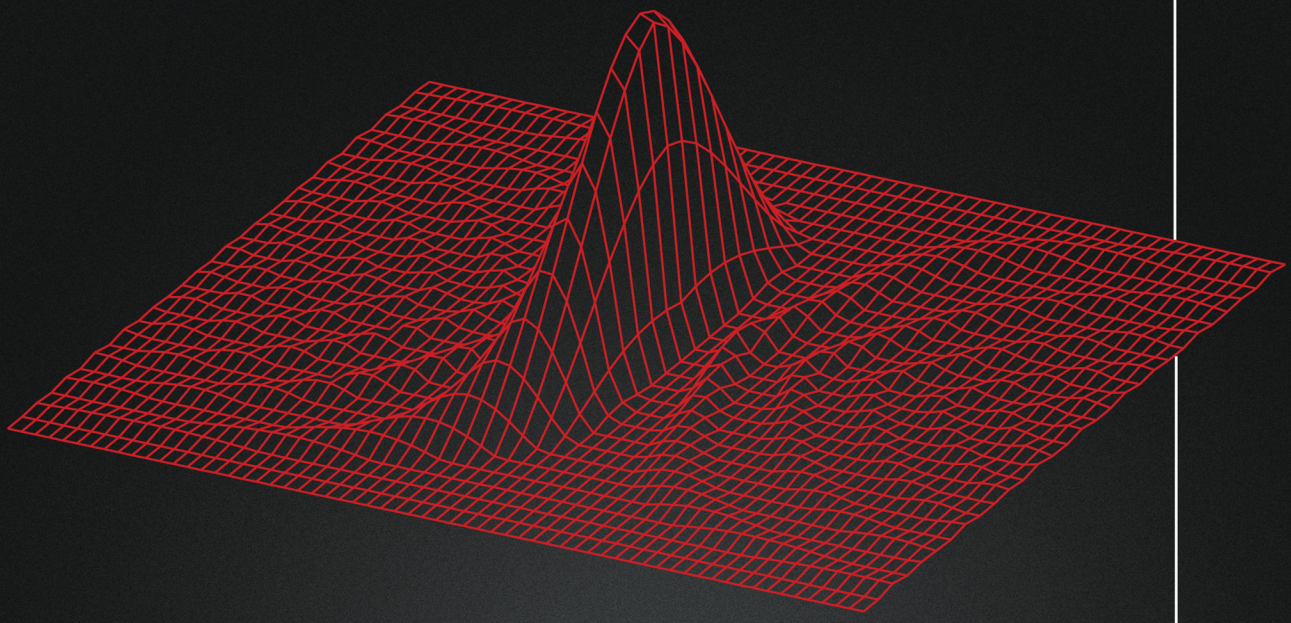

SECOND EDITION

QUANTUM MECHANICS II

Advanced Topics

S. Rajasekar

R. Velusamy

CRC Press
Taylor & Francis Group

Quantum Mechanics II

Quantum Mechanics II: Advanced Topics offers a comprehensive exploration of the state-of-the-art in various advanced topics of current research interest. A follow-up to the authors' introductory book ***Quantum Mechanics I: The Fundamentals,*** this book expounds basic principles, theoretical treatment, case studies, worked-out examples and applications of advanced topics including quantum technologies.

A thoroughly revised and updated this unique volume presents an in-depth and up-to-date progress on the growing topics including latest achievements on quantum technology. In the second edition six new chapters are included and the other ten chapters are extensively revised.

Features

- Covers classical and quantum field theories, path integral formalism and supersymmetric quantum mechanics.
- Highlights coherent and squeezed states, Berry's phase, Aharonov—Bohm effect and Wigner function.
- Explores salient features of quantum entanglement and quantum cryptography.
- Presents basic concepts of quantum computers and the features of no-cloning theorem and quantum cloning machines.
- Describes the theory and techniques of quantum tomography, quantum simulation and quantum error correction.
- Introduces other novel topics including quantum versions of theory of gravity, cosmology, Zeno effect, teleportation, games, chaos and steering.
- Outlines the quantum technologies of ghost imaging, detection of weak amplitudes and displacements, lithography, metrology, teleportation of optical images, sensors, batteries and internet.
- Contains several worked-out problems and exercises in each chapter.

Quantum Mechanics II: Advanced Topics addresses various currently emerging exciting topics of quantum mechanics. It emphasizes the fundamentals behind the latest cutting-edge developments to help explain the motivation for deeper exploration. The book is a valuable resource for graduate students in physics and engineering wishing to pursue research in quantum mechanics.

Taylor & Francis
Taylor & Francis Group
http://taylorandfrancis.com

Quantum Mechanics II

Advanced Topics

Second Edition

S. Rajasekar and R. Velusamy

CRC Press
Taylor & Francis Group
Boca Raton London New York

CRC Press is an imprint of the
Taylor & Francis Group, an **informa** business
A CHAPMAN & HALL BOOK

Second edition published 2023
by CRC Press
4 Park Square, Milton Park, Abingdon, Oxon, OX14 4RN

and by CRC Press
6000 Broken Sound Parkway NW, Suite 300, Boca Raton, FL 33487-2742

© 2023 S. Rajasekar and R. Velusamy

First edition published by CRC Press 2014

CRC Press is an imprint of Informa UK Limited

The right of S. Rajasekar and R. Velusamy to be identified as authors of this work has been asserted in accordance with sections 77 and 78 of the Copyright, Designs and Patents Act 1988.

All rights reserved. No part of this book may be reprinted or reproduced or utilised in any form or by any electronic, mechanical, or other means, now known or hereafter invented, including photocopying and recording, or in any information storage or retrieval system, without permission in writing from the publishers.

For permission to photocopy or use material electronically from this work, access www.copyright.com or contact the Copyright Clearance Center, Inc. (CCC), 222 Rosewood Drive, Danvers, MA 01923, 978-750-8400. For works that are not available on CCC please contact mpkbookspermissions@tandf.co.uk

Trademark notice: Product or corporate names may be trademarks or registered trademarks, and are used only for identification and explanation without intent to infringe.

British Library Cataloguing-in-Publication Data
A catalogue record for this book is available from the British Library

Library of Congress Cataloging-in-Publication Data

Names: Rajasekar, S. (Shanmuganathan), 1963- author. | Velusamy, R., 1952- author.
Title: Quantum mechanics / S. Rajasekar, R. Velusamy.
Description: Second edition. | Boca Raton : CRC Press, 2022. | Includes bibliographical references and index. | Contents: v. 1. The fundamentals -- v. 2. Advanced topics. | Summary: "Quantum Mechanics I: The Fundamentals provides a graduate-level account of the behavior of matter and energy at the molecular, atomic, nuclear, and sub-nuclear levels. It covers basic concepts, mathematical formalism, and applications to physically important systems. This fully updated new edition addresses many topics not typically found in books at this level, including: Bound state solutions of quantum pendulum Morse oscillator Solutions of classical counterpart of quantum mechanical systems A criterion for bound state Scattering from a locally periodic potential and reflection-less potential Modified Heisenberg relation Wave packet revival and its dynamics An asymptotic method for slowly varying potentials Klein paradox, Einstein-Podolsky-Rosen (EPR) paradox, and Bell's theorem Delayed-choice experiments Fractional quantum mechanics Numerical methods for quantum systems A collection of problems at the end of each chapter develops students' understanding of both basic concepts and the application of theory to various physically important systems. This book, along with the authors' follow-up Quantum Mechanics II: Advanced Topics, provides students with a broad, up-to-date introduction to quantum mechanics. Print Versions of this book also include access to the ebook version"-- Provided by publisher.
Identifiers: LCCN 2022021033 | ISBN 9780367769987 (v. 1 ; hardback) | ISBN 9780367776367 (v. 1 ; paperback) | ISBN 9781003172178 (v. 1 ; ebook) | ISBN 9780367770006 (v. 2 ; hardback) | ISBN 9780367776428 (v. 2 ; paperback) | ISBN 9781003172192 (v. 2 ; ebook)
Subjects: LCSH: Quantum theory.
Classification: LCC QC174.12 .R348 2022 | DDC 530.12--dc23/eng20220518
LC record available at https://lccn.loc.gov/2022021033

ISBN: 978-0-367-77000-6 (hbk)
ISBN: 978-0-367-77642-8 (pbk)
ISBN: 978-1-003-17219-2 (ebk)

DOI: 10.1201/9781003172192

Typeset in CMR10 font
by KnowledgeWorks Global Ltd.

Publisher's note: This book has been prepared from camera-ready copy provided by the authors.

To our teachers.

Taylor & Francis
Taylor & Francis Group
http://taylorandfrancis.com

Contents

Preface **xiii**

About the Authors **xvii**

1 Quantum Field Theory **1**
1.1 Introduction . . . 1
1.2 Why Quantum Field Theory? . . . 1
1.3 What is a Field? . . . 2
1.4 Classical Field Theory . . . 3
1.5 Quantum Equations for Fields . . . 7
1.6 Quantization of Nonrelativistic Wave Equation . . . 8
1.7 Electromagnetic Field in Vacuum . . . 12
1.8 Interaction of Charged Particles with Electromagnetic Field . . . 17
1.9 Quantization of Klein–Gordon Equation . . . 20
1.10 Quantization of Dirac Field . . . 25
1.11 Gauge Field Theories . . . 27
1.12 Concluding Remarks . . . 29
1.13 Bibliography . . . 29
1.14 Exercises . . . 30

2 Path Integral Formulation **33**
2.1 Introduction . . . 33
2.2 Time Evolution of Wave Function and Propagator . . . 34
2.3 Path Integral Representation of Propagator . . . 35
2.4 Connection Between Propagator and Classical Action . . . 36
2.5 Schrödinger Equation From Path Integral Formulation . . . 39
2.6 Transition Amplitude of a Free Particle . . . 40
2.7 Systems with Quadratic Lagrangian . . . 42
2.8 Path Integral Version of Ehrenfest's Theorem . . . 48
2.9 Concluding Remarks . . . 48
2.10 Bibliography . . . 49
2.11 Exercises . . . 50

3 Supersymmetric Quantum Mechanics **51**
3.1 Introduction . . . 51
3.2 Supersymmetric Potentials . . . 52
3.3 Relations Between the Eigenstates of Two Supersymmetric Hamiltonians 58
3.4 Hierarchy of Supersymmetric Hamiltonians . . . 61
3.5 Applications . . . 62
3.6 Generation of Complex Potentials with Real Eigenvalues . . . 66
3.7 Concluding Remarks . . . 71
3.8 Bibliography . . . 71

3.9 Exercises . . . 73

4 Coherent and Squeezed States **75**
4.1 Introduction . . . 75
4.2 The Uncertainty Product of Harmonic Oscillator . . . 76
4.3 Coherent States: Definition, Uncertainty Product and Physical Meaning . . . 78
4.4 Generation and Properties of Coherent States . . . 80
4.5 Spin Coherent States . . . 86
4.6 Coherent States of Position-Dependent Mass Systems . . . 87
4.7 Squeezed States . . . 89
4.8 Deformed Oscillators and Nonlinear Coherent States . . . 94
4.9 Concluding Remarks . . . 98
4.10 Bibliography . . . 98
4.11 Exercises . . . 102

5 Berry's Phase, Aharonov–Bohm and Sagnac Effects **105**
5.1 Introduction . . . 105
5.2 Derivation of Berry's Phase . . . 106
5.3 Origin and Properties of Berry's Phase . . . 108
5.4 Classical Analogue of Berry's Phase . . . 109
5.5 Berry's Phase in Solid State Physics . . . 111
5.6 Examples and Effects of Berry's Phase . . . 113
5.7 Applications of Berry's Phase . . . 114
5.8 Experimental Verification of Berry's Phase . . . 116
5.9 Pancharatnam's Work . . . 117
5.10 Cumulants Associated with Geometric Phases . . . 118
5.11 The Aharonov–Bohm Effect . . . 119
5.12 Sagnac Effect . . . 123
5.13 Concluding Remarks . . . 126
5.14 Bibliography . . . 127
5.15 Exercises . . . 129

6 Phase Space Picture and Canonical Transformations **131**
6.1 Introduction . . . 131
6.2 Squeeze and Rotation in Phase Space . . . 132
6.3 Linear Canonical Transformations . . . 134
6.4 Wigner Function . . . 135
6.5 Time Evolution of the Wigner Function . . . 139
6.6 Applications . . . 142
6.7 Advantages of the Wigner Function . . . 146
6.8 Concluding Remarks . . . 147
6.9 Bibliography . . . 147
6.10 Exercises . . . 149

7 Quantum Entanglement **151**
7.1 Introduction . . . 151
7.2 States in Classical Mechanics . . . 152
7.3 Quantum Entangled States . . . 153
7.4 Mixed States . . . 156
7.5 Bipartite Systems . . . 158

7.6 Separability Criteria . . . 161
7.7 Multipartite Entanglement . . . 165
7.8 Quantifying Entanglement . . . 166
7.9 Applications of Entanglement . . . 171
7.10 Concluding Remarks . . . 173
7.11 Bibliography . . . 174
7.12 Exercises . . . 177

8 Quantum Decoherence 179
8.1 Introduction . . . 179
8.2 Decoherence and Interference Damping . . . 180
8.3 Interaction of a Detector on the Double-Slit Experiment . . . 181
8.4 Decoherence Due to Phase Randomization . . . 182
8.5 Position Decoherence Due to Environmental Scattering . . . 185
8.6 Master Equations . . . 187
8.7 Decoherence Models . . . 191
8.8 Decoherence Experiments . . . 192
8.9 The Role of Decoherence in the Interpretation of Quantum Mechanics . . . 195
8.10 Concluding Remarks . . . 198
8.11 Bibliography . . . 198
8.12 Exercises . . . 200

9 Quantum Computers 201
9.1 Introduction . . . 201
9.2 What is a Quantum Computer? . . . 201
9.3 Why is a Quantum Computer? . . . 204
9.4 Fundamental Properties . . . 205
9.5 Quantum Algorithms . . . 213
9.6 Testing Quantum Computers Using Grover's Algorithm . . . 220
9.7 Features of Quantum Computation . . . 221
9.8 Quantum Computation Through NMR . . . 221
9.9 Why is Making a Quantum Computer Extremely Difficult? . . . 222
9.10 Concluding Remarks . . . 223
9.11 Bibliography . . . 223
9.12 Exercises . . . 225

10 Quantum Cryptography 229
10.1 Introduction . . . 229
10.2 Standard Cryptosystems . . . 229
10.3 Quantum Cryptography–Basic Principle . . . 231
10.4 Types of Quantum Cryptography . . . 233
10.5 Multiparty Quantum Secret Sharing . . . 239
10.6 Applications of Quantum Cryptography . . . 241
10.7 Implementation and Limitations . . . 242
10.8 Fiber-Optical Quantum Key Distribution . . . 243
10.9 Quantum Cheque Scheme . . . 243
10.10 Concluding Remarks . . . 246
10.11 Bibliography . . . 247
10.12 Exercises . . . 248

11 No-Cloning Theorem and Quantum Cloning Machines **251**
11.1 Introduction . . . 251
11.2 Proof of No-Cloning Theorem . . . 251
11.3 No-Broadcasting Theorem . . . 253
11.4 No-Cloning and No-Superluminar Signalling . . . 255
11.5 Quantum Cloning Machines . . . 256
11.6 Quantum Telecloning . . . 261
11.7 Other No-Go Theorems . . . 263
11.8 Concluding Remarks . . . 264
11.9 Bibliography . . . 264
11.10 Exercises . . . 265

12 Quantum Tomography **267**
12.1 Introduction . . . 267
12.2 Pauli Problem . . . 268
12.3 Recovery of Density Matrix from Wigner Function . . . 270
12.4 Optical Homodyne Tomography . . . 273
12.5 Qubit Quantum Tomography . . . 274
12.6 Experimental Measure of Polarization of a Photonic Qubit . . . 277
12.7 Multiqubit Tomography . . . 279
12.8 Quantum Process Tomography . . . 280
12.9 Conclusion . . . 283
12.10 Bibliography . . . 283
12.11 Exercises . . . 285

13 Quantum Simulation **287**
13.1 Introduction . . . 287
13.2 Limitations of Classical Computers in Simulating Quantum Systems . . . 288
13.3 Quantum Simulators . . . 289
13.4 Analog Quantum Simulators . . . 290
13.5 Digital Quantum Simulators . . . 291
13.6 Theory of Quantum Simulation of the Schrödinger Equation . . . 293
13.7 Quantum Simulators Using Quantum Computers . . . 294
13.8 Quantum Circuits . . . 295
13.9 Quantum Circuits for Final Measurements . . . 299
13.10 Concluding Remarks . . . 300
13.11 Bibliography . . . 300
13.12 Exercises . . . 302

14 Quantum Error Correction **305**
14.1 Introduction . . . 305
14.2 Sources of Errors in Quantum Information Processing . . . 305
14.3 Difficulties of Using Classical Error Correction Techniques to QEC . . . 308
14.4 Digitization of Quantum Errors . . . 310
14.5 QEC Mechanisms Using Quantum Redundancy . . . 310
14.6 QEC with Stabilizer Codes . . . 314
14.7 The Surface Code . . . 317
14.8 Practical Issues in the Implementation of QEC Codes . . . 319
14.9 Concluding Remarks . . . 322
14.10 Bibliography . . . 322
14.11 Exercises . . . 324

15 Some Other Advanced Topics **327**
15.1 Introduction . . . 327
15.2 Quantum Theory of Gravity . . . 327
15.3 Quantum Cosmology . . . 331
15.4 Quantum Zeno Effect . . . 337
15.5 Quantum Teleportation . . . 343
15.6 Quantum Games . . . 346
15.7 Quantum Pseudo-Telepathy Games . . . 352
15.8 Quantum Steering . . . 358
15.9 Quantum Diffusion . . . 359
15.10 Quantum Chaos . . . 362
15.11 Concluding Remarks . . . 366
15.12 Bibliography . . . 367
15.13 Exercises . . . 374

16 Quantum Technologies **375**
16.1 Introduction . . . 375
16.2 Quantum Entangled Photons . . . 376
16.3 Ghost Imaging . . . 378
16.4 Detection of Weak Amplitude Object . . . 379
16.5 Entangled Two-Photon Microscopy . . . 381
16.6 Detection of Small Displacements . . . 382
16.7 Quantum Lithography . . . 384
16.8 Quantum Metrology . . . 386
16.9 Quantum Teleportation of Optical Images . . . 389
16.10 Quantum Sensors . . . 389
16.11 Quantum Batteries . . . 394
16.12 Quantum Internet . . . 397
16.13 Concluding Remarks . . . 399
16.14 Bibliography . . . 400
16.15 Exercises . . . 406

Solutions to Selected Exercises **407**

Index **411**

Taylor & Francis
Taylor & Francis Group
http://taylorandfrancis.com

Preface

Quantum mechanics is the study of the behaviour of matter and energy at the molecular, atomic, nuclear levels and even at sub-nuclear level. This book is intended to provide a broad introduction to fundamental and advanced topics of quantum mechanics. Volume I is devoted to basic concepts, mathematical formalism and application to physically important systems. Volume II covers most of the advanced topics of current research interest in quantum mechanics. Both the volumes are primarily developed as texts at the graduate level and also as reference books. In addition to worked-out examples, numerous collection of exercises are included at the end of each chapter. Solutions are available to confirmed instructors upon request to the publisher. Some of the exercises serve as a mode of understanding and highlighting the significances of basic concepts while others form application of theory to various physically important systems/problems. Developments made in recent years on various mathematical treatments, theoretical methods, their applications and experimental observations are pointed out wherever necessary and possible and moreover they are quoted with references so that readers can refer them for more details.

Volume I consists of 23 chapters and 7 appendices. Chapter 1 summarizes the needs for the quantum theory and its early development (old quantum theory). Chapters 2 and 3 provide the basic mathematical framework of quantum mechanics. Schrödinger wave mechanics and operator formalism are introduced in these chapters. Chapters 4 and 5 are concerned with the analytical solutions of bound states and scattering states, respectively, of certain physically important microscopic systems. The basics of matrix mechanics, Dirac's notation of state vectors and Hilbert space are elucidated in chapter 6. The next chapter gives the Schrödinger, Heisenberg and interaction pictures of time evolution of quantum mechanical systems. Description of time evolution of ensembles by means of density matrix is also described. Chapter 8 is concerned with Heisenberg's uncertainty principle. A brief account of wave function in momentum space and wave packet dynamics are presented in chapters 9 and 10, respectively. Theory of angular momentum is covered in chapter 11. Chapter 12 is devoted exclusively to the theory of hydrogen atom.

Chapters 13 through 16 are mainly concerned with approximation methods such as time-independent and time-dependent perturbation theories, WKB method and variational method. The elementary theory of elastic scattering is presented in chapter 17. Identical particles are treated in chapter 18. The next chapter presents quantum theory of relativistic particles with specific emphasize on Klein–Gordon equation, Dirac equation and its solution for a free particle, a particle in a box (Klein paradox) and hydrogen atom.

Quantum mechanics has novel concepts like wave-particle duality, the uncertainty principle and wave function collapse due to measurement done. Chapter 20 examines the strange consequences of role of measurement through the paradoxes of EPR and a thought experiment of Schrödinger. A brief sketch of Bell's inequality and the quantum mechanical examples violating it are given. With reference to wave-particle duality modified double slit experiments, referred as delayed-choice experiments, have been proposed and performed to identify whether a microscopic particle decides to behave as a particle or wave at the slits itself irrespective of the later path. These experiments and their outcomes are presented in chapter 21. The next chapter introduces and covers the various features of fractional

quantum mechanics where in the Schrödinger equation the space derivative or the time derivative or both can be fractional.

Considering the rapid growth of numerical techniques in solving physical problems and significances of simulation studies in describing complex phenomena, the final chapter is devoted for a detailed description of numerical computation of bound state eigenvalues and eigenfunctions, transmission and reflection probabilities of scattering potentials, transition probabilities of quantum systems in the presence of external fields and electronic distribution of atoms. Some supplementary and background materials are presented in the appendices.

The pedagogic features of volume I of the book, which are not usually found in textbooks at this level, are the presentation of bound state solutions of Morse oscillator, quantum pendulum, Pöschl–Teller potential, damped and forced linear harmonic oscillator, solutions of classical counter part of quantum mechanical systems considered, criterion for bound state, scattering from a locally periodic potential and reflectionless potential, modified Heisenberg relation, quaternionic quantum mechanics, wave packet revival and its dynamics, hydrogen atom in D-dimension, alternate perturbation theories, an asymptotic method for slowly varying potentials, Klein paradox, EPR paradox, Bell's theorem, delayed-choice experiments, fractional quantum mechanics and numerical methods for quantum systems.

The volume II consists of 16 chapters. Chapter 1 describes the basic ideas of both classical and quantum field theories. Quantization of nonrelativistic equation, electromagnetic field, Klein–Gordon equation and Dirac field is given. The formulation of quantum mechanics in terms of path integrals is presented in chapter 2. Application of it to free particle and undamped and damped linear harmonic oscillators are considered. In chapter 3 some illustrations and interpretation of supersymmetric potentials and partners are presented. A simple general procedure to construct all the supersymmetric partners of a given quantum mechanical systems with bound states is described. The method is then applied to a few interesting system. A method to generate complex potentials with real eigenvalues is presented. The next chapter is concerned with coherent and squeezed states. Construction of these states and their characteristic properties are enumerated. Chapter 5 is devoted to Berry's phase, Aharonov–Bohm and Sagnac effects. Their origin, properties, effects and experimental demonstration are presented. The features of Wigner distribution function are elucidated in chapter 6.

In composite quantum systems, entanglement is a kind of correlation between subsystems with no classical counterpart. The definition, detection, classification, quantification and the application of quantum entanglement are covered in chapter 7. The next chapter discusses the concept of quantum decoherence, its models, experimental studies on it and its significance in the interpretation of quantum mechanics. There is a growing interest on quantum computing. Basic aspects of quantum computing are presented in chapter 9. Deutsch–Jozsa algorithm of finding whether a function is constant or not, Grover's search algorithm and Shor's efficient quantum algorithm for integer factorization and evaluation of discrete logarithms are described. Chapter 10 deals with quantum cryptography. Basic principles of classical cryptography and quantum cryptography and features of a few quantum cryptographic systems are discussed.

Chapter 11 presents no-cloning theorem concerned with the impossibility of copying a quantum state without destroying the original state and the features of quantum cloning machines. Learning the state of a quantum system by appropriate measurements is known as quantum tomography. An overview of the relevant theory and techniques of quantum tomography is provided in chapter 12. Simulating or emulating less controllable quantum systems through some controllable quantum systems is the aim of quantum simulation. Chapter 13 is devoted to the theoretical and experimental aspects of quantum simulation. The next chapter is concerned with quantum error correction (QEC), which is foundational in quantum computing and quantum information processing due to the presence of noise

and interaction of the systems with the environment and the measurement devices. Basic ideas of QEC, setting and using of QEC codes and practical issues in the implementation of QEC codes are covered.

A brief introduction to other advanced topics such as quantum gravity, quantum cosmology, quantum Zeno effect, quantum teleportation, quantum games, quantum diffusion and quantum chaos is presented in chapter 15. The last chapter gives features of some of the recent technological applications of quantum mechanics. Particularly, promising applications of quantum mechanics in ghost imaging, detection of weak amplitude objects and small displacements, entangled two-photon microscopy, lithography, metrology, teleportation of optical images and quantum sensors, batteries and internet are briefly discussed.

In the second edition of both the volumes, comprehensive revision of the chapters in the first edition and extensive enlargement through the addition of two chapters in volume I and six chapters in volume II have been made. Other chapters in the first edition are updated by including the advancements witnessed in the past several years. Key revision to the volume I includes new sections/subsections on Morse oscillator, damped and forced linear harmonic oscillators, moments of linear harmonic oscillator, two-dimensional exactly solvable systems, quaternionic quantum mechanics, condition for a wave function to possess the minimum uncertainty product, wave packet revival of a particle in a box potential, density matrix of a spin-1/2 system and two new chapters on delayed-choice experiments and fractional quantum mechanics.

In volume II six new chapters on quantum entanglement, quantum decoherence, no-cloning theorem and quantum cloning machines, quantum tomography, quantum simulation and QEC are presented. Further, some notable newly added topics in other chapters are application of path integral formulation to linearly damped systems, generation of complex supersymmetric potentials with real eigenvalues, coherent states of position-dependent mass systems, spin coherent states, Zak phase, cumulants with geometric phases, Aharonov–Bohm effect in electrodynamics, testing quantum computers using Grover's algorithm, multi-photon and mult-stage protocol for cryptography, quantum cheque scheme, quantum cosmology, quantum batteries, quantum sensors and quantum internet. Typographical errors occurred in the first edition of both the volumes are corrected in the second edition.

During the preparation of this book, we have received great supports from many colleagues, students and friends. In particular, we are grateful to Prof. N. Arunachalam, Prof. K.P.N. Murthy, Prof. M. Daniel, Dr. S. Sivakumar, Mr. S. Kanmani, Dr. V. Chinnathambi, Dr. P. Philominathan, Dr. K. Murali, Dr. S.V.M. Sathyanarayana, Dr. K. Thamilmaran, Dr.T. Arivudainambi and Dr.V.S. Nagarathinam for their suggestions and encouragement. It is a great pleasure to thank Dr. V.M. Gandhimathi, Dr. V. Ravichandran, Dr. S. Jeyakumari, Dr. G. Sakthivel, Dr. M. Santhiah, Dr. R. Arun, Dr. C. Jeevarathinam, Dr. R. Jothimurugan, Dr. K. Abirami and Dr. S. Rajamani for typesetting some of the chapters. We thank the senior publishing editor Luna Han, commissioning editor for physics Carolina Antunes, editorial assistants Betsy Byers and Danny Kielty, and Michael Davidson, production editor at Taylor & Francis for various suggestions and careful editing of the manuscript, and their team members for smooth handling of the publication process. Finally, we thank our family members for their unflinching support, cooperation and encouragement during the course of preparation of this work.

Tiruchirapalli
July, 2022

S. Rajasekar
R. Velusamy

Taylor & Francis
Taylor & Francis Group
http://taylorandfrancis.com

About the Authors

Shanmuganathan Rajasekar was born in Thoothukudi, Tamilnadu, India in 1962. He received his B.Sc. and M.Sc. in Physics, both from St. Joseph's College, Tiruchirapalli. He was awarded Ph.D. degree from Bharathidasan University in 1992 under the supervision of Prof.M. Lakshmanan. In 1993, he joined as a Lecturer at the Department of Physics, Manonmaniam Sundaranar University, Tirunelveli. In 2003, the book on *Nonlinear Dynamics: Integrability, Chaos and Patterns* written by Prof. M. Lakshmanan, and the author was published by Springer. In 2005, he joined as a Professor at the School of Physics, Bharathidasan University. In 2016 Springer has published the book on Nonlinear Resonances written by Prof. Miguel A.F. Sanjuan and the author. In 2021 Professors U.E. Vincent, P.V.E. McClintock, I.A. Khovanov, and the author compiled and edited two issues of Philosophical Transactions of the Royal Society A on the theme Vibrational and Stochastic Resonances in Driven Nonlinear Systems. He has also edited a book on Recent Trends in Chaotic, Nonlinear and Complex Dynamics with Professors Jan Awrejecewicz and Minvydas Ragulskis published by World Scientific in 2022. His recent research focuses on nonlinear dynamics with a special emphasize on nonlinear resonances. He has authored or coauthored more than 120 research papers in nonlinear dynamics.

Ramiah Velusamy was born in Srivilliputhur, Tamilnadu, India in the year 1952. He received his B.Sc. degree in Physics from the Ayya Nadar Janaki Ammal College, Sivakasi in 1972 and M.Sc. in Physics from the P.S.G. Arts and Science College, Coimbatore in 1974. He worked as a demonstrator in the Department of Physics in P.S.G. Arts and Science College during 1974–1977. He received M.S. Degree in Electrical Engineering at Indian Institute of Technology, Chennai in the year 1981. In the same year, he joined in Ayya Nadar Janaki Ammal College as an Assistant Professor in Physics. He was awarded M.Phil. degree in Physics in the year 1988. He retired in the year 2010. His research topics are quantum confined systems and wave packet dynamics.

Taylor & Francis
Taylor & Francis Group
http://taylorandfrancis.com

1

Quantum Field Theory

1.1 Introduction

Classical field theory makes it feasible to study about the fields within the formulation of classical mechanics. The application of quantum mechanics to fields leads to quantum field theory (QFT) [1,2]. The essential principles of QFT were developed by Paul Adrien Maurice Dirac, Wolfgang Joseph Pauli, Richard Phillips Feynman and others during 1920–1950. *What are the salient features of QFT? What does it impart to our knowledge that was not present already in classical field theory and in quantum mechanics?* The basic characteristic ideas of QFT are two fold:

1. The dynamical degrees of freedom are operators, functions of space and time and they satisfy appropriate commutation relations.
2. The interactions of the fields are essentially local. So, the equations of motion and the corresponding commutation relations in space-time depend only on the behaviour of the fields and their derivatives at the point of consideration.

Relativistic and nonrelativistic systems can be quantized in the Schrödinger, Heisenberg and interaction pictures. Schrödinger picture is rarely considered in QFT because in most cases Heisenberg picture is considerably easier to perform quantization. In QFT the Klein–Gordon (KG), Dirac and Maxwell equations describing spin-0, 1/2 and 1 particles, respectively, need to be quantized. The predictions of QFT are found to be in best agreement with experimental observations in all physics. It is a powerful tool for particle physics and condensed matter physics, many body problems in superconductivity, theory of metals and quantum Hall effect.

In the present chapter first we indicate the need for QFT. We describe the basic ideas involved in the classical field theory (CFT). Next, we obtain quantum equations for fields and quantize the nonrelativistic Schrödinger equation and electromagnetic field in vacuum. We discuss the interaction of charged particles and the electromagnetic field in the frame work of QFT. Then we quantize KG and Dirac equations.

1.2 Why Quantum Field Theory?

In quantum mechanics space and time are considered differently. Here time appears as a parameter while space coordinates become operators and are observables. Further, in the quantum theory the total number of particles are assumed to be remain the same. But there are situations where the number of particles is changed. Consider the following problems.

DOI: 10.1201/9781003172192-1

1. In certain processes particles are created and destroyed. An example is β-decay where a neutron decays into a proton, an electron and an anti-neutrino. This decay process is represented as $\mathrm{n} \rightarrow \mathrm{p} + \mathrm{e}^- + \overline{\gamma}_\mathrm{e}$. A neutron is annihilated while the particles p and e^- and $\overline{\gamma}_e$ are created. The total number of particles is not conserved.
2. In relativistic theory according to Einstein's mass-energy relation $E = mc^2$ new particles can be created from energy. For example, if an electron and a positron collide with enough high energy then an additional electron-positron pair would be created: $\mathrm{e}^- + \mathrm{e}^+ \rightarrow \mathrm{e}^- + \mathrm{e}^+ + \mathrm{e}^- + \mathrm{e}^+$. In this process the total number of particles is changed due to the creation of new particles.
3. In the problem of interaction of electromagnetic field with a system, we handle the system as quantum mechanical while the field as classical. However, we treat the absorption and emission of radiation as absorption and emission of photons. In this case the number of particles change.
4. The negative energy states in Dirac equation imply the existence of antiparticles are created in various processes.
5. In certain processes the initial and final states contain same particles but in the intermediate states creation and annihilation of other particles occur. The final results are affected by the processes in the intermediate states.

The quantum theory must include the above possibilities that alter the number of particles in the system and creation and annihilation of particles. This is done in QFT. In the correspondence limit $\hbar \rightarrow 0$, nonrelativistic Schrödinger equation reduces to classical mechanics but not to relativistic equation. The Dirac equation has no ground state. For a system of identical particles the wave function must be symmetric or antisymmetric with respect to exchange the coordinates of the particles. This makes the wave function highly complex. These problems can be resolved by considering quantum fields rather than particles.

1.3 What is a Field?

The concept of field was originally introduced in classical theory to account for the interaction between two systems separated by a finite distance. For example, in classical physics the electric field $\mathbf{E}(\mathbf{X}, t)$ is a three-component function and the interaction between two charged systems 1 and 2 is viewed as the interaction of the system 2 with the created electric field of system 1.

A function $\phi(\mathbf{X})$ that depends on one or more variables $\mathbf{X}$ is called a *field variable* or simply a field. A field is an entity and not a particle present in space. The field of a system carries momentum, energy and other observables. A field depends on space coordinates but can vary with time also. We can write the field variable as $\phi(\mathbf{X}, t)$. The mathematical equations describing the connection between $\mathbf{X}$, t and ϕ are the *field equations*. A theory describing a system in terms of one or more fields is called a *field theory*. The position and momentum variables of a classical particle are fields and the equation of motion is the field equation. Thus, classical mechanics is a field theory. We can treat the components of electric and magnetic fields as variables and the Maxwell equations as field equations. Therefore, electromagnetism is a field theory.

The field amplitude $\phi(\mathbf{X}, t)$ may vary from point to point in space and their values at different points are independent of each other. In field theory, each of the values of the space coordinates are treated as generalized coordinates. So, the field has an infinite

number of degrees of freedom. Therefore, it can be considered analogous to a system with an infinite number of particles. In quantum theory the field concept takes a new dimension. The basic idea of QFT is that we associate particles with field such as the electromagnetic field (photon).

1.4 Classical Field Theory

Before we get into the problem of quantization in quantum mechanics, first we discuss some basic methods involved in the formulation of classical field theories. Quantization of a classical field turns a classical field into an operator capable of creating particles from a vacuum [3]. Quantization of classical equations of motion of a system refers to the replacement of numerical functions representing the positions and momenta by operators obeying prescribed commutation relations. A notable point is that results of quantum mechanics follow from this prescription. *How do we obtain field equations?* Generally, they are derived from a variational principle. In this principle, starting from the Lagrangian we construct a quantity called *action* and obtain its stationary value.

1.4.1 Lagrangian Formalism

In classical mechanics the Lagrangian L is denoted as $L(q, \dot{q}, t)$. We consider it as a spatial integral of some function of a field. The integrand have the dimensions of Lagrangian density ($\mathcal{L}$). We denote the fields as ϕ^A. Different values of A yields different fields. For simplicity we drop the superscript A and denote the fields as ϕ.

We write L as

$$L(\phi, \dot{\phi}) = \int \mathcal{L}(\phi, \dot{\phi}, \partial\phi/\partial x)\, \mathrm{d}x\,, \tag{1.1}$$

where L is assumed to depend on ϕ and $\dot{\phi}$. ϕ takes the role of coordinate q in $L(q, \dot{q}, t)$. $\mathcal{L}$ is assumed to depend on space derivative also because space coordinates are also independent parameters. Relation between $\mathcal{L}$ and equations of motion exists.

In the Lagrangian formulation, we begin from the action S

$$\begin{aligned} S &= \int_{t_1}^{t_2} L\, \mathrm{d}t = \int_{t_1}^{t_2} \mathrm{d}t \int_{x_1}^{x_2} \mathrm{d}x \mathcal{L}(\phi, \dot{\phi}, \partial\phi/\partial x) \\ &= \int_{\Omega} \mathcal{L}\, \mathrm{d}\tau\,, \quad \mathrm{d}\tau = \mathrm{d}x\, \mathrm{d}t\,, \end{aligned} \tag{1.2}$$

where Ω specifies the space-time region of our interest and t_1 and t_2 are the initial and end values of time. Often Ω is chosen to be all space-time. S given by Eq. (1.2) is simply a number. In general, S will change if the field is changed and hence it is called a *functional*. We assume the periodic boundary condition $\phi(x + L) = \phi(x)$.

The principle of least action, which states that among all possible motions the system follows the one for which S is extremum, is used to find the equations of motion. In field theory the principle of least action says that the system evolves through fields that make the action S stationary against small variations of the fields. Suppose we vary the fields ϕ slightly around the true fields ϕ' and write

$$\phi'(x, t) = \phi(x, t) + \delta\phi(x, t)\,. \tag{1.3}$$

For fixed t_1 and t_2 we have $\delta\phi(x,t_1) = \delta\phi(x,t_2) = 0$. Consequently, the change in S, δS, becomes zero to the first-order in $\delta\phi$ making $\delta S = S' - S$. We write

$$\begin{aligned}\delta S &= \int (\mathcal{L}' - \mathcal{L})\,\mathrm{d}\tau \\ &= \int \delta\mathcal{L}\,\mathrm{d}x\,\mathrm{d}t \\ &= \int_{-L/2}^{L/2}\int_{t_1}^{t_2}\left[\frac{\partial\mathcal{L}}{\partial\phi}\,\delta\phi + \frac{\partial\mathcal{L}}{\partial\dot{\phi}}\,\delta\dot{\phi} + \frac{\partial\mathcal{L}}{\partial(\partial\phi/\partial x)}\,\delta(\partial\phi/\partial x)\right]\mathrm{d}x\,\mathrm{d}t, \end{aligned} \tag{1.4}$$

where $\delta\dot{\phi} = \dot{\phi}' - \dot{\phi} = \dot{\delta}\phi$ and

$$\delta\left(\frac{\partial\phi}{\partial x}\right) = \frac{\partial\phi'}{\partial x} - \frac{\partial\phi}{\partial x} - \frac{\partial}{\partial x}(\delta\phi)\,. \tag{1.5}$$

Further,

$$\frac{\partial\mathcal{L}}{\partial\dot{\phi}}\,\delta\dot{\phi} = \frac{\partial\mathcal{L}}{\partial\dot{\phi}}\,\dot{\delta}\phi = \frac{\partial}{\partial t}\left(\frac{\partial\mathcal{L}}{\partial\dot{\phi}}\,\delta\phi\right) - \left[\frac{\partial}{\partial t}\left(\frac{\partial\mathcal{L}}{\partial\dot{\phi}}\right)\right]\delta\phi \tag{1.6}$$

and

$$\begin{aligned}\frac{\partial\mathcal{L}}{\partial(\partial\phi/\partial x)}\delta\left(\frac{\partial\phi}{\partial x}\right) &= \frac{\partial\mathcal{L}}{\partial(\partial\phi/\partial x)}\,\frac{\partial}{\partial x}(\delta\phi) \\ &= \frac{\partial}{\partial x}\left(\frac{\partial\mathcal{L}}{\partial(\partial\phi/\partial x)}\delta\phi\right) - \frac{\partial}{\partial x}\left(\frac{\partial\mathcal{L}}{\partial(\partial\phi/\partial x)}\right)\delta\phi. \end{aligned} \tag{1.7}$$

Then Eq. (1.4) becomes

$$\begin{aligned}\delta S = \int_{-L/2}^{L/2}\int_{t_1}^{t_2}\Bigg\{&\frac{\partial\mathcal{L}}{\partial\phi}\,\delta\phi + \frac{\partial}{\partial t}\left(\frac{\partial\mathcal{L}}{\partial\dot{\phi}}\,\delta\phi\right) - \frac{\partial}{\partial t}\left(\frac{\partial\mathcal{L}}{\partial\dot{\phi}}\right)\delta\phi \\ &+\frac{\partial}{\partial x}\left(\frac{\partial\mathcal{L}}{\partial(\partial\phi/\partial x)}\,\delta\phi\right) - \left[\frac{\partial}{\partial x}\left(\frac{\partial\mathcal{L}}{\partial(\partial\phi/\partial x)}\right)\right]\delta\phi\Bigg\}\,\mathrm{d}x\,\mathrm{d}t. \end{aligned} \tag{1.8}$$

We have the following results:

$$\int_{t_1}^{t_2}\frac{\partial}{\partial t}\left(\frac{\partial\mathcal{L}}{\partial\dot{\phi}}\right)\delta\phi\,\mathrm{d}t = \frac{\partial\mathcal{L}}{\partial\dot{\phi}}\,\delta\phi\Big|_{t_1}^{t_2} = 0\,, \tag{1.9a}$$

$$\int_{-L/2}^{L/2}\frac{\partial}{\partial x}\left(\frac{\partial\mathcal{L}}{\partial(\partial\phi/\partial x)}\,\delta\phi\right)\mathrm{d}x = \frac{\partial\mathcal{L}}{\partial(\partial\phi/\partial x)}\,\delta\phi\Big|_{-L/2}^{L/2} = 0\,. \tag{1.9b}$$

Use of these results in Eq. (1.8) leads to

$$\delta S = \int_{-L/2}^{L/2}\int_{t_1}^{t_2}\left[\frac{\partial\mathcal{L}}{\partial\phi} - \frac{\partial}{\partial t}\left(\frac{\partial\mathcal{L}}{\partial\dot{\phi}}\right) - \frac{\partial}{\partial x}\left(\frac{\partial\mathcal{L}}{\partial(\partial\phi/\partial x)}\right)\right]\delta\phi\,\mathrm{d}x\,\mathrm{d}t. \tag{1.10}$$

We require $\delta S = 0$ for any arbitrary variation $\delta\phi$. This implies that the terms in the square-bracket in Eq. (1.10) should be zero for all values of (x,t). This gives

$$\frac{\partial\mathcal{L}}{\partial\phi} - \frac{\partial}{\partial t}\left(\frac{\partial\mathcal{L}}{\partial\dot{\phi}}\right) - \frac{\partial}{\partial x}\left(\frac{\partial\mathcal{L}}{\partial(\partial\phi/\partial x)}\right) = 0\,. \tag{1.11}$$

Equation (1.11) is the classical field equation and is called *Euler–Lagrange equation* for the Lagrangian density. This equation is the condition for the action to be stationary. Thus, in field theory there is a relation between the Lagrangian density and equations of motion.

Equation (1.11) in covariant form reads as

$$\partial_\mu \frac{\partial \mathcal{L}}{\partial(\partial_\mu \phi)} = \frac{\partial \mathcal{L}}{\partial \phi}\,. \tag{1.12}$$

For the field equations to be relativistically invariant the requirement is that the equations must be in covariant form, that is, in all inertial frame the equations should have the same form. The field equation obtainable from $\mathcal{L}$ is covariant if $\mathcal{L}$ is a relativistically scalar density, that is,

$$\mathcal{L}'(\phi', \dot{\phi}', \nabla'\phi', t') = \mathcal{L}(\phi, \dot{\phi}, \nabla\phi, t)\,, \tag{1.13}$$

where prime and unprime refer to two inertial frames. The dependence of Lagrangian density on x is only through the fields ϕ. If it explicitly depends on x then the relativistic invariance will be violated. Since $\mathrm{d}\mathbf{X}\,\mathrm{d}t = \mathrm{d}x\,\mathrm{d}y\,\mathrm{d}z\,\mathrm{d}t$ is relativistically invariant we have

$$S' = \int \mathcal{L}'\,\mathrm{d}\mathbf{X}\,\mathrm{d}t' = \int \mathcal{L}\,\mathrm{d}\mathbf{X}\,\mathrm{d}t = S\,. \tag{1.14}$$

So, action is unchanged under the Lorentz transformation. The equations of motion have the same form in both the coordinate systems and are thus covariant as given by Eq. (1.12).

The invariance of a system under continuous symmetry transformations leads to continuity equations and conservation laws. The derivation of the conservation laws from the invariance of the Lagrangian density is known as *Noether theorem*. This theorem states that every continuous transformation that leaves the action S unchanged leads to a conservation law. For example, the conservation of four-momentum and of angular momentum follows from the invariance of the Lagrangian density $\mathcal{L}$ under translations and rotations, respectively.

Solved Problem 1:

Given the Lagrangian density of a one-dimensional string of linear mass density μ and Young's modulus Y, $\mathcal{L} = (1/2)\left[\mu\dot{q}^2 - Y(\partial q/\partial x)^2\right]$, where $q(x)$ is the displacement of the string, use the Euler–Lagrange equation to find the wave equation.

For the Euler–Lagrange Eq.(1.11) with $\phi = q$, we get

$$\frac{\partial \mathcal{L}}{\partial q} = 0\,, \quad \frac{\partial}{\partial t}\left(\frac{\partial \mathcal{L}}{\partial \dot{q}}\right) = \frac{\partial}{\partial t}\mu\dot{q} = \mu\ddot{q}\,, \tag{1.15}$$

$$\frac{\partial}{\partial x}\left(\frac{\partial \mathcal{L}}{\partial(\partial q/\partial x)}\right) = \frac{\partial}{\partial x}\left(-Y\frac{\partial q}{\partial x}\right) = -Y\frac{\partial^2 q}{\partial x^2}\,. \tag{1.16}$$

Then the Euler–Lagrange equation is

$$\mu\ddot{q} - Y\frac{\partial^2 q}{\partial x^2} = 0 \;\text{ or }\; \frac{\partial^2 q}{\partial t^2} = \frac{Y}{\mu}\frac{\partial^2 q}{\partial x^2} \tag{1.17}$$

which is the wave equation.

1.4.2 Hamiltonian Formalism

Quantization is much more straight-forward in the Hamiltonian formalism. The Hamiltonian formalism is based on the Legendre transform of the Lagrangian with respect to $\dot{\phi}$. Given

a function $f(x)$, introduce a new variable $p = \mathrm{d}f/\mathrm{d}x$ in place of x and replace f by $g(p) = px - f$. $g(p)$ is called *Legendre transform* of $f(x)$. We have $x = \partial g/\partial p$. The Legendre transform of $L(\phi, \dot{\phi}, t)$ gives π (the canonical conjugate momentum) in place of $\dot{\phi}$ (velocity).

Let us consider $H(t, \phi, p) = p\dot{\phi} - L$, where H is the Hamiltonian. π and $\dot{\phi}$ are related by the equation $p = \partial L/\partial\dot{\phi}$. If the volume is divided into a number of small cells with the volume of ith cell as $\delta\tau_i$ then the derivatives of L with respect to ϕ and $\dot{\phi}$ at a point (cell) are denoted as $\overline{\partial}L/\overline{\partial}\phi$ and $\overline{\partial}L/\overline{\partial}\dot{\phi}$ and are called *functional derivatives*. In this case the Euler–Lagrange equation becomes

$$\frac{\overline{\partial}L}{\overline{\partial}\phi} - \frac{\partial}{\partial t}\left(\frac{\overline{\partial}L}{\overline{\partial}\dot{\phi}}\right) = 0\,. \tag{1.18}$$

In analogy with the classical Hamiltonian $H = \sum p_i\dot{q}_i - L$ we write in terms of the fields ϕ_i, $H = \sum p_i\dot{\phi}_i - L$. We define the momentum density as

$$\pi(x) = \frac{\overline{\partial}L}{\overline{\partial}\dot{\phi}} = \frac{\partial\mathcal{L}}{\partial\dot{\phi}}\,. \tag{1.19}$$

The momenta p_i are given by

$$p_i = \pi_i\delta\tau_i = \frac{\partial\mathcal{L}_i}{\partial\dot{\phi}_i}\,\delta\tau_i\,. \tag{1.20}$$

Then

$$H = \sum p_i\dot{\phi}_i - L = \sum \pi_i\delta\tau_i\dot{\phi}_i - \sum \mathcal{L}_i\delta\tau_i = \sum\left(\pi_i\dot{\phi}_i - \mathcal{L}_i\right)\delta\tau_i\,. \tag{1.21}$$

In the continuum limit, letting $\delta\tau_i \to 0$, Eq. (1.21) becomes

$$H = \int(\pi\dot{\phi} - \mathcal{L})\,\mathrm{d}\tau = \int\mathcal{H}\,\mathrm{d}\tau\,, \tag{1.22a}$$

where

$$\mathcal{H}(\phi, \nabla\phi, \pi) = \pi\dot{\phi} - \mathcal{L}(\phi, \dot{\phi}, \nabla\phi) \tag{1.22b}$$

is called *Hamiltonian density*. $\mathcal{L}$ is a function of ϕ, $\dot{\phi}$ and $\nabla\phi$ while $\mathcal{H}$ is a function of ϕ, $\nabla\phi$ and π. δH is written as

$$\delta H = \int_V\left[\frac{\overline{\partial}H}{\overline{\partial}\pi}\,\delta\pi + \frac{\overline{\partial}H}{\overline{\partial}\phi}\,\delta\phi\right]\,\mathrm{d}\tau\,, \tag{1.23a}$$

where

$$\frac{\overline{\partial}H}{\overline{\partial}\phi} = \frac{\partial\mathcal{H}}{\partial\phi} - \sum_k\frac{\partial}{\partial x_k}\left(\frac{\partial\mathcal{H}}{\partial(\partial\phi/\partial x_k)}\right)\,, \tag{1.23b}$$

$$\frac{\overline{\partial}H}{\overline{\partial}\pi} = \frac{\partial\mathcal{H}}{\partial\pi} - \sum_k\frac{\partial}{\partial x_k}\left(\frac{\partial\mathcal{H}}{\partial(\partial\pi/\partial x_k)}\right)\,. \tag{1.23c}$$

Now, we derive the classical equations of motion. We obtain

$$\begin{aligned}
\delta L &= \int\left[\frac{\overline{\partial}L}{\overline{\partial}\phi}\,\delta\phi + \frac{\overline{\partial}L}{\overline{\partial}\dot{\phi}}\,\delta\dot{\phi}\right]\mathrm{d}\tau \\
&= \int\left[\dot{\pi}\delta\phi + \pi\delta\dot{\phi}\right]\mathrm{d}\tau \\
&= \int\left[\dot{\pi}\delta\phi + \delta(\pi\dot{\phi}) - \dot{\phi}\delta\pi\right]\mathrm{d}\tau \\
&= \int\left[\dot{\pi}\delta\phi + \delta(\mathcal{H} + \mathcal{L}) - \dot{\phi}\delta\pi\right]\mathrm{d}\tau \\
&= \delta H + \delta L + \int(\dot{\pi}\delta\phi - \dot{\phi}\delta\pi)\mathrm{d}\tau\,.
\end{aligned} \tag{1.24}$$

Or

$$\delta H = \int \left(\dot{\phi} \delta\pi - \dot{\pi} \delta\phi \right) \mathrm{d}\tau \,. \tag{1.25}$$

Comparison of Eqs. (1.23a) and (1.25) yields

$$\dot{\phi} = \frac{\overline{\partial} H}{\overline{\partial} \pi} \,, \quad \dot{\pi} = -\frac{\overline{\partial} H}{\overline{\partial} \phi} \,. \tag{1.26}$$

Solved Problem 2:

Find the Hamiltonian equation for time evolution of a function, say, $\mathbf{F}(\phi, \pi, t)$.

We express $\mathbf{F}$ as a volume integral of the functional density $\mathcal{F}(\phi, \pi, t)$. We find

$$\begin{aligned} \frac{\mathrm{d}\mathbf{F}}{\mathrm{d}t} &= \frac{\partial \mathbf{F}}{\partial t} + \int \left(\frac{\partial \mathcal{F}}{\partial \phi} \dot{\phi} + \frac{\partial \mathcal{F}}{\partial \pi} \dot{\pi} \right) \mathrm{d}\tau \\ &= \frac{\partial \mathbf{F}}{\partial t} + \int \left(\frac{\overline{\partial} \mathcal{F}}{\overline{\partial} \phi} \dot{\phi} + \frac{\overline{\partial} \mathcal{F}}{\overline{\partial} \pi} \dot{\pi} \right) \mathrm{d}\tau \\ &= \frac{\partial \mathbf{F}}{\partial t} + \int \left(\frac{\overline{\partial} \mathcal{F}}{\overline{\partial} \phi} \frac{\overline{\partial} H}{\overline{\partial} \pi} - \frac{\overline{\partial} \mathcal{F}}{\overline{\partial} \pi} \frac{\overline{\partial} H}{\overline{\partial} \phi} \right) \mathrm{d}\tau \\ &= \frac{\partial \mathbf{F}}{\partial t} + \{\mathbf{F}, H\} \,, \end{aligned} \tag{1.27}$$

where $\{\mathbf{F}, H\}$ is the Poisson bracket of $\mathbf{F}$ and H.

1.5 Quantum Equations for Fields

Classical field is a quantity varying continuously in space-time and its evolution is described by certain wave equation. In contrast to this, the quantum field is an operator and it creates states of definite momentum and energy. *How do we obtain quantum equations for fields?* The starting point is the field equations. In quantum mechanics the classical field ϕ is a wave field (here onwards we use ψ in place of ϕ) and ψ_i and π_i should be Hermitian. Here i denotes the cell number.

Similar to the commutation relations $[q_i, q_j] = 0$, $[p_i, p_j] = 0$ and $[q_i, p_j] = \mathrm{i}\hbar\delta_{ij}$ we write

$$[\psi(\mathbf{r}, t), \psi(\mathbf{r}', t)] = 0 \,, \tag{1.28a}$$

$$[\pi(\mathbf{r}, t), \pi(\mathbf{r}', t)] = 0 \,, \tag{1.28b}$$

$$[\psi(\mathbf{r}, t), \pi(\mathbf{r}', t)] = \mathrm{i}\hbar\delta^3(\mathbf{r} - \mathbf{r}') \,. \tag{1.28c}$$

As an alternative, ψ can be expanded in a complete orthonormal set of functions, say, u_k, as $\psi(\mathbf{r}, t) = \sum a_k(t) u_k(\mathbf{r})$. Here a_k are the field coordinates. The field equations can be expressed in terms of either ψ or a_k. Further, applying periodic boundary conditions, we can expand ψ in Fourier series and treat the Fourier coefficients as operators obeying the commutation relations.

Let us denote the components of field ψ as $\psi_1, \psi_2, \ldots$. Then the Lagrangian density of the field is

$$\mathcal{L} = \mathcal{L}(\psi_1, \psi_2, \ldots, \nabla\psi_1, \nabla\psi_2, \ldots, t). \tag{1.29}$$

The canonically conjugate momentum of π_j is given as

$$\pi_j = \frac{\overline{\partial} L}{\overline{\partial}\dot{\psi}_j} = \frac{\partial \mathcal{L}}{\partial \dot{\psi}_j} \,. \tag{1.30}$$

Further,

$$\mathcal{H} = \sum_j \pi_j \dot{\psi}_j - \mathcal{L} \,. \tag{1.31}$$

Then the Hamiltonian equations are

$$\dot{\psi}_j = \frac{\overline{\partial} H}{\overline{\partial}\pi_j} \,, \quad \dot{\pi}_j = -\frac{\overline{\partial} H}{\overline{\partial}\psi_j} \,, \quad j = 1, 2, \ldots \,. \tag{1.32}$$

The equation of motion of a dynamical variable F_j is written as

$$\frac{\mathrm{d}F_j}{\mathrm{d}t} = \frac{\partial F_j}{\partial t} + \frac{1}{\mathrm{i}\hbar} [F_j, H] \,. \tag{1.33}$$

The commutation relations (1.28) take the form

$$[\psi_j(\mathbf{r}, t), \psi_{j'}(\mathbf{r}', t)] = 0 \,, \tag{1.34a}$$

$$[\pi_j(\mathbf{r}, t), \pi_{j'}(\mathbf{r}', t)] = 0 \,, \tag{1.34b}$$

$$[\psi_j(\mathbf{r}, t), \pi_{j'}(\mathbf{r}', t)] = \mathrm{i}\hbar \delta^3_{jj'}(\mathbf{r} - \mathbf{r}') \,. \tag{1.34c}$$

In QFT ψ is generally complex: $\psi = \psi_1 + \mathrm{i}\psi_2$. The commutation relations are now given by Eqs. (1.34) with $j = 1, 2$. It can be shown that the field Eqs. (1.11) obtained by independent variations of ψ_1 and ψ_2 are equivalent to those obtained by independent variations of ψ and ψ^*.

1.6 Quantization of Nonrelativistic Wave Equation

Let us apply the quantization technique developed in the previous section to the nonrelativistic Schrödinger equation

$$\mathrm{i}\hbar \frac{\partial \psi}{\partial t} = -\frac{\hbar^2}{2m} \nabla^2 \psi + V\psi \,. \tag{1.35}$$

Equation (1.35) is obtained from classical Hamiltonian by replacing the dynamical variables q and p by their corresponding operators. This is called *first quantization*. Quantization of the Schrödinger equation by replacing the wave function by an operator is known as *second quantization*, the term coined by Dirac. QFT is the quantization of the quantum mechanical wave equation.

On what basis did Dirac introduce the notion of second quantization? If we write $\psi = \sum C_a \psi_a$ then $\sum |C_a|^2 = 1$. This is for a single particle. For a set of N such independent particles we have $\sum |C_a \sqrt{N}|^2 = N$. In this case $|C_a|^2$ is the probable number of particles in the state ψ_a and hence it must be an integer. This requirement is the basic motivation for Dirac's introduction of second quantization [1].

1.6.1 Lagrangian and Hamiltonian Densities Associated with the Schrödinger Equation

Let us first treat Eq. (1.35) as representing a classical wave field. *What are the Lagrangian and Hamiltonian densities associated with Eq. (1.35)?* We can show that

$$\mathcal{L} = \mathrm{i}\hbar\psi^*\dot{\psi} - \frac{\hbar^2}{2m}\nabla\psi^*\cdot\nabla\psi - V(\mathbf{r},t)\psi^*\psi \tag{1.36}$$

leads to the Schrödinger Eq. (1.35). The momentum π canonically conjugate to ψ and $\overline{\pi}$ are given by

$$\pi = \frac{\partial\mathcal{L}}{\partial\dot{\psi}} = \mathrm{i}\hbar\psi^*, \quad \overline{\pi} = \frac{\partial\mathcal{L}}{\partial\dot{\psi}^*} = 0\,. \tag{1.37}$$

In this case $[\psi^*(\mathbf{r},t),\overline{\pi}(\mathbf{r}',t)] = 0$ and hence ψ^* and $\overline{\pi}$ cannot be regarded as a pair of canonically conjugate variables. Further, $\pi^\dagger \neq \overline{\pi}$.

Next, it is easy to show that the Schrödinger equation follows from the Hamiltonian formulation of field description. The Hamiltonian density $\mathcal{H}$ given by Eq. (1.22b) becomes

$$\mathcal{H} = \pi\dot{\psi} - \mathcal{L} = -\frac{\mathrm{i}\hbar}{2m}\nabla\pi\cdot\nabla\psi - \frac{\mathrm{i}}{\hbar}V\pi\psi\,. \tag{1.38}$$

Then

$$H = \int\mathcal{H}\,\mathrm{d}\tau = \int\left(\frac{\hbar^2}{2m}\nabla\psi^\dagger\nabla\psi + V\psi^\dagger\psi\right)\mathrm{d}\tau\,. \tag{1.39}$$

We obtain

$$\dot{\psi} = \frac{\overline{\partial}H}{\overline{\partial}\pi} = \frac{\partial\mathcal{H}}{\partial\pi} - \nabla\left(\frac{\partial\mathcal{H}}{\partial\nabla\pi}\right) = -\frac{\mathrm{i}}{\hbar}V\psi + \frac{\mathrm{i}\hbar}{2m}\nabla^2\psi \tag{1.40a}$$

and

$$\dot{\pi} = \frac{\overline{\partial}H}{\overline{\partial}\psi} = \frac{\partial\mathcal{H}}{\partial\psi} - \nabla\left(\frac{\partial\mathcal{H}}{\partial\nabla\psi}\right) = -\frac{\mathrm{i}}{\hbar}V\pi + \frac{\mathrm{i}\hbar}{2m}\nabla^2\pi\,. \tag{1.40b}$$

We can rewrite Eqs. (1.40) in the standard form of Schrödinger equation.

1.6.2 Number, Creation and Annihilation Operators

Let us define an operator N as

$$N = \int_{-\infty}^{\infty}\psi^\dagger\psi\,\mathrm{d}\tau\,. \tag{1.41}$$

N gives the number of particles in the field and is a Hermitian. The equation of motion of N is

$$\mathrm{i}\hbar\frac{\mathrm{d}N}{\mathrm{d}t} = [N,H] = 0\,. \tag{1.42}$$

We define a representation of N in which it is diagonal. Since N is Hermitian its eigenvalues are real. We consider the expansion

$$\psi(\mathbf{r},t) = \sum C_k(t)u_k(\mathbf{r})\,, \quad \psi^\dagger(\mathbf{r},t) = \sum C_l^\dagger u_l^*(\mathbf{r})\,, \tag{1.43a}$$

where C_k are operators given by

$$C_k(t) = \int_{-\infty}^{\infty}u_k^*(\mathbf{r})\psi(\mathbf{r},t)\,\mathrm{d}\tau \tag{1.43b}$$

and $u_k(\mathbf{r})$ form an orthonormal set of functions. We obtain

$$[C_k, C_l] = \left[C_k^\dagger, C_l^\dagger\right] = 0\,, \quad \left[C_k, C_l^\dagger\right] = \delta_{kl}\,. \tag{1.44}$$

Now,

$$\begin{aligned} N &= \int_{-\infty}^{\infty} \psi^\dagger \psi \,\mathrm{d}\tau \\ &= \int_{-\infty}^{\infty} \sum_k C_k^\dagger u_k^* \sum_l C_l u_l \,\mathrm{d}\tau \\ &= \sum_k C_k^\dagger C_k \\ &= \sum_k N_k\,, \quad N_k = C_k^\dagger C_k\,. \end{aligned} \tag{1.45}$$

It is easy to verify that N_k's commute with other N_k's so that they can be diagonalized.

Suppose we write

$$C_k = \frac{1}{\sqrt{2}}\,(x_k + \mathrm{i}p_k)\,, \quad C_k^\dagger = \frac{1}{\sqrt{2}}\,(x_k - \mathrm{i}p_k) \tag{1.46a}$$

which gives

$$x_k = \frac{1}{\sqrt{2}}\left(C_k + C_k^\dagger\right)\,, \quad p_k = -\frac{\mathrm{i}}{\sqrt{2}}\left(C_k - C_k^\dagger\right)\,. \tag{1.46b}$$

We find

$$N_k = C_k^\dagger C_k = \frac{1}{2}\left(x_k^2 + p_k^2\right) - \frac{1}{2}\,. \tag{1.47}$$

For the harmonic oscillator we have

$$H = \frac{1}{2}p_k^2 + \frac{1}{2}q_k^2\,, \quad E_n = n + \frac{1}{2}\,, \tag{1.48}$$

where we have set $\hbar = 1$, $\omega = 1$ and $m = 1$. Comparison of Eqs. (1.47) and (1.48) we get

$$N_k = n_k, \quad n_k = 0, 1, 2, \ldots\,. \tag{1.49}$$

Further,

$$C_k|n_k\rangle = \sqrt{n_k}\,|n_k - 1\rangle\,, \tag{1.50a}$$

$$C_k^\dagger|n_k\rangle = \sqrt{n_k + 1}\,|n_k + 1\rangle\,. \tag{1.50b}$$

The operator C_k lowers the eigenvalue of n_k by 1 while $C_k^\dagger$ raises it by 1. Therefore, C_k and $C_k^\dagger$ are annihilation and creation operators for the state k of the field.

From Eqs. (1.39), (1.43a) and (1.43b) we get

$$H = \sum_{l,k} C_l^\dagger C_k \left[\int_{-\infty}^{\infty} \frac{\hbar^2}{2m} \nabla u_l^* \cdot \nabla u_k + V u_l^* u_k\right] \mathrm{d}\tau\,. \tag{1.51}$$

Using integration by parts and applying the boundary conditions on the surface at infinity we get

$$\int_{-\infty}^{\infty} \frac{\hbar^2}{2m} \nabla u_l^* \cdot \nabla u_k \,\mathrm{d}\tau = \int_{-\infty}^{\infty} u_l^* \left(-\frac{\hbar^2}{2m}\nabla^2\right) u_k \,\mathrm{d}\tau\,. \tag{1.52}$$

Then Eq. (1.51) becomes

$$\begin{aligned} H &= \sum_{l,k} C_l^\dagger C_k \int_{-\infty}^{\infty} u_l^* \left(-\frac{\hbar^2}{2m}\nabla^2 + V \right) u_k \, \mathrm{d}\tau \\ &= \sum_{l,k} C_l^\dagger C_k E_k \int_{-\infty}^{\infty} u_l^* u_k \, \mathrm{d}\tau \\ &= \sum_k N_k E_k \,. \end{aligned} \tag{1.53}$$

So, in the number representation, the ket $|n_1, n_2, \ldots, n_k, \ldots\rangle$ has the energy eigenvalue $\sum_k n_k E_k$. In the representation $|n_1, n_2, \ldots, n_k, \ldots\rangle$ of the field, the number of particles in each state k is a positive integer or zero. The commutation relations (1.44) lead to the theory of many particles that obey Bose–Einstein statistics. The commutation relations (1.44) follow if the state ket $|n_1, n_2, \ldots\rangle$ is symmetric with respect to exchange of two particles.

1.6.3 Systems of Fermions

The commutation relations of the field operators lead us to describe a system of bosons. One must find a quantum field formulation to yield a theory of particles that obey Fermi–Dirac statistics. For fermions, the Pauli exclusion principle postulates that the occupation number n_k be only either 0 or 1 and that the state function $|n_1, n_2, \ldots\rangle$ be antisymmetric with respect to the interchange of any two indistinguishable particles. Ernst Pascual Jordan and Eugene Paul Wigner obtained the QFT to describe a fermion field by replacing the commutator brackets (1.44) with the anticommutator brackets

$$[C_k, C_l]_+ = C_k C_l + C_l C_k = 0 \,, \tag{1.54a}$$

$$\left[C_k^\dagger, C_l^\dagger\right]_+ = C_k^\dagger C_l^\dagger + C_l^\dagger C_k^\dagger = 0 \,, \tag{1.54b}$$

$$\left[C_k, C_l^\dagger\right]_+ = C_k C_l^\dagger + C_l^\dagger C_k = \delta_{kl} \,. \tag{1.54c}$$

Now, consider the occupation number operator $N_k = C_k^\dagger C_k$ and $N_k^2 = C_k^\dagger C_k C_k^\dagger C_k$. From (1.54c) we obtain $C_k C_k^\dagger = I - C_k^\dagger C_k$. Then we get

$$N_k^2 = C_k^\dagger \left(I - C_k^\dagger C_k \right) C_k = C_k^\dagger C_k = N_k \,. \tag{1.55}$$

If N_k is in diagonal form with the eigenvalues n_k', n_k'',..., then Eq. (1.55) gives

$$(n_k')^2 = n_k' \,, \quad (n_k'')^2 = n_k'' \,, \quad \ldots \,. \tag{1.56}$$

So, the eigenvalues $n_k', n_k'', \ldots$ must all have either 0 or 1, thus satisfying the Pauli's exclusion principle.

1.7 Electromagnetic Field in Vacuum

In this section we take up the problem of quantization of an electromagnetic field in a vacuum, where ρ (charge density) and $\mathbf{J}$ (current density) are zero. We obtain classical field equations and convert them into quantum field equations.

1.7.1 Lagrangian and Hamiltonian Equations

The Maxwell's equations in a vacuum are

$$\nabla \times \mathbf{E} + \frac{1}{c}\frac{\partial \mathbf{H}_B}{\partial t} = 0\,, \tag{1.57a}$$

$$\nabla \times \mathbf{H}_B - \frac{1}{c}\frac{\partial \mathbf{E}}{\partial t} = 0\,, \tag{1.57b}$$

$$\nabla \cdot \mathbf{E} = 0\,, \tag{1.57c}$$

$$\nabla \cdot \mathbf{H}_B = 0\,. \tag{1.57d}$$

The scalar and vector potentials are defined through the equations

$$\mathbf{E} = -\frac{1}{c}\frac{\partial \mathbf{A}}{\partial t} - \nabla\phi\,, \tag{1.58a}$$

$$\mathbf{H}_B = \nabla \times \mathbf{A}\,. \tag{1.58b}$$

Equations (1.58a) and (1.58b) do not specify unique potentials for $\mathbf{A}$ and ϕ as gauge transformations of $\mathbf{A}$ and ϕ give the same electric and magnetic fields.

Let us assume the Lagrangian density as

$$\mathcal{L} = \frac{1}{8\pi}\left(\frac{1}{c}\frac{\partial \mathbf{A}}{\partial t} + \nabla\phi\right)^2 - \frac{1}{8\pi}\left(\nabla \times \mathbf{A}\right)^2\,. \tag{1.59}$$

Treating A_x, A_y, A_z and ϕ as field variables, the Euler–Lagrange equation takes the form

$$\frac{\partial \mathcal{L}}{\partial A_\mu} - \sum_{k=x,y,z}\frac{\partial}{\partial x_k}\left(\frac{\partial \mathcal{L}}{\partial\left(\frac{\partial A_\mu}{\partial x_k}\right)}\right) - \frac{\partial}{\partial t}\frac{\partial \mathcal{L}}{\partial \dot{A}_\mu} + \frac{\partial \mathcal{L}}{\partial \phi} - \sum_{k=x,y,k}\frac{\partial \mathcal{L}}{\partial\left(\frac{\partial \phi}{\partial x_k}\right)} - \frac{\partial}{\partial t}\frac{\partial \mathcal{L}}{\partial \dot{\phi}} = 0\,. \tag{1.60}$$

Equating the variations of $\mathbf{A}$ and ϕ separately to zero we get

$$\nabla \times (\nabla \times \mathbf{A}) + \frac{1}{c}\frac{\partial}{\partial t}\left(\frac{1}{c}\frac{\partial \mathbf{A}}{\partial t} + \nabla\phi\right) = 0\,, \tag{1.61a}$$

$$\nabla \cdot \left(\frac{1}{c}\frac{\partial \mathbf{A}}{\partial t} + \nabla\phi\right) = 0\,. \tag{1.61b}$$

Using Eqs. (1.58), the Eq. (1.61a) becomes Eq. (1.57b). Equation (1.61b) is simply Eq. (1.57c). Operating $\nabla\cdot$ on both sides of Eq. (1.58b) we get (1.57d). Similarly, from Eq. (1.58a), taking $\nabla\times$ on both sides, we obtain Eq. (1.57a).

Next, we explain the Hamiltonian formalism. The momentum canonically conjugate to $\mathbf{A}$ is

$$\pi = \frac{\partial \mathcal{L}}{\partial \dot{\mathbf{A}}} = \frac{1}{4\pi c}\left[\frac{1}{c}\frac{\partial \mathbf{A}}{\partial t} + \nabla\phi\right]\,. \tag{1.62}$$

The momentum canonically conjugate to ϕ is $\pi_\phi = \partial\mathcal{L}/\partial\dot{\phi} = 0$. That is, ϕ is not a field variable and hence we eliminate it from $\mathcal{H}$. We obtain

$$\begin{aligned}\mathcal{H} &= \pi\cdot\dot{\mathbf{A}} - \mathcal{L}\\ &= \pi\cdot\frac{\partial\mathbf{A}}{\partial t} - \mathcal{L}\\ &= \pi\cdot\left(4\pi c^2\pi - c\nabla\phi\right) - \frac{1}{8\pi}\left(\frac{1}{c}\frac{\partial\mathbf{A}}{\partial t} + \nabla\phi\right)^2 + \frac{1}{8\pi}\left(\nabla\times\mathbf{A}\right)^2\\ &= 2\pi c^2\pi^2 - c\,\pi\cdot\nabla\phi + \frac{1}{8\pi}\left(\nabla\times\mathbf{A}\right)^2 . \end{aligned} \tag{1.63}$$

The Hamilton's equations of motion are

$$\dot{\mathbf{A}} = \frac{\partial\mathcal{H}}{\partial\pi} \Rightarrow \frac{\partial\mathbf{A}}{\partial t} = 4\pi c^2\pi - c\nabla\phi\,, \tag{1.64a}$$

$$\dot{\pi} = -\frac{\partial\mathcal{H}}{\partial\mathbf{A}} \Rightarrow \frac{\partial\pi}{\partial t} = -\frac{1}{4\pi}\nabla\times\left(\nabla\times\mathbf{A}\right). \tag{1.64b}$$

Using Eq. (1.64a) in (1.56a) we get $\mathbf{E} = -4\pi c\pi$. Substituting $\pi = -\mathbf{E}/(4\pi c)$ and $\nabla\times\mathbf{A} = \mathbf{H}_B$ in Eq. (1.64b) we get Eq. (1.57b). The definitions of $\mathbf{E}$ and $\mathbf{H}_B$ given by Eqs. (1.58) satisfy Eqs. (1.57a) and (1.57d). Equation (1.57c) cannot be obtained through the Hamiltonian formalism. However, we can say that we wish to have the solutions with $\nabla\cdot\mathbf{E} = 0$ which implies $\nabla\cdot\pi = 0$. We can show that if $\nabla\cdot\mathbf{E} = 0$ or $\nabla\cdot\pi = 0$ is valid at one instant of time, then this condition is valid at all times. We have from (1.64b)

$$\nabla\cdot\dot{\pi} = \frac{\partial}{\partial t}\nabla\cdot\pi = -\frac{1}{4\pi}\nabla\cdot\left(\nabla\times\nabla\times\mathbf{A}\right) = 0\,. \tag{1.65}$$

Since $\nabla\cdot\left(\nabla\times\nabla\times\mathbf{A}\right)$ is zero at all times, $\nabla\cdot\pi = 0$ is satisfied for all times. It is easy to show that

$$H = \int\mathcal{H}\,\mathrm{d}^3x = \frac{1}{8\pi}\int\left(\mathbf{E}^2 + \mathbf{H}_B^2\right)\,\mathrm{d}^3x\,. \tag{1.66}$$

Solved Problem 3:

Verify that the equations of motion for $\mathbf{A}$ and π, $\partial\mathbf{A}/\partial t = 4\pi c^2\pi$, $\partial\pi/\partial t = -(1/4\pi)\nabla\times(\nabla\times\mathbf{A})$, are in agreement with the Maxwell's equations.

Taking curl on both sides of Eq. (1.58a) we get

$$\begin{aligned}\nabla\times\mathbf{E} &= -\frac{1}{c}\frac{\partial}{\partial t}\nabla\times\mathbf{A} - \nabla\times\nabla\phi\\ &= -\frac{1}{c}\frac{\partial}{\partial t}\nabla\times\mathbf{A}\\ &= -\frac{1}{c}\frac{\partial\mathbf{H}_B}{\partial t}\end{aligned} \tag{1.67a}$$

which is Eq. (1.57a). Next, taking curl on Eq. (1.58b) we get

$$\begin{aligned}\nabla\times\mathbf{H}_B &= \nabla\times\left(\nabla\times\mathbf{A}\right)\\ &= -4\pi\frac{\partial\pi}{\partial t}\\ &= -4\pi\frac{\partial}{\partial t}\left(\frac{1}{4\pi c^2}\frac{\partial\mathbf{A}}{\partial t}\right)\\ &= \frac{1}{c}\frac{\partial\mathbf{E}}{\partial t}\end{aligned} \tag{1.67b}$$

which is Eq. (1.57b). Next, taking divergence on Eq. (1.58a) we obtain

$$\nabla \cdot \mathbf{E} = -\frac{1}{c}\nabla \cdot \frac{\partial \mathbf{A}}{\partial t} = -4\pi \nabla \cdot \pi = 0 \tag{1.67c}$$

and is Eq. (1.57c). Finally, taking divergence on Eq. (1.58b) we get $\nabla \cdot \mathbf{H}_B = \nabla \cdot (\nabla \times \mathbf{A}) = 0$ which is Eq. (1.57d).

1.7.2 Quantum Equations

To quantize the field, we use the commutation relations (1.28). With $\phi = 0$ we get the commutation relations for the field operators as

$$[A_j(\mathbf{r},t), A_k(\mathbf{r}',t)] = [\pi_j(\mathbf{r},t), \pi_k(\mathbf{r}',t)] = 0\,, \tag{1.68a}$$

$$[A_j(\mathbf{r},t), \pi_k(\mathbf{r}',t)] = \mathrm{i}\hbar\delta_{jk}\delta^3(\mathbf{r}-\mathbf{r}')\,, \quad j,k = x,y,z. \tag{1.68b}$$

The equation of motion of $\mathbf{A}$ is

$$\begin{aligned} \mathrm{i}\hbar\frac{\partial \mathbf{A}}{\partial t} &= [\mathbf{A}(\mathbf{r},t), \mathcal{H}] \\ &= \left[\mathbf{A}, 2\pi c^2\pi^2 + \frac{1}{8\pi}(\nabla \times \mathbf{A})^2 - c\,\pi \cdot \nabla\phi\right] \\ &= 2\pi c^2\left[\mathbf{A}, \pi^2\right] + \frac{1}{8\pi}\left[\mathbf{A}, (\nabla \times \mathbf{A})^2\right] - c\left[\mathbf{A}, \pi \cdot \nabla\phi\right]. \end{aligned} \tag{1.69}$$

Because ϕ is not a field variable we set the last term in the above equation, by choosing a gauge, with $\phi = 0$.

We find

$$\left[\mathbf{A}, \pi^2\right] = 2\mathrm{i}\hbar\delta^3(\mathbf{r}-\mathbf{r}')\pi'\,, \tag{1.70a}$$

$$\left[\mathbf{A}, (\nabla \times \mathbf{A})^2\right] = \mathbf{A}(\nabla \times \mathbf{A})^2 - (\nabla \times \mathbf{A})^2\mathbf{A} = 0\,. \tag{1.70b}$$

Then

$$\mathrm{i}\hbar\frac{\partial \mathbf{A}}{\partial t} = \mathrm{i}4\pi c^2\hbar\delta^3(\mathbf{r}-\mathbf{r}')\pi'\,. \tag{1.71}$$

Integrating the above equation with respect to $\mathbf{r}'$ we get

$$\frac{\partial \mathbf{A}}{\partial t} = 4\pi c^2\pi\,. \tag{1.72a}$$

The above equation is Eq. (1.64a) with $\phi = 0$. The equation of motion of π is

$$\begin{aligned} \mathrm{i}\hbar\frac{\partial \pi}{\partial t} &= [\pi, \mathcal{H}] \\ &= 2\pi c^2\left[\pi, \pi^2\right] + \frac{1}{8\pi}\left[\pi, (\nabla \times \mathbf{A})^2\right] - c\left[\pi, \pi \cdot \nabla\phi\right] \\ &= \frac{1}{8\pi}\left[\pi, (\nabla \times \mathbf{A})^2\right] \\ &= -\frac{\mathrm{i}\hbar}{4\pi}\nabla \times (\nabla \times \mathbf{A}) \end{aligned}$$

or

$$\frac{\partial \pi}{\partial t} = -\frac{1}{4\pi}\nabla \times (\nabla \times \mathbf{A}) \tag{1.72b}$$

which is Eq. (1.64b). From Eq. (1.72a) we get $\nabla \cdot (\partial \mathbf{A}/\partial t) = 4\pi c^2 \nabla \cdot \pi$. Since $\nabla \cdot \pi = 0$ at all times, $\nabla \cdot (\partial \mathbf{A}/\partial t) = \partial(\nabla \cdot \mathbf{A})/\partial t = 0$. Hence, $[\mathbf{A}(\mathbf{r}, t), \nabla' \cdot \pi(\mathbf{r}', t)] = 0$. But, if we use the quantum condition (1.68a) we get

$$[A_x(\mathbf{r}, t), \nabla' \cdot \pi(\mathbf{r}', t)] = \mathrm{i}\hbar \frac{\partial}{\partial x'} \delta^3(\mathbf{r} - \mathbf{r}') \,. \tag{1.72c}$$

This inconsistency arises since $\mathbf{A}$ is not experimentally measurable and hence it is not a physical quantity. This inconsistency will be removed if the commutation relations are given in terms of the experimentally measurable quantities $\mathbf{E}$ and $\mathbf{H}$.

1.7.3 Occupation Number Representation of Electromagnetic Field

Since the scalar potential $\phi = 0$, using (1.58) in (1.57b) we get

$$\nabla \times \nabla \times \mathbf{A} + \frac{1}{c^2} \frac{\partial^2 \mathbf{A}}{\partial t^2} = 0 \,. \tag{1.73}$$

Since $\nabla \times \nabla \times \mathbf{A} = \nabla(\nabla \cdot \mathbf{A}) - \nabla^2 \mathbf{A}$, in the gauge $\nabla \cdot \mathbf{A} = 0$, Eq. (1.73) gives the d'Alembert equation

$$\nabla^2 \mathbf{A} = \frac{1}{c^2} \frac{\partial^2 \mathbf{A}}{\partial t^2} \,. \tag{1.74}$$

If we assume that the electromagnetic field is confined to a large box of size of volume V with side length L and that it satisfies the periodic boundary conditions with period L then the general free solution to Eq. (1.74) can be given as a Fourier transform

$$\mathbf{A}(\mathbf{r}, t) = \frac{1}{\sqrt{V}} \sum_k \sum_{\lambda=1}^{2} \epsilon_{\mathbf{k}\lambda} A_{\mathbf{k}\lambda} \, \mathrm{e}^{\mathrm{i}\mathbf{k}\cdot\mathbf{r}} \,, \quad A_{\mathbf{k}\lambda} = A^*_{-\mathbf{k}\lambda} \,. \tag{1.75}$$

Similarly, $\pi(\mathbf{r}, t)$ can be given as

$$\pi(\mathbf{r}, t) = \frac{1}{\sqrt{V}} \sum_k \sum_{\lambda=1}^{2} \epsilon_{\mathbf{k}\lambda} \pi_{\mathbf{k}\lambda} \mathrm{e}^{-\mathrm{i}\mathbf{k}\cdot\mathbf{r}} \,, \quad \pi_{\mathbf{k}\lambda} = \pi^*_{-\mathbf{k}\lambda} \,. \tag{1.76}$$

where the components of the wave vector $\mathbf{k}$ take on an infinite series of discrete values due to the boundary conditions

$$\mathbf{k}_i = \frac{2\pi n_i}{L} \,, \quad i = x, y, z, \;\; n_i = 0, \pm 1, \pm 2 \ldots \,. \tag{1.77}$$

The $\epsilon_{\mathbf{k}\lambda}$ are real unit polarization vectors.

Since the electromagnetic wave in free space is transverse in nature and has two independent polarizations, the polarization vectors satisfy the conditions

$$\mathbf{k} \cdot \epsilon_{\mathbf{k}\lambda} = 0, \quad \epsilon_{\mathbf{k}\lambda} \cdot \epsilon_{\mathbf{k}\lambda'} = \delta_{\lambda\lambda'}, \quad \lambda, \; \lambda' = 1, 2. \tag{1.78}$$

This classical description can be changed to quantum description by replacing $\mathbf{A}_{\mathbf{k}\lambda}$ and $\pi_{\mathbf{k}\lambda}$ into operators satisfying the commutation relations

$$[\mathbf{A}_{\mathbf{k}\lambda}, \pi_{\mathbf{k}'\lambda'}] = \mathrm{i}\hbar \delta_{\mathbf{k}\mathbf{k}'} \delta_{\lambda\lambda'} \,. \tag{1.79}$$

These operators can be expressed in terms of the boson (photon) creation operator $\mathbf{a}^\dagger_{\mathbf{k}\lambda}$ and annihilation operator $\mathbf{a}_{\mathbf{k}\lambda}$ as

$$\mathbf{A}_{\mathbf{k}\lambda}(t) = \left(\frac{2\pi\hbar c^2}{\omega(k)}\right)^{1/2}\left[\mathbf{a}_{\mathbf{k}\lambda}(t) + \mathbf{a}^\dagger_{-\mathbf{k}\lambda}(t)\right], \tag{1.80a}$$

$$\pi_{\mathbf{k}\lambda}(t) = \mathrm{i}\left(\frac{\hbar\omega(k)}{8\pi c^2}\right)^{1/2}\left[\mathbf{a}^\dagger_{\mathbf{k}\lambda}(t) - \mathbf{a}_{-\mathbf{k}\lambda}(t)\right]. \tag{1.80b}$$

The vector potential (1.75) satisfies Eq. (1.74) if

$$\mathbf{A}_{\mathbf{k}\lambda}(t) = \mathbf{A}_{\mathbf{k}\lambda}(0)\,\mathrm{e}^{-\mathrm{i}\omega(k)t}. \tag{1.81}$$

Substituting (1.75) and (1.81) in (1.74) we get the dispersion relation $\omega(k) = c|\mathbf{k}|$.

The commutation relations (1.68a) then lead to the commutation relations

$$\left[\mathbf{a}_{\mathbf{k}\lambda}(t), \mathbf{a}^\dagger_{\mathbf{k}'\lambda'}(t)\right] = \delta_{\mathbf{k}\mathbf{k}'}\delta_{\lambda\lambda'}, \tag{1.82a}$$

$$[\mathbf{a}_{\mathbf{k}\lambda}(t), \mathbf{a}_{\mathbf{k}'\lambda'}(t)] = \left[\mathbf{a}^\dagger_{\mathbf{k}\lambda}(t), \mathbf{a}^\dagger_{\mathbf{k}'\lambda'}(t)\right] = 0. \tag{1.82b}$$

Using the transformation (1.80), we can get the vector potential operator $\mathbf{A}$ and its conjugate momentum operator π in terms of photon creation and annihilation operators as

$$\mathbf{A}(\mathbf{r},t) = \sum_k \sum_{\lambda=1}^{2}\left(\frac{2\pi\hbar c^2}{V\omega(k)}\right)^{1/2}\epsilon_{\mathbf{k}\lambda}\mathrm{e}^{\mathrm{i}\mathbf{k}\cdot\mathbf{r}}\left[\mathbf{a}_{\mathbf{k}\lambda}(t) + \mathbf{a}^\dagger_{-\mathbf{k}\lambda}(t)\right], \tag{1.83a}$$

$$\pi(\mathbf{r},t) = \mathrm{i}\sum_k \sum_{\lambda=1}^{2}\left(\frac{\hbar\omega(k)}{8\pi c^2 V}\right)^{1/2}\epsilon_{\mathbf{k}\lambda}\mathrm{e}^{-\mathrm{i}\mathbf{k}\cdot\mathbf{r}}\left[\mathbf{a}^\dagger_{\mathbf{k}\lambda}(t) - \mathbf{a}^\dagger_{-\mathbf{k}\lambda}(t)\right]. \tag{1.83b}$$

We have from Eq. (1.63), with $\phi = 0$, the Hamiltonian density

$$\mathcal{H} = 2\pi c^2\pi^2 + \frac{1}{8\pi}(\nabla\times\mathbf{A})^2. \tag{1.84}$$

Since

$$(\mathbf{k}\times\epsilon_{\mathbf{k}\lambda})\cdot(\mathbf{k}\times\epsilon_{\mathbf{k}\lambda'}) = |\mathbf{k}|^2\delta_{\lambda\lambda'}, \quad \int_V \mathrm{e}^{\mathrm{i}(\mathbf{k}-\mathbf{k}')\cdot\mathbf{r}}\mathrm{d}^3r = V\delta_{\mathbf{k}\mathbf{k}'} \tag{1.85}$$

substituting (1.83) in (1.84) and integrating over the volume V we get the Hamiltonian of the electromagnetic field as

$$H = \sum_k \sum_{\lambda=1}^{2}\hbar\omega(k)\left(\mathbf{a}^\dagger_{\mathbf{k}\lambda}\mathbf{a}_{\mathbf{k}\lambda} + \frac{1}{2}\right). \tag{1.86}$$

Comparing Eq. (1.86) with the Hamiltonian $H = \hbar\omega\left(a^\dagger a + \frac{1}{2}\right)$ of a linear harmonic oscillator we identify $\mathbf{a}^\dagger_{\mathbf{k}\lambda}\mathbf{a}_{\mathbf{k}\lambda}$ as the number operator of the photon with momentum $\hbar\mathbf{k}$, energy $\hbar\omega(k)$ and polarization λ. The Planck's quantum hypothesis follows from Eq. (1.86) as it says that the energy associated with each plane electromagnetic wave is an integer multiple of the fundamental quantum $\hbar\omega = h\nu = \hbar kc$. As the summation extends up to infinity, the sum of the zero-point energy $\hbar\omega/2$ gives infinity. This infinite zero-point energy does

not lead to any difficulty as the interaction depends only on the change of the occupation number $n_{\mathbf{k}\lambda}$. The quantization of the electromagnetic field corresponds to the creation or annihilation of elementary excitations, namely photon with energy $\hbar\omega$, momentum $\hbar\mathbf{k}$ and polarization $\epsilon_{\mathbf{k}\lambda}$.

We notice that the field equation for $A(\mathbf{r},t)$ shows that the coefficients $\mathbf{a}_{\mathbf{k}\lambda}$ obey the classical harmonic oscillator equation. $A(\mathbf{r},t)$ is a vector operator-valued field with $\mathbf{a}_{\mathbf{k}\lambda}$ and $\mathbf{a}^{\dagger}_{\mathbf{k}\lambda}$ of the kth field mode satisfying the Heisenberg equations of motion for a set of quantum harmonic oscillators. As $A(\mathbf{r},t)$ defines an operator for every point $\mathbf{r}$ in space, it is called a field. $\mathbf{r}$ is not an operator but a parameter. In nonrelativistic quantum physics we can speak about $\langle\mathbf{r}\rangle$ whereas in QFT we can speak about $\langle\mathbf{A}(\mathbf{r},t)\rangle$ but not $\langle\mathbf{r}\rangle$ because $\mathbf{r}$ is not an observable.

$\mathbf{A}$ operates on ψ and creates and destroys photons. As pointed out in [4] $\mathbf{A}$ is a physically meaningful field since it has a measurable expectation value at each and every point $\mathbf{r}$ in space. That is, a quantized classical field does not cease to be a field.

Quantum fields possess a particle-like property which classical fields do not possess. Notice that quantum fields are made of quanta. Thus, quanta cannot vanish but must be instantly created and destroyed (like particles). As quanta carry energy and momenta, they can hit like a particle.

1.8 Interaction of Charged Particles with Electromagnetic Field

In this section we consider the QFT of interaction of charged particles with an electromagnetic field.

1.8.1 Lagrangian and Hamiltonian Equations

The Schrödinger equation for a particle of mass m and charge e in an electromagnetic field is given by

$$\begin{aligned} \mathrm{i}\hbar\frac{\partial\psi}{\partial t} &= -\frac{\hbar^2}{2m}\nabla^2\psi + \frac{\mathrm{i}e\hbar}{mc}(\mathbf{A}\cdot\nabla)\psi + \frac{\mathrm{i}e\hbar}{2mc}(\nabla\cdot\mathbf{A})\psi \\ &\quad + \frac{e^2}{2mc^2}\,\mathbf{A}^2\psi + e\phi\psi + V\psi\,. \end{aligned} \tag{1.87}$$

The Maxwell's equations of motion are

$$\nabla\times\mathbf{E} + \frac{1}{c}\frac{\partial\mathbf{H}_B}{\partial t} = 0\,, \tag{1.88a}$$

$$\nabla\times\mathbf{H}_B - \frac{1}{c}\frac{\partial\mathbf{E}}{\partial t} = \frac{4\pi}{c}\,\mathbf{J}\,, \tag{1.88b}$$

$$\nabla\cdot\mathbf{E} = 4\pi\rho\,, \tag{1.88c}$$

$$\nabla\cdot\mathbf{H}_B = 0\,. \tag{1.88d}$$

The continuity equation is $\partial\rho/\partial t + \nabla\cdot\mathbf{J} = 0$.

The Lagrangian density of the problem is obtained by combining the $\mathcal{L}$ of nonrelativistic Schrödinger equation and of Maxwell's equations given by Eqs. (1.36) and Eq. (1.59),

respectively, and with the transformation

$$\mathrm{i}\hbar\frac{\partial\psi}{\partial t} \rightarrow \left(\mathrm{i}\hbar\frac{\partial}{\partial t} - e\phi\right)\psi\,, \tag{1.89a}$$

$$-\mathrm{i}\hbar\nabla\psi \rightarrow \left(-\mathrm{i}\hbar\nabla - \frac{e}{c}\mathbf{A}\right)\psi\,, \tag{1.89b}$$

$$\mathrm{i}\hbar\nabla\psi^* \rightarrow \left(\mathrm{i}\hbar\nabla - \frac{e}{c}\mathbf{A}\right)\psi^*\,. \tag{1.89c}$$

The resulting $\mathcal{L}$ is

$$\begin{aligned}\mathcal{L} &= \psi^*\left(\mathrm{i}\hbar\frac{\partial}{\partial t} - e\phi\right)\psi - \frac{1}{2m}\left(\mathrm{i}\hbar\nabla - \frac{e}{c}\mathbf{A}\right)\psi^*\cdot\left(-\mathrm{i}\hbar\nabla - \frac{e}{c}\mathbf{A}\right)\psi \\ &\quad -V\psi^*\psi + \frac{1}{8\pi}\left(\frac{1}{c}\frac{\partial\mathbf{A}}{\partial t} + \nabla\phi\right)^2 - \frac{1}{8\pi}(\nabla\times\mathbf{A})^2\,.\end{aligned} \tag{1.90}$$

Similarly, using the transformation (1.89), we get

$$\rho = e\psi^*\psi\,, \tag{1.91a}$$

$$\begin{aligned}\mathbf{J} &= \frac{e\hbar}{2m\mathrm{i}}\left[\psi^*\frac{1}{-\mathrm{i}\hbar}\left(-\mathrm{i}\hbar\nabla\psi - \frac{e}{c}\mathbf{A}\psi\right) - \frac{1}{\mathrm{i}\hbar}\psi\left(\mathrm{i}\hbar\nabla\psi^* - \frac{e}{c}\mathbf{A}\psi^*\right)\right] \\ &= \frac{e\hbar}{2m\mathrm{i}}\left[\psi^*\nabla\psi - \psi\nabla\psi^*\right] - \frac{e^2}{mc}\mathbf{A}\psi^*\psi\,.\end{aligned} \tag{1.91b}$$

The momentum canonically conjugate to ψ is $\mathrm{i}\hbar\psi^*$ and that of $\mathbf{A}$ is

$$\pi = \frac{1}{4\pi c}\left(\frac{1}{c}\frac{\partial\mathbf{A}}{\partial t} + \nabla\phi\right)\,. \tag{1.92}$$

The Hamiltonian H is given by

$$\begin{aligned}H &= \int\left(\mathrm{i}\hbar\psi^*\frac{\partial\psi}{\partial t} + \pi\cdot\frac{\partial\mathbf{A}}{\partial t}\right)\mathrm{d}^3x - L \\ &= \int\left\{\frac{1}{2m}\left[\left(\mathrm{i}\hbar\nabla - \frac{e}{c}\mathbf{A}\right)\psi^*\right]\cdot\left[\left(-\mathrm{i}\hbar\nabla - \frac{e}{c}\mathbf{A}\right)\psi\right] + e\phi\psi^*\psi\right. \\ &\quad \left. +V\psi^*\psi + 2\pi c^2\pi^2 + \frac{1}{8\pi}(\nabla\times\mathbf{A})^2 - c\,\pi\cdot\nabla\phi\right\}\mathrm{d}^3x\,.\end{aligned} \tag{1.93}$$

The integrand in Eq. (1.93) is $\mathcal{H}$. Then we obtain

$$\frac{\partial\mathbf{A}}{\partial t} = \frac{\partial\mathcal{H}}{\partial\pi} = 4\pi c^2\pi - c\nabla\phi\,, \tag{1.94a}$$

$$\frac{\partial\pi}{\partial t} = \frac{\partial\mathcal{H}}{\partial\mathbf{A}} = -\frac{1}{4\pi}\nabla\times(\nabla\times\mathbf{A}) + \frac{1}{c}\,\mathbf{J}\,. \tag{1.94b}$$

It can be shown that H will be independent of ϕ. Consider the last term in Eq. (1.93). We get

$$-c\int\pi\cdot\nabla\phi\,\mathrm{d}^3x = c\int\phi\nabla\cdot\pi\,\mathrm{d}^3x = -\int\phi\rho\,\mathrm{d}^3x = -e\int\phi\psi^*\psi\,\mathrm{d}^3x \tag{1.95}$$

since $c\nabla\cdot\pi = -(1/4\pi)\nabla\cdot\mathbf{E} = -\rho = -e\psi^*\psi$. Hence,

$$\begin{aligned}H &= \int\left\{\frac{1}{2m}\left[\left(\mathrm{i}\hbar\nabla - \frac{e}{c}\,\mathbf{A}\right)\psi^*\right]\cdot\left[\left(-\mathrm{i}\hbar\nabla - \frac{e}{c}\,\mathbf{A}\right)\psi\right] + V\psi^*\psi\right. \\ &\quad \left. +2\pi c^2\pi^2 + \frac{1}{8\pi}\,(\nabla\times\mathbf{A})^2\right\}\mathrm{d}^3x\end{aligned} \tag{1.96}$$

and is independent of ϕ.

Let us assume that $\pi = \pi_1 + \pi_2$, where π_1 and π_2 represent solenoidal and irrotational parts. We have $\nabla \cdot \pi_1 = 0$ and $\nabla \times \pi_2 = 0$. We write $\pi_2 = (1/(4\pi c))\nabla\phi$ so that $\nabla \times \pi_2 = 0$. Then

$$\begin{aligned}\int \pi^2 \, \mathrm{d}^3x &= \int \left(\pi_1^2 + \pi_2^2 + 2\pi_1 \cdot \pi_2\right) \mathrm{d}^3x \\ &= \int \left[\pi_1^2 + \frac{1}{4\pi c}\left(2\pi_1 + \pi_2\right) \cdot \nabla\phi\right] \mathrm{d}^3x \\ &= \int \pi_1^2 \, \mathrm{d}^3x - \frac{1}{4\pi c}\int \phi \nabla \cdot \left(2\pi_1 + \pi_2\right) \mathrm{d}^3x \\ &= \int \pi_1^2 \, \mathrm{d}^3x - \frac{1}{4\pi c}\int \phi \nabla \cdot \pi_2 \mathrm{d}^3x \, . \end{aligned} \tag{1.97}$$

Using (1.95) we get

$$2\pi c^2 \int \pi^2 \, \mathrm{d}^3x = 2\pi c^2 \int \pi_1^2 \, \mathrm{d}^3x + \frac{1}{2}\int \phi\rho \, \mathrm{d}^3x \, . \tag{1.98}$$

From $\pi_2 = (1/4\pi c)\nabla\phi$ we get

$$\nabla^2\phi = 4\pi c \nabla \cdot \pi_2 = 4\pi c(-\rho/c) = -4\pi\rho \, . \tag{1.99}$$

Its solution is

$$\phi(\mathbf{r}, t) = \int \frac{\rho(\mathbf{r}', t)}{|\mathbf{r} - \mathbf{r}'|} \, \mathrm{d}^3x' \, . \tag{1.100}$$

Using Eqs. (1.98) and (1.100) we get

$$\begin{aligned} H &= \int \left\{ \frac{1}{2m}\left[\left(\mathrm{i}\hbar\nabla - \frac{e}{c}\mathbf{A}\right)\psi^*\right] \cdot \left[\left(-\mathrm{i}\hbar\nabla - \frac{e}{c}\mathbf{A}\right)\psi\right] \right. \\ &\quad \left. + V\psi^*\psi + \left[2\pi c^2\pi_1^2 + \frac{1}{8\pi}(\nabla \times \mathbf{A})^2\right] \right\} \mathrm{d}^3x \\ &\quad + \frac{1}{2}\int\int \frac{\rho(\mathbf{r}, t)\rho(\mathbf{r}', t)}{|\mathbf{r} - \mathbf{r}'|} \, \mathrm{d}^3x \, \mathrm{d}^3x' . \end{aligned} \tag{1.101}$$

1.8.2 Quantization of the Fields

The equation of motion of a quantum dynamical variable is given by Eq. (1.33). The required Hamiltonian is given by Eq. (1.101) except the integrand in the last term is replaced by

$$\begin{aligned}\rho(\mathbf{r}, t)\rho(\mathbf{r}', t) &= e^2\psi^\dagger\psi\psi'^\dagger\psi' \\ &= e^2\psi^\dagger\psi\psi'^\dagger\psi' - e^2\psi^\dagger\psi'^\dagger\psi\psi' + e^2\psi^\dagger\psi'^\dagger\psi\psi' \\ &= e^2\psi^\dagger\psi'\delta^3(\mathbf{r} - \mathbf{r}') + e^2\psi^\dagger\psi'^\dagger\psi\psi' \, . \end{aligned} \tag{1.102}$$

Then

$$\begin{aligned}\frac{1}{2}\int\int \frac{\rho\rho'}{|\mathbf{r} - \mathbf{r}'|} \, \mathrm{d}^3x \mathrm{d}^3x' &= \frac{1}{2}\, e^2 \int\int \frac{\psi^\dagger\psi'}{|\mathbf{r} - \mathbf{r}'|}\, \delta^3(\mathbf{r} - \mathbf{r}') \, \mathrm{d}^3x \, \mathrm{d}^3x' \\ &\quad + \frac{1}{2}\, e^2 \int\int \frac{\psi^\dagger\psi'^\dagger\psi\psi'}{|\mathbf{r} - \mathbf{r}'|} \, \mathrm{d}^3x \, \mathrm{d}^3x' \, . \end{aligned} \tag{1.103}$$

The first term on the right-side of the above equation is infinity unless $\psi^\dagger\psi' = 0$ and hence

$$\frac{1}{2}\int\int \frac{\rho\rho'}{|\mathbf{r} - \mathbf{r}'|} \, \mathrm{d}^3x \, \mathrm{d}^3x' = \frac{1}{2}\, e^2 \int\int \frac{\psi^\dagger\psi'^\dagger\psi\psi'}{|\mathbf{r} - \mathbf{r}'|} \, \mathrm{d}^3x \, \mathrm{d}^3x' \, . \tag{1.104}$$

The quantization equations of motion can be obtained from (1.33) by modifying (1.101) by replacing the last integral of it by Eq. (1.104).

1.9 Quantization of Klein–Gordon Equation

Let us take up the problem of quantization of KG equation.

1.9.1 Klein–Gordon Equation for Real Field

Consider the Lagrangian density

$$\mathcal{L} = \frac{1}{2}\dot{\psi}^2 - \frac{1}{2}m^2\psi^2 - \frac{1}{2}(\nabla\psi)^2 \tag{1.105}$$

in natural units $\hbar = c = 1$. Then L is $\int \mathcal{L}\,\mathrm{d}\tau$. Defining the canonical momentum as $\pi = \partial\mathcal{L}/\partial\dot{\psi}$, we obtain

$$\mathcal{H} = \pi\dot{\psi} - \mathcal{L} = \frac{1}{2}\left(\pi^2 + m^2\psi^2 + (\nabla\psi)^2\right) . \tag{1.106}$$

The Euler–Lagrange equation is

$$\psi_{tt} - \nabla^2\psi + m^2\psi = 0\,. \tag{1.107}$$

Defining $\partial^2 = \partial^2/\partial t^2 - \nabla^2$ the Eq. (1.107) can be rewritten as

$$\partial^2\psi + m^2\psi = 0\,. \tag{1.108}$$

It is the KG equation.

1.9.1.1 Second Quantization

Now, quantize the KG equation. We obtain the equation $\pi = \dot{\psi}$ and Eq. (1.108) from Heisenberg equation of motion. The commutation relations are

$$[\psi(\mathbf{r},t), \pi(\mathbf{r}',t)] = \mathrm{i}\hbar\delta^3(\mathbf{r}-\mathbf{r}')\,, \tag{1.109a}$$

$$[\psi(\mathbf{r},t), \psi(\mathbf{r}',t)] = [\pi(\mathbf{r},t), \pi(\mathbf{r}',t)] = 0\,. \tag{1.109b}$$

The field $\psi(\mathbf{r},t)$ represents an infinite number of operators and they give the values of the field at various positions $\mathbf{r}$ in space and then conjugate operators $\pi(\mathbf{r},t)$.

The equation of motion of ψ is given by

$$\begin{aligned}
\dot{\psi} &= \frac{1}{\mathrm{i}\hbar}[\psi, H] \\
&= \frac{1}{\mathrm{i}\hbar}\left[\psi, \int \mathcal{H}\,\mathrm{d}^3x\right] \\
&= \frac{1}{\mathrm{i}\hbar}\left[\psi, \frac{1}{2}\int \left(\pi'^2 + (\nabla'\psi')^2 + m^2\psi'^2\right)\,\mathrm{d}^3x'\right] .
\end{aligned}$$

Since $[\nabla'\psi', \psi] = 0$ and $[\psi, \psi'] = 0$ we get

$$\begin{aligned}
\dot{\psi} &= \frac{1}{\mathrm{i}\hbar}\left[\psi, \frac{1}{2}\int \pi'^2\,\mathrm{d}^3x'\right] \\
&= \frac{1}{2\mathrm{i}\hbar}\int \left\{[\psi,\pi']\,\pi' + \pi'\,[\psi,\pi']\right\}\,\mathrm{d}^3x' \\
&= \frac{1}{2\mathrm{i}\hbar}\left\{\int 2\mathrm{i}\hbar\delta^3(\mathbf{r}-\mathbf{r}')\pi'\,\mathrm{d}^3x'\right\} \\
&= \pi(\mathbf{r})\,.
\end{aligned} \tag{1.110}$$

Next,

$$\begin{aligned}\dot{\pi} &= \frac{1}{\mathrm{i}\hbar}[\pi, H] \\ &= \frac{1}{\mathrm{i}\hbar}\left[\pi, \frac{1}{2}\int\left(\pi'^2 + \left(\nabla'\psi'\right)^2 + m^2\psi'^2\right)\mathrm{d}^3x'\right] \\ &= \frac{1}{\mathrm{i}\hbar}\left[\pi, \frac{1}{2}\int\left(\left(\nabla'\psi'\right)^2 + m^2\psi'^2\right)\mathrm{d}^3x'\right] \\ &= \frac{1}{2\mathrm{i}\hbar}\left\{\left[\pi, \int\left(\nabla'\psi'\right)^2\mathrm{d}^3x'\right] + \left[\pi, \int m^2\psi'^2\,\mathrm{d}^3x'\right]\right\}. \end{aligned} \tag{1.111}$$

For an operator $f(\mathbf{r})$ we have the result

$$\int f'\left[\pi, \frac{\partial\psi'}{\partial x'^j}\right]\mathrm{d}^3x' = \mathrm{i}\hbar\frac{\partial f}{\partial x^j}. \tag{1.112}$$

Then Eq. (1.111) becomes

$$\dot{\pi} = \nabla^2\psi - m^2\psi. \tag{1.113}$$

Substituting $\pi = \dot{\psi}$ in the above equation we get the KG equation.

1.9.1.2 Spectrum of KG Equation

To compute the spectrum consider the KG equation in Fourier space. We write

$$\psi(\mathbf{r}, t) = \frac{1}{(2\pi)^3}\int\psi(\mathbf{p}, t)\,\mathrm{e}^{\mathrm{i}\mathbf{p}\cdot\mathbf{r}}\,\mathrm{d}^3p. \tag{1.114}$$

Then the KG equation becomes

$$\frac{\partial^2\psi(\mathbf{p}, t)}{\partial t^2} + \left(|\mathbf{p}|^2 + m^2\right)\psi(\mathbf{p}, t) = 0. \tag{1.115}$$

Defining $E_{\mathbf{p}}^2 = |\mathbf{p}|^2 + m^2$, Eq. (1.115) takes the form $\psi_{tt} + E_{\mathbf{p}}^2\psi = 0$. It is the harmonic oscillator equation. For the harmonic oscillator (with $m = 1$, $\hbar = 1$)

$$H = \frac{1}{2}\mathbf{p}^2 + \frac{1}{2}\omega_0^2\psi^2, \tag{1.116}$$

and

$$\psi = \frac{1}{\sqrt{2\omega_0}}(a + a^\dagger), \quad \mathbf{p} = -\mathrm{i}\sqrt{\frac{\omega_0}{2}}\,(a - a^\dagger). \tag{1.117}$$

In analogy with Eq. (1.80) we write

$$\psi(\mathbf{r}) = \frac{1}{(2\pi)^3}\int\frac{1}{\sqrt{2E_{\mathbf{p}}}}\left(a_{\mathbf{p}}\,\mathrm{e}^{\mathrm{i}\mathbf{p}\cdot\mathbf{r}} + a_{\mathbf{p}}^\dagger\,\mathrm{e}^{-\mathrm{i}\mathbf{p}\cdot\mathbf{r}}\right)\mathrm{d}^3p, \tag{1.118a}$$

$$\pi(\mathbf{r}) = -\frac{\mathrm{i}}{(2\pi)^3}\int\sqrt{\frac{E_{\mathbf{p}}}{2}}\left(a_{\mathbf{p}}\,\mathrm{e}^{\mathrm{i}\mathbf{p}\cdot\mathbf{r}} - a_{\mathbf{p}}^\dagger\,\mathrm{e}^{-\mathrm{i}\mathbf{p}\cdot\mathbf{r}}\right)\mathrm{d}^3p. \tag{1.118b}$$

We use the abstract operator method to determine the energy eigenpairs. We started with ψ and π and now switch to a and $a^\dagger$. We can use the commutation relations (1.109) to find the commutation relations between a and $a^\dagger$. We thus invert Eqs. (1.118) and express a and $a^\dagger$ in terms of ψ and π. Then the use of (1.109) gives

$$\left[a_{\mathbf{p}}, a_{\mathbf{p}'}^\dagger\right] = (2\pi)^3\delta^3(\mathbf{p} - \mathbf{p}'), \tag{1.119a}$$

$$\left[a_{\mathbf{p}}, a_{\mathbf{p}}^\dagger\right] = \left[a_{\mathbf{p}}^\dagger, a_{\mathbf{p}'}^\dagger\right] = 0 \tag{1.119b}$$

and

$$\begin{aligned}[\psi,\pi'] &= -\frac{\mathrm{i}}{2(2\pi)^6}\sqrt{\frac{E_{\mathbf{p}'}}{E_{\mathbf{p}}}}\int\left\{\left[a^\dagger_{-\mathbf{p}},a_{\mathbf{p}'}\right]-\left[a_{\mathbf{p}},a^\dagger_{-\mathbf{p}'}\right]\right\}\\ &\qquad\times\mathrm{e}^{\mathrm{i}(\mathbf{p}\cdot\mathbf{r}+\mathbf{p}'\cdot\mathbf{r}')}\,\mathrm{d}^3p\,\mathrm{d}^3p'\\ &= \mathrm{i}\delta^3(\mathbf{r}-\mathbf{r}')\,. \end{aligned}\tag{1.119c}$$

We note that $a_{\mathbf{p}}$ annihilates $|0\rangle$: $a_{\mathbf{p}}|0\rangle=0$ for all $\mathbf{p}$ and the state $|0\rangle$ has $E=0$. The other states can be obtained by acting $a_{\mathbf{p}}$ on $|0\rangle$. The eigenvalue of H with the state $(a^\dagger_{\mathbf{p}})^n|0\rangle$ is $nE_{\mathbf{p}}$.

For relativistic KG equation the charge and current densities are $\rho=(1/(mc^2))\,E\psi^*\psi$ and $\mathbf{J}=(\hbar/(2m\mathrm{i}))\,[\psi^*\nabla\psi-\psi\nabla\psi^*]$, respectively. For a real field ($\psi=\psi^*$), the operator ψ becomes a Hermitian as $\psi=\psi^\dagger$. Hence, the charge density operator ρ and the current density operator $\mathbf{J}$ vanish. Therefore, the KG equation for real scalar field when quantized applicable to a neutral particle alone. Also, ψ transforms as a scalar (pseudo-scalar) under Lorentz transformations and hence the spin of the KG field is zero. So, the real KG field ψ describes neutral pion π^0 that has zero spin and mass. But if neutral spin zero particles with mass possess additional degrees of freedom like hypercharge then they cannot be described by a real KG field.

Solved Problem 4:

Given the Eqs. (1.118) and (1.106) and starting from $H=\int\mathcal{H}\mathrm{d}^3x$ express H in terms of the ladder operators. Also, find $\langle\psi|H|\psi\rangle$.

We obtain

$$\begin{aligned}H &= \int\mathcal{H}\,\mathrm{d}^3x\\ &= \frac{1}{2}\int\left[\pi^2+(\nabla\psi)^2+m^2\psi^2\right]\,\mathrm{d}^3x\\ &= \frac{1}{(2\pi)^6}\int\mathrm{d}^3x\int\mathrm{d}^3p\int\mathrm{d}^3p'\mathrm{e}^{\mathrm{i}(\mathbf{p}+\mathbf{p}')\cdot\mathbf{r}}\\ &\qquad\times\left\{\frac{\sqrt{E_{\mathbf{p}}E_{\mathbf{p}'}}}{4}\left(a_{\mathbf{p}}-a^\dagger_{-\mathbf{p}}\right)\left(a_{\mathbf{p}'}-a^\dagger_{-\mathbf{p}'}\right)\right.\\ &\qquad\left.+\frac{-\mathbf{p}\cdot\mathbf{p}'+m^2}{4\sqrt{E_{\mathbf{p}}E_{\mathbf{p}'}}}\left(a_{\mathbf{p}}+a^\dagger_{-\mathbf{p}}\right)\left(a_{\mathbf{p}'}+a^\dagger_{-\mathbf{p}'}\right)\right\}\\ &= \frac{1}{(2\pi)^3}\int\mathrm{d}^3p\,E_{\mathbf{p}}\left(a^\dagger_{\mathbf{p}}a_{\mathbf{p}}+\frac{1}{2}\left[a_{\mathbf{p}},\,a^\dagger_{\mathbf{p}}\right]\right)\,. \end{aligned}\tag{1.120}$$

Simplifying the right-side of the above equation we get

$$H = \frac{1}{(2\pi)^3}\int\mathrm{d}^3p\,E_{\mathbf{p}}a^\dagger_{\mathbf{p}}a_{\mathbf{p}}+\frac{1}{2}\int E_{\mathbf{p}}\,\mathrm{d}^3p\,.\tag{1.121}$$

The expectation value $\langle0|H|0\rangle=(1/2)\int E_{\mathbf{p}}\,\mathrm{d}^3p$ is infinite. This is because there is an oscillator for each value of momentum. Hence, contribution from all the oscillators is infinite. We cannot detect this infinite energy shift experimentally because in experiments we measure only the energy difference from the ground state of H. That is, the last term in the above equation has no observable effect and hence we discard it. Then

$$H = \frac{1}{(2\pi)^3}E_{\mathbf{p}}\int\mathrm{d}^3p\,a^\dagger_{\mathbf{p}}a_{\mathbf{p}}\,.\tag{1.122}$$

Next, we find

$$\langle\psi|H|\psi\rangle = \frac{E_{\mathbf{p}}}{(2\pi)^3}\int\langle\psi|a^\dagger_{\mathbf{p}}a_{\mathbf{p}}|\psi\rangle\,\mathrm{d}^3p = \frac{E_{\mathbf{p}}}{(2\pi)^3}\int||a_{\mathbf{p}}|\psi\rangle||^2\,\mathrm{d}^3p \tag{1.123}$$

which is always positive and $\langle 0|H|0\rangle = 0$. Hence, the ground state $|0\rangle$ is the lowest energy state.

1.9.2 Klein–Gordon Equation with Complex Scalar Field

We have seen that the KG equation for real field, on quantization describes creation and annihilation of chargeless particles with mass. Another KG field is a complex field $\psi(\mathbf{r},t)$ that may be regarded as made up of two independent real scalar fields $\psi_1(\mathbf{r},t)$ and $\psi_2(\mathbf{r},t)$:

$$\psi(\mathbf{r},t) = \frac{1}{\sqrt{2}}\,(\psi_1 + \mathrm{i}\psi_2)\;,\quad \psi^*(\mathbf{r},t) = \frac{1}{\sqrt{2}}\,(\psi_1 - \mathrm{i}\psi_2)\;. \tag{1.124}$$

The Lagrangian density for such a field is

$$\mathcal{L} = \dot{\psi}\dot{\psi}^* - m^2\psi\psi^* - (\nabla\psi)(\nabla\psi^*) \tag{1.125}$$

$$= \sum_{i=1}^{2}\frac{1}{2}\left[(\dot{\psi}_i)^2 - (\nabla\psi_i)^2 - m^2\psi_i^2\right]\;. \tag{1.126}$$

Then the conjugate momentum densities are given by

$$\pi_i = \frac{\partial\mathcal{L}}{\partial\dot{\psi}_i} = \dot{\psi}_i\,. \tag{1.127}$$

The Hamiltonian density is $\mathcal{H} = \sum_{i=1}^{2}\pi_i\dot{\psi}_i - \mathcal{L}$ and the total Hamiltonian becomes

$$H = \sum_{i=1}^{2}\left\{\int\left[(\dot{\psi}_i)^2 + (\nabla\psi_i)^2 + m^2\psi_i^2\right]\mathrm{d}^3\tau\;. \tag{1.128}$$

Using the classical field Eq. (1.11) we can show that the Lagrangian density (1.127) leads to the KG equations

$$\frac{\partial^2\psi_i}{\partial t^2} - \nabla^2\psi_i + m^2\psi_i = 0\,,\quad i = 1,2\,. \tag{1.129}$$

A plane wave solution of (1.129) is

$$u_k(\mathbf{r},t) = \frac{1}{\sqrt{V}\,\sqrt{2\omega}}\mathrm{e}^{\mathrm{i}(\mathbf{k}\cdot\mathbf{r}-\omega t)}\,, \tag{1.130}$$

where $\omega^2 = k^2 + m^2$. In order to quantize the field, ψ_1 and ψ_2 are regarded as operators. We expand them in terms of u_k as

$$\psi_i(\mathbf{r},t) = \frac{1}{\sqrt{V}}\sum_k\frac{1}{\sqrt{2\omega}}\left[a_i(\mathbf{k})\,\mathrm{e}^{\mathrm{i}(\mathbf{k}\cdot\mathbf{r}-\omega t)} + a_i^\dagger(\mathbf{k})\,\mathrm{e}^{-\mathrm{i}(\mathbf{k}\cdot\mathbf{r}-\omega t)}\right]\,. \tag{1.131}$$

Since ψ_i are real, the second term (the Hermitian conjugate of the first term) is also included in Eq. (1.131). We make use of the following commutation relations to quantize the fields ψ_i:

$$\left[a_i(\mathbf{k}), a_j^\dagger(\mathbf{k}')\right] = \delta_{ij}\delta(\mathbf{k}-\mathbf{k}')\,, \tag{1.132a}$$

$$[a_i(\mathbf{k}), a_j(\mathbf{k}')] = \left[a_i^\dagger(\mathbf{k}), a_j^\dagger(\mathbf{k}')\right] = 0\,. \tag{1.132b}$$

Then according to the previous section this complex field will represent two types of particles of spin zero.

From (1.131) and (1.124) we get

$$\psi = \frac{1}{\sqrt{V}} \sum_k \frac{1}{\sqrt{2\omega}} \left[a(\mathbf{k})\, \mathrm{e}^{\mathrm{i}(\mathbf{k}\cdot\mathbf{r}-\omega t)} + b^\dagger(\mathbf{k})\, \mathrm{e}^{-\mathrm{i}(\mathbf{k}\cdot\mathbf{r}-\omega t)} \right] , \tag{1.133}$$

where

$$a(\mathbf{k}) = \frac{1}{\sqrt{2}}[a_1(\mathbf{k}) - \mathrm{i}a_2(\mathbf{k})] , \quad b(\mathbf{k}) = \frac{1}{\sqrt{2}}[a_1(\mathbf{k}) + \mathrm{i}a_2(\mathbf{k})] . \tag{1.134}$$

Using Eq. (1.134) we can prove that a, b and their Hermitian conjugates satisfy the commutation rules

$$[a(\mathbf{k}), a^\dagger(\mathbf{k}')] = [b(\mathbf{k}), b^\dagger(\mathbf{k}')] = \delta(\mathbf{k} - \mathbf{k}') . \tag{1.135}$$

All other combinations of the commutation brackets are zero.

The operators $a^\dagger(\mathbf{k})$ and $a(\mathbf{k})$ create and annihilate one type of particle while $b^\dagger(\mathbf{k})$ and $b(\mathbf{k})$ create and annihilate the second type of particle. $n_a(\mathbf{k}) = a^\dagger(\mathbf{k})a(\mathbf{k})$ and $n_b(\mathbf{k}) = b^\dagger(\mathbf{k})b(\mathbf{k})$ are the occupation number operators of these two types of particles. The continuity equation $\nabla \cdot \mathbf{J} + \partial\rho/\partial t = 0$ gives

$$\mathbf{J} = \mathrm{i}e\left[(\nabla\psi^*)\psi - (\nabla\psi)\psi^*\right] , \tag{1.136a}$$

$$\rho = -\mathrm{i}e(\psi\dot{\psi}^* - \psi^*\dot{\psi}) . \tag{1.136b}$$

From Eq. (1.136a), the total charge of the field is computed as

$$Q = \int_V \rho\, \mathrm{d}^3\mathbf{r} = -\mathrm{i}e \int_V (\psi\dot{\psi}^* - \psi^*\dot{\psi})\, \mathrm{d}^3\mathbf{r} . \tag{1.137}$$

Substituting (1.133) in (1.137) and using the commutation relation (1.135), we obtain

$$Q = e\sum_k [n_a(\mathbf{k}) - n_b(\mathbf{k})] . \tag{1.138}$$

The a particles have a charge e and the b particles have $-e$. Except for the sign of their charge these particles possess identical properties. The interchange of a and b changes only the sign of Q. In relativistic QFT, every charge particle is automatically accompanied by an antiparticle with opposite charge. This is a general result in field theory and also applicable to particles with other spin values. The meson π^+ and π^- with spin zero are described by the complex KG field. However, the charge need not necessarily be an electrical charge. The neutral mesons K^0 and $\overline{K}^0$ are also described by the complex KG field as they have opposite hypercharge: $Y = 1$ for the K^0 and $Y = -1$ for the $\overline{K}^0$. The hypercharge is an intrinsic degree of freedom like charge, and they are related to electrical charge Q, the isospin I_z, the strangeness S and the baryon number N by $Y = 2(Q - I_z)$ and $S = Y - N$.

Substituting (1.130) in (1.128) and using the relations (1.132), (1.134) and (1.135) we get

$$\begin{aligned} H &= \sum_k [a^\dagger(\mathbf{k})a(\mathbf{k}) + b^\dagger(\mathbf{k})b(\mathbf{k})]\omega(\mathbf{k}) + \sum_k \omega_k I \\ &= \sum_k \left[n_a(\mathbf{k}) + \frac{1}{2} \right] \omega(\mathbf{k}) + \sum_k \left[n_b(\mathbf{k}) + \frac{1}{2} \right] \omega(\mathbf{k}) . \end{aligned} \tag{1.139}$$

The energy of the vacuum state $|00\rangle$ is $E_0 = \sum_k \omega(\mathbf{k})$ and is known as zero-point energy. Though it diverges, it is not a problem because only energy differences are measurable and are finite.

1.10 Quantization of Dirac Field

Quantization of the Dirac equation is analogous to quantization of Maxwell's equations. The result is the quantized electron-positron field.

The Lagrangian density for the Dirac equation

$$\mathrm{i}\hbar\frac{\partial\psi}{\partial t} = -\mathrm{i}\hbar c\ (\alpha\cdot\nabla)\,\psi + \beta mc^2\psi \tag{1.140}$$

is

$$\mathcal{L} = \overline{\psi}(\mathrm{i}\overline{\partial} - m)\psi\,, \quad \overline{\psi} = \psi^\dagger\gamma^0\,, \quad \overline{\partial} = \gamma^\mu\partial_\mu\,, \tag{1.141a}$$

where we set $\hbar = 1$ and $c = 1$ and the γ-matrices are

$$\gamma^0 = \beta = \begin{pmatrix} I & 0 \\ 0 & -I \end{pmatrix}, \quad \gamma^\mu = \begin{pmatrix} 0 & \sigma_\mu \\ \sigma_\mu & 0 \end{pmatrix}. \tag{1.141b}$$

We start by showing that the Lagrangian density (1.141a) leads to the Dirac equation. The action S is given by

$$S = \int \mathcal{L}\,\mathrm{d}^4x = \int \psi^\dagger\gamma^0(\mathrm{i}\overline{\partial} - m)\psi\,\mathrm{d}^4x\,. \tag{1.142}$$

The variation in S is

$$\delta S = \int \delta\psi^\dagger\gamma^0(\mathrm{i}\overline{\partial} - m)\psi\,\mathrm{d}^4x = 0\,, \tag{1.143a}$$

where

$$\delta\psi^\dagger = (\delta\psi_1^*,\,\delta\psi_2^*,\,\delta\psi_3^*,\,\delta\psi_4^*)\,. \tag{1.143b}$$

In Eq. (1.143b) all the components of $\gamma^0(\mathrm{i}\overline{\partial} - m)\psi$ should be zero. Multiplying by γ^0 from left we get the Dirac equation $(\mathrm{i}\overline{\partial} - m)\psi = 0$.

The field conjugate to the nth component of ψ is

$$\begin{aligned} p_n = \frac{\partial\mathcal{L}}{\partial\dot{\psi}_n} &= \frac{\partial}{\partial\dot{\psi}_n}\left(\overline{\psi}\gamma^\mu\mathrm{i}\partial_\mu\psi - m\overline{\psi}\psi\right) \\ &= \frac{\partial}{\partial\dot{\psi}_n}\left(\overline{\psi}\gamma^\mu\mathrm{i}\partial_\mu\psi\right) \\ &= \frac{\partial}{\partial\dot{\psi}_n}\left(\overline{\psi}\gamma^0\mathrm{i}\partial_0\psi + \ldots\right)\,. \end{aligned} \tag{1.144}$$

Or

$$\begin{aligned} p_n &= \frac{\partial}{\partial\dot{\psi}_n}\left(\overline{\psi}\gamma^0\mathrm{i}\frac{\partial\psi}{\partial t}\right) \\ &= \frac{\partial}{\partial\dot{\psi}_n}\left(\psi^\dagger(\gamma^0)^2\mathrm{i}\frac{\partial\psi}{\partial t}\right) \\ &= \frac{\partial}{\partial\dot{\psi}_n}(\psi^\dagger\mathrm{i}\dot{\psi}) \\ &= \frac{\partial}{\partial\dot{\psi}_n}(\mathrm{i}\psi_n^\dagger\dot{\psi}_n) \\ &= \mathrm{i}\psi_n^\dagger\,. \end{aligned} \tag{1.145}$$

Therefore, we write $\pi = \mathrm{i}\psi^\dagger$. We notice that there is no field conjugate to $\dot{\psi}_n^\dagger$ as $\mathcal{L}$ is independent of $\dot{\psi}_n^\dagger$.

We obtain the Hamiltonian density as

$$\mathcal{H} = \psi^\dagger \mathrm{i}\partial_0 \psi\,, \quad \mathrm{i}\partial_0 = -\mathrm{i}\alpha\cdot\nabla + m\beta\,. \tag{1.146}$$

$\mathrm{i}\partial_0$ is the Dirac Hamiltonian. The total momentum is

$$\pi = -\int p_n \nabla\psi_n \,\mathrm{d}^3x = -\int \mathrm{i}\psi_n^*\nabla\psi_n\,\mathrm{d}^3x = \int \psi^\dagger(-\mathrm{i}\nabla\psi)\,\mathrm{d}^3x\,. \tag{1.147}$$

The total Hamiltonian is

$$H = \int \mathcal{H}\,\mathrm{d}^3x = \mathrm{i}\int \psi^\dagger\partial_0\psi\,\mathrm{d}^3x\,. \tag{1.148}$$

We separate the four-component Dirac wave function into two pairs of mutually complex conjugate function as

$$\begin{pmatrix} \psi^{(1)} \\ \psi^{(2)} \end{pmatrix} \text{ and } \begin{pmatrix} \psi^{(3)} = \psi^{(1)*} \\ \psi^{(4)} = \psi^{(2)*} \end{pmatrix}. \tag{1.149}$$

For a free electron field, the plane wave solutions are

$$\psi^{(i)} = u_i\,\mathrm{e}^{\mathrm{i}(\mathbf{k}\cdot\mathbf{r}-\omega t)}\,, \quad i = 1,2 \tag{1.150a}$$

$$\psi^{(j)} = u_j\,\mathrm{e}^{-\mathrm{i}(\mathbf{k}\cdot\mathbf{r}-\omega t)}\,, \quad j = 3,4 \tag{1.150b}$$

and the energy eigenvalues are

$$E_k = \omega(k) = \pm\sqrt{k^2+m^2}\,. \tag{1.151}$$

To quantize the Dirac field for free particles we need to expand ψ and $\psi^\dagger$ in the complete set of plane waves (1.150) and replace ψ and $\psi^\dagger$ by their operator forms

$$\psi(x,t) = \frac{1}{\sqrt{V}}\sum_k\sum_{i=1}^{2}\Big[a_i(\mathbf{k})u_i(\mathbf{k})\mathrm{e}^{\mathrm{i}(\mathbf{k}\cdot\mathbf{r}-\omega t)} + b_i^\dagger(\mathbf{k})u_i^*(\mathbf{k})\mathrm{e}^{-\mathrm{i}(\mathbf{k}\cdot\mathbf{r}-\omega t)}\Big]\,, \tag{1.152a}$$

$$\psi^\dagger(x,t) = \frac{1}{\sqrt{V}}\sum_k\sum_{i=1}^{2}\Big[a_i^\dagger(\mathbf{k})u_i^\dagger(\mathbf{k})\mathrm{e}^{-\mathrm{i}(\mathbf{k}\cdot\mathbf{r}-\omega t)} + b_i(\mathbf{k})\widetilde{u}_i(\mathbf{k})\mathrm{e}^{\mathrm{i}(\mathbf{k}\cdot\mathbf{r}-\omega t)}\Big]\,, \tag{1.152b}$$

where u_i, u_i^* are column matrices, $u_s^\dagger = \widetilde{u}_s^*$, $\widetilde{u}_s$ are row matrices. *What are* $a_i(\mathbf{k})$, $a_i^\dagger(\mathbf{k})$, $b_i(\mathbf{k})$ *and* $b_i^\dagger(\mathbf{k})$*?* $a_i(\mathbf{k})$ and $a_i^\dagger(\mathbf{k})$ are the annihilation and creation operators, respectively, of electrons in the state with charge $-e$, momentum $\mathbf{k}$ and energy $\omega(\mathbf{k})$. $b_i(\mathbf{k})$ and $b_i^\dagger(\mathbf{k})$ are the annihilation and creation operators, respectively, of positrons in the state with charge e, momentum $\mathbf{k}$ and energy $\omega(\mathbf{k})$.

Substituting ψ and $\psi^\dagger$ in (1.148) and adopting commutation relations between the field operators $a_i(\mathbf{k})$, $a_i^\dagger(\mathbf{k})$, $b_i(\mathbf{k})$ and $b_i^\dagger(\mathbf{k})$ we get

$$H = \sum_k\sum_{i=1}^{2}\omega(\mathbf{k})[a_i^\dagger(\mathbf{k})a_i(\mathbf{k}) - b_i^\dagger(\mathbf{k})b_i(\mathbf{k})] \tag{1.153}$$

and the total charge as

$$Q = e \sum_k \sum_{i=1}^{2} [a_i^\dagger(\mathbf{k}) a_i(\mathbf{k}) + b_i^\dagger(\mathbf{k}) b_i(\mathbf{k})] \,. \tag{1.154}$$

We note from (1.153) that the field Hamiltonian would not be positive definite whereas the total charge will be always positive definite. There will be no lower bound to the energy. A system described by this Hamiltonian would not be stable. The excitation of the particle of the operator $b_i^\dagger(\mathbf{k})$ would reduce energy. The way out of this dilemma is to use the anticommutation rules:

$$\{a_i(\mathbf{k}), a_{i'}(\mathbf{k}')\} = \delta_{ii'}\delta_{kk'} \,, \tag{1.155a}$$
$$\{b_i(\mathbf{k}), b_{i'}(\mathbf{k}')\} = \delta_{ii'}\delta_{kk'} \,, \tag{1.155b}$$
$$\{a_i(\mathbf{k}), a_{i'}(\mathbf{k}')\} = \{b_i(\mathbf{k}), b_{i'}(\mathbf{k}')\} = 0 \,, \tag{1.155c}$$
$$\{a_i(\mathbf{k}), b_{i'}(\mathbf{k}')\} = \left\{a_i(\mathbf{k}), b_{i'}^\dagger(\mathbf{k}')\right\} = 0 \,. \tag{1.155d}$$

Using the relations (1.155) we get from (1.148),

$$H = \sum_k \sum_{i=1}^{2} \omega(\mathbf{k}) [a_i^\dagger(\mathbf{k}) a_i(\mathbf{k}) + b_i^\dagger(\mathbf{k}) b_i(\mathbf{k})] \,, \tag{1.156a}$$

$$Q = -\sum_k \sum_{i=1}^{2} [a_i^\dagger(\mathbf{k}) a_i(\mathbf{k}) - b_i^\dagger(\mathbf{k}) b_i(\mathbf{k})] \,. \tag{1.156b}$$

If $|0\rangle$ is the vacuum state then

$$H = \sum_k \sum_{i=1}^{2} \omega(\mathbf{k}) \left[N_{i-}(\mathbf{k}) + N_{i+}(\mathbf{k})\right] \,, \tag{1.157}$$

where $N_{i-}(\mathbf{k})$ is the occupation number for electrons and $N_{i+}(\mathbf{k})$ are the occupation number for positrons.

1.11 Gauge Field Theories

In realistic quantum mechanics we have the difficulties in interpreting the KG equation and the Dirac equation as single-particle wave equations. Single-particle wave functions are commonly used to describe systems when the number of particles is conserved. Relativistic consideration leads to creation and annihilation of particle-amplitude pairs. In such situations, we have found that the wave function is identified as a field. The wave function and its canonical momentum become operators which satisfy the usual communication relations. When we quantize the classical Maxwell field of electromagnetism, photons with spin-1 emerge as the quantum of the electromagnetic field, and so the theory describes a system with any number of particles. Quantization of KG equation and the Dirac fields lead to quanta which have spin-0 and spin-1/2, respectively.

A QFT is usually expressed in a Lagrangian formulation. The symmetries of Lagrangian density leads to conservation laws through the use of Noether's theorem. Symmetry principles play an important role in physics. A transformation of a physical system that acts the

same way everywhere and at all times is said to have a global symmetry. Due to invariance of laws of physics under spatial, rotational and time transformations, linear momentum, angular momentum and energy are, respectively, conserved. Due to the invariance under a change in phase of the wave functions of charged particles, electric charge is conserved. These are examples of global symmetry. Another important symmetry is the gauge (local) symmetry. We have seen that under a gauge transformation of the electromagnetic potentials, the electric and magnetic fields do not change. Gauge invariance forces the existence of special particles, gauge bosons.

QFTs incorporate quantum concepts for fields as well as particles. Conventional particles, such as electrons, are reinterpreted as states of the quantum field. The most important QFTs for describing elementary particle physics are gauge theories. The classic idea of gauge theory was given by Hermann Weyl. Gauge field theories have revolutionized our understanding of elementary particle interactions during the second half of twentieth century.

1.11.1 Quantum Electrodynamics

The quantum version of Maxwell theory known as quantum electrodynamics (QED) gives an extremely accurate account of electromagnetic fields and force. QED improved the accuracy for certain earlier quantum theory predictions by second-orders of magnitude as well as predicting new splitting of energy levels. QED is an ablelian gauge theory with symmetry graph $U(1)$. Electromagnetic field is the gauge field which mediates the interaction between the charged spin-1/2 fields. It was developed in the late 1940s by Richard Phillips Feynman, Julian Seymour Schwinger and Shinichiro Tomonaga independently. Under QED, charged particles interact by exchange of virtual photons, that do not exit inside the interaction and only serve as carriers of momentum and force.

In the 1960, a formulation of QED led to the unification of theories of weak and electromagnetic interactions by making use of $SU(2) \times U(1)$ gauge group. Sheldon Glashow, Mohammad Abdus Salam and Steven Weinberg independently proposed a unified electro-weak theory which is based on the exchange of four particles: the photon for electromagnetic interaction, two charged W particles and a neutral z particle for weak interaction.

1.11.2 Quantum Chromodynamics

Quantum chromodynamics (QCD) describes the string or 'color' force that binds quarks to form baryons and mesons. QCD is a non-abelian gauge theory invariant under $SU(3)$. There are three different charges (colors) in strong interaction unlike in QED, where there is only one charge (electric). In QCD there are eight types of generalized electromagnetic fields $(\mathbf{E}_\alpha, \mathbf{B}_\alpha)$, $\alpha = 1, 2, \ldots, 8$. The associated quanta are called *gluons* G_α. They are massless spin-1 objects. The exchange of gluons between quarks bind or glue the quarks together to form the neutron or proton. That is, the interaction is governed by gluons.

1.11.3 The Standard Model

The standard model (SM) of high energy physics essentially consists of two parts [5]: (i) Electro-weak dynamics unifying electromagnetic and weak interactions and (ii) chromodynamics governing strong interactions. Gravity has been left out in SM. Analogous to electrodynamics, in electro-weak dynamics there are four types of generalized electromagnetic fields denoted as $(\mathbf{E}_i, \mathbf{B}_i)$, $i = 1, 2, 3, 4$. One of $(\mathbf{E}_i, \mathbf{B}_i)$ being the Faraday–Maxwell electromagnetic field. There are four electro-weak quanta also called *electro-weak gauge bosons*. One of them is the photon (γ) which mediates electromagnetic interaction while the three others W^+, W^- and Z mediate weak interaction.

According to the SM the constituents of the universe are classified into field sector and particle sector. In the field sector, there are twelve gauge fields γ, W^+, W^-, Z, G_1, G_2, ..., G_8. The quanta of them are essentially particles with spin 1 (bosons). The particle sector consists of spin 1/2 particles (fermions). It is noteworthy to point out that fields have their quanta that are particles and in *QFT* each particle in the particle sector has its quantum field. For example, electron is the quanta of the electron field. Thus, QFT unifies field and particle concepts [5].

1.12 Concluding Remarks

Quantum electrodynamics was the first successful QFT to be developed in the middle of the last century and it described completely with high accuracy all electromagnetic interactions. In the next few decades, it was extended to describe weak and strong interactions. It has now been proved that quantum fields provide the appropriate framework to describe a wide class of phenomena and interactions. Though QFT is mainly used by particle physicists to shed light on the fundamental particles of matter and their interactions, condensed matter physicists also make use of it widely. There are two methods to quantize the fields. One is the canonical quantization of the field. Another method which is predominately used is the functional method based on path integral formulation of quantum mechanics developed by Feynman. It has been found that the path integral method is found to be superior to the canonical method in many respects to describe gauge fields. A preliminary study of numerical evaluation of QFT has been reported [6–8].

1.13 Bibliography

[1] S.S. Schweber, *QED and the Men Who Made It?: Dyson, Feynman, Schwinger and Tomonaga.* University Press, Hyderabad, 2001.

[2] S. Weinberg, *The Quantum Theory of Fields.* Volumes I to III. Cambridge University Press, Cambridge, 2000.

[3] M. Daniel, *Phys. Edu.* 41:119, 2006.

[4] A. Hobson, *Am. J. Phys.* 81:211, 2013.

[5] G. Rajasekaran, *Resonance* 17:956, 2012.

[6] C. Bell, *Numerical methods in quantum field theories.* Preprint, 2011; https://physics.nd.edu/assets/118521/bell_christopher.pdf.

[7] R. Easther, D.D. Ferrante, G.S. Guralnik and D. Petrov, A review of two novel numerical methods in QFT. *arXiv.hep-lat*/0306038, 27 June 2003.

[8] S. Garcia, G.S. Guralnik and J. Lawson, *Phys. Lett. B* 322:119, 1994.

1.14 Exercises

1.1 If $\psi = \psi_1 + \mathrm{i}\psi_2$, show that the Lagrange equation obtained by independent variation of ψ and ψ^* are equivalent to those obtained by variations of ψ_1 and ψ_2.

1.2 Obtain the Euler–Lagrange equation for

$$\mathcal{L} = \frac{1}{2}\dot{\psi}^2 - \frac{1}{2}m^2\psi^2 - \frac{1}{2}\left(\frac{\partial\psi}{\partial x}\right)^2.$$

Also, obtain the corresponding Hamiltonian density.

1.3 Show that the Lagrangian density $\mathcal{L} = \mathrm{i}\hbar\psi^*\dot{\psi} - (\hbar^2/2m)\nabla\psi^* \cdot \nabla\psi - V(\mathbf{r}, t)\psi^*\psi$ leads to the Schrödinger equation.

1.4 Find the Euler–Lagrange equation corresponding to the Lagrangian density

$$\mathcal{L} = -\frac{1}{2}\left(\frac{\partial\phi}{\partial x_\mu}\frac{\partial\phi}{\partial x_\mu} + m^2\phi\right),\ \mu = 1, 2, 3, 4.$$

1.5 Rewrite the Euler–Lagrange field equation in terms of L.

1.6 Given the $H = \int[(\hbar^2/2m)\nabla\psi^* \cdot \nabla\psi + V\psi^*\psi]\,\mathrm{d}\tau$ obtain the equation of motion of the operator ψ in the Heisenberg picture.

1.7 Consider two Lagrangian densities $\mathcal{L}$ and $\mathcal{L}'$ which differ by the divergence of some function of the fields as $\mathcal{L}' = \mathcal{L} + \partial_\mu F^\mu(\phi)$. Show that the equations of motion obtained from $\mathcal{L}'$ and $\mathcal{L}$ would be identical.

1.8 If $\psi = (\psi_1 + \mathrm{i}\psi_2)/\sqrt{2}$, find the relations between the canonically conjugate momenta π, $\overline{\pi}$, π_1 and π_2 corresponding to ψ, ψ^*, ψ_1 and ψ_2, respectively.

1.9 Prove the commutation relations $[C_k, C_l] = \left[C_k^\dagger, C_l^\dagger\right] = 0$ and $\left[C_k, C_l^\dagger\right] = \delta_{kl}$.

1.10 Determine the relation between the vacuum state $|0\rangle = |00\ldots\rangle$ and the state $|n_1 n_2 \ldots\rangle$.

1.11 Show that N_k and N_l commute.

1.12 Assuming $\int f'[\pi, \partial\psi'/\partial x'^j]\,\mathrm{d}^3x' = \mathrm{i}\hbar\partial f/\partial x^j$ find out

(a) $[\pi, \int(\nabla'\psi')^2\,\mathrm{d}^3x']$ and (b) $[\pi, \int m^2\psi'^2\,\mathrm{d}^3x']$.

1.13 For the electromagnetic field in vacuum show that $[\mathbf{A}, \pi^2] = 2\mathrm{i}\hbar\delta^3(\mathbf{r} - \mathbf{r}')\pi'$.

1.14 Find the time dependence of the operator $\mathbf{a}_{\mathbf{k}\lambda}$ in the Heisenberg representation and show that the operators of the electric field $\mathbf{E}$ and the magnetic induction $\mathbf{H}_B$ are given by

$$\mathbf{E} = \mathrm{i}\sum_{\mathbf{k}}\sum_{\lambda=1}^{2}\left(\frac{2\pi\hbar\omega(\mathbf{k})}{V}\right)^{1/2}\epsilon_{\mathbf{k}\lambda}\,\mathrm{e}^{\mathrm{i}\mathbf{k}\cdot\mathbf{r}}\left(\mathbf{a}_{\mathbf{k}\lambda} - \mathbf{a}^\dagger_{-\mathbf{k}\lambda}\right) \text{ and}$$

$$\mathbf{H}_B = \mathrm{i}\sum_{\mathbf{k}}\sum_{\lambda=1}^{2}\left(\frac{2\pi\hbar c^2}{V\omega(\mathbf{k})}\right)^{1/2}(\mathbf{k}\times\epsilon_{\mathbf{k}\lambda})\,\mathrm{e}^{\mathrm{i}\mathbf{k}\cdot\mathbf{r}}\left(\mathbf{a}_{\mathbf{k}\lambda} - \mathbf{a}^\dagger_{-\mathbf{k}\lambda}\right).$$

1.15 Show that $\langle\phi_n|\nabla|\phi_m\rangle = -(m\omega_{nm}/\hbar)\mathbf{r}_{nm}$.

1.16 Given the $\mathcal{L} = \psi^\dagger\gamma^0(\overline{\partial} - m)\psi$ obtain the Hamiltonian density of the Dirac field.

1.17 Express H of Dirac field in terms of ladder operators.

1.18 For the electromagnetic field in vacuum determine $H = \int \mathcal{H}\, \mathrm{d}^3x$, where $\mathcal{H} = 2\pi c^2 \pi^2 + \dfrac{1}{8\pi}(\nabla \times \mathbf{A})^2 - c\pi \cdot \nabla\phi$.

1.19 Obtain the values of the commutators $[E_j, H_{Bj'}]$, where $j, j' = x, y, z$. Then find the equations of motion of $\mathbf{E}$ and $\mathbf{B}$.

1.20 For the $\mathbf{E}$ and $\mathbf{H}_B$ of the previous exercise find $\dfrac{\partial}{\partial t}\nabla \cdot \mathbf{E}$ and $\dfrac{\partial}{\partial t}\nabla \cdot \mathbf{H}_B$.

Taylor & Francis
Taylor & Francis Group
http://taylorandfrancis.com

2

Path Integral Formulation

2.1 Introduction

The conventional approach to quantum mechanics begins with the classical Hamiltonian and changes observables to noncommuting operators. Canonically conjugate observables have to be noncommuting operators in order to satisfy the Heisenberg uncertainty principle. The dynamics of a quantum mechanical system is given by the time-dependent Schrödinger equation. In the early 1940s, Richard Feynman realized that it would be possible to construct a quantum model using the classical Lagrangian approach (a method closely related to the action integral). Paul Adrien Maurice Dirac had earlier pointed out that e^{it} times the Lagrangian was analogous to a transformation function for the wave function in which the wave function at one instant could be related to the wave function at a next instant in a time interval of t by multiplying with such an exponential function. Feynman found the exponential phase factor to be the action S which is the time integral of the Lagrangian. Further, he noticed that it was necessary to perform integrals over all space variables at every instant of time to find the transition amplitudes. He developed a way for describing and evaluating the integration using the idea of *integral over all paths*. In Feynman's approach, the particles are described using amplitudes calculated along the paths they may or may not follow. These amplitudes behave like waves, their phase changes as the quantum system moves along the path and the amplitudes for all paths superpose and interfere. This interference between all paths is called as *sum-over-histories* and the resulting amplitude is connected in the same way that the amplitude of a wave function is linked to probability as magnitude-squared.

Generally, the quantum mechanics based on the Schrödinger equation is preferred for a system of particles. But path integral formulation of quantum mechanics [1–6] finds applications in more complicated situations, particularly, in quantum field theory (QFT). There are two widely used approaches to QFT. The first is based on field operators and the canonical quantization of these operator fields which was discussed in chapter 1. The second approach uses the path integral formulation of quantum mechanics. A path integral description of field theory is used in high energy physics. The main development in high energy particle physics has been the emergence of gauge field theory as the basic framework for theories of weak, electromagnetic and strong interactions. Path integral method is highly appropriate for describing the gauge field theory. Path integrals also play a role in some of the theories of quantum gravity. For example, in string theory, path integral can be used to calculate the probability of given string interactions. In quantum cosmology, proposals for the origin of universe are formulated using path integrals. In this framework, the probability of the evolution of the universe into a certain state results from the sum over all possibilities for how such an evolution might take place. Further, it gives a physically appealing and intuitive approach of looking at quantum mechanics. We can understand the classical limit of quantum mechanics in a clear way with path integrals.

DOI: 10.1201/9781003172192-2

We shall discuss the formulation of quantum mechanics in terms of path integrals as it is the basis on which the field theory is developed.

2.2 Time Evolution of Wave Function and Propagator

Consider the one-dimensional time-dependent Schrödinger equation

$$\mathrm{i}\hbar\frac{\partial}{\partial t}\psi(x,t) = H\psi(x,t)\ , \tag{2.1}$$

where $\psi(x,t)$ is the wave function in Schrödinger picture and the Hamiltonian H is independent of time. The purpose of solving the Schrödinger equation lies in finding the time evolution operator which is able to generate the time translation of the given system. The time evolution operator transforms the state at, say, $t = 0$ to a future time t as

$$|\psi(t)\rangle = U(t)|\psi(0)\rangle\ . \tag{2.2}$$

As H is independent of time in the Schrödinger picture, from Eqs. (2.1) and (2.2), we get for $t > 0$,

$$U(t) = \mathrm{e}^{-(\mathrm{i}/\hbar)Ht}\ . \tag{2.3}$$

More explicitly, we write

$$U(t) = \theta(t)\,\mathrm{e}^{-(\mathrm{i}/\hbar)Ht}\ , \tag{2.4a}$$

where

$$\theta(t) = \begin{cases} 1, & \text{for } t > 0 \\ 1/2, & \text{for } t = 1/2 \\ 0, & \text{for } t < 0. \end{cases} \tag{2.4b}$$

The time evolution operator appear as the Green's function for the Schrödinger equation and satisfies

$$\left(\mathrm{i}\hbar\frac{\partial}{\partial t} - H\right)U(t) = \mathrm{i}\hbar\delta(t)\ . \tag{2.5}$$

Determination of this operator is equivalent to finding its matrix elements in a given basis.

In the coordinate basis $|x\rangle$, we define

$$\hat{x}|x\rangle = x|x\rangle. \tag{2.6}$$

Denote the state in which the particle is at $t = 0$ as $|x_i\rangle$. *What is the probability amplitude A for a particle to be in $|x_f\rangle$ at some time t?* It is given by

$$A = K(x_f,t;x_i,0) = \left\langle x_f\middle|\mathrm{e}^{-(\mathrm{i}/\hbar)Ht}\middle|x_i\right\rangle\ . \tag{2.7}$$

K is called the *propagator* from $|x_i\rangle$ to $|x_f\rangle$. K is also called *Feynman's kernel*. It is the transition amplitude between the states $|x_i\rangle$ and $|x_f\rangle$ determined at two times $t_0 = 0$ and $t_0 + t$. Further,

$$\psi(x,t) = \int \mathrm{d}x_i\, K(x_f,t;x_i,0)\psi(x_i,0)\ . \tag{2.8}$$

Equation (2.8) indicates the way in which the particle or the transition amplitude propagates from $(x_i, t = 0)$ to (x_f, t). That is, K has details about the evolution of quantum systems. Equation (2.8) indicates that $\psi(x,t)$ can be determined from K.

In the next section, we obtain an expression for the propagator K in the form of a summation (or integral) over all possible paths between $|x_i\rangle$ and $|x_f\rangle$.

2.3 Path Integral Representation of Propagator

Let us begin by dividing the time interval 0 to t into two intervals: 0 to t_1 and t_1 to t. Writing

$$\mathrm{e}^{-(\mathrm{i}/\hbar)Ht} = \mathrm{e}^{-(\mathrm{i}/\hbar)H(t-t_1)}\mathrm{e}^{-(\mathrm{i}/\hbar)Ht_1} \tag{2.9}$$

the propagator K becomes

$$K = \left\langle x_f \middle| \mathrm{e}^{-(\mathrm{i}/\hbar)H(t-t_1)}\mathrm{e}^{-(\mathrm{i}/\hbar)Ht_1} \middle| x_i \right\rangle . \tag{2.10}$$

Because $\int \mathrm{d}x_1 |x_1\rangle\langle x_1| = 1$ we write

$$\begin{aligned} K &= \left\langle x_f \middle| \mathrm{e}^{-(\mathrm{i}/\hbar)H(t-t_1)} \int \mathrm{d}x_1 |x_1\rangle\langle x_1| \, \mathrm{e}^{-(\mathrm{i}/\hbar)Ht_1} \middle| x_i \right\rangle \\ &= \int \mathrm{d}x_1 \, K(x_f, t; x_1, t_1) K(x_1, t_1; x_i, 0) . \end{aligned} \tag{2.11}$$

We point out that this is simply an expression of the quantum rule for combining amplitudes. It is an expression of the composition property of the propagator K. More precisely, when a system undergoes transition from $|x_i\rangle$ to $|x_f\rangle$ then it must be somewhere at an intermediate time t_1. Denoting the state at t_1 as $|x_1\rangle$ we are able to compute the amplitude for the propagator through the state $|x_1\rangle$ and integrate over all possible states. The fact that this scheme applies to amplitudes rather than probabilities is a striking feature of quantum mechanics.

Now, suppose we divide the time interval t into N (large) steps with an infinitesimal step size $\delta t = t/N$. Then the propagator K becomes

$$\begin{aligned} K &= \left\langle x_f \middle| \mathrm{e}^{-(\mathrm{i}/\hbar)Ht} \middle| x_i \right\rangle \\ &= \left\langle x_f \middle| \left(\mathrm{e}^{-(\mathrm{i}/\hbar)H\delta t} \right)^N \middle| x_i \right\rangle \\ &= \left\langle x_f \middle| \mathrm{e}^{-(\mathrm{i}/\hbar)H\delta t}\mathrm{e}^{-(\mathrm{i}/\hbar)H\delta t} \ldots \mathrm{e}^{-(\mathrm{i}/\hbar)H\delta t} \middle| x_i \right\rangle . \end{aligned} \tag{2.12}$$

Using the closure property $\int \mathrm{d}x_j |x_j\rangle\langle x_j| = 1$, we obtain

$$\begin{aligned} K &= \left\langle x_f \middle| \mathrm{e}^{-(\mathrm{i}/\hbar)H\delta t} \int \mathrm{d}x_{N-1} |x_{N-1}\rangle\langle x_{N-1}| \mathrm{e}^{-(\mathrm{i}/\hbar)H\delta t} \right. \\ &\quad \times \int \mathrm{d}x_{N-2} |x_{N-2}\rangle\langle x_{N-2}| \mathrm{e}^{-(\mathrm{i}/\hbar)H\delta t} \ldots \int \mathrm{d}x_2 |x_2\rangle\langle x_2| \mathrm{e}^{-(\mathrm{i}/\hbar)H\delta t} \\ &\quad \left. \times \int \mathrm{d}x_1 |x_1\rangle\langle x_1| \mathrm{e}^{-(\mathrm{i}/\hbar)H\delta t} \middle| x_i \right\rangle \\ &= \int \mathrm{d}x_1 \ldots \mathrm{d}x_{N-1} \left\langle x_f \middle| \mathrm{e}^{-(\mathrm{i}/\hbar)H\delta t} \middle| x_{N-1} \right\rangle \\ &\quad \times \left\langle x_{N-1} \middle| \mathrm{e}^{-(\mathrm{i}/\hbar)H\delta t} \middle| x_{N-2} \right\rangle \ldots \left\langle x_1 \middle| \mathrm{e}^{-(\mathrm{i}/\hbar)H\delta t} \middle| x_i \right\rangle \\ &= \left(\prod_{j=1}^{N-1} \int \mathrm{d}x_j \right) \left\langle x_f \middle| \mathrm{e}^{-(\mathrm{i}/\hbar)H\delta t} \middle| x_{N-1} \right\rangle \\ &\quad \times \left\langle x_{N-1} \middle| \mathrm{e}^{-(\mathrm{i}/\hbar)H\delta t} \middle| x_{N-2} \right\rangle \ldots \left\langle x_1 \middle| \mathrm{e}^{-(\mathrm{i}/\hbar)H\delta t} \middle| x_i \right\rangle . \end{aligned} \tag{2.13}$$

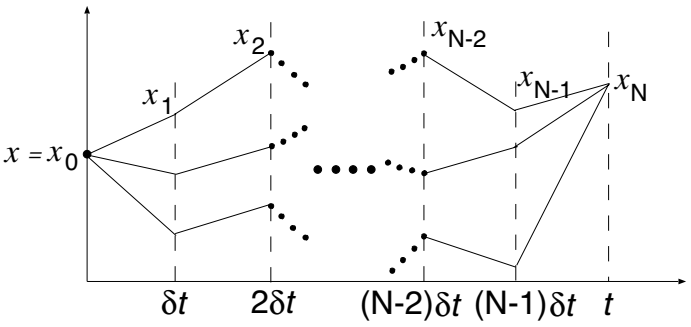

FIGURE 2.1
Representation of transition amplitude (propagator) as a sum over all N small steps.

In Eq. (2.13) the initial and final states (corresponding to $j = 0$ and N, respectively) are not integrated over. Defining $|x_0\rangle = |x_i\rangle$, $|x_N\rangle = |x_f\rangle$ the above equation is rewritten as

$$K = \left(\prod_{j=1}^{N-1} \int \mathrm{d}x_j \right) K_{x_N, x_{N-1}} K_{x_{N-1}, x_{N-2}} \ldots K_{x_2, x_1} K_{x_1, x_0} \, . \tag{2.14}$$

The above equation indicates that K or the amplitude A is the integral of the amplitude of all N-step paths. This is illustrated in Fig. 2.1. K is essentially summed over all possible paths of the propagator or amplitude for each path:

$$K = \sum_{\text{paths}} A_{\text{path}} \, , \tag{2.15a}$$

where

$$\sum_{\text{paths}} = \prod_{j=1}^{N-1} \int \mathrm{d}x_j \, , \quad A_{\text{path}} = \prod_{j=1}^{N} K_{x_j, x_{j-1}} \, . \tag{2.15b}$$

It must be noted that none of the paths are left out. That is, the path integral extends over all possible paths. These paths may be differentiable, nondifferentiable, smooth and nonsmooth. Further, the paths need not obey the classical equation of motion.

2.4 Connection Between Propagator and Classical Action

What is the connection between K and the classical action S? To obtain the relation between K and S consider the factor $\left\langle x_{j+1} \middle| \mathrm{e}^{-(\mathrm{i}/\hbar) H \delta t} \middle| x_j \right\rangle$. For simplicity let the system be a one-dimensional free particle with the operator $H = p^2/2m$. The momentum eigenfunction for a free particle in the Schrödinger picture is given by

$$\langle x|p\rangle = \frac{1}{\sqrt{2\pi\hbar}} \, \mathrm{e}^{\mathrm{i}px/\hbar} \, . \tag{2.16}$$

It is found to satisfy the normalization condition

$$\int \mathrm{d}p \, |p\rangle\langle p| = 1 \, . \tag{2.17}$$

Inserting the complete set of $|p\rangle$ we get K_{x_{j+1},x_j} as

$$\begin{aligned} K_{x_{j+1},x_j} &= \langle x_{j+1}|\mathrm{e}^{-(\mathrm{i}/\hbar)\delta t(\widehat{p}^2/2m)}|x_j\rangle \\ &= \int \mathrm{d}p\,\langle x_{j+1}|\mathrm{e}^{-(\mathrm{i}/\hbar)\delta t(\widehat{p}^2/2m)}|p\rangle\langle p|x_j\rangle\ . \end{aligned} \tag{2.18}$$

We have

$$\widehat{p}|p\rangle = p|p\rangle\ ,\quad \mathrm{e}^{-(\mathrm{i}/\hbar)\delta t(\widehat{p}^2/2m)}|p\rangle = \mathrm{e}^{-(\mathrm{i}/\hbar)\delta t(p^2/2m)}|p\rangle\ . \tag{2.19}$$

Substituting Eq. (2.19) in (2.18), we obtain

$$K_{x_{j+1},x_j} = \frac{1}{2\pi}\int \mathrm{d}p\,\mathrm{e}^{-(\mathrm{i}/\hbar)\delta t(p^2/2m)}\langle x_{j+1}|p\rangle\langle p|x_j\rangle\ . \tag{2.20}$$

The integral over p is known as a *Gaussian integral*. Integrating over p leads to the result [2]

$$K_{x_{j+1},x_j} = \Big(\frac{m}{2\pi\mathrm{i}\hbar\delta t}\Big)^{1/2}\mathrm{e}^{(\mathrm{i}m/2\hbar)(x_{j+1}-x_j)^2/\delta t}\ . \tag{2.21}$$

Substituting (2.21) in (2.13), we obtain

$$K = \Big(\frac{m}{2\pi\mathrm{i}\hbar\delta t}\Big)^{N/2}\prod_{j=0}^{N-1}\int \mathrm{d}x_j\exp\left\{(\mathrm{i}m\delta t/2\hbar)\sum_{j=0}^{N-1}\left[(x_{j+1}-x_j)/\delta t\right]^2\right\}\ . \tag{2.22}$$

In the limit $\delta t\to 0$, we write $\dot{x}_j = (x_{j+1}-x_j)/\delta t$ and replace $\delta t\sum_{j=0}^{N-1}$ by $\int_0^t \mathrm{d}t$. Further, we define

$$\int \mathcal{D}x(t) = \lim_{N\to\infty}\Big(\frac{m}{2\pi\mathrm{i}\hbar\delta t}\Big)^{N/2}\prod_{j=0}^{N-1}\int \mathrm{d}x_j\ . \tag{2.23}$$

$\int \mathcal{D}x(t)$ is considered as a definition of the functional measure over the space of $x(t)$. $\mathcal{D}x(t)$ represents the element of integration. Now, in the limit $\delta t\to 0$, we write Eq. (2.22) in a compact form as

$$K = \int \mathcal{D}x(t)\,\mathrm{e}^{(\mathrm{i}/\hbar)\int_0^t m\dot{x}^2/2\,\mathrm{d}t}\ . \tag{2.24}$$

The integral in the above equation is seen as over all $x(t)$ and $\dot{x}(t)$. Remember that the quantities in the integral are not operators.

When $H = p^2/(2m) + V(x,t)$ we have

$$K = \int \mathcal{D}x(t)\,\mathrm{e}^{(\mathrm{i}/\hbar)\int_0^t\left[(1/2)m\dot{x}^2 - V(x,t)\right]\mathrm{d}t}\ . \tag{2.25}$$

The Lagrangian is $L = T - V = m\dot{x}^2/2 - V(x,t)$ and $\int^t L\mathrm{d}t = S[x(t)]$, where S is called the *classical action*. Hence, for motion along the arbitrary path $x(t)$, Eq. (2.25) becomes

$$K = \int \mathcal{D}x(t)\,\mathrm{e}^{(\mathrm{i}/\hbar)S[x(t)]}\ . \tag{2.26}$$

This is *Feynman's path integral* or *Feynman's kernel* for the transition amplitude. In the above equation, the propagator is written as sum over all possible phase trajectories and weighted by the classical action S. In the classical limit of $S \gg \hbar$, the quantity $S/\hbar$ varies rapidly between neighboring points and the destructive interference occurs. On the other hand, along the classical path the action takes extremum and constructive interference happens among the neighboring paths. Consequently, contribution to the integral comes

from the paths close to the classical paths. This shows how classical mechanics is recovered from quantum mechanics [7] in the limit $\hbar \to 0$.

In the expression (2.26), the path $x(t)$ is unrestricted except at x_i and x_f. $x(t)$ is not the only one selected by the classical equation of motion, that is, not just a path for which S is minimum. In the limit $\delta t \to 0$, the integrals are over the intermediate points $(x_1, x_2, \ldots, x_{N-1})$, therefore, consider all paths from x_i to x_f. In the path integral $\mathcal{D}x(t)$, the end points are fixed where the intermediate points are integrated over the entire space. Any spatial configuration of the intermediate points gives a trajectory between the initial and final points. Therefore, according to path integral *the transition amplitude between an initial and a final state is the sum over all paths, connecting the two points, with the weight factor* $\mathrm{e}^{(\mathrm{i}/\hbar)S[x(t)]}$. We know that in classical mechanics the classical action determines the dynamics. The classical system takes only a path on which the action S is minimum. In quantum mechanics, all the possible paths contribute to the transition amplitude.

Note that the transformation matrix $\langle x_f | \mathrm{e}^{-(\mathrm{i}/\hbar)Ht} | x_i \rangle$ is the propagator $K(x_f, t; x_i, 0)$. K contains the complete dynamics of the system. The path integral (2.26) gives a description of finding K directly. If ψ is the wave function then K propagates ψ through the integral equation

$$\psi(x,t) = \int K(x,t;x',0)\psi(x',0)\,\mathrm{d}x', \quad t > 0. \tag{2.27}$$

K is thus the Green's function of the Schrödinger equation and Eq. (2.27) provides the equivalence between the analytical approach of Schrödinger and Feynman's geometric approach.

Solved Problem 1:

Using the BCH (Baker–Campbell–Hausdorff) theorem

$$\mathrm{e}^P \mathrm{e}^Q = \exp(P + Q + \frac{1}{2}[P,Q] + \frac{1}{2}([P,[P,Q]] - [Q,[P,Q]]) + \ldots) \tag{2.28}$$

show that $\mathrm{e}^{-\mathrm{i}H\delta t/\hbar} \approx \mathrm{e}^{-\mathrm{i}T\delta t/\hbar}\mathrm{e}^{-\mathrm{i}V\delta t/\hbar}$ for $\delta t \to 0$. Hence, establish the result

$$K = \int \mathcal{D}x(t)\, \exp\left(\frac{\mathrm{i}}{\hbar}\int_0^t \left[\frac{1}{2}m\dot{x}^2 - V(x)\right]\mathrm{d}t\right). \tag{2.29}$$

We have $H = T + V$ and $\mathrm{e}^{-\mathrm{i}H\delta t/\hbar} = \mathrm{e}^{-\mathrm{i}\delta t(T+V)/\hbar}$. Substituting $P = -\mathrm{i}\delta tT/\hbar$ and $Q = -\mathrm{i}\delta tV/\hbar$, we find that $[P,Q]$ varies as δt^2 and $[P,[P,Q]]$ and $[Q,[P,Q]]$ vary as δt^3. So, for $\delta t \to 0$, we can write $\mathrm{e}^P\mathrm{e}^Q \approx \mathrm{e}^{P+Q}$. Hence, $\mathrm{e}^{-\mathrm{i}H\delta t/\hbar} \approx \mathrm{e}^{-\mathrm{i}T\delta t/\hbar}\mathrm{e}^{-\mathrm{i}V\delta t/\hbar}$. Then

$$\langle x_{j+1} | \mathrm{e}^{-\mathrm{i}H\delta t/\hbar} | x_j \rangle = \langle x_{j+1} | \mathrm{e}^{-\mathrm{i}T\delta t/\hbar}\mathrm{e}^{-\mathrm{i}V(x)\delta t/\hbar} | x_j \rangle\,. \tag{2.30}$$

As

$$\mathrm{e}^{-\mathrm{i}V(x)\delta t/\hbar}|x_j\rangle = \mathrm{e}^{-\mathrm{i}V(x_j)\delta t/\hbar}|x_j\rangle \tag{2.31}$$

we get

$$\langle x_{j+1} | \mathrm{e}^{-\mathrm{i}H\delta t/\hbar} | x_j \rangle = \langle x_{j+1} | \mathrm{e}^{-\mathrm{i}T\delta t/\hbar} | x_j \rangle \mathrm{e}^{-\mathrm{i}V(x_j)\delta t/\hbar}\,. \tag{2.32}$$

Substituting

$$\langle x_{j+1} | \mathrm{e}^{-\mathrm{i}T\delta t/\hbar} | x_j \rangle = \left(\frac{m}{2\pi\mathrm{i}\hbar\delta t}\right)^{1/2} \mathrm{e}^{(\mathrm{i}m/2\hbar)(x_{j+1}-x_j)^2/\delta t} \tag{2.33}$$

we get

$$\begin{aligned} K &= \left\langle x_{j+1}\middle|\mathrm{e}^{-\mathrm{i}T\delta t/\hbar}\middle|x_j\right\rangle \\ &= \left(\frac{m}{2\pi\mathrm{i}\hbar\delta t}\right)^{N/2}\prod_{j=0}^{N-1}\int \mathrm{d}x_j \\ &\quad \times\exp\left\{\frac{\mathrm{i}\delta t}{\hbar}\sum_{j=0}^{N-1}\frac{m}{2}\left[\frac{x_{j+1}-x_j}{\delta t}\right]^2 - V(x_j)\right\} . \end{aligned} \tag{2.34}$$

In the limit $\delta t \to 0$, we get

$$K = \int \mathcal{D}x(t)\,\mathrm{e}^{(\mathrm{i}/\hbar)\int_0^t[(1/2)m\dot{x}^2 - V(x)]\mathrm{d}t} . \tag{2.35}$$

2.5 Schrödinger Equation From Path Integral Formulation

We ask: *Is the path integral formulation an equivalent picture of nonrelativistic quantum mechanics?* Inside the path integral we have classical functions and functionals rather than operators. As a result simple classical manipulations of the path integral leads to quantum mechanical identities. For example, we recover the time-dependent Schrödinger equation. Because the Schrödinger equation is a differential equation, we need to obtain the propagator for an infinitesimal variation of time δt from $t = 0$. The propagator for an infinitesimal change δt is obtained from Eq. (2.25) as

$$\begin{aligned} K(x_f, t+\delta t; x_i, t) &= \left(\frac{m}{2\pi\mathrm{i}\hbar\delta t}\right)^{1/2}\exp\left\{\frac{\mathrm{i}}{\hbar}\delta t\left[\frac{m}{2}\left(\frac{x_f - x_i}{\delta t}\right)^2\right.\right. \\ &\quad \left.\left. -V\left(\frac{x_f + x_i}{2}\right)\right]\right\} . \end{aligned} \tag{2.36}$$

Substituting (2.36) in (2.27) we get

$$\begin{aligned} \psi(x, t+\delta t) &= \left(\frac{m}{2\pi\mathrm{i}\hbar\delta t}\right)^{1/2}\int_{-\infty}^{\infty}\psi(x', t) \\ &\quad \times\exp\left\{\frac{\mathrm{i}m}{2\hbar\delta t}(x-x')^2 - \frac{\mathrm{i}\delta t}{\hbar}V\left(\frac{x+x'}{2}\right)\right\}\mathrm{d}x'. \end{aligned} \tag{2.37}$$

Introduction of $\xi = x' - x$ gives

$$\begin{aligned} \psi(x, t+\delta t) &= \left(\frac{m}{2\pi\mathrm{i}\hbar\delta t}\right)^{1/2}\int_{-\infty}^{\infty}\psi(x+\xi, t) \\ &\quad \times\exp\left\{\frac{\mathrm{i}m}{2\hbar\delta t}\xi^2 - \frac{\mathrm{i}\delta t}{\hbar}V\left(x+\frac{\xi}{2}\right)\right\}\mathrm{d}\xi . \end{aligned} \tag{2.38}$$

For $\delta t \to 0$ and large ξ, $\mathrm{e}^{[\mathrm{i}\,m/(2\hbar\delta t)]\xi^2}$ would oscillate and all such contributions will average out to zero. This term will contribute to the integral only if $0 \le |\xi| \le (2\pi\hbar\delta t/m)^{1/2}$. Thus, $\xi \to 0$ as $\delta t \to 0$. Now, expand ψ and the integrand in power series. It is enough to consider terms of order δt. The result is

$$\begin{aligned} \psi(x,t) + \epsilon\frac{\mathrm{d}\psi}{\mathrm{d}t} &= \left(\frac{m}{2\pi\mathrm{i}\hbar\delta t}\right)^{1/2}\int_{-\infty}^{\infty}\mathrm{e}^{\mathrm{i}m\xi^2/(2\hbar\delta t)}\left[1 - \frac{\mathrm{i}\delta t}{\hbar}V(x,t)\right] \\ &\quad \times\left[\psi(x,t) + \xi\frac{\partial\psi}{\partial x} + \frac{1}{2}\xi^2\frac{\partial^2\psi}{\partial x^2}\right]\mathrm{d}\xi . \end{aligned} \tag{2.39}$$

Using the results

$$\int_{-\infty}^{\infty} \mathrm{e}^{\mathrm{i}m\xi^2/(2\hbar\delta t)}\mathrm{d}\xi = \left(\frac{2\pi\mathrm{i}\hbar\delta t}{m}\right)^{1/2}, \tag{2.40a}$$

$$\int_{-\infty}^{\infty} \xi\mathrm{e}^{\mathrm{i}m\xi^2/(2\hbar\delta t)}\mathrm{d}\xi = 0\,, \tag{2.40b}$$

$$\int_{-\infty}^{\infty} \xi^2\mathrm{e}^{\mathrm{i}m\xi^2/(2\hbar\delta t)}\mathrm{d}\xi = \frac{\mathrm{i}\hbar\delta t}{m}\left(\frac{2\pi\mathrm{i}\hbar\delta t}{m}\right)^{1/2} \tag{2.40c}$$

in Eq. (2.39) we obtain

$$\psi + \delta t\frac{\partial\psi}{\partial t} = \psi - \frac{\mathrm{i}\delta t}{\hbar}V\psi - \frac{\hbar\delta t}{2\mathrm{i}m}\frac{\partial^2\psi}{\partial x^2} \tag{2.41}$$

which gives the Schrödinger equation

$$-\frac{\hbar}{\mathrm{i}}\frac{\partial\psi}{\partial t} = -\frac{\hbar^2}{2m}\frac{\partial^2\psi}{\partial x^2} + V\psi\,. \tag{2.42}$$

The path integral formalism contains the Schrödinger equation and is equivalent to it. There are other ways to show this equivalence. It is also possible to begin with the Schrödinger picture [4].

2.6 Transition Amplitude of a Free Particle

As an example of the path integral method, consider the simplest system, a free particle.

Let us compute K by the path integral approach. From Eq. (2.22)

$$K = \lim_{\substack{N\to\infty\\ \delta t\to 0}} \left(\frac{m}{2\pi\mathrm{i}\hbar\delta t}\right)^{N/2} \int\cdots\int \exp\left\{\frac{\mathrm{i}m}{2\hbar\delta t}\sum_{i=1}^{N}(x_i - x_{i-1})^2\right\} \times \mathrm{d}x_1\ldots\mathrm{d}x_{N-1}. \tag{2.43}$$

Defining $s_i = [m/(2\hbar\delta t)]^{1/2}x_i$ we rewrite the above K as

$$K = \lim_{\substack{N\to\infty\\ \delta t\to 0}} \left(\frac{m}{2\pi\mathrm{i}\hbar\delta t}\right)^{N/2} \left(\frac{2\hbar\delta t}{m}\right)^{(N-1)/2} \times \int\cdots\int \mathrm{d}s_1\ldots\mathrm{d}s_{N-1}\exp\left\{\mathrm{i}\sum_{i=1}^{N}(s_i - s_{i-1})^2\right\}. \tag{2.44}$$

Integration with respect to s_1 gives

$$\begin{aligned}\int \mathrm{d}s_1\,\mathrm{e}^{\mathrm{i}[(s_1-s_0)^2+(s_2-s_1)^2]} &= \int \mathrm{d}s_1\,\mathrm{e}^{\mathrm{i}\left[2(s_1-(s_0+s_2)/2)^2+(s_2-s_0)^2/2\right]}\\ &= \mathrm{e}^{\mathrm{i}(s_2-s_0)^2/2}\int \mathrm{d}s_1\,\mathrm{e}^{\mathrm{i}2(s_1-(s_0+s_2)/2)^2}\\ &= \left(\frac{\mathrm{i}\pi}{2}\right)^{1/2}\mathrm{e}^{\mathrm{i}(s_2-s_0)^2/2}\,.\end{aligned} \tag{2.45}$$

Next, consider the $\int [.]\, \mathrm{d}s_1\, \mathrm{d}s_2$. We have

$$\begin{aligned}
&\int\int \mathrm{d}s_1\, \mathrm{d}s_2\, \mathrm{e}^{\mathrm{i}\left[(s_1-s_0)^2+(s_2-s_1)^2+(s_3-s_2)^2\right]} \\
&= \left(\frac{\mathrm{i}\pi}{2}\right)^{1/2} \int \mathrm{d}s_2\, \mathrm{e}^{\mathrm{i}\left[(s_2-s_0)^2/2+(s_3-s_2)^2\right]} \\
&= \left[\frac{(\mathrm{i}\pi)^2}{3}\right]^{1/2} \mathrm{e}^{\mathrm{i}(s_3-s_0)^2/3} \,. \qquad (2.46)
\end{aligned}$$

Continuation of this recursion $N-1$ times, Eq. (2.44) becomes

$$\begin{aligned}
K &= \lim_{\substack{N\to\infty \\ \delta t\to 0}} \left(\frac{m}{2\pi\mathrm{i}\hbar\delta t}\right)^{N/2} \left(\frac{2\hbar\delta t}{m}\right)^{(N-1)/2} \left(\frac{(\mathrm{i}\pi)^{N-1}}{N}\right)^{1/2} \mathrm{e}^{\mathrm{i}(s_N-s_0)^2/N} \\
&= \lim_{\substack{N\to\infty \\ \delta t\to 0}} \left(\frac{m}{2\pi\mathrm{i}\hbar N\delta t}\right)^{1/2} \mathrm{e}^{\mathrm{i}m(x_f-x_i)^2/(2\hbar N\delta t)} \,. \qquad (2.47)
\end{aligned}$$

As $N\delta t = t$, we rewrite the above equation as

$$K(x_f,t;x_i,0) = \left(\frac{m}{2\pi\mathrm{i}\hbar t}\right)^{1/2} \mathrm{e}^{\mathrm{i}m(x_f-x_i)^2/(2\hbar t)} \,. \qquad (2.48)$$

We can prove that the K obtained from path integral obeys the equation

$$\mathrm{i}\hbar\frac{\partial K}{\partial t} = -\frac{\hbar^2}{2m}\frac{\partial^2 K}{\partial x_f^2} \,. \qquad (2.49)$$

From Eq. (2.48), the propagator to go from $(0,0)$ to a point (x,t) is

$$K(x,t;0,0) = \left(\frac{m}{2\pi\mathrm{i}\hbar t}\right)^{1/2} \mathrm{e}^{\mathrm{i}mx^2/(2\hbar t)} \,. \qquad (2.50)$$

We notice that $K(x,t;0,0)$ changes with the distance x and t. Because of the phase factor it oscillates as x and t vary. The amplitude of the propagator depends only on time t. In fact, the propagator for a quadratic Lagrangian system is proved to be

$$K(x_f,t_f;x_i,t_i) = F(t_f-t_i)\, \mathrm{e}^{(\mathrm{i}/\hbar)S(x_f,t_f;x_i,t_i)} \,, \qquad (2.51)$$

where S is the classical action and $F(t_f-t_i)$ is a function of the difference of time between the two points. For the free particle, from Eq. (2.48), we find

$$F(t_f-t_i) = \left(\frac{m}{2\pi\mathrm{i}\hbar(t_f-t_i)}\right)^{1/2} \qquad (2.52)$$

and the classical action

$$S = \frac{m(x_f-x_i)^2}{2(t_f-t_i)} \,. \qquad (2.53)$$

Solved Problem 2:

Calculate the propagator $K(x_f,T;x_i,0)$ from ordinary quantum mechanics.

We obtain

$$\begin{aligned} K &= \langle x_f | \mathrm{e}^{-\mathrm{i}Ht/\hbar} | x_i \rangle \\ &= \left\langle x_f \middle| \mathrm{e}^{-\mathrm{i}tp^2/(2m\hbar)} \int \frac{\mathrm{d}p}{2\pi} \middle| p \right\rangle \langle p | x_i \rangle . \end{aligned}$$

That is,

$$\begin{aligned} K &= \int \frac{\mathrm{d}p}{2\pi} \mathrm{e}^{-\mathrm{i}tp^2/(2m\hbar)} \langle x_f | p \rangle \langle p | x_i \rangle \\ &= \int \frac{\mathrm{d}p}{2\pi} \mathrm{e}^{-\mathrm{i}tp^2/(2m\hbar) + \mathrm{i}(x_f - x_i)p} \\ &= \left(\frac{m}{2\pi \mathrm{i}\hbar t} \right)^{1/2} \mathrm{e}^{\mathrm{i}m(x_f - x_i)^2/(2\hbar t)} . \end{aligned} \tag{2.54}$$

Solved Problem 3:

Show that the classical action for a free particle is $S = \dfrac{m}{2} \dfrac{(x_f - x_i)^2}{(t_f - t_i)}$.

For a free particle $V = 0$ and $L = m\dot{x}^2/2 = E$ a constant. We have

$$S = \int_{t_i}^{t_f} L \, \mathrm{d}t = L(t_f - t_i) = \frac{1}{2} m \dot{x}^2 (t_f - t_i) . \tag{2.55}$$

Since $\dot{x} = (x_f - x_i)/(t_f - t_i)$ we get

$$S = \frac{m}{2} \frac{(x_f - x_i)^2}{(t_f - t_i)} . \tag{2.56}$$

2.7 Systems with Quadratic Lagrangian

We discuss a mathematical technique for a system which has the Lagrangian of the form

$$L = a(t)\dot{x}^2 + b(t)\dot{x}x + c(t)x^2 + d(t)\dot{x} + e(t)x + f(t) . \tag{2.57}$$

Then we apply the method to the undamped harmonic oscillator, the linearly damped harmonic oscillator and a particle in a uniform gravitational field with linear damping.

2.7.1 Mathematical Technique

For the systems with L of the form (2.57) the path integrals will have the variables appearing up to the second degree in an exponent. These integrals are called *Gaussian integrals*. The action S will be at most quadratic in $x(t)$.

The transition amplitude for the system to go from the initial position (x_i, t_i) to the final position (x_f, t_f) is given by

$$K = \int \mathcal{D}x(t) \, \mathrm{e}^{(\mathrm{i}/\hbar)S[x(t)]} = \int_{x_i}^{x_f} \mathcal{D}x(t) \, \mathrm{e}^{(\mathrm{i}/\hbar) \int_{t_i}^{t_f} L(\dot{x}, x, t) \, \mathrm{d}t} . \tag{2.58}$$

Let $x_{\rm CM}(t)$ be a classical path with the action $S = \int L\,{\rm d}t$ is extremum. So, the classical action for the two points (from x_i to x_f) is given by

$$S_{\rm CM}(x_f, x_i) = S(x_{\rm CM}(t))\ . \tag{2.59}$$

We represent $x(t)$ in terms of the classical path $x_{\rm CM}(t)$ and a new variable $\eta(t)$: $x(t) = x_{\rm CM}(t) + \eta(t)$. $\eta(t)$ is the deviation of $x(t)$ from $x_{\rm CM}(t)$. As the two end points x_i and x_f are same for $x(t)$ and $x_{\rm CM}(t)$ we have

$$\eta(t_i) = \eta(t_f) = 0\ . \tag{2.60}$$

As at each time t we have x and η differ by a constant ${\rm d}x_i = {\rm d}\eta_i$ for each point t_i. So, we write

$$\mathcal{D}x(t) = \mathcal{D}y(t)\ . \tag{2.61}$$

Using Eq. (2.57), the action integral is written as

$$\begin{aligned} S[x(t)] &= S\left(x_{\rm CM}(t) + \eta(t)\right) \\ &= \int_{t_i}^{t_f} \left[a\left(\dot{x}_{\rm CM} + \dot{\eta}\right)^2 + b\left(\dot{x}_{\rm CM} + \dot{\eta}\right)\left(x_{\rm CM} + \eta\right) + \ldots\right] {\rm d}t. \end{aligned} \tag{2.62}$$

(Substitution of $\eta = \dot{\eta} = 0$ in the above equation gives the $S[x_{\rm CM}(t)]$). Expand the integrands and write the right-side of (2.62) as the integrals corresponding to $S[x_{\rm CM}(t)]$ plus the others. Because the derivative of S with respect to $x_{\rm CM}$ is zero (S is extremum), the integrals over linear terms in η vanishes and only the quadratic terms present. Then Eq. (2.62) becomes

$$S[x(t)] = S\left[x_{\rm CM}(t)\right] + \int_{t_i}^{t_f} \left[a(t)\dot{\eta}^2 + b(t)\dot{\eta}\eta + c(t)\eta^2\right] {\rm d}t\ . \tag{2.63}$$

S is a function of the parameters $(x_f, t_f; x_i, t_i)$ and is also called *2-point action function*. Using (2.60), (2.61) and (2.63), we get

$$\begin{aligned} K(x_f, t_f; x_i, t_i) &= {\rm e}^{({\rm i}/\hbar)S[x_{\rm CM}(t)]} \int_0^0 \mathcal{D}\eta(t) \\ &\quad \times {\rm e}^{({\rm i}/\hbar)\int_{t_i}^{t_f}\left[a(t)\dot{\eta}^2 + b(t)\dot{\eta}\eta + c(t)\eta^2\right]{\rm d}t}\ . \end{aligned} \tag{2.64}$$

Since all possible paths $\eta(t)$ begin from and return to the point $\eta = 0$, the integral over paths is a function only of times at the end points. Hence, K takes the form

$$K(x_f, t_f; x_i, t_i) = {\rm e}^{({\rm i}/\hbar)S[x_{\rm CM}(t)]} F(t_i, t_f)\ . \tag{2.65}$$

To determine K we need to find the classical action integral and the function $F(t_i, t_f)$.

2.7.2 Undamped Harmonic Oscillator

The Langrangian of the one-dimensional undamped harmonic oscillator is

$$L = \frac{1}{2}m\dot{x}^2 - \frac{1}{2}m\omega^2 x^2. \tag{2.66}$$

Then

$$S[x(t)] = \int_{t_i}^{t_f} L(\dot{x}, x, t)\,{\rm d}t = \int_{t_i}^{t_f} \left(\frac{1}{2}m\dot{x}^2 - \frac{1}{2}m\omega^2 x^2\right) {\rm d}t\ . \tag{2.67}$$

The paths over which the integral in the above equation is to be carried out go from $x(t=t_i)=x_i$ to $x(t=t_f)=x_f$. Then the propagator is given by

$$K(x_f,t_f;x_i,t_i)=\int_{x_i}^{x_f}\mathcal{D}x(t)\,\mathrm{e}^{(\mathrm{i}/\hbar)\int_{t_i}^{t_f}\frac{1}{2}m(\dot{x}^2-\omega^2x^2)\,\mathrm{d}t}\ . \tag{2.68}$$

Using the method given in the previous section, we get from Eq. (2.64)

$$\begin{aligned} K(x_f,T;x_i,0) &= \mathrm{e}^{(\mathrm{i}/\hbar)S[x_{\mathrm{CM}}(t)]}\int_0^0\mathcal{D}\eta(t)\mathrm{e}^{(\mathrm{i}/\hbar)\int_0^T m(\dot{\eta}-\omega^2\eta^2)/2\mathrm{d}t} \\ &= \mathrm{e}^{(\mathrm{i}/\hbar)S[x_{\mathrm{CM}}(t)]}F(T)\ , \end{aligned} \tag{2.69a}$$

where

$$F(T)=\int_0^0\mathcal{D}\eta(t)\mathrm{e}^{(\mathrm{i}/\hbar)\int_0^T m(\dot{\eta}-\omega^2\eta^2)/2\mathrm{d}t} \tag{2.69b}$$

and $x_{\mathrm{CM}}(t)$ is the solution of

$$\ddot{x}_{\mathrm{CM}}+\omega^2x_{\mathrm{CM}}=0\ ,\quad x_{\mathrm{CM}}(t_i)=x_i,\ \ x_{\mathrm{CM}}(t_f)=x_f\ . \tag{2.69c}$$

We can make change of variables in the path integral to $\eta(t)$. Since all paths $\eta(t)$ go from 0 at $t=0$ and 0 at $t=T$, the fluctuations at any point on the trajectory is represented as a Fourier series:

$$\eta(t)=\sum_n a_n\sin(n\pi t/T)\ . \tag{2.70}$$

Then we convert the integrals with respect to η into the integrals with respect to a_n by a linear transformation of $\eta(t)$ to a_n with the Jacobian J. The Jacobian is a constant, independent of ω, m and $\hbar$. So, it will appear as a multiplying constant in K.

From Eqs. (2.70) we find that

$$\begin{aligned} \int_0^T\dot{\eta}^2\,\mathrm{d}t &= \sum_{n,m}\int_0^T\mathrm{d}t\,a_na_m\left(\frac{n\pi}{T}\right)\left(\frac{m\pi}{T}\right)\cos\left(\frac{n\pi t}{T}\right)\cos\left(\frac{m\pi t}{T}\right) \\ &= \frac{T}{2}\sum_n\left(\frac{n\pi}{T}\right)^2a_n^2\ . \end{aligned} \tag{2.71}$$

Similarly, we also obtain

$$\int_0^T\eta^2\,\mathrm{d}t=\sum_{n,m}\int_0^T\mathrm{d}t\,a_na_m\sin\left(\frac{n\pi t}{T}\right)\sin\left(\frac{m\pi t}{T}\right)=\frac{T}{2}\sum_n a_n^2\ . \tag{2.72}$$

Suppose the time T is divided into steps of length δt. Then there are finite number N of the coefficients a_n. In this case Eq. (2.69b) is written as

$$\begin{aligned} F(T) &= \lim_{\substack{N\to\infty\\ \delta t\to 0}} A\int\mathrm{d}a_1\,\mathrm{d}a_2\ldots\mathrm{d}a_{N-1} \\ &\qquad\times\exp\left\{\frac{\mathrm{i}}{2\hbar}\sum_{n=1}^{N-1}\left[\frac{T}{2}\left(\frac{n\pi}{T}\right)^2ma_n^2-\frac{T}{2}m\omega^2a_n^2\right]\right\} \\ &= \lim_{\substack{N\to\infty\\ \delta t\to 0}} A\int\mathrm{d}a_1\,\mathrm{d}a_2\ldots\mathrm{d}a_{N-1} \\ &\qquad\times\exp\left\{\frac{\mathrm{i}mT}{4\hbar}\sum_{n=1}^{N-1}\left[\left(\frac{n\pi}{T}\right)^2-\omega^2\right]a_n^2\right\}\ . \end{aligned} \tag{2.73}$$

Any possible factor coming from the Jacobian due to the change of variables from η to a_n has to be taken into account in the constant A. Since Eq. (2.73) has only Gaussian integrals, they are evaluated individually. For example,

$$\begin{aligned}\int \mathrm{d}a_n \exp\left\{\frac{\mathrm{i}mT}{4\hbar}\left[\left(\frac{n\pi}{T}\right)^2-\omega^2\right]a_n^2\right\} &= \left(\frac{4\pi\mathrm{i}\hbar}{mT}\right)^{1/2}\left[\left(\frac{n\pi}{T}\right)^2-\omega^2\right]^{-1/2} \\ &= \left(\frac{4\pi\mathrm{i}\hbar}{mT}\right)^{1/2}\left(\frac{n\pi}{T}\right)^{-1}\left[1-\left(\frac{\omega T}{n\pi}\right)^2\right]^{-1/2}. \end{aligned} \tag{2.74}$$

Using (2.74) in Eq. (2.73) we get

$$F(T) = \lim_{\substack{\omega\to 0\\ N\to\infty}} B\prod_{n=1}^{N-1}\left[1-\left(\frac{\omega T}{n\pi}\right)^2\right]^{-1/2}. \tag{2.75}$$

Using the identity

$$\lim_{N\to\infty}\prod_{n=1}^{N-1}\left[1-\left(\frac{\omega T}{n\pi}\right)^2\right] = \frac{\sin\omega T}{\omega T} \tag{2.76}$$

we get

$$F(T) = \lim_{\substack{N\to\infty\\ \omega\to 0}} B\left(\frac{\omega T}{\sin\omega T}\right)^{1/2} = C\left(\frac{\omega T}{\sin\omega T}\right)^{1/2}. \tag{2.77}$$

As $\omega\to 0$, the harmonic oscillator reduces to a free particle. The $F(T)$ for a free particle is given by Eq. (2.52). So,

$$F(T) = \lim_{\omega\to 0} C\left(\frac{\omega T}{\sin\omega T}\right)^{1/2} = \left(\frac{m}{2\pi\mathrm{i}\hbar T}\right)^{1/2}. \tag{2.78}$$

Thus,

$$C = \left(\frac{m}{2\pi\mathrm{i}\hbar T}\right)^{1/2}. \tag{2.79}$$

Substituting (2.79) in (2.78) we get

$$F(T) = \left(\frac{m\omega}{2\pi\mathrm{i}\hbar\sin\omega T}\right)^{1/2}. \tag{2.80}$$

We can show that for one-dimensional harmonic oscillator, the classical action is

$$S[x_{\mathrm{CM}}(t)] = \frac{m\omega}{2\sin\omega T}\left[(x_i^2+x_f^2)\cos\omega T - 2x_ix_f\right]. \tag{2.81}$$

Substituting (2.80) and (2.81) in Eq. (2.69a) we get the kernel as

$$\begin{aligned} K(x_f,T;x_i,0) &= \left(\frac{m\omega}{2\pi\mathrm{i}\hbar\sin\omega T}\right)^{1/2} \\ &\quad\times\exp\left\{\frac{\mathrm{i}m\omega}{2\hbar\sin\omega T}[(x_i^2+x_f^2)\cos\omega T - 2x_ix_f]\right\}. \end{aligned} \tag{2.82}$$

In the limit $\omega\to 0$, Eq. (2.82) reduces to the free particle transition amplitude given by Eq. (2.48).

2.7.3 Linearly Damped Harmonic Oscillator

Dissipative phenomena with a quantum origin manifest themselves in many different situations and hence the study of dissipative systems and their quantization is of a great theoretical and practical value. Many dissipative systems can be modelled as a linearly damped harmonic oscillator. Hence, many different approaches have been followed in the past to solve the Schrödinger equation for the linearly damped harmonic oscillator which contains a velocity term as a damping factor in its Hamiltonian. Even though various solutions of the Schrödinger equation were obtained for the linearly damped harmonic oscillator, it was found that all those kinds of solutions always violated the uncertainty relation [8–10], one of the fundamental laws of quantum mechanics. However, in 1987, Um, Yeon and Kahng [11] evaluated the exact quantum mechanical solution for the linearly damped harmonic oscillator using the path integral formulation without violating any fundamental law of quantum mechanics.

Consider the Lagrangian

$$L(x,\dot{x},t) = \mathrm{e}^{2\gamma t}\left(\frac{1}{2}m\dot{x}^2 - \frac{1}{2}m\omega_0^2 x^2\right). \tag{2.83}$$

Here ω_0 is the natural frequency of the system and m is the mass of the oscillating particle. Using the Euler–Lagrange's equation of motion

$$\frac{\mathrm{d}}{\mathrm{d}t}\left(\frac{\partial L}{\partial \dot{x}}\right) - \frac{\partial L}{\partial x} = 0 \tag{2.84}$$

we get the equation of motion for the linearly damped harmonic oscillator

$$\ddot{x} + 2\gamma\dot{x} + \omega_0^2 x = 0. \tag{2.85}$$

The classical solution of Eq. (2.85) is

$$x_{\mathrm{CM}}(t) = C_1\mathrm{e}^{a_1 t} + C_2\mathrm{e}^{a_2 t}, \tag{2.86}$$

where $a_1 = -\gamma - \mathrm{i}\Omega$, $a_2 = -\gamma + \mathrm{i}\Omega$ with $\Omega = \sqrt{\omega_0^2 - \gamma^2}$. The integration constants C_1 and C_2 are evaluated using the conditions that the particle moves from the position x_i at the time t_i to the position x_f at the time t_f.

We have seen in sec. 2.7, for the systems with quadratic Lagrangian, the propagator takes the form given by Eq. (2.65). As the Lagrangian given by Eq. (2.83) is quadratic in form we have to find the classical action integral

$$S_{\mathrm{CM}} = S_{\mathrm{CM}}(x_f,t_f;x_i,t_i) = \int_{t_i}^{t_f} L\left(x_{\mathrm{CM}},\dot{x}_{\mathrm{CM}},t\right)\mathrm{d}t \tag{2.87}$$

and the function $F(t_i,t_f)$. Substituting Eq. (2.86) in Eq. (2.87) and integrating in the limit $t_i \to t_f$, we obtain the classical action as

$$\begin{aligned} S_{\mathrm{CM}} \;=\; & \frac{m\Omega}{2\sin\Omega(t_f-t_i)}\Big[\left(x_i^2\mathrm{e}^{2\gamma t_i} + x_f^2\mathrm{e}^{2\gamma t_f}\right)\cos\Omega(t_f-t_i) \\ & -2x_i x_f \mathrm{e}^{2\gamma(t_i+t_f)}\Big] + \frac{m\gamma}{2}\left[x_i^2\mathrm{e}^{2\gamma t_i} - x_f^2\mathrm{e}^{2\gamma t_f}\right]. \end{aligned} \tag{2.88}$$

$F(t_i,t_f)$ can be obtained [12] using

$$F(t_i,t_f) = \left(\frac{\mathrm{i}}{2\pi\hbar}\frac{\partial^2 S_{\mathrm{CM}}}{\partial x_f \partial x_i}\right)^{1/2}. \tag{2.89}$$

Substituting Eq. (2.88) in (2.89) we get

$$F(t_i, t_f) = \left(\frac{m\Omega e^{\gamma(t_i+t_f)}}{2\pi i\hbar \sin \Omega(t_i - t_f)} \right)^{1/2}. \tag{2.90}$$

The complete kernal for the linearly damped harmonic oscillator is

$$K(x_f, t_f; x_i, t_i) = \left(\frac{m\Omega e^{\gamma(t_i+t_f)}}{2\pi i\hbar \sin \Omega(t_i - t_f)} \right)^{1/2} e^{(i/\hbar)S_{CM}}. \tag{2.91}$$

In the limit $\gamma \to 0$ and substituting $t_i = 0$ and $t_f = T$, we obtain Eq. (2.82) corresponding to the linear harmonic oscillator.

The application of the path integral formulation to the driven damped harmonic oscillator has been studied [12].

2.7.4 Particle in a Uniform Gravitational Field with Linear Damping

The equation of motion of a particle moving in a viscous medium under uniform gravitational field is given by

$$m\ddot{x} + \gamma\dot{x} = mg, \tag{2.92}$$

where γ is the damping coefficient and g is the acceleration due to gravity. The classical solution of Eq. (2.92) is given by

$$x_{CM}(t) = A + Be^{-\Lambda t} + \frac{g}{\Lambda}t, \tag{2.93}$$

where $\Lambda = \gamma/m$, A and B are the integration constants. Using the conditions $x_{CM}(t_i) = x_i$ and $x_{CM}(t_f) = x_f$ we find

$$A = \frac{\left[\left(x_i e^{-\Lambda t_f} - x_f e^{-\Lambda t_i} \right) - \frac{g}{\Lambda} \left(t_i e^{-\Lambda t_f} - t_f e^{-\Lambda t_i} \right) \right]}{\left(e^{-\Lambda t_f} - e^{-\Lambda t_i} \right)}, \tag{2.94a}$$

$$B = \frac{\left[(x_f - x_i) - \frac{g}{\Lambda} (t_f - t_i) \right]}{\left(e^{-\Lambda t_f} - e^{-\Lambda t_i} \right)}. \tag{2.94b}$$

Consider the Lagrangian

$$L(x, \dot{x}, t) = \left(\frac{1}{2} m\dot{x}^2 + mgx \right) e^{\Lambda t}. \tag{2.95}$$

Using the Euler-Lagrangian Eq. (2.84) we obtain Eq. (2.92). Substituting $L(x_{CM}, \dot{x}_{CM}, t)$ in Eq. (2.87) and integrating, we obtain [13]

$$\begin{aligned} S_{CM}(x_f, t_f; x_i, t_i) = {} & \frac{m\Lambda e^{\Lambda(t_i+t_f)}}{2\left(e^{\Lambda t_f} - e^{\Lambda t_i} \right)} \left[x_f - x_i - \frac{g}{\Lambda} (t_f - t_i) \right]^2 \\ & + \frac{mg}{\Lambda} \left(x_f e^{\Lambda t_f} - x_i e^{\Lambda t_i} \right) \\ & + \frac{mg^2}{2\Lambda^3} \left(e^{-\Lambda t_i} - e^{-\Lambda t_f} \right). \end{aligned} \tag{2.96}$$

Since the Lagrangian Eq. (2.95) is in quadratic form the propagator is given by Eq. (2.65). Substituting Eq. (2.96) in Eq. (2.89) we get

$$F(t_i, t_f) = \left(\frac{m\Lambda e^{\Lambda(t_i+t_f)}}{2\pi i\hbar \left(e^{\Lambda t_f} - e^{\Lambda t_i} \right)} \right)^{1/2}. \tag{2.97}$$

So, we obtain the propagator for a particle under a uniform gravitational field in a viscous medium as

$$K\left(x_f, t_f; x_i, t_i\right) = \left(\frac{m\Lambda \mathrm{e}^{\Lambda(t_i+t_f)}}{2\pi \mathrm{i}\hbar\left(\mathrm{e}^{\Lambda t_f} - \mathrm{e}^{\Lambda t_i}\right)}\right)^{1/2} \mathrm{e}^{\mathrm{i}S_{\mathrm{CM}}/\hbar}. \tag{2.98}$$

This equation gives the propagator of a free particle when $g = 0$ and $\Lambda \to 0$.

2.8 Path Integral Version of Ehrenfest's Theorem

Introducing a shift $x(t) \to x(t) + u(t)$, $u(t_i = 0) = 0$, $u(t_f = T) = 0$ we write

$$\begin{aligned} K &= \int_{x_i}^{x_f} \mathcal{D}x(t)\, \mathrm{e}^{(\mathrm{i}/\hbar)S[x(t)]} \\ &= \int_{x_i}^{x_f} \mathcal{D}x(t)\, \mathrm{e}^{(\mathrm{i}/\hbar)S[x(t)+u(t)]}\ . \end{aligned} \tag{2.99}$$

Letting, $u(t) = \delta x(t)$ and $S[x(t) + \delta x(t)] = S[x(t)] + \delta S[x(t)]$, we obtain

$$K = \int_{x_i}^{x_f} \mathcal{D}x(t)\, \delta S[x(t)] \mathrm{e}^{(\mathrm{i}/\hbar)S[x(t)]} = 0\ . \tag{2.100}$$

That is, the path integral of a total derivative is zero:

$$\int_{x_i}^{x_f} \mathcal{D}x(t)\, \frac{\delta}{\delta x(t)} \mathrm{e}^{(\mathrm{i}/\hbar)S[x(t)]} = 0\ . \tag{2.101}$$

Because the variation of the action with $\delta x(t)$ vanishes at the end points we have the Euler–Lagrange equations

$$\delta S[x(t)] = \int_{t_i}^{t_f} \mathrm{d}t\, \left(\frac{\partial L}{\partial x} - \frac{\mathrm{d}}{\mathrm{d}t}\frac{\partial L}{\partial \dot{x}}\right) \delta x(t)\ . \tag{2.102}$$

Equation (2.102) in Eq. (2.100) gives

$$\int_{x_i}^{x_f} \mathcal{D}x(t)\, \left(\frac{\partial L}{\partial x} - \frac{\mathrm{d}}{\mathrm{d}t}\frac{\partial L}{\partial \dot{x}}\right) \mathrm{e}^{(\mathrm{i}/\hbar)S[x(t)]} = 0 \tag{2.103}$$

and is the path integral version of Ehrenfest's theorem [14].

2.9 Concluding Remarks

In this chapter we presented a brief introduction of path integral formalism. Note that $K(x_f, t_f; x_i, t_i)$ is the probability amplitude of finding a particle at x_f at t_f starting from x_i at t_i. Further $|K(x_f, t_f; x_i, t_i)|^2$ is the probability of finding the particle at x_f at t_f. It has found applications in the study of intense laser-atom interactions [15], equilibrium isotope effects [16], vibrational-rotational free energies [17] and one-dimensional chains [18]. A new type of seismic imaging based on Feynman path integrals for wave form modelling

is found to be capable of producing accurate subsurface images without any need for a reference velocity model [19]. Berry's phase for systems with nondegenerate and degenerate energy levels has been obtained through the path integral formalism [20]. A numerical method based on the density actions to compute path integral was presented [21]. Numerical implementation of path integral with application to harmonic oscillator was discussed by Marsden [22]. A Monte Carlo method for numerical computation of path integral was reported [23]. Numerical evaluation of path integral for quantum dissipative systems was presented [24].

2.10 Bibliography

[1] R.P. Feynman, *Rev. Mod. Phys.* 20:367, 1948.

[2] R.P. Feynman and A.R. Hibbs, *Quantum Mechanics and Path Integrals.* McGraw-Hill, New York, 1965.

[3] D.C. Khandekar, S.V. Lawande and K.V. Bhagwat, *Path Integral Methods and Their Applications*. World Scientific, Singapore, 2002.

[4] R. MacKenzie, Path integral methods and applications. *arXiv: quant-ph/4090 v1*, 24 April 2000.

[5] A. Das, *Field Theory - A Path Integral Approach.* World Scientific, Singapore, 2006.

[6] A. Zee, *Quantum Field Theory in a Nutshell.* Princeton University Press, Princeton, 2010.

[7] P. Storey and C.C. Tannoudji, *J. Phys. II France* 4:1999, 1994.

[8] P. Havas, *Bull. Am. Phys. Soc.* 1:337, 1956.

[9] I.R. Svinin, *Teor. Mat. Fiz.* 27:2037, 1972.

[10] C.I. Um and K.H. Yeon, *J. Korean Phys. Soc.* 41:594, 2002.

[11] C.I. Um, K.H. Yeon and W.H. Kahng, *J. Phys. A. Math. Gen.* 20:611, 1987.

[12] K.H. Yeon, S.S. Kim, Y.M. Moon, S.K. Hong, C.F. Um and T.F. George, *J. Phys. A. Math. Gen.* 34:7719, 2001.

[13] D. Jain, A. Das and S. Kar, *Am. J. Phys.* 75:259, 2007.

[14] M. Blau, *Notes on (Semi-) advanced quantum mechanics: The path integral approach to quantum mechanics.* Preprint, 2006; http://www.blau.itp.unibe.ch/lecturesPI.pdf

[15] P. Salieres, B. Carre, L. Le Deroff, F. Grasbon, G.G. Paulus, H. Walther, R. Kopold, W. Becker, D.B. Milosevic, A. Sanpera and M. Lewenstein, *Science* 292:902, 2001.

[16] T. Zimmermann and J. Vanicek, *J. Chem. Phys.* 131:024111, 2009.

[17] S.L. Mielke and D.G. Truhlar, *J. Phys. Chem. A* 113:4817, 2009.

[18] M.C. Bohm, J. Schulte and L. Utrera, *Phys. Status Solidi* 176:401, 2006.

[19] E. Landa, S. Fomel and T.J. Moser, *Geophys. Prospecting* 54:491, 2006.

[20] M.A. Alves and M.T. Thomaz, *Am. J. Phys.* 75:552, 2007.

[21] R.J. Creswick, *Mod. Phys. Lett. B* 9:693, 1995.

[22] N.D. Madsen, *Numerical methods project: Feynman path integrals in quantum mechanics.* Preprint, 2009.

[23] R. Govin Jha, *On the numerical simulations of Feynman's path integrals using Markov chain Monte Carlo with Metropolis–Hastings algorithm.* M.Sc. project submitted to St. Xavier's College, Kolkata, India, 2012.

[24] N. Makri, *J. Math. Phys.* 36:2430, 1995.

2.11 Exercises

2.1 (a) Show by direct substitution that the free particle kernel $K(x_f, t; x_i, 0)$ satisfies the differential equation $\mathrm{i}\hbar\partial K/\partial t = -(\hbar^2/2m)\partial^2 K/\partial x_f^2$.

(b) Find the wavelength λ of oscillation of $K(x, t; 0, 0)$ of a free particle at large values of x at a fixed time.

(c) Show that for a fixed distance x, the frequency of oscillation of $K(x, t; 0, 0)$ at large values of t is given by $\nu = E/h$, where E is the classical energy of the free particle.

2.2 Obtain the classical action for one-dimensional undamped linear harmonic oscillator.

2.3 Express the propagator in terms of eigenstates.

2.4 Similar to the quantum statistical function $Z(\beta) = \mathrm{Tr}\,\mathrm{e}^{-\beta H}$ we can introduce the quantum mechanical partition function as $Z(t_f, t_i) = \mathrm{Tr}\,U(t_f, t_i)$. Obtain the path integral form of it.

2.5 Obtain the propagator for a particle of mass m confined within a box potential $V(x) = 0$ for $|x| < a$ and ∞ for $|x| > a$.

2.6 Making use of the propagator of free particle write the propagator for a particle of mass confined to a ring of radius R.

2.7 Find the propagator for a particle falling under a constant gravitational field.

2.8 Given the Lagrangian $\mathrm{e}^{2\gamma t}\left[\frac{1}{2}m_0\dot{x}^2 - \frac{1}{2}m_0\omega_0^2 x^2\right]$ obtain the (Caldirola–Kanai) Hamiltonian with time-dependent mass $m(t) = m_0\mathrm{e}^{2\gamma t}$.

2.9 Determine the evolution of the initial Gaussian wave packet

$$\psi(x, 0) = \left(\frac{1}{2\pi\sigma_0^2}\right)^{1/4} \mathrm{e}^{-(x_i - a)^2/(4\sigma_0^2)}$$

in the linearly damped harmonic oscillator.

2.10 Find the equation of motion of the system with the Lagrangian $L = \left(\frac{1}{2}m\dot{x}^2 + \frac{mg}{2\Lambda}\right)\mathrm{e}^{2\Lambda x}$. By a suitable transformation converts the given L into the quadratic form and then construct the propagator K [13].

3

Supersymmetric Quantum Mechanics

3.1 Introduction

In elementary particle physics, supersymmetry is a symmetry relating fermions and bosons. Fermions are the particles with half-integral spin. Bosons are the particles with intrinsic angular momentum and integral spin. Supersymmetry is a new symmetry of matter and it renders the masses of elementary particles compatible with gravitation. One of the prime predictions of it is that all the known elementary particles have partners called *superparticles*. Every fermion has a bosonic superpartner and vice-versa. For example, fermionic quarks[1] are partners of bosonic squarks[2]. That is, quarks and squarks belong to the same irreducible representation of supersymmetry. Some other supersymmetric pairs of particles are photon-photrino, lepton-slepton and graviton-gravitino. It has been hoped that supersymmetric theories would be able to unify all the known forces. Hermann Nicolai first defined supersymmetry for nonrelativistic quantum systems [1]. Applications of supersymmetry have been found in quantum mechanics, nuclear and condensed matter physics. Supersymmetric technique [2–9] can be employed to analytically solvable potentials to determine bound state eigenspectra and scattering matrix.

Time-independent Schrödinger equation of certain physically interesting potentials are exactly solved. Eigenfunctions and eigenvalues of possible stationary states are obtained. An intriguing question is: *Given a potential $V(x)$ with energy eigenvalues E_n, are there other potentials with the same energy eigenvalues?* Using supersymmetric quantum mechanics [2–5] one can show that for a potential $V(x)$, there exists a one (continuous) parameter (λ) set of potentials $\widehat{V}(x)$ isospectral to $V(x)$ for $0 < \lambda \leq \infty$ or $-\infty \leq \lambda \leq -1$ while for $\lambda = 0$ or -1 $\widehat{V}(x)$ has one bound state less than $V(x)$. The potentials $\widehat{V}(x)$ are called *supersymmetric partners* of $V(x)$.

The study of supersymmetry in quantum mechanics has three important applications:

1. So far several physically interesting potentials are solved exactly and their eigenvalues and eigenfunctions are determined. Employing supersymmetric theory, isospectral potentials of several exactly solvable potentials can be identified.
2. For a new system one can identify whether its potential is an isospectral to any of the known exactly solved systems. If it is not an isospectral then one can proceed to solve it exactly or numerically.
3. For all the potentials studied the superpartner V_n is given by $V_n(x) = V_1 + R(x)$. That is, there are certain spacial types of perturbations $R(x)$ for which the eigenstates can be determined exactly through simple formulas.

In this chapter some illustrations and interpretations of supersymmetry in quantum

[1] Quarks are the basic building blocks of hadrons.

[2] Squark is a hypothetical boson superpartner of a quark. Its electric charge and mass are $-1/3$ and 988 times, respectively, those of an electron. Its strangeness is -1.

DOI: 10.1201/9781003172192-3

mechanics are presented. Particularly, the notions of supersymmetric potentials and partners are defined. The features of supersymmetric partners are brought out. Next, a simple procedure to construct all the supersymmetric partners of a given quantum mechanical system whose all bound states are known is described. Then the technique is applied to linear harmonic oscillator and particle in a box. Construction of complex potentials with real eigenvalues is presented.

3.2 Supersymmetric Potentials

In this section the basic idea of supersymmetry in quantum mechanics is discussed. As shown below, a given one-dimensional time-independent Hamiltonian H_1 with potential V_1 can be rewritten in terms of the operators A^+ and A^- as $A^+A^- + \epsilon$, where ϵ is a constant. The operator A^-A^+ helps to identify a new potential V_2 and a Hamiltonian $H_2 = A^-A^+ + \epsilon$. V_2 and H_2 are called *supersymmetric potential* and *supersymmetric Hamiltonian*, respectively.

3.2.1 Factorization of the Schrödinger Equation

Consider a one-dimensional nonrelativistic Hamiltonian of the form

$$H_1 = -\frac{1}{2}\frac{\mathrm{d}^2}{\mathrm{d}x^2} + V_1(x)\,, \tag{3.1}$$

where $V_1(x)$ is a potential with at least one bound state. Let $\phi_0(x)$ and E_0 be the ground state eigenfunction and energy of H_1, respectively. Then the ground state Schrödinger equation is

$$H_1\phi_0 = \left(-\frac{1}{2}\frac{\mathrm{d}^2}{\mathrm{d}x^2} + V_1(x)\right)\phi_0 = E_0\phi_0\,, \tag{3.2}$$

where $\hbar^2/m$ is set to unity for simplicity. From the above equation we write

$$V_1(x) - E_0 = \frac{1}{2\phi_0}\frac{\mathrm{d}^2\phi_0}{\mathrm{d}x^2} = \frac{\phi_0''}{2\phi_0}\,. \tag{3.3}$$

Let us define

$$A^{\pm} = \frac{1}{\sqrt{2}}\left(\pm\frac{\mathrm{d}}{\mathrm{d}x} + \overline{V}(x)\right)\,, \tag{3.4}$$

where $\overline{V}(x)$ is to be determined. A^+ is the adjoint of A^-. (*Are the operators A^- and A^+ Hermitian?*) Now, consider $A^+A^- + \epsilon$. It is given by

$$\begin{aligned} A^+A^- + \epsilon &= -\frac{1}{2}\frac{\mathrm{d}^2}{\mathrm{d}x^2} + \frac{1}{2}\frac{\mathrm{d}\overline{V}}{\mathrm{d}x} + \frac{1}{2}\overline{V}\frac{\mathrm{d}}{\mathrm{d}x} - \frac{1}{2}\overline{V}\frac{\mathrm{d}}{\mathrm{d}x} + \frac{1}{2}\overline{V}^2 + \epsilon \\ &= -\frac{1}{2}\frac{\mathrm{d}^2}{\mathrm{d}x^2} + \frac{1}{2}\frac{\mathrm{d}\overline{V}}{\mathrm{d}x} + \frac{1}{2}\overline{V}^2 + \epsilon \\ &= H_1 + \frac{1}{2}\frac{\mathrm{d}\overline{V}}{\mathrm{d}x} + \frac{1}{2}\overline{V}^2 - V_1 + \epsilon\,. \end{aligned} \tag{3.5}$$

The choice

$$\frac{1}{2}\frac{\mathrm{d}\overline{V}}{\mathrm{d}x} + \frac{1}{2}\overline{V}^2 - V_1 + \epsilon = 0 \tag{3.6}$$

allows us to write

$$H_1 = A^+A^- + \epsilon\,. \tag{3.7}$$

Equation (3.6) is known as *Riccati equation*. Note that the second-order differential form of H_1 given by Eq. (3.1) is reexpressed as the product of two first-order differential operators A^+ and A^- plus a constant ϵ. In the case of harmonic oscillator A^+ and A^- are creation and annihilation operators, respectively, and $\epsilon = E_0$ is the ground state energy. The condition given by Eq. (3.6) is satisfied if

$$\overline{V}(x) = \frac{\phi_0'}{\phi_0} \quad \text{and} \quad \epsilon = E_0\,. \tag{3.8}$$

Substitution of (3.8) in (3.6) gives $\phi_0'' + 2\,(E_0 - V_1(x))\,\phi_0 = 0$ which is the time-independent Schrödinger Eq. (3.2). Without loss of generality, the ground state energy can be chosen as zero also. Thus, any Hamiltonian H_1 of the form of Eq. (3.1) with a ground state (ϕ_0, E_0) can be factorized as Eq. (3.7) with $\epsilon = E_0$ and

$$A^{\pm} = \frac{1}{\sqrt{2}}\left(\pm\frac{\mathrm{d}}{\mathrm{d}x} + \frac{\phi_0'}{\phi_0}\right)\,. \tag{3.9}$$

In Eq. (3.7) H_1 is expressed as $A^+A^- + \epsilon$. *What will happen if we consider A^-A^+ instead of A^+A^-?* Particularly, we ask: *Does the new Hamiltonian $H_2 = A^-A^+ + E_0$ have any interesting feature?* The following interesting results are obtained with the operator A^-A^+ [4,5].

1. If ϕ is an eigenfunction of A^+A^- then $A^-\phi$ is an eigenfunction of A^-A^+.
2. The eigenvalues of A^-A^+ are the eigenvalues of A^+A^- (except its ground state eigenvalue is missing in A^-A^+). That is, the Hamiltonians $H_1 = A^+A^-$ and $H_2 = A^-A^+$ are *isospectral* except for the ground state.
3. $A^-A^+ + E_0$ defines a new Hamiltonian H_2 and a simple connection exists between the eigenstates of H_1 and H_2.

The above results are obtained explicitly in the next subsection.

Solved Problem 1:

Assume that the Hamiltonian $H = \frac{1}{2}p_x^2 + V(x)$ can be written as $H_1 = A^-A^+ + \epsilon$, where $A^{\pm} = \frac{1}{\sqrt{2}}\left(\pm\frac{\mathrm{d}}{\mathrm{d}x} + W(x)\right)$. Obtain an equation for $W(x)$. For $V = V_1(x) = \frac{1}{2}x^2$ determine a $W(x)$ and ϵ. Also, find the eigenvalues of $H_2 = A^+A^- + \epsilon$.

We obtain $H_1 = A^-A^+ + \epsilon$ as

$$\begin{aligned} H_1 &= \frac{1}{2}\left(-\frac{\mathrm{d}}{\mathrm{d}x} + W\right)\left(\frac{\mathrm{d}}{\mathrm{d}x} + W\right) + \epsilon \\ &= \frac{1}{2}p_x^2 - \frac{1}{2}\frac{\mathrm{d}W}{\mathrm{d}x} + \frac{1}{2}W^2 + \epsilon. \end{aligned} \tag{3.10}$$

Equating H to H_1 we get

$$\frac{\mathrm{d}W}{\mathrm{d}x} - W^2 + 2V(x) - 2\epsilon = 0. \tag{3.11}$$

For $V = V_1(x) = \frac{1}{2}x^2$ Eq. (3.11) becomes

$$\frac{\mathrm{d}W}{\mathrm{d}x} - W^2 + x^2 - 2\epsilon = 0. \tag{3.12}$$

The solution $W = x$ gives $\epsilon = \dfrac{1}{2}$. Thus,

$$H_1 = A^- A^+ + \frac{1}{2} = \frac{1}{2}p_x^2 + \frac{1}{2}x^2 = H. \tag{3.13}$$

Next,

$$H_2 = A^+ A^- + \epsilon = \frac{1}{2}p_x^2 + \frac{1}{2}x^2 + 1 = \frac{1}{2}p_x^2 + V_2(x), \tag{3.14}$$

where $V_2(x) = \dfrac{1}{2}x^2 + 1 = V_1 + 1$.

The eigenvalues of H_1 are $E_n^{(1)} = \left(n + \frac{1}{2}\right)$. As $H_2 = H_1 + 1$ the eigenvalues of H_2 are the eigenvalues of H_1 plus 1. That is, $E_n^{(2)} = E_n^{(1)} + 1 = n + \dfrac{3}{2}$. $E = E_0^{(1)} = \dfrac{1}{2}$ is missing in the eigenvalues of H_2.

3.2.2 Eigenvalues and Eigenfunctions of $A^- A^+$

A^+ and A^- act as raising and lowering operators, respectively. $A^-\phi_n$ leads to $(n-1)$th state. Multiplication of the eigenvalue equation $A^+A^-\phi = E\phi$ from left by A^- gives

$$A^- A^+ (A^-\phi) = E(A^-\phi)\,. \tag{3.15}$$

Thus, the eigenvalue of $A^- A^+$ is E while its eigenfunction is $A^-\phi$. Therefore, if ϕ_n is an eigenfunction of H_1 then the eigenfunction of $A^- A^+$ is $A^-\phi_n$. Because of $A^-\phi_0 = 0$, the above statement breaks down at $n = 0$ (ground state).

3.2.3 Supersymmetric Partner Potentials

The operator $A^- A^+$ is written as

$$\begin{aligned}
A^- A^+ &= \frac{1}{2}\left(-\frac{\mathrm{d}}{\mathrm{d}x} + \frac{\phi_0'}{\phi_0}\right)\left(\frac{\mathrm{d}}{\mathrm{d}x} + \frac{\phi_0'}{\phi_0}\right) \\
&= \frac{1}{2}\left[-\frac{\mathrm{d}^2}{\mathrm{d}x^2} - \frac{\mathrm{d}}{\mathrm{d}x}\frac{\phi_0'}{\phi_0} - \frac{\phi_0'}{\phi_0}\frac{\mathrm{d}}{\mathrm{d}x} + \frac{\phi_0'}{\phi_0}\frac{\mathrm{d}}{\mathrm{d}x} + \left(\frac{\phi_0'}{\phi_0}\right)^2\right] \\
&= -\frac{1}{2}\frac{\mathrm{d}^2}{\mathrm{d}x^2} - \frac{1}{2}\frac{\phi_0''}{\phi_0} + \frac{1}{2}\left(\frac{\phi_0'}{\phi_0}\right)^2 \\
&= -\frac{1}{2}\frac{\mathrm{d}^2}{\mathrm{d}x^2} + \frac{1}{2}\frac{\phi_0''}{\phi_0} - \frac{\mathrm{d}^2}{\mathrm{d}x^2}\ln\phi_0 \\
&= -\frac{1}{2}\frac{\mathrm{d}^2}{\mathrm{d}x^2} + V_1(x) - E_0 - \frac{\mathrm{d}^2}{\mathrm{d}x^2}\ln\phi_0\,.
\end{aligned} \tag{3.16}$$

Defining

$$V_2(x) = V_1(x) - \frac{\mathrm{d}^2}{\mathrm{d}x^2}\ln\phi_0 \tag{3.17}$$

Eq. (3.16) can be rewritten as

$$A^- A^+ + E_0 = -\frac{1}{2}\frac{\mathrm{d}^2}{\mathrm{d}x^2} + V_2(x)\,. \tag{3.18}$$

Thus, from a given potential $V_1(x)$ with the known ground state eigenfunction ϕ_0 another potential $V_2(x)$ can be constructed through Eq. (3.17). The potentials $V_1(x)$ and $V_2(x)$ are called *supersymmetric partner potentials* [2–5].

The Hamiltonian H_2 corresponding to $V_2(x)$ is given by (refer Eq. (3.18))

$$H_2 = -\frac{1}{2}\frac{\mathrm{d}^2}{\mathrm{d}x^2} + V_2(x) = A^- A^+ + E_0\,. \tag{3.19}$$

Equation (3.19) implies that the eigenspectra of H_2 are simply those of $A^-A^+ + E_0$. The Hamiltonians H_1 and H_2 whose potentials are V_1 and V_2, respectively, are called *supersymmetric partners*. H_1 and H_2 share the same eigenvalue spectra except that the ground state of H_1 is missing in H_2. The operators A^- and its adjoint A^+ act as transformation operators between the Hamiltonians H_1 and H_2 as $A^+H_2 = H_1A^+$ and $A^-H_1 = H_2A^+$.

Solved Problem 2:

For a system with N-spatial dimension, $N > 1$ show that if the ground state is nondegenerate it is not possible to find A such that the Hamiltonian cannot be factorized as $H = A^+A^- + E_0$, where E_0 is the ground state energy.

Suppose that it is possible to find A^- with $H = A^+A^- + E_0$. A^- must be a function of $\partial/\partial x_k$, $k = 1, 2, \ldots, N$, otherwise, it is impossible for us to reconstruct the kinetic energy term of H. ϕ_0 is the ground state eigenfunction of H if and only if $A^-\phi_0 = 0$. But $A^-\phi_0 = 0$ is a partial differential equation with N variables, $N > 1$. It will have more than one linearly independent solution ϕ_0. That is, E_0 is degenerate which is contradictory to our assumption that E_0 is nondegenerate. For a nondegenerate ground state energy H cannot be factorized as $A^+A^- + E_0$.

3.2.4 Why are H_1 and H_2 Called Supersymmetric Partners?

Now, we bring out the origin for calling H_1 and H_2 as supersymmetric partners. The term *supersymmetry* was earlier used to denote a symmetry associated with certain field theories which allows transformations between the field components with spins differing by $\hbar/2$. In our discussion the word supersymmetry is used in a general sense. In field theory it is used to describe systems subjected to an underlying algebra and can be obtained from the algebra of supersymmetry.

Let us define the operators Q^+, Q^- and H_s as

$$Q^+ = \begin{pmatrix} 0 & 0 \\ A^- & 0 \end{pmatrix}, \quad Q^- = \begin{pmatrix} 0 & A^+ \\ 0 & 0 \end{pmatrix}, \quad H_\mathrm{s} = \begin{pmatrix} H_1 & 0 \\ 0 & H_2 \end{pmatrix}. \tag{3.20}$$

In supersymmetric quantum mechanics $Q^\pm$ are anticommuting:

$$\left\{Q^+, Q^+\right\}_+ = \left\{Q^-, Q^-\right\}_+ = 0\,. \tag{3.21}$$

We can easily verify that Q^+, Q^- and H_s satisfy the following so-called *supersymmetric commutation* if we take the ground state energy as zero (for a proof of these relations see the exercises 10 and 11 at the end of this chapter)

$$\left\{Q^-, Q^+\right\}_+ = Q^-Q^+ + Q^+Q^- = H_\mathrm{s}\,, \tag{3.22a}$$

$$\left[H_\mathrm{s}, Q^-\right] = H_\mathrm{s}Q^- - Q^-H_\mathrm{s} = 0\,, \tag{3.22b}$$

$$\left[H_\mathrm{s}, Q^+\right] = 0\,. \tag{3.22c}$$

Because of this the Hamiltonians H_1 and H_2 are called *supersymmetric partner Hamiltonians*. H_1 and H_2 can be viewed, respectively, as fermionic and bosonic components of the supersymmetric Hamiltonian $H_{\rm s}$. The term supersymmetric Hamiltonian means in the sense that a Hamiltonian defined in terms of Q^+ and Q^- that satisfy the same algebra of the generators of the supersymmetry in field theory.

Equations (3.22b) and (3.22c) point out the invariance of the Hamiltonian under the symmetry. Further, they imply that Q^- and Q^+ are conserved. Equation (3.21) states that Q^- and Q^+ are fermion-like and express their anticommutator property. It moreover conveys that the square of the generators is zero. Through Eq. (3.22a) time transformation can be generated by means of a transformation in the Q^- direction followed by one in the Q^+ direction.

As the potentials $V_1(x)$ and $V_2(x)$ are interconnected it is worth it to ask: *Are the eigenfunctions and eigenvalues of the Hamiltonians H_1 and H_2 related? If so, how are they related? Is it possible to determine systematically the eigenvalues and eigenfunctions of one of the Hamiltonians from the known eigenstates of the other?* Interestingly, simple relations exist between the eigenstates of H_1 and H_2 and will be established in the next section.

3.2.5 An Example for Supersymmetric Hamiltonian

If $Q^{\pm}$ are taken as anticommuting operators, then $H_{\rm s}$ contains coordinates quantized by commutators and anticommutators. They are mixed by supersymmetry transformation. As an example, consider a particle with spin. The position and spin-orientation form a pair of such coordinates. Consider

$$Q^- = \frac{1}{\sqrt{2}}(-{\rm i}p + \overline{V}(x))\sigma_-\,, \quad Q^+ = \frac{1}{\sqrt{2}}({\rm i}p + \overline{V}(x))\sigma_+ \tag{3.23}$$

in which x and p are Bose degrees of freedom whereas σ_+ and σ_- are Fermi degrees of freedom. The quantum condition for x and p is $[x, p] = {\rm i}$. For σ_+ and σ_- we have the anticommutative relations

$$\{\sigma_+, \sigma_-\}_+ = \{\sigma_-, \sigma_+\}_+ = 1\,, \quad \{\sigma_-, \sigma_-\}_+ = \{\sigma_+, \sigma_+\}_+ = 0\,. \tag{3.24}$$

Hence, as $\sigma_+^2 = \sigma_-^2 = 0$, we obtain

$$\left\{Q^+, Q^+\right\}_+ = 2Q^{+2} = ({\rm i}p + \overline{V})^2\sigma_+^2 = 0\,, \tag{3.25a}$$

$$\left\{Q^-, Q^-\right\}_+ = 2Q^{-2} = (-{\rm i}p + \overline{V})^2\sigma_-^2 = 0\,. \tag{3.25b}$$

Then

$$\begin{aligned} H_{\rm s} &= Q^-Q^+ + Q^+Q^- \\ &= \frac{1}{2}\left(p^2 + \overline{V}^2\right)\{\sigma_-, \sigma_+\}_+ - \frac{1}{2}\frac{\partial\overline{V}}{\partial x}\,[\sigma_-, \sigma_+] \\ &= \frac{1}{2}\left(p^2 + \overline{V}^2\right) + \frac{1}{2}\sigma_z\frac{\partial\overline{V}}{\partial x}\,. \end{aligned} \tag{3.26}$$

The Hamiltonian H_s given by (3.26) contains H_1 and H_2 and are known as Bose and Fermi sectors, respectively. These two possess the same energy levels as they are partner Hamiltonians except for the ground state of H_1.

3.2.6 Supersymmetric Oscillator

The Hamiltonian of a bosonic oscillator in one-dimension with a natural frequency ω is given by ($\hbar = 1$)

$$H_{\rm B} = \frac{1}{2}\omega \left(a_{\rm B}^{+} a_{\rm B} + 1\right) , \tag{3.27}$$

where the creation and annihilation operators satisfy $\left[a_{\rm B}, a_{\rm B}^{+}\right]_{-} = 1$ with all others vanishing. A fermionic oscillator is described by the Hamiltonian

$$H_{\rm F} = \omega \left(a_{\rm F}^{+} a_{\rm F} - \frac{1}{2}\right) , \tag{3.28}$$

where the $a_{\rm F}^{+}$ and $a_{\rm F}$ satisfy the anticommutative relations

$$\left\{a_{\rm F}, a_{\rm F}\right\}_{+} = 0 = \left\{a_{\rm F}^{+}, a_{\rm F}^{+}\right\}_{+} , \quad \left\{a_{\rm F}, a_{\rm F}^{+}\right\}_{+} = 1 . \tag{3.29}$$

A system consisting of a bosonic and a fermionic oscillators with the same natural frequency ω is known as a *supersymmetric oscillator*. From Eqs. (3.27) and (3.28), its Hamiltonian can be written as

$$H = H_{\rm B} + H_{\rm F} = \omega \left(a_{\rm B}^{+} a_{\rm B} + a_{\rm F}^{+} a_{\rm F}\right) . \tag{3.30}$$

$a_{\rm B}^{+} a_{\rm B}$ is simply the bosonic number operator $n_{\rm B}$ whereas $a_{\rm F}^{+} a_{\rm F}$ is the fermionic number operator $n_{\rm F}$. If $|n_{\rm B}, n_{\rm F}\rangle$ are the eigenstates of H, then

$$H|n_{\rm B}, n_{\rm F}\rangle = \omega \left(n_{\rm B} + n_{\rm F}\right) |n_{\rm B}, n_{\rm F}\rangle \tag{3.31}$$

with $n_{\rm B} = 0, 1, \ldots$ and $n_{\rm F} = 0, 1$. Note that the eigenvalues of the fermionic number operator are 0 and 1 and are consistent with the Pauli principle. On the other hand, the eigenvalues of the bosonic number operator can take any positive integer values.

Let us consider

$$Q^{-} = \sqrt{\omega}\, a_{\rm B}^{+} a_{\rm F} , \quad Q^{+} = \sqrt{\omega}\, a_{\rm F}^{+} a_{\rm B} . \tag{3.32}$$

We obtain

$$\left\{Q^{-}, Q^{-}\right\}_{+} = 2\omega a_{\rm B}^{+} a_{\rm F} a_{\rm B}^{+} a_{\rm F} = 2\omega \left(a_{\rm B}^{+}\right)^{2} \left(a_{\rm F}\right)^{2} . \tag{3.33}$$

Since $\left\{a_{\rm F}, a_{\rm F}\right\}_{+} = 0$ we have $a_{\rm F}^{2} = 0$. Hence, $\left\{Q^{-}, Q^{-}\right\}_{+} = 0$. Similarly, $\left\{Q^{+}, Q^{+}\right\}_{+} = 0$. So, Q^{-} and Q^{+} are anticommuting. We have

$$\begin{aligned} \left\{Q^{-}, Q^{+}\right\}_{+} &= Q^{-} Q^{+} + Q^{+} Q^{-} \\ &= \omega \left\{a_{\rm B}^{+} a_{\rm F}, a_{\rm F}^{+} a_{\rm B}\right\}_{+} \\ &= \omega \left(a_{\rm B}^{+} a_{\rm F} a_{\rm F}^{+} a_{\rm B} + a_{\rm F}^{+} a_{\rm B} a_{\rm B}^{+} a_{\rm F}\right) . \end{aligned} \tag{3.34}$$

Using the commutator relations (3.29), we get

$$\left\{Q^{-}, Q^{+}\right\}_{+} = \omega \left(a_{\rm B}^{+} a_{\rm B} + a_{\rm F}^{+} a_{\rm F}\right) = H . \tag{3.35}$$

Also,

$$\begin{aligned} \left[Q^{-}, H\right]_{-} &= \left[\sqrt{\omega}\, a_{\rm B}^{+} a_{\rm F}, \omega \left(a_{\rm B}^{+} a_{\rm B} + a_{\rm F}^{+} a_{\rm F}\right)\right] \\ &= \omega^{3/2} \left(-a_{\rm B}^{+} a_{\rm F} + a_{\rm B}^{+} a_{\rm F}\right) \\ &= 0 . \end{aligned} \tag{3.36}$$

Similarly, one can prove that

$$\left[Q^{+}, H\right] = 0 . \tag{3.37}$$

Q^- and Q^+ defined by Eq. (3.32) are conserved quantities of the system. So, Eqs. (3.35)–(3.37) define an algebra involving commutators and anticommutators. Such an algebra is known as *graded Lie algebra* and defines the infinitesimal form of the supersymmetric transformations.

Solved Problem 3:

The two-dimensional Hamiltonian for an electron subjected to a constant electric field $\mathbf{B} = B_z\mathbf{k}$ is given by $H_\mathrm{s} = \frac{1}{2}\left(\pi_x^2 + \pi_y^2 - eB\sigma_z\right)$, where $\pi_x = P_x - eA_x$, $\pi_y = P_y - eA_y$ and $\mathbf{A}$ is the vector potential defined by $\mathbf{B} = \nabla \times \mathbf{A}$. The supercharges are defined by $A^\pm = \pi_\pm\sigma_\mp/\sqrt{2}$, where $\sigma_\pm = (\sigma_x \pm \mathrm{i}\sigma_y)/2$. Show that Q^-, Q^+ and H_s satisfy the supersymmetric commutation relation

$$[H_\mathrm{s}, Q^-] = H_\mathrm{s}Q^- - Q^-H_\mathrm{s} = 0,\ [H_\mathrm{s}, Q^+] = 0. \tag{3.38}$$

We obtain

$$\begin{aligned}
\left[H_\mathrm{s}, Q^-\right] &= H_\mathrm{s}Q^- - Q^-H_\mathrm{s} \\
&= \frac{1}{2\sqrt{2}}\begin{pmatrix} \pi_-\pi_+ & 0 \\ 0 & \pi_+\pi_- \end{pmatrix}\begin{pmatrix} 0 & 1 \\ 0 & 0 \end{pmatrix} \\
&\quad -\frac{\pi_-}{2\sqrt{2}}\begin{pmatrix} 0 & 1 \\ 0 & 0 \end{pmatrix}\begin{pmatrix} \pi_-\pi_+ & 0 \\ 0 & \pi_+\pi_- \end{pmatrix} \\
&= \begin{pmatrix} 0 & 0 \\ 0 & 0 \end{pmatrix}.
\end{aligned} \tag{3.39}$$

Similarly, one can show the other relation.

3.3 Relations Between the Eigenstates of Two Supersymmetric Hamiltonians

In this section we bring out the relations between the eigenvalues and eigenfunctions of the supersymmetric Hamiltonians H_1 and H_2 [4,5]. Let $\phi_n^{(1)}$ and $\phi_n^{(2)}$ denote the eigenfunctions of H_1 and H_2, respectively, with the eigenvalues $E_n^{(1)}$ and $E_n^{(2)}$, where $n = 0, 1, 2, \ldots$. Operation of H_2 on $A^-\phi_n^{(1)}$ gives

$$\begin{aligned}
H_2\left(A^-\phi_n^{(1)}\right) &= \left(A^-A^+ + E_0^{(1)}\right)\left(A^-\phi_n^{(1)}\right) \\
&= A^-\left[\left(A^+A^- + E_0^{(1)}\right)\phi_n^{(1)}\right] \\
&= A^-\left(H_1\phi_n^{(1)}\right) \\
&= E_n^{(1)}A^-\phi_n^{(1)}, \quad n = 1, 2, \ldots .
\end{aligned} \tag{3.40}$$

This relation breaks-down at $n = 0$ because of $A^-\phi_n^{(1)} = 0$.

Similarly, operation of H_1 on $A^+\phi_n^{(2)}$ leads to

$$\begin{aligned} H_1\left(A^+\phi_n^{(2)}\right) &= \left(A^+A^- + E_0^{(1)}\right)\left(A^+\phi_n^{(2)}\right) \\ &= A^+\left[(A^-A^+)\phi_n^{(2)}\right] + E_0^{(1)}A^+\phi_n^{(2)} \\ &= A^+H_2\phi_n^{(2)} \\ &= E_n^{(2)}A^+\phi_n^{(2)}\,. \end{aligned} \tag{3.41}$$

Equation (3.40) implies that if $\phi_n^{(1)}$ is the eigenfunction of the Hamiltonian H_1 with the eigenvalue $E_n^{(1)}$ then $A^-\phi_n^{(1)}$ is the eigenfunction of H_2 with the same eigenvalue $E_n^{(1)}$ except for the ground state. Similarly, if $\phi_n^{(2)}$ is the eigenfunction of H_2 with the eigenvalue $E_n^{(2)}$ then $A^+\phi_n^{(2)}$ is the eigenfunction of H_1 with the same eigenvalue $E_n^{(2)}$. $A^+\phi_n^{(2)}$ creates $(n+1)$th eigenstate of H_1 with the eigenvalue $E_n^{(2)}$. But the eigenvalue of $(n+1)$th state of H_1 is designated as $E_{n+1}^{(1)}$. Hence, one has the relation $E_n^{(2)} = E_{n+1}^{(1)}$, $n = 0, 1, 2, \ldots$. This relation indicates that $A^-\phi_{n+1}^{(1)}$ leads to the eigenfunction of nth eigenstate of H_2. Consequently, one can write $\phi_n^{(2)} \propto A^-\phi_{n+1}^{(1)}$ or

$$\phi_n^{(2)} = \alpha A^-\phi_{n+1}^{(1)}\,, \tag{3.42}$$

where α is a constant. α can be determined using the normalization condition for $\phi_n^{(2)}$.

One has

$$\begin{aligned} 1 &= \int_{-\infty}^{\infty}\left(\phi_n^{(2)}\right)^*\phi_n^{(2)}\,\mathrm{d}x \\ &= \alpha^2\int_{-\infty}^{\infty}\left(A^-\phi_{n+1}^{(1)}\right)^*\left(A^-\phi_{n+1}^{(1)}\right)\mathrm{d}x \\ &= \alpha^2\int_{-\infty}^{\infty}\left(\phi_{n+1}^{(1)}\right)^*(A^+A^-)\phi_{n+1}^{(1)}\,\mathrm{d}x \\ &= \alpha^2\int_{-\infty}^{\infty}\left(\phi_{n+1}^{(1)}\right)^*\left(H_1 - E_0^{(1)}\right)\phi_{n+1}^{(1)}\,\mathrm{d}x \\ &= \alpha^2\left(\int_{-\infty}^{\infty}\left(\phi_{n+1}^{(1)}\right)^*H_1\phi_{n+1}^{(1)}\,\mathrm{d}x - E_0^{(1)}\right), \end{aligned} \tag{3.43}$$

where in the last equation the result $\displaystyle\int_{-\infty}^{\infty}\left(\phi_{n+1}^{(1)}\right)^*\phi_{n+1}^{(1)}\,\mathrm{d}x = 1$ is used. Now, from the eigenvalue equation

$$H_1\phi_{n+1}^{(1)} = E_{n+1}^{(1)}\phi_{n+1}^{(1)} \tag{3.44}$$

one obtains

$$\int_{-\infty}^{\infty}\left(\phi_{n+1}^{(1)}\right)^*H_1\phi_{n+1}^{(1)}\,\mathrm{d}x = E_{n+1}^{(1)}\int_{-\infty}^{\infty}\left(\phi_{n+1}^{(1)}\right)^*\phi_{n+1}^{(1)}\,\mathrm{d}x = E_{n+1}^{(1)}\,. \tag{3.45}$$

Then Eq. (3.43) gives $\alpha = \left(E_{n+1}^{(1)} - E_0^{(1)}\right)^{-1/2}$. Equation (3.42) expresses $\phi_n^{(2)}$ in terms of $\phi_{n+1}^{(1)}$. It is possible to express $\phi_{n+1}^{(1)}$ in terms of $\phi_n^{(2)}$. For this purpose considering $A^+\phi_n^{(2)}$ one has

$$\phi_{n+1}^{(1)} = \beta\left(A^+\phi_n^{(2)}\right), \tag{3.46}$$

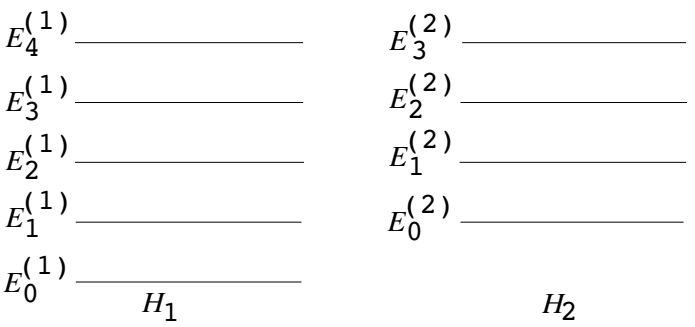

FIGURE 3.1
Schematic diagram of arrangement of eigenvalues of the supersymmetric H_1 and H_2.

where β is to be determined. Again the normalization condition of $\phi_{n+1}^{(1)}$ gives

$$1 = \int_{-\infty}^{\infty} \left(\phi_{n+1}^{(1)}\right)^* \phi_{n+1}^{(1)} \, \mathrm{d}x = \beta^2 \left(E_n^{(2)} - E_0^{(1)}\right) . \tag{3.47}$$

Then $\beta = \left(E_n^{(2)} - E_0^{(1)}\right)^{-1/2}$.

In summary, the relations between the eigenvalues and eigenfunctions of $H_1 = -\frac{1}{2}\frac{\mathrm{d}^2}{\mathrm{d}x^2} + V_1 = A^+A^- + \epsilon$ and $H_2 = -\frac{1}{2}\frac{\mathrm{d}^2}{\mathrm{d}x^2} + V_2 = A^-A^+ + \epsilon$ are

$$E_n^{(2)} = E_{n+1}^{(1)} , \tag{3.48}$$

$$\phi_n^{(2)} = \left(E_{n+1}^{(1)} - E_0^{(1)}\right)^{-1/2} A^- \phi_{n+1}^{(1)} , \tag{3.49}$$

$$\phi_{n+1}^{(1)} = \left(E_n^{(2)} - E_0^{(1)}\right)^{-1/2} A^+ \phi_n^{(2)} , \quad n = 0, 1, 2, \ldots . \tag{3.50}$$

Equation (3.48) implies that the potentials V_1 and V_2 have the same eigenvalue spectrum except that the ground state of V_1 is missing in V_2. The mapping of spectra of H_1 and H_2 is depicted in Fig. 3.1. Once the eigenfunctions of H_1 are known then the eigenfunctions of H_2 can be determined from Eq. (3.49). The above two are the connection between the supersymmetric potentials V_1 and V_2. The step-like ladder structure of the eigenvalue spectrum (Fig. 3.1) and the one-to-one relationships between the eigenfunctions in Eqs. (3.49)–(3.50) are the characteristic features of supersymmetric systems in one-dimension.

The hallmarks of the supersymmetric potentials V_1 and V_2 are:

1. If the eigenfunction $\phi_{n+1}^{(1)}$ of H_1 is normalized then $\phi_n^{(2)}$ of H_2 is also normalized.
2. The operator A^- converts an eigenfunction of H_1 into an eigenfunction of H_2 with the same energy.
3. A^+ converts an eigenfunction of H_2 into an eigenfunction of H_1 with the same energy. A^+ and A^- essentially connect the eigenstates of different energies of supersymmetric partner potentials.
4. The operator A^- destroys a node, that is, $\phi_{n+1}^{(1)}$ has $(n+1)$ nodes whereas $\phi_n^{(2)}$ has n nodes only.

5. The operator A^+ creates a node.
6. The eigenvalue of nth state of H_2 is determined by calculating the $(n+1)$th state of H_1.

Solved Problem 4:

For the Rosen–Morse potential $V_1 = A^2 - A\left(A - \beta/\sqrt{2}\right)\text{sech}^2\beta x$ the eigenvalues and ground state eigenfunction are $E_n^{(1)} = A^2 - \left(A - n\beta/\sqrt{2}\right)^2$ and $\phi_0^{(1)} \propto (\text{sech}\beta x)^{\sqrt{2}A/\beta}$. Obtain the supersymmetric partner V_2 of V_1.

We obtain

$$\begin{aligned} V_2 &= V_1 - \frac{\mathrm{d}^2}{\mathrm{d}x^2}\ln\phi_0^{(1)} \\ &= V_1 + \sqrt{2}\,A\beta\,\text{sech}^2\beta x \\ &= A^2 - A\left(A - \frac{3\beta}{\sqrt{2}}\right)\text{sech}^2\beta x \end{aligned} \tag{3.51}$$

and

$$E_n^{(2)} = E_{n+1}^{(1)} = A^2 - \left[A - \frac{(n+1)\beta}{\sqrt{2}}\right]^2 . \tag{3.52}$$

3.4 Hierarchy of Supersymmetric Hamiltonians

The procedure described in the previous section to find the Hamiltonian H_2 can be easily iterated to generate a Hamiltonian hierarchy with supersymmetric property [4,5]. That is, the mth member (H_m) of the hierarchy has the same eigenvalue spectrum as the first member H_1, except for missing the $(m-1)$ eigenvalues of H_1.

Suppose that H_1 (Eq. (3.1)) with $V_1(x)$ admits M bound states. Then as shown in sec. 3.2.3 the partner H_2 and V_2 are given by Eqs. (3.19) and (3.17), respectively. For convenience, let us rewrite them as

$$H_1 = -\frac{1}{2}\frac{\mathrm{d}^2}{\mathrm{d}x^2} + V_1 = A_1^+ A_1^- + E_0^{(1)}\,, \tag{3.53a}$$

$$A_1^\pm = \frac{1}{\sqrt{2}}\left(\pm\frac{\mathrm{d}}{\mathrm{d}x} + \frac{1}{\phi_0^{(1)}}\frac{\mathrm{d}}{\mathrm{d}x}\phi_0^{(1)}\right) \tag{3.53b}$$

and

$$H_2 = -\frac{1}{2}\frac{\mathrm{d}^2}{\mathrm{d}x^2} + V_2 = A_1^- A_1^+ + E_0^{(1)}\,, \tag{3.54a}$$

$$V_2 = V_1 + \left[A_1^-, A_1^+\right] = V_1 - \frac{\mathrm{d}^2}{\mathrm{d}x^2}\ln\phi_0^{(1)}\,. \tag{3.54b}$$

Also,

$$E_n^{(2)} = E_{n+1}^{(1)}\,, \quad n = 0, 1, 2, \ldots, m-2 \tag{3.54c}$$

$$\phi_n^{(2)} = \left(E_{n+1}^{(1)} - E_0^{(1)}\right)^{-1/2} A_1^-\phi_{n+1}^{(1)}\,. \tag{3.54d}$$

The Hamiltonian H_2 can be factorized in terms of its ground state $(\phi_0^{(2)}, E_0^{(2)})$ as

$$H_2 = -\frac{1}{2}\frac{\mathrm{d}^2}{\mathrm{d}x^2} + V_2 = A_2^+ A_2^- + E_0^{(2)}\,, \tag{3.55a}$$

$$A_2^\pm = \frac{1}{\sqrt{2}}\left(\pm\frac{\mathrm{d}}{\mathrm{d}x} + \frac{1}{\phi_0^{(2)}}\frac{\mathrm{d}}{\mathrm{d}x}\phi_0^{(2)}\right). \tag{3.55b}$$

The factorization of H_2 results in a new supersymmetric partner H_3

$$H_3 = A_2^- A_2^+ + E_0^{(2)}\,. \tag{3.56}$$

Repeating the above one can generate a hierarchy of Hamiltonians. The nth Hamiltonian takes the form

$$H_n = -\frac{1}{2}\frac{\mathrm{d}^2}{\mathrm{d}x^2} + V_n = A_n^+ A_n^- + E_0^{(n)} = A_{n-1}^- A_{n-1}^+ + E_0^{(n-1)}\,, \tag{3.57a}$$

where

$$A_n^\pm = \frac{1}{\sqrt{2}}\left(\pm\frac{\mathrm{d}}{\mathrm{d}x} + \frac{1}{\phi_0^{(n)}}\frac{\mathrm{d}}{\mathrm{d}x}\phi_0^{(n)}\right) \tag{3.57b}$$

and

$$\begin{aligned} V_n &= V_{n-1} - \frac{\mathrm{d}^2}{\mathrm{d}x^2}\ln\phi_0^{(n-1)} \\ &= V_1 - \frac{\mathrm{d}^2}{\mathrm{d}x^2}\ln\left(\phi_0^{(1)}\phi_0^{(2)}\ldots\phi_0^{(n-1)}\right), \quad n = 2,3,\ldots,m. \end{aligned} \tag{3.57c}$$

The eigenvalues obey the condition

$$E_m^{(n)} = E_{m+1}^{(n-1)} = \ldots = E_{n+m-1}^{(1)}\,, \quad \begin{matrix} m=0,1,\ldots,m-n, \\ n=2,3,\ldots,m. \end{matrix} \tag{3.58}$$

The eigenfunctions are given by

$$\begin{aligned} \phi_m^{(n)} &= \left\{\prod_{i=1}^{n-1}\left(E_{n+m-1}^{(1)} - E_{n-i}^{(1)}\right)A_{n-i}^-\right\} \\ &\quad \times \left(E_{n+m-1}^{(1)} - E_0^{(1)}\right)^{-1/2}\phi_{n+m-1}^{(1)}. \end{aligned} \tag{3.59}$$

The above equations state that the excited states of H_1 can be calculated from the ground states of the hierarchy of H_n. Figure 3.2 depicts the eigenvalue spectra of H_1, H_2 and H_3.

3.5 Applications

Let us construct all possible supersymmetric partners of a few interesting quantum mechanical systems.

3.5.1 Linear Harmonic Oscillator

The Hamiltonian, the potential and the eigenstates of the linear harmonic oscillator are given by (after setting $\hbar = 1$ and $m = 1$)

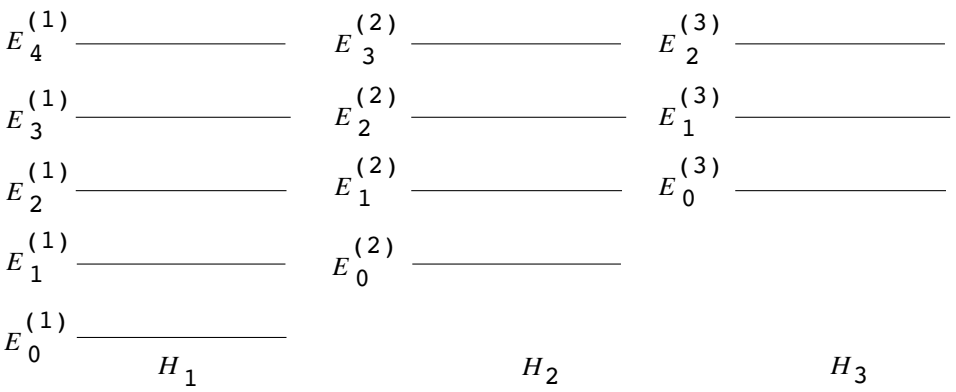

FIGURE 3.2
The alignment of eigenvalue spectra of the supersymmetric Hamiltonians H_1, H_2 and H_3.

$$H_1 = -\frac{1}{2}\frac{\mathrm{d}^2}{\mathrm{d}x^2} + V_1(x)\,, \quad V_1(x) = \frac{1}{2}\omega^2 x^2 \tag{3.60a}$$

$$E_m^{(1)} = \left(m + \frac{1}{2}\right)\omega\,, \quad m = 0, 1, 2, \ldots \tag{3.60b}$$

$$\phi_0^{(1)} = \left(\frac{\omega}{\sqrt{\pi}}\right)^{1/2} \mathrm{e}^{-\omega x^2/2}, \tag{3.60c}$$

$$\phi_1^{(1)} = 2\left(\frac{\omega}{2\sqrt{\pi}}\right)^{1/2} \omega x \mathrm{e}^{-\omega x^2/2}, \tag{3.60d}$$

$$\phi_2^{(1)} = 2\left(\frac{\omega}{8\sqrt{\pi}}\right)^{1/2} (2\omega x^2 - 1)\mathrm{e}^{-\omega x^2/2}, \ldots\,. \tag{3.60e}$$

The operators $A_1^{\pm}$ are obtained as

$$A_1^{\pm} = \frac{1}{\sqrt{2}}\left(\pm\frac{\mathrm{d}}{\mathrm{d}x} + \frac{1}{\phi_0^{(1)}}\frac{\mathrm{d}}{\mathrm{d}x}\phi_0^{(1)}\right) = \frac{1}{\sqrt{2}}\left(\pm\frac{\mathrm{d}}{\mathrm{d}x} - \omega x\right)\,. \tag{3.60f}$$

3.5.1.1 First Supersymmetric Partner H_2

The supersymmetric partner H_2, V_2, $E^{(2)}$ and $\phi^{(2)}$ can be obtained from Eqs. (3.57)–(3.59) with $n = 2$. The potential V_2 is determined as

$$V_2(x) = V_1 - \frac{\mathrm{d}^2}{\mathrm{d}x^2}\ln \mathrm{e}^{-\omega x^2/2} = V_1 + \omega\,. \tag{3.61a}$$

The Hamiltonian H_2 is then given by

$$H_2 = -\frac{1}{2}\frac{\mathrm{d}^2}{\mathrm{d}x^2} + V_1 + \omega\,. \tag{3.61b}$$

Its eigenvalues are

$$E_n^{(2)} = E_{n+1}^{(1)} = \left(n + \frac{3}{2}\right)\omega\,, \quad n = 0, 1, 2, \ldots\,. \tag{3.61c}$$

The eigenfunctions are

$$\begin{aligned}\phi_n^{(2)} &= \frac{1}{\sqrt{2}}\left[\left(n+\frac{3}{2}\right)\omega-\frac{1}{2}\omega\right]^{-1/2}\left(-\frac{\mathrm{d}}{\mathrm{d}x}-\omega x\right)\phi_{n+1}^{(1)} \\ &= -\frac{1}{\sqrt{2}}\left[(n+1)\omega\right]^{-1/2}\left(\frac{\mathrm{d}}{\mathrm{d}x}+\omega x\right)\phi_{n+1}^{(1)}\,. \end{aligned} \tag{3.61d}$$

When $n=0$ (ground state)

$$\phi_0^{(2)} = -\frac{2}{\sqrt{2\omega}}\left(\frac{\mathrm{d}}{\mathrm{d}x}+\omega x\right)\left(\frac{\omega}{2\sqrt{\pi}}\right)^{1/2}\omega x\mathrm{e}^{-\omega x^2/2} = \frac{\mathrm{e}^{-\omega x^2/2}}{\pi^{1/4}}\,. \tag{3.61e}$$

The operators $A_2^{\pm}$ are found to be

$$A_2^{\pm} = \frac{1}{\sqrt{2}}\left(\pm\frac{\mathrm{d}}{\mathrm{d}x}+\frac{1}{\phi_0^{(2)}}\frac{\mathrm{d}}{\mathrm{d}x}\phi_0^{(2)}\right) = \frac{1}{\sqrt{2}}\left(\pm\frac{\mathrm{d}}{\mathrm{d}x}-\omega x\right)\,. \tag{3.61f}$$

3.5.1.2 Second Supersymmetric Partner H_3

The potential V_3 is obtained as

$$V_3 = V_2 - \frac{\mathrm{d}^2}{\mathrm{d}x^2}\ln\phi_0^{(2)} = V_2+\omega = V_1+2\omega\,. \tag{3.62a}$$

Then

$$H_3 = -\frac{1}{2}\frac{\mathrm{d}^2}{\mathrm{d}x^2}+V_1+2\omega\,, \tag{3.62b}$$

$$E_n^{(3)} = \left(n+\frac{5}{2}\right)\omega\,,\quad n=0,1,2,\ldots \tag{3.62c}$$

$$A_3^{\pm} = \frac{1}{\sqrt{2}}\left(\pm\frac{\mathrm{d}}{\mathrm{d}x}-\omega x\right)\,. \tag{3.62d}$$

$\phi_n^{(3)}$ can be obtained from Eq. (3.59).

3.5.1.3 $(N-1)$th Supersymmetric Partner

By inspecting the Eqs. (3.60)–(3.62) one can write

$$V_N = V_1+(N-1)\omega\,, \tag{3.63a}$$

$$H_N = -\frac{1}{2}\frac{\mathrm{d}^2}{\mathrm{d}x^2}+V_N\,, \tag{3.63b}$$

$$E_n^{(N)} = \left(n+N-\frac{1}{2}\right)\omega\,,\quad n=0,1,\ldots \tag{3.63c}$$

$$A_N^{\pm} = \frac{1}{\sqrt{2}}\left(\pm\frac{\mathrm{d}}{\mathrm{d}x}-\omega x\right)\,,\quad N=2,3,\ldots\,. \tag{3.63d}$$

The Hamiltonian hierarchy shifts the potential up in units of $\hbar\omega$. The nice result is that the linear harmonic oscillator potential $V_1=\omega x^2/2$ and the potentials $\omega x^2/2+(N-1)\omega$ where $N=2,3,\ldots$ share the same energy levels except for the lower states.

3.5.2 Linear Harmonic Oscillator in an Electric Field

Consider the linear harmonic oscillator system subjected to an external electric field. The Hamiltonian and the potential of the system are

$$H_1 = -\frac{1}{2}\frac{\mathrm{d}^2}{\mathrm{d}x^2} + \frac{1}{2}\omega^2 x^2 - \alpha x\,, \quad \alpha = eE \tag{3.64a}$$

$$V_1 = \frac{1}{2}\omega^2 x^2 - \alpha x\,. \tag{3.64b}$$

This system is an exactly solvable system. Its eigenvalues and eigenfunctions are given by

$$E_n^{(1)} = \left(n + \frac{1}{2}\right)\omega - \frac{1}{2}\alpha\omega^2\,, \tag{3.64c}$$

$$\phi_n^{(1)} = \left(\frac{\omega}{\pi}\right)^{1/4}\left(\frac{1}{2^n n!}\right)^{1/2} \mathrm{e}^{-\omega(x-\alpha)^2/2} H_n\left(\frac{\omega}{x-\alpha}\right)\,, \tag{3.64d}$$

where H_n's are Hermite polynomials. The ground state eigenfunction is

$$\phi_0^{(1)} = \left(\frac{\omega}{\pi}\right)^{1/4} \mathrm{e}^{-\omega(x-\alpha)^2/2}\,. \tag{3.64e}$$

The potential V_1 and $\phi_0^{(1)}$ lead to the following result:

$$V_N = \frac{1}{2}\omega^2(x-\alpha)^2 - \frac{1}{2}\omega^2\alpha + (N-1)\omega\,, \quad N = 2, 3, \ldots \tag{3.65a}$$

$$E_n^{(N)} = \left(n + N - \frac{1}{2}\right)\omega - \frac{1}{2}\omega^2\alpha\,, \tag{3.65b}$$

$$A_N^{\pm} = \frac{1}{\sqrt{2}}\left(\pm\frac{\mathrm{d}}{\mathrm{d}x} - \omega(x-\alpha)\right)\,. \tag{3.65c}$$

3.5.3 Linear Harmonic Oscillator with a Shifted Potential

Consider the Hamiltonian

$$H_1 = -\frac{1}{2}\frac{\mathrm{d}^2}{\mathrm{d}x^2} + V_1(x)\,, \quad V_1(x) = \frac{1}{2}\omega^2\left(x - \frac{\sqrt{2}\,b}{\omega}\right)^2\,. \tag{3.66a}$$

It is also an exactly solvable system. Its eigenvalues and eigenfunctions are

$$E_n^{(1)} = n\omega\,, \tag{3.66b}$$

$$\phi_n^{(1)} = \left(\frac{\omega}{2^n n!\pi}\right)^{1/2} \mathrm{e}^{-\omega(x-\sqrt{2}\,b/\omega)^2/2} H_n\left(\omega x - \sqrt{2}\,b\right)\,. \tag{3.66c}$$

The ground state eigenfunction is $\phi_0^{(1)} = \left(\frac{\omega}{\pi}\right)^{1/2} \mathrm{e}^{-\omega(x-\sqrt{2}\,b/\omega)^2/2}$. We obtain

$$V_N = V_1 + \frac{(2N-3)\omega}{2}\,, \quad E_n^{(N)} = (n+N-1)\omega\,, \tag{3.67a}$$

$$A_N^{\pm} = \frac{1}{\sqrt{2}}\left(\pm\frac{\mathrm{d}}{\mathrm{d}x} - \omega x + \sqrt{2}\,b\right)\,. \tag{3.67b}$$

3.5.4 Particle in a Box

As another system, consider a particle in a box governed by the potential

$$V_1(x) = \begin{cases} 0, & |x| < a \\ \infty, & |x| > a\,. \end{cases} \tag{3.68}$$

It has two types of exactly solved eigenstates and are represented by $\cos k_n x$ and $\sin k_n x$. For the eigenfunctions of the form of cosine function we have

$$E_n^{(1)} = \frac{\pi^2(n+1)^2}{8a^2}\,, \quad \phi_n^{(1)} \sim \cos\frac{\pi(2n+1)x}{2a}\,, \tag{3.69a}$$

$$A_1^{\pm} = \frac{1}{\sqrt{2}}\left(\pm\frac{\mathrm{d}}{\mathrm{d}x} - \frac{\pi}{2a}\tan\frac{\pi x}{2a}\right)\,. \tag{3.69b}$$

It is easy to obtain [4,5]

$$V_N(x) = V_1(x) + \frac{\pi^2}{8a^2}N(N-1)\sec^2\frac{\pi x}{2a}\,, \tag{3.70a}$$

$$E_n^{(N)} = \frac{\pi^2(N+n)^2}{8a^2}\,, \quad N = 1, 2, \ldots, \;\; n = 0, 1, \ldots\,. \tag{3.70b}$$

Thus, the box potential V_1 given by Eq. (3.68) leads to a sequence of $\sec^2(\pi x/(2a))$ potentials with increasing strength.

3.6 Generation of Complex Potentials with Real Eigenvalues

Certain complex potentials with real eigenvalues or combination of real and complex eigenvalues are identified [10–16]. A method for constructing complex potentials with real eigenvalues has been developed based on the connection between a second-order equation of the Schrödinger type and the so-called nonlinear Ermakov equation [16]. In this approach the solutions of the Ermakov equation is used to set-up complex potentials which share their eigenvalue spectrum with a given solvable real-valued potential. We present this approach in this section.

3.6.1 Complex Wave Function

Consider the Hermitian Hamiltonian

$$H = -\frac{1}{2}\frac{\mathrm{d}^2}{\mathrm{d}x^2} + V(x). \tag{3.71}$$

With $\psi(x) = u(x)$ it is desired to solve the eigenvalue equation

$$u'' + 2(\epsilon - V(x))u = 0, \tag{3.72}$$

where u is complex and not necessarily normalizable.

Assume the solution of (3.72) as

$$u(x) = u_0 \mathrm{e}^{\int^x \beta(y)\mathrm{d}y}, \tag{3.73}$$

where u_0 is an arbitrary complex constant and $\beta(x)$ is a complex function to be determined. Substitution of (3.73) in (3.72) results in

$$\beta' + \beta^2 + 2(\epsilon - V) = 0. \tag{3.74}$$

Now, factorize the Hamiltonian (3.71) by considering

$$A^{\pm} = \frac{1}{\sqrt{2}} \left(\pm \frac{\mathrm{d}}{\mathrm{d}x} + \beta \right). \tag{3.75}$$

In terms of $A^{\pm}$

$$H = A^+ A^- + \epsilon = \frac{1}{2} \left(-\frac{\mathrm{d}^2}{\mathrm{d}x^2} + \beta' + \beta^2 \right) + \epsilon = -\frac{1}{2} \frac{\mathrm{d}^2}{\mathrm{d}x^2} + V \tag{3.76}$$

and

$$\begin{aligned} \widetilde{H} &= A^- A^+ + \epsilon \\ &= -\frac{1}{2} \frac{\mathrm{d}^2}{\mathrm{d}x^2} + \frac{1}{2} \left(-\beta' + \beta^2 \right) + \epsilon \\ &= -\frac{1}{2} \frac{\mathrm{d}^2}{\mathrm{d}x^2} + V - \beta' \\ &= -\frac{1}{2} \frac{\mathrm{d}^2}{\mathrm{d}x^2} + \widetilde{V}, \quad \widetilde{V} = V(x) - \beta'(x) \end{aligned} \tag{3.77}$$

with β being the solution of Eq. (3.74).

If $\beta = \beta_{\mathrm{R}} + \mathrm{i}\beta_{\mathrm{I}}$ then

$$u(x) = \phi_0 \mathrm{e}^{\int^x \beta_{\mathrm{R}} \mathrm{d}y} \mathrm{e}^{\mathrm{i} \int^x \beta_{\mathrm{I}} \mathrm{d}y} = \phi(x) \mathrm{e}^{\mathrm{i}\nu(x)}, \tag{3.78a}$$

where

$$\phi(x) = \phi_0 \mathrm{e}^{\int^x \beta_{\mathrm{R}}(y) \mathrm{d}y}, \quad \nu(x) = \int^x \beta_{\mathrm{I}}(y) \mathrm{d}y + \nu_0 \tag{3.78b}$$

and ϕ_0 and ν_0 are integration constants. From Eq. (3.74) the equations for β_{R} and β_{I} are obtained as

$$\beta_{\mathrm{R}}' + \beta_{\mathrm{R}}^2 - \beta_{\mathrm{I}}^2 + 2(\epsilon - V) = 0, \tag{3.79a}$$

$$\beta_{\mathrm{I}}' + 2\beta_{\mathrm{R}}\beta_{\mathrm{I}} = 0. \tag{3.79b}$$

Equation (3.79b) can be rewritten as

$$\beta_{\mathrm{R}} = -\frac{1}{2} \frac{\mathrm{d}}{\mathrm{d}x} \ln \beta_{\mathrm{I}}. \tag{3.80}$$

Defining $\beta_{\mathrm{I}} = \lambda / \alpha^2(x)$ with λ being an integration constant and substituting it in Eq. (3.80), we obtain

$$\beta_{\mathrm{R}} = \frac{\alpha'}{\alpha} = \frac{\mathrm{d}}{\mathrm{d}x} \ln \alpha(x). \tag{3.81}$$

What is the requirement for β_{R} and β_{I} to be real?

Now,

$$\beta = \beta_{\mathrm{R}} + \mathrm{i}\beta_{\mathrm{I}} = (\ln \alpha(x))' + \frac{\mathrm{i}\lambda}{\alpha^2(x)}. \tag{3.82}$$

Next, find an equation for α. Use of the above $\beta_{\rm R}$and $\beta_{\rm I}$ in Eq. (3.79a) gives

$$\alpha'' - M\alpha - \frac{\lambda_0}{\alpha^3} = 0, \quad M = 2(V-\epsilon), \;\; \lambda_0 = \lambda^2. \tag{3.83}$$

Equation (3.83) is the *Ermakov equation* [16]. When $\lambda = 0$ Eq. (3.83) becomes the Schrödinger equation.

In terms of α the function $u(x)$ is given by

$$\begin{aligned} u(x) &= \phi_0 \mathrm{e}^{\int^x \frac{\mathrm{d}}{\mathrm{d}y} \ln\alpha(y)\mathrm{d}y} \mathrm{e}^{\mathrm{i}\int^x (\lambda/\alpha^2)\mathrm{d}y} \mathrm{e}^{\mathrm{i}\nu_0} \\ &= \phi_0 \mathrm{e}^{\mathrm{i}\nu_0} \mathrm{e}^{\ln\alpha(x)} \mathrm{e}^{\mathrm{i}\lambda\int^x (1/\alpha^2)\mathrm{d}y} \\ &= \phi_0 \mathrm{e}^{\mathrm{i}\nu_0} \alpha(x) \mathrm{e}^{\mathrm{i}\lambda\int^x (1/\alpha^2)\mathrm{d}y} \\ &= \alpha(x) \mathrm{e}^{\pm\mathrm{i}\sqrt{\lambda_0}\int^x (1/\alpha^2(y))\mathrm{d}y}, \end{aligned} \tag{3.84}$$

where $\phi_0 \mathrm{e}^{\mathrm{i}\nu_0}$ is set to unity and $\lambda = \pm\sqrt{\lambda_0}$ is used.

3.6.2 New Real and Complex Superpotentials

Consider Eq. (3.82) with real λ and $\alpha(x)$ is the solution of Eq. (3.83). We have the following superpotentials.

Case 1: $\lambda = 0$**.**

When $\lambda = 0$ Eq. (3.82) gives $\beta = (\ln\alpha)'$, a conventional real-valued superpotential.

Case 2: $\lambda_\pm = \pm\mathrm{i}\sqrt{|\lambda_0|}$**,** $\lambda_0 < 0$**.**

$\lambda_\pm$ are pure imaginary for $\lambda_0 < 0$ and

$$\beta_\pm = (\ln\alpha(x))' \pm \frac{\sqrt{|\lambda_0|}}{\alpha^2}. \tag{3.85}$$

Case 3: $\lambda_\pm = \pm\sqrt{\lambda_0}$**,** $\lambda_0 > 0$**.**

In this case

$$\beta_\pm = (\ln\alpha(x))' \pm \mathrm{i}\frac{\sqrt{\lambda_0}}{\alpha^2}. \tag{3.86}$$

3.6.3 New Complex Potentials and Their Eigenspectra

With $A^\pm$ given by Eq. (3.75) we have $H = A^+A^- + \epsilon = -\frac{1}{2}\frac{\mathrm{d}^2}{\mathrm{d}x^2} + V$ and $\widetilde{H} = A^-A^+ + \epsilon = -\frac{1}{2}\frac{\mathrm{d}^2}{\mathrm{d}x^2} + \widetilde{V}$ where the new complex potential is given by (refer Eq. (3.77))

$$\begin{aligned} \widetilde{V} &= V(x) - \beta'(x) \\ &= V(x) - \frac{\mathrm{d}^2}{\mathrm{d}x^2}\ln\alpha(x) - \frac{\mathrm{d}}{\mathrm{d}x}\frac{\mathrm{i}\lambda}{\alpha^2} \\ &= V(x) - \frac{\mathrm{d}^2}{\mathrm{d}x^2}\ln\alpha(x) + \mathrm{i}2\lambda\frac{\alpha'(x)}{\alpha^3(x)}. \end{aligned} \tag{3.87}$$

Using Eq. (3.74) we can also write

$$\widetilde{V} = V(x) - \beta'(x) = \frac{1}{2}\beta' + \frac{1}{2}\beta^2 + \epsilon. \tag{3.88}$$

We note that

$$\widetilde{H}^{\dagger} = \left(-\frac{1}{2}\frac{\mathrm{d}^2}{\mathrm{d}x^2} + \widetilde{V}\right)^{\dagger} = -\frac{1}{2}\frac{\mathrm{d}^2}{\mathrm{d}x^2} + \widetilde{V}^* \neq \widetilde{H}. \tag{3.89}$$

That is, $\widetilde{H}$ is not a self-adjoint operator. On the other hand, we notice that

$$\widetilde{H}A^- = (A^-A^+ + \epsilon)A^- = A^-(A^+A^- + \epsilon) = A^-H, \tag{3.90a}$$

and

$$HA^+ = A^+\widetilde{H}. \tag{3.90b}$$

If ψ_E in $H\psi_E = E\psi_E$ is normalized then for $\epsilon \neq E$ the $\widetilde{\psi}_E$ in $\widetilde{H}\widetilde{\psi}_E = E\widetilde{\psi}_E$ is proportional to $A^-\psi_E$ and $\widetilde{\psi}_E$ can be normalized for appropriate choice of u-functions. The eigenfunction $\widetilde{\psi}_\epsilon = C_l u^{-1}$ of $\widetilde{H}$ with C_l an arbitrary constant and satisfying $A^+\widetilde{\psi}_\epsilon = 0$ is not considered by the transformation Eqs. (3.90). Considering Eq. (3.84) we write $|\widetilde{\psi}_\epsilon|^2 = |C_l|^2/\alpha^2$. If $\widetilde{\psi}_\epsilon$ is normalizable then it has to be included in the set $\left\{\widetilde{\psi}_{\mathrm{E}}\right\}$. Then $\widetilde{H}$ is almost isospectral to H.

3.6.4 Solutions of Ermakov Equation

If the integral of the equation $u'' - Mu = 0$ is known then we can determine the integral of Eq. (3.83) and vice-versa. Further, the complete solution of $u'' - Mu = 0$ can be obtained once a particular solution of Eq. (3.83) is known.

The solution of the Ermakov Eq. (3.83) is

$$\alpha(x) = z(x)\left[\frac{\lambda_0}{C_1} + C_1\left(\int^x z^{-2}(y)\mathrm{d}y + \frac{C_0}{C_1}\right)^2\right]^{1/2}, \tag{3.91}$$

where C_0 and C_1 are integration constants and $z(x)$ is the solution of the homogeneous equation $u'' - Mu = 0$. The second solution of Eq. (3.83) is

$$\nu(x) = z(x)q(x), \quad q(x) = W_0\int^x z^{-2}(y)\mathrm{d}y. \tag{3.92}$$

$z(x)$ and $\nu(x)$ are linearly independent if the Wronskian $W(z,\nu) = z\nu' - z'\nu$ is a constant. When $\lambda_0 = 0$ the function $\alpha(x)$ given by Eq. (3.91) becomes the general solution of $u'' - Mu = 0$. In terms of z and ν

$$\begin{aligned}\alpha(x) &= \left[\frac{C_1}{W_0^2}\nu^2 + 2\frac{C_0}{W_0}\nu z + \left(\frac{\lambda_0 + C_0^2}{C_1}\right)z^2\right]^{1/2} \\ &= \left[a\nu^2 + b\nu z + cz^2\right]^{1/2}.\end{aligned} \tag{3.93}$$

For

$$a = C_1/W_0^2, \quad c = \left(\lambda_0 + C_0^2\right)/C_1 \tag{3.94}$$

we have

$$W(z,\nu) = W_0, \quad b^2 - 4ac = -\frac{4\lambda_0}{W_0^2}, \quad b = \pm\frac{2C_0}{W_0}. \tag{3.95}$$

3.6.5 Examples

Let us construct supersymmetric partner complex potentials with energies of free particle and linear harmonic oscillator.

1. Free Particle

For a free particle $V(x) = 0$, $z = \mathrm{e}^{\mathrm{i}kx}$, $\nu = \mathrm{e}^{-\mathrm{i}kx}$, $k^2 = \epsilon \geq 0$ and $W(z, \nu) = -2\mathrm{i}k$. Considering Eqs. (3.94) and (3.95) the function $\alpha(x)$ given by Eq. (3.93) becomes

$$\alpha(x) = \left[a\mathrm{e}^{-2\mathrm{i}kx} + c\mathrm{e}^{2\mathrm{i}kx} + 2\sqrt{ac + \frac{\lambda^2}{4k^2}} \right]^{1/2} . \tag{3.96}$$

For $a = c = 1/2$

$$\alpha(x) = [\cos 2kx + \gamma]^{1/2} , \quad \gamma = \sqrt{1 + \frac{\lambda^2}{k^2}} . \tag{3.97}$$

Then from Eq. (3.82)

$$\beta = \frac{-k \sin 2kx + \mathrm{i}\lambda}{\cos 2kx + \gamma}, \quad \widetilde{V} = \frac{2k^2(1 + \gamma \cos 2kx) - \mathrm{i}2\lambda k \sin 2kx}{(\cos 2kx + \gamma)^2} . \tag{3.98}$$

Further, the missing state is $\widetilde{\psi}_\epsilon = C_\epsilon / u = C_\epsilon / \alpha(x)$ and

$$P_\epsilon(x; \lambda) = |\widetilde{\psi}_\epsilon|^2 = \frac{|C_\epsilon|^2}{\cos 2kx + \gamma} . \tag{3.99}$$

We notice that for real values of k and λ the integral $\int_{-\infty}^{\infty} P_\epsilon(x; \lambda) \mathrm{d}x$ is not finite. We obtained complex periodic potentials $\widetilde{V}$ and they do not have bound states. For $a = -c = \mathrm{i}/2$ we have $\alpha(x) = (\sin 2kx + \gamma)^{1/2}$.

2. Linear Harmonic Oscillator

For the linear harmonic oscillator with $V(x) = x^2$ we can use [16]

$$z = {}_1F_1 \left(\frac{1 - \epsilon}{4}, \frac{1}{2}; x^2 \right) \mathrm{e}^{-x^2/2}, \quad \nu = {}_1F_1 \left(\frac{3 - \epsilon}{4}, \frac{3}{2}; x^2 \right) x\mathrm{e}^{-x^2/2}, \tag{3.100}$$

where ${}_1F_1(a, c; z)$ denotes the confluent hypergeometric function and $W(z, \nu) = -1/2$. For the choice $\epsilon = -1$

$$z = \mathrm{e}^{x^2/2}, \quad \nu = \frac{\sqrt{\pi}}{2} \mathrm{e}^{x^2/2} \mathrm{Erf}(x), \tag{3.101}$$

where $\mathrm{Erf}(x) = \dfrac{2}{\sqrt{\pi}} \displaystyle\int_0^x \mathrm{e}^{-t^2} \mathrm{d}t$ is the error function and $\mathrm{Erf}'(x) = \dfrac{2}{\sqrt{\pi}} \mathrm{e}^{-x^2}$. Then

$$\alpha(x) = \mathrm{e}^{x^2/2} \left[a\mathrm{Erf}^2(x) + b\mathrm{Erf}(x) + c \right]^{1/2} . \tag{3.102}$$

Assume that a, b, $c > 0$. As $\mathrm{Erf}(x) \in [-1, 1]$ the function $\alpha(x)$ is real and has no zeros for $c > b^2/(4a)$. $\widetilde{\psi}_\epsilon$ is therefore normalizable. Next,

$$\beta = \frac{\alpha'}{\alpha} + \mathrm{i}\frac{\lambda}{\alpha^2} = 2x + \frac{1}{\sqrt{\pi}\alpha^2} \left[b + 2a\mathrm{Erf}(x) + \mathrm{i}\lambda\sqrt{\pi} \right] , \tag{3.103}$$

$$\beta' = 2 + \frac{\mathrm{d}}{\mathrm{d}x} \left[\frac{b + 2a\mathrm{Erf}(x) + \mathrm{i}\lambda\sqrt{\pi}}{\sqrt{\pi}\,\alpha^2} \right] \tag{3.104}$$

and

$$\widetilde{V} = V - \beta' = x^2 - 2 - \frac{\mathrm{d}}{\mathrm{d}x}\left[\frac{b + 2a\mathrm{Erf}(x) + \mathrm{i}\lambda\sqrt{\pi}}{\sqrt{\pi}\,\alpha^2}\right] \tag{3.105}$$

Any set of nonnegative parameters $\{a, b, c > b^2/(4a)\}$ gives supersymmetric partner potentials $\widetilde{V}$ of the harmonic oscillator potential $V(x) = x^2$.

3.7 Concluding Remarks

In this chapter, we have demonstrated that if one of the partner systems (the Hamiltonians) can be solved completely, by calculating the energy levels and the eigenfunctions, then the supersymmetry formalism enables us to solve the partner problem. The supersymmetry quantum mechanics has been generalized to generate supersymmetric partners from the superpotential defined by higher excited eigenstates. For details see ref. [17]. Supersymmetry of certain periodic potentials has also been studied [18]. The method has been applied to position-dependent mass quantum systems [19–23] and bilayer graphene [24]. We note that for the three linear harmonic oscillators considered in sec. 3.5 their supersymmetric potentials are independent of x (which is not the case for a particle in a box). Therefore, the shape of V_N, $N > 1$ are the same as that of V_1. They differ only in the parameters that appear in them. Such a pair of supersymmetric potentials are called *shape invariant potentials* [7,8]. For a pair of supersymmetric potentials V_1 and V_2 to be shape invariant they must satisfy the requirement $V_2(x; a_0) = V_1(x; a_1) + R(a_1)$, where a_0 is a set of parameters, a_1 is a function of a_0, that is $a_1 = f(a_0)$, and $R(a_1)$ is independent of x. For the linear harmonic oscillator $R(a_1) = \omega$, $a_0 = \omega$ and $a_1 = \omega$. Algebraic nature [25,26] and generation [27–31] of shape invariant potentials, inter-relations between additive shape invariant superpotentials [32] and exactly solvable new class of potentials with finite discrete energies [33] have been reported.

For a wide class of shape invariant Hamiltonians the interpolation of the two supersymmetric partner Hamiltonians $H = A^+A^-$ and $H_\mathrm{s} = (1 - s)A^+A^- + sA^-A^+$, $0 \le s \le 1$, also retains shape invariance [34]. The Hamiltonian H_s has the same form as the original Hamiltonian with shifted coupling constants and a shifted ground state energy. It has been shown that the potential $V_1 = x^2 + 8(2x^2 - 1)/(2x^2 + 1)^2$ is a supersymmetric partner of the linear harmonic oscillator $V_2 = x^2 + 5$ [35]. Eigenpairs of a nonpolynomial oscillator is obtained by supersymmetric formalism [35]. The eigenvalues for oscillators with quadratic and sextic anharmonicities have been calculated by applying supersymmetry formalism [36]. Supersymmetric partners of the trigonometric Pöschl–Teller potentials have also been obtained [37]. In [24,38] supersymmetric quantum mechanics is employed to solve the effective Hamiltonian for electrons in bilayer graphene.

3.8 Bibliography

[1] H. Nicolai, *J. Phys. A: Math. Gen.* 9:1497, 1976.

[2] M. Bernstein and L.S. Brown, *Phys. Rev. Lett.* 52:1933, 1984.

[3] A.A. Andrianov, N.V. Borisov and M.V. Ioffe, *Phys. Lett. A* 105:19, 1984.

[4] C.V. Sukumar, *J. Phys. A* 18:L57, 1985.

[5] C.V. Sukumar, *J. Phys. A* 18:2917, 1985.

[6] R.W. Haymaker and A.R.P. Rau, *Am. J. Phys.* 54:928, 1986.

[7] R. Dutt, A. Khare and U.P. Sukhatme, *Am. J. Phys.* 56:163, 1988.

[8] A. Khare and U. Sukhatme, *Phys. News* 22:35, 1991.

[9] A. Valance, T.J. Morgan and H. Bergeron, *Am. J. Phys.* 58:487, 1990.

[10] D. Baye, G. Levai and J.M. Sparenberg, *Nucl. Phys. A* 599:435, 1996.

[11] F. Cannata, G. Junker and J. Trost, *Phys. Lett. A* 246:219, 1998.

[12] A.A. Andrianov, M.V. Ioffe, F. Cannata and J.P. Dedonder, *Int. J. Mod. Phys. A* 14:2675, 1999.

[13] B. Bagchi, S. Mallik and C. Quesne, *Int. J. Mod. Phys. A* 16:2859, 2001.

[14] D.J. Fernandez, R. Munoz and A. Ramos, *Phys. Lett. A* 308:11, 2003.

[15] N. Fernandez-Garcia and O. Rosas-Ortiz, *J. Phys. Conf. Ser.* 128:012044, 2008.

[16] O. Rosas-Ortiz, O. Castanos and D. Schuch, *J. Phys. A: Math. Theor.* 48:445302, 2015.

[17] W. Kwong and J.L Rosner, *Prog. Theor. Phys.* 86:366, 1986.

[18] A. Khare and U. Sukhatme, *J. Phys. A* 37:10037, 2004.

[19] A.R. Plastino, A. Rigo, M. Casas, F. Garcias and A. Plastino, *Phys. Rev. A* 60:4398, 1999.

[20] B. Gonul, O. Ozer, B. Gonul and F. Uzgun, *Mod. Phys. Lett. A* 17:2453, 2002.

[21] C. Quesne, *Ann. Phys.* 321:1221, 2006.

[22] A. Ganguly and L.M. Nieto, *J. Phys. A* 40:7265, 2007.

[23] T. Tanaka, *J. Phys. A* 39:219, 2006.

[24] D.J. Fernandez, J.D. Garcia and D.O-Campa, *J. Phys. A: Math. Theor.* 54:245302, 2021.

[25] A.B. Balantekin, *Phys. Rev. A* 57:4188, 1998.

[26] A.B. Balantekin, M.A. Candido Ribeiro and A.N.F. Aleixo, *J. Phys. A* 32:2785, 1999.

[27] J. Bougie, A. Gangopadhyaya and J.V. Mallow, *Phys. Rev. Lett.* 105:210402, 2010.

[28] J.F. Carinena and A. Ramos, *Rev. Math. Phys.* 12:1279, 2000.

[29] A. Gangopadhyaya and J.V. Mallow, *Int. J. Mod. Phys. A* 23:4959, 2008.

[30] S. Odake and R. Sasaki, *Phys. Lett. B* 682:130, 2009.

[31] A. Ramos, *J. Phys. A: Math. Theor.* 44:342001, 2011.

[32] J.V. Mallow, A. Gangopadhyaya, J. Bougie and C. Rasinariu, *Phys. Lett. A* 384:126129, 2020.

[33] J. Benbourenane and H. Eleuch, *Results in Phys.* 17:103034, 2020.

[34] S. Odake, Y. Pehlivan and R. Sasaki, *J. Phys. A* 40:11973, 2007.

[35] J.M. Fellows and R.A. Smith, *J. Phys. A* 42:335303, 2009.

[36] B. Chakrabarti, *J. Phys. A* 41:405301, 2008.

[37] A. Contreras-Astorga and D.J. Fernandez, *J. Phys. A* 41:475303, 2008.

[38] Y. Concha, A. Huet, A. Raya and D. Valenzuela, *Mat. Res. Express* 5:065607, 2018.

3.9 Exercises

3.1 What is the condition for two potentials V_1 and V_2 to be supersymmetric partners?

3.2 Obtain the supersymmetric partner Hamiltonian of $H_1 = A^+A^-$, where $A^\pm = (\pm ip + v(x))/\sqrt{2}$ [9]. Here p is the momentum operator and $v(x)$ is a Hermitian operator of a one-dimensional system.

3.3 For two supersymmetric partner Hamiltonians H_1 and H_2 discuss the condition for (a) $E_n^{(1)} = E_{n+1}^{(2)}$ and (b) $E_n^{(2)} = E_n^{(1)}$, where $E_n^{(1)}$ and $E_n^{(2)}$ are the eigenvalues of H_1 and H_2, respectively, [5].

3.4 Determine the values of $A^+H_2 - H_1A^+$ and $A^-H_1 - H_2A^+$.

3.5 Show that $[A^-, A^+] = -\dfrac{\mathrm{d}^2}{\mathrm{d}x^2}\ln\phi_0$. Hence, show that it is a function of x for potentials which are not harmonic.

3.6 A one-dimensional Hamiltonian $H = -\dfrac{\hbar^2}{2m}\dfrac{\mathrm{d}^2}{\mathrm{d}x^2} + V(x)$ can be written as $H = A^+A^- + E_0$, where E_0 is the ground state energy and

$$A^- = \frac{\hbar}{\sqrt{2m}}\left(\frac{\mathrm{d}}{\mathrm{d}x} - \frac{1}{\phi_0}\frac{\mathrm{d}\phi_0}{\mathrm{d}x}\right), \quad A^+ = \frac{\hbar}{\sqrt{2m}}\left(-\frac{\mathrm{d}}{\mathrm{d}x} - \frac{1}{\phi_0}\frac{\mathrm{d}\phi_0}{\mathrm{d}x}\right)$$

with ϕ_0 as the ground state eigenfunction. With the help of the above determine whether the ground state energy level of a one-dimensional Hamiltonian is degenerate or nondegenerate.

3.7 Factorize the Hamiltonian in N-dimensions with the potential $V(x_1, x_2, \ldots, x_N)$ [5].

3.8 Find out the effect of A^- on $\phi_0^{(1)}$.

3.9 Based on supersymmetry transformation show that all the discrete energy levels of a one-dimensional system are nondegenerate. Extend your argument for a system with N-spatial dimension [H.F. Chau, *Am. J. Phys.* 63:1005, 1995].

3.10 Obtain the values of $\{Q^-, Q^+\}$, $\{Q^+, Q^+\}$ and $\{Q^-, Q^-\}$, where $Q^+ = \begin{pmatrix} 0 & A^+ \\ 0 & 0 \end{pmatrix}$ and $Q^- = \begin{pmatrix} 0 & 0 \\ A^- & 0 \end{pmatrix}$.

3.11 For the Q^+ and Q^- given in the previous exercise show that $[H_\mathrm{s}, Q^-] = 0$.

3.12 The two-dimensional Hamiltonian for an electron subjected to a constant electric field $\mathbf{B} = B_z\mathbf{k}$ is given by $H_\mathrm{s} = \dfrac{1}{2}\left(\pi_x^2 + \pi_y^2 - eB\sigma_z\right)$, where $\pi_x = P_x - eA_x$, $\pi_y = P_y - eA_y$ and $\mathbf{A}$ is the vector potential defined by $\mathbf{B} = \nabla \times \mathbf{A}$. The supercharges are defined by $A^\pm = \pi_\pm\sigma_\mp/\sqrt{2}$, where $\sigma_\pm = (\sigma_x \pm \mathrm{i}\sigma_y)/2$. Find out $\{Q^-, Q^+\}$.

3.13 Show that $H_\mathrm{s} = \dfrac{1}{2}p^2 + \dfrac{1}{2}\overline{V}^2 + \dfrac{1}{2}\sigma_z\dfrac{\mathrm{d}\overline{V}}{\mathrm{d}x} + E_0$.

3.14 Show that $\overline{V} = -\omega x$ gives two partner harmonic oscillator Hamiltonians with the zero-point energy shifted by ω. Hence, find the ground state eigenfunctions and energy of both Hamiltonians.

3.15 Show that the two supersymmetric partners of the step function $\overline{V}(x) = \theta(x) - \theta(-x)$ are the attractive and repulsive δ-potentials.

3.16 Determine the first supersymmetric partner potential and its energy eigenvalues of the attractive potential [5] $V_1 = -\lambda_1 \text{sech}^2 x$, $\lambda_1 > 0$ assuming

$$E_n^{(1)} = -\frac{1}{2}\left[Q - \left(n + \frac{1}{2}\right)\right]^{1/2}, \quad n = 0, 1, \ldots, m \leq \left(Q_1 - \frac{1}{2}\right) \text{ and}$$

$$\phi_0^{(1)} = \text{sech} x^{(Q_1 - \frac{1}{2})}, \quad Q_1 = \left(2\lambda_1 + \frac{1}{4}\right)^{1/2} \geq \frac{1}{2}.$$

3.17 Given the normalized ground state eigenfunction corresponding to the ground state energy $E_0^{(1)} = 0$ for the potential $V_1 = (1 - 2\text{sech}^2 x)/2$, as $\phi_0^{(1)} = (1/\sqrt{2})\text{sech} x$ show that its supersymmetric partner potential V_2 corresponds to a free particle. Find the remaining normalized eigenfunctions for the potential V_1.

3.18 Obtain the supersymmetric partner V_2 of hydrogen atom.

3.19 For the Hamiltonian $H = \frac{1}{2}p_x^2 + V_1(x)$, $V_1(x) = \frac{1}{2}x^2 + \frac{\lambda(\lambda - 1)}{2x^2}$ identify A^+ and A^- operators so that $H_1 = A^- A^+ + \epsilon$. Also, find the potential V_2 in the Hamiltonian $H_2 = A^+ A^- + \epsilon = \frac{1}{2}p_x^2 + V_2(x)$.

3.20 Consider a free particle with unphysical energy eigenvalues $E = k^2 < 0$. Determine the complex potentials with real spectra.

4

Coherent and Squeezed States

4.1 Introduction

Certain superposition (linear combination) of energy eigenfunctions of linear harmonic oscillators are called *coherent states* because they are of significance in optics for the representation of coherent light waves. A hallmark of coherent states is that the variances (squares of the uncertainties) of x and p_x are constant in time and further their product becomes the minimum value allowed by the Heisenberg uncertainty principle. On the other hand, some linear combinations of harmonic oscillator energy functions give rise to *squeezed states*. A curious property of squeezed states is that the variances of x and p_x oscillate in time 180° out of phase with one another with the frequency twice of the oscillator. The wave packet of a coherent state possesses a minimum uncertainty. $\langle x \rangle$ and $\langle p_x \rangle$ have the same oscillatory forms as in the classical case. That is, a coherent state at macroscopic scales would reproduce the classical motion. The coherent states have also been called *minimum uncertainty coherent states*, the *Schrödinger coherent states* or the *Glauber coherent states* [1–7]. The squeezed states are sometimes referred to in the literature as two-photon coherent states.

Why is the study of coherent and squeezed states important? They provide promising measurement results better than those usually expected from the Heisenberg uncertainty principle. This is certainly the case where optical interferometers are used to detect very weak forces such as gravitational wave detection [8], in optical communications [9], photon detection techniques, atomic spectroscopy, optical wave guide tap, noise free amplification, high-resolution spectroscopy, quantum communications and low-light-level microscopy, etc. [10]. The radiative properties of atoms are highly sensitive to their contact with the environment or the vacuum reservoir. If a normal vacuum reservoir is replaced with a squeezed one, then it is possible to considerably reduce the line width of emission and absorption spectra and this is very useful in enhancing the resolution in laser spectroscopy of atoms. Note that the light from a laser is a coherent state. In optical fields coherent states are used for dealing with the photon statistics and coherent properties. Now, coherent and squeezed states form the basic language for quantum optics.

In this chapter some basic aspects of coherent and squeezed states are presented. We obtain the Heisenberg uncertainty relation for the harmonic oscillator states and show that it is a minimum for ground state. Next, we define coherent states and show that they are the minimum uncertainty product states. A physical interpretation of coherent states is then given. We outline a method for constructing coherent states from ground state. We list some important properties of coherent states. Finally, we discuss the squeezed states.

DOI: 10.1201/9781003172192-4

4.2 The Uncertainty Product of Harmonic Oscillator

Let us calculate the uncertainties in the position and momentum of the linear harmonic oscillator corresponding to the number states and also for various linear combinations of them. The uncertainties are normally characterized by the variances:

$$\text{var}(x) = (\Delta x)^2 = \langle x^2\rangle - \langle x\rangle^2 , \tag{4.1a}$$

$$\text{var}(p) = (\Delta p_x)^2 = \langle p_x^2\rangle - \langle p_x\rangle^2 . \tag{4.1b}$$

These averages can be calculated when $\psi(x,t)$ of an oscillator is known. The integrals for $\langle x\rangle$, $\langle x^2\rangle$, $\langle p_x\rangle$ and $\langle p_x^2\rangle$ are often tedious to calculate in x-representation. However, they can be easily calculated as follows making use of ladder operators a and $a^\dagger$.

We represent the energy eigenfunctions of harmonic oscillator by a Dirac ket $|n\rangle$. We have

$$a|0\rangle = 0 , \quad |n\rangle = \frac{\left(a^\dagger\right)^n |0\rangle}{\sqrt{n!}} , \tag{4.2a}$$

$$a^\dagger = \sqrt{n+1}\,|n+1\rangle , \quad a|n\rangle = \sqrt{n}|n-1\rangle , \tag{4.2b}$$

$$\langle n|n'\rangle = \delta(n,n') , \quad \sum_{n=0}^{\infty} |n\rangle\langle n| = I , \tag{4.2c}$$

where I is the identity operator and

$$a = \frac{1}{\sqrt{2m\omega\hbar}}\,(m\omega x + \mathrm{i}p_x), \quad a^\dagger = \frac{1}{\sqrt{2m\omega\hbar}}\,(m\omega x - \mathrm{i}p_x). \tag{4.3}$$

Setting m, ω and $\hbar$ as unity we have

$$x = \frac{1}{\sqrt{2}}\left(a + a^\dagger\right) , \quad p_x = -\frac{\mathrm{i}}{\sqrt{2}}\left(a - a^\dagger\right) . \tag{4.4}$$

Squaring of the above equation gives

$$x^2 = \frac{1}{2}\left(a^\dagger a + aa^\dagger + aa + a^\dagger a^\dagger\right) , \tag{4.5a}$$

$$p_x^2 = \frac{1}{2}\left(a^\dagger a + aa^\dagger - aa - a^\dagger a^\dagger\right) . \tag{4.5b}$$

Now,

$$\langle x\rangle = \langle\psi|x|\psi\rangle = \left\langle\psi\right|\left[\left(a + a^\dagger\right)/\sqrt{2}\right]\left|\psi\right\rangle , \tag{4.6a}$$

$$\langle p_x\rangle = \langle\psi|p_x|\psi\rangle = \left\langle\psi\right|\left[\left(a - a^\dagger\right)/(\mathrm{i}\sqrt{2}\,)\right]\left|\psi\right\rangle . \tag{4.6b}$$

The operators $a \pm a^\dagger$ operating on $|n\rangle$ give linear combinations of $|n-1\rangle$ and $|n+1\rangle$. When $|\psi\rangle$ is a number state then the right-sides of Eqs. (4.6) produce terms such as $\langle n|n-1\rangle$ and $\langle n|n+1\rangle$. These terms become zero by orthogonality. Therefore, $\langle x\rangle = \langle p_x\rangle = 0$. But Δx and Δp_x of the number states are not equal to zero as shown below.

From Eq. (4.5a), we obtain

$$\langle x^2\rangle = \langle n|[(a^\dagger a + aa^\dagger + aa + a^\dagger a^\dagger)/2]|n\rangle . \tag{4.7}$$

Since $a^\dagger a|n\rangle = n|n\rangle$ and $a^\dagger a - a^\dagger a = 1$, the first two terms in the right-side of Eq. (4.7) are combined to give

$$a^\dagger a + aa^\dagger = 2a^\dagger a + 1 = 2n + 1\,. \tag{4.8}$$

The contribution coming from the last two operators in Eq. (4.7) is zero because they generate terms that are proportional to $|n-2\rangle$ and $|n+2\rangle$ and are orthogonal to $\langle n|$. Thus,

$$\langle x^2\rangle = \langle n|(2n+1)/2|n\rangle = n + \frac{1}{2}\,. \tag{4.9}$$

Similarly,

$$\langle p_x^2\rangle = n + \frac{1}{2}\,. \tag{4.10}$$

Now,

$$\Delta x = \left(\langle x^2\rangle - \langle x\rangle^2\right)^{1/2} = \left(n+\frac{1}{2}\right)^{1/2}, \tag{4.11a}$$

$$\Delta p_x = \left(\langle p_x^2\rangle - \langle p_x\rangle^2\right)^{1/2} = \left(n+\frac{1}{2}\right)^{1/2} \tag{4.11b}$$

so that

$$\Delta x \Delta p_x = n + \frac{1}{2}\,. \tag{4.12}$$

Equations (4.12) gives the Heisenberg uncertainty principle for the number states of the harmonic oscillator. Its minimum value is 1/2 corresponding to $n = 0$, the ground state (vacuum state). The ground state, $n = 0$, is thus called a *minimum uncertainty state*.

We write a most general state, a linear combination of the number states as

$$\psi(x,t) = \sum_{n=0}^{\infty} C_n(t)|n\rangle\,, \tag{4.13}$$

where $C_n(t)$ are generally complex numbers and the x-dependence is in $|n\rangle$. Now, determine $C_n(t)$'s. Substitution of Eq. (4.13) and $H = n + 1/2$ in the Schrödinger equation $\mathrm{i}\partial\psi/\partial t = H\psi$ gives

$$\mathrm{i}\frac{\mathrm{d}}{\mathrm{d}t}C_n(t) = \left(n+\frac{1}{2}\right)C_n(t)\,, \quad n = 0, 1, 2, \ldots\,. \tag{4.14}$$

The solution of Eq. (4.14) is

$$C_n(t) = C_n(0)\mathrm{e}^{-\mathrm{i}(n+\frac{1}{2})t}\,. \tag{4.15}$$

The probability of measuring n quanta in the oscillator is $|C_n|^2$ and is independent of time.

Now, an interesting and important question is: *Is the energy linear combination state ψ a minimum product state like the vacuum state?* The answer is no. Not every linear combination state is a minimum product state. There are special sets of $C_n(t)$ leading to minimum product states; one such a remarkable set is the coherent state. The squeezed states described in sec. 4.7 are a more general class of minimum product states.

4.3 Coherent States: Definition, Uncertainty Product and Physical Meaning

A state $|\alpha(t)\rangle$ satisfying the time-dependent Schrödinger equation of a system is called a *coherent state* of the system if it satisfies the conditions [11]

$$\text{(i)} \quad \langle\alpha(t)|x|\alpha(t)\rangle = x_{\rm CM}(t)\,, \tag{4.16}$$

$$\text{(ii)} \quad \langle\alpha(t)|H|\alpha(t)\rangle = E_{\rm CM}\,. \tag{4.17}$$

where 'CM' stands for classical mechanics. In the following we show that if the state $|\alpha\rangle$ is an eigenstate of the annihilation operator a then the condition (i) is satisfied.

4.3.1 Proof of $\langle\alpha|a|\alpha\rangle = \alpha$

The classical coordinate $x_{\rm CM}(t)$ of the oscillator is

$$x_{\rm CM}(t) = \lambda\left[\alpha {\rm e}^{-{\rm i}t} + \alpha^* {\rm e}^{{\rm i}t}\right]\,, \tag{4.18}$$

where $\alpha = |\alpha|{\rm e}^{{\rm i}\theta}$ is a complex number, λ is an appropriately chosen number and $E_{\rm CM} = |\alpha|^2$. The real numbers $|\alpha|$ and θ are the amplitude and phase of α and $0 \le |\alpha| < \infty$, $0 < \theta \le 2\pi$. For the linear harmonic oscillator, from Eq. (4.4), we have $x = x_0(a + a^\dagger)$, $x_0 = 1/\sqrt{2}$. As

$$|\psi(t)\rangle = {\rm e}^{-{\rm i}Ht/\hbar}|\psi(0)\rangle \tag{4.19}$$

and H commutes with $a^\dagger a$, $|\alpha(t)\rangle$ is written as

$$|\alpha(t)\rangle = {\rm e}^{-{\rm i}ta^\dagger a}|\alpha(0)\rangle = {\rm e}^{-{\rm i}ta^\dagger a}|\alpha\rangle\,. \tag{4.20}$$

Then

$$\langle x\rangle = x_{\rm CM}(t) = x_0\big\langle\alpha\big|{\rm e}^{{\rm i}ta^\dagger a}(a + a^\dagger){\rm e}^{-{\rm i}ta^\dagger a}\big|\alpha\big\rangle\,. \tag{4.21}$$

Using the operator identity

$${\rm e}^{\xi a^\dagger a} f(a, a^\dagger){\rm e}^{-\xi a^\dagger a} = f\left(a{\rm e}^{-\xi}, a^\dagger {\rm e}^{\xi}\right) \tag{4.22}$$

in Eq. (4.21), (with $\xi = {\rm i}t$), we obtain

$$\begin{aligned} x_{\rm CM}(t) &= x_0\big\langle\alpha\big|\left(a{\rm e}^{-{\rm i}t} + a^\dagger {\rm e}^{{\rm i}t}\right)|\alpha\big\rangle \\ &= x_0\langle\alpha|a|\alpha\rangle{\rm e}^{-{\rm i}t} + x_0\langle\alpha|a^\dagger|\alpha\rangle{\rm e}^{{\rm i}t}\,. \end{aligned} \tag{4.23}$$

Comparison of Eqs. (4.18), with $\lambda = x_0$, and (4.23) gives

$$\langle\alpha|a|\alpha\rangle = \alpha\,, \quad \langle\alpha|a^\dagger|\alpha\rangle = \alpha^*\,. \tag{4.24}$$

Thus, the condition (i) leads to $\langle\alpha|a|\alpha\rangle = \alpha$ which proves that $|\alpha\rangle$ is the eigenfunction of the operator a. Further, $\langle n\rangle = \langle\alpha|A^\dagger a|\alpha\rangle = \langle|\alpha a^\dagger|\alpha\rangle = \alpha\alpha^*\langle\alpha|\alpha\rangle = |\alpha|^2$. $|\alpha\rangle$ does not contain a fixed number of quanta,

4.3.2 Uncertainty Product of Coherent States [12]

For a coherent state the expectation values of x and p_x are obtained as

$$\langle x\rangle = \langle\alpha|(a+a^\dagger)/\sqrt{2}|\alpha\rangle = \frac{1}{\sqrt{2}}\left(\alpha \mathrm{e}^{-\mathrm{i}t} + \alpha^* \mathrm{e}^{\mathrm{i}t}\right) \tag{4.25a}$$

$$\langle p_x\rangle = \langle\alpha|(a-a^\dagger)/(\mathrm{i}\sqrt{2}\,)|\alpha\rangle = \frac{1}{\mathrm{i}\sqrt{2}}\left(\alpha \mathrm{e}^{-\mathrm{i}t} - \alpha^* \mathrm{e}^{\mathrm{i}t}\right) . \tag{4.25b}$$

For real eigenvalues α, $\langle x\rangle$ and $\langle p_x\rangle$ become

$$\langle x\rangle = \sqrt{2}\,\alpha\cos t\,, \quad \langle p_x\rangle = -\sqrt{2}\,\alpha\sin t\,. \tag{4.26}$$

In Eq. (4.26) $\langle x\rangle$ is exactly the classical limit for a harmonic oscillator with amplitude $\sqrt{2}\,\alpha$ such that the energy is $x_0^2/2$.

Next,

$$\begin{aligned}\langle x^2\rangle &= \langle\alpha|(a^\dagger a + aa^\dagger + aa + a^\dagger a^\dagger)/2|\alpha\rangle \\ &= \frac{1}{2}\left(\alpha^*\alpha + \alpha^*\alpha + 1 + \alpha^2 \mathrm{e}^{-2\mathrm{i}t} + \alpha^{*2}\mathrm{e}^{2\mathrm{i}t}\right) , \qquad (4.27a)\\ \langle p_x^2\rangle &= \langle\alpha|(a^\dagger a + aa^\dagger - aa - a^\dagger a^\dagger)/2|\alpha\rangle \\ &= \frac{1}{2}\left(\alpha^*\alpha + \alpha^*\alpha + 1 - \alpha^2 \mathrm{e}^{-2\mathrm{i}t} - \alpha^{*2}\mathrm{e}^{2\mathrm{i}t}\right) . \qquad (4.27b)\end{aligned}$$

For real α

$$\langle x^2\rangle = \frac{1}{2} + 2\alpha^2\cos^2 t\,, \quad \langle p_x^2\rangle = \frac{1}{2} + 2\alpha^2\sin^2 t\,. \tag{4.28}$$

Replacement of $|\alpha^2|$ by $\langle n\rangle$ gives

$$\langle x\rangle = \sqrt{2\langle n\rangle}\,\cos t\,, \quad \langle x^2\rangle = 2\langle n\rangle\cos^2 t + \frac{1}{2}\,, \tag{4.29a}$$

$$\langle p_x\rangle = -\sqrt{2\langle n\rangle}\,\sin t\,, \quad \langle p_x^2\rangle = 2\langle n\rangle\sin^2 t + \frac{1}{2}\,. \tag{4.29b}$$

Then

$$(\Delta x)^2 = \langle x^2\rangle - \langle x\rangle^2 = \frac{1}{2}\,, \quad (\Delta p_x)^2 = \langle p_x^2\rangle - \langle p_x\rangle^2 = \frac{1}{2}. \tag{4.30}$$

That is, $(\Delta x)(\Delta p_x) = 1/2$. Thus, the coherent states are minimum uncertainty states. Note that this minimum product is identical to the minimum uncertainty product of the ground state. Further, observe that $(\Delta x)^2$ and $(\Delta p_x)^2$, that is $\mathrm{Var}(x)$ and $\mathrm{Var}(p)$, are independent of the average number of quanta in the state and also time. If we do not set m, $\hbar$ and ω to unity then $(\Delta x)^2 = \hbar/(2m\omega)$, $(\Delta p_x)^2 = \hbar m\omega/2$ and $\Delta x\Delta p_x = \hbar/2$.

4.3.3 Physical Meaning of Coherent States

Referring to (4.13), a coherent state is mathematically, a linear superposition of the number states. *What is the physical meaning of it?* To bring out the physical meaning of it let us compute the coefficients C_n in the linear superposition given by Eq. (4.13) [12]. Substitution of (4.13) in $a|\alpha\rangle = \alpha|\alpha\rangle$ gives

$$a\sum_{n=0}^{\infty} C_n|n\rangle = \sum_{n=0}^{\infty} C_n\sqrt{n}|n-1\rangle = \alpha\sum_{n=0}^{\infty} C_n|n\rangle\,, \tag{4.31a}$$

where $C_n = C_n(0)$. More explicitly,

$$C_1\sqrt{1}\,|0\rangle + C_2\sqrt{2}\,|1\rangle + C_3\sqrt{3}\,|2\rangle + \cdots = \alpha C_0|0\rangle + \alpha C_1|1\rangle + \alpha C_2|2\rangle + \cdots . \tag{4.31b}$$

Equating the coefficients of $|i\rangle$, $i = 0, 1, \ldots$ on both sides gives

$$C_1 = \alpha C_0\,,\;\; C_2 = \frac{\alpha C_1}{\sqrt{2}},\;\ldots\,,\;\; C_n = \frac{\alpha C_{n-1}}{\sqrt{n}} = \frac{C_0\alpha^n}{\sqrt{n!}}\,. \tag{4.32}$$

To evaluate C_0 we use the normalization condition:

$$1 = \sum_{n=0}^{\infty} |C_n|^2 = |C_0|^2 \sum_{n=0}^{\infty} \frac{(|\alpha|^2)^n}{n!} = |C_0|^2\, \mathrm{e}^{|\alpha|^2}. \tag{4.33}$$

The above equation gives

$$|C_0| = \mathrm{e}^{-|\alpha|^2/2}\,. \tag{4.34}$$

Since $|C_n|^2$ represents the probability P_n of measuring an energy equal to $(n + 1/2)$ (that is, n quanta in the system), we write

$$P_n = |C_n|^2 = \frac{\mathrm{e}^{-|\alpha|^2}}{n!}\,\left(|\alpha|^2\right)^n = \frac{\mathrm{e}^{-\langle n\rangle}\langle n\rangle^n}{n!}\,, \tag{4.35}$$

where $\langle n\rangle = |\alpha|^2$ is used. We note that $|\alpha\rangle$ does not contain a fixed number of quanta. However, because $\langle n\rangle = |\alpha|^2$, the average energy in $|\alpha\rangle$ is $\left(|\alpha|^2 + 1/2\right)$.

Equation (4.35) represents Poisson distribution. Experimentally, a single-mode laser light can be regarded as an approximate coherent light, and is found to have Poisson counting statistics. Thus, physically a coherent state $|\alpha\rangle$ is a linear combination of number states with $|C_n|^2$ representing the probabilities of measuring n quanta in a Poisson distribution with $|\alpha|^2$ being the average number of quanta.

4.4 Generation and Properties of Coherent States

In the following we show that coherent states can be generated from ground state with the help of the displacement operator $D(\alpha)$ [11]. Then we enumerate properties of coherent states.

4.4.1 Expression for Coherent States

From Eqs. (4.13), (4.32) and (4.35) the expression for the coherent state is

$$|\alpha\rangle = \sum_{n=0}^{\infty} C_n(t)|n\rangle = \mathrm{e}^{-|\alpha|^2/2} \sum_n \frac{\alpha^n}{\sqrt{n!}}\,|n\rangle\,, \tag{4.36}$$

where $|n\rangle$ is the nth excited state of the linear harmonic oscillator. The state $|\alpha\rangle$ is normalized: $\langle\alpha|\alpha\rangle = 1$. In Eq. (4.36) $\mathrm{e}^{-|\alpha|^2/2}$ is the normalization constant. In coordinate representation

$$|n\rangle = \left(\frac{1}{\sqrt{\pi}\,2^n n!}\right)^{1/2} H_n(x)\,\mathrm{e}^{-x^2/2} \tag{4.37}$$

and the expression for $|\alpha\rangle$ becomes

$$|\alpha\rangle = \left(\frac{1}{\pi}\right)^{1/4} \mathrm{e}^{-[\mathrm{Im}(\alpha)]^2}\, \mathrm{e}^{-(x-\sqrt{2}\,\alpha)^2/2}\,, \tag{4.38}$$

where α is a complex number and the above wave function is Gaussian.

4.4.2 Generation of Coherent States from Ground State

Let us consider the operators a' and $a'^{\dagger}$ defined by

$$a' = a + \alpha\,, \quad a'^{\dagger} = a^{\dagger} + \alpha^* \tag{4.39}$$

and the displacement operator $D(\alpha)$ through

$$a' = D^{\dagger}(\alpha) a D(\alpha)\,, \quad a'^{\dagger} = D^{\dagger}(\alpha) a^{\dagger} D(\alpha) \tag{4.40a}$$

with

$$D(\alpha)D^{\dagger}(\alpha) = D^{\dagger}(\alpha)D(\alpha) = I\,. \tag{4.40b}$$

Suppose $|\alpha'\rangle$ is the state given by

$$|\alpha'\rangle = D^{\dagger}(\alpha)|\alpha\rangle\,, \quad \langle\alpha'(t)| = \langle\alpha(t)|D(\alpha)\,. \tag{4.41}$$

Now, evaluate $\langle\alpha'|a'|\alpha'\rangle$:

$$\begin{aligned}
\langle\alpha'|a'|\alpha'\rangle &= \langle\alpha|D(\alpha)a'D^{\dagger}(\alpha)|\alpha\rangle \\
&= \langle\alpha|D(\alpha)D^{\dagger}(\alpha)aD(\alpha)D^{\dagger}(\alpha)|\alpha\rangle \\
&= \langle\alpha|a|\alpha\rangle \\
&= \alpha\langle\alpha|\alpha\rangle \\
&= \alpha\langle\alpha'|\alpha'\rangle \\
&= \langle\alpha'|\alpha|\alpha'\rangle\,.
\end{aligned} \tag{4.42}$$

That is,

$$\langle\alpha'|a' - \alpha|\alpha'\rangle = 0 = \langle\alpha'|a|\alpha'\rangle\,. \tag{4.43}$$

Similarly, $\langle\alpha'|a^{\dagger}|\alpha'\rangle = 0$.

The Hamiltonian of the oscillator is $H = a^{\dagger}a$. Define $H' = a'^{\dagger}a'$. Then

$$\langle H\rangle = \langle\alpha(t)|H|\alpha(t)\rangle = \langle\alpha(t)|D(\alpha)H'D^{\dagger}(\alpha)|\alpha(t)\rangle = \langle\alpha'(t)|H'|\alpha'(t)\rangle. \tag{4.44a}$$

Substituting $H' = a'^{\dagger}a'$, we obtain

$$\begin{aligned}
\langle H\rangle &= \langle\alpha'|a'^{\dagger}a'|\alpha'\rangle \\
&= \langle\alpha'|(a^{\dagger} + \alpha^*)(a + \alpha)|\alpha'\rangle \\
&= \langle\alpha'|a^{\dagger}a|\alpha'\rangle + |\alpha|^2\langle\alpha'|\alpha'\rangle + \alpha^*\langle\alpha'|a|\alpha'\rangle + \alpha\langle\alpha'|a^{\dagger}|\alpha'\rangle \\
&= \langle\alpha'|a^{\dagger}a|\alpha'\rangle + |\alpha|^2\langle\alpha'|\alpha'\rangle \\
&= |\alpha|^2 + \langle\alpha'|H|\alpha'\rangle \\
&= E_{\mathrm{CM}} + \langle\alpha'|H|\alpha'\rangle\,.
\end{aligned} \tag{4.44b}$$

That is,

$$\langle\alpha(t)|H|\alpha(t)\rangle = E_{\rm CM} + \langle\alpha'|H|\alpha'\rangle\,. \tag{4.45}$$

If the condition (ii) given by Eq.(4.17) is imposed in the above equation, we get

$$0 = \langle\alpha'|H|\alpha'\rangle = \langle\alpha'|a^\dagger a|\alpha'\rangle\,. \tag{4.46}$$

This is valid only if $|\alpha'\rangle = |0\rangle$. Then from Eq. (4.41), we obtain

$$|\alpha'\rangle = D^\dagger(\alpha)|\alpha\rangle\,, \quad |0\rangle = D^\dagger(\alpha)|\alpha\rangle\,, \quad D(\alpha)|0\rangle = |\alpha\rangle\,. \tag{4.47}$$

Hence, the coherent state given by Eq. (4.20) becomes

$$|\alpha(t)\rangle = \mathrm{e}^{-\mathrm{i}ta^\dagger a}|\alpha\rangle = \mathrm{e}^{-\mathrm{i}ta^\dagger a}D(\alpha)|0\rangle\,. \tag{4.48}$$

Thus, *the displacement operator $D(\alpha)$ acting on the vacuum state $|0\rangle$ of the oscillator generates a coherent state*.

4.4.3 Explicit Form of $D(\alpha)$

Let us proceed to find an explicit form for $D(\alpha)$. For this purpose assume that

$$D(\alpha) = \mathrm{e}^{\mathrm{i}h(\alpha)} \tag{4.49}$$

where $h(\alpha)$ is a Hermitian operator assumed to be existing.

From Eqs. (4.39) and (4.40) we have

$$a + \alpha = a' = D^\dagger(\alpha)aD(\alpha) = \mathrm{e}^{-\mathrm{i}h(\alpha)}a\mathrm{e}^{\mathrm{i}h(\alpha)}\,, \tag{4.50a}$$

$$a^\dagger + \alpha^* = \mathrm{e}^{\mathrm{i}h(\alpha)}a^\dagger\mathrm{e}^{\mathrm{i}h(\alpha)}\,. \tag{4.50b}$$

Use of the operator identity

$$\mathrm{e}^A B\mathrm{e}^{-A} = B + [A,B] + \frac{1}{2}[A,[A,B]] + \ldots \tag{4.51}$$

gives

$$\mathrm{e}^{-\mathrm{i}h(\alpha)}a\mathrm{e}^{\mathrm{i}h(\alpha)} = a + \alpha = a - \mathrm{i}[h(\alpha), a] + \ldots \tag{4.52a}$$

and similarly

$$\mathrm{e}^{\mathrm{i}h(\alpha)}a^\dagger\mathrm{e}^{\mathrm{i}h(\alpha)} = a^\dagger + \alpha^* = a^\dagger - \mathrm{i}[h(\alpha), a^\dagger] + \ldots\,. \tag{4.52b}$$

Equation (4.52a) implies that

$$[h(\alpha), a] = \mathrm{i}\alpha\,, \quad [h(\alpha), a^\dagger] = \mathrm{i}\alpha^*\,. \tag{4.53}$$

The above equation gives (verify)

$$h(\alpha) = \mathrm{i}\alpha a^\dagger - \mathrm{i}\alpha^* a = -\mathrm{i}\alpha a^\dagger + \mathrm{i}\alpha^* a\,. \tag{4.54}$$

Now,

$$D(\alpha) = \mathrm{e}^{\mathrm{i}h(\alpha)} = \mathrm{e}^{\alpha a^\dagger - \alpha^* a}\,. \tag{4.55}$$

Solved Problem 1:

Given $|\alpha\rangle = D(\alpha)|0\rangle$ show that the coherent state $|\alpha\rangle$ is the eigenstate of a with eigenvalue α.

We obtain

$$\begin{aligned} a|\alpha\rangle &= aD(\alpha)|0\rangle \\ &= D(\alpha)(a+\alpha)|0\rangle \\ &= D(\alpha)a|0\rangle + \alpha D(\alpha)|0\rangle \\ &= \alpha D(\alpha)|0\rangle \\ &= \alpha|\alpha\rangle\,, \end{aligned} \tag{4.56}$$

where we used Eq. (4.47c). This equation states that the coherent state $|\alpha\rangle$ is the eigenstate of a with eigenvalue α.

We would like to know the time evolution of $|\alpha\rangle$. This is determined in the following.

4.4.4 Time Evolution of $|\alpha\rangle$

From Eqs. (4.55) and (4.56) we write

$$a|\alpha\rangle = a\,\mathrm{e}^{\alpha a^\dagger - \alpha^* a}|0\rangle\,. \tag{4.57}$$

We have

$$|\alpha(x,0)\rangle = D(\alpha)|0\rangle = \mathrm{e}^{\alpha a^\dagger - \alpha^* a}|0\rangle\,. \tag{4.58}$$

Since $H = \left(a^\dagger a + 1/2\right)$, applying the time evolution operator $\mathrm{e}^{-\mathrm{i}Ht} = \mathrm{e}^{-\mathrm{i}(a^\dagger a+1/2)t}$ to $|\alpha(x,0)\rangle$ we get

$$\begin{aligned} |\alpha(x,t)\rangle &= \mathrm{e}^{-\mathrm{i}(a^\dagger a+1/2)t}|\alpha(x,0)\rangle \\ &= \mathrm{e}^{-|\alpha|^2/2}\sum_{n=0}^{\infty}\frac{\alpha^n}{\sqrt{n!}}\,\mathrm{e}^{-\mathrm{i}(a^\dagger a+1/2)t}|n\rangle \\ &= \mathrm{e}^{-(|\alpha|^2+\mathrm{i}t)/2}\sum_{n=0}^{\infty}\frac{\alpha^n \mathrm{e}^{-\mathrm{i}nt}}{\sqrt{n!}}\,|n\rangle \\ &= \mathrm{e}^{-\mathrm{i}t/2}|\alpha(t)\rangle \end{aligned} \tag{4.59a}$$

with

$$\alpha(t) = \alpha(x,0)\,\mathrm{e}^{-\mathrm{i}t}\,. \tag{4.59b}$$

Substitution of Eq. (4.58) for $|\alpha(x,0)\rangle$ in Eq. (4.59a) gives

$$|\alpha(x,t)\rangle = \mathrm{e}^{-\mathrm{i}t/2}\mathrm{e}^{\alpha(t)a^\dagger - \alpha^*(t)a}|0\rangle\,. \tag{4.60}$$

With $|0\rangle = (1/\pi)^{1/4}\mathrm{e}^{-x^2/2}$ the above equation is worked out as

$$\begin{aligned} |\alpha(x,t)\rangle &= \left(\frac{1}{\pi}\right)^{1/4}\mathrm{e}^{-[x-\sqrt{2}\,|\alpha(0)|\cos(t-\theta)]^2/2} \\ &\quad\times\mathrm{e}^{-\mathrm{i}[\sqrt{2}\,|\alpha(0)|x\sin(t-\theta)}\,\mathrm{e}^{\mathrm{i}|\alpha(0)|^2\sin 2(t-\theta)}\,\mathrm{e}^{-\mathrm{i}t/2}\,. \end{aligned} \tag{4.61}$$

Then

$$|\,|\alpha(x,t)\rangle\,|^2 = \frac{1}{\sqrt{\pi}}\,\mathrm{e}^{-[x-\sqrt{2}\,|\alpha(0)|\,\cos(t-\theta)]^2}\,. \tag{4.62}$$

This coherent state is

1. a Gaussian wave packet,
2. does not spread out and
3. oscillate in amplitude without change of shape.

Such a state can be regarded as a particle moving in the way of a mass on a spring. On the other hand, in the theory of radiation, it is the changing electric field strength. These states represent a standing electromagnetic wave with its amplitude oscillating sinusoidally in phase through the enclosure.

4.4.5 Generalized Coherent States of Linear Harmonic Oscillator

We note that the peak of the probability density of the coherent state $|\alpha(x,t)\rangle$ follows the sinusoidal trajectory of the classical particle. So, the coherent state can be considered as a displaced ground state. Interestingly, it has been pointed out that the coherent state can be generalized to include other energy eigenstates [13–14]. That is, we can introduce *generalized coherent states* (GCSs) in which any energy eigenstate can also be displaced with the probability density oscillates similar to classical trajectory.

Consider the wave function [13–15]

$$\begin{aligned} |n,\alpha\rangle &= \frac{(1/\pi)^{1/4}}{2^{n/2}\sqrt{n!}}\mathrm{e}^{-(x-\langle x\rangle)^2/2}H_n(x-\langle x\rangle) \\ &\quad\times\mathrm{e}^{\mathrm{i}[-(n+\frac{1}{2})t+x\langle p_x\rangle-\langle x\rangle\langle p_x\rangle/2]} \end{aligned} \tag{4.63a}$$

which is the solution of the time-dependent Schrödinger equation of the linear harmonic oscillator with

$$\langle x\rangle = \sqrt{2}|\alpha|\cos(t-\theta), \qquad \langle p_x\rangle = -\sqrt{2}|\alpha|\sin(t-\theta). \tag{4.63b}$$

The choice $\alpha = 0$ corresponds to the energy eigenstates of linear harmonic oscillator. The GCSs combine the quantum number containing classical features and the quantum number containing quantum features. That is, the α part of the GCS behaves that of a coherent state where as that of a number state is reflected by n part of GCS.

Equation (4.63) gives coherent state for $n = 0$. For large α, $x(t) = |\alpha|\sqrt{2}\cos(t-\theta)$ (ω is chosen as 1) can be viewed as the classical trajectory approximation to the coherent state at macroscopic energies [15]. Figure 4.1 depicts $||n,\alpha\rangle|^2$ for $n = 0, 1, 2$ with $\alpha = 2$. The difference between $|n,\alpha\rangle$ and $|n\rangle$ is that [15] the x-dependence of the amplitude of $|n,\alpha\rangle$ is displaced by the time-dependent $\langle x\rangle$ while the phase displacement is $x\langle p_x\rangle - \langle x\rangle\langle p_x\rangle/2$. Further, the probability density $||n,\alpha\rangle|^2$ retains the shape of $|n,0\rangle$, however, oscillates in time and follows a classical trajectory.

For $|n,\alpha\rangle$ we can define $a_\alpha = a - \alpha\mathrm{e}^{-\mathrm{i}t}$ and $[a_\alpha, a_\alpha^\dagger] = 1$. It is easy to obtain

$$a_\alpha|n,\alpha\rangle = \sqrt{n}\,\mathrm{e}^{-\mathrm{i}t}|n-1,\alpha\rangle, \quad a_\alpha^\dagger|n,\alpha\rangle = \sqrt{n+1}\,\mathrm{e}^{\mathrm{i}t}|n+1,\alpha\rangle. \tag{4.64}$$

Then the displacement of a is realized by the operator

$$D(\alpha) = \exp[\alpha\mathrm{e}^{-\mathrm{i}t}a^\dagger - a^*\mathrm{e}^{\mathrm{i}t}a], \tag{4.65a}$$

$$D^\dagger(-\alpha)aD(-\alpha) = a - \alpha\mathrm{e}^{-\mathrm{i}t} = a_\alpha. \tag{4.65b}$$

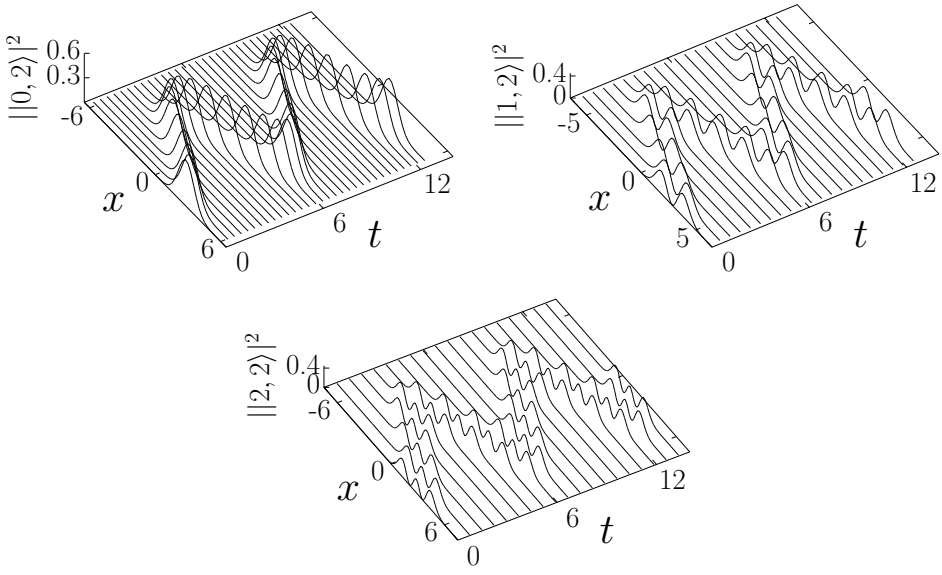

FIGURE 4.1
Plot of $||n,\alpha\rangle|^2$ of linear harmonic oscillator versus x and t for $n = 0, 1, 2$ with $\alpha = 2$. $|n,\alpha\rangle$ is given by Eq. (4.63).

Then $|n,\alpha\rangle = D(\alpha)|n,0\rangle$ with

$$\sum_{n=0}^{\infty} |n,\alpha\rangle\langle n,\alpha| = I, \quad \frac{1}{\pi}\int |n,\alpha\rangle\langle n,\alpha| \mathrm{d}^2\alpha = I. \tag{4.66}$$

4.4.6 Properties of Coherent States

We now enumerate the properties of coherent states:

1. Coherent states are eigenstates of the annihilation operator: $a|\alpha\rangle = \alpha|\alpha\rangle$.
2. They are created from the vacuum state through the unitary displacement operator: $\mathrm{e}^{\alpha a^\dagger - \alpha^* a}|0\rangle = |\alpha\rangle$.
3. Coherent states are minimum uncertainty product states, $\Delta x \Delta p_x = \hbar/2$, with Δx and Δp_x equal to those of the vacuum state.
4. Expectation values of x and p_x are nonzero but are oscillating.
5. $\langle x\rangle$ lags with $\langle p_x\rangle$ by 90° as in a classical oscillator.
6. The oscillation amplitude of average values of x and p_x are proportional to $\sqrt{\langle n\rangle}$ like those amplitudes in a classical system are proportional to $\sqrt{E}$.
7. The uncertainties Δx in x and Δp_x in p_x are equal (=1/2) and independent of time. Further, $\Delta x \Delta p_x = \hbar/2$.
8. The coherent states obey Poisson distribution.
9. For any complete set $|i\rangle$, the requirement for completeness is $\int |i\rangle\langle i| \, \mathrm{d}^2 i = 1$. But we find $\int |\alpha\rangle\langle\alpha| \, \mathrm{d}^2\alpha = \pi$ which states that the set $|\alpha\rangle$ is an over complete set.

10. $|n\rangle$ has a definite number of particles but an uncertain phase. In contrast to this $|\alpha\rangle$ has an uncertain number of particles but a definite phase.

For further details on coherent states the reader may refer to refs. [1–3].

Solved Problem 2:

Find whether two different coherent states $|\alpha\rangle$ and $|\beta\rangle$ are orthogonal or not.

From Eq. (4.36), we obtain

$$\begin{aligned}\langle\alpha|\beta\rangle &= \mathrm{e}^{-|\alpha|^2/2}\,\mathrm{e}^{-|\beta|^2/2}\sum_n\sum_m \frac{(\alpha^{*n}\beta^m)\,\langle n|m\rangle}{\sqrt{n!m!}} \\ &= \mathrm{e}^{-\left(|\alpha|^2+|\beta|^2\right)/2}\sum \frac{(\alpha^*\beta)^n}{\sqrt{n!n!}} \\ &= \mathrm{e}^{-\left(|\alpha|^2+|\beta|^2\right)/2}\mathrm{e}^{\alpha^*\beta} \end{aligned} \tag{4.67}$$

which is nonzero. Note that $|\langle\alpha|\beta\rangle|^2 = \mathrm{e}^{-|\alpha-\beta|^2}$.

Solved Problem 3:

Determine the time evolution of a coherent state.

With $H_0 = \omega(a^\dagger a + \frac{1}{2})$ ($\hbar = 1$) we find

$$\mathrm{e}^{-\mathrm{i}H_0 t}|\alpha\rangle = \mathrm{e}^{-|\alpha|^2/2}\mathrm{e}^{-\mathrm{i}\omega t/2}\sum_{n=0}^{\infty}\frac{\alpha^n \mathrm{e}^{-\mathrm{i}n\omega t}}{\sqrt{n!}}\,|n\rangle = \mathrm{e}^{-\mathrm{i}\omega t/2}|\mathrm{e}^{-\mathrm{i}\omega t}\alpha\rangle\,. \tag{4.68}$$

That is, the time evolution of any coherent state remains within the set $\{|\alpha\rangle\}$.

4.5 Spin Coherent States

A particular quantum state of a spin system which most closely resemble a classical spin is termed as a *spin coherent state* [16–19].

Let us consider a spin with a total angular momentum quantum number s. s can be $0, \frac{1}{2}, 1, \ldots$ where we set $\hbar = 1$. Denote $|sm\rangle$ as the z-angular momentum eigenstates with $m = -s, -s+1, \ldots, s$. $|ss\rangle$ is the maximal angular momentum state. With the spin operator S one can easily verify that

$$S_x|ss\rangle = \left(\frac{s}{2}\right)^{1/2}|s, s-1\rangle, \quad S_y|ss\rangle = \mathrm{i}\left(\frac{s}{2}\right)^{1/2}|s, s-1\rangle, \tag{4.69a}$$

$$S_z|ss\rangle = s|ss\rangle, \quad \langle ss|S_x|ss\rangle = \langle ss|S_y|ss\rangle = 0, \tag{4.69b}$$

$$\langle ss|S_z|ss\rangle = s, \quad \langle ss|S|ss\rangle = s\mathrm{e}_z, \tag{4.69c}$$

where e_z is the unit vector along the z-direction.

Now, denote $\mathbf{s} = (s, \theta, \phi)$ be a vector of length s and direction (θ, ϕ) in spherical polar coordinates. The spin coherent state $|\mathbf{s}\rangle$ is defined [19] as the state obtained by rotating the state $|ss\rangle$ by an angle θ about y-axis counterclockwise and then by an angle ϕ about the z-axis. $|\mathbf{s}\rangle$ is given by

$$|\mathbf{s}\rangle = |s\theta\phi\rangle = \mathrm{e}^{\mathrm{i}\phi S_z}\mathrm{e}^{\mathrm{i}\theta S_y}|ss\rangle. \tag{4.70}$$

We find $\langle \mathbf{s}|\mathbf{S}|\mathbf{s}\rangle = \mathbf{s}$. It is to be noted that $|\mathbf{s}\rangle$ is not an eigenstate of $\mathbf{S}$ because $\mathbf{S}|\mathbf{s}\rangle \neq \mathbf{s}|\mathbf{s}\rangle$.

For a state $|\psi\rangle$ one can use the spin coherent state as a basis and define the *spin function* (the spin-coherent -state-representation function) as

$$F(\theta,\phi) = \sqrt{\frac{2s+1}{4\pi}}\,\langle s\theta\phi|\psi\rangle, \tag{4.71}$$

where $\sqrt{(2s+1)/(4\pi)}$ is the normalization factor. In many ways F behaves like a wave function. Though a time-dependent Schrödinger equation for $F(\theta,\phi,t)$ can be set-up, $|F(\theta,\phi,t)|^2$ is not the probability distribution of outcomes of measuring $\mathbf{S}$.

One can show that [19]

$$\begin{aligned}\langle s\theta\phi|s\theta'\phi'\rangle &= \sum_{m=-s}^{s} \frac{(2s)!}{(s+m)!(s-m)!}\,[\cos(\theta/2)\cos(\theta'/2)]^{s+m} \\ &\quad\times [\sin(\theta/2)\sin(\theta'/2)]^{s-m}\,\mathrm{e}^{\mathrm{i}m(\phi-\phi')}\end{aligned} \tag{4.72}$$

and

$$\begin{aligned}F_{sm}(\theta,\phi) &= \left[\frac{2s+1}{4\pi}\frac{(2s)!}{(s+m)!(s-m)!}\right]^{1/2}[\cos(\theta/2)]^{s+m} \\ &\quad\times [\sin(\theta/2)]^{s-m}\,\mathrm{e}^{\mathrm{i}m\phi}.\end{aligned} \tag{4.73}$$

The spin function of the spin coherent state $|\mathbf{s}'\rangle = |s\theta'\phi'\rangle$ is

$$F_{\theta'\phi'}(\theta,\phi) = \left(\frac{2s+1}{4\pi}\right)^{1/2}\langle s\theta\phi|s\theta'\phi'\rangle. \tag{4.74}$$

That is,

$$F_{\mathbf{s}'}(\mathbf{s}) = \left(\frac{2s+1}{4\pi}\right)^{1/2}\langle \mathbf{s}|\mathbf{s}'\rangle. \tag{4.75}$$

The largest magnitude of F is at $\mathbf{s} = \mathbf{s}'$ and decays away from it.

For $|\psi(t)\rangle$ we write $F(\theta,\phi,t) = \langle s\theta\phi|\psi(t)\rangle$ and

$$\frac{\partial}{\partial t}F(\theta,\phi,t) = -\mathrm{i}\int_0^{\pi}\mathrm{d}\theta'\sin\theta'\int_0^{2\pi}\mathrm{d}\phi'\langle s\theta\phi|H|s\theta'\phi'\rangle F(\theta',\phi',t) \tag{4.76}$$

(*how?*).

4.6 Coherent States of Position-Dependent Mass Systems

This section is concerned with the coherent states of position-dependent mass (PDM) systems [20]. Such systems are found wide range of applications in physics [21–26].

The classical Hamiltonian of a PDM system is of the form

$$H = \frac{1}{2m(x)}p_x^2 + V(x,\alpha), \tag{4.77}$$

where α is a parameter used to specify the range, strength and diffuseness of V. H can be quantized by considering

$$\begin{aligned}\widehat{H} &= -\frac{1}{2m(x)}\frac{\mathrm{d}^2}{\mathrm{d}x^2} - \left(\frac{1}{2m(x)}\right)'\frac{\mathrm{d}}{\mathrm{d}x} + V(x,\alpha) \\ &= A^+(\alpha)A^-(\alpha) + E_0, \end{aligned} \tag{4.78}$$

where

$$A^+ = \frac{1}{\sqrt{2m(x)}}\frac{\mathrm{d}}{\mathrm{d}x} + W(x,\alpha), \tag{4.79a}$$

$$A^- = -\frac{1}{\sqrt{2m(x)}}\frac{\mathrm{d}}{\mathrm{d}x} - \left(\frac{1}{2m(x)}\right)' + W(x,\alpha) \tag{4.79b}$$

and W represents the supersymmetric potential. As $[A^+, A^-]$ depends on x the operators A^+ and A^- are not ladder operators. Therefore, introduce new operators whose commutator does not depend on dynamical variables. For this purpose we consider

$$A^+(\alpha_1)A^-(\alpha_1) - A^-(\alpha_2)A^+(\alpha_2) = R(\alpha_1), \tag{4.80}$$

where $\alpha_1 = \alpha$, $\alpha_2 = \alpha_1 + \eta$ and $R(\alpha_1)$ is the remainder term. Here

$$T^{-1}(\alpha_1)R(\alpha_n)T(\alpha_1) = R(\alpha_{n-1}), \tag{4.81}$$

where

$$T(\alpha_1)|\phi(\alpha_1)\rangle = |\phi(\alpha_2)\rangle, \quad T(\alpha_1)T^{-1}(\alpha_1) = 1. \tag{4.82}$$

Next, introduce $L_\pm(\alpha_1)$ as

$$L_-(\alpha_1) = T^{-1}(\alpha_1)A^+(\alpha_1), \quad L_+(\alpha_1) = A^-(\alpha_1)T(\alpha_1). \tag{4.83}$$

It is easy to verify that $[L_-(\alpha_1), L_+(\alpha_1)] = R(\alpha_0)$. Further, $R(\alpha_n)L_+(\alpha_1) = L_+(\alpha_1)R(\alpha_{n-1})$. Then the eigenvalues of $\widehat{H}$ (Eq. (4.77)) are given by

$$E_n = \sum_{k=1}^{n} R(\alpha_k) + E_0. \tag{4.84}$$

The eigenstates of $\widehat{H}$ can be obtained by considering

$$L_+(\alpha_1)|\phi_n\rangle = \left[\sum_{k=1}^{n+1} R(\alpha_k)\right]^{1/2} |\phi_{n+1}\rangle, \tag{4.85a}$$

$$L_-(\alpha_1)|\phi_n\rangle = \left[\sum_{k=1}^{n} R(\alpha_k)\right]^{1/2} |\phi_{n-1}\rangle. \tag{4.85b}$$

We obtain

$$|\phi_n\rangle = \frac{1}{\sqrt{\rho_n}}\left[L_+(\alpha_1)\right]^n |\phi_0\rangle, \tag{4.86a}$$

where

$$\rho_n = [R(\alpha_n) + R(\alpha_{n-1}) + \ldots + R(\alpha_1)]\ldots[R(\alpha_1)]. \tag{4.86b}$$

Coherent states $|z\rangle$ are given by

$$L_-|z\rangle = z|z\rangle, \quad |z\rangle = \sum_{n=0}^{\infty} C_n|\phi_n\rangle. \tag{4.87}$$

It is easy to show that

$$|z\rangle = \left(\sum_{n=0}^{\infty} \frac{(|z|^2)^n}{\rho_n}\right)^{-1/2} \sum_{n=0}^{\infty} \frac{z^n}{\sqrt{\rho^n}}|\phi_n\rangle. \tag{4.88}$$

4.7 Squeezed States

We noticed that for coherent states $(\Delta x)^2$ and $(\Delta p_x)^2$ are constant in time. In the following we consider a general linear combination state for which these uncertainties oscillate sinusoidally in time [12].

4.7.1 Definition

A state is said to be *squeezed* if its oscillating variances (or uncertainties) are smaller than the variances (or uncertainties) of the ground state. When the minimum value of the product of the variances become 1/4 then the state is referred to as a minimum uncertainties squeezed state.

A squeeze operator is defined as

$$S(r,\phi) = S(z) = \mathrm{e}^{(z^* a^2 - z a^{\dagger 2})/2}\,, \tag{4.89}$$

where the complex factor z has the form $z = r\mathrm{e}^{2\mathrm{i}\phi}$. The real numbers r and ϕ are called the *squeeze factor* and *squeeze angle*, respectively, of a squeezed state. r and ϕ are defined as $0 \le r < \infty$, $-\pi/2 < \phi \le \pi/2$. A squeezed state is denoted as $|\alpha, z\rangle$ or $|\beta\rangle$. It is generated by acting the displacement operator $D(\alpha)$ on the squeezed vacuum state $S(z)|0\rangle$:

$$|\beta\rangle = D(\alpha)S(z)|0\rangle\,. \tag{4.90}$$

Squeezing states are experimentally realized only in special linear combination states generated by certain nonlinear processes including parametric amplification, four-wave mixing and so on [27–33].

In classical mechanics, the average value of a sinusoidally varying quantity is written as $\langle x\rangle = 2\mathrm{Re}(A\mathrm{e}^{-\mathrm{i}t})$. The quantity $A\mathrm{e}^{-\mathrm{i}t}$ and $A^*\mathrm{e}^{\mathrm{i}t}$ are called *classical phasors*. When A and A^* are treated as input phasors then a general property of a nonlinear device is to produce a negative and positive frequency output phasors denoted as B and B^*. B and B^* are linear combination of A and A^*, that is,

$$B = \mu A + \nu A^*\,, \quad B^* = \mu^* A^* + \nu^* A\,, \tag{4.91}$$

where μ and ν are complex numbers. We can introduce operators to represent B and B^* as

$$b = \mu a + \nu a^\dagger\,, \quad b^\dagger = \mu^* a^\dagger + \nu^* a\,, \tag{4.92}$$

where $|\mu|^2 - |\nu|^2 = 1$. These operators possess certain interesting properties. It is possible to

set-up eigenfunctions of b by a similar manner used to obtain Eq. (4.36). The eigenfunctions of b are called *squeezed states*.

From Eq. (4.92) we write

$$\nu^* b = \nu^* \mu a + \nu^* \nu a^\dagger, \quad \mu b^\dagger = \mu\mu^* a^\dagger + \mu\nu^* a\,. \tag{4.93}$$

From the above equation we find

$$a^\dagger = \mu b^\dagger - \nu^* b, \quad a = \mu^* b - \nu b^\dagger\,. \tag{4.94}$$

4.7.2 Construction of Squeezed States

If we assume that a squeezed state $|\beta\rangle$ is an eigenstate of b with eigenvalue β then the eigenvalue equation is

$$b|\beta\rangle = \beta|\beta\rangle\,. \tag{4.95}$$

Let us choose

$$|\beta\rangle = \sum_{n=0}^{\infty} C_n|n\rangle\,. \tag{4.96}$$

Then Eq. (4.95) using Eq. (4.92) for b, gives

$$(\mu a + \nu a^\dagger)\sum_{n=0}^{\infty} C_n|n\rangle = \beta \sum_{n=0}^{\infty} C_n|n\rangle\,, \tag{4.97}$$

where C_n's are at time $t = 0$. Operating $\mu a + \nu a^\dagger$ on each term in $\sum C_n|n\rangle$ we arrive at the result

$$\mu \sum_{n=1}^{\infty} \sqrt{n}\, C_n|n-1\rangle + \nu \sum_{n=0}^{\infty} \sqrt{n+1}\, C_n|n+1\rangle = \beta \sum_{n=0}^{\infty} C_n|n\rangle\,. \tag{4.98a}$$

That is,

$$\begin{aligned} &\mu(C_1|0\rangle + \sqrt{2}\, C_2|1\rangle + \ldots) + \nu(C_0|1\rangle + \sqrt{2}\, C_1|2\rangle + \ldots) \\ &\quad = \beta(C_0|0\rangle + C_1|1\rangle + \ldots)\,. \end{aligned} \tag{4.98b}$$

Equating the coefficients of $|i\rangle$, $i = 0, 1, \ldots$ in both sides we get

$$C_n = \frac{\beta C_{n-1} - \nu\sqrt{n-1}\, C_{n-2}}{\mu\sqrt{n}}\,, \quad n = 1, 2, \ldots. \tag{4.99}$$

For fixed values of μ, ν and β starting with an arbitrary value of C_0 the values of the other C_n's can be calculated recursively from Eq. (4.99). The value of C_0 is fixed by the normalization condition $\sum_{n=0}^{\infty} |C_n|^2 = 1$.

Solved Problem 4:

Determine $\langle n\rangle$ for squeezed states.

We obtain $\langle n\rangle = \langle\beta|n|\beta\rangle$ as

$$\begin{aligned} \langle n\rangle &= \langle\beta|a^\dagger a|\beta\rangle \\ &= \langle\beta|(\mu b^\dagger - \nu^* b)(\mu^* b - \nu b^\dagger)|\beta\rangle \\ &= (\mu\beta - \nu\beta)(\mu^*\beta^* - \nu^*\beta^*) + |\nu|^2 \\ &= \beta^2(\mu - \nu)^2 + \nu^2\,. \end{aligned} \tag{4.100}$$

TABLE 4.1
Comparison of expectation values and variances of coherent and squeezed states.

Quantity	Coherent state	Squeezed state
$\langle n \rangle$	α^2	$\beta^2(\mu-\nu)^2+\nu^2$
$\langle x \rangle$	$\sqrt{2}\,\alpha\cos t$	$\sqrt{2}\,\beta(\mu-\nu)\cos t$
$\langle p_x \rangle$	$-\sqrt{2}\,\alpha\sin t$	$-\sqrt{2}\,\beta(\mu-\nu)\sin t$
$(\Delta n)^2$	α^2	$\beta^2(\mu-\nu)^4+2\mu^2\nu^2$
$(\Delta x)^2$	$1/2$	$(\mu^2+\nu^2-2\mu\nu\cos 2t)/2$
$(\Delta p_x)^2$	$1/2$	$(\mu^2+\nu^2+2\mu\nu\cos 2t)/2$

4.7.3 Expectation Values and Uncertainty Product

Table 4.1 summarizes the expectation values and the variances of x, p_x and n for both the coherent and the squeezed states (for the case of β, μ and ν being real). Δx and Δp_x of squeezed states oscillate with t. $(\Delta x)^2(\Delta p_x)^2$ is

$$(\Delta x)^2(\Delta p_x)^2 = \frac{1}{4}\left[(\mu^2+\nu^2)^2 - 4\mu^2\nu^2\cos^2 2t\right]\,. \tag{4.101}$$

The product of the variances also oscillates with time. The state $|\beta\rangle$ is a Gaussian wave packet. As it evolves its shape remains Gaussian but the width varies periodically. As Δx decreases, Δp_x increases and vice-versa. It cannot be treated as a minimum uncertainty wave packet because $\Delta x \Delta p_x$ is not always $\hbar/2$. However, we can choose the values of β, μ and ν such that, for part of the oscillatory cycle, $(\Delta x)^2$ or $(\Delta p_x)^2$ is less than $\hbar/2$ (the value corresponding to the vacuum state).

Suppose we choose $|\mu|^2 - |\nu|^2 = 1$. In this case at $t = 0, \pi/2, \pi, \ldots$

$$(\Delta x)^2(\Delta p_x)^2 = \frac{1}{4}\left[(\mu^2+\nu^2)^2 - 4\mu^2\nu^2\right] = \frac{1}{4}\,. \tag{4.102}$$

The minimum value of $(\Delta x)(\Delta p_x)$ is $1/2$ and the state is called a *minimum uncertainty squeezed state*. Let us consider the following two cases.

Case 1: $t = 0, \pi, 3\pi, \ldots$

From table 4.1 we note that when $t = 0, \pi, 3\pi, \ldots$ Δx and Δp_x assume their minimum and maximum values, respectively. They are given by

$$(\Delta x)^2 \to (\Delta x)^2_{\rm min} = \frac{1}{2}(\mu-\nu)^2\,, \tag{4.103a}$$

$$(\Delta p_x)^2 \to (\Delta p_x)^2_{\rm max} = \frac{1}{2}(\mu+\nu)^2\,, \tag{4.103b}$$

$$\Delta x \Delta p_x = \frac{1}{2}\,. \tag{4.103c}$$

Case 2: $t = \pi/2, 3\pi/2, \ldots$

When $t = \pi/2, 3\pi/2, \ldots$ Δx becomes a maximum value while Δp_x attains minimum:

$$(\Delta x)^2 \to (\Delta x)^2_{\max} = \frac{1}{2}(\mu + \nu)^2 , \tag{4.104a}$$

$$(\Delta p_x)^2 \to (\Delta p_x)^2_{\min} = \frac{1}{2}(\mu - \nu)^2 , \tag{4.104b}$$

$$\Delta x \Delta p_x = \frac{1}{2} . \tag{4.104c}$$

In both the cases we observe that $\Delta x \Delta p_x$ is minimum. However, Δx and Δp_x attains two extreme values. That is, the product $\Delta x \Delta p_x$ takes a minimum value $1/2$ only at the times that one variance is minimum whereas the other is maximum. In other words, in a squeezed state, the quantum variations in one observable are reduced below their value in a minimum uncertainty state at the expense of increased variations in the conjugate observable so that the uncertainty relation is not violated. This is a special property of squeezed states. Thus, the basic hallmark of squeezing is the reduction of quantum variations in the variances of the observables within the Heisenberg's uncertainty principle. Recall the corresponding property of a coherent state. For this state the fluctuations in the variances are equal and their product is the Heisenberg's minimum uncertainty relation.

The special property of squeezed state has an important application. In normal radiation field, as a consequence of the uncertainty principle, we cannot predict with desired accuracy, for example, both the amplitude and the phase of the electric field. The random variations restrict them to a certain minimum uncertainty, and as a result the product of the two is constrained by the Heisenberg's uncertainty principle. In a squeezed state, one of these characteristics can be well known, at the expense of large variances in the other. The suggestion is to make use of the well known component to perform a measurement of a physical quantity, which can then be known more accurately than if it were being measured by a randomly varying field. The detection of gravitation waves is a notable use for squeezed states. In such a device, squeezed light can be utilized to detect the minute vibrations generated in a metal bar by a gravitational wave.

4.7.4 Properties of Squeezed States

We summarize some of the characteristic properties of squeezed states.

1. $\langle x \rangle$ and $\langle p_x \rangle$ are nonzero and oscillating in time.
2. The variances of x and p_x oscillate in time 180° out of phase with one another with a frequency twice the frequency of the oscillator.
3. At any time, one variance becomes smaller than the square-root of the minimum uncertainty product.
4. A squeezed wave packet is sharply peaked initially then spread out and comes to its original state periodically.
5. Like coherent states, squeezed states can be represented by infinite series.
6. Quantum noise is not randomly distributed in phase.

4.7.5 Example

Let us consider the time evolution of the wave function of the linear harmonic oscillator given by

$$\psi(x,t) = \int G(x,x',t')\psi(x',0)\mathrm{d}x' \,, \tag{4.105a}$$

where

$$\begin{aligned} G(x,x',t) &= \left(\frac{m\nu}{2\pi\hbar|\sin\nu t|}\right)^{1/2} \\ &\quad \times\exp\left(\frac{\mathrm{i}m\nu}{2\hbar\sin\nu t}\left[(x^2+x'^2)\cos\nu t - 2xx'\right]\right) \end{aligned} \tag{4.105b}$$

with $\nu = \sqrt{mk}$. If at $t=0$, $\psi(x',0) = \delta(x'-x_0)$ then at $t = \pi/2\nu, \pi/\nu$ we have $\psi(x,0) = \delta(x-x_0)$ and

$$\psi\left(x,\frac{\pi}{2\nu}\right) = \sqrt{\frac{m\nu}{2\pi\hbar}}\,\mathrm{e}^{\mathrm{i}m\nu x_0 x/\hbar}, \quad \psi\left(x,\frac{\pi}{\nu}\right) = \delta(x+x_0)\,. \tag{4.106}$$

That is, the system will return to a sharp state every half period. This points out the possibility of a stroboscopic measurement, where we can make observations on the oscillator at time $t = 0, \pi/\nu, 2\pi/\nu, \ldots$ so that there is no limitation due to the width of the ground state wave function.

Solved Problem 5:

Show that $U = \mathrm{e}^{\xi(a^2 - a^{\dagger 2})/2}$, where $\mathrm{e}^{\xi} = \mu + \nu$ transforms a coherent state into a squeezed state. (Assume that $b = UaU^{\dagger}$ and $a = U^{\dagger}bU$.)

Assume that $|\alpha\rangle$ is a coherent state. Then $a|\alpha\rangle = \alpha|\alpha\rangle$. Let U transform $|\alpha\rangle$ into $|\beta\rangle$: $|\beta\rangle = U|\alpha\rangle$. We have to prove that $|\beta\rangle$ is an eigenstate of the operator b. Consider $U|\alpha\rangle = |\beta\rangle$. We get $\langle\beta| = \langle\alpha|U^{\dagger}$. Also,

$$\langle\beta|b|\beta\rangle = \langle\alpha|U^{\dagger}bU|\alpha\rangle\,. \tag{4.107}$$

Since $b = UaU^{\dagger}$, $a = U^{\dagger}bU$ we get

$$\langle\beta|b|\beta\rangle = \langle\alpha|a|\alpha\rangle = \alpha\langle\alpha|\alpha\rangle = \alpha\,. \tag{4.108}$$

Hence, $|\beta\rangle$ is an eigenstate of the operator b. Therefore, U transform the coherent state $|\alpha\rangle$ into a squeezed state $|\beta\rangle$.

4.7.6 Certain Squeezed States

One can define the *squeezed-entangled-state* (SES) as [34]

$$|\psi_{\mathrm{SES}}\rangle = \mathcal{N}(|z,0\rangle + |0,z\rangle), \quad \mathcal{N} = \frac{1}{\sqrt{2}\left(1+\frac{1}{\cosh|z|}\right)^{1/2}}\,. \tag{4.109}$$

For a large squeezing regime, $|z| \gg 1$ we have $\mathcal{N} \approx 1/\sqrt{2}$. The *squeezed cat state* (SCS) is defined as [34]

$$|\psi_{\mathrm{SCS}}\rangle = \mathcal{N}S(z)(|\alpha\rangle + |-\alpha\rangle), \quad \mathcal{N} = \frac{1}{\sqrt{2}\sqrt{1+\mathrm{e}^{-2\alpha^2}}}. \tag{4.110}$$

Experimentally, the SCSs have been generated [35–36].

4.8 Deformed Oscillators and Nonlinear Coherent States

The eigenstates of an operator $f(\hat{n})a$, where $f(\hat{n})$ is an operator-valued function of $\hat{n}$, are defined through

$$f(\hat{n})a|\alpha, f\rangle = \alpha|\alpha, f\rangle\,. \tag{4.111}$$

The eigenstates $|\alpha, f\rangle$ are called *nonlinear coherent states* [37–39] and are nonclassical. These states have been introduced in the study of deformed oscillators whose frequency depends on its energy.

4.8.1 Deformed Operators

For the harmonic oscillator

$$a = \frac{1}{\sqrt{2}}\left(x + \frac{\mathrm{d}}{\mathrm{d}x}\right),\quad a^\dagger = \frac{1}{\sqrt{2}}\left(x - \frac{\mathrm{d}}{\mathrm{d}x}\right),\quad \hat{n} = a^\dagger a, \tag{4.112}$$

where we have set the mass and $\hbar$ as unity, the Hamiltonian $H = p_x^2/2 + x^2/2$ is expressed in terms of a and $a^\dagger$ as

$$H = \frac{1}{2}\left(aa^\dagger + a^\dagger a\right) = \left(a^\dagger a + \frac{1}{2}\right)\,. \tag{4.113}$$

Now, deform the operators a and $a^\dagger$ with an operator-valued function, say, $f(\hat{n})$, and define two operators A and $A^\dagger$ as

$$A = af(\hat{n}) = f(\hat{n}+1)a,\quad A^\dagger = f^\dagger(\hat{n})a^\dagger = a^\dagger f^\dagger(\hat{n}+1)\,. \tag{4.114}$$

When f is chosen as real and nonnegative then $f^\dagger = f$. The commutator of A and $A^\dagger$ is worked out as

$$\begin{aligned}
[A, A^\dagger] &= AA^\dagger - A^\dagger A \\
&= af(\hat{n})f^\dagger(\hat{n})a^\dagger - f^\dagger(\hat{n})a^\dagger a f(\hat{n}) \\
&= f(\hat{n}+1)aa^\dagger f^\dagger(\hat{n}+1) - f^\dagger(\hat{n})nf(\hat{n}) \\
&= f(\hat{n}+1)(a^\dagger a + 1)f^\dagger(\hat{n}+1) - nf^\dagger(\hat{n})f(\hat{n}) \\
&= (n+1)f(\hat{n}+1)f^\dagger(\hat{n}+1) - nf^\dagger(\hat{n})f(\hat{n})\,.
\end{aligned} \tag{4.115a}$$

Also, we have

$$AA^\dagger + A^\dagger A = (n+1)f(\hat{n}+1)f^\dagger(\hat{n}+1) + nf^\dagger(\hat{n})f(\hat{n})\,. \tag{4.115b}$$

Notice that $[A, A^\dagger] \neq 1$ which means that the transformation from a to A is noncanonical.

In analogy with the Hamiltonian in Eq. (4.113) introduce a Hamiltonian in terms of the deformed operators A and $A^\dagger$ as

$$H_{\mathrm{M}} = \frac{1}{2}\left(AA^\dagger + A^\dagger A\right)\,. \tag{4.116}$$

The above Hamiltonian was introduced by Man'ko et al [38]. The oscillators represented by the above Hamiltonian is termed as f-deformed oscillators or simply f-oscillators. The

eigenstates of $H_{\rm M}$ are the same as that of the H given by Eq. (4.113). This is because f is a function of $\hat{n}$. The eigenvalues of the above Hamiltonian are

$$E_n = \frac{1}{2}\left[(n+1)f(n+1)f^\dagger(n+1) + nf(n)f^\dagger(n)\right] . \tag{4.117}$$

Energy values are nonlinear functions of n. Deformed oscillators are realized as realistic systems such as matter-radiation interaction and polyatomic molecules. In polyatomic molecule the potential energy between the atoms has anharmonic terms. We can regard the deformed oscillators as a kind of anharmonic oscillator and in this sense they are appropriate to describe the vibrations of polyatomic molecules [40].

4.8.2 Examples of Deformed Oscillators

Consider the classical oscillator with $H = (p_x^2 + x^2)/2$. In terms of

$$\alpha = \frac{1}{\sqrt{2}}\left(x + \mathrm{i}p_x\right), \quad \alpha^* = \frac{1}{\sqrt{2}}\left(x - \mathrm{i}p_x\right) \tag{4.118}$$

(for which the Poisson bracket $\{\alpha, \alpha^*\} = -\mathrm{i}$) the above H becomes $H = \alpha\alpha^*$. Introduce two new variables [38]

$$\beta = \sqrt{\frac{\sinh(\lambda\alpha\alpha^*)}{\alpha\alpha^*\sinh\lambda}}\,\alpha, \quad \beta^* = \sqrt{\frac{\sinh(\lambda\alpha\alpha^*)}{\alpha\alpha^*\sinh\lambda}}\,\alpha^* . \tag{4.119}$$

Now, we have

$$\{\beta, \beta^*\} = -\frac{\mathrm{i}\lambda}{\sinh\lambda}\sqrt{1 + |\beta|^4\sinh\lambda} = -\frac{\mathrm{i}\lambda}{\sinh\lambda}\sqrt{1 + \sinh^2|\alpha|^2} \tag{4.120}$$

and $H = \beta\beta^*$. The equation of motion of β is

$$\dot{\beta} = \{\beta, H\} = -\frac{\mathrm{i}\lambda}{\sinh\lambda}\sqrt{1 + |\beta|^4\sinh^2\lambda} . \tag{4.121}$$

Its solution is

$$\begin{aligned}\beta(t) &= \beta(0)\exp\left(-\frac{\mathrm{i}\lambda t}{\sinh\lambda}\sqrt{1 + |\beta(0)|^4\sinh^2\lambda}\right) \\ &= \beta(0)\exp\left(-\frac{\mathrm{i}\lambda t}{\sinh\lambda}\cosh(\lambda\alpha\alpha^*)\right) .\end{aligned} \tag{4.122}$$

Or we write

$$\beta(t) = \beta(0)\mathrm{e}^{-\mathrm{i}\omega t}, \quad \omega = \frac{\lambda}{\sinh\lambda}\cosh(\lambda\alpha\alpha^*) , \tag{4.123}$$

where ω is the frequency of oscillation of β. The Hamiltonian of this system in terms of α and α^* is

$$H = \frac{\sinh(\lambda\alpha\alpha^*)}{\sinh\lambda} . \tag{4.124}$$

We note that both the energy and the frequency of oscillation grow with $\alpha\alpha^*$ due to the deformation function used. Application of $\alpha \to a$ to Eq. (4.119) makes β to be the A given by Eq. (4.114a) with

$$f(\hat{n}) = \sqrt{\frac{\sinh(\lambda\hat{n})}{\sinh(\lambda)\hat{n}}} . \tag{4.125}$$

Suppose $\mathrm{e}^\lambda = q$. Then we find that $[A, A^\dagger] = q^{-a^\dagger a}$. The system is called a *q-deformed oscillator*.

4.8.3 Nonlinear Coherent States

We can say that nonlinear coherent states are the eigenstates of the deformed annihilation operator A:

$$A|\alpha, f\rangle = \alpha|\alpha, f\rangle. \tag{4.126}$$

Let us express $|\alpha, f\rangle$ as

$$|\alpha, f\rangle = \sum_{n=0}^{\infty} C_n|n\rangle\,, \tag{4.127}$$

where we have written $|\hat{n}\rangle$ as $|n\rangle$. To determine C_n, substitute (4.127) in (4.126). Premultiplying by $\langle m|$ and replace A by $af(n)$ give (verify)

$$\sum \langle m|f(n)C_n\sqrt{n}\,|n-1\rangle = \alpha \sum C_n\langle m|n\rangle\,. \tag{4.128}$$

The above equation yields the recursion relation

$$C_{n+1}\sqrt{n+1}\,f(n+1) = \alpha C_n\,. \tag{4.129}$$

That is,

$$C_{n+1} = \frac{\alpha C_n}{\sqrt{n+1}\,f(n+1)}\,. \tag{4.130}$$

Replacing n by $n-1$ successively gives

$$C_n = \frac{\alpha C_{n-1}}{\sqrt{n}\,f(n)} = \frac{\alpha^2 C_{n-2}}{\sqrt{n(n-1)}\,f(n)f(n-1)} \ldots = \frac{\alpha^n C_0}{\sqrt{n!}\,[f(n)]!}\,. \tag{4.131}$$

The normalization condition $\langle\alpha, f|\alpha, f\rangle = 1$ yields

$$C_0 = \left(\sum_{n=1}^{\infty} \frac{|\alpha|^{2n}}{n!\,|\,[f(n)\,]!|^2}\right)^{-1/2} = N_{f,\alpha}\,. \tag{4.132}$$

In order to have $0 < |N_{f,\alpha}| < \infty$ the requirement is

$$|\alpha| \leq \lim_{n\to\infty} n|f(n)|^2. \tag{4.133}$$

Similar to the coherent states $|\alpha\rangle$, two distinct nonlinear coherent states $|\alpha, f\rangle$ and $|\beta, f\rangle$ are not orthogonal since

$$\langle\alpha, f|\beta, f\rangle = N_{f,\alpha}N_{f,\beta}\sum_{n=0}^{\infty} \frac{(\alpha^*\beta)^n}{n!\,|\,[f(n)]!\,|^2} \neq 0. \tag{4.134}$$

It has been shown that in wave guide arrays with certain types of coupling coefficients the light evolution can be used to obtain classical analogue of nonlinear coherent states [41].

4.8.4 Photon Added Coherent States

Nonlinear coherent states are realized in a trapped ion [39] and in an interaction of a two-level atom with a cavity field [42].

The photon-added coherent states, denoted as $|\alpha, m\rangle$, given by

$$|\alpha, m\rangle = \frac{(a^\dagger)^m|\alpha\rangle}{\sqrt{\langle\alpha|a^m(a^\dagger)^m|\alpha\rangle}}\,, \tag{4.135}$$

where m is a nonnegative integer, is a nonlinear state. These states possess phase squeezing and sub-Poissonian statistics. These states are realized where two level atom with a ground state and excited state interacts with a single-mode cavity field. Suppose we define the operator representing the transition from ground state $|g\rangle$ to the excited state $|e\rangle$ as $\hat{\sigma}_+$ and $\hat{\sigma}_-$ is that of $|e\rangle \to |g\rangle$. If g is the coupling constant then the Hamiltonian of the system is [42]

$$H_{\text{int}} = \hbar g(\hat{\sigma}_+ a + \hat{\sigma}_- a^\dagger)\,. \tag{4.136}$$

For a detailed discussion on $|\alpha, -m\rangle$ and its squeezing features and about photon-added coherent states one may refer to refs. [43–45].

4.8.5 Certain Other Coherent States

Let us point out some of the coherent states introduced and the connection of them to the nonlinear coherent states [46]. Klauder, Penson and Sixdeniers (KPS) [47] introduced the states

$$|\alpha\rangle_{\text{KPS}} = N(|\alpha|^2)^{-1/2}\sum_{n=0}^{\infty}\frac{z^n}{\rho(n)}\,|n\rangle\,, \quad N(|\alpha|^2) = \sum_{n=0}^{\infty}\frac{|\alpha|^{2n}}{\rho(n)}, \tag{4.137}$$

where $\rho(0) = 1$. For KPS states $f(n) = \sqrt{e_n/n}$.

The Gazeau–Klauder (GK) coherent states [48] are defined as

$$|J, \gamma\rangle = N(J)^{-1/2}\sum_{n=0}^{\infty}\frac{J^{n/2}\mathrm{e}^{-\mathrm{i}e_n\gamma}}{\sqrt{\rho(n)}}\,|n\rangle, \quad N(J) = \sum_{n=0}^{\infty}\frac{J^n}{\rho(n)}\,, \tag{4.138}$$

where $\rho(0) = 1$, $J \geq 0$ and $-\infty < \gamma < \infty$. In Eq. (4.138a) $|n\rangle$ are the eigenstates of H:

$$H|n\rangle = E_n|n\rangle = e_n|n\rangle, \quad n = 0, 1, 2, \ldots \tag{4.139}$$

where $\hbar$ is set unity and $\rho(n) = (e_n)!$.

The Penson and Solomon [49] coherent states assume the form

$$|q, \alpha\rangle_{\text{PS}} = \left[N(q, |\alpha|^2\right]^{-1/2}\sum_{n=0}^{\infty}\frac{q^{n(n-1)/2}}{\sqrt{n!}}\,\alpha^n|n\rangle\,, \tag{4.140}$$

where $0 \leq q \leq 1$. It can be shown that for these states $f(n) = q^{1-n}$.

Another type of coherent state given by Barut and Girardello [50] is

$$|\alpha, \kappa\rangle_{\text{BG}} = N(|z|^2)^{-1/2}\sum_{n=0}^{\infty}\frac{z^n}{\sqrt{n!}}\,\frac{|n\rangle}{\sqrt{n+2\kappa}}, \quad \kappa = 1, 3/2, 2, \ldots\,. \tag{4.141}$$

For these states

$$f(n) = \sqrt{n+2\kappa-1}, \quad H = n(n+2\kappa-1), \quad n = 0, 1, 2, \ldots\,. \tag{4.142}$$

4.9 Concluding Remarks

Coherent states were constructed for many interesting potentials including infinite well and Poschl-Teller potentials [51] and Morse potential [52,53]. The coherent states of a free particle [54], a harmonic oscillator with time-dependent frequency [55,56], harmonic oscillator driven by a periodic external force [57], generalized time-dependent harmonic oscillator [58], damped and force harmonic oscillator [59], charged particle in a time-dependent electromagnetic field [60,61] and general potentials [62–64] and graphene [65–67] have been investigated. For discussion on coherent states of hydrogen atom see ref. [68].

Delayed luminescence of biological systems has been characterized in terms of coherent states [69]. Coherent states based on quantum key distribution [70], teleportation [71,72], quantum cryptography [73,74], quantum computation [75,76], secure communication [77] and characterization of quantum optical processes [78,79] have been investigated. Storage and transmission [80], cloning [81–83] and generation via cross phase-modulation in a double electromagnetically induced transparency regime [84] of coherent states were reported.

Squeezed states in a Bose-Einstein condensate [85,86], Jaynes-Cummins model [87], nanomechanical resonators [88], de Sitter vacuum [89], time-dependent harmonic oscillator [90], generalized parametric oscillator [91,92] and two mechanical oscillators [93] were obtained. Use of squeezed states in quantum cryptography [94], quantum distribution of keys [95,96], extended coherence time [97], quantum engineering [98], teleportation [99], optics [100,101], detection of gravitational waves [102,103], quantum metrology [104–108] and laser interferometers [109] have been analyzed. Nonclassical and decoherence properties [110,111], purification [112] and observation with strong photon-number oscillations [113] of squeezed states have been discussed.

4.10 Bibliography

[1] E. Schrödinger, *Naturwiss.* 14:664, 1926.

[2] J.R. Klauder and B.S. Skagerstam, *Coherent States–Applications in Physics and Mathematical Physics.* World Scientific, Singapore, 1985.

[3] A. Perelomov, *Generalized Coherent States and Their Applications.* Springer, New York, 1986.

[4] M.O. Scully and M.S. Zubairy, *Quantum Optics.* Cambridge University Press, Cambridge, 1998.

[5] A. Joshi and S.V. Lawande, *Current Science* 82:816, 2002.

[6] M.M. Nieto and L.M. Simmons, *Phys. Rev. Lett.* 41:207, 1978.

[7] B. Bagchi, R. Ghosh and A. Khare, *Int. J. Mod. Phys. A* 35:2030011, 2020.

[8] D.F. Walls, *Nature* 306:141, 1983.

[9] J.H. Shapiro, H.P. Yuen and J.A. Machado Mata, *IEEE Trans. Inf. Theory* 25:179, 1979.

[10] See for example, the special issues on squeezed states of light: *J. Mod. Opt.* 34:709, 1987; *J. Opt. Soc. Am. B* 4:1450, 1987.

[11] S. Howard and S.K. Roy, *Am. J. Phys.* 55:1109, 1987.

[12] R.W. Henry and S.C. Glotzer, *Am. J. Phys.* 56:318, 1988.

[13] I.R. Senitzky, *Phys. Rev.* 95:1115, 1954.

[14] M.F. Marhic, *Lett. Nuovo Cim.* 22:376, 1978.

[15] T.G. Philbin, *Am. J. Phys.* 82:742, 2014.

[16] J.M. Radcliffe, *J. Phys. A* 4:313, 1971.

[17] A. Auerbach, *Interacting Electrons and Quantum Magnetism*. Springer, New York, 1998.

[18] P.K. Aravind, *Am. J. Phys.* 67:899, 1999.

[19] Y.L. Loh and M. Kim, *Am. J. Phys.* 83:30, 2015.

[20] O.N. Amir and S. Iqbal, *Commun. Theor. Phys.* 66:615, 2016.

[21] O. Von Roos, *Phys. Rev. B* 27:7547, 1983.

[22] M.R. Geller and W. Kohn, *Phys. Rev. Lett.* 70:3103, 1993.

[23] A.R. Plastino, A. Rigo, M. Casas, F. Garcias and A. Plastino, *Phys. Rev. A* 60:4318, 1999.

[24] A.J. Peter and K. Navaneetha Krishnana, *Physica E* 40:2747, 2008.

[25] N. Amir and S. Iqbal, *Commun. Theor. Phys.* 62:790, 2014.

[26] N. Amir and S. Iqbal, *J. Math. Phys.* 57:062105, 2016.

[27] H.P. Yuen and J.H. Shapiro, *Opt. Lett.* 4:334, 1979.

[28] R.E. Slusher, L.W. Hollberg, B. Yurke, J.C. Mertz and J.F. Valley, *Phys. Rev. Lett.* 55:2409, 1985.

[29] R.M. Shelby, M.D. Levenson, S.H. Perlmutter, R.G. DeVoe and D.F. Walls, *Phys. Rev. Lett.* 57:691, 1986.

[30] Ling-An Wu, H.J. Kimble, J.L. Hall and H. Wu, *Phys. Rev. Lett.* 57:2520, 1986.

[31] M.N. Maeda, P. Kumar and J.H. Shapiro, *J. Opt. Soc. Am. B* 4:1501, 1987.

[32] S. Machida and Y. Yamamoto, *Phys. Rev. Lett.* 60:792, 1988.

[33] D.M. Greenberger and A. Zeilinger, *Phys. World*, September 1995 pp.33.

[34] P.A. Knott, T.J. Proctor, A.J. Hayes, J.P. Cooling and J.A. Dunningham, *Phys. Rev. A* 93:033859, 2016.

[35] A. Ourjoumtsev, H. Jeong, R. Tualle-Brouri and P. Grangier, *Nature* 448:784, 2007.

[36] J. Etesse, M. Bouilland, B. Kanseri and R. Tualle-Brouri, *Phys. Rev. Lett.* 114:193602, 2015.

[37] V.I. Man'ko, Wigner function, squeezing, Schrödinger cats and tomography. In Proceedings of the IV Wigner Symposium. Eds.: N.M. Atakishiyev, T.H. Seligman and K.B. Wolf. World Scientific, Signapore, 1996, pp. 148-157.

[38] V.I. Man'ko, G. Marmo, F. Zaccaria and E.C.G. Sudarshan, *Phys. Scr.* 55:528, 1997.

[39] R.L. de Matos and W. Vogel, *Phys. Rev. A* 54:4560, 1996.

[40] D. Bonatsos and C. Daskaloyannis, *Phys. Rev. A* 46:75, 1992; 48:3611, 1992.

[41] A.P. Loreto and D.N. Christodoulides, *Opt. Commun.* 284:1833, 2011.

[42] G.S. Agarwal and K. Tara, *Phys. Rev. A* 43:492, 1991.

[43] S. Sivakumar, *J. Phys. A: Math. Gen.* 32:3441, 1999.

[44] S. Sivakumar, *J. Opt. B: Quantum Semiclass. Opt.* 2:R61, 2000.

[45] S. Sivakumar, *Phys. Rev. A* 83:035802, 2011.

[46] R. Roknizadeh and M.K. Tavassoly, *J. Phys. A: Math. Gen.* 37:8111, 2004.

[47] J.R. Klauder, K.A. Penson and J.M. Sixdeniers, *Phys. Rev. A* 64:013817, 2001.

[48] J.P. Gazeau and J.R. Klauder, *J. Phys. A: Math. Gen.* 32:123, 1999.

[49] K.A. Penson and A.I. Solomon, *J. Math. Phys.* 40:2354, 1999.

[50] A.O. Barut and L. Girardello, *Commun. Math. Phys.* 21:41, 1971.

[51] J.P. Antoine, J.P. Gazeau, P. Monceau, J.R. Klauder and K.A. Penson, *J. Math. Phys.* 42:2349, 2001.

[52] M.G. Benedict and B. Molnar, *Phys. Rev. A* 60:1737(R), 1999.

[53] M. Angelova and V. Hussin, *J. Phys. A* 41:304016, 2008.

[54] M. Maamache, A. Khatir, H. Lakehal and J.R. Choi, *Sci. Rep.* 6:30538, 2016.

[55] J.R. Ray, *Phys. Rev. D* 25:3417, 1982.

[56] K.H. Yeon and C.I. Um, *J. Korean Phys. Soc.* 25:567, 1992.

[57] L.O. Castanos and A. Zuniga-Segundo, *Am. J. Phys.* 87:815, 2019.

[58] J.R. Choi, *Pramana J. Phys.* 62:13, 2004.

[59] V.V. Dodonov and V.I. Man'ko, *Phys. Rev. A* 20:550, 1979.

[60] I.A. Malkin, V.I. Man'ko and D.A. Trifonov, *Phys. Rev. D* 2:1371, 1970.

[61] V.V. Dodonov, I.A. Malkin and V.I. Man'ko, *Physica* 59:241, 1972.

[62] M.M. Nieto and L.M. Simmons Jr., *Phys. Rev. Lett.* 41:207, 1978.

[63] L. Parker, *Phys. Rev. D* 19:438, 1979.

[64] M.M. Nieto and L.M. Simmons Jr., *Phys. Rev. D* 20:1321, 1332, 1342, 1979.

[65] E. Diaz-Bautista and D.J. Fernandez, *Eur. Phys. J. Plus* 132:499, 2017.

[66] E. Diaz-Bautista, J. Negro and P. Roy, *Physica E* 96:17, 2018.

[67] D.J. Fernandez and D.I. Martinez-Moreno, *Eur. Phys. J. Plus* 135:739, 2020.

[68] J.R. Klauder, *J. Phys. A* 29:L293, 1996.

[69] F.A. Popp and Y. Yan, *Phys. Lett. A* 293:93, 2002.

[70] F. Grosshans, G. Van Assche, J. Wenger, R. Brouri, N.J. Cerf and Ph. Grangier, *Nature* 421:238, 2003.

[71] S.J. van Enk and O. Hirota, *Phys. Rev. A* 64:022313, 2001.

[72] X. Wang, *Phys. Rev. A* 64:022303, 2001.

[73] F. Grosshans and P. Grangier, *Phys. Rev. Lett.* 88:057902, 2002.

[74] X.B. Wang, *Phys. Rev. A* 72:012322, 2005.

[75] H. Jeong and M.S. Kim, *Phys. Rev. A* 65:042305, 2002.

[76] T.C. Ralph, A. Gilchrist, G.J. Milburn, W.J. Munro and S. Glancy, *Phys. Rev. A* 68:042319, 2003.

[77] G.A. Barbosa, E. Corndorf, P. Kumar and H.P. Yuen, *Phys. Rev. Lett.* 90:227901, 2003.

[78] S.R. Keshari, A. Scherer, A. Mann, A.T. Rezakhani, A.I. Lvovsky and B.C. Sanders, *New J. Physics* 13:013006, 2011.

[79] M. Lobino, D. Korystov, C. Kupchak, E. Figueroa, B.C. Sanders and A.I. Lvovsky, *Science* 322:563, 2008.

[80] K. Hammerer, M.M. Wolf, E.S. Polzik and J.I. Cirac, *Phys. Rev. Lett.* 94:150503, 2005.

[81] S.L. Braunstein, N.J. Cerf, S. Iblisdir, P. van Loock and S. Massar, *Phys. Rev. Lett.* 86:4938, 2001.

[82] U.L. Andersen, V. Josse and G. Leuchs, *Phys. Rev. Lett.* 94:240503, 2005.

[83] N.J. Cerf, O. Kruger, P. Navez, R.F. Werner and M.M. Wolf, *Phys. Rev. Lett.* 95:070501, 2005.

[84] M. Paternostro, M.S. Kim and B.S. Ham, *Phys. Rev. A* 67:023811, 2003.

[85] C. Orzel, A.K. Tuchman, M.L. Fenselau, M. Yasuda and M.A. Kasevich, *Science* 291:2386, 2001.

[86] A. Lamacraft, *Nat. Phys.* 8:254, 2012.

[87] P. Meystre and M.S. Zubairy, *Phys. Lett. A* 89:390, 1982.

[88] P. Rabl, A. Shnirman and P. Zoller, *Phys. Rev. B* 70:205304, 2004.

[89] M.B. Einhorn and F. Larsent, *Phys. Rev. D* 68:064002, 2003.

[90] K.H. Yeon, H.J. Kim, C.I. Um, T.F. George and L.N. Pandey, *Phys. Rev. A* 50:1035, 1994.

[91] S.A. Buyukasik and Z. Cayic *J. Math. Phys.* 60:062104, 2019.

[92] S.A. Buyukasik and Z. Cayic *J. Phys.: Conf. Series* 1194:012018, 2019.

[93] F. Xue, Y. Liu, C.P. Sun and F. Nori, *Phys. Rev. B* 76:064305, 2007.

[94] M. Hillery, *Phys. Rev. A* 61:022309, 2000.

[95] N.J. Cerf, M. Levy and G. Van Assche, *Phys. Rev. A* 63:052311, 2001.

[96] D. Gottesman and J. Preskill, *Phys. Rev. A* 63:022309, 2001.

[97] W. Li, A.K. Tuchman, H.C. Chien and M.A. Kasevich, *Phys. Rev. Lett.* 98:040402, 2007.

[98] H. Vahlbruch, S. Chelkowski, K. Danzmann and R. Schnabel, *New J. Phys.* 9:371, 2007.

[99] G. Adesso and G. Chiribella, *Phys. Rev. Lett.* 100:170503, 2008.

[100] Y. Yamamoto and H.A. Haus, *Rev. Mod. Phys.* 58:1001, 1986.

[101] C.M. Caves, *Phys. Rev. D* 23:1693, 1981.

[102] H. Vahlbruch, S. Chelkowski, B. Hage, A. Franzen, K. Danzmann and R. Schnabel, *Phys. Rev. Lett.* 97:011101, 2006.

[103] S.S.Y. Chua, B.J.J. Slagmolen, D.A. Shaddock and D.E. McClell, *Class. Quantum Grav.* 31:183001, 2014.

[104] H. Vahlbruch, S. Chelkowski, K. Danzmann and R. Schnabel, *New J. Phys.* 9:371, 2007.

[105] J.P. Dowling, *Contemp. Phys.* 49:125, 2008.

[106] R. Schnabel, N. Mavalvala, D.E. McClell and P.K. Lam, *Nature Commun.* 1:121, 2010.

[107] P.M. Anisimov, G.M. Raterman, A. Chiruvelli, W.N. Plick, S.D. Huver, H. Lee and J.P. Dowling, *Phys. Rev. Lett.* 104:103602, 2010.

[108] V. Giovannetti, S. Lloyd and L. Maccone, *Nature Photonics* 5:222, 2011.

[109] R. Schnabel, *Phys. Rep.* 684:1 2017.

[110] A. Biswas and G.S. Agarwal, *Phys. Rev. A* 75:032104, 2007.

[111] K. Zelaya, S. Dey and V. Hussin, *Phys. Lett. A* 382:3369, 2018.

[112] A. Franzen, B. Hage, J. DiGuglielmo, J. Fiurasek and R. Schnabel, *Phys. Rev. Lett.* 97:150505, 2006.

[113] M. Mehmet, H. Vahlbruch, N. Lastzka, K. Danzmann and R. Schnabel, *Phys. Rev. A* 81:013814, 2010.

[114] R. Roman-Ancheyta, O. de los Santos-Sanchez and J. Recamier, *J. Phys. A: Math. Theor.* 44:435304, 2011.

4.11 Exercises

4.1 Show that $|n\rangle = \dfrac{(a^\dagger)^n|0\rangle}{\sqrt{n!}}$.

4.2 Find whether the operators a and $a^\dagger$ are Hermitian.

4.3 Show that the ground state of linear harmonic oscillator with the new set of annihilation and creation operators $b = a - z$ and $b^\dagger = a^\dagger - z^*$ (z is a complex number) is a coherent state.

4.4 Find out whether the ground state of a simple harmonic oscillator driven by a constant force F is a coherent state.

4.5 Show that in configuration space the coherent states are just displaced ground state of the harmonic oscillator given by $\phi(x) = (m\omega/\pi\hbar)^{1/4}\mathrm{e}^{-m\omega(x-x_0)^2/(2\hbar)}$.

4.6 Express the coherent state $|\alpha\rangle = \mathrm{e}^{-|\alpha|^2/2}\sum_n \dfrac{\alpha^n}{\sqrt{n!}}|n\rangle$ in terms of the vacuum state $|0\rangle$.

4.7 Show that the creation operator $a^\dagger$ does not possess eigenfunctions.

4.8 Compute the values of

(a) $\langle\alpha|\alpha\rangle$, (b) $(1/\pi)\int|\alpha\rangle\langle\alpha|\,\mathrm{d}^2\alpha$, (c) $|\,|\alpha\rangle - |\alpha'\rangle\,|^2$ and (d) $\langle n\rangle$.

4.9 Using the identity $\mathrm{e}^A B\,\mathrm{e}^{-A} = B + [A,B] + \dfrac{1}{2!}[A,[A,B]] + \ldots$ determine $D^\dagger(\alpha)aD(\alpha) = \mathrm{e}^{-\alpha a^\dagger + \alpha^* a}a\,\mathrm{e}^{\alpha a^\dagger - \alpha^* a}$.

4.10 Using the identity given in the previous exercise show that $D^\dagger(\alpha) = D^{-1}(\alpha) = D(-\alpha)$.

4.11 Using the Weyl identity $\mathrm{e}^{A+B} = \mathrm{e}^{-[A,B]/2}\,\mathrm{e}^A\,\mathrm{e}^B$ which is valid for any two operators A and B satisfying the relations $[A,[A,B]] = [B,[A,B]] = 0$ show that the coherent state $|\alpha\rangle$ can be written in an equivalent form $|\alpha\rangle = \mathrm{e}^{-(|\alpha|^2-\alpha^2)/2}\,\mathrm{e}^{-\mathrm{i}\sqrt{2}\,\alpha p_x}|0\rangle$.

4.12 Starting from $|\alpha(x,t)\rangle = \mathrm{e}^{-\mathrm{i}t/2}\,|\alpha(t)\rangle$, where $\alpha(t) = \alpha(x,0)\,\mathrm{e}^{-\mathrm{i}t}$ determine $|\,|\alpha(x,t)\rangle\,|^2$.

4.13 The energy eigenvalues and eigenfunctions of the Pöschl–Teller potential $V(x) = V_0 \tan^2(ax)$, where a is the range of the potential are

$$\begin{aligned} E_n &= \frac{1}{2}\hbar^2 a^2 \left(n^2 + 2n\lambda + \lambda\right), \quad \lambda(\lambda+1) = \frac{2V_0}{\hbar^2 a^2} \\ \psi_n^{\lambda}(x) &= \sqrt{\frac{a(\lambda+n)\Gamma(2\lambda+n)}{\Gamma(n+1)}}\, \sqrt{\cos ax}\, P^{\frac{1}{2}-\lambda}_{n+\lambda-\frac{1}{2}}(\sin ax). \end{aligned}$$

Obtain the ladder operators and construct the coherent states [114].

4.14 For coherent states calculate $\langle x\rangle$, $\langle x^2\rangle$, $\langle p_x\rangle$, $\langle p_x^2\rangle$, $(\Delta x)^2$ and $(\Delta p_x)^2$.

4.15 Compute $\langle n\rangle$, $\langle n^2\rangle$ and then $(\Delta n)^2$ for coherent states.

4.16 Determine the coherent states of a linear harmonic oscillator with the potential $V(x) = \frac{1}{2}m(x)\alpha^2 x^2$, where $m(x) = 1/(1-(\lambda x)^2)$ and $x^2 \leq 1/\lambda^2$ [20].

4.17 For a system with $V(x) = \frac{1}{2}m(x)\alpha^2 x^2$, $m(x) = 1/(1+\lambda x^2)$, construct its coherent states [20].

4.18 Calculate $\langle x\rangle$, $\langle p_x\rangle$, $\langle n\rangle$, $(\Delta x)^2$, $(\Delta p_x)^2$ and $(\Delta n)^2$ for squeezed states.

4.19 Show that the transformation $a = \mu b - \nu b^\dagger$, $a^\dagger = \lambda b^\dagger - \nu b$ with the condition $\lambda^2 - \nu^2 = 1$ leads to squeezed states.

4.20 Given the transformation $b = \mu a + \nu a^\dagger$, $b^\dagger = \mu a^\dagger + \nu a$, where μ and ν are real numbers that are related by the condition $\mu^2 - \nu^2 = 1$, prove that the operators a and b are related by a unitary transformation $b = UaU^\dagger$ where $U = \mathrm{e}^{\xi(a^2 - a^{\dagger 2})/2}$ and $\mathrm{e}^{\xi} = \mu + \nu$. Also, show that U transform a coherent state into a squeezed state.

Taylor & Francis
Taylor & Francis Group
http://taylorandfrancis.com

5

Berry's Phase, Aharonov–Bohm and Sagnac Effects

5.1 Introduction

Consider a quantum mechanical system beginning at a time t_i with an eigenstate $\psi_n(\mathbf{x}, t_i)$. Suppose its potential is slowly changing. We assume that $\partial H/\partial t$ is very small. Then according to adiabatic approximation the wave function ψ of the system is given by

$$\psi(t) = \sum_n a_n(t)\psi_n(t)\, \mathrm{e}^{-\mathrm{i}\int_{t_i}^{t} E_n(t')\,\mathrm{d}t'} \,, \tag{5.1}$$

where a_n's are unknown to be determined, E_n is the energy eigenvalue of nth state and $\sum$ runs over all possible states. The phase factor $-\mathrm{i}\int_{t_i}^{t} E_n(t')\,\mathrm{d}t'$ is called the *dynamical phase*. In adiabatic approximation the initial state $\psi_n(t_i)$ changes into $\psi_n(t, t_i)$ without combination with other states. Hence, Eq. (5.1) can be written as

$$\psi(t) = \mathrm{e}^{\mathrm{i}\eta(t,t_i)}\, \psi_n(t) \,. \tag{5.2}$$

Usually, the phase factor $\eta(t, t_i)$ is set to zero as only $\psi\psi^*$ is measurable. It has been assumed that $\eta(t, t_i)$ does not give any observable effect.

In 1984 Michael Victor Berry of Bristol University in the U.K. made a very surprising observation about the evolution of a quantum system in an energy eigenstate under the action of a Hamiltonian $H = H(R_i(t))$. Here H is a function of adiabatically (slowly) varying parameters $R_i(t)$, with period T, representing a circuit C in the parameter space. He investigated the evolution of the system by adiabatic approximation. Berry got a fascinating result. After a certain time interval T the system came back to the initial eigenstate. However, there is a phase factor [1]

$$\mathrm{e}^{-\mathrm{i}\int_{t_i}^{t_f} E_n(t)\,\mathrm{d}t}\, \mathrm{e}^{\mathrm{i}\phi_n(C)} \,. \tag{5.3}$$

The first phase in Eq. (5.3) is same as the one in Eq. (5.2). $\phi_n(C)$ gives an additional phase and is a function of C. That is, this phase factor depends on the path of the circuit. Different circuits give rise to different phases. Therefore, we cannot adjust it or set it to zero. His discovery is indeed both deep and beautiful. This phase factor $\phi_n(C)$ is named in his honor as *Berry's phase*. It is also called *geometric phase*.

Soon after, many generalizations including relaxing the adiabatic conditions and connecting it to corresponding classical phenomena, experimental observations and applications of the Berry's phase have been reported. Interestingly, a very close analogy to Berry's phase had been discovered by Shivaramakrishnan Pancharatnam [2,3] in 1956 at the Raman Research Institute in Bangalore in the topic of polarization of optics. Later, Berry reevaluated and placed in perspective this pioneering work done in India. Using the ideas proposed by Pancharatnam, Rajendra Bhandari and Joseph Samuel [4] have shown that a geometric phase can be defined for noncyclic and nonunitary evolution. Ji et al [5] constructed an

DOI: 10.1201/9781003172192-5

exact wave function of a time-dependent harmonic oscillator using the Heisenberg picture approach. They examined the wave function for the τ-periodic Hamiltonian and found the cyclic initial state and the corresponding Berry's phase. The phenomenon of geometric phase and its applications have been studied to a remarkably wide range of problems in particle physics, quantum field theory, condensed matter physics, atomic and nuclear physics.

There are two other quantum effects which have been most widely discussed. The Aharonov–Bohm effect predicts that a charged particle can be influenced by a magnetic field even if the particle is not in the region of nonzero field strength. For example, suppose an electron is sent towards an infinite, perfectly shielded cylinder of radius R, with a homogeneous field inside, then it would acquire a phase proportional to the magnetic flux. In 1913 Georges Sagnac demonstrated that a beam of light split into two such that one part travelled clock-wise and the other part counter-clock-wise around a rotating circular ring.

In this chapter, first the derivation of Berry's phase is presented. This is followed by a brief discussion on its origin and properties. Next, a classical analogue of Berry's phase is brought out. Then, a few examples and effects of the geometric phase are given. A simple interferometric demonstration of the geometric phase is described. The work of Pancharatnam is briefly outlined. The Aharonov–Bohm and Sagnac effects are also discussed in detail.

5.2 Derivation of Berry's Phase

Let us consider a Hamiltonian $H(R_i(t))$, $i = 1, 2, \ldots, k$ which is a function of a set of parameters $R_i(t)$ [1,6]. It can be a time-dependent vector field. In this case $k = 3$ and $R_i(t)$ are the independent components of the field vector. Assume that the rate of change of $R_i(t)$ is much slower than $\Delta E_n(t)$ such that the adiabatic approximation is applicable.

The Schrödinger equation of the problem is (with $\hbar = 1$ for simplicity)

$$\mathrm{i}\frac{\partial \psi}{\partial t} = H(R_i(t))\psi \; . \tag{5.4}$$

The solution of the above equation can be written as (refer to exercise 1 at the end of this chapter)

$$W = \psi(\mathbf{x}, t) = \psi_n(\mathbf{x}, t)\mathrm{e}^{-\mathrm{i}\int_{t_i}^{t_f} E_n(t)\,\mathrm{d}t}\,\mathrm{e}^{\mathrm{i}\phi_n(t)} \; . \tag{5.5}$$

To determine $\phi_n(t)$, substitute Eq. (5.5) in Eq. (5.4). Then multiply the resultant equation by ψ_n^*, replace $H\psi_n$ by $E_n\psi_n$ and obtain

$$\mathrm{i}\frac{\partial W}{\partial t}\psi_n^* = E_n\psi_n\psi_n^*\,\mathrm{e}^{-\mathrm{i}\int_{t_i}^{t_f} E_n(t)\,\mathrm{d}t}\mathrm{e}^{\mathrm{i}\phi_n(t)} \; . \tag{5.6}$$

Performing the partial derivative in the above equation we get

$$\dot{\phi}_n\psi_n\psi_n^* = \mathrm{i}\dot{\psi}_n\psi_n^* \; . \tag{5.7}$$

Integration of the above equation with respect to spatial variables gives

$$\dot{\phi}_n = \mathrm{i}\int \psi_n^*\dot{\psi}_n\,\mathrm{d}^3x \; , \tag{5.8}$$

where $\int_{-\infty}^{\infty}\psi_n^*\psi_n\,\mathrm{d}^3x = 1$ is used. If R_i's are independent of time then $\psi_n(\mathbf{x}, t)$ would be time-independent. Therefore, we write $\psi_n(\mathbf{x}, t) = \psi_n(\mathbf{x}, R_i(t))$. When $k = 1$ in $R_i(t) = 1, 2, 3, \ldots, k$ then

$$\dot{\psi}_n = \frac{\partial \psi_n}{\partial R_1}\frac{\mathrm{d}R_1}{\mathrm{d}t} = \frac{\partial \psi_n}{\partial R_1}\dot{R}_1 \; . \tag{5.9}$$

For the case of $k > 1$

$$\dot{\psi}_n = (\nabla_{R_i}\psi_n)\,\dot{R}_i \tag{5.10}$$

and Eq. (5.8) becomes

$$\dot{\phi}_n = \mathrm{i}\int \sum_{i=1}^{k} \psi_n^*(\mathbf{x}, R_i(t))\,[\nabla_{R_i}\psi_n(\mathbf{x}, R_i(t))]\,\dot{R}_i(t)\,\mathrm{d}^3x\,. \tag{5.11}$$

Let

$$\mathbf{R}(t) = \begin{pmatrix} R_1(t) \\ R_2(t) \\ \vdots \\ R_k(t) \end{pmatrix} \tag{5.12}$$

be a k-component column vector. Defining the nth eigenstate as $|n;\mathbf{R}\rangle$ and noting that integration is with respect to $\mathbf{x}$, Eq. (5.11) is rewritten as

$$\dot{\phi}_n = \mathrm{i}\langle n;\mathbf{R}|\nabla_{\mathbf{R}}|n;\mathbf{R}\rangle\cdot\dot{\mathbf{R}}\,. \tag{5.13}$$

So far we noticed nothing new. In fact for a long time the presence of the phase ϕ_n in addition to the phase factor given by Eq. (5.2) has been well known. Generally, it was assumed that we could eliminate ϕ_n by properly redefining the phase of the eigenstates. However, Berry pointed out if $\mathbf{R}(t_f) = \mathbf{R}(t_i)$ so that $|n;\mathbf{R}(t_f)\rangle$ interfere with $|n;\mathbf{R}(t_i)\rangle$ then such a phase is observable. Integration of Eq. (5.13) from t_i to t_f gives

$$\begin{aligned} \phi_n(t) &= \mathrm{i}\int_{t_i}^{t_f}\langle n;\mathbf{R}|\nabla_{\mathbf{R}}|n;\mathbf{R}\rangle\cdot\frac{\mathrm{d}\mathbf{R}}{\mathrm{d}t}\,\mathrm{d}t \\ &= \mathrm{i}\oint\langle n;\mathbf{R}|\nabla_{\mathbf{R}}|n;\mathbf{R}\rangle\cdot\mathrm{d}\mathbf{R}\,. \end{aligned} \tag{5.14}$$

The $\phi_n(t)$ given by Eq. (5.14) is called *Berry's phase* [1] or *geometric phase*. $\phi_n(t)$ is an *observable* and cannot be eliminated. It has a geometric character and depends on the history of the quantum system from t_i to t_f. We define the phase angle ϕ_n in terms of an integral over a vector-valued function as

$$A_n(\mathbf{R}) = \mathrm{i}\langle n;\mathbf{R}|\nabla_{\mathbf{R}}|n;\mathbf{R}\rangle \tag{5.15}$$

which is called *Berry's vector potential* or *Berry's connection* [1,6].

In classical physics, an object rotated by an integral number of complete revolutions about an axis should return to its initial state. The operator for rotation through $2m\pi$ radians, where m is an integer, is essentially equivalent to the identity operation. Its effect cannot be observed. But as shown above in quantum mechanics, the wave function of a system may not come back to its initial phase after its parameters are cycled around a circuit.

Solved Problem 1:

Using the normalization condition of $\psi_n(t)$, show that the Berry's phase $\mathrm{i}\int_{t_i}^{t}\langle n|\partial/\partial t'|n\rangle\,\mathrm{d}t'$ is real.

Since $\psi_n(t)$ is normalized we have $\dfrac{\partial}{\partial t}\langle n(t)|n(t)\rangle = 0$. That is,

$$\left\langle\frac{\partial}{\partial t}\psi_n(t)\middle|\psi_n(t)\right\rangle + \left\langle\psi_n(t)\middle|\frac{\partial}{\partial t}\middle|\psi_n(t)\right\rangle = 0 \tag{5.16}$$

$$\left\langle\psi_n(t)\middle|\frac{\partial}{\partial t}\middle|\psi_n(t)\right\rangle^* + \left\langle\psi_n(t)\middle|\frac{\partial}{\partial t}\middle|\psi_n(t)\right\rangle = 0\,. \tag{5.17}$$

Hence, the real part of $\langle n|\partial/\partial t|n\rangle = 0$. Therefore, $\langle n|\partial/\partial t|n\rangle$ is imaginary. Thus, $\mathrm{i}\int_{t_i}^{t}\langle n|\partial/\partial t|n\rangle\,\mathrm{d}t'$ is real.

5.3 Origin and Properties of Berry's Phase

Berry's phase arises when a system evolves in configuration space. The origin of the phase can be easily understood by the following illustration given by Levi [7]. Suppose we hold our arm straight against our side vertically downward and point our thumb in the forward direction. Lift the arm sideways so that it levels with the shoulder. Next, we rotate the arm in the forward direction and make it stick straight-out in front of us. Then, we drop the arm back to our side. Now, our thumb no longer juts out forward but directs in toward our side. Notice that, our arm has undergone one completion of a trajectory and came back to its starting point. But the thumb has been rotated about 90° relative to its original direction. There is no local change but a global change has been made.

We can regard our thumb as the state vector of a system that is coupled to a slowly changing environment which is our arm. If this system changes adiabatically then we expect that the state vector should return back to its initial state after a cyclic evolution in parameter space. But it might be multiplied by a phase factor. Part of this phase will be the dynamic phase arising from the time-dependence of the Hamiltonian. Further, the phase would be associated with a rotation of the state vector, locally about an axis which is perpendicular to the surface. The remaining part of the phase factor resulting from the cycling of our arms is a Berry's phase.

Some of the properties of Berry's phase are listed below:

1. The size of the phase is a function of the path taken and sensitive to the features of its topology.
2. It is nonintegrable and single-valued, that is $\phi(t_f) \neq \phi(t_i)$. Repeated traversals of a circuit builds-up ϕ.
3. In electromagnetic theory, the magnetic vector potential $\mathbf{A}$ and the magnetic field $\mathbf{B}$ are related as $\mathbf{B} = \nabla \times \mathbf{A}$ and $\mathbf{A}$ is given by

$$\mathbf{A}(\mathbf{r}_2) = \frac{\mu_0}{4\pi}\int \frac{\mathbf{J}(\mathbf{r}_1)}{|\mathbf{r}_2 - \mathbf{r}_1|}\,\mathrm{d}\tau\ . \tag{5.18}$$

   Here $\mathbf{J}(\mathbf{r}_1)$ is the current density. Now, define a quantity $\mathbf{A}_n(\mathbf{R})$ as

$$\mathbf{A}_n(\mathbf{R}) = \mathrm{i}\langle n;\mathbf{R}|\nabla_{\mathbf{R}}|n;\mathbf{R}\rangle\ . \tag{5.19}$$

   Note that in Eq. (5.19) the right-side is an n-dimensional volume integral. Thereby comparing Eqs. (5.18) and (5.19) we can regard $\mathbf{A}_n(\mathbf{R})$ as vector potential-like a quantity. Then, in terms of $\mathbf{A}_n(\mathbf{R})$, Eq. (5.14) is written as

$$\phi_n = \oint \mathbf{A}_n(\mathbf{R})\,\mathrm{d}\mathbf{R}\ . \tag{5.20}$$

   That is, ϕ_n is written in terms of a vector potential-like quantity.
4. The vector potential is arbitrary to the extent that the gradient of some scalar function Λ can be added. Then $\mathbf{B}$ is unchanged by the transformation

$$\mathbf{A} = \mathbf{A}' = \mathbf{A} + \nabla\Lambda\ . \tag{5.21}$$

The transformation Eq. (5.21) is the well known *gauge transformation*. Suppose the phase of the eigenstate is redefined as

$$|n;\mathbf{R}\rangle \rightarrow |n;\mathbf{R}\rangle\, \mathrm{e}^{\mathrm{i}\theta(\mathbf{R})}, \tag{5.22}$$

where $\theta(\mathbf{R})$ is an arbitrary phase. Then

$$\mathbf{A}_n(\mathbf{R}) \rightarrow \mathbf{A}_n(\mathbf{R}) + \nabla_{\mathbf{R}}\theta(\mathbf{R})\ . \tag{5.23}$$

Equation (5.23) is analogous to the gauge transformation.

Solved Problem 2:

Show that Berry's phase satisfies the property that an observable cannot depend on the choice of gauge.

A line integral can be transformed into a surface integral (by the Stoke's theorem)

$$\oint \mathbf{B}\cdot \mathrm{d}\mathbf{l} = \int_{\mathrm{S}} \nabla\times\mathbf{B}\cdot \mathrm{d}\mathbf{S}\ . \tag{5.24}$$

Using the above, Eq. (5.14) becomes

$$\phi_n = \oint \mathbf{A}_n(\mathbf{R})\cdot \mathrm{d}\mathbf{R} = \int_{\mathrm{S}} \nabla_{\mathbf{R}}\times\mathbf{A}_n(\mathbf{R})\cdot \mathrm{d}\mathbf{S}\ . \tag{5.25}$$

Replacement of $\mathbf{A}_n$ by its gauge (Eq. (5.23)) gives

$$\phi_n = \int_{\mathrm{S}} \nabla_{\mathbf{R}}\times[\mathbf{A}_n(\mathbf{R}) + \nabla_{\mathbf{R}}\theta(\mathbf{R})]\cdot \mathrm{d}\mathbf{S} = \int_{\mathrm{S}} \nabla_{\mathbf{R}}\times\mathbf{A}_n(\mathbf{R})\cdot \mathrm{d}\mathbf{S}\,. \tag{5.26}$$

ϕ_n given by Eqs. (5.25) and (5.26) are the same. Hence, ϕ_n does not depend on the choice of the gauge. Equation (5.26) can be rewritten as

$$\phi_n = \int_{\mathrm{S}} \mathbf{B}_n(\mathbf{R})\cdot \mathrm{d}\mathbf{S}\ , \quad \mathbf{B}_n(\mathbf{R}) = \nabla_{\mathbf{R}}\times\mathbf{A}_n(\mathbf{R})\ . \tag{5.27}$$

$\mathbf{B}_n(\mathbf{R})$ appears as a field-like quantity with ϕ_n being the flux of it through the surface. $\mathbf{B}_n(\mathbf{R})$ is called *Berry's curvature* and is the Berry's phase per unit area.

5.4 Classical Analogue of Berry's Phase

Many classical phenomena have corresponding quantum mechanical analogue. Therefore, it is natural to identify a classical analogue of Berry's phase. *Is there a classical system which when taken around a closed path in a parameter space develops a factor similar to Berry's phase?* Interestingly, rotation by an angle equivalent to Berry's phase can be realized by using classical mechanics without referring to quantum mechanics [8]. This is possible when the adiabatic transformation can be reduced to a coordinate transformation. As an example, let us consider the classical case of rotation of polarization in twisted optical fibers.

Consider a particle restricted to move on a two-dimensional plane. The potential $V = V(r)$ is assumed to be cylindrically symmetric. A unit vector $\mathbf{S}$ represents the orientation of the two-dimensional plane. $\mathbf{S}$ is perpendicular to the plane. Suppose $\mathbf{S}$ is slowly changed

by means of an applied force. The charge is along a closed path and $\mathbf{S}$ returns to its initial value after some time. The time evolution of $\mathbf{S}$ is given by

$$\frac{\mathrm{d}\mathbf{S}}{\mathrm{d}t} = \chi\mathbf{N}\,, \quad \frac{\mathrm{d}\mathbf{N}}{\mathrm{d}t} = -\chi\mathbf{S} + \tau\mathbf{B}\,, \quad \frac{\mathrm{d}\mathbf{B}}{\mathrm{d}t} = -\tau\mathbf{N}\,, \tag{5.28}$$

where $\mathbf{N}$ and $\mathbf{B}$ are normal and binormal unit vectors, respectively. χ and τ are the curvature and the torsion of a curve, respectively. χ and τ are assumed to be small.

Let us introduce the following two basis vectors

$$\mathbf{U}_1 = \cos\phi\,\mathbf{N} - \sin\phi\,\mathbf{B}\,, \quad \mathbf{U}_2 = \sin\phi\,\mathbf{N} + \cos\phi\,\mathbf{B}\,, \tag{5.29}$$

and define

$$\frac{\mathrm{d}\phi}{\mathrm{d}t} = \tau(t)\,. \tag{5.30}$$

Differentiation of $\mathbf{U}_1$ and $\mathbf{U}_2$ give

$$\begin{aligned}
\frac{\mathrm{d}\mathbf{U}_1}{\mathrm{d}t} &= \dot{\mathbf{N}}\cos\phi - \mathbf{N}\sin\phi\,\dot{\phi} - \dot{\mathbf{B}}\sin\phi - \mathbf{B}\cos\phi\,\dot{\phi} \\
&= \dot{\mathbf{N}}\cos\phi - \tau\mathbf{N}\sin\phi - \dot{\mathbf{B}}\sin\phi - \tau\mathbf{B}\cos\phi \\
&= -\chi\cos\phi\,\mathbf{S} + \tau\mathbf{B}\cos\phi - \tau\mathbf{N}\sin\phi + \tau\mathbf{N}\sin\phi - \tau\mathbf{B}\cos\phi \\
&= -\chi\cos\phi\,\mathbf{S}\,, \qquad (5.31a) \\
\frac{\mathrm{d}\mathbf{U}_2}{\mathrm{d}t} &= -\chi\sin\phi\,\mathbf{S}\,. \qquad (5.31b)
\end{aligned}$$

In a local inertial frame, introduce a vector $\mathbf{X} = u_1\mathbf{v}_1 + u_2\mathbf{v}_2$ with $\ddot{\mathbf{X}} = -\widehat{\mathbf{X}}\mathrm{d}V/\mathrm{d}r$, where $V = V(r)$ and $r^2 = u_1^2 + u_2^2$. Then we have

$$\ddot{u}_1 = -\frac{\mathrm{d}V}{\mathrm{d}u_1} - \chi^2\left(u_1\cos^2\phi + u_2\sin\phi\cos\phi\right)\,, \tag{5.32a}$$

$$\ddot{u}_2 = -\frac{\mathrm{d}V}{\mathrm{d}u_2} - \chi^2\left(u_1\sin\phi\cos\phi + u_2\sin^2\phi\right)\,. \tag{5.32b}$$

Note that the transformation becomes adiabatic for slowly changing $\mathbf{S}$. Hence, for sufficiently small χ we can neglect the terms containing χ^2 in Eq. (5.32). Then Eqs. (5.32) become $\ddot{u}_i = -\mathrm{d}V/\mathrm{d}u_i$, $i = 1, 2$. This equation is identical to the equation of motion of a particle of unit mass with $\mathbf{S}$ being time-independent. Consider the direction of $\mathbf{S}$. Suppose it is transformed along a closed curve into itself. Then at the end of the curve $\mathbf{U}_1$ and $\mathbf{U}_2$ differ from $\mathbf{N}$ and $\mathbf{B}$. They differ by a rotation angle ϕ. From Eq. (5.30) ϕ is obtained as

$$\phi = \int \tau(t)\,\mathrm{d}t\,. \tag{5.33}$$

This phase is the classical analogue of Berry's phase and is called *Hannay angle* [8].

The Hannay theorem establishes that, if a classical system is taken around a closed path in parameter space then an angle variable gives a geometric phase. That is, in addition to the angle predicted in the adiabatic limit by the unperturbed Hamiltonian there exists another phase shift. This phase shift is (i) independent of the initial conditions of the system and (ii) the duration of cycle of adiabatic change.

5.5 Berry's Phase in Solid State Physics

Energy spectra of solids display band structures, particularly, in the form of piece-wise continuous. In each continuous piece the energy is a function of Bloch quasimomentum $\mathbf{k}$ and $\mathbf{k}$ varies in the Brillouin zone which can be treated as a parameter space. The Bloch function $\psi_{nk}(\mathbf{r})$ can acquire a Berry's phase [9]. In the Brillouin zone $\mathbf{k}$ can be varied along a direction and the path is closed when the edge of the zone is reached. For an one-dimensional solid the Brillouin zone is defined over $[-\pi/a, \pi/a]$, where a is the lattice constant and the edges are at $-\pi/a$ and π/a. By means of an appropriate perturbation, for example, applied electric field or magnetic fied k can be allowed to vary through the entire zone. The Berry's phase in one-dimension is usually called *Zak phase* and is used for a better understanding of electric polarization in dielectrics [10], protected edge states [11,12] and Wannier–Stark ladders [9,13] and integer quantum Hall effect [14].

5.5.1 Theoretical Consideration

The Schrödinger equation for an one-dimensional Bloch electron subjected to a vector potential $A(t)$ is given by

$$\mathrm{i}\hbar\frac{\partial\psi}{\partial t} = \left[\frac{1}{2m}\left(p - \frac{e}{c}A(t)\right)\right]^2\psi + V(x)\psi, \quad V(x+a) = V(x), \tag{5.34}$$

where $A(t)$ is assumed to be varying adiabatically with t. It is desired to solve the equation

$$\left[\frac{1}{2m}\left(p - \frac{e}{c}A(t)\right)^2 + V(x)\right]\psi_{nl}(x) = E_n(t)\psi_{nl}(x). \tag{5.35}$$

We look for solution of the form

$$\psi_{nl}(x) = \mathrm{e}^{\mathrm{i}kx}u_{nk(t)}(x), \quad k(t) = k - \frac{e}{\hbar c}A(t) \tag{5.36}$$

and u is the periodic part of ψ_{nl}. The equation for $u_{nk(t)}$ is

$$\left[\frac{1}{2m}\left(p + \hbar k - \frac{e}{c}A(t)\right)^2 + V(x)\right]u_{nk(t)} = E_n(k(t))u_{nk(t)}. \tag{5.37}$$

Then $\psi(x,t)$, the solution of Eq. (5.34), can be written as

$$\psi(x,t) = \exp\left[\mathrm{i}\gamma_n(t) - \frac{\mathrm{i}}{\hbar}\int_0^t E_n(k(t'))\mathrm{d}t'\right]\psi_{nl}. \tag{5.38}$$

In Eq. (5.38) $\gamma_n(t)$ is a phase corresponding to the energy band n. Substitution of (5.38) in (5.34) leads to [9]

$$\gamma_n = \int_{-\pi/a}^{\pi/a} X_{nn}(k)\mathrm{d}k, \tag{5.39a}$$

where

$$X_{nn}(k) = \frac{2\pi\mathrm{i}}{a}\int_0^a u_{nk}^*(x)\frac{\partial}{\partial k}u_{nk}(x)\mathrm{d}x. \tag{5.39b}$$

Equation (5.39a) provides the Berry's phase for the nth energy band. γ_n can also be expressed in terms of the so-called *Wannier function* $a_n(x)$ of a particular band.

For an energy band n its band center is defined as [15]

$$q_n = \frac{a}{2\pi}\int_{-\pi/a}^{\pi/a} X_{nn}(k)\mathrm{d}k. \tag{5.40}$$

Thus, we have $\gamma_n = (2\pi/a)q_n$. It is to be noted that a homogeneous electric field E_F with frequency sufficiently smaller than the relevant band gaps can gives rise to adiabatic $A(t)$. We can obtain such a field from $A(t) = -c\int_0^t E_\mathrm{F}(t')\mathrm{d}t'$. In this case k is given by $\hbar\dot{k} = -cE_\mathrm{F}(t)$ [16]. In general different energy bands acquire different Berry's phase due to the applied field. Suppose, γ_n and $\gamma_{n'}$ correspond to the bands n and n', respectively. By means of an interference experiment with electrons from the bands n and n' it is possible to measure the difference between γ_n and $\gamma_{n'}$.

5.5.2 Direct Measurement of the Zak Phase

An experimental measurement of Zak phase in a dimerized optical lattice with two sites per unit cell has been reported [17]. Depending on the parameter values the system can mimic either conjugated diatomic polymers or polyacetylene. The Hamiltonian of the system is

$$H = -\sum_n \left(Ja_n^\dagger b_n + J'a_n^\dagger b_{n-1} + \mathrm{h.c.}\right) + \Delta\sum_n \left(a_n^\dagger a_n - b_n^\dagger b_n\right), \tag{5.41}$$

where h.c. denotes Hermitian conjugate of the preceeding terms, $a_n^\dagger$ and $b_n^\dagger$ are the particle creation operators for an atom on the sublattice sites a_n and b_n, respectively, in the nth lattice cell. J and J' are the modulated tunnelling amplitudes within the unit cell and Δ characterizes the energy offset between neighbouring lattice sites.

For $\Delta = 0$ the system is a polyacetylene and there are two phases denoted as D1 with $J > J'$ and D2 with $J < J'$. A consequence of the different topological character of the phases is seen in the difference in their Zak phases: $\delta\phi_\mathrm{Zak} = \pi$. When $\Delta \neq 0$ the model is a linearly conjugated diatomic polymer and in this case the difference of the Zak phases is fractional in units of π.

Experimental realization of the H given by (5.39) is achieved by loading a BEC of ^{87}Rb into a 1D optical superlattice potential. To form this potential two standing optical waves of $\lambda_\mathrm{s} = 767\,\mathrm{nm}$ and $\lambda_\mathrm{l} = 1534\,\mathrm{nm}$ were superimposed leading to a lattice potential $V(x) = V_\mathrm{l}\sin^2(2k_\mathrm{l}x + \phi/2) + V_\mathrm{s}\sin^2(k_\mathrm{l}x + \pi/2)$, $k_\mathrm{l} = 2\pi/\lambda_\mathrm{l}$. Switching between $\phi = 0$ and $\phi = \pi$ leads to $\Delta = 0$ while $\Delta \neq 0$ for tuning ϕ away from 0 and π. For $\Delta = 0$ the Zak phases are found to be same for the lower and upper bands: $\phi_\mathrm{Zak}^\mathrm{D1} = \pi/2$. When the configuration was changed from D1 to D2 then $\phi_\mathrm{Zak}^\mathrm{D2} = -\pi/2$. The difference in the two phases is $\delta\phi_\mathrm{Zak} = \pi$.

It has been pointed out that the phase shift consists of geometric phase ϕ_Zak, dynamical phase $\phi_\mathrm{dyn} = \int(E(t)/\hbar)\mathrm{d}t$ and a phase ϕ_Z due to Zeeman energy of the atom in an external magnetic field. Zak phase was isolated in the experiment using a three step process. For details see ref. [17]. In [18] an optical system consisting of lattices of circularly curved optical waveguides has been suggested for observation of Zak phase. In this system photons exhibit Bloch oscillations in different Bloch bands. For some reports on experimental measurement of Zak phase one may refer the refs. [19–22].

5.6 Examples and Effects of Berry's Phase

In this section a few examples of physical systems where Berry's phase is observed and certain interesting observable effects of Berry's phase are presented.

5.6.1 Examples of Berry's Phase

1. The precision of a neutron in a magnetic field

A rotation of spin axis of the neutron through 360° results in a phase shift of π.

2. Systems with spins

Phase shifts can be introduced into systems by coupling the spins to a slowly changing magnetic field. These have been noticed in nuclear-magnetic-resonance interferometry. Optical measurements have detected phase shifts. The phase shifts arise as the orientation of the light changes through a complete cycle. The geometric phase has been observed in the spectra of trimers such as Na_3.

3. Spin-1 particles

A spin-1 particle can have a phase factor of -1 under some rotations which return to its initial state classically. For example, the direction of a magnetic field can be rotated slowly through a cone of apex angle 120° in such a way that the magnetic moment of the spin follows it adiabatically. After the magnetic field has come back to its original direction, the wave function of the spin acquires a change in its sign relative to that of an identical spin which has remained in an unchanged magnetic field. This sign change can manifest itself in the destructive interference between the spins of the two beams.

4. Foucault pendulum

A simple example is the Foucault pendulum, a simple two-dimensional harmonic pendulum with an added Coriolis force. An experimental set-up of this system is available at Griffith Observatory in Los Angeles. The direction of the swing of the pendulum does not return back to its initial value when the pendulum completes its one-day trip around a circle of latitude (of Los Angeles). The geometric phase is the solid angle swept out by the pendulum axis during one revolution of the earth. This is a classical system.

5. System of three hydrogen atoms

Consider a system of three hydrogen atoms. It has two electronic potential energy surfaces. They come together at a conical intersection. It represents a configuration where the three hydrogen atoms essentially form an equilateral triangle. The system distorts when it moves away from the intersection point. Moreover, the two electronic wave functions are distinct. For each configuration of the nuclei we can determine the electronic wave function. Permit the nuclear environment to evolve adiabatically. The reactants reach one another, interact and retreat. As the nuclear coordinates change slowly the state vector moves adiabatically over the electronic potential energy surface. If the energy of the system is sufficiently low then the state moves completely on the lower energy surface. But it appears that the upper energy surface indeed can influence the reaction through the geometric phase.

5.6.2 Effects of Berry's Phase

The presence of a geometric phase gives rise to observable effects in many physical and chemical systems. Some of the observed effects of geometric phases are pointed out in the following.

1. In trimers such as Na_3, the geometric phase causes the quantum number of angular momentum to be half-integer instead of the expected integer value.
2. In certain chemical reactions the geometric phase leads to observable effects. For example, in $H+H_2 \rightarrow H_2+H$ reaction the total cross-section computed without geometric phase is different from the experimental result.
3. Geometric phase is used to describe certain classical systems, for example the kinematics of deformable bodies.
4. The presence of geometric phase indicates that eigenstates of quantum systems are not single-valued through continuation of parameters in the Hamiltonian. This is in contrast to the single-valuedness requirement of wave functions under continuation of position coordinates (*why?*).
5. An effective optical activity of a helically wound single-mode optical fiber has been predicted.

5.7 Applications of Berry's Phase

The concept of Berry's phase has been used in the study of quantized Hall effect, the spin statistics properties of quasiparticle excitations, the rotation of photon polarization in helical optical fibers, etc. [23,24]. We discuss two applications of Berry's phase in solid state physics. The presence of Berry's phase affects Bloch systems [9,25].

5.7.1 Semiclassical Equations of Motion

Taking into account the geometric phase, the semiclassical equations of motion for a Bloch electron are [26].

$$\dot{\mathbf{k}} = \frac{\mathbf{F}}{\hbar} , \quad \dot{\mathbf{r}} = \frac{1}{\hbar}\frac{\partial \epsilon(\mathbf{k})}{\partial \mathbf{k}} - \dot{\mathbf{k}} \times \Omega(\mathbf{k}) , \tag{5.42}$$

where $\mathbf{r}$ is the position of the electron, $\mathbf{k}$ is the crystal momentum (or wave vector), $\epsilon(\mathbf{k})$ is the band structure (which can be changed by the magnetic field) and $\mathbf{F}$ is the total force on the Bloch electron. The Berry curvature of a Bloch state $|\mathbf{k}\rangle$ is defined as [27]

$$\Omega(\mathbf{k}) = \mathrm{i}\langle \nabla_{\mathbf{k}} u_{\mathbf{k}}| \times |\nabla_{\mathbf{k}} u_{\mathbf{k}}\rangle , \tag{5.43}$$

where $u_{\mathbf{k}}$ is the periodic part of the Bloch function.

We write

$$\begin{aligned} \dot{\mathbf{k}} \cdot \mathbf{a} &= \dot{\mathbf{k}} \cdot \frac{\mathrm{d}\dot{\mathbf{r}}}{\mathrm{d}t} \\ &= \dot{\mathbf{k}} \cdot \frac{\mathrm{d}}{\mathrm{d}t}\left(\frac{1}{\hbar}\frac{\partial \epsilon}{\partial \mathbf{k}} - \dot{\mathbf{k}} \times \Omega(\mathbf{k})\right) \\ &= \dot{k}_i \dot{k}_j \left(\frac{1}{\hbar}\frac{\partial^2 \epsilon}{\partial k_i \partial k_j} - \epsilon_{jmn}\dot{k}_m \frac{\partial \Omega_n}{\partial k_i}\right) , \end{aligned} \tag{5.44}$$

where ϵ_{jmn} is the Levi–Civita permutation symbol.

To define an inverse effective mass tensor $\mathcal{M}^{-1}$ we identify a proportionality constant between acceleration and external force. From (5.44) we write

$$\left[\mathcal{M}^{-1}\right]_{ij} = \frac{1}{\hbar}\left(\frac{1}{\hbar}\frac{\partial^2\epsilon}{\partial k_i \partial k_j} - \epsilon_{jmn}\dot{k}_m \frac{\partial \Omega_n}{\partial k_i}\right) . \tag{5.45}$$

The dimensions of this tensor is inverse mass. We have $\mathbf{F} = \hbar\dot{\mathbf{k}}$. Since $\mathcal{M}^{-1}$ depends upon $\dot{\mathbf{k}}$ it depends on $\mathbf{F}$. That is, the acceleration in such a system depends on $\mathbf{F}$ and also on $|\mathbf{F}|^2$.

5.7.2 Cyclotron Effective Mass

The effective mass of a Bloch electron determined by a cyclotron resonance experiment is called the *cyclotron effective mass* m^*. The presence of $\Omega(\mathbf{k})$ affects m^*. A charged particle of mass m in a magnetic field exhibits cyclotron motion with an angular frequency $\omega_c = qB/(mc)$. For Bloch systems the Bloch electrons with m^* undergo such a cyclotron motion. In the presence of the applied field, the $\Omega(\mathbf{k})$ prescribe k-space orbits. Writing $\mathbf{F} = -(e/c)\dot{\mathbf{r}} \times \mathbf{B}$ and then eliminating $\dot{\mathbf{r}}$ from the equations of motion we get

$$\dot{\mathbf{k}} = -\frac{\dfrac{e}{\hbar c}\left[\dfrac{1}{\hbar}\dfrac{\partial \epsilon(\mathbf{k})}{\partial \mathbf{k}} \times \mathbf{B}\right]}{\left[1 + \dfrac{e}{\hbar c}\left(\mathbf{B} \cdot \Omega(\mathbf{k})\right)\right]} . \tag{5.46}$$

The time taken from $\mathbf{k}_1$ to $\mathbf{k}_2$ (using Eq. (5.46)) is

$$\begin{aligned}
\Delta t &= \int_{\mathbf{k}_1}^{\mathbf{k}_2} \frac{1}{|\dot{\mathbf{k}}|}\,\mathrm{d}k \\
&= \frac{\hbar^2 c}{e|\mathbf{B}|}\int_{\mathbf{k}_1}^{\mathbf{k}_2}\left(\left|\frac{\partial \epsilon(\mathbf{k})}{\partial \mathbf{k}}\right|_{\perp}\right)^{-1}\mathrm{d}k \\
&\quad + \frac{\hbar}{|\mathbf{B}|}\int_{\mathbf{k}_1}^{\mathbf{k}_2}\left(\mathbf{B}\cdot\Omega(\mathbf{k})\right)\left(\left|\frac{\partial \epsilon(\mathbf{k})}{\partial \mathbf{k}}\right|_{\perp}\right)^{-1}\mathrm{d}k .
\end{aligned} \tag{5.47}$$

In Eq. (5.47) $\left|\dfrac{\partial \epsilon(\mathbf{k})}{\partial \mathbf{k}}\right|_{\perp}$ is the component of $\left|\dfrac{\partial \epsilon(\mathbf{k})}{\partial \mathbf{k}}\right|$ perpendicular to $\mathbf{B}$. The second term in the right-side of Eq. (5.47) can be rewritten as

$$I = \hbar\int_{\mathbf{k}_1}^{\mathbf{k}_2}\frac{\mathbf{B}\cdot\Omega(\mathbf{k})}{|\mathbf{B}|}\left(\left|\frac{\partial \epsilon_{\mathrm{M}}(\mathbf{k})}{\partial \mathbf{k}}\right|_{\perp}\right)^{-1}\mathrm{d}k , \tag{5.48}$$

where $\mathbf{B}\cdot\Omega(\mathbf{k})/|\mathbf{B}| = \Omega(\mathbf{k})_{parallel}$ is the component parallel to the magnetic field. We can show that

$$\Delta t = \frac{\hbar^2 c}{e|\mathbf{B}|}\frac{\partial A}{\partial \epsilon} + I , \tag{5.49}$$

where A is the area swept out from $\mathbf{k}_1$ to $\mathbf{k}_2$ on the ϵ_{M} surface. For a free electron the period is $2\pi mc/(e|\mathbf{B}|)$ and

$$m^* = \frac{\hbar^2}{2\pi}\frac{\partial A}{\partial \epsilon} + \frac{e|\mathbf{B}|}{2\pi c}I . \tag{5.50}$$

The result indicates that the cyclotron effective mass depends on the applied magnetic field.

To test the dependence of m^* on the magnetic field let us consider a cyclotron resonance experiment with $\omega_c = qB/(mc)$ to find m^*. Assume that the experiment is performed with

a field $\mathbf{B}$ and then with $-\mathbf{B}$. m^* measured in the two cases differs by an amount twice I. For $\Omega(\mathbf{k}) = \Omega$ we find

$$I = \frac{\hbar}{|\mathbf{B}|} \int_{\mathbf{k}_1}^{\mathbf{k}_2} (\mathbf{B} \cdot \Omega(\mathbf{k})) \left(\left| \frac{\partial \epsilon(\mathbf{k})}{\partial \mathbf{k}} \right|_{\perp} \right)^{-1} \mathrm{d}k = \frac{\hbar}{|\mathbf{B}|} (\mathbf{B} \cdot \Omega) \frac{\partial A}{\partial \epsilon} \,. \tag{5.51}$$

Then

$$m^* = \frac{\hbar^2}{2\pi} \left(1 + \frac{e}{\hbar c} (\mathbf{B} \cdot \Omega) \right) \frac{\partial A}{\partial \epsilon} \,. \tag{5.52}$$

The rough value of $|\Omega|$ is $\sim a^2$, where a is the lattice constant. For $B \sim 1\mathrm{T}$, $a \sim 2.5\,\text{Å}$ and $e = 4.8 \times 10^{-10}$ esu the correction term is $\sim 10^{-4}$ and is large enough in experiments [25]. Berry curvature is important for noninversion symmetric materials for which $\Omega(\mathbf{k})$ does not vanish. Even inversion symmetric materials [28] (for example, single-layer graphene) have displayed the presence of nonzero Berry's phase.

5.8 Experimental Verification of Berry's Phase

Experimental observation of Berry's phase was reported initially by Delacretaz et al. [29]. Then several experimental demonstration of Berry's phase were done [4,24,30–37] in NMR, molecular physics, optics and neutron spin rotation. In optics geometric phases were observed with classical light fields [30,36,38] and with single photons [39,40]. For pairs of identically polarized photons doubling of the geometric phase compared to single photon experiments was observed [41].

A typical measurement of geometric phase is as follows. The light beam is split into two channels. One channel is taken as a reference. In the other channel a set of transformations act. When the beams are recombined the relative phase arises in the interference pattern. The following is a brief summary of the experiment performed by Bhandari and Samuel [4,31–33] at Raman Research Institute, Bangalore.

The experimental set-up used to observe Berry's phase is given in [31–33]. A linearly polarized beam from a He-Ne laser is split into two beams by a beam splitter. The measurement beam is taken along a cycle of polarization transformations through the following three components:

1. A quarter-wave plate (QWP1) oriented with its principal axes at 45° to the electric vector in the beam.
2. A half-wave plate (HWP) with its axes oriented at an angle $90° + \alpha/2$ to that of QWP1.
3. A linear polarizer LP.

The above cycle of transformations can be represented on the Poincaré sphere as shown in Fig. 5.1. These three processes represent the path APBQA. Steps 1, 2 and 3 correspond to the parts AP, PBQ and QA, respectively. In these processes the beam gets a geometric phase. Its magnitude is half the solid angle subtended at the center of the sphere by the area APBQA.

The absolute value of the acquired phase is not easy to determine because it would be buried in a larger magnitude dynamical phase. However, it is possible to measure the change in the geometric phase by changing the circuit from APBQA to APCQA. This can be achieved by rotating the HWP plate about the beam axis through an angle θ. This is

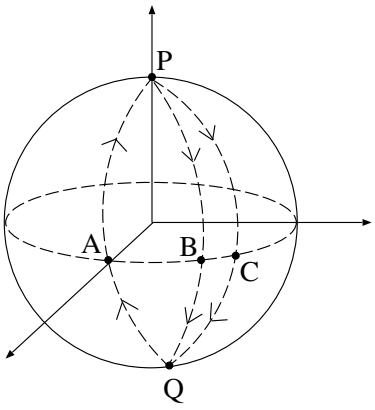

FIGURE 5.1
Circuits on the Poincaré sphere corresponding to the experiment.

recorded by a laser interferometer system in the experiment. The sign of the phase change depends upon the direction of rotation of the HWP.

The HWP was rotated into two full rotations in one sense and then two full rotations in the opposite sense. The phase is found to change with the angle of rotation of the HWP. Further, the change in the phase is found to continue after a full rotation of the HWP and moreover returned to the original value after an equivalent amount of reverse rotation. This is attributed to geometric phase.

5.9 Pancharatnam's Work

Pancharatnam[1] studied the interference patterns produced in plates of an anisotropic crystal [2]. He was concerned with the problem of defining the phase difference between two beams in different polarization states. He considered the intensity determined by the linear superposition of the two beams. The intensity varied sinusoidally when the phase of one beam is varied linearly. The intensity was maximum when the beams were in phase.

A phase shift was noticed when a beam had been taken from one polarization state to another polarization state, then to a third polarization state, and finally back to its original state. The magnitude of the phase shift depended on the geometry of the cycle. The above process was represented on the Poincaré sphere by Pancharatnam.

The states of polarization are represented as points on the Poincaré sphere as shown in Fig. 5.2 [37]. The poles correspond to left- and right-handed circular polarizations with the rotation by 180° in a 360° circuit. All other points mark elliptic polarizations. The polarization attached with any point on the Poincaré sphere $\widehat{r}$ is $\widehat{r} \cdot \sigma$, where $\widehat{r}$ is a unit vector with polar angles θ and ϕ and σ is the vector of Pauli spin matrices. The important result of studies of Pancharatnam is that the phase change associated with a circuit C on the Poincaré sphere was half of the solid angle subtended at the center of the sphere by C.

[1]Pancharatnam was a nephew of Sir Chandrasekhara Venkata Raman. When he wrote about polarized light, he was only 22 years old. In spite of this brilliant beginning, his life ended at the age of 35.

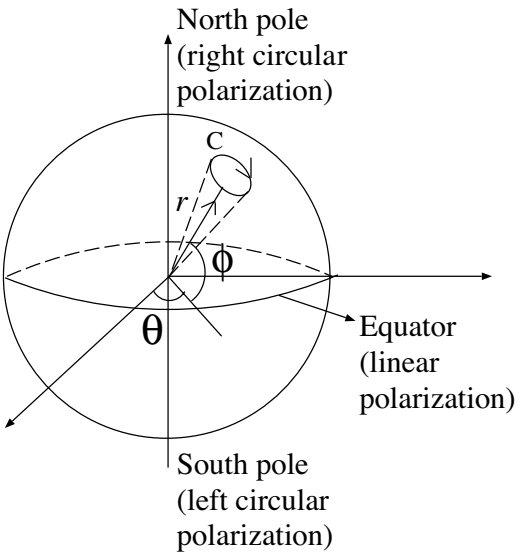

FIGURE 5.2
Poincaré sphere representation of polarization states. (Reproduced from P. Hariharan, *Am. J. Phys.* 61:591, 1993 with permission of the American Association of Physics Teachers.)

5.10 Cumulants Associated with Geometric Phases

Equation (5.14) gives the Berry's phase as an integral over a closed curve of the parameters $\mathbf{R}$. But the most general way to obtain the Berry's phase is to write it in the discrete representation as was done originally by Pancharatnam and then to take the continuous limit. Valentine Bargmann [42] obtained first the discrete Berry's phase. If we have the Hamiltonian $H(\mathbf{R})$ depending on the parameters $\mathbf{R}$ then for the nth eigenstate $|n, \mathbf{R}\rangle$ we have the Schrödinger equation

$$H(\mathbf{R})|n, \mathbf{R}\rangle = E_n(\mathbf{R})|n, \mathbf{R}\rangle. \tag{5.53}$$

If we consider M points in the parameter space $\{\mathbf{R}_I\}$ then we can form the quantity

$$\phi_n = -\text{I.P.}\left[\ln \prod_{I=0}^{M-1} \langle n, \mathbf{R}_I | n, \mathbf{R}_{I+1}\rangle\right], \tag{5.54}$$

where $|n, \mathbf{R}_M\rangle = |M, \mathbf{R}_0\rangle$ (cyclic). If the points $\{\mathbf{R}_I\}$ are points on the closed curve then taking the continuous limits gives Eq. (5.14).

It has been shown that [43] when the product in Eq. (5.54) associated with an adiabatic cycle is equated to a cumulant expansion and the continuous limit is taken then a series of physically well defined quantities result. These quantities are the integrals around the adiabatic cycle of the parameters. The first-order term gives the Berry's phase and the higher-order terms give the associated cumulants.

If we consider a cyclic curve parametrized according to a scalar χ then the product in Eq. (5.54) is $\prod_{I=0}^{M-1} \langle n, \chi_I | n, \chi_{I+1}\rangle$. If Λ is the length of the curve which is evenly spaced with

a grid of $\Delta\chi$ then one can write [43]

$$\prod_{I=0}^{M-1} \langle n, \chi_I | n, \chi_{I+1} \rangle = \exp\left[\sum_{m=1}^{\infty} \frac{(\mathrm{i}\Delta\chi)^m}{m!} C_m \right]. \tag{5.55}$$

Using the Taylor's series expansion

$$|n, \chi_{I+1}\rangle = |n, \chi_I\rangle + \Delta\chi \partial_\chi |n, \chi_I\rangle + \frac{(\Delta\chi)^2}{2!} \partial_\chi^2 |n, \chi_I\rangle + \ldots \tag{5.56}$$

on the left-side of Eq. (5.55) we can equate the powers of $\Delta\chi$ term by term to obtain the cumulants C_m. Equating the first-order term gives

$$C_1 = -\mathrm{i} \sum_{I=0}^{M-1} \Delta\chi \gamma_1(\chi_I), \quad \gamma_1^I(\chi) = \langle n, \chi | \partial_\chi^I | n, \chi \rangle \tag{5.57}$$

and the second-order term gives

$$C_2 = -\sum_{I=0}^{M-1} \Delta\chi \left[\gamma_2(\chi_I) - \gamma_1^2(\chi_I) \right]. \tag{5.58}$$

Similarly, we can find higher-order cumulants C_m. Taking the continuous limit ($\Delta\chi \to 0$, $M \to \infty$, Λ fixed) one can get

$$C_1 = -\mathrm{i} \int_0^\Lambda \gamma_1 \mathrm{d}\chi, \quad C_2 = -\int_0^\Lambda \left[\gamma_2 - \gamma_1^2 \right] \mathrm{d}\chi, \tag{5.59a}$$

$$C_3 = \mathrm{i} \int_0^\Lambda \left[\gamma_3 - 3\gamma_2\gamma_1 + 2\gamma_1^2 \right] \mathrm{d}\chi, \tag{5.59b}$$

$$C_4 = \int_0^\Lambda \left[\gamma_4 - 3\gamma_2^2 - 4\gamma_3\gamma_1 + 12\gamma_1^2\gamma_2 - 6\gamma_1^4 \right] \mathrm{d}\chi. \tag{5.59c}$$

As can be seen from Eq. (5.14) C_1 gives the Berry's phase. We have already proved that Berry's phase is gauge invariant. C_m's are also gauge invariant [43] and hence they are physically significant. Further, the cumulants give information about the underlying probability distribution associated with Berry's phase [43].

5.11 The Aharonov–Bohm Effect

Apart from the nonlocality displayed by the entangled states of two or many particles experiment of EPR, quantum mechanics possesses nonlocality for single particle states. The most notable of this is the *Aharonov–Bohm effect* [44–48] predicted in 1959 [47] and confirmed experimentally many times [49–52].

5.11.1 Physical Significance of Electromagnetic Potentials

We know that the electromagnetic fields are produced by potentials. In classical electrodynamics

$$\mathbf{E} = -\nabla\phi - \frac{1}{c}\frac{\partial \mathbf{A}}{\partial t}, \tag{5.60a}$$

$$\mathbf{B} = \nabla \times \mathbf{A}, \tag{5.60b}$$

where $\mathbf{A}$ and ϕ are vector and scalar potentials. The fields $\mathbf{E}$ and $\mathbf{B}$ are unaffected by the transformation (see exercise 3 at the end of this chapter)

$$\mathbf{A} \to \mathbf{A}' = \mathbf{A} + \nabla\chi \,, \tag{5.61a}$$

$$\phi \to \phi' = \phi - \frac{1}{c}\frac{\partial\chi}{\partial t} \,, \tag{5.61b}$$

where $\chi = \chi(\mathbf{x}, t)$ is an arbitrary scalar function. This change of the potentials, called *gauge transformation* has no effect on a physical result. Thus, in classical mechanics, the potentials are generally treated as book-keeping devices. They are assumed to have no physical significance or effects. A particle with no force acts on it will feel no effect. This is not the case in quantum mechanics. Yakir Aharonov and David Joseph Bohm (1959) [47] showed that in quantum mechanics there are situations, where the potentials indeed have physical significance. They predicted that diffraction of charged particles would be affected by electromagnetic potentials under conditions though the electromagnetic fields are absent.

Consider the Hamiltonian of a particle in an electromagnetic field given by

$$H = \frac{1}{2m}\left(\mathbf{p} - \frac{q}{c}\mathbf{A}\right)^2 + q\phi \,, \tag{5.62}$$

where m is the mass of the particle, $\mathbf{p}$ is the momentum operator of the particle, $\mathbf{A}$ and ϕ are operators. The Schrödinger equation of the system is

$$\mathrm{i}\hbar\frac{\partial\psi}{\partial t} = \frac{1}{2m}\left(\frac{\hbar}{\mathrm{i}}\nabla - \frac{q}{c}\mathbf{A}\right)^2\psi + q\phi\psi \,. \tag{5.63}$$

The changes to the vector and scalar potentials, Eq. (5.61), are accompanied by a change in the phase of the wave function ψ. That is, the change of potentials given by Eq. (5.61) change the phase of the wave function even when the fields are not present. Nothing of this kind is realized in classical physics.

We note that the Schrödinger Eq. (5.63) is unchanged by the substitution of Eq. (5.61) and

$$\psi \to \psi' = \psi\, \mathrm{e}^{\mathrm{i}q\chi/(\hbar c)} \tag{5.64}$$

(verify). These sets of transformations are called gauge transformations in quantum mechanics.

5.11.2 Aharonov–Bohm Experiment

The Aharonov–Bohm experiment consists of splitting an electron beam, passing around both sides of a solenoid and then recombining the beam. This is shown in Fig. 5.3a. An experimental set-up is depicted in Fig. 5.3b. It essentially consists of a source of charged particles and a double slit diffraction apparatus. A long solenoid (surrounded by a cylindrical shield impenetrable to the charged particles) is kept perpendicular to the plane of the figure and its position is such that particles cannot reach it. A magnetic field is set inside the solenoid. Note that the field is zero outside the solenoid. However, there is a circular potential and it advances the wave front of one electron beam while it retards the other. When the two beams recombine, there will be a manifestation of a phase-shift between them. This is known as *Aharonov–Bohm effect*. The phase-shift depends on the magnetic flux through the closed path of the electron beams. This can be easily shown as follows.

Suppose $\psi_0(\mathbf{x}, t)$ is the solution of the Schrödinger equation. Outside the solenoid $\mathbf{B} = \nabla \times \mathbf{A} = 0$. However, $\mathbf{A}$ is not zero everywhere as $\nabla \times \mathbf{A}$ can be zero with $\mathbf{A} \neq 0$. For

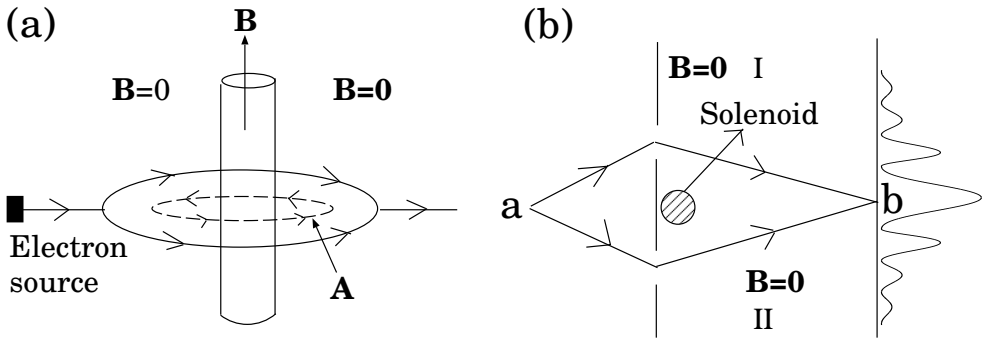

FIGURE 5.3
Schematic sketch of the Aharonov–Bohm experiment. (a) Splitting of an electron beam by circulating vector potential outside the solenoid. (b) Experimental arrangement.

example, if $\mathbf{A}$ is a gradient of a scalar function or a constant vector then $\nabla \times \mathbf{A} = 0$. Applying Stokes' theorem to any path surrounding the cylinder, we obtain

$$\oint \mathbf{A} \cdot \mathrm{d}\mathbf{x} = \int\int (\nabla \times \mathbf{A}) \cdot \mathrm{d}S = \int\int \mathbf{B} \cdot \mathrm{d}S = \phi \,. \tag{5.65}$$

Consequently, if the magnetic flux ϕ through the cylinder is nonzero then $\mathbf{A} \neq 0$ on every path that encloses the cylinder. Then according to the gauge transformation we have

$$\psi = \psi^{(0)}\, \mathrm{e}^{\mathrm{i}q\Lambda/(\hbar c)} \,, \tag{5.66}$$

where $\psi^{(0)}$ is the zero-potential solution. Let us apply the above technique to the regions I and II of Fig. 5.3b. In the region I

$$\psi_{\mathrm{I}} = \psi_{\mathrm{I}}^{(0)}\, \mathrm{e}^{\mathrm{i}q\Lambda_1/(\hbar c)} \,, \quad \Lambda_1(\mathbf{x}, t) = \int \mathbf{A} \cdot \mathrm{d}\mathbf{x} \,. \tag{5.67}$$

The integral in Eq. (5.67) is along a path within the region I. ψ in II can be written in a form similar to Eq. (5.67).

The wave function at the point b is a superposition of contributions from both slits:

$$\psi_{\mathrm{b}} = \psi_{\mathrm{I}}^{(0)} \mathrm{e}^{\mathrm{i}q\Lambda_1/(\hbar c)} + \psi_{\mathrm{II}}^{(0)} \mathrm{e}^{\mathrm{i}q\Lambda_2/(\hbar c)} \,. \tag{5.68}$$

Here, for Λ_1 the integration path is a to b through the region I. For Λ_2 it is through the region II. The interference pattern depends on the relative phase of the two terms in Eq. (5.68), $\mathrm{e}^{\mathrm{i}q(\Lambda_1 - \Lambda_2)/(\hbar c)}$. $(\Lambda_1 - \Lambda_2)$ is the difference between the integrals along paths on either side of the cylinder. It is equivalent to an integral around a closed path surrounding the cylinder given by $\oint \mathbf{A} \cdot \mathrm{d}\mathbf{x} = \phi$. Therefore, the interference pattern is sensitive to ϕ inside of the cylinder, even though the particles do not pass through the region where $\mathbf{B} \neq 0$. That is, the potential makes a track of the continuity of every happenings throughout space and more significantly affects the wave function. This is a *nonlocal effect*.

5.11.3 Experimental Observation of Aharonov–Bohm Effect

In 1962 Bayh [50,53] recorded the Aharonov–Bohm effect on a photographic film. A 40 KV electron beam was split and recombined by a system of three electrostatic biprisms. A tiny

tungsten coil was inserted (acted as Aharonov–Bohm solenoid) between the first and second biprism at a place, where the separation of the electron beam was at its maximum. A photographic film was attached to a small electric motor. The motor advanced the film with a rate proportional to the rate of increase of current in the coil windings. The film was shielded except for a 0.5 mm wide slit oriented perpendicular to the interference pattern. There was a well defined value of magnetic flux through the solenoid. The interference pattern was recorded on the film. The resulting pattern showed continuous lateral displacement of the fringes.

Tonomura et al [54,55] constructed small toroidal magnets such that the magnetic field was practically zero outside them. The magnets were impenetrable [55] and covered by superconducting layers so that leakage of the magnetic field outside the magnets was forbidden. An electron wave packet was sent toward the magnet and then superimposed behind it with a reference electron wave packet. This resulted in an interference pattern. The experiments were set in a way that the reference electron wave packet was not influenced by the magnet. Furthermore, the wave packets of electron and the reference electron interfered behind the magnet alone. The observed interference patterns provided clear evidence of the Aharonov–Bohm effect.

There is an electric potential equivalent for the Aharonov–Bohm effect. It involves passing an electron beam through a spatially homogeneous electric potential varying in time. This can produce a potential but not a force. There is an equivalent effect for a time-dependent potential. This effect can be produced in a neutron interferometer. In this device the neutron beam can be split by centimeter and coherently recombined. In one of the split beams the interaction of the neutron magnetic moment with a magnetic field produces a homogeneous potential. This in turn, when the beams were recombined, gives rise to a phase-shift between the two amplitudes. The above effect was observed by Antony Klein's and Sam Werner's groups.

5.11.4 Features of Aharonov–Bohm Effect

We list some of the features of the Aharonov–Bohm effect.

1. The Aharonov–Bohm effect is a topological effect. That is, the effect depends on the flux encircled by the paths of the particle but the paths never approach the region of the flux.
2. The effect depends on the dimensionless ratio $q\phi/\hbar c$. If the charge of the particle is zero then no effect occurs. This is verified experimentally using neutrons.
3. The particle never enters the region in which $\mathbf{B} \neq 0$. Therefore, the trajectory cannot be deflected by the magnetic field inside the cylinder. In quantum mechanics this is true on the average. The ensemble average rate of change of velocity of the particle is
$$\left\langle \frac{\mathrm{d}\mathbf{v}}{\mathrm{d}t} \right\rangle = \frac{1}{2}\left(\frac{q}{mc}\right)\langle\psi|\mathbf{v}\times\mathbf{B} - \mathbf{B}\times\mathbf{v}|\psi\rangle\ . \tag{5.69}$$
Since $\psi(\mathbf{x}) \neq 0$ if $\mathbf{B} \neq 0$ and $\mathbf{B}(\mathbf{x}) = 0$ if $\psi(\mathbf{x}) = 0$ we have $\langle \mathrm{d}\mathbf{v}/\mathrm{d}t\rangle = 0$. The flux ϕ affects the motion of individual particles but the net deflection is zero.
4. The positions of the fringes pattern shift as ϕ is varied. Their intensities also change so that the centroid of the pattern remains the same.
5. If the flux ϕ were quantized in multiples of $2\pi\hbar c/q$ then the phase factor $\mathrm{e}^{\mathrm{i}qc/(\hbar c)}$ is 1. Then there would be no observable dependence of the interference pattern on ϕ. That is, in Aharonov–Bohm effect ϕ is not quantized. Note that it is quantized in superconductivity.

For more discussion on the Aharonov–Bohm effect one may refer to ref. [56].

5.11.5 Aharonov–Bohm Effect in Quantum Electrodynamics

In this section we present the possibility of occurrence of quantum electrodynamic Aharonov–Bohm effect wherein a charge interacts with a potential arising due to a quantized electromagnetic field with no overlapping of field with the charge [57].

We consider a system where a superconducting charge qubit is located at the middle of a ring-shaped cavity with a node. The qubit state can be formed by means of Josephson junction tunnelling with superconducting reservoir. In this set-up the electromagnetic field not directly overlaps the qubit. Denote the Hamiltonians of the qubit, the single mode cavity and their interaction as $H_{\rm q}$, $H_{\rm c}$ and $H_{\rm int}$, respectively. The Hamiltonian of the system is

$$H = H_{\rm q} + H_{\rm c} + H_{\rm int}. \tag{5.70}$$

In diagonalized form [57] $H_{\rm q}$ is

$$H_{\rm q} = E_{\rm g}|{\rm g}\rangle\langle{\rm g}| + E_{\rm e}|{\rm e}\rangle\langle{\rm e}|, \tag{5.71a}$$

where

$$|{\rm g}\rangle = \cos(\gamma/2)|0\rangle + \sin(\gamma/2)|1\rangle, \tag{5.71b}$$

$$|{\rm e}\rangle = -\sin(\gamma/2)|0\rangle + \cos(\gamma/2)|1\rangle, \tag{5.71c}$$

$$\gamma = \tan^{-1}\left[\frac{E_{\rm J}}{E_{\rm c}(1-2n_{\rm g})}\right]. \tag{5.71d}$$

Here $E_{\rm J}$ is the effective Josephson coupling, $E_{\rm c}$ is the charging energy of a single Cooper pair and $n_{\rm g}$ is the gate-dependent parameter. $H_{\rm c}$ is given by $H_{\rm c} = \hbar\omega\left(a^\dagger a + \frac{1}{2}\right)$ with $a^\dagger$ being creation operator for creating a photon of frequency ω. $H_{\rm int}$ is given by $H_{\rm int} = \widehat{q}V$, where $\widehat{q} = 2e|1\rangle\langle 1| = e\sin\gamma(\sigma_+ + \sigma_-)$ with $\sigma_+ = |{\rm e}\rangle\langle{\rm g}|$ and $\sigma_- = |{\rm g}\rangle\langle{\rm e}|$.

The scalar potential at the location of qubit denoted as $V(t)$ is obtained as [57] $V(t) = V_1(t) + V_2(t)$, where $V_1(t)$ is the contribution from the surface charges of the inner conductor of the cavity and $V_2(t)$ is from that of the outer conductor. They are

$$V_i(t) = V_i^{(0)}\left(a{\rm e}^{-{\rm i}\omega(t-\rho_i/c)} + a^\dagger{\rm e}^{{\rm i}\omega(t-\rho_i/c)}\right), \quad i = 1, 2 \tag{5.72}$$

where ρ_1 and ρ_2 are the inner and the outer radii of the cavity and $V_i^{(0)}$'s are the amplitudes. V_1 and V_2 do not cancel. We can obtain

$$H_{\rm int} = \hbar g(\sigma_+ + \sigma_-)\left(a{\rm e}^{{\rm i}\theta} + a^\dagger{\rm e}^{-{\rm i}\theta}\right), \quad hg = -qV_0/2. \tag{5.73}$$

The point is that the cavity field and the non-overlapping qubit interact. The amplitude of interaction is $qV_0/2$. This is the manifestation of the Aharonov–Bohm effect for a quantum electrodynamic potential. This interaction leads to Stark and Lamb shifts and vacuum Rabi splitting of the eigenfrequency, $\omega_\pm = \omega + \frac{\Delta}{2} \pm \frac{\Omega_{\rm R}}{2}$, with a vacuum Rabi frequency $\Omega_{\rm R} = \sqrt{4g^2 + \Delta^2}$, where $\Delta = \omega_{\rm q} - \omega$.

5.12 Sagnac Effect

Generally, a fully Galilean invariant theory, (that is, for the comoving observer all physically relevant parameters are the same as for a corresponding observer in rest) will not predict

an observable effect of the rotation. One may think that nonrelativistic quantum mechanics is a Galilean invariant theory, that is it is independent of relativistic consideration. But the way in which the phase of the wave function transforms is incompatible with the behaviour of classical waves under Galilei transformations. Consequently, the Schrödinger wave mechanics can make predictions that have a relativistic character and cannot be expected from a Galilean invariant theory.

5.12.1 The Transformation of the Phase

The phase of a wave at a point with coordinate x at time t is given by $\phi = (p_x x - Et)/\hbar = (m/\hbar)(vx - v^2 t/2)$. Here v is the velocity of the particle. Consider a Galilean frame (x', t') moving with a velocity $-u$ with respect to the frame (x, t) then $x' = x+ut$, $t' = t$, $v' = v+u$. Now,

$$\phi = \frac{m}{\hbar}\left(v'x' - \frac{1}{2}v'^2 t' - ux' + \frac{1}{2}u^2 t'\right) . \tag{5.74}$$

On the other hand, in the moving frame the phase is

$$\phi' = \frac{m}{\hbar}\left(v'x' - \frac{1}{2}v'^2 t'\right) . \tag{5.75}$$

From Eqs. (5.74) and (5.75) we get the transformation law for the phase as

$$\phi' = \phi + \frac{m}{\hbar}\left(ux' - \frac{1}{2}u^2 t'\right) . \tag{5.76}$$

Thus, if $\psi(x, t)$ is a solution of the Schrödinger equation in the inertial frame (x, t) then that of the Schrödinger equation in (x', t') frame is

$$\psi'(x', t') = \psi(x' - ut, t)\, \mathrm{e}^{\mathrm{i}\frac{m}{\hbar}(ux' - \frac{1}{2}u^2 t')} . \tag{5.77}$$

5.12.2 Galilean Invariance

The transformation of the wave function given by Eq. (5.77) corresponds to a (projective) representation of the group of Galilei transformations. Moreover, the Schrödinger equation is invariant under the transformations. The momentum transformation is from p_x to $p_x + mu$. The fulfilment of the above two conditions is sufficient to argue that the Schrödinger theory is Galilean invariant. This means that the only effect on the wave functions is multiplication by a phase factor. However, the detection probabilities phenomena remain the same irrespective of the choice of the frame used for prediction. But this argument is inconsistent with the Sagnac effect discussed below.

5.12.3 Sagnac Effect

Consider a disk made to rotate around its center. A device on the disk emits two signals of same kind simultaneously. The signals travel with same velocity in opposite directions. Further, they are allowed to travel along the same circular path with the center in the middle of the disk. The signals are detected and compared once they come to the point of emission. Now, the question is: *Will the rotation of the disk influence the measurement of the detector?*

From Galilean invariance it is to be noted that a comoving observer on the disk would observe the departure of both the signals with the same speed. The time taken for the

signals to meet at the point of emission after one complete revolution is $2\pi R/v$, where R and v are the radius of the circular plate and the speed of the signals, respectively. There is no effect on both the arrival time and the phase relation of the signals due to rotation.

What will happen if we include the relativistic effect? In the case of the relativistic version, the observer of the rotating disk would see the departure of the signals with oppositely directed speeds namely v' and $-v$, in their respective momentary inertial frames. If x and t are the coordinates of a momentary inertial frame moving along with a segment of the moving disk then for the comoving observer at the position of the detector we have

$$t' = \frac{\left(t + \dfrac{\omega R x}{c^2}\right)}{\left(1 - \dfrac{\omega^2 R^2}{c^2}\right)^{1/2}} . \tag{5.78}$$

For the signal moving in the same direction of the rotating disk, the time $\Delta t_1'$ required for one revolution is

$$\Delta t_1' = \int \mathrm{d}t + \frac{2\pi\omega R^2}{c^2\sqrt{1 - (\omega^2 R^2/c^2)}} . \tag{5.79}$$

For the other signal

$$\Delta t_2' = \int \mathrm{d}t - \frac{2\pi\omega R^2}{c^2\sqrt{1 - (\omega^2 R^2/c^2)}} . \tag{5.80}$$

The integral $\int \mathrm{d}t$ represent the total time measured from the successive momentary inertial frames. This time is $2\pi R/(v\sqrt{1 - (\omega^2 R^2/c^2)})$. Then the difference in arrival time is

$$\Delta t_1' - \Delta t_2' = \frac{4\pi\omega R^2}{c^2\sqrt{1 - (\omega^2 R^2/c^2)}} . \tag{5.81}$$

The time difference Δt is connected with a phase difference

$$\Delta\phi = 2\pi\nu\Delta t = \frac{8\pi^2\omega R^2\nu}{c^2\sqrt{1 - (\omega^2 R^2/c^2)}} . \tag{5.82}$$

The appearance of

1. a difference in arrival times and
2. an associated phase difference

when the total system is in rotation is called the *Sagnac effect* [58–60]. The origin of the effect is completely relativistic.

The Sagnac effect was verified experimentally. The phase-shift in the interference of two coherent light beams manifesting due to the rotation of the apparatus was first observed by Georges Sagnac in 1913 [58] and then by Albert Abraham Michelson and Henry G. Gale in 1925 [60]. The same effect in the interference of neutron beams due to the rotation of earth has also been observed [61]. The Sagnac effect is used, for example, in inertial guidance systems and global navigation systems. This effect is utilized in many applications related to the measurement of rotation rates. In the Global Positioning System (GPS), a Sagnac correction has to be taken into account because a rotating clock (on board a satellite) experiences loss of synchronization at each turn with itself.

5.12.4 The Quantum Sagnac Effect

In quantum theory, two particles with opposite velocities can be represented by wave packets with opposite group velocities. Because the velocities transform as per a Galilei transformation the rotation of the disk gives no effect on the time needed by the wave packets to reach the detector. However, for the phases there is a difference. The point is that the observer of the disk should not carry out the calculations using $\phi = (p_x x - Et)/\hbar$ but should take into account of the correction term $m(ux' - u^2 t/2)/\hbar$. The phase difference at the detector is given by

$$\Delta\phi = \frac{4\pi m\omega R^2}{\hbar} = 4\pi R^2 \frac{\omega}{\hbar}\frac{h\nu}{c^2} = 4\pi R^2 \frac{\omega}{h/2\pi}\frac{h\nu}{c^2} = \frac{8\pi^2\omega R^2\nu}{c^2} \,. \tag{5.83}$$

Thus, in addition to the relativistic correction factor $1/\sqrt{1-\omega^2R^2/c^2}$, the phase-shift $\Delta\phi$ given by Eq. (5.82) is expected on the relativistic theory.

Interestingly, the phase-shift gives an observable effect. Suppose ψ_1 and ψ_2 are the wave packets without rotation of the disk. Then, when the disk is made to rotate the total wave function at the detector is $N(\psi_1 e^{i\phi_1} + \psi_2 e^{i\phi_2})$ with N being a normalization constant. As a result, the probability to detect a particle is $\propto |\psi_1|^2 + |\psi_2|^2 + 2\mathrm{Re}[\psi_1\psi_2^* e^{i(\phi_1-\phi_2)}]$. The Sagnac phase-shift is consequently reflected in the counting of particles in the detector. The effect has been verified experimentally in neutron interferometry, where the rotation of the earth has been proved detectable in this way [58].

5.13 Concluding Remarks

It has been shown that in two vertically coupled InGaAs/GaAs quantum dots Berry's phase can be changed from 0 to 2π or 2π to 0 by applying an external bias voltage [62]. A method was proposed for detecting spin-entangled electrons using Berry's phase [63]. It is possible to observe geometric phase with polarization changes, where the initial and final states are different. This kind of polarization is called *noncyclic* and represented by non-closed paths on the Poincaré sphere. Both theoretically and experimentally the phase on the optical elements is found to depend on a linear or nonlinear or on a singular way [64]. Berry's phase has a significant role in the tunnelling of nano magnetic clusters. For a cluster with a half-integer degenerate spin states tunnelling between two states is suppressed by the Berry's phase resulting from the destructive interference of different tunnelling paths [65,66]. Detection of Berry's phase in graphene [67], semiconductors [68] and in anisotropic insulators [69] have been reported.

Berry's phase is found to effect the center of the line for hydrogenic emitters in plasmas [70]. For a review on the effects of Berry's phase on electronic properties see ref. [71]. Progress on Berry's phase optical elements has been presented [72]. Broadband THz emitters based on Berry's phase nonlinear metasurfaces exhibiting unique optical functions was experimentally realized [73]. In quantum field theory we can consider Berry's phase of various states associated with the adiabatic variation of parameters such as masses and coupling. For some details of Berry's phase in quantum field theory see the refs. [74,75].

The role of tunnelling and associated forces on the Aharonov–Bohm effect has been reported [76]. The Aharonov–Bohm effect was explained without using the potentials but treating the source of the potentials in the framework of quantum theory [77]. The Sagnac effect has been studied in resonant microcavities [78] and light propagation in a wave guide [79] also.

5.14 Bibliography

[1] M.V. Berry, *Proc. Royal Soc. London A* 392:45, 1984.

[2] S. Pancharatnam, *Proc. Indian Acad. Sciences A* 44:247, 1956.

[3] S. Ramaseshan and R. Nityananda, *Current Science* 55:1225, 1986.

[4] J. Samuel and R. Bhandari, *Phys. Rev. Lett.* 60:2339, 1988.

[5] J.Y. Ji, J.K. Kim, S.P. Kim and K.S. Soh, *Phys. Rev. A* 52:3352, 1995.

[6] B.R. Holstein, *Am. J. Phys.* 57:1079, 1989.

[7] B.G. Levi, *Phys. Today* 46:17, 1993.

[8] M. Kugler and S. Shtrikman, *Phys. Rev. D* 37:934, 1988.

[9] J. Zak, *Phys. Rev. Lett.* 62:2747, 1989.

[10] R.D. King-Smith and D. Vanderbilt, *Phys. Rev. B* 47:1651, 1993.

[11] S. Ryu and Y. Hatsugai, *Phys. Rev. Lett.* 89:077002, 2002.

[12] P. Delplace, D. Ullmo and G. Montambaux, *Phys. Rev. B* 84:195452, 2011.

[13] D. Xiao, M.C. Chang and Q. Niu, *Rev. Mod. Phys.* 82:1959, 2010.

[14] J.E. Avron, D. Osadchy and R.Seiler, *Phys. Today* 56:38, 2003.

[15] J. Zak, *Phys. Rev. Lett.* 48:359, 1982.

[16] C. Kittel, *Quantum Theory of Solids*. Wiley, New York, 1963.

[17] M. Atala, M. Aidelsburger, J.T. Barreiro, D. Abanin, T. Kitagawa, E. Demler and I. Bloch, *Nat. Phys.* 9:795, 2013.

[18] S. Longhi, *Opt. Lett.* 38:3716, 2013.

[19] Q. Wang, M. Xiao, H. Liu, Sh. Zhu and C.T. Chan, *Phys. Rev. B* 93:041415, 2016.

[20] W. S. Gao, M. Xiao, C.T. Chan and W.Y. Tam, *Optics Letters* 40:5259, 2015.

[21] W. Zhu, Y. Ding, J. Ren, Y. Sun, Y. Li, H. Jiang and H. Chen, *Phys. Rev. B* 97:195307, 2018.

[22] F. Cardano, A. D'Errico, A. Dauphin, M. Maffei, B. Piccirillo, C. de Lisio, G. De Filippis, V. Cataudella, E. Santamato, L. Marrucci, M. Lewenstein and P. Massignan, *Nat. Commun.* 8:15516, 2017.

[23] R. Jackiw, *Atom. Mol. Phys.* 21:71, 1988.

[24] R.Y. Chiao and Y.S. Wu, *Phys. Rev. Lett.* 57:933, 1986.

[25] M.J. Rave and W.C. Kerr, *Eur. J. Phys.* 31:15, 2010.

[26] G. Sundaram and Q. Niu, *Phys. Rev. B* 59:14915, 1999.

[27] R. Resta, *J. Phys. Condens. Matter* 12:R107, 2000.

[28] Y. Zhang, Y.W. Tan, H.L. Stormer and P. Kim, *Nature* 438:201, 2005.

[29] G. Delacretaz, E.R. Grant, R.L. Whetten, L. Woste and J.W. Zwanziger, *Phys. Rev. Lett.* 56:2598, 1986.

[30] A. Tomita and R.Y. Chiao, *Phys. Rev. Lett.* 57:937, 1986.

[31] R. Bhandari, *Phys. Lett. A* 133:1, 1988.

[32] R. Bhandari and J. Samuel, *Phys. Rev. Lett.* 60:1211, 1988.

[33] R. Bhandari, *Current Science* 59:1159, 1990.

[34] R. Simon, H.J. Kimble and E.C.G. Sudarshan, *Phys. Rev. Lett.* 61:19, 1988.

[35] T.H. Chyba, L.J. Wang, L. Mandel and R. Simon, *Opt. Lett.* 13:562, 1988.

[36] R.Y. Chiao, A. Antaramian, K.M. Ganga, H. Jiao, S.R. Wilkinson and H. Nathel, *Phys. Rev. Lett.* 60:1214, 1988.

[37] P. Hariharan, *Am. J. Phys.* 61:591, 1993.

[38] H. Jiao, S.R. Wilkinson, R.Y. Chiao and H. Nathel, *Phys. Rev. A* 39:3475, 1989.

[39] P.G. Kwiat and R.Y. Chiao, *Phys. Rev. Lett.* 66:588, 1991.

[40] T.P. Grayson, J.R. Torgerson and G.A. Barbosa, *Phys. Rev. A* 49:626, 1994.

[41] J. Brendel, W. Dultz and W. Martienssen, *Phys. Rev. A* 52:2551, 1995.

[42] V. Bargmann, *J. Math. Phys.* 5:862, 1964.

[43] B. Hetenyi and M. Yahyavi, *Eur. Phys. Lett.* 105:40005, 2014.

[44] L.E. Ballentine, *Quantum Mechanics – A Modern Development.* World Scientific, Singapore, 1998.

[45] D.M. Greenberger and A. Zeilinger, *Phys. World*, September 1995, pp.33.

[46] S. Olariu and I.I. Popescu, *Rev. Mod. Phys.* 57:339, 1985.

[47] Y. Aharonov and D. Bohm, *Phys. Rev.* 115:485, 1959.

[48] J. Anandan, *Science* 297:1656, 2002.

[49] R.G. Chambers, *Phys. Rev. Lett.* 5:3, 1960.

[50] W. Bayh, *Z. Physik* 169:492, 1962.

[51] N. Osakabe, T. Matsuda, T. Kawasaki, J. Endo, A. Tonomura, S. Yano and H. Yamada, *Phys. Rev. A* 34:815, 1986.

[52] A. van Oudenaarden, M.H. Devoret, Yu.V. Nazarov and J.E. Mooij, *Nature* 391:768, 1998.

[53] M.P. Silverman, *More than One Mystery: Explorations in Quantum Interference.* Springer, Berlin, 1995.

[54] A. Tonomura, T. Matsuda, R. Suzuki, A. Fukuhara, N. Osakabe, H. Umezaki, J. Endo, K. Shinagawa, Y. Sugita and H. Fujiwara, *Phys. Rev. Lett.* 48:1443, 1982.

[55] A. Tonomura, N. Osakabe, T. Matsuda, T. Kawasaki, J. Endo, S. Yano and H. Yamada, *Phys. Rev. Lett.* 56:792, 1986.

[56] M. Ballesteros and R. Weder, *J. Math. Phys.* 50:122108, 2009.

[57] Y.W. Kim and K. Kang, *Quantum electrodynamic Aharonov–Bohm effect of charge qubit*. *arxiv:1506.07961v1 [quant-ph]*, 26 June 2015.

[58] G. Sagnac, *Comptes Rendus* 157:708, 1410, 1913.

[59] J. Anandan, *Phys. Rev. D* 24:338, 1981.

[60] A.A. Michelson and H.G. Gale, *Astrophys. J.* 61:140, 1925.

[61] S.A. Werner, J.L. Staudenmann and R. Colella, *Phys. Rev. Lett.* 42:1103, 1979.

[62] H. Wang and K.D. Zhu, *Europhys. Lett.* 82:60006, 2008.

[63] X. Zhao, T.C.A. Yeung, Y.B. Yu, C.H. Kam and Y.Q. Li, *Europhys. Lett.* 82:10005, 2008.

[64] T. van Dijk, H.F. Schouten, W. Ubachs and T.D. Visser, *Opt. Exp.* 18:10796, 2010.

[65] D. Loss, D.P. DiVincenzo and G. Grinstein, *Phys. Rev. Lett.* 69:3232, 1992.

[66] J. von Delft, C.L. Henley, *Phys. Rev. Lett.* 69:3236, 1992.

[67] A.F. Young, Y.Z. Zhang and P. Kim, *Experimental manifestation of Berry phase in graphene*. In Physics of Graphene. Eds.: H. Aoki and M. Dresselhaus. Springer, New York, 2014 pp. 3-27.

[68] M. Murakawa, M.S. Bahramy, M. Tokunaga, Y. Kohama, C. Bell, Y. Kaneko, N. Nagosa, H.Y. Hwang and Y. Tokura, *Science* 342:1490, 2013.

[69] K.I. Imura, Y. Takane and A. Tanaka, *Phys. Rev. B* 84:195406, 2011.

[70] M. Difallah, M.T. Meftah and N. Bedida, *Phys. Scr.* 85:055012, 2012.

[71] D. Xiao, M.C. Chang and Q. Niu, *Rev. Mod. Phys.* 82:1959, 2010.

[72] Y.H. Lee, G. Tan, T. Zhan, Y. Weng, G. Liu, F. Gou, F. Peng, N.V. Tabiryan, S. Gauza, and S.T. Wu, *Opt. Data Process Storage* 3:79, 2017.

[73] C. McDonnell, J. Deng, S. Sideris, T. Ellenbogen and G. Li *Nat. Commun.* 2021.

[74] M. Baggio, V. Narchos, K. Papadodimas, *J. High Energy Phys.* 4:062, 2017.

[75] P.S. Hsin, A. Kapustin and R. Thorngren, *Phys. Rev. B* 102:245113, 2020.

[76] G.C. Hegerfeldt and J.T. Neumann, *J. Phys. A* 41:155305, 2008.

[77] L. Vaidman, *Phys. Rev. A* 86:040101, 2012.

[78] S. Sunada and T. Harayama, *Phys. Rev. A* 74:021801(R), 2006.

[79] R. Wang, Y. Zheng and A. Yao, *Phys. Rev. Lett.* 93:143901, 2004.

5.15 Exercises

5.1 Under the adiabatic approximation show that

$$\frac{\mathrm{d}a_n}{\mathrm{d}t} = -\Big\langle \psi_n(t)\Big|\frac{\partial}{\partial t}\Big|\psi_n(t)\Big\rangle a_n(t).$$

Also, prove that

$$\eta(t,t_i) = -\frac{1}{\hbar}\int_{t_i}^{t} E_n(t')\,\mathrm{d}t + \mathrm{i}\int_{t_i}^{t}\Big\langle n(t')\Big|\frac{\partial}{\partial t'}\Big|n(t')\Big\rangle\,\mathrm{d}t',$$

where the last term in the above is called the Berry's phase.

5.2 The time evolution of a physical system described by a time-dependent Hamiltonian $H(t)$ is given by the Schrödinger equation $\mathrm{i}\hbar\mathrm{d}\psi(t)/\mathrm{d}t = H(t)\psi(t)$. Defining the time evolution of a state vector as $\psi(t) = U^\dagger\psi(0)$ show that $U^\dagger$ satisfies $\mathrm{i}\hbar\mathrm{d}U^\dagger(t)/\mathrm{d}t = H(t)U^\dagger(t)$ and $U^\dagger(t) = I - (\mathrm{i}/\hbar)\int_0^t H(t')U^\dagger(t')\,\mathrm{d}t'$. Then find $U^\dagger(t)$ if $H(t)$ commutes at different times, $[H(t), H(t')] = 0$.

5.3 Show that the gauge transformations $\mathbf{A} \to \mathbf{A}' = \mathbf{A} + \nabla\chi$, $\phi \to \phi' = \phi - (1/c)\partial\chi/\partial t$ leave $\mathbf{E}$ and $\mathbf{B}$ unchanged.

5.4 A current carrying long solenoid of radius R has a constant magnetic field $\mathbf{B}$ parallel to the axis of the solenoid (z-direction) inside and zero field outside. That does not mean that the vector potential outside the solenoid is zero. Find the magnetic field produced by the vector potential $\mathbf{A} = \mathbf{B}\rho\phi/2$ if $\rho \leq R$ and $\mathbf{A} = \mathbf{B}R^2\phi/(2\rho)$ if $\rho \geq R$.

5.5 Show that for the region in which magnetic field vanishes, the vector potential $\mathbf{A}$ is defined by the scalar function $\chi(\mathbf{r})$ given by $\chi(\mathbf{r}) = \int \mathbf{A} \cdot \mathrm{d}\mathbf{l}$.

5.6 The Hamiltonian of a spin-1/2 particle in an applied magnetic field ($\mathbf{R}(\mathbf{t})$) is

$$H(\mathbf{R}(\mathbf{t})) = -\tfrac{\mu}{\mathbf{2}}\sigma \cdot \mathbf{R}(\mathbf{t}) = -\tfrac{\mu}{\mathbf{2}} \begin{pmatrix} z(t) & x(t) - \mathrm{i}y(t) \\ x(t) + \mathrm{i}y(t) & -z(t) \end{pmatrix}.$$

Obtain the Berry's phase. Verify the result with the representation $| \uparrow, \mathbf{R}\rangle = \begin{pmatrix} \cos(\theta/2) \\ \sin(\theta/2)\mathrm{e}^{\mathrm{i}\phi} \end{pmatrix}$ for a spinor in the direction of $\hat{R}$ represented in terms of the polar angles θ and ϕ.

5.7 In a typical measurement of geometric phase the light beam is made to split into two. One is treated as reference while on the other group transformations are employed. The two beams are then recombined. Interference pattern is realized due to the relative phase. What does the relative phase refer to in the above?

5.8 In the Hamiltonian of a spin-1/2 particle in an applied field given in the exercise 5.6 assume that the z-component of the field is fixed and the projection on the (x, y)-plane is performing rotation, that is, $\theta =$ a constant and $\phi = \omega t$. Evaluate the Berry's phase and the associated cumulants by defining an adiabatic cycle in which ϕ rotates from 0 to 2π for both its two eigenstates.

5.9 Calculate the Zak phase of two-dimensional dimerized configurations governed by the Hamiltonian [10]

$$H = -\sum_n \left(J a_n^\dagger b_n + J' a_n^\dagger b_{n-1} + \text{h.c.}\right) + \Delta \sum_n \left(a_n^\dagger a_n - b_n^\dagger b_n\right)$$

with usual notations.

5.10 Starting from $\mathbf{B}_n(\mathbf{R}) = -\mathrm{Im} \sum_{n' \neq n} \langle \nabla n | n' \rangle \times \langle n' | \nabla n \rangle$ arrive at the result

$$\mathbf{B}_n(\mathbf{R}) = -\mathrm{Im} \sum_{n' \neq n} \frac{\langle n | \nabla H | n' \rangle \times \langle n' | \nabla H | n \rangle}{(E_n - E_{n'})^2}.$$

6

Phase Space Picture and Canonical Transformations

6.1 Introduction

Given the wave function $\psi(x,t)$ we compute the probability density function $\rho(x,t) = |\psi(x,t)|^2$ and easily visualize the distribution. Knowing $\psi(x,t)$ the distribution in momentum p_x is given by

$$\sigma(p_x,t) = |\chi(p_x,t)|^2 = \left|\frac{1}{\sqrt{2\pi}}\int_{-\infty}^{\infty}\psi(x,t)\mathrm{e}^{-\mathrm{i}kx}\,\mathrm{d}x\right|^2, \tag{6.1}$$

where $\chi(p_x,t)$ is the momentum wave function. The momentum distribution is difficult to visualize from the given $\psi(x,t)$. Thus, we wish to have a function that can display the probability distribution in the variables x and p_x simultaneously. Recall that, in classical mechanics phase space is used to visualize the solutions of systems. For quantum mechanical systems Eugene Paul Wigner introduced a quantum analogue of a phase space probability distribution called *Wigner distribution function* or *phase space picture* [1–8]. The idea is that every state of a quantum system is describable by a distribution (or function) on the classical phase space. In the phase space picture, starting from the Schrödinger wave function, we are able to construct the Wigner distribution function in terms of x and p_x. It does not represent a joint probability distribution for x and p_x because the uncertainty principle disallows the simultaneous determination of these variables with desired accuracy.

Using the Wigner distribution function [1,2] it is possible to perform a canonical transformation in quantum mechanics. The phase space picture is a useful candidate to illustrate the transition from classical to quantum mechanics. We note that classical mechanics deals with trajectories in phase space. In contrast to this quantum mechanics is concerned with probabilities. If it is desired to compare the classical mechanics and quantum mechanics, we need to focus on ensembles of trajectories in phase space for the classical case while density distribution in x and p_x (or Wigner function) for the quantum case.

The phase space approach finds applications in modern optics. In quantum optics, coherent state is represented by the circles and squeezed states by ellipses. They are generally in the two-dimensional phase space. In the Schrödinger representation, the position and momentum operators are represented by noncommuting operators and consequently the phase space concept is incompatible with this representation. However, in the Wigner phase space representation the circles and ellipses are defined in a very compact manner. In this chapter we present some of the features of the phase space picture.

DOI: 10.1201/9781003172192-6

6.2 Squeeze and Rotation in Phase Space

Let us first define the term squeeze [9] in phase space. For this purpose consider a circle centered about the origin in x and p_x coordinate system. Suppose we elongate the x-axis by multiplying it by a real number > 1 and contract the p_x-axis by dividing it by the same number. This circle is transformed into an ellipse. However, the areas of both are the same. This is a squeezing process. Squeezing can be performed in an arbitrary direction by combining the above operation with rotation about the origin.

In the above squeezing process, the x and p_x are changed, essentially, underwent translations. The coordinate transformation representing it is

$$x' = x + 0 \cdot p_x + u \ , \quad p'_x = 0 \cdot x + p_x + v. \tag{6.2a}$$

In matrix form the translation matrix $T(u, v)$ is given by

$$T(u,v) = \begin{pmatrix} x' \\ p'_x \\ 1 \end{pmatrix} = \begin{pmatrix} 1 & 0 & u \\ 0 & 1 & v \\ 0 & 0 & 1 \end{pmatrix} \begin{pmatrix} x \\ p_x \\ 1 \end{pmatrix} . \tag{6.3}$$

If u and v are set to zero then Eq. (6.3) is a linear homogeneous transformation. An example of linear transformation is the rotation around the origin through an angle $\theta/2$:

$$R(\theta/2) = \begin{pmatrix} x' \\ p'_x \\ 1 \end{pmatrix} = \begin{pmatrix} \cos(\theta/2) & -\sin(\theta/2) & 0 \\ \sin(\theta/2) & \cos(\theta/2) & 0 \\ 0 & 0 & 1 \end{pmatrix} \begin{pmatrix} x \\ p_x \\ 1 \end{pmatrix} . \tag{6.4}$$

(*When does the order of the matrix* $R(\theta/2)$ *become* 2×2*?*) Another example is the squeeze along the x-axis. Here, the circle is deformed into the ellipse and the elongation is along the x-axis. Now, x becomes $\mathrm{e}^{\lambda/2}x$ while $p_x \to \mathrm{e}^{-\lambda/2}p_x$, where λ is the deformation parameter. The matrix form of squeezing is [9]

$$S_x(\lambda) = \begin{pmatrix} x' \\ p'_x \\ 1 \end{pmatrix} = \begin{pmatrix} \mathrm{e}^{\lambda/2} & 0 & 0 \\ 0 & \mathrm{e}^{-\lambda/2} & 0 \\ 0 & 0 & 1 \end{pmatrix} \begin{pmatrix} x \\ p_x \\ 1 \end{pmatrix} . \tag{6.5}$$

Observe that the elongation along the x-axis is necessarily accompanied by the contraction along the p_x-axis. $S_x(\lambda)$ deforms the circle into ellipse with $\mathrm{e}^{-\lambda}x^2 + \mathrm{e}^{\lambda}p_x^2 = 1$. We know that a canonical transformation followed by another one is also a canonical transformation. As a consequence, an appropriate form of the transformation matrix can be a product of matrices T, R and S_x representing translation, rotation and squeezes, respectively. Let us simplify this by making use of the generators of the transformation matrices.

Solved Problem 1:

Consider a circle described by $(x-a)^2 + (p_x - b)^2 = 1$ which is not centered about the origin. Determine the effect of the squeezing along the direction that gives an angle $\theta/2$ with the x-axis with the deformation parameter η.

With the applied squeeze the given circle becomes a tilted ellipse with

$$\begin{aligned} &\mathrm{e}^{-\eta}\left[(x-a')\cos(\theta/2) + (p_x - b')\sin(\theta/2)\right]^2 \\ &\quad + \mathrm{e}^{\eta}\left[(x-a')\sin(\theta/2) - (p_x - b')\cos(\theta/2)\right]^2 = 1 \ . \end{aligned} \tag{6.6}$$

We can write

$$\begin{pmatrix} a' \\ b' \end{pmatrix} = \begin{pmatrix} \cosh\frac{\eta}{2} + \sinh\frac{\eta}{2}\cos\theta & \sinh\frac{\eta}{2}\sin\theta \\ \sinh\frac{\eta}{2}\sin\theta & \cosh\frac{\eta}{2} - \sinh\frac{\eta}{2}\cos\theta \end{pmatrix} \begin{pmatrix} a \\ b \end{pmatrix} . \tag{6.7}$$

6.2.1 Generators of the Transformation Matrices

For the translation matrix $T(u, v)$ of Eq. (6.3) the generator is

$$T(u,v) = \mathrm{e}^{-\mathrm{i}(uN_1+vN_2)}, \quad N_1 = \begin{pmatrix} 0 & 0 & \mathrm{i} \\ 0 & 0 & 0 \\ 0 & 0 & 0 \end{pmatrix}, \quad N_2 = \begin{pmatrix} 0 & 0 & 0 \\ 0 & 0 & \mathrm{i} \\ 0 & 0 & 0 \end{pmatrix} . \tag{6.8}$$

Next, the rotation matrix $R(\theta/2)$ is written as

$$R(\theta/2) = \mathrm{e}^{-\mathrm{i}\theta L} , \quad L = \begin{pmatrix} 0 & -\mathrm{i}/2 & 0 \\ \mathrm{i}/2 & 0 & 0 \\ 0 & 0 & 0 \end{pmatrix} . \tag{6.9}$$

The squeeze matrix S_x is generated by

$$S_x = \mathrm{e}^{-\mathrm{i}\lambda K_1} , \quad K_1 = \begin{pmatrix} \mathrm{i}/2 & 0 & 0 \\ 0 & -\mathrm{i}/2 & 0 \\ 0 & 0 & 0 \end{pmatrix} . \tag{6.10}$$

The matrix generating the squeeze in the direction making $\pi/4$ with x-axis is

$$K_2 = \begin{pmatrix} 0 & \mathrm{i}/2 & 0 \\ \mathrm{i}/2 & 0 & 0 \\ 0 & 0 & 0 \end{pmatrix} . \tag{6.11}$$

Solved Problem 2:

Show that the coordinate transformation operator $T(a) = \mathrm{e}^{-\mathrm{i}ap_x/\hbar}$ corresponds to a spatial translation and find the generators for coordinate translation.

We know that $[x, f(p_x)] = \mathrm{i}\hbar\partial f/\partial p_x$. Therefore, $[x, T(a)] = \mathrm{i}\hbar\partial T(a)/\partial p_x = aT(a)$. That is,

$$xT(a) = T(a)x + aT(a) = T(a)(x + a) . \tag{6.12}$$

Let $|x'\rangle$ be the eigenkets of x operator: $x|x'\rangle = x'|x'\rangle$. Further,

$$xT(a)|x'\rangle = T(a)(x + a)|x'\rangle = (x' + a)T(a)|x'\rangle . \tag{6.13}$$

$T(a)|x'\rangle$ is an eigenket of x with eigenvalue $(x' + a)$. Hence, $T(a)|x'\rangle = |x' + a\rangle$. $T(a)$ corresponds to a spatial translation. For an infinitesimal transformation, $a \to \delta a \to 0$, $T(a) \approx 1 - \mathrm{i}\delta a p_x/\hbar$. Comparing it with the equation $xT(a) = T(a)(x + a)$ the generators for translation transformation along x-direction is given by $N_1 = p_x/\hbar = -\mathrm{i}\partial/\partial x$.

6.2.2 Commutation Relations of N_1, N_2, L, K_1 and K_2

The matrices N_1, N_2, L, K_1 and K_2 obey the following set of commutation relations which are easy to verify:

$$[K_1,\, N_1] = \frac{\mathrm{i}}{2}N_1\,, \quad [K_1,\, N_2] = -\frac{\mathrm{i}}{2}N_2, \tag{6.14a}$$

$$[K_2,\, N_1] = \frac{\mathrm{i}}{2}N_2\,, \quad [K_2,\, N_2] = \frac{\mathrm{i}}{2}N_1, \tag{6.14b}$$

$$[K_1,\, K_2] = -\mathrm{i}L\,, \quad [N_1,\, N_2] = 0\,, \tag{6.14c}$$

$$[K_1,\, L] = -\mathrm{i}K_2\,, \quad [K_2,\, L] = \mathrm{i}K_1\,, \tag{6.14d}$$

$$[N_1,\, L] = \frac{\mathrm{i}}{2}N_2\,, \quad [N_2,\, L] = -\frac{\mathrm{i}}{2}N_1\,. \tag{6.14e}$$

6.3 Linear Canonical Transformations

For a function that is real and defined in the phase space of x and p_x we can do area-preserving canonical transformations [6]. An example of such a function is the Wigner probability distribution to be considered in the next section. First consider linear canonical transformations applicable to a function of x and p_x. *How do we obtain them?* This is achieved converting the matrix generators considered in the previous section into differential forms.

When a unitary operator $U(\alpha_1, \alpha_2, \ldots, \alpha_r)$ performs an infinitesimal transformation associated with a Lie group, then $U = 1 - \mathrm{i}\sum_{l=1}^{r} \delta_{\alpha_l} G_l$, where the operators G_l are called *generators of the Lie group*. For the spatial translation group, the generators are the components of the momentum operator. In the case of the three rotational translational group, the components of the angular momentum are the generators. When the translation is in momentum space then the operators of the position coordinates are the required generators.

The generators of translations in x and p_x space and rotation about the z-axis are [6]

$$N_1 = -\mathrm{i}\frac{\partial}{\partial x}\,, \quad N_2 = -\mathrm{i}\frac{\partial}{\partial p_x} \quad L_z = \frac{\mathrm{i}}{2}\left(p_x\frac{\partial}{\partial x} - x\frac{\partial}{\partial p_x}\right)\,. \tag{6.15}$$

The generators of squeezes along the x-axis and along the direction making 45° angle are

$$K_1 = \frac{\mathrm{i}}{2}\left(x\frac{\partial}{\partial x} - p_x\frac{\partial}{\partial p_x}\right)\,, \quad K_2 = \frac{\mathrm{i}}{2}\left(x\frac{\partial}{\partial p_x} + p_x\frac{\partial}{\partial x}\right)\,. \tag{6.16}$$

The operators in Eqs. (6.15)-(6.16) obey the commutation relations, Eqs. (6.14). Therefore, we use the matrix formalism of classical mechanics considered in the previous section in the phase space picture of quantum mechanics.

The Poisson brackets and canonical transformations are part of the effective formulation of classical mechanics. In quantum mechanics the Poisson bracket becomes commutator. We ask: *Why are canonical transformations not discussed for example, in the Schrödinger picture?* This is because in phase space, the translation operators x and p_x do not commute with each other. Further, the wave function is a function of x or p_x and not both. In fact, the following transformations on $\psi(x,t)$ lead to the transformations [9] given in

Eq. (6.15)–(6.16):

$$\widehat{N}_1 = -\mathrm{i}\frac{\partial}{\partial x}\,, \quad \widehat{N}_2 = x\,, \quad \widehat{L} = \frac{1}{4}\left[x^2 - \left(\frac{\partial}{\partial x}\right)^2\right]\,, \tag{6.17a}$$

$$\widehat{K}_1 = -\frac{\mathrm{i}}{4}\left(2x\frac{\partial}{\partial x} + 1\right)\,, \quad \widehat{K}_2 = \frac{1}{4}\left[x^2 + \left(\frac{\partial}{\partial x}\right)^2\right]\,. \tag{6.17b}$$

These operators are all Hermitian in the Schrödinger picture. However, the question is whether they satisfy the commutation relations (6.14). They satisfy all the commutation relations except one. For $\widehat{N}_1$ and $\widehat{N}_2$ (and N_1 and N_2)

$$\left[\widehat{N}_1,\, \widehat{N}_2\right] = -\mathrm{i} \;\text{ while }\; [N_1,\, N_2] = 0\,. \tag{6.18}$$

N_1 and N_2 commute with each other whereas $\widehat{N}_1$ and $\widehat{N}_2$ do not. $\left[\widehat{N}_1,\, \widehat{N}_2\right] = -\mathrm{i}$ causes a factor of modulus unity when the translation along p_x is commuted with that along the x-direction. The point is that the set of linear canonical transformations in the Schrödinger picture is not the same as that in classical theory. Further, N_1, N_2 and L form the two-dimensional Euclidean group. On the other hand, $\widehat{N}_1$, $\widehat{N}_2$ and $\widehat{L}$ require the identity operator to form a group.

6.4 Wigner Function

In this section we introduce the Wigner function, point out the properties of it and work it for two quantum systems.

6.4.1 Definition

If $\psi(x,t)$ is a solution of the Schrödinger equation

$$\mathrm{i}\frac{\partial\psi}{\partial t} = -\frac{1}{2m}\frac{\partial^2\psi}{\partial x^2} + V(x)\psi\,, \tag{6.19}$$

where $\hbar$ is set to unity then we are able to construct a function $W(x,p_x,t)$

$$W(x,p_x,t) = \frac{1}{\pi}\int_{-\infty}^{\infty}\psi^*(x+s,t)\psi(x-s,t)\,\mathrm{e}^{2\mathrm{i}p_x s}\,\mathrm{d}s\,. \tag{6.20}$$

This distribution function is defined over the two-dimensional phase space of x and p_x and is called *phase space distribution function* or *Wigner distribution function* or simply *Wigner function*. Eugene Wigner introduced this function in the early 1930s in the study of quantum corrections. The Wigner function is seen as the Fourier transform of the product of the shifted ψ and its complex conjugate ψ^*. It is a real function of x and p_x. Since $W(x,p_x)$ has a one-to-one correspondence with ψ_x, it completely represents a quantum state. It is meaningful to regard W as a probability distribution function in the phase space with the coordinates x and p_x.

6.4.2 Properties of Wigner Function

The integrand in Eq. (6.20) measures the correlation between ψ and ψ^* in a Fourier space. The Wigner function has several remarkable properties that are summarized below:

1. $W = W^*$ (verify). W is pure real and may be positive or negative. It is not a probability distribution function because it may take on both positive and negative values.
2. Knowing W the positive probability distribution function in the $(x,\, p_x)$ coordinates are given by

$$\begin{aligned} P_{\rm QM}(x,t) &= |\psi(x,t)|^2 \\ &= \int_{-\infty}^{\infty} W(x,p_x,t)\mathrm{d}p_x, \qquad (6.21a) \\ P_{\rm QM}(p_x,t) &= |\chi(p_x,t)|^2 \\ &= \int_{-\infty}^{\infty} W(x,p_x,t)\mathrm{d}x, \qquad (6.21b) \end{aligned}$$

   where χ is the momentum wave function. Integration over p_x gives the position distribution $|\psi(x)|^2$. On the other hand, integration over x yields the momentum distribution $|\chi(p_x)|^2$. Interestingly, W encodes both coordinate space probability and momentum space probability in a state represented by ψ.
3. The absolute square of the inner product of two wave functions $\psi(x,t)$ and $\phi(x,t)$ is given by

$$\frac{1}{2\pi}|(\phi,\psi)|^2 = \int_{-\infty}^{\infty}\int_{-\infty}^{\infty} W_\psi W_\phi \,\mathrm{d}x\,\mathrm{d}p_x \,. \qquad (6.22)$$

   $|(\phi,\psi)|^2$ is positive but becomes zero when ψ and ϕ are orthogonal.
4. Conventional representations give information about either position or momentum. In contrast, the Wigner representation gives details about both position and momentum.
5. From Eq. (6.20) the following translation property is evident. When $\psi(x,t) \to \psi(x-\alpha,t)$ then $W(x,p_x,t) \to W(x-\alpha,p_x,t)$: a shift in ψ introduces a corresponding shift in W. If $\psi(x,t) \to \psi(x,t)\mathrm{e}^{\mathrm{i}\alpha x}$ then $W(x,p_x,t)$ becomes $W(x,p_x-\alpha,t)$. A shift in momentum wave function gives a corresponding shift in p_x of W.
6. *How do we find the wave function from the Wigner function?* Given $W(x,p_x,t)$ we compute $\psi(x,t)$ through a two-step process:
   (a) Find the Fourier transform $\overline{W}$ of W:

$$\begin{aligned} \overline{W}(x,s,t) &= \frac{1}{\pi}\int_{-\infty}^{\infty} W(x,p_x,t)\,\mathrm{e}^{-2\mathrm{i}p_x s}\,\mathrm{d}p_x \\ &= \frac{1}{\pi}\psi^*(x+s,t)\,\psi(x-s,t) \,. \qquad (6.23) \end{aligned}$$

   (b) Choose an arbitrary point x_0 at which $\overline{W}(x_0,0,t) \neq 0$ and compute $\psi(x,t)$. When $x = (x+x_0)/2$ and $s = (-x+x_0)/2$

$$\overline{W}\left(\frac{x+x_0}{2},\, \frac{-x+x_0}{2},\, t\right) = \frac{1}{\pi}\psi^*(x_0,t)\psi(x,t) \,. \qquad (6.24)$$

   Then

$$\psi(x,t) = \frac{\pi}{\psi^*(x_0,t)}\overline{W}\left(\frac{x+x_0}{2},\, \frac{-x+x_0}{2},\, t\right) \,. \qquad (6.25)$$

The choice $x = x_0$, $s = 0$ yields $\overline{W}(x_0, 0, t) = (1/\pi)\psi^*(x_0, t)\ \psi(x_0, t)$. This in turn gives

$$\psi^*(x_0, t) = \frac{\pi \overline{W}(x_0, 0, t)}{\psi(x_0, t)} \ . \tag{6.26}$$

Substitution of this expression in Eq. (6.25) leads to

$$\psi(x, t) = \frac{\overline{W}\left(\frac{x + x_0}{2}, \frac{-x + x_0}{2}, t\right)}{\overline{W}(x_0, 0, t)\psi(x_0, t)} \ . \tag{6.27}$$

The noteworthy observation is that W is pure real while ψ is generally complex. Thus, from the real function W it is possible to compute a complex function ψ.

7. We write $W = \dfrac{1}{\pi}\displaystyle\int_{-\infty}^{\infty} \psi_1^*(x)\psi_2(x)\mathrm{d}s$. Then $|W| \leq 1/\pi$ and hence W cannot take arbitrarily large values.
8. For identical particles, if ψ is either symmetric or antisymmetric with respect to the exchange of x's and p_x's then W is symmetric:

$$W(x_1, p_{x_1}, x_2, p_{x_2}) = W(x_2, p_{x_2}, x_1, p_{x_1}). \tag{6.28}$$

For a system with N states ψ is represented by N complex numbers ($2N$ real numbers) with an overall phase ambiguity. For this same system W needs N^2 real numbers.
9. The Wigner function is useful when the process of extracting desired information from it is easier than obtaining from ψ. For example, from the property (3) the momentum density is computed from W by an integration of it over position. Whereas the momentum density is computed from ψ through the square of a Fourier transform. Several problems, particularly in quantum optics, are in this category [10,11].
10. *Is it possible to measure $W(x, p_x)$ of a quantum mechanical particle?* Because the probability distribution of an observable corresponds to an integral over $W(x, p_x)$, a single measurement cannot yield localized values of $W(x, p_x)$. We consider an observable whose average value is proportional to $W(x, p_x)$. We can perform a large number of repeated measurements on that observable by preparing a particle in the same quantum state. Then it is possible to construct the Wigner distribution by averaging the observable [10,12,13].

Solved Problem 3:

Starting from $W(x, p_x, t) = \dfrac{1}{\pi}\displaystyle\int_{-\infty}^{\infty} \psi^*(x + s, t)\psi(x - s, t)\mathrm{e}^{2\mathrm{i}p_x s}\,\mathrm{d}s$ obtain $P_{\mathrm{QM}}(x, t)$.

We obtain

$$\begin{aligned} P_{\mathrm{QM}}(x, t) &= \int_{-\infty}^{\infty} \frac{1}{\pi} \int_{-\infty}^{\infty} \psi^*(x + s, t)\psi(x - s, t)\mathrm{e}^{2\mathrm{i}p_x s}\,\mathrm{d}s\,\mathrm{d}p_x \\ &= \int_{-\infty}^{\infty} \psi^*(x + s, t)\psi(x - s, t)\delta(s)\,\mathrm{d}s \\ &= \psi^*(x + s, t)\psi(x - s, t)|_{s=0} \\ &= \psi^*(x, t)\psi(x, t) \\ &= |\psi(x, t)|^2 \ . \end{aligned} \tag{6.29}$$

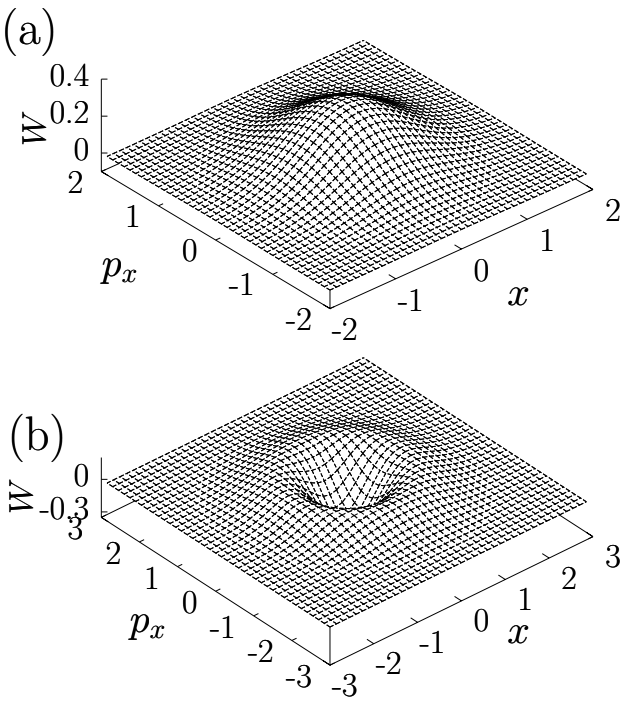

FIGURE 6.1
Wigner function for the harmonic oscillator. The subplots (a) and (b) are for the ground and first excited states, respectively.

6.4.3 Wigner Function for Harmonic Oscillator and Particle in a Box

Many standard potentials were analyzed using the Wigner distribution. Examples include harmonic oscillator, Morse potential, Coulomb potential, infinite height square-well potential, etc. [14–22].

Let us determine W for the one-dimensional linear harmonic oscillator ground state [22] with the wave function $\psi_0(x) = (1/\pi)^{1/4} \mathrm{e}^{-x^2/2}$. We find

$$\begin{aligned} W &= \frac{1}{\pi} \int_{-\infty}^{\infty} \psi_0^*(x+s)\psi_0(x-s)\, \mathrm{e}^{2\mathrm{i}p_x s}\, \mathrm{d}s \\ &= \frac{1}{\pi^{3/2}} \mathrm{e}^{-(x^2+p_x^2)} \int_{-\infty}^{\infty} \mathrm{e}^{(p_x+\mathrm{i}s)^2}\, \mathrm{d}s \\ &= \frac{1}{\pi}\, \mathrm{e}^{-(x^2+p_x^2)}\,. \end{aligned} \tag{6.30}$$

Figures 6.1a and 6.1b show the Wigner function for the ground state and first excited state of the linear harmonic oscillator.

For a particle in a box potential $V(x) = 0$ for $0 \le x \le L$ and ∞ otherwise we have $\psi_n(x) = \sqrt{2/L}\, \sin(n\pi x/L)$. First determine the limits of integration in Eqs. (6.20) (with

$t = 0$). Because $\psi_n(x \pm s)$ are always zero in the interval $[0, L]$ we must consider $0 \le x+s \le L$ and $0 \le x - s \le L$, that is, $-x \le s \le x$ for $0 \le x \le L/2$ and $-(L-x) \le s \le (L-x)$ for $L/2 \le x \le L$. For $0 \le x \le L/2$ we find [22]

$$\begin{aligned} W &= \frac{1}{\pi}\int_{-x}^{x} \psi_n^*(x+s)\psi_n(x-s)\mathrm{e}^{2ip_x s}\,\mathrm{d}s \\ &= \frac{2}{\pi L}\int_{-x}^{x} \sin[n\pi(x+s)/L]\sin[n\pi(x-s)/L]\mathrm{e}^{2ip_x s}\,\mathrm{d}s \\ &= \frac{2}{\pi L}\left\{\frac{\sin[2(p_x - n\pi/L)u]}{4(p_x - n\pi/L)} + \frac{\sin[2(p_x + n\pi/L)u]}{4(p_x + n\pi/L)}\right. \\ &\qquad \left. -\frac{1}{2p_x}\cos(2n\pi u/L)\,\sin(2p_x u)\right\}, \end{aligned} \tag{6.31}$$

where $u = x$ for $0 \le x \le L/2$. For the interval $L/2 \le x \le L$ in the above x and u are to be replaced by $L - x$. Figure 6.2 presents three examples of the Wigner function for $n = 1$, 5 and 10 with $L = 1$. For clarity $W > 0$ alone is shown in Fig. 6.2. W is almost everywhere positive for $n = 1$. For $n \gg 1$ (as shown for $n = 5$ and 10) the patterns are surprising. We can clearly observe the triangular form of the *fin*-shaped pattern along $p_x = \pm p_n$ axes. There are *spines* along the $p_x = 0$ axes. Both these structures are features of the system.

6.5 Time Evolution of the Wigner Function

With $\hbar = 1$ and $m = 1$ from Eq. (6.20) the time evolution of W is

$$\begin{aligned} \frac{\partial W}{\partial t} &= \frac{1}{\pi}\int_{-\infty}^{\infty} \mathrm{e}^{2\mathrm{i}p_x s}\left[\psi(x-s,t)\frac{\partial}{\partial t}\psi^*(x+s,t)\right. \\ &\qquad \left. +\psi^*(x+s,t)\frac{\partial}{\partial t}\psi(x-s,t)\right]\mathrm{d}s\,. \end{aligned} \tag{6.32}$$

The time derivative terms in the right-side of Eq. (6.32) can be replaced by space derivative term using the equations

$$\mathrm{i}\frac{\partial}{\partial t}\psi(x-s,t) = -\frac{1}{2}\frac{\partial^2}{\partial x^2}\psi(x-s,t) + V(x-s)\psi(x-s,t)\,, \tag{6.33a}$$

$$-\mathrm{i}\frac{\partial}{\partial t}\psi^*(x+s,t) = -\frac{1}{2}\frac{\partial^2}{\partial x^2}\psi^*(x+s,t) + V(x+s)\psi^*(x+s,t)\,. \tag{6.33b}$$

Then Eq. (6.32) becomes

$$\frac{\partial W}{\partial t} = \frac{\partial W_T}{\partial t} + \frac{\partial W_V}{\partial t}\,, \tag{6.34a}$$

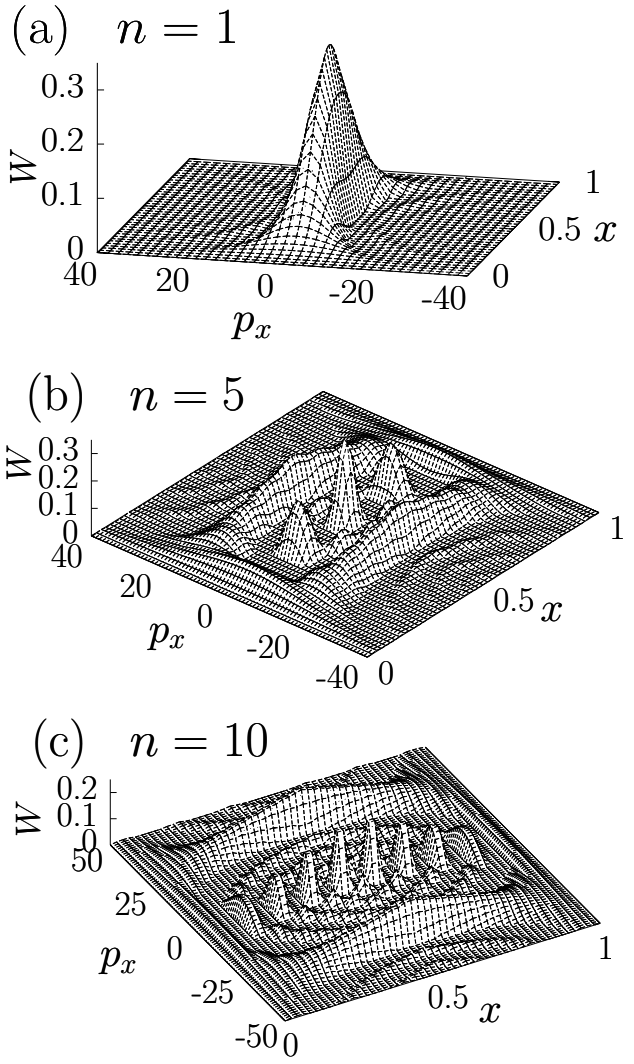

FIGURE 6.2
Wigner function for the particle in the box potential for three energy eigenstates. $W < 0$ is suppressed for easy visualization.

where

$$\frac{\partial W_T}{\partial t} = \frac{1}{2\pi \mathrm{i}} \int_{-\infty}^{\infty} \mathrm{e}^{2\mathrm{i}p_x s} \left[\psi(x-s,t) \frac{\partial^2}{\partial x^2} \psi^*(x+s,t) - \psi^*(x+s,t) \frac{\partial^2}{\partial x^2} \psi(x-s,t) \right] \mathrm{d}s \,, \tag{6.34b}$$

$$\frac{\partial W_V}{\partial t} = \frac{\mathrm{i}}{\pi} \int_{-\infty}^{\infty} \mathrm{e}^{2\mathrm{i}p_x s} \left[V(x+s) - V(x-s) \right] \times \psi^*(x+s,t) \psi(x-s,t) \mathrm{d}s \,. \tag{6.34c}$$

Consider $\partial W_T/\partial t$. The term $\partial^2/\partial x^2$ in Eq. (6.34b) can be rewritten suitably as $\partial^2/\partial x \partial s$ and then integrated by parts [23]:

$$\begin{aligned}
\frac{\partial W_T}{\partial t} &= \frac{1}{2\pi \mathrm{i}} \int_{-\infty}^{\infty} \mathrm{e}^{2\mathrm{i}p_x s} \left[\psi(x-s,t) \frac{\partial^2}{\partial x \partial s} \psi^*(x+s,t) \right. \\
&\qquad \left. + \psi^*(x+s,t) \frac{\partial^2}{\partial x \partial s} \psi(x-s,t) \right] \mathrm{d}s \\
&= \frac{1}{2\pi \mathrm{i}} \int_{-\infty}^{\infty} \mathrm{e}^{2\mathrm{i}p_x s} \frac{\partial}{\partial x} \psi^*(x+s,t) \frac{\partial}{\partial x} \psi(x-s,t) \mathrm{d}s \\
&\quad - \frac{p_x}{\pi} \int_{-\infty}^{\infty} \mathrm{e}^{2\mathrm{i}p_x s} \psi(x-s,t) \frac{\partial}{\partial x} \psi^*(x+s,t) \mathrm{d}s \\
&\quad - \frac{1}{2\pi \mathrm{i}} \int_{-\infty}^{\infty} \mathrm{e}^{2\mathrm{i}p_x s} \frac{\partial}{\partial x} \psi^*(x+s,t) \frac{\partial}{\partial x} \psi(x-s,t) \mathrm{d}s \\
&\quad - \frac{p_x}{\pi} \int_{-\infty}^{\infty} \mathrm{e}^{2\mathrm{i}p_x s} \psi^*(x+s,t) \frac{\partial}{\partial x} \psi(x-s,t) \mathrm{d}s \\
&= -\frac{p_x}{\pi} \int_{-\infty}^{\infty} \mathrm{e}^{2\mathrm{i}p_x s} \frac{\partial}{\partial x} \left(\psi^*(x+s,t) \psi(x-s,t) \right) \mathrm{d}s \\
&= -p_x \frac{\partial W}{\partial x} \qquad (6.35a)
\end{aligned}$$

Next, if $V(z)$ is analytic, it can be expressed as a Taylor series as

$$V(x+s) - V(x-s) = \sum_{n=\text{odd}} \frac{2s^n}{n!} \frac{\partial^n V}{\partial x^n} \,. \qquad (6.36)$$

Substituting it in Eq. (6.34c) and replacing s^n by $\left(\frac{1}{2\mathrm{i}} \frac{\partial}{\partial p_x} \right)^n$ (outside the integral), we obtain

$$\frac{\partial W_V}{\partial t} = \sum_{n=\text{odd}} \frac{(-\mathrm{i})^{n-1}}{2^{n-1} n!} \frac{\partial^n V}{\partial x^n} \frac{\partial^n W}{\partial p_x^n} \,. \qquad (6.37)$$

Now, we write

$$\frac{\partial W}{\partial t} = -p_x \frac{\partial W}{\partial x} + \sum_{n=0}^{\infty} \frac{\mathrm{i}^{2n}}{2^n (2n+1)!} \left(\frac{\partial}{\partial x} \right)^{2n+1} V(x) \left(\frac{\partial}{\partial p_x} \right)^{2n+1} W \,. \qquad (6.38)$$

We use the Schrödinger equation to determine $\psi(x,t)$ from a given $\psi(x,0)$. Then obtain $W(x,p_x,t)$ by solving Eqs. (6.34a) and (6.38). Notably, ψ and W obtained for given initial conditions are indeed unique because the Schrödinger equation and Eqs. (6.34a) and (6.38) are linear and first-order in time t. Because Eqs. (6.34a) and (6.38) are obtained from Schrödinger equation these solutions have the one-to-one relations.

If $\hbar$ and m are not set to unity then in Eq. (6.38) $\hbar^{2n}$ enters inside the summation as

$$\frac{\partial W}{\partial t} = -\frac{p_x}{m} \frac{\partial W}{\partial x} + \frac{\partial V}{\partial x} \frac{\partial W}{\partial p_x} + O(\hbar^2) \,. \qquad (6.39)$$

The above equation, neglecting the terms containing $\hbar^2$ and higher powers of $\hbar^2$, is the classical Liouville equation. The motion of W in phase space is that of classical case under the influence of $V(x)$. When we add higher derivatives of V then they give rise to a diffusion-like dynamics.

For the harmonic oscillator with $V(x) = kx^2/2$, the Eq. (6.39) becomes

$$\frac{\partial W}{\partial t} = -p_x \frac{\partial W}{\partial x} + kx \frac{\partial W}{\partial p_x} \,. \tag{6.40}$$

It is the classical Liouville equation for the linear harmonic oscillator. Hence, the W of the harmonic oscillator obeys the classical Liouville equation, even if the state is not nearly classical ($\hbar$ not $\to 0$).

6.6 Applications

The phase space picture of quantum mechanics became a research tool in modern optics. Coherent and squeezed states [2] and uncertainty relation for the spreading wave packet [3] are described more precisely in this picture. The canonical transformations in the phase space representation is a very vital theoretical tool in many branches of physics [1,4–6], particularly, to study Lorentz transformations while applying canonical transformations in phase space that correspond to processes in optics laboratories [3]. In the infinite height potential video sequences [24] of the evolution of Wigner functions for a wave function of a wave packet and its mirror wave packet is constructed. This and other related studies explored the fascinating patterns called *quantum carpets* [25–30] (patterns in space-time density plot) of probability density $|\psi(x,t)|^2$. W is exploited to study entanglement of correlated systems and the phase space sub-Planck structures of quantum interference [31,32]. Wigner functions have been reconstructed experimentally for quantum states of light, vibrational modes of molecules and superposition of diffracted cold atoms by a double slit [12]. A method to compute W for hydrogen atom has been developed [33]. A discrete Wigner function based on mutually unbiased bases has been defined [34–36] and it received great interest and has been used in a wide range of problems [37–40].

It is possible to write a light field as a Wigner distribution blurred by a kernel that can be reduced to a delta function at the geometric optics limit. This demonstrates the equivalence between the Wigner distribution and light field at that limit. In signal processing studies, the Wigner distribution is seen as a distribution on position and frequency of a signal.

In this section we present the application of the canonical transformations and phase space distribution function in the study of wave packet spread and coherent and squeezed states.

6.6.1 Wave Packet Spread

Let us consider the wave packet spread of a free particle with unit mass [6]. Suppose the initial ($t = 0$) momentum distribution is

$$g(k) = \left(\frac{1}{\pi}\right)^{1/4} \mathrm{e}^{-k^2/2} \,. \tag{6.41}$$

Let us compute $W(x, p_x, t)$. The scheme is this. First, determine $\psi(x,t)$ and $\psi(x,0)$. Use Eq. (6.20) to find $W(x, p_x, 0)$. Then solve Eq. (6.38) to get the time development of $W(x, p_x, 0)$.

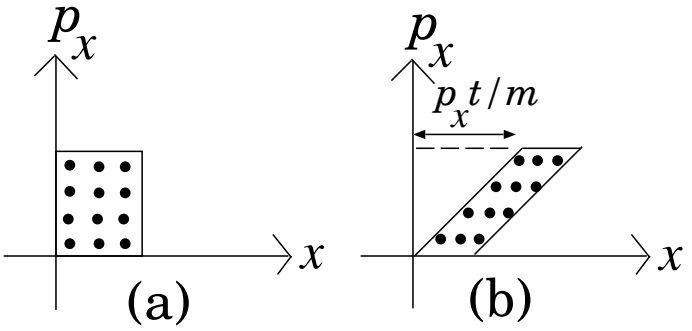

FIGURE 6.3
(a) A box of initial condition at $t = 0$. (b) Shear of the box in (a) in time t.

For the free particle

$$\begin{aligned}\psi(x,t) &= \int_{-\infty}^{\infty} g(k)\,\mathrm{e}^{-\mathrm{i}(kx-Et)}\,\mathrm{d}k \\ &= \int_{-\infty}^{\infty} g(k)\,\mathrm{e}^{-\mathrm{i}\left(kx-k^2t/2\right)}\,\mathrm{d}k \\ &= \left(\frac{1}{\pi}\right)^{1/4}\frac{1}{(1+\mathrm{i}t)^{1/2}}\,\mathrm{e}^{-x^2/[2(1+\mathrm{i}t)]}\,. \end{aligned} \tag{6.42}$$

Therefore,

$$\psi(x,0) = \left(\frac{1}{\pi}\right)^{1/4}\mathrm{e}^{-x^2/2}\,. \tag{6.43}$$

Next, from Eq. (6.20)

$$\begin{aligned} W(x,p_x,0) &= \frac{1}{\pi}\int_{-\infty}^{\infty}\psi^*(x+s,0)\psi(x-s,0)\mathrm{e}^{2\mathrm{i}p_x s}\,\mathrm{d}s \\ &= \frac{1}{\pi^{3/2}}\mathrm{e}^{-(x^2+p_x^2)}\int_{-\infty}^{\infty}\mathrm{e}^{(p_x+\mathrm{i}s)^2}\,\mathrm{d}s \\ &= \frac{1}{\pi}\mathrm{e}^{-(x^2+p_x^2)}\,. \end{aligned} \tag{6.44}$$

Equation (6.38) for the free particle is $\partial W/\partial t = -p_x \partial W/\partial x$ which implies

$$W(x,p_x,t) = W\left(x - p_x t, p_x, 0\right)\,. \tag{6.45}$$

Therefore, using Eq. (6.44), we obtain

$$W(x,p_x,t) = \frac{1}{\pi}\mathrm{e}^{-[x-p_x t]^2-p_x^2}\,. \tag{6.46}$$

The time evolution of the solution, (6.45), is depicted in Fig. 6.3. Every point in the phase space moves with velocity proportional to p_x in the x-direction. This transformation is area-preserving. The box undergoes a shear, however, its volume remains the same with time. *What does it imply?*

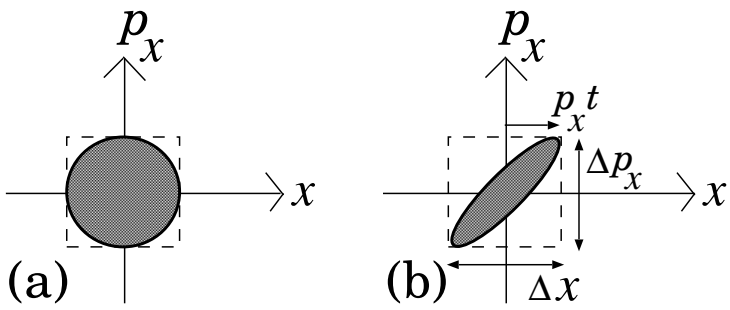

FIGURE 6.4
(a) W given by (6.46) at $t = 0$. (b) W at a time t.

Consider the $W(x, p_x, t)$ given by Eq. (6.46). It is a circle at $t = 0$ (Fig. 6.4). As time increases, the circle deforms a tilted ellipse preserving its area. The distribution is concentrated in the region where the exponent becomes < 1 in magnitude. This region is the region of uncertainty and is called *error box*. *What do we infer from the area-preserving property?* In the Schrödinger picture as time advances, the spatial distribution $\rho(x)$ or Δx becomes widespread. This is called the *wave packet spread*. On the other hand, in the phase space picture of quantum mechanics, the uncertainty is defined in terms of the volume of the error box that is invariant. Many of the results would be difficult to obtain from the Schrödinger equation. Thus, a deeper understanding is achieved about the wave packet spread.

The above mentioned elliptic deformation is a canonical transformation. The transformation matrix and the generator for it are

$$\begin{pmatrix} x' \\ p'_x \end{pmatrix} = \begin{pmatrix} 1 & t \\ 0 & 1 \end{pmatrix} \begin{pmatrix} x \\ p_x \end{pmatrix}, \quad G = \begin{pmatrix} 0 & \mathrm{i} \\ 0 & 0 \end{pmatrix} . \tag{6.47}$$

This yields $\mathrm{e}^{-\mathrm{i}tG} = \begin{pmatrix} 1 & t \\ 0 & 1 \end{pmatrix}$. We note that this G is $K_2 - L$.

6.6.2 Linear Harmonic Oscillator

For the linear harmonic oscillator the classical motion in x, p_x space is

$$x_0 = x \cos \omega t - \frac{1}{\omega} p_x \sin \omega t \,, \quad p_{x0} = p_x \cos \omega t + \omega x \sin \omega t \,, \tag{6.48}$$

where x_0 and p_{x0} are the values of x and p_x at $t = 0$. Thus, if the Wigner function $W(x, p_x, 0)$ corresponds to $t = 0$ then at $t > 0$

$$W(x, p_x, t) = W\left(x \cos \omega t - \frac{1}{\omega} p_x \sin \omega t, p_x \cos \omega t + \omega x \sin \omega t, 0 \right) . \tag{6.49}$$

It is noteworthy to mention that for the harmonic oscillator the analysis with exponentials and Hermite polynomials is concerned with the quantum state which can be prepared. It has nothing to do with the physics of the time development of initial state [23].

6.6.3 Coherent and Squeezed States

It is straight-forward to evaluate the Wigner function for the coherent state of the harmonic oscillator given by

$$|\alpha\rangle = \left(\frac{1}{\pi}\right)^{1/4} \mathrm{e}^{-[\mathrm{Im}(\alpha)]^2}\ \mathrm{e}^{-(x-\sqrt{2}\,\alpha)^2/2}\ , \tag{6.50}$$

where $\alpha = (a + \mathrm{i}b)/\sqrt{2}$ with a and b are real constants. The result is [2]

$$W(x, p_x) = \frac{1}{\pi}\mathrm{e}^{-(x-a)^2-(p_x-b)^2}\ . \tag{6.51}$$

This function is concentrated in a circular region governed by the equation

$$(x - a)^2 + (p_x - b)^2 = 1\ . \tag{6.52}$$

The Wigner function moves around its path in phase space, whereas its projection on the x-axis moves back and forth without an unchanging profile. If $\alpha = 0$, then $a = b = 0$ and hence the above circle becomes centered around the origin $x^2 + p_x^2 = 1$. This is the vacuum (zero photon) state. Therefore, the study of the Wigner function for the harmonic oscillator is equivalent to the study of a circle. The canonical transformation consists of translations, rotation and area-preserving elliptic deformations of this circle. These transformations are straight-forward under the translation along the x-axis by an amount a. In this case the circle becomes $(x - a)^2 + p_x^2 = 1$ with the centre $(a, 0)$. That is, the coherent state has a Gaussian distribution in phase space and it can be represented by a circle.

If we multiply α by $\mathrm{e}^{\mathrm{i}\theta/2}$, the circle given by Eq. (6.52) becomes rotated around the origin so that

$$(x - a')^2 + (p_x - b')^2 = 1\ , \tag{6.53}$$

where

$$\begin{pmatrix} a' \\ b' \end{pmatrix} = \begin{pmatrix} \cos\theta/2 & -\sin\theta/2 \\ \sin\theta/2 & \cos\theta/2 \end{pmatrix} \begin{pmatrix} a \\ b \end{pmatrix}\ . \tag{6.54}$$

Then the Wigner function is

$$R(\theta)T(a, b)W(x, p_x) = \frac{1}{\pi}\mathrm{e}^{(x-a')^2+(p_x-b')^2}\ . \tag{6.55}$$

Let us elongate (squeeze) the translated circle given by Eq. (6.52) in the x-direction. This means $x \to x\mathrm{e}^{\lambda/2}$ and $p_x \to p_x\mathrm{e}^{-\lambda/2}$. The result is the deformed ellipse described by

$$\mathrm{e}^{-\lambda}\left(x - a\mathrm{e}^{\lambda/2}\right)^2 + \mathrm{e}^{\lambda}\left(p_x - b\mathrm{e}^{-\lambda/2}\right)^2 = 1\ . \tag{6.56}$$

Figure 6.5 depicts coherent and squeezed states in Wigner phase space. Here b is chosen as zero. The circle around the origin in Fig. 6.5a represents the ground state harmonic oscillator. The one about $(a, 0)$ corresponds to coherent state. This circle can be elongated along the x-direction. The resulting ellipse is for the squeezed state with a real parameter ($a \neq 0$, $b = 0$) (Fig. 6.5b). This ellipse can be rotated through an angle $\theta/2$ (Fig. 6.5c). This rotated ellipse corresponds to the squeezed state with a complex parameter ($a \neq 0$, $b \neq 0$). A squeezed state has a Gaussian distribution in phase space like the coherent state. Unlike the case of coherent states the distribution for a squeezed state is elliptic. The circle in phase space for the coherent state is linearly deformed in such a way that the area is preserved.

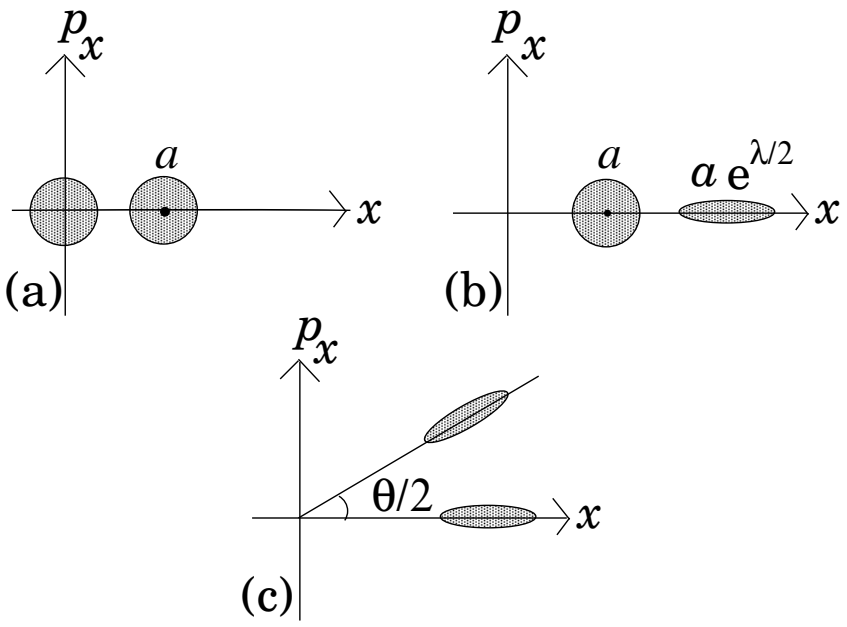

FIGURE 6.5
Representation of coherent and squeezed states in the Wigner phase space. For details see the text.

6.7 Advantages of the Wigner Function

The Wigner function has the following advantages in quantum optics.

1. Both the position and momentum variables are C numbers (real and complex numbers) in this representation. The W for the coherent and squeezed states is a Gaussian function of these C number variables. This Gaussian form can be described by circles and ellipses in phase space.
2. Canonical transformations can be performed on the Gaussian form of the distribution function which makes the mathematics simpler. For example, in the Schrödinger picture the uncertainty product for a squeezed state is not always minimal. But it is always minimal in the Wigner representation.
3. It is possible to calculate the expectation values and transition probabilities directly from W [2]. Due to the symmetry properties in phase space the calculations are simpler than in the Schrödinger representation.
4. The basic advantage of the Wigner function is that the translation operators commute with each other in phase space whereas the translation operators x and p_x in the Schrödinger representation do not commute with each other.

6.8 Concluding Remarks

Wigner distribution has been constructed for a time-dependent quadratic Hamiltonian system [41] and certain position-dependent mass systems [42]. The Wigner function has been used in quantum optics to explain the partial coherence associated with radioactivity [43]. It is used to bridge the gap between simple ray tracing and the full wave analysis of the system in the modelling of optical systems such as telescopes or fiber telecommunications devices. In signal analysis it has been used to represent a time-varying electrical signal, mechanical vibration, or sound wave. For the purposes of musical synthesis deriving from timbre morphing, the increased accuracy of the Wigner distribution representation will allow more accurate extraction of those features which characterize musical timbre [44]. The open-system Wigner function approach has proved to be of use in understanding the behaviour of resonant-tunnelling diodes. This technique permits evaluation of steady-state behaviour in the form of the curve, and calculations of the large-signal transient response and small-signal ac response [45]. It was shown that the Wigner domain may provide a better understanding of the sampling process than the traditional Fourier domain [46].

In quantum mechanics, linear combinations of wave functions $\psi(x,t)$ that satisfy the Schrödinger equation are also the solutions of it. When the transformation is made to the corresponding Wigner functions and the $x - p_x$ space, this linearity is lost. This is demonstrated for nonlinear Duffing oscillator as a classical system and as a quantum system has been presented [47]. It has been pointed out that the distinction between classical and quantum is not simply the distinction between large and small, but the extent to which we know the distribution [23]. If we pin down the distribution in phase space, either due to the details of preparation, details of evolution, or fineness of measurement, to details approaching $\Delta x \Delta p_x \approx \hbar$, the quantum nature will emerge.

Monte Carlo simulation study of resonant tunnelling diode operation [48] and nonequilibrium electron transport [49] have been analyzed through Wigner function approach. Tunnelling in deca-nanometer MOSFET was studied using Monte Carlo method for the Wigner transport equation [50]. For recent developments on Wigner function approaches in different fields one may refer to the ref. [51].

6.9 Bibliography

[1] E. Wigner, *Phys. Rev.* 40:749, 1932.

[2] N. Mukunda, *Am. J. Phys.* 47:192, 1979.

[3] S. Stenholm, *Eur. J. Phys.* 1:244, 1980.

[4] N.L. Balazs and B.K. Jennings, *Phys. Rep.* 104:347, 1984.

[5] M. Hillery, R.F. O'Connell, M.O. Scully and E.P. Wigner, *Phys. Rep.* 106:121, 1984.

[6] Y.S. Kim and E.P. Wigner, *Am. J. Phys.* 58:439, 1990.

[7] H.W. Lee, *Phys. Rep.* 259:147, 1995.

[8] T. Padmanabhan, *Resonance*, October 2009, pp.934.

[9] D. Han, Y.S. Kim and M.E. Noz, *Phys. Rev. A* 37:807, 1988.

[10] D. Leibfried, T. Pfau and C. Monroe, *Phys. Today* 51:22, 1998.

[11] Y.S. Kim and W.W. Zachary (Eds.) *The Physics of Phase Space.* Springer, Berlin, 1987.

[12] U. Leonhardt, *Measuring the Quantum State of Light.* Cambridge University Press, New York, 1997.

[13] W. Schleich and M. Raymer (Eds.) Special Issue of *J. Mod. Opt.* 44 (11,12), 1977.

[14] J.P. Dahl and M. Springborg, *Mol. Phys.* 47:1001, 1982.

[15] M. Springborg and J.P. Dahl, *Phys. Rev. A* 36:1050, 1987.

[16] M. Springborg, *Theor. Chim. Acta (Berlin)* 63:349, 1983.

[17] G. Mourgues, J.C. Andrieux and M.R. Feix, *Eur. J. Phys.* 5:112, 1984.

[18] J.P. Dahl and M. Springborg, *J. Chem. Phys.* 88:4535, 1988.

[19] M. Casas, H. Krivine and J. Martorell, *Eur. J. Phys.* 12:105, 1991.

[20] H.W. Lee, *Phys. Rep.* 25:259, 1995.

[21] A.M. Ozorio de Almeida, *Phys. Rep.* 295:265, 1998.

[22] M. Belloni, M.A. Doncheski and R.W. Robinett, *Am. J. Phys.* 72:1183, 2004.

[23] W.B. Case, *Am. J. Phys.* 76:937, 2008.

[24] O.M. Friesch, I. Marzoli and W.P. Schleich, *New J. Phys.* 2:4.1-4.11, 2000.

[25] M.V. Berry, *J. Phys. A* 29:6617, 1996.

[26] F. Groβmann, J.M. Rost and W.P. Schleich, *J. Phys. A* 30:L277, 1997.

[27] P. Stifter, C. Leichtle, W.P. Schleich and J. Marklov, *Z. Naturforsch A. Phys. Sci.* 52a:377, 1997.

[28] I. Marzoli, F. Saif, B. Birula, O.M. Friesch, A.E. Kaplan and W.P. Schleich, *Acta Phys. Slov.* 48:323, 1998.

[29] W. Loinaz and T.J. Newman, *J. Phys. A* 32:8889, 1999.

[30] M.J.W. Hall, M.S. Reineker and W.P. Schleich, *J. Phys. A* 32:8275, 1999.

[31] B.G. Englert and K. Wodkiewicz, *Int. J. Quantum Inform.* 1:153, 2003.

[32] W.H. Zurek, *Nature* 412:712, 2001.

[33] L. Praxmeyer, J. Mostowski and K. Wodkiewicz, *J. Phys. A* 39:14143, 2006.

[34] W.K. Wootters, *Ann. Phys.* 176:1, 1987.

[35] K.S. Gibbons, M.J. Hoffman and W.K. Wootters, *Phys. Rev. A* 70:062101, 2004.

[36] T. Baron, *Europhys. Lett.* 88:10002, 2009.

[37] M. Koniorczyk, V. Buzek, and J. Janszky, *Phys. Rev. A* 64:034301, 2001.

[38] J.P. Paz, A.J. Roncaglia and M. Saraceno, *Phys. Rev. A* 72:012309, 2005.

[39] U. Leonhardt, *Phys. Rev. A* 53:2998, 1996.

[40] P. Bianucci, C. Miquel, J.P. Paz and M. Saraceno, *Phys. Lett. A* 297:353, 2002.

[41] J.R. Choi and K.H. Yeon, *Phys. Scr.* 78:045001, 2008.

[42] A. de S. Dutra and J.A. de Oliveira, *Phys. Scr.* 78:035009, 2008.

[43] A. Walther, *J. Opt. Soc. Am.* 58:1256, 1968.

[44] D.J. Furlong and C.J. Hope, *Time-frequency distributions for timbre morphing: The Wigner distribution versus the STFT*. In Procceedings of the SBCMIV, 4th Symposium of Brasilian Computer Music, Brasilia, Brasil, August 1997.

[45] W.R. Frensley, *Rev. Mod. Phys.* 62:745, 1990.

[46] A. Stern and B. Javidi, *J. Opt. Soc. Am. A* 21:360, 2004.

[47] I. Katz, A. Retzker, R. Straub and R. Lifshitz, *Phys. Rev. Lett.* 99:040404, 2007.

[48] L. Shifren, C. Ringhofer and D.K. Ferry, *IEEE Trans. Elect. Dev.* 50:769, 2003.

[49] C. Jacoboni and P. Bordone, *Rep. Prog. Phys.* 67:1044, 2044.

[50] A. Gehring and H. Kosina, *J. Comp. Elec.* 4:67, 2005.

[51] J. Weinbub and D.K. Ferry, *Appl. Phys. Rev.* 5:041104, 2018.

6.10 Exercises

6.1 If $N_1 = \begin{pmatrix} 0 & 0 & \mathrm{i} \\ 0 & 0 & 0 \\ 0 & 0 & 0 \end{pmatrix}$ and $N_2 = \begin{pmatrix} 0 & 0 & 0 \\ 0 & 0 & \mathrm{i} \\ 0 & 0 & 0 \end{pmatrix}$ prove that $T(u,v) = \mathrm{e}^{-\mathrm{i}(uN_1+vN_2)}$ becomes $\begin{pmatrix} 1 & 0 & u \\ 0 & 1 & v \\ 0 & 0 & 1 \end{pmatrix}$.

6.2 Given $L = \begin{pmatrix} 0 & -\mathrm{i}/2 & 0 \\ \mathrm{i}/2 & 0 & 0 \\ 0 & 0 & 0 \end{pmatrix}$ determine $R(\theta/2)(= \mathrm{e}^{-\mathrm{i}\theta L})$.

6.3 Write the Wigner distribution in momentum space.

6.4 Show that the momentum transformation operator $k(p_0) = \mathrm{e}^{\mathrm{i}xp_0/\hbar}$ corresponds to a momentum translation and find the generators for momentum translation.

6.5 Show that $W^* = W$.

6.6 Find the Fourier transform $\overline{W}$ of W.

6.7 For a free particle wave function

$$\psi(x,t) = \frac{1}{\left[\sqrt{\pi}\,(1+\mathrm{i}t)\right]^{1/2}} \mathrm{e}^{\mathrm{i}p_0(x-x_0)} \mathrm{e}^{-\mathrm{i}p_0^2 t/2} \times \mathrm{e}^{-(x-x_0-p_0 t)^2 / [2(1+\mathrm{i}t)]}$$

find the Wigner function $W(x, p_x, t)$.

6.8 If $\psi = A\psi_1 + B\psi_2 = (A/\pi^{1/4})\mathrm{e}^{-x^2/2}\mathrm{e}^{\mathrm{i}p_A x} + (B/\pi^{1/4})\mathrm{e}^{-x^2/2}\mathrm{e}^{\mathrm{i}p_B x}$ find its Wigner function.

6.9 Show that for $\psi_n(x,t) = u_n(x)\mathrm{e}^{-\mathrm{i}E_n t}$ the Wigner function W is time-independent.

6.10 Obtain the Wigner function for the first excited state of a linear harmonic oscillator.

Taylor & Francis
Taylor & Francis Group
http://taylorandfrancis.com

7

Quantum Entanglement

7.1 Introduction

Entanglement, first coined by Schrödinger as *Verschränkung*, is a phenomenon where a strong correlation exists between the subsystems of a composite state, regardless of the distance between them [1]. He observed that the maximal knowledge of a whole system does not necessarily include knowledge of all its subsystems even if they are totally divided from each other and do not influence each other at the present time. Quantum systems display many new features like superposition of quantum states, interference, tunnelling which are unknown in classical systems even for a single particle system. There are further differences that manifest themselves in composite quantum systems in the form of entanglement which is a type of correlation between particles that have no classical counterpart. Schrödinger first recognized a feature implying the existence of global states of composite systems that cannot be written as a product of the states of individual systems. This phenomenon is known as *entanglement* [1]. Entanglement between two states refers to the situation that *if one state is changed then the other state changes automatically*.

Consider a particle with two states $|0\rangle$ and $|1\rangle$. It may be a photon with vertical polarization state or horizontal polarization state. Or it may be an electron with spin-up state or spin-down state. Now, think of a composite system of two such particles. First, note that each of the two vector spaces is spanned by similar sets of two basis vectors: $\{|0\rangle, |1\rangle\}$ and $\{|0\rangle, |1\rangle\}$. Since the composite system space of two particles is produced by tensor product $\mathcal{H}_1 \otimes \mathcal{H}_2 = \mathcal{H}$, we get

$$\begin{bmatrix} |0\rangle \\ |1\rangle \end{bmatrix} \otimes [|0\rangle \ |1\rangle] = \begin{bmatrix} |0\rangle_1|0\rangle_2 & |0\rangle_1|1\rangle_2 \\ |1\rangle_1|0\rangle_2 & |1\rangle_1|1\rangle_2 \end{bmatrix} = \begin{bmatrix} |00\rangle & |01\rangle \\ |10\rangle & |11\rangle \end{bmatrix} . \tag{7.1}$$

Thus, $\{|00\rangle, |01\rangle, |10\rangle, |11\rangle\}$ are the set of the four basis vector of the new entangled space $\mathcal{H}$. A linear combination of them may yield entangled states. For example, the Bell states

$$|\psi^{\pm}\rangle = \frac{1}{\sqrt{2}}(|01\rangle \pm |10\rangle), \quad |\phi^{\pm}\rangle = \frac{1}{\sqrt{2}}(|00\rangle \pm |11\rangle) \tag{7.2a}$$

are entangled. Suppose $|0\rangle$ and $|1\rangle$ denote the spin-down and spin-up states, respectively, of a particle along any direction $\mathbf{n}$ then for the above specified state the spin for neither particle is determined. It could be up or down along any direction, during its propagation. However, if one particle is found to be spin-up (down) in a measurement along a particular direction then the other one must be spin-down (up) along that direction immediately, irrespective of the distance between the two particles.

Entanglement was used by Einstein, Podolsky and Rosen (EPR) to argue that quantum mechanics was incomplete as it did not describe reality [2]. Bell developed the local hidden variable model (LHVM) in order to incorborate the EPR idea of deterministic world into quantum mechanics. Bell proved that LHVM has to satisfy some inequalities (known as *Bell inequalities*) on statistical correlations in experiments involving two particle systems

DOI: 10.1201/9781003172192-7

[3]. It was proved experimentally that these Bell inequalities are violated for some entangled states of two particle systems, thus establishing that it is impossible to simulate quantum correlations within any classical formulation. The entangled states violating a Bell inequality are termed as *nonlocal*.

Violation of Bell inequality proved that quantum formulation is nonlocal in nature. (For more details refer Volume I, Chapter 20.) Entanglement of more than two particles also leads to a contradiction with LHVM [4]. Initially Bell's work made the study of quantum entanglement important for understanding the formulation of quantum theory. But in the last three decades, entanglement has come to be realized as a potentially valuable resource. It has been found that one can perform many tasks that are otherwise impossible to do with classical systems using entangled states. Entanglement finds wide application in the development of quantum information theory. Quantum information processings like quantum cryptography, quantum teleportation, quantum error correction codes and quantum computation depend mainly on the use of entangled states.

There are three fundamental issues concerned with entanglement:

1. Theoretical and experimental detection of entanglement.
2. Reversing the degradation of entanglement.
3. Characterization, classification, controlling and quantification of entanglement.

In this chapter after reviewing states in classical mechanics we shall discuss the fundamental aspects of characterization of quantum entanglement like the definition, the detection, the classification and quantification of entanglement. Using density matrices we define entanglement in mixed states and that of a bipartite pure state. We discuss the determination of entanglement of bipartite pure state by means of Schmidt coefficients. We present criteria to identify the separability of quantum states. Then we consider full and partial separabilities of quantum states of multipartite systems. Then we diiscuss the measures of entanglement. Finally, we briefly discuss the applications of quantum entanglement.

7.2 States in Classical Mechanics

In the following we briefly review the notions of various kinds of states in classical mechanics and we mainly follow the ref. [5].

A state of a classical system is represented by a point, say, x_0, in an appropriate phase space X. We can represent a state by means of a scalar valued function. That is, $f : X \to \mathbb{R}$, $f(x) = 1$ for $x = x_0 \in X$ otherwise 0. It can be treated as a probability density function in X. Such a state is termed as a *pure state*. A *mixed state* is one with $f(x_k) = p_k > 0$, $k = 1, 2, \ldots, n$ with $\sum p_k = 1$ and $f(x_k) = 0$ for $k > n$. A mixed state refers to a situation wherein the system can be in any one of the set of finite number of points with $p_k > 0$. One can easily show that a mixed state can be generated by a set of pure states.

A vector space can be formed by the set of all scalar valued functions on X. Suppose define a set of vectors as $S = \{v_i : 1 \leq i \leq k\}$. We can define a vector space of the form $\sum_{i=1}^{k} a_i v_i$, $0 \leq a_i \leq 1$, $1 \leq i \leq k$, $\sum_{i=1}^{k} a_i = 1$ as a convex combination of vectors from S. For a state f on X we write $f(x_i) = p_i > 0$, $\{x_i : 1 \leq i \leq n\}$ and $\sum_{i=1}^{n} p_i = 1$ or $f = \sum_{i=1}^{n} p_i f_{x_i}$ where f_{x_i} represent pure states for $1 \leq i \leq n$. We note that f is a pure state or a convex combination of pure states.

Let us consider a system with two particles: particle-1with phase space X and particle-2 with phase space Y. The phase space of the composite system is $X \times Y$. Denote the pure

states of the subsystems X and Y as f_{x_0} and g_{y_0}, respectively. $f_{x_0} \otimes g_{y_0} = f_{x_0} \times g_{y_0}$. The tensor product of pure states of the subsystems is given by

$$\begin{aligned} [f_{x_0} \times g_{x_0}](x,y) &= f_{x_0}(x) \times g_{y_0}(y) \\ &= \delta_{x_0 x} \times \delta_{y_0 y} \\ &= \begin{cases} 1, & \text{if } x = x_0,\ y = y_0 \\ \\ 0, & \text{otherwise.} \end{cases} \end{aligned} \tag{7.3}$$

The composite states $f_{x_0} \otimes f_{y_0}$ are termed as *product state*. From the above it is clear that for a composite system, each pure state is of the form of a product of pure states of the subsystems. (*Is it true for quantum systems?)*

Suppose the state of a composite system is, say, expressed as $\sum_{i=1}^{n} p_i f_i \otimes g_i$ with $\{f_i\}$ and $\{g_i\}$ are the states of the subsystems. Such a state is called a *separable state*. A nonseparable state is termed as an entangled state. Further, a state which is not expressible as a convex combination of product states is essentially referred as an entangled state.

As noted earlier, each and every classical state is either a pure state or a convex combination of pure states. Moreover, a pure state is a product state for a composite system. Therefore, classical composite states are separable states implying that classically no entangled state exists.

7.3 Quantum Entangled States

Consider a quantum system-1 described by a finite dimensional Hilbert space $\mathcal{H}_1$. The state of the system $|\psi_1\rangle$ is described by a vector in $\mathcal{H}_1$. If $\{|u_i\rangle,\ i = 1, 2, \ldots, n\}$ form the basis of the n-dimensional Hilbert space $\mathcal{H}_1$ then the state vector can be written as a linear combination of the kets $|u_i\rangle$ as

$$|\psi_1\rangle = \sum_{i=1}^{n} a_i |u_i\rangle, \quad \sum |a_i|^2 = 1. \tag{7.4}$$

As the ket $|\psi_1\rangle$ represents a vector in $\mathcal{H}_1$, it is called a *pure state*. Similarly, a second quantum system-2 described by the Hilbert space $\mathcal{H}_2$ of dimension m will have a pure state

$$|\psi_2\rangle = \sum_{j=1}^{m} b_j |v_j\rangle, \quad \sum |b_j|^2 = 1, \tag{7.5}$$

where the orthonormal kets $\{|v_j\rangle,\ j = 1, 2, \ldots, m\}$ span $\mathcal{H}_2$.

Next, consider a biparticle composite quantum system comprising the two subsystems-1 and 2. The total Hilbert space of the composite system $\mathcal{H}$ is a tensor product of the two subsystem spaces $\mathcal{H} = \mathcal{H}_1 \otimes \mathcal{H}_2$. The Hilbert space $\mathcal{H}$ consists of all vectors that can be written as a superposition in the form

$$|\psi\rangle = \sum_{i=1}^{n} \sum_{j=1}^{m} C_{ij} \left(|u_i\rangle \otimes |v_j\rangle\right) \tag{7.6}$$

for some choice of the complex coefficients and $|u_i\rangle \otimes |v_j\rangle = |u_i\rangle|v_j\rangle$. $|\psi\rangle$ cannot be in general regarded as a product of the states of individual subsystems

$$|\psi\rangle \neq |\psi_1\rangle \otimes |\psi_2\rangle. \tag{7.7}$$

If $|\psi\rangle$ is not a direct product as given by Eq. (7.7) then the state $|\psi\rangle$ is said to be *entangled*.

If we consider N separate systems each described in the Hilbert space $\mathcal{H}_i$, $i = 1, 2, \ldots, N$ then according to quantum theory, the total Hilbert space of the composite system is a tensor product of the subsystem spaces $\mathcal{H} = \overset{N}{\underset{i=1}{\otimes}} \mathcal{H}_i$. Then according to the superposition principle, the total state of the system is [6]

$$|\psi\rangle = \sum_{\mathbf{i}_N} C_{\mathbf{i}_N} |\mathbf{i}_N\rangle, \quad \mathbf{i}_N = i_1, i_2, \ldots, i_N \tag{7.8a}$$

in which $\mathbf{i}_N$ is the multi-index and

$$|\mathbf{i}_N\rangle = |i_1\rangle \otimes |i_2\rangle \otimes \ldots\ldots \otimes |i_N\rangle \tag{7.8b}$$

with $|i_i\rangle$ is the orthonormal basis of $\mathcal{H}_i$ for the ith subsystem. In general, $|\psi\rangle$ is not a product of the states of individual subsystems:

$$|\psi\rangle \neq |\psi_1\rangle \otimes |\psi_2\rangle \otimes \ldots\ldots \otimes |\psi_N\rangle. \tag{7.9}$$

$|\psi_i\rangle$ is a pure state in the Hilbert space $\mathcal{H}_i$ of the ith subsystem. If $|\psi\rangle$ is not the direct product of the pure states of the subsystems, then $|\psi\rangle$ is said to be *entangled*. If

$$|\psi\rangle = |\psi_1\rangle \otimes |\psi_2\rangle \otimes \ldots\ldots \otimes |\psi_N\rangle \tag{7.10}$$

then $|\psi\rangle$ is not entangled and is said to be *separable*. If $|\psi\rangle$ is separable then the local measurement outcomes on different subsystems are uncorrelated with each other and depend only on the states of each respective subsystems.

Example:

Consider a biparticle separable system $|\psi\rangle = |\psi_1\rangle \otimes |\psi_2\rangle$ and assume a Hermitian operator O_1 that operates only on $\mathcal{H}_1$. Since a local measurement is done on system-1, we can consider the local observable as $O_1 \otimes \mathbb{1}$ which will operate O_1 on the system-1 and leave the system-2 unaffected due to the identity operator $\mathbb{1}$. Since O_1 operates on $|\psi_1\rangle$, it will project an eignestate of O_1, but the state $|\psi_2\rangle$ will be unaffected due to the $\mathbb{1}$ operation. If later on, we perform a local operation $\mathbb{1} \otimes O_2$ on system-2, it will project an eigenstate of O_2, leaving the state $|\psi_1\rangle$ unaffected. This result will be independent of the first result. Hence, the local measurement outcomes on different subsystems are uncorrelated with each other and depend only on the states of each respective subsystems. On the other hand, if $|\psi\rangle \neq |\psi_1\rangle \otimes |\psi_2\rangle$, then the local measurements on one subsystem will affect the state of the other subsystem and hence the measurements will be correlated.

In the above we considered entanglement between separate systems. An example of this is the singlet state of, say, two spins-$\frac{1}{2}$; $|\uparrow\rangle_1|\downarrow\rangle_2 - |\downarrow\rangle_1|\uparrow\rangle_2$. One may think of another type of entanglement between different properties of a single system. An example is entangling external motional ($|x_1\rangle$, $|x_2\rangle$) and ($|\uparrow\rangle, |\downarrow\rangle$): $|x_1\rangle|\uparrow\rangle + |x_2\rangle|\downarrow\rangle$. In this book we are concerned with the former type.

Consider the entangled state of two spin-$\frac{1}{2}$ particles given by

$$|\psi\rangle = \frac{1}{\sqrt{2}} \left(|\uparrow\rangle_1|\downarrow\rangle_2 - |\downarrow\rangle_1|\uparrow\rangle_2\right). \tag{7.11}$$

The above ψ states that either electron-1 will posses spin-up and electron-2 will posses spin-down or electron-1 will posses spin-down and electron-2 will posses spin-up. This ψ

can be treated as containing a complete knowledge of the two-spin system but no definite information about the spin property of each electron.[1]

Solved Problem 1:

Identify entangled states of the two qubit system from the following states by finding whether they are factorizable into a tensor product state or not.
(i) $\frac{1}{\sqrt{2}}(|11\rangle_{\rm AB} + |10\rangle_{\rm AB})$. (ii) $\frac{1}{\sqrt{2}}(|11\rangle_{\rm AB} + |00\rangle_{\rm AB})$.

The normalized states of particle A in H_2 are $\frac{1}{\sqrt{a^2+b^2}}(a|1\rangle_{\rm A} + b|0\rangle_{\rm A})$ and that for particle B are $\frac{1}{\sqrt{c^2+d^2}}(c|1\rangle_{\rm B} + d|0\rangle_{\rm B})$. Therefore, the tensor product space $H_{2\rm A} \otimes H_{2\rm B}$ is

$$\begin{aligned} H_{2\rm A} \otimes H_{2\rm B} \quad = \quad & \frac{1}{\sqrt{a^2+b^2}\sqrt{c^2+d^2}}\,[ac|11\rangle_{\rm AB} + ad|10\rangle_{\rm AB} \\ & + bc|01\rangle_{\rm AB} + bd|00\rangle_{\rm AB}]\ . \end{aligned} \tag{7.12}$$

The determinant of the coefficients is

$$\begin{vmatrix} ac & ad \\ bc & bd \end{vmatrix} = 0\ . \tag{7.13}$$

Thus, if the determinant of the coefficients vanishes then the tensor product state is factorizable and it is not an entangled state. If the determinant of the coefficients is not zero for a state then it is an entangled state.

Case (i): $\frac{1}{\sqrt{2}}(|11\rangle_{\rm AB} + |10\rangle_{\rm AB})$

The determinant of the coefficients is

$$\frac{1}{\sqrt{2}}\begin{vmatrix} 1 & 1 \\ 0 & 0 \end{vmatrix} = 0\ . \tag{7.14}$$

Hence, it is not an entangled state.

Case (ii): $\frac{1}{\sqrt{2}}(|11\rangle_{\rm AB} + |00\rangle_{\rm AB})$

For this case the determinant of the coefficients becomes

$$\frac{1}{\sqrt{2}}\begin{vmatrix} 1 & 0 \\ 0 & 1 \end{vmatrix} = \frac{1}{\sqrt{2}} \neq 0\ . \tag{7.15}$$

It is an entangled state.

Interference effect and state projection accompanying measurement can be used to create an entanglement between two separated particles [7]. For example, consider qubits of two ions. They can be encoded in hyperfine levels of the electronic ground states and prepared in the superposition states $\frac{1}{2}(|{\rm g}\rangle + |{\rm e}\rangle)$, where $|{\rm g}\rangle$ and $|{\rm e}\rangle$ represent ground and excited states, respectively. These qubits undergo simultaneously single-photon scattering when excited by

[1] In [E. Santos, *Eur. J. Phys.* 37:055402, 2016] Santos regarded this as: it is like a student claiming to have complete knowledge of a whole subject matter but no knowledge at all about every lesson.

short laser pulses. The frequencies (say, red and blue) of the emitted photons are correlated with the qubit states:

$$|\psi_{1,2}\rangle = \frac{1}{\sqrt{2}}\left[|\mathrm{g}\rangle_{1,2}|\mathrm{blue}\rangle + |\mathrm{e}\rangle_{1,2}|\mathrm{red}\rangle\right]. \tag{7.16}$$

We can then send the photons simultaneously through a 50:50 beam splitter and detect them using two detectors A and B. If photons are found simultaneously detected at A and B then it implies the projection of the ions into the Bell state

$$|\psi_{\mathrm{final}}\rangle = \frac{1}{\sqrt{2}}\left[|\mathrm{g}\rangle_1|\mathrm{e}\rangle_2 - |\mathrm{e}\rangle_1|\mathrm{g}\rangle_2\right]. \tag{7.17}$$

Note that here the atoms did not interact directly. This scheme is useful for entanglement assisted communication between ion locations, say 1 and 2.

7.4 Mixed States

A pure state state is a vector or a ray in Hilbert space. But usually we encounter only mixed states rather than pure states. In that case we cannot define entanglement for mixed state as equivalent to being nonproduct state as defined for pure state by Eq. (7.9). As mixed state is described by density matrix, entanglement of a mixed state is also defined using density matrices.

7.4.1 Density Operator

The density operator (matrix) is used to describe the state of a quantum system in a more general way than provided by the state vector of the Hilbert space. It is more useful to describe an ensemble of mixed states for which a state vector cannot be formed. (For more information on density operator, refer Chapter 7, Volume I.) If p_i is the probability for the qubit to be in the state $|\psi_i\rangle$ then the density operator is defined as

$$\rho = \sum_i p_i|\psi_i\rangle\langle\psi_i| = \sum_i p_i\rho_i, \quad \sum_i p_i = 1. \tag{7.18}$$

If we choose an arbitrary orthonormal basis $\{|u_j\rangle\}$ then $\sum_j |u_j\rangle\langle u_j| = \mathbb{1}$. In such a basis the density matrix element is given by

$$\rho_{kl} = \sum_i p_i\langle u_k|\psi_i\rangle\langle\psi_i|u_l\rangle. \tag{7.19}$$

The expectation value of any observable O with matrix element $O_{kl} = \langle u_k|O|u_l\rangle$ is given by $\langle O\rangle = \mathrm{Tr}(\rho O)$, where Tr is the trace of the matrix.

The density matrix is Hermitian and its trace is equal to 1. The density operator of a pure state $|\psi\rangle$ is given by $\rho = |\psi\rangle\langle\psi|$, $\rho^2 = |\psi\rangle\langle\psi|\psi\rangle\langle\psi| = \rho$. Hence, $\mathrm{Tr}(\rho^2) = 1$ as $\mathrm{Tr}(\rho) = 1$. For a mixed state one can show that $0 < \mathrm{Tr}(\rho^2) < 1$ (see the solved problem 2).

Solved Problem 2:

Consider the density matrix in the z-basis for a 50:50 mixture of spin-up and spin-down in the z-direction of the state $\frac{1}{2}(|0\rangle + |1\rangle)$. Show that $\mathrm{Tr}(\rho^2) < 1$ for mixed state.

We have $\rho_{\uparrow\downarrow} = \frac{1}{2}(|0\rangle\langle 0| + |1\rangle\langle 1|)$. As $|0\rangle = \begin{bmatrix} 1 \\ 0 \end{bmatrix}$ and $|1\rangle = \begin{bmatrix} 0 \\ 1 \end{bmatrix}$ we get

$$|0\rangle\langle 0| = \begin{bmatrix} 1 \\ 0 \end{bmatrix} \otimes \begin{bmatrix} 1 & 0 \end{bmatrix} = \begin{bmatrix} 1 & 0 \\ 0 & 0 \end{bmatrix} \tag{7.20a}$$

$$|1\rangle\langle 1| = \begin{bmatrix} 0 \\ 1 \end{bmatrix} \otimes \begin{bmatrix} 0 & 1 \end{bmatrix} = \begin{bmatrix} 0 & 0 \\ 0 & 1 \end{bmatrix}. \tag{7.20b}$$

That is,

$$\rho_{\uparrow\downarrow} = \frac{1}{2}\begin{bmatrix} 1 & 0 \\ 0 & 0 \end{bmatrix} + \frac{1}{2}\begin{bmatrix} 0 & 0 \\ 0 & 1 \end{bmatrix} = \frac{1}{2}I. \tag{7.21}$$

Hence,

$$\rho_{\uparrow\downarrow}^2 = \frac{1}{4}I^2 = \frac{1}{4}I \text{ and } \mathrm{Tr}\left(\rho_{\uparrow\downarrow}^2\right) = \frac{1}{2} < 1. \tag{7.22}$$

Thus, $\mathrm{Tr}\left(\rho_{\uparrow\downarrow}^2\right) < 1$ for mixed state.

7.4.2 Bloch Sphere

As any 2×2 matrix can be written as a linear combination of the unit matrix and the Pauli matrices σ_x, σ_y and σ_z, an arbitrary single qubit density matrix can be written as [8]

$$\rho = \frac{1}{2}\left[I + \mathbf{P} \cdot \boldsymbol{\sigma}\right], \tag{7.23}$$

where $\mathbf{P}$ is an arbitrary real vector of length $|\mathbf{P}| < 1$. $|\mathbf{P}|$ is the radius of a sphere called *Bloch sphere*. We get from Eq. (7.23) $\mathrm{Tr}\left(\rho^2\right) = \frac{1}{2}\left(1 + |\mathbf{P}|^2\right)$. For $|\mathbf{P}| = 1$, $\mathrm{Tr}\left(\rho^2\right) = 1$. The pure states are on the surface of the Bloch sphere, where as mixed states with $|\mathbf{P}| < 1$ are inside the sphere.

7.4.3 Reduced Density Matrix

Consider a biparticle composite system consisting of system-1 and system-2. Let ρ be the density matrix of the composite system on $\mathcal{H} = \mathcal{H}_1 \otimes \mathcal{H}_2$ describing a statistical ensemble of the combined system. Then the reduced density matrices for the subsystems 1 and 2 are defined as

$$\rho_1 = \mathrm{Tr}_2(\rho), \quad \rho_2 = \mathrm{Tr}_1(\rho). \tag{7.24}$$

For ρ_1, the trace is performed over $\mathcal{H}_2$ only and for ρ_2, the trace is performed over $\mathcal{H}_1$ only. This is known as *partial trace*.

If the kets $|a_1\rangle$ and $|a_2\rangle$ belong to $\mathcal{H}_1$ and $|b_1\rangle$ and $|b_2\rangle$ belong to $\mathcal{H}_2$ then the partial trace can be defined as follows:

$$\mathrm{Tr}_1\left(|a_1\rangle\langle a_2| \otimes |b_1\rangle\langle b_2|\right) = \left(\mathrm{Tr}|a_1\rangle\langle a_2|\right)|b_1\rangle\langle b_2|, \tag{7.25}$$

$$\mathrm{Tr}_2\left(|a_1\rangle\langle a_2| \otimes |b_1\rangle\langle b_2|\right) = |a_1\rangle\langle a_2|\left(\mathrm{Tr}|b_1\rangle\langle b_2|\right). \tag{7.26}$$

This rule combined with linearity enables to compute partial traces in all the cases. The physical meaning of the reduced density matrix of a subsystem is that it describes everything

that is accessible by local operations in that particular subsystem. One can construct a general pure state as a linear combination of pure states in $\mathcal{H}$ as

$$|\psi\rangle = \frac{1}{\sqrt{2}}\left(|\psi_1\rangle \otimes |\psi_2\rangle + |\phi_1\rangle \otimes |\phi_2\rangle\right), \quad |\psi_i\rangle \neq |\phi_i\rangle,\ i = 1, 2. \tag{7.27}$$

Suppose we make a measurement of a local observable O_1 for the subsystem-1. As the operator O_1 operates on $\mathcal{H}_1$, it will not affect the states $|\psi_2\rangle$ and $|\phi_2\rangle$ of $\mathcal{H}_2$. Hence, the expectation value observed for system-1 will be $\langle O_1\rangle = \langle\psi|O_1 \otimes \mathbb{1}_2|\psi\rangle$. Using Eq. (7.19) we get

$$\langle O_1\rangle = \mathrm{Tr}\left(O_1 \otimes \mathbb{1}_2\rho\right), \tag{7.28}$$

where the density matrix of the composite system is $\rho = |\psi\rangle\langle\psi|$. Then

$$\langle O_1\rangle = \mathrm{Tr}\left(O_1 \otimes \mathbb{1}_2|\psi\rangle\langle\psi|\right) = \mathrm{Tr}_1\left(O_1 \mathrm{Tr}_2|\psi\rangle\langle\psi|\right). \tag{7.29}$$

Using Eq. (7.24) we obtain $\langle O_1\rangle = \mathrm{Tr}_1\left(O_1\rho_1\right)$, where $\mathrm{Tr}_{1,2}$ denotes the partial trace over the first/second subsystem and $\rho_1 = \mathrm{Tr}_2\rho$ is the reduced matrix of the first subsystem. Thus, ρ_1 as defined by Eq. (7.24) describes completely the subsystem-1 and ρ_2 describes completely the subsystem-2.

7.5 Bipartite Systems

We shall consider finite-dimensional *bipartite* quantum systems which are composed of two distinct subsystems 1 and 2, described by the Hilbert space $\mathcal{H} = \mathcal{H}_1 \otimes \mathcal{H}_2$. For example, consider a particle with two states $|0\rangle$ and $|1\rangle$. It may be a photon with vertical polarization state or horizontal polarization state. Or it may be an electron with spin-up state or spin-down state.

7.5.1 Basis Vectors

Now, consider a composite system of two such particles. We must note that each of the two vector spaces is spanned by similar set of two basis vectors: $\{u_i\} = \{|0\rangle_1,\ |1\rangle_1\}$ and $\{v_j\} = \{|0\rangle_2,\ |1\rangle_2\}$. Then any pure state in the Hilbert space $\mathcal{H}$ can be written as Eq. (7.6), that is,

$$|\psi\rangle = \sum_{i=1}^{2}\sum_{j=1}^{2} C_{ij}|u_i\rangle \otimes |v_j\rangle, \quad \sum_{i,j=1}^{2} |C_{ij}|^2 = 1. \tag{7.30}$$

Since

$$\begin{bmatrix} u_1 \\ u_2 \end{bmatrix} = \begin{bmatrix} |0\rangle_1 \\ |1\rangle_1 \end{bmatrix}, \quad \begin{bmatrix} v_1 \\ v_2 \end{bmatrix} = \begin{bmatrix} |0\rangle_2 \\ |1\rangle_2 \end{bmatrix} \tag{7.31}$$

we obtain

$$\begin{bmatrix} u_1 \\ u_2 \end{bmatrix} \otimes \begin{bmatrix} v_1 \\ v_2 \end{bmatrix} = \begin{bmatrix} |0\rangle_1 \\ |1\rangle_1 \end{bmatrix} \otimes \begin{bmatrix} |0\rangle_2 \\ |1\rangle_2 \end{bmatrix} = \begin{bmatrix} |0\rangle_1|0\rangle_2 \\ |0\rangle_1|1\rangle_2 \\ |1\rangle_1|0\rangle_2 \\ |1\rangle_1|1\rangle_2 \end{bmatrix} = \begin{bmatrix} |00\rangle \\ |01\rangle \\ |10\rangle \\ |11\rangle \end{bmatrix}. \tag{7.32}$$

Therefore, $|00\rangle$, $|01\rangle$, $|10\rangle$ and $|11\rangle$ are the four basis vectors spanning the Hilbert space $\mathcal{H}$ of the bipartite system.

7.5.2 Bipartite Entanglement in Pure State

Any linear combination of the basis vectors of $\mathcal{H}$ will give a pure state. We have already defined by Eq. (7.7) the entanglement of pure states as a pure state in $\mathcal{H}$ which cannot be written as the product of the pure states of the Hilbert space of the two subsystems. If we can write $|\psi\rangle = |\psi_1\rangle \otimes |\psi_2\rangle$, where $|\psi_1\rangle$ and $|\psi_2\rangle$ are pure states in $\mathcal{H}_1$ and $\mathcal{H}_2$, and $|\psi\rangle$ is a pure state in $\mathcal{H}$ then $|\psi\rangle$ is said to be *separable*. A linear combination of the basis vectors in $\mathcal{H}$ may yield entangled states. For example, the Bell states given by Eq. (7.2) are entangled. Note that measurement at only one of the subsystems leads to finding it with equal proabability in the state $|0\rangle$ or $|1\rangle$. That is, the states provide no knowledge about the subsystems. On the other hand, the states are pure as a whole thereby giving maximal knowledge about the whole system.

One can define the entanglement of a bipartite pure state in terms of the density matrices also. Suppose for a pure state $|\psi\rangle$, its density matrix $\rho = |\psi\rangle\langle\psi| \neq \rho_1 \otimes \rho_2$, where $\rho_1 = |\psi_1\rangle\langle\psi_1|$ and $\rho_2 = |\psi_2\rangle\langle\psi_2|$ are the density matrices of the subsystems 1 and 2, respectively. As $\rho \neq \rho_1 \otimes \rho_2$, if a local measurement is performed in any of the subsystem it leads to a state reduction of the whole composite system state $|\psi\rangle$, not only on the subsystem on which the measurement has been done. Thus, the probabilities for the outcomes on local measurements on one subsystem are influenced by prior measurements of the other subsystem even if the two subsystems are well separated. For pure states the two subsystems are entangled if $\rho \neq \rho_1 \otimes \rho_2$ and separable if $\rho = \rho_1 \otimes \rho_2$.

7.5.3 Schmidt Decomposition

One can find a special basis representation of bipartite state $|\psi\rangle$ performing Schmidt decomposition [9–11]. The coordinates in this represenation called the *Schmidt coefficients* completely determine the entanglement of the bipartite pure state. Schmidt decomposition is obtained using singular-value decomposition (SVD) of linear algebra. In SVD method of linear algebra, any arbitrary matrix $A \in C^{m\times n}$ of rank k can be always expressed as $A = VDU^\dagger$, where $V \in C^{m\times m}$, $U = C^{n\times n}$ and the diagonal matrix $D = [d_{ij}] \in C^{m\times n}$. The nonvasishing elements of D are the so-called *singular-values* a_i:

$$d_{11} = a_1, \;\; d_{22} = a_2, \;\; \ldots, \;\; d_{kk} = a_k \tag{7.33}$$

which are the square-root of the eigenvalues of $AA^\dagger$. The columns of V and U are the eigenvectors of $AA^\dagger$ and $A^\dagger A$, respectively. Using SVD we can perform Schmidt decomposition for the bipartite pure state

$$|\psi\rangle = \sum_{i=1}^{m}\sum_{j=1}^{n} C_{ij}|i_1\rangle|j_2\rangle, \tag{7.34}$$

where $|i_1\rangle$ is the orthonormal basis of $\mathcal{H}_1$ of dimension m and $|j_2\rangle$ is the orthonormal basis of $\mathcal{H}_2$ of dimension n and C_{ij} is the matrix element of the matrix $[C]^{m\times n}$. Applying SVD to the matrix $[C]$, we obtain

$$\begin{aligned}
|\psi\rangle &= \sum_{i=1}^{m}\sum_{j=1}^{n} \left[VDU^\dagger\right]_{ij} |i_1\rangle|j_2\rangle \\
&= \sum_{i=1}^{m}\sum_{j=1}^{n}\sum_{l=1}^{k} V_{il} D_{ll} U^\dagger_{lj} |i_1\rangle|j_2\rangle \\
&= \sum_{l=1}^{k} a_l \left(\sum_{i=1}^{m} V_{il}|i_1\rangle\right)\left(\sum_{j=1}^{n} U^*_{jl}|j_2\rangle\right).
\end{aligned} \tag{7.35}$$

Since $\sum_{i=1}^{m} V_{il}|i_1\rangle$ is a linear combination of the basis vectors $|i_1\rangle$ in $\mathcal{H}_1$ it gives an another vector $|l_1\rangle$ in $\mathcal{H}_1$. Similarly, $\sum_{j=1}^{n} U_{jl}^{*}|j_2\rangle$ gives the ket $|l_2\rangle$ in $\mathcal{H}_2$. We find from Eq. (7.35), $|\psi\rangle$ is obtained in a transformed basis (Schmidt basis) $|l_1\rangle|l_2\rangle$ as

$$|\psi\rangle = \sum_{l=1}^{k} a_l|l_1\rangle|l_2\rangle = \sum_{l} \sqrt{p_l}\,|l_1\rangle|l_2\rangle, \tag{7.36}$$

where the singular-values $a_l = \sqrt{p_l}$. It can be proved that p_l are the nonzero elements of the spectra of either reduced density matrix ρ_1 and ρ_2. Since $|\psi\rangle$ is normalized

$$\sum_{l=1}^{k} |a_l|^2 = \sum_{l=1}^{k} p_l = 1. \tag{7.37}$$

$\sqrt{p_l}$ are known as the *Schmidt coefficients of the state* and are real and positive [12]. *What do these Schmidt coefficients represent?* (See the exercise 7 at the end of this chapter.) k is called the *Schmidt rank* of the pure bipartite state. k is equal to the number of nonzero Schmidt coefficients. We have [12]

$$k \leq \min(\dim(\mathcal{H}_1), \dim(\mathcal{H}_2)). \tag{7.38}$$

The Schmidt coefficients are invariant under any local unitary transformation. As the entanglement is in general both qualitatively and quantitatively invariant under local unitary transformations, Schmidt coefficients are considered to determine completely the entanglement of bipartite pure state.

$|\psi\rangle$ is separable if it is a product state. From Eq. (7.37) we observe that for a product state, there must be only one nonzero value of the Schmidt coefficient $\sqrt{p_l} = 1$. Otherwise, a bipartite pure state is entangled. That is, from Eq. (7.37), for any pure product state the Schmidt rank $k = 1$ while $k > 1$ for entangled state. Therefore, a pure state can be determined whether it is separable or entangled by diagonalizing its reduced density matrix.

Solved Problem 3:

Given the pure bipartite state $|\psi\rangle = \frac{1}{\sqrt{3}}(|00\rangle + |01\rangle + |10\rangle)$ find ρ_1 and ρ_2 and hence the Schmidt coefficients. Does $|\psi\rangle$ represent an entangled state?

We obtain

$$\begin{aligned}
\rho_1 &= \mathrm{Tr}_2|\psi\rangle\langle\psi| \\
&= \mathrm{Tr}_2 \frac{1}{3}(|0\rangle_1|0\rangle_2 + |0\rangle_1|1\rangle_2 + |1\rangle_1|0\rangle_2) \\
&\quad \times ({}_2\langle 0|\,{}_1\langle 0| + {}_2\langle 1|\,{}_1\langle 0| + {}_2\langle 0|\,{}_1\langle 1|)\,.
\end{aligned} \tag{7.39}$$

Since trace is taken in state-2 and $\mathrm{Tr}_2(|a_1\rangle\langle a_2|) = \langle a_2|a_1\rangle$ we get

$$\mathrm{Tr}_2|0\rangle_2\,{}_2\langle 0| = 1, \quad \mathrm{Tr}_2|1\rangle_2\,{}_2\langle 1| = 1, \tag{7.40a}$$

$$\mathrm{Tr}_2|0\rangle_2\,{}_2\langle 1| = 0, \quad \mathrm{Tr}_2|1\rangle_2\,{}_2\langle 0| = 0. \tag{7.40b}$$

Then using $|0\rangle = \begin{bmatrix} 1 \\ 0 \end{bmatrix}$ and $|1\rangle = \begin{bmatrix} 0 \\ 1 \end{bmatrix}$, we find

$$\begin{aligned}
\rho_1 &= \frac{1}{3}[|0\rangle_1\,{}_1\langle 0| + |1\rangle_1\,{}_1\langle 0| + |0\rangle_1\,{}_1\langle 0| + |0\rangle_1\,{}_1\langle 1| + |1\rangle_1\,{}_1\langle 1|] \\
&= \frac{1}{3}\left[2\begin{pmatrix} 1 \\ 0 \end{pmatrix} \otimes \begin{pmatrix} 1 & 0 \end{pmatrix} + \begin{pmatrix} 0 \\ 1 \end{pmatrix} \otimes \begin{pmatrix} 1 & 0 \end{pmatrix}\right. \\
&\quad \left. + \begin{pmatrix} 1 \\ 0 \end{pmatrix} \otimes \begin{pmatrix} 0 & 1 \end{pmatrix} + \begin{pmatrix} 0 \\ 1 \end{pmatrix} \otimes \begin{pmatrix} 0 & 1 \end{pmatrix}\right] \\
&= \begin{bmatrix} 2/3 & 1/3 \\ 1/3 & 1/3 \end{bmatrix}.
\end{aligned} \tag{7.41}$$

The eigenvalues of ρ_1 are $\lambda_1 = p_1 = \frac{1}{2} + \frac{1}{2}\sqrt{\frac{5}{9}}$ and $\lambda_2 = p_2 = \frac{1}{2} - \frac{1}{2}\sqrt{\frac{5}{9}}$. Similarly,

$$\rho_2 = \mathrm{Tr}_1|\psi\rangle\langle\psi| = \begin{bmatrix} 2/3 & 1/3 \\ 1/3 & 1/3 \end{bmatrix}. \tag{7.42}$$

We note that $\rho_1 = \rho_2$ and the Schmidt coefficients are $\frac{1}{2} + \frac{1}{2}\sqrt{\frac{5}{9}}$ and $\frac{1}{2} - \frac{1}{2}\sqrt{\frac{5}{9}}$. As there are more than one nonzero Schmidt coefficients, $|\psi\rangle$ is entangled.

7.5.4 Bipartite Entanglement in Mixed State

We have so far considered only bipartite entanglement in pure states. But only mixed states are mostly encountered in real experiments since it is hardly possible to isolate a system with its environment. As we have seen earlier, the separability of pure states can be easily checked using Schmidt decomposition. But it is much more difficult to decide whether a given mixed state is entangled or not. As a mixed state is defined by a density matrix, we cannot define entanglement of mixed states to be nonproduct states as we defined for the case of pure states. A mixed state of n systems is separable if the density matrix of the composite system can be written as a convex combination of the product states [13]

$$\rho = \sum_{i=1}^{l} p_i \rho_1^i \otimes \rho_2^i \otimes \ldots \otimes \rho_n^i, \tag{7.43}$$

where ρ_j^i is the density matrix of the jth subsystem of the state vector $|i_j\rangle$ in the Hilbert space $\mathcal{H}_j$ and $0 < p_i < 1$ such that $\sum_{i=1}^{l} p_i = 1$. In general $\langle i_j|i'_j\rangle \neq \delta_{ii'}$. Thus, a mixed state is entangled if

$$\rho \neq \sum_{i=1}^{l} p_i \rho_1^i \otimes \rho_2^i \otimes \ldots \otimes \rho_n^i. \tag{7.44}$$

Hence, a bipartite mixed state is entangled if

$$\rho \neq \sum_{i=1}^{l} p_i \rho_1^i \otimes \rho_2^i. \tag{7.45}$$

Using the above definition alone one cannot normally check whether a given mixed state ρ is separable or not.

7.6 Separability Criteria

It is of primary importance to test whether a given quantum state is separable or entangled. A pure state is separable if there exists a decomposition of this state into product state. A mixed state is separable if there exists a decomposition of this state into a convex sum as given by Eq. (7.43). It is not an easy task to find such a decomposition. Hence, some other criteria are used to distinguish separable states from entangled states. There are

separability criteria for pure states which discriminate the separable and entangled states unambiquously. But for mixed states, such tools are available only for low-dimensional systems. For higher-dimensional systems only partial information about separability can be obtained using these criteria.

7.6.1 The Peres Criterion

The Peres criterion [14] known as *positive partial transpose* (PPT) criterion is an important criterion to find the separability of mixed states at least for low-dimensional systems. It states that the partial transpose of any separable state must be a positive semidefinite matrix. The partial transpose of a mathematical operator is a mathematical operation that treats the state as a product state and transposes one subsystem. If $\rho = \rho_1 \otimes \rho_2$ then $\rho^{\mathrm{T}_2} = \rho_1 \otimes \rho_2^{\mathrm{T}}$. The matrix elements of ρ transform under the partial transpose operation of the subsystem-2 as

$$\langle m|\mu|\rho^{\mathrm{T}_2}|n\rangle|\nu\rangle = \langle m|\nu|\rho|n\rangle|\mu\rangle. \tag{7.46}$$

The Peres criterion is easily proved for a bipartite system. The condition of separability is

$$\rho = \sum_i p_i \rho_1^i \otimes \rho_2^i. \tag{7.47}$$

The partial transpose of the state with respect to subsystem-2 gives

$$\rho^{T_2} = \sum_i p_i \rho_1^i \otimes \rho_2^{i\mathrm{T}}. \tag{7.48}$$

Since the transpose operator does not change the characteristics like positivity, unit trace and Hermiticity, $\rho_2^{i\mathrm{T}}$ also represents a state. Hence, Eq. (7.48) represents a separable state like Eq. (7.47). The set of states with PPT is identical to the set of separable states only in 2×2 and 2×3 dimensions [15].

As an example, we consider a *Wigner state* which is a $d \times d$ dimensional bipartite quantum state that is invariant under any unitary operation of the form $U \otimes U^*$. If ρ is the density matrix of such a state then

$$\rho = (U \otimes U^*)\, \rho \left(U^\dagger \otimes U^{*\dagger}\right). \tag{7.49}$$

For example, a Wigner state is defined by the density matrix

$$\rho = \alpha|\psi^-\rangle\langle\psi^-| + \frac{1-\alpha}{4}\mathbb{1} \otimes \mathbb{1}. \tag{7.50}$$

The interval for the parameter α is decided by the requirement $\mathrm{Tr}\rho = 1$. Since $|\psi^-\rangle = \frac{1}{\sqrt{2}}(|01\rangle - |10\rangle)$, we obtain

$$\rho = \begin{bmatrix} (1-\alpha)/4 & 0 & 0 & 0 \\ 0 & (1+\alpha)/4 & -\alpha/2 & 0 \\ 0 & -\alpha/2 & (1+\alpha)/4 & 0 \\ 0 & 0 & 0 & (1-\alpha)/4 \end{bmatrix}. \tag{7.51}$$

As $\mathrm{Tr}\rho = 1$, it represents a quantum state. It can be proved that all eigenvalues of ρ given by Eq. (7.51) are positive for the range $-1 \leq \alpha \leq 1$. Taking the partial transpose of Eq. (7.51) with respect to the subsystem-2 we get

$$\rho^{\mathrm{T}} = \begin{bmatrix} (1-\alpha)/4 & 0 & 0 & -\alpha/2 \\ 0 & (1+\alpha)/4 & 0 & 0 \\ 0 & 0 & (1+\alpha)/4 & 0 \\ -\alpha/2 & 0 & 0 & (1-\alpha)/4 \end{bmatrix}. \tag{7.52}$$

The eigenvalues of this matrix are $\lambda_1 = \lambda_2 = \lambda_3 = (1+\alpha)/4$ and $\lambda_4 = (1-3\alpha)/4$. The last eigenvalue will be negative if $\alpha > 1/3$. Since the eigenvalues of ρ are positive for the range $-1 \leq \alpha \leq 1$ and one of the eigenvalues of ρ^{T_2} is negative if $\alpha > 1/3$, by applying PPT criterion we find for the given Wigner state

$$-1 \leq \alpha \leq \frac{1}{3} \longrightarrow \rho \text{ is separable}, \quad \frac{1}{3} \leq \alpha \leq 1 \longrightarrow \rho \text{ is entangled}. \tag{7.53}$$

It can be seen that the PPT condition is equivalent to demanding the positivity of the operator $[\mathbb{1} \otimes \mathrm{T}_2]\rho$. The transposition map T_2 acting on the subsystem-2 is a positive (P) map but it is not completely positive (CP). It has been noted that any P but not CP map Λ provides a nontrivial necessary separability criterion in the form

$$[\mathbb{1}_1 \otimes \Lambda_2]\,\rho \geq 0. \tag{7.54}$$

The state ρ is separable *if and only if* the above condition is satisfied for all P and not CP maps Λ [15].

7.6.2 Entanglement Witnesses

For dimensions greater than $2 \otimes 2$ and $2 \otimes 3$, one can still use PPT to find separable states. For higher-dimensional systems all states with negative partial transpose are entangled but there are entangled states with a PPT. Therefore, PPT is not a reliable tool to detect separability for such cases. In fact, there exists no single separability condition for higher-dimensional systems.

There are several tools available to detect quantum entanglement. Among them *entanglement witnesses* are extensively used for characterizing quantum entanglement. Terhal [16] introduced the term entanglement witnesses for operators detecting quantum entanglement states. It is found that any entangled state can be detected by some entanglement witnesses. A full classification of states of composite quantum system can be done from the knowledge of entanglement witnesses.

Entanglement witnesses (say W) are observables (Hermitian). They have at least one negative eigenvalue and a nonnegative mean value on product states. If $|\psi_1\rangle|\psi_2\rangle$ represents any arbitrary product state $|\psi\rangle$ then W satisfy the nonnegative condition $\langle\psi|W|\psi\rangle > 0$. The state represented by the density matrix ρ is separable if it has a nonnegative mean value

$$\mathrm{Tr}(W\rho) \geq 0. \tag{7.55}$$

That is, the state ρ is entangled *if and only if*

$$\mathrm{Tr}(W\rho) < 0. \tag{7.56}$$

For example, the Hermitian swap operator

$$V = \sum_{i=0}^{d-1}\sum_{j=0}^{d-1} |i\rangle\langle j| \otimes |j\rangle\langle i| \tag{7.57}$$

is the entanglement witness for the $d \otimes d$ case. $|i\rangle$ and $|j\rangle$ are the d-basis vectors of $\mathcal{H}_1$ and $\mathcal{H}_2$.

An entanglement witness W is *decomposable* if it can be written as

$$W = \alpha P + (1 - \alpha) Q^{\mathrm{T}_1}, \tag{7.58}$$

where P and Q are some positive operators and T_1 is a partial transpose on subsystem-1 [16]. Decomposable entanglement witnesses cannot detect entanglement of PPT states. There exists some witness W for detection of any entangled state. But there is no general method for construction of entanglement witnesses.

The map condition (7.54) is equivalent to the set of witness condition (7.55). But any simple witness condition is much weaker than the condition given by the map Λ. For example, the transposition map T detects all entanglements in the two-qubit case, where as the swap operator V defined by Eq. (7.57) does not detect entanglement of any symmetric pure state.

An entanglement witness W_1 is finer than W_2 if and only if the entanglement of any ρ detected by W_2 is also detected by W_1. If there is no witness finer than W then it is called *optimal*. Typical W is defined [17,18] for the Hilbert subspace $\mathcal{P}_W$ by the condition

$$\{|\phi_1\rangle|\phi_2\rangle : \langle\phi_1|\langle\phi_2|W|\phi_1\rangle|\phi_2\rangle = 0\}. \tag{7.59}$$

How many witnesses have to be measured to arrive at a conclusion? A conclusive answer may not be obtained if we consider the expectation values of the witnesses one by one [19]. We can use the expectation values of properly chosen witnesses jointly. In this case $d^2 - 1$ witnesses are required for a d-dimensional system. It is possible to reduce this number by making use of all the information collected when computing the expectation values of the witnesses measured successively.

Entanglement witnesses have been useful in experimental detection of entanglement because entanglement witnesses are observables [6]. It has been used in quantum optics [20,21], quantum cryptography [22], nanophysics [23], cluster states [24] and hidden nonlocality [25], a few to mention. The witness-family-based entanglement detection scheme has been introduced [18] and verified [26]. An experimental method for detecting a collective universal witness that is a necessary and sufficient measure of two-photon polarization entanglement was proposed [27].

7.6.3 Bell Inequalities

As the separable states do not violate any Bell inequality, they can be used to detect separability of a state. But it has been found that all entangled states do not violate a Bell inequality [13,28]. The Bell inequalities can be considered as nonoptimal witnesses as they are not able to detect all entangled states. The relation between Bell inequalities and witnesses was first studied by Terhal [16]. The Bell inequality derived by Clauser, Hone, Shimony and Holf (CHSH) [29] provides a way of detecting experimentally the LHVM.

Consider a correlation experiment in which variables (A_1, A_2) are measured in subsystem-1 and the variables (B_1, B_2) are measured in spatially separated subsystem-2 of a whole system. Further, assume that A_1, A_2, B_1 and B_2 can take only ± 1 values. Then for LHVM to be valid the inequality to be satisfied is

$$|E(A_1, B_1) + E(A_1, B_2) + E(A_2, B_1) - E(A_2, B_2)| \leq 2, \tag{7.60}$$

where $E(A_i, B_j)$ is the expectation of the correlation experiment $A_i B_j$. If we consider the CHSH operator

$$B_{\mathrm{CHSH}} = A_1 \otimes (B_1 + B_2) + A_2 \otimes (B_1 - B_2), \tag{7.61}$$

where $A_1 = \mathbf{a}_1 \cdot \boldsymbol{\sigma}$, $A_2 = \mathbf{a}_2 \cdot \boldsymbol{\sigma}$, $B_1 = \mathbf{b}_1 \cdot \boldsymbol{\sigma}$ and $B_2 = \mathbf{b}_2 \cdot \boldsymbol{\sigma}$, where $\boldsymbol{\sigma} = (\sigma_x, \sigma_y, \sigma_z)$ is the vector of Pauli spin operators, $\mathbf{a} = (a_x, a_y, a_z)$ and $\mathbf{b} = (b_x, b_y, b_z)$ are the unit vectors describing the measurements in subsystem-1 and subsystem-2, respectively. If a state defined by the density matrix ρ admits the LHVM then the CHSH inequality

$$|\mathrm{Tr}\,(B_{\mathrm{CHSH}}\,\rho)\,| \leq 0 \tag{7.62}$$

is satisfied. As separable states admit LHVM, one can define CHSH-type witness

$$W_{\mathrm{CHSH}} = 2I - B_{\mathrm{CHSH}}. \tag{7.63}$$

A Bell observable is a *double witness* as it detects both entanglement and nonlocality.

A special case of the CHSH inequality is the Freedman's inequality. For a detailed discussion on it one may refer to [30].

7.7 Multipartite Entanglement

Multipartite entanglement theory is much complex compared to the bipartite case. One cannot generalize the results of bipartite entanglement to multipartite entanglement. The multipartite entanglement exhibits a variety of forms which are not easily distinguishable and are very difficult to identify them. Just like in bipartite case we can define full separability for the multipartite cases. But unlike in bipartite case we can define many types of partial separability.

For discussions on nonlinear separability criteria, general separability criteria based on uncertainty relation, separability criterion in terms of covariance matrices and the use of uncertainty relation in detecting entanglement one may refer to the refs. [6,31–35].

7.7.1 Full Separability

Consider a n-partite composite system in the Hilbert space $\mathcal{H} = \mathcal{H}_1 \otimes \mathcal{H}_2 \otimes \ldots \otimes \mathcal{H}_n$. The full separability of the n-partite system is defined if the state ρ in $\mathcal{H}$ can be written as Eq. (7.43), where l in this equation is $\leq \dim\mathcal{H}^2$. Such a defined set of n-separable state is *convex and closed*. For example, the three-qubit state

$$\rho = p|0\rangle\langle 0|^{\otimes 3} + (1-p)|1\rangle\langle 1|^{\otimes 3} \tag{7.64}$$

is fully separable.

A n-partite pure state is fully separable only if it is a product of the pure states of the n-elementary subsystems. Thus, one can compute the reduced density matrices of the subsystems and check whether they are pure or not. However, this simple separability condition is violated in many ways. For example, in multipartite case, the pure states admit only rarely the Schmidt decomposition. The generalized entangled Greenberger-Horne-Zeilinger (GHZ) state

$$|\mathrm{GHZ}\rangle_d^{(n)} = \frac{1}{\sqrt{d}} \sum_{i=0}^{d-1} |i\rangle^{\otimes n} \tag{7.65}$$

admits Schmidt decomposition. For the three-qubit GHZ state

$$|\mathrm{GHZ}\rangle_2^{(3)} = \frac{1}{\sqrt{2}} \left(|0\rangle|0\rangle|0\rangle + |1\rangle|1\rangle|1\rangle\right) \tag{7.66}$$

one can perform Schmidt decomposition. But the entangled state

$$|W\rangle = \frac{1}{\sqrt{3}}\left(|0\rangle|0\rangle|1\rangle + |0\rangle|1\rangle|0\rangle + |1\rangle|0\rangle|0\rangle\right) \tag{7.67}$$

which has an entangled subsystem, does not admit Schmidt decomposition. Thus, a fully separable n-partite state must be the direct product of the n-state vectors of the subsystems as

$$|\psi\rangle = |\psi_1\rangle \otimes |\psi_2\rangle \otimes \ldots \otimes |\psi_n\rangle. \tag{7.68}$$

7.7.2 Partial Separability

Violation of condition (7.68) cannot be considered as the decomposition of n-partite entanglement. When classifying the entanglement in multipartite system, one must take into account the number and nature of entangled subsystems. For example, a triqubit pure state can be classified as

1. fully separable state,
2. biseparable state and
3. fully entangled state.

Even for fully entangled triqubit pure state, classification can be done by means of local operation and classification with nonzero probability [36]. It is found that any fully entangled triqubit state can be converted into one of the two standard forms, namely, the GHZ state (Eq. (7.66)) or the *W-state* (Eq. (7.67)).

A complete hierarchic classification of a family of states based on the separability properties of the partitions of the systems into subsystems has been proposed [37,38]. A k-separable state with n-particles ($n \geq k$) is defined if a pure state ρ in $\mathcal{H}$ can be written as $\rho = \rho_1 \otimes \rho_2 \otimes \ldots \otimes \rho_k$, where ρ_j is the density matrix of the jth part of the partition. A mixed state ρ is k-separable if

$$\rho = \sum_{i=1}^{M} p_i \rho_1^{(i)} \otimes \rho_2^{(i)} \otimes \ldots \otimes \rho_k^{(i)}. \tag{7.69}$$

In the hierarchic classification, all possible partitions of k parts for all k ($k \in (2, 3, \ldots, n)$) are considered and then each partition is detected whether the given state is k-separable or not. We have to continue the procedure starting with $k = n$, continuing with $k = n-1$, $n-2$, ... until $k = 2$. At each level k we need to consider all possible partitions of k-separability. Note that the different levels of this structure are not independent of each other. The study of partial separable states are important as different types of partially separable states have been used for many different applications.

Hyper-entanglement refers to the simultaneous entanglement in more than one degree of freedom. It includes polarization-momentum, polarization-time-bin, polarization-spatial modes-energy-time entanglements and so on [39–41].

7.8 Quantifying Entanglement

It is in general possible to detect whether a quantum state is entangled or not. But the amount of entanglement cannot be easily determined for general mixed states.

Quantification of entanglement is very much needed in many applications of entanglement. But there exists no measure of entanglement which satisfies all the properties of a good measure of entanglement. Consequently, many different measures of entanglement are considered for quantifying entanglement. These measures are considered with different motivations and they have their own strengths and weaknesses.

7.8.1 Entanglement Measure

If we have an entangled state ρ then the entanglement measure $E(\rho)$ maps ρ into a single real number. Therefore, $E(\rho)$ is defined as the map: $E(\rho): \ \rho \leftrightarrow x$ such that $x \in \mathbb{R}$. The measure $E(\rho)$ must satisfy the following four conditions:

1. $E(\rho) = 0$ if the state ρ is separable.
2. Any local unitary transformation $U_1 \otimes U_2$ will not change $E(\rho)$, that is,

$$E(\rho) = E\left(U_1 \otimes U_2 \rho U_1^\dagger \otimes U_2^\dagger\right). \tag{7.70}$$

3. Local operation (LO), classical communication (CC) and sub-selection (SS) do not increase entanglement [42,43]. Hence, if $\rho \xrightarrow{\text{LOCCSS}} \sum_i p_i \rho_i$ then

$$E(\rho) \geq \sum_i p_i E(\rho_i). \tag{7.71}$$

4. If $\rho = \rho_1 \times \rho_2$ then $E(\rho) = E(\rho_1) + E(\rho_2)$.

Sometimes additional requirements for entanglement measures like convexity, additivity, continuity are imposed [44]. For pure bipartite states von Neumann entropy of entanglement is accepted as a canonical measure. Several measures are considered for mixed states.

7.8.2 Von Neumann Entropy of Entanglement

The quantum counterpart of Shannon entropy of information theory is the von Neumann entropy which is defined for a quantum state ρ as

$$S(\rho) = -\text{Tr}\left(\rho \log_2 \rho\right). \tag{7.72}$$

As it maps a density matrix into a number, it can be a measure of the entanglement of the state ρ. $S(\rho)$ also satisfies all the four conditions of measure. Von Neumann entropy is interpreted as a measure of unpredictability of measurement of quantum state.

If ρ_1 and ρ_2 are the density operators of subsystems of the composite system ρ then the conditional von Neumann entropy is given by

$$S\left(\rho_1|\rho_2\right) = S\left(\rho\right) - S\left(\rho_2\right). \tag{7.73}$$

The conditional entropy can be negative. Therefore, the entropy of the subsystem may be greater than the entropy of the joint system. Hence, the knowledge (information) of the joint system is greater than that of the subsystem. This is true only for entangled states. As log can be extended on operators one can use the spectral decomposition of ρ to obtain

$$S(\rho) = -\sum_{i=1}^{n} \lambda_i \log_2 \lambda_i, \tag{7.74}$$

where λ_i are the eigenvalues of ρ.

Solved Problem 4:

Show that $S(\rho_1) = S(\rho_2) > S(\rho)$ for the Bell's state $|\psi^+\rangle = \frac{1}{\sqrt{2}}(|00\rangle + |11\rangle)$.

We obtain

$$\begin{aligned} |\psi^+\rangle &= \frac{1}{\sqrt{2}}(|0\rangle \otimes |0\rangle + |1\rangle \otimes |1\rangle) \\ &= \frac{1}{\sqrt{2}}\left(\begin{pmatrix} 1 \\ 0 \end{pmatrix} \otimes \begin{pmatrix} 1 \\ 0 \end{pmatrix} + \begin{pmatrix} 0 \\ 1 \end{pmatrix} \otimes \begin{pmatrix} 0 \\ 1 \end{pmatrix}\right) \\ &= \frac{1}{\sqrt{2}} \begin{bmatrix} 1 \\ 0 \\ 0 \\ 1 \end{bmatrix}. \end{aligned} \tag{7.75}$$

Then ρ and ρ_1 are obtained as

$$\rho = |\psi^+\rangle\langle\psi^+| = \frac{1}{2} \begin{bmatrix} 1 \\ 0 \\ 0 \\ 1 \end{bmatrix} \otimes \begin{bmatrix} 1 & 0 & 0 & 1 \end{bmatrix} = \begin{bmatrix} 1/2 & 0 & 0 & 1/2 \\ 0 & 0 & 0 & 0 \\ 0 & 0 & 0 & 0 \\ 1/2 & 0 & 0 & 1/2 \end{bmatrix} \tag{7.76}$$

and

$$\begin{aligned} \rho_1 &= \mathrm{Tr}_2(\rho) \\ &= \frac{1}{2}\left(\begin{pmatrix} 1 \\ 0 \end{pmatrix} \otimes \begin{pmatrix} 1 & 0 \end{pmatrix} + \begin{pmatrix} 0 \\ 1 \end{pmatrix} \otimes \begin{pmatrix} 0 & 1 \end{pmatrix}\right) \\ &= \frac{1}{2}\begin{pmatrix} 1 & 0 \\ 0 & 1 \end{pmatrix} = \frac{1}{2}I. \end{aligned} \tag{7.77}$$

Similarly, we can find $\rho_2 = I/2$. ρ has eigenvalues 1, 0, 0, 0 and ρ_1 and ρ_2 have eigenvalues 1/2, 1/2.

We obtain $S(\rho) = -\sum_{i=1}^{4} \lambda_i \log_2 \lambda_i = -1 \times \log_2 1 = 0$ and $S(\rho_1) = S(\rho_2) = -\frac{1}{2}\log_2 \frac{1}{2} - \frac{1}{2}\log_2 \frac{1}{2} = 1$. Thus, $S(\rho_1) = S(\rho_2) > S(\rho)$.

7.8.3 Distillable Entanglement and Entanglement Cost

Many applications of quantum information theory like quantum teleportation uses the pure maximally entangled state − Bell state $|\psi^+\rangle$. But we usually get only mixed state due to imperfection of operational coupling with environment and decoherence. The question of obtaining the maximally entangled states from the *noisy* mixed state was considered in [45] and established a paradigm for purification of entanglement by means of LOCC operations. This process is called *entanglement distillation*.

Suppose two distant parties share n copies of a bipartite noisy mixed state ρ. Then they can perform some LOCC and obtain in turn k ($< n$) copies of the systems in a state which is very close to the pure maximally entangled state. A sequence of LOCC operations to obtain this entanglement purification is called *entangled distillation protocal*. The efficiency with which one can achieve this process of distillation defines an asymptotic entanglement measure known as *distillable entanglement* $E_{\mathrm{D}}(\rho)$. It gives the best rate at which one can transform $\rho^{\otimes n}$ into k singlets.

The distillable entanglement is the supremum of such states over all distillation protocals (Λ). It is defined as [44]

$$E_{\mathrm{D}}(\rho) = \sup\left\{r : \lim_{n\to\infty}\left[\inf_{\Lambda}\left|\left|\Lambda\left(\rho^{\otimes n}\right) - \Phi\left(2^{rn}\right)^{+}\right|\right|\right] = 0\right\}, \tag{7.78}$$

where $\Phi\left(2^{rn}\right)^{+} = \left(|\phi_{+}\rangle\langle\phi_{+}|\right)^{\otimes rn}$ and $||\cdot||$ is the trace norm and Λ are the trace preserving LOCC operations. Because of the complexity of this variational definition very little progress has been made in computing $E_{\mathrm{D}}(\rho)$. It equals the entropy of entanglement for pure states.

We note that entangled states allowing the creation of a maximally entangled state by LOCC opeations in at least one bipartition of the composite system are essentially *distillable*. A distillable state can be transformable into a nonlocal state using only LOCC. However, not every nonlocal state is distillable. For a PPT state the distillable entanglement is zero. The entangled states with zero distillable entanglement are termed as *bound entangled states* [46]. Such states are though entangled but not distillable.

Another useful entanglement measure is the *entanglement cost* $E_{\mathrm{C}}(\rho)$ which is duel to $E_{\mathrm{D}}(\rho)$. $E_{\mathrm{C}}(\rho)$ defines the maximally possible rate r at which we can convert blocks of maximally entangled state using LOCC (Λ) operations to obtain many copies of ρ such that the approximations become vanishingly small in the limit of large block sizes. $E_{\mathrm{C}}(\rho)$ is the reverse of $E_{\mathrm{D}}(\rho)$. It is defined as [44]

$$E_{\mathrm{C}}(\rho) = \inf\left\{r : \left[\inf_{\Lambda}\left|\left|\rho^{\otimes n} - \Lambda\left(\Phi\left(2^{rn}\right)^{+}\right)\right|\right|\right] = 0\right\}, \tag{7.79}$$

This quantity is also very difficult to compute. $E_{\mathrm{D}}(\rho)$ and $E_{\mathrm{C}}(\rho)$ are two most important measures for entanglement of bipartite mixed states. These two are equal for pure states.

7.8.4 Entanglement of Formation and Concurrence

There are other two well defined quantitative measures of entanglement, namely, *entanglement of formation* (EoF) [42,45] and *concurrence* [47,48]. EoF for a bipartite state ρ is defined as the partial entropy with respect to the subsystems as

$$E_{\mathrm{f}}(\rho) = -\mathrm{Tr}\left(\rho_1 \log_2 \rho_1\right) = -\mathrm{Tr}\left(\rho_2 \log_2 \rho_2\right). \tag{7.80}$$

$E_{\mathrm{f}}(\rho)$ vanishes only for product states. For a mixed state $E_{\mathrm{f}}(\rho)$ is defined by the convex roof as

$$E_{\mathrm{f}}(\rho) = \min_{(p_i|\rho_i)} \sum_{p_i} E_{\mathrm{f}}(\rho_i) \tag{7.81}$$

for all possible realizations. We have

$$\rho = \sum_i p_i \rho_i, \quad p_i \geq 0, \quad \sum_i p_i = 1. \tag{7.82}$$

Therefore, ρ is separable only if $E_{\mathrm{f}}(\rho) = 0$. $E_{\mathrm{f}}(\rho)$ defined by Eq. (7.81) satisfies all the essential requirements of a good entanglement measure. But it is extremely difficult to calculate $E_{\mathrm{f}}(\rho)$ as one has to find the minimum of the calculation Eq. (7.81) for all possible realizations.

One feature that distinguishes E_{f} from E_{D} is that E_{f} will be zero only if ρ is separable whereas E_{D} can be zero even for nonseparable states. Though E_{f} is in general very difficult to calculate there exists general formulas for certain systems and certain classes of states.

For example, for 2×2 systems $E_{\rm f}$ can be expressed in terms of concurrence $C(\psi)$ which is expressed for a pure state ψ as

$$C(\psi) = |\langle \psi^* | \sigma_y \otimes \sigma_y | \psi \rangle|. \tag{7.83}$$

$|\psi^*\rangle$ is the complex conjugate of $|\psi\rangle$. If $|\psi\rangle = \sum_{i,j} \psi_{ij} |ij\rangle$ in the basis of $|ij\rangle = \{|00\rangle, |01\rangle, |10\rangle, |11\rangle\}$ then

$$|\psi^*| = \sum_{i,j} \psi_{ij} \langle ij|. \tag{7.84}$$

For an arbitrary two-qubit pure state $|\psi\rangle = \alpha|00\rangle + \beta|01\rangle + \gamma|10\rangle + \delta|11\rangle$ we obtain $C(\psi) = 2|\alpha\delta - \beta\gamma|$ with $|\alpha|^2 + |\beta|^2 + |\gamma|^2 + |\delta|^2 = 1$ (see the solved problem 5 below). On the other hand, for $|\psi'\rangle = \alpha|00\rangle + \beta|11\rangle$ the concurrence is $C(\psi') = 2|\alpha\beta|$ with $|\alpha|^2 + |\beta|^2 = 1$.

Solved Problem 5:

Show that concurrence for a pure state $|\psi\rangle = \alpha|00\rangle + \beta|01\rangle + \gamma|10\rangle + \delta|11\rangle$ is equal to $2|\alpha\delta - \beta\gamma|$.

We obtain

$$\sigma_y \otimes \sigma_y = \begin{bmatrix} 0 & 0 & 0 & -1 \\ 0 & 0 & 1 & 0 \\ 0 & 1 & 0 & 0 \\ -1 & 0 & 0 & 0 \end{bmatrix}. \tag{7.85}$$

We write $|\psi\rangle = \begin{bmatrix} \alpha \\ \beta \\ \gamma \\ \delta \end{bmatrix}$, $|\psi^*\rangle = \begin{bmatrix} \alpha^* \\ \beta^* \\ \gamma^* \\ \delta^* \end{bmatrix}$ and $\langle \psi^*| = \begin{bmatrix} \alpha & \beta & \gamma & \delta \end{bmatrix}$. Then we obtain

$$\begin{aligned} \langle \psi^* | \sigma_y \otimes \sigma_y | \psi \rangle &= \begin{bmatrix} \alpha & \beta & \gamma & \delta \end{bmatrix} \begin{bmatrix} 0 & 0 & 0 & -1 \\ 0 & 0 & 1 & 0 \\ 0 & 1 & 0 & 0 \\ -1 & 0 & 0 & 0 \end{bmatrix} \begin{bmatrix} \alpha \\ \beta \\ \gamma \\ \delta \end{bmatrix} \\ &= 2(\beta\gamma - \alpha\delta). \end{aligned} \tag{7.86}$$

Therefore, $|\langle \psi^* | \sigma_y \otimes \sigma_y | \psi \rangle| = 2|\beta\gamma - \alpha\delta| = 2|\alpha\delta - \beta\gamma|$.

The concurrence of mixed states is defined by the corresponding convex roof like Eq. (7.81) as

$$C(\rho) = \min_{\{p_i, \rho_i\}} \sum_i p_i C(\rho_i) \tag{7.87}$$

with $p_i > 0$ and $\sum_i p_i = 1$.

Consider a 2×2 system. For such a system, $E_{\rm f}$ can be given as a function of $C(\rho)$ as

$$E_{\rm f} = \varepsilon(C), \quad \varepsilon(C) = h\left(\frac{1 + \sqrt{1 - C^2}}{2}\right) \tag{7.88a}$$

with

$$h(x) = -x \log_2 x - (1 - x) \log_2 (1 - x). \tag{7.88b}$$

As E_f increases monotonically with C we can treat C as a measure of entanglement. If we calculate the minimum of $C(\rho)$ by Eq. (7.87), using C defined by Eq. (7.83), for the states ψ_i, then the minimum of E_f as defined by Eq.(7.81) can be found by using the relation (7.88).

Measurement of the concurrence with linear optics [49], trapped ions [50], cross-Kerr nonlinearity [51] and its detection in atomic-qubit pure state [52] and cavity QED system [53] have been reported.

7.8.5 Entanglement Negativity

Another measure of entanglement is the entanglement *negativity* $\mathcal{N}^{A|B}$ [54–56]. It quantifies the amount of entanglement between the parts A and B if they are in a state ρ_{AB}. $\mathcal{N}^{A|B}$ is the absolute value of the sum of negative eigenvalues of $\rho_{AB}^{T_A}$, where T_A represents partial transpose with respect to the subsystem A. That is,

$$\mathcal{N}^{A|B} = \frac{1}{2}\left[||\rho_{AB}^{T_A}||_1 - 1\right], \tag{7.89}$$

where $||X||_1 = \mathrm{Tr}\sqrt{X^\dagger X}$.

7.9 Applications of Entanglement

In this section we enumerate some of the promising applications of entanglement.

1. The philosophical debates on quantum entanglement started by the EPR paradox was brought to a conclusion by Bell's theorem and numerous experimental verifications of Bell's inequalities. But it was found later that it is a new resource which can be exploited to perform many tasks that cannot be performed by any classical resources [57]. It was found that the entangled states can be used in a variety of real-world applications.

2. Ekert [58] found that entangled states along with the Bell inequalities can be used to produce a private cryptographic key. He discovered entangled-based quantum key distribution. It is different from the original BB84 scheme which directly uses quantum communication (refer chapter 10 for more information on quantum cryptography).

3. **Quantum Dense Coding**: Another important application of quantum entanglement is the quantum dense coding [59]. According to classical information theory, if we want to send a message in the form of N distinguishable states then the maximum number of different messages we have to send is N. That is, we can send at most $\log_2 N$ bits of information. Qubit can thus carry at most only one bit of classical information. But dense coding allows us to communicate two classical bits by sending one a *priori* entangled qubit.

   In Bennett and Wiesner's idea of dense coding the sender and receiver, say Alice and Bob, share an entangled single state

$$|\psi_1\rangle = \frac{1}{\sqrt{2}}\left(|0\rangle|0\rangle + |1\rangle|1\rangle\right). \tag{7.90}$$

Suppose Alice wants to tell Bob any one of the four events $k \in (1, 2, 3, 4)$. Alice performs one of the four unitary operations $\sigma = \mathbb{1}$, $\sigma_2 = \sigma_z$, $\sigma_3 = \sigma_x$ and $\sigma_4 = \sigma_y$ and return half of the entangled states back to Bob transforming $|\psi_1\rangle$ into one of the four original signal states

$$|\psi_1\rangle = \mathbb{1} \otimes \mathbb{1}|\psi_1\rangle = \frac{1}{\sqrt{2}}\left(|00\rangle + |11\rangle\right), \tag{7.91a}$$

$$|\psi_2\rangle = \mathbb{1} \otimes \sigma_z|\psi_1\rangle = \frac{1}{\sqrt{2}}\left(|00\rangle - |11\rangle\right), \tag{7.91b}$$

$$|\psi_3\rangle = \mathbb{1} \otimes \sigma_x|\psi_1\rangle = \frac{1}{\sqrt{2}}\left(|01\rangle + |10\rangle\right), \tag{7.91c}$$

$$|\psi_4\rangle = \mathbb{1} \otimes \sigma_y|\psi_1\rangle = \frac{1}{\sqrt{2}}\left(|01\rangle - |10\rangle\right) \tag{7.91d}$$

which Bob can discriminate and identify them as they are orthogonal states. (For the proof of the relations (7.91) see the exercise 7.20 at the end of this chapter.) In this way acting locally only on a single two-state system, Alice can send two bits of classical information to Bob. The first experimental implementation of quantum dense coding was reported in [60].

4. **Entangled two-photon microscopy**: Microscopy based on classical sources of light are considerably noisy because of the photons arriving randomly in time and position. The two-photon laser scanning fluorescence microscopy (TPLSM) is found to be more efficient. This technique uses a highly focused optical beam in order to localize the region from which fluorescence is observed. For classical light the rate of simultaneous absorption of 2 photons is proportional to ϕ^2, where ϕ is the optical photon flux density. Thus, in TPLSM, the rate of two-photon absorption is proportional to ϕ^2. TPLSM needs the utility of high photon flux density sources (such as femtosecond pulsed lasers), to make sure that two photons have a significantly considerable probability of reaching simultaneously and resulting in an absorption.

   Entangled photon microscopy (EPM) using quantum photon pairs as source was proposed [61]. EPM offers several advantages over TPLSM. In EPM, the entangled photons' arrival times are correlated. As a result the two-photon absorption rate is substantially enhanced. This process depends linearly on the photon flux density [62]. Consequently, lower values of the photon flux density are also used in EPM. It has been realized that correlated two-photon absorption dominates over random two-photon absorption in the case of small values of photon-flux density (below a critical photon flux density ϕ_c). If ϕ_c is sufficiently large, EPM has a number of features rendering it superior to TPLSM.

5. A quantum state cannot be copied due to no cloning theorem (refer chapter 11). However, Alice can send qubit to Bob if the qubit is simultaneously erased in Alice's site. That is, a quantum state can be transformed from one place to another but it cannot be copied from one pace to another. This is the principle of quantum teleportation. It has been found that [45] using maximally entangled state quantum teleportation can be done (refer sec. 15.5).

6. Quantum entanglement has led to development of many quantum technologies like ghost images, entangled two-photon microscopy, quantum lithography, quantum metrology which are all discussed extensively in chapter 15.

7. It is generally believed that entanglement plays a role in speeding-up of quantum computation though there is no common agreement on the role of entanglement in quantum computation. Entanglement is also found to be useful for reducing the complexity of classical communication [63,64].

8. Entanglement is used in clock synchronization [65–67], frequency standard improvement [68] and in entanglement-assisted orientation in space [69].

9. Entanglement has also given new insights for understanding many physical phenomena like super-radiance [70,71], superconductivity of disordered systems [72,73] and quantum phase transition [74–76].

10. Entanglement can be utilized to produce states that permit to measure some parameters while suppressing others. For example, to obtain a precise quadrupole moment of, say, a $^{40}Ca^{+}$ ion, we can perform spectroscopy on an entangled state of couple of ions which depend on the quadrupole moment with insensitiveness to fluctuations in the magnetic field [77].

7.10 Concluding Remarks

Though quantum entanglement is a new resource having potentials for many applications which can never be done using any classical resource, it is quite complex and usually fragile to the environment. It is really difficult to study both conceptually and mathematically as it is endowed with rich structure. We have given only the basic ideas on the definition, detection, quantification and some applications of quantum entanglement.

For more information on the different methods of detection of entanglement, one can refer the review articles [6,12]. The ref. [6] reviews the various aspects of entanglement like its characterization, detection, distillation, quantification, various manifestations of entanglement via Bell inequalities, entropic inequalities, entanglement witnesses and quantum cryptography. It also discusses the role of entanglement in quantum communication, manipulation of quantum entanglement, irreversebility, monogamy, entanglement decay and entanglement in continuous variable systems. A review on the theory of entanglement measures is presented in [44].

Many criteria like reduction criterion, positive partial transpose positive maps, entanglement witnesses and criterion for qualitative characterization of bipartite quantum entanglement have been discuseed [78]. For more information on EoF and the related concepts of concurrence one may refer [79]. An overview of the quantitative theory of entanglement has been reported [80]. For a discussion on pictorial examples of entangled wave functions one may refer to [82]. Undergratuate level laboratory experiments with entangled photons have been discussed in the refs. [83–90].

Research on different aspects of quantum entanglement is very active as not only its philosophical features are interesting but also it has very large potential for application in every day life. The study of entanglement is pursued vigorously by scientific community as it has been proved experimentally that entanglement lies at the heart of many future quantum technologies.

7.11 Bibliography

[1] E. Schrödinger, *Proc. Cambridge Philos. Soc.* 31:555, 1935.

[2] A. Einstein, B. Podolsky and N. Rosen, *Phys. Rev.* 47:777, 1935.

[3] J.S. Bell, *Physics* 1:195, 1964.

[4] D.M. Greenberger, M.A. Horne and A. Zeilinger, *Going beyond Bell's theorem*. In Bell's Theorem, Quantum Theory and Conceptions of the Universe. Kluwer Academic, Dordrecht, 1989.

[5] S. Kanmani, Entangled states: Classical versus quantum. *arXiv:0907. 1784v1 [quant-ph]*, 10 July 2009.

[6] R. Horodecki, P. Horodecki, M. Horodecki and K. Horodecki, *Rev. Mod. Phys.* 81:865, 2009.

[7] D.L. Moehring, P. Maunz, S. Olmschenk, K.C. Younge, D.N. Matsukevich, L.M. Duan and C. Monroe, *Nature* 449:68, 2007.

[8] D. Sarkar, *Quantum entanglement - Fundamental aspects*, preprint. https://www.iopb.res.in/∼iscqi/talks/dsarkar.pdf.

[9] A. Ekert and P.L. Knight, *Am. J. Phys.* 63:415, 1995.

[10] H.A. Carteret, A. Higuchi and A. Sudbery, *J. Math. Phys.* 41:7932, 2000.

[11] A. Acín, A. Andrianov, L. Costa, E. Jane, J.I. Latorre and R. Tarrach, *Phys. Rev. Lett.* 85:1560, 2000.

[12] O. Guhns and G. To'th, *Phys. Rep.* 474:1, 2009.

[13] R.F. Werner, *Phys. Rev. A* 40:4277, 1989.

[14] A. Peres, *Phys. Rev. Lett.* 77:1413, 1996.

[15] M. Horodecki, P. Horodecki and R. Horodecki, *Phys. Lett. A* 223:1, 1996.

[16] B.W. Terhal, *Phys. Lett. A* 271:319, 2000.

[17] M. Lewenstein, B. Kraus, J.I. Cirac and P. Horodecki, *Phys. Rev. A* 62:052310, 2000.

[18] M. Lewenstein, B. Kraus, P. Horodecki and J.I. Cirac, *Phys. Rev. A* 63:044304, 2001.

[19] H. Zhu, Y. Teo and B.Z. Englert, *Phys. Rev. A* 81:052339, 2010.

[20] M. Stobinska and K. Wodkiewicz, *Phys. Rev. A* 71:032304, 2005.

[21] M. Stobinska and K. Wodkiewicz, *Int. J. Mod. Phys. B* 20:1504, 2006.

[22] M. Curty, O. Guhne, M. Lewenstein and N. Lutkenhaus, *Phys. Rev. A* 71:022306, 2005.

[23] M. Blaauboer and D.P. DiVincenzo, *Phys. Rev. Lett.* 95:160402, 2005.

[24] G. Vallone, E. Pomarico, P. Mataloni, F. De Martini and V. Berardi, *Phys. Rev. Lett.* 98:180502, 2007.

[25] L. Masanes, Y.C. Liang and A.C. Doherty, *Phys. Rev. Lett.* 100:090403, 2008.

[26] J. Dai, Y.L. Len, Y.S. Teo, B.G. Englerted and L.A. Krivitsky, *Phys. Rev. Lett.* 113:170402, 2014.

[27] K. Bartkiewicz, P. Horodecki, K. Lemr, A. Miranowicz and K. Zyczkowski, *Phys. Rev. A* 91:032315, 2015.

[28] R.F. Werner and M.M. Wolf, *Phys. Rev. A* 64:032112, 2001.

[29] J.F. Clauser, M.A. Horne, A. Shimony and R.A. Holt, *Phys. Rev. Lett.* 23:880, 1969.

[30] J. Brody and C. Selton, *Am. J. Phys.*, 86:412, 2018.

[31] H. Hald, J.L. Sorensen, C. Schori and E. S. Polzik, *Phys. Rev. Lett.* 83:1319, 1999.

[32] V. Giobannettic, S. Mancini, D. Vitali and P. Tombesi, *Phys. Rev. A*, 67:022320, 2003.

[33] A.R.U. Devi, R. Prabhu and A.K. Rajagopal, *Phys. Rev. Lett.* 98:060501, 2007.

[34] O. Guhne, P. Hyllus, O. Gittsovich and J. Eisert, *Phys. Rev. Lett.* 99:130504, 2007.

[35] P. Badziag, C. Brukner, W. Laskowski, T. Baterek and M. Zukowski, *Phys. Rev. Lett.* 100:140403, 2008.

[36] C.H. Bennett, S. Popescu, D. Rohrlich, J.A. Smolin and A.V. Thapliyal, *Phys. Rev. A* 63:012307, 2001.

[37] W. Dur, J.I. Cirac and R. Tarrach, *Phys. Rev. Lett.* 83:3562, 1999.

[38] W. Dur and J.I. Cirac, *Phys. Rev. A* 61:042314, 2000.

[39] J.T. Barreiro, N.K. Langford, N.A. Peters and P.G. Kwiat, *Phys. Rev. Lett.* 95:260501, 2005.

[40] M. Barbieri, C. Cinelli, P. Mataloni and F. De Martini, *Phys. Rev. A* 72:052110, 2005.

[41] B.L. Hu and Y.B. Zhan, *Phys. Rev. A* 82:054301, 2010.

[42] C.H. Bennett, D.P. DiVincenzo, J.A. Smolin and W.K. Wootters, *Phys. Rev. A* 54:3824, 1996.

[43] V. Vedral, M.B. Plenio, M.A. Rippin and P.L. Knight, *Phys. Rev. Lett.* 78:2275, 1997.

[44] M.B. Plenio and S.S. Virmani, *Quantum Infor. & Comput.* 7:1, 2007.

[45] C.H. Bennett, G. Brassard, S. Popescu, B. Schumacher, J.A. Smolin and W.K. Wootters, *Phys. Rev. Lett.* 76:722, 1996.

[46] M. Horodecki, P. Horodecki and R. Horodecki, *Phys. Rev. Lett.* 80:5239, 1998.

[47] S. Hill and W.K. Wooters, *Phys. Rev. Lett.* 78:5022, 1997.

[48] W.K. Wooters, *Phys. Rev. Lett.* 80:2245, 1998.

[49] S.P. Walborn, P.H. Souto Ribeiro, L. Davidovich, F. Mintert and A. Buchleitner, *Nature* 440:1022, 2006.

[50] R.C. Yand, X. Lin, Z.P. Huang and H.C. Li, *Commun. Theor. Phys.* 51:252, 2009.

[51] L.H. Zhang, Q. Yang, M. Yang, W. Song and Z.L. Cao, *Phys. Rev. A* 88:062342, 2013.

[52] G. Romero, C.E. Lopez, F. Lastra, F. Solano and J.C. Retamal, *Phys. Rev. A* 75:032303, 2007.

[53] S.M. Lee, S.W. Ji, H.W. Lee and M. Suhail Zubairy, *Phys. Rev. A* 77:040301, 2008.

[54] K. Zyczkowski, P. Hododecki, A. Sanpera and M. Lewenstein, *Phys. Rev. A* 58:883, 1998.

[55] G. Vidal and R.F. Werner, *Phys. Rev. A* 65:032314, 2002.

[56] J. Lee, M.S. Kim, Y.J. Park and S. Lee, *J. Mod. Opt.* 47:2151, 2000.

[57] C.H. Bennett, *Phys. Scr.* T76:210, 1998.

[58] A.K. Ekert, *Phys. Rev. Lett.* 67:661, 1991.

[59] C.H. Bennett and S. Wiesner, *Phys. Rev. Lett.* 69:2881, 1992.

[60] K. Mattle, H. Weinfurter, P.G. Kwiat and A. Zeilinger, *Phys. Rev. Lett.* 76:4656, 1996.

[61] M.C. Teich and B.E.A. Saleh, *Ceskoslovensky Cosopis Pro Fygiku* 47:3, 1997.

[62] H. Fei, B. Jost, S. Popescu, B. Saleh and M. Teich, *Phys. Rev. Lett.* 78:1679, 1997.

[63] C. Brukner, M. Zukowski, J.W. Pan and A. Zeilinger, *Phys. Rev. Lett.* 92:127901, 2004.

[64] M. Epping and C. Brukner, *Phys. Rev. A* 87:032305, 2013.

[65] V. Giovannetti, S. Lloyd and L. Maccone, *Nature* 412:417, 2001.

[66] V. Giovannetti, S. Lloyd and L. Maccone, *Phys. Rev. A* 65:022309, 2002.

[67] E.O. Ilo-Okeke, L. Tessler, J.P. Dowling and T.Byrnes, *AIP Conf. Proc.* 2241:020011, 2020.

[68] S.F. Huelga, C. Macchiavello, T. Pellizzari and A.K. Ekert, M.B. Plenio and I. Cirac, *Phys. Rev. Lett.* 79:3865, 1997.

[69] C. Brunker, N. Paunkovic, T. Rudolph and V. Vedral, *Int. J. Quant. Inform.* 04:365, 2006.

[70] P. Solano, P. Barberis-Blostein, F.K. Fatemi, L.A. Orozco and S.L. Rolston, *Nat. Commun.* 8:1857, 2017.

[71] P. Longo, C. Keitel and J. Evers, *Sci. Rep.* 6:23628, 2016.

[72] J. Borchmann, A. Farrell, S. Matsuura and T. Pereg-Barnea, *Phys. Rev. B* 90:235150, 2014.

[73] G.A. Canella and V.V. França, *Physica A* 545:123646, 2020.

[74] T.J. Osborne and M.A. Nielsen, *Quan. Infor. Process.* 1:45, 2002.

[75] S.B. Li, Z.X. Xu, J.H. Dai and J.B. Xu, *Phys. Rev. B* 73:184411, 2006.

[76] KL.S. Lima, *Solid State Commun.* 309:113836, 2020.

[77] C.F. Roos, M. Chwalla, K. Kim, M. Riebe and R. Blatt, *Nature* 443:316, 2006.

[78] D. Kurzzyk, *Theor. Appl. Infor.* 24:135, 2012.

[79] W.K. Wooters, *Quant. Infor. Comput.* 1:27, 2001.

[80] C. Eltschka and J. Siewert, *J. Phys. A* 47:424005, 2014.

[81] D.V. Schroeder, *Am. J. Phys.* 85:812, 2017.

[82] H.M. Bharath and V. Ravishankar, *Phys. Rev. A* 89:062110, 2014.

[83] M. Beck, *Quantum Mechanics: Theory and Experiment*. Oxford University Press, Oxford, 2012.

[84] D. Dehlinger and M.W. Mitchell, *Am. J. Phys.* 70:898, 2002.

[85] D. Dehlinger and M.W. Mitchell, *Am. J. Phys.* 70:903, 2002.

[86] J.A. Carlson, M.D. Olmstead and M. Beck, *Am. J. Phys.* 74:180, 2006.

[87] E.J. Galvez, *Am. J. Phys.* 78:510, 2010.

[88] J. Carvioto-Logos, P. Gustavo Armendariz, V. Velazquez, E. Lopez-Moreno, M. Grether and E.J. Galvez, *Eur. J. Phys.* 33:1843, 2012.

[89] E. Dederick and M. Beck, *Am. J. Phys.* 82:962, 2014.

[90] M.N. Beck and M. Beck, *Am. J. Phys.* 84:87, 2016.

7.12 Exercises

7.1 Given an arbitrary density matrix $\rho = \begin{bmatrix} a & b \\ c & d \end{bmatrix}$ of the state with a basis $|\uparrow\rangle$ and $|\downarrow\rangle$, show that the probabilities to find $|\uparrow\rangle$ and $|\downarrow\rangle$ are given by the diagonal elements of ρ.

7.2 Show that in the z-basis, the density matrix of a fifty-fifty mixture of spin-up ($\uparrow$) and spin-down ($\downarrow$) in the z-direction is the same as a fifty-fifty mixture of the spin-up ($\rightarrow$) and spin-down ($\leftarrow$) in the x-direction.

7.3 Identify the entangled states of the two qubit system from the following states by finding whether they are factorizable into a tensor product state or not.

(a) $\frac{1}{2}\left(|11\rangle_{\mathrm{AB}} + |10\rangle_{\mathrm{AB}} + |01\rangle_{\mathrm{AB}} + |00\rangle_{\mathrm{AB}}\right)$,

(b) $\frac{1}{2}\left(|11\rangle_{\mathrm{AB}} + |10\rangle_{\mathrm{AB}} - |01\rangle_{\mathrm{AB}} + |00\rangle_{\mathrm{AB}}\right)$.

7.4 For the entangled state $|\psi\rangle_{\mathrm{AB}} = \left(|11\rangle_{\mathrm{AB}} + |00\rangle_{\mathrm{AB}}\right)/\sqrt{2}$ of two particles find the spin-up and spin-down probabilities for both the particles in x, y and z directions.

7.5 Using density matrices show that the pure state $|\psi\rangle = |\psi_1\rangle \otimes |\psi_2\rangle$, where $\psi_1 = \frac{1}{\sqrt{2}}\left(|0\rangle_1 + |1\rangle_1\right)$ and $\psi_2 = \frac{1}{\sqrt{2}}\left(|0\rangle_2 + |1\rangle_2\right)$ are separable.

7.6 Using density matrices show that the pure state $|\phi^+\rangle = \frac{1}{\sqrt{2}}\left[|00\rangle + |11\rangle\right]$ is entangled.

7.7 In the Schmidt basis $|l_1\rangle|l_2\rangle$ one can write $|\psi\rangle = \sum_{l=1}^{k} \sqrt{p_l}\,|l_1\rangle|l_2\rangle$. Prove that p_l are the eigenvalues of the reduced matrices ρ_1 and ρ_2.

7.8 By evaluating the Schmidt coefficients show that $|\psi\rangle = \frac{1}{\sqrt{2}}(|01\rangle + |11\rangle)$ is a product state and $|\psi^+\rangle = \frac{1}{\sqrt{2}}(|01\rangle + |10\rangle)$ is an entangled state.

7.9 Prove the completeness relation $\sum_i |i\rangle\langle i| = \mathbb{1}$ for an orthonormal basis $|i\rangle$ in a vector space. Then show that for any two vectors $|a_1\rangle$ and $|a_2\rangle$, $\mathrm{Tr}(|a_1\rangle\langle a_2|) = \langle a_2|a_1\rangle$.

7.10 For the pure state $|\psi\rangle = \frac{1}{\sqrt{2}}\left[\sin\theta\left(|00\rangle + |11\rangle\right) + \cos\theta\left(|01\rangle + |10\rangle\right)\right]$ perform Schmidt decomposition and find the value of θ for which we get product state.

7.11 If a state ρ has an equivalent separable finite dimensional state ρ' then ρ is said to admit classical simulation. If a state ρ does not admit classical simulation then it is said to be an *exceptional*. Show that all partially entangled pure states are exceptional [82].

7.12 Using PPT criterion show that the Bell state $|\psi^+\rangle = \frac{1}{\sqrt{2}}(|00\rangle + |11\rangle)$ is entangled.

7.13 Show that $W = \alpha I - |\psi_{\text{ent}}\rangle\langle\psi_{\text{ent}}|$ is a witness operator.

7.14 If $|w\rangle = |00\rangle \cos(\alpha/2) + |11\rangle \sin(\alpha/2)$ with $\sin\alpha \neq 0$ find the eigenkets of the witness $W = (|w\rangle\langle w|)^{\text{T}_2}$, where Tr_2 denotes the partial transposition on the second qubit.

7.15 Find the swap operator V for a pair of qubits in the basis $|00\rangle$, $|01\rangle$, $|10\rangle$ and $|11\rangle$. Show that it has at least one negative eigenvalue.

7.16 Show that the swap operator V found in the previous exercise satisfies the non-negative condition $\langle\psi|V|\psi\rangle > 0$ for an arbitrary product state $|\psi\rangle$.

7.17 Show that the swap operator V of the exercise 7.15 detects the entanglement for the Bell state $|\psi^-\rangle = \frac{1}{\sqrt{2}}(|10\rangle - |01\rangle)$ and not that of the symmetric Bell state $|\psi^+\rangle = \frac{1}{\sqrt{2}}(|10\rangle + |01\rangle)$.

7.18 Show that one cannot discriminate between entangled and separable states in the tripartite case by taking partial traces of the subsystems of the tripartite entangled states $|\text{GHZ}\rangle$ and $|W\rangle$.

7.19 Consider a spectral basis $|e_1\rangle = |\phi^+\rangle$, $|e_2\rangle = \text{i}|\phi^-\rangle$, $|e_3\rangle = \text{i}|\psi^+\rangle$ and $|e_4\rangle = |\psi^-\rangle$, where $|\phi^\pm\rangle$ and $|\psi^\pm\rangle$ are the Bell's states given by $|\phi^\pm\rangle = \frac{1}{\sqrt{2}}(|00\rangle \pm |11\rangle)$ and $|\psi^\pm\rangle = \frac{1}{\sqrt{2}}(|01\rangle \pm |10\rangle)$. If the concurrence C is defined for a pure state ψ as $C(\psi) = \left|\sum_i \langle e_i|\psi\rangle^2\right|$ show that $C(\psi) = \left|\langle\psi^*|\sigma_y \otimes \sigma_y|\psi\rangle\right|$.

7.20 Prove the relations (7.91).

8

Quantum Decoherence

8.1 Introduction

Quantum coherence is concerned with the fact that objects have both wave- and particle-like properties. When the wave nature of a particle got splitted into two then these two waves interfere coherently with each other and form a single state. The resulting state is essentially the superposition of the two states. *How is it different from quantum entanglement?* Decoherence is considered as the loss of information from a system due to its coupling with the surroundings. The study of decoherence was initially considered in statistical mechanics as a result of interaction of the systems with environment. It entered into quantum theory as a measuring instrument interacts with the system concerned in a measurement.

Quantum decoherence plays an important role in the interpretation of quantum mechanics. Decoherence is an important quantum phenomenon which has wide applications both theoretical and experimental. Quantum decoherence helps to know the fundamental reasons of understanding the very nature of quantum mechanics, the measurement process and the boundary between quantum and classical behaviour. Decoherence brings a quantum system into an apparant classical system. Decoherence is often thought that it will lead to the solution of some of the fundamental questions in quantum mechanics, namely, the measurement problem, the quantum to classical transition and also the quantum arrow of time.

The quantum information processing fields like quantum computers, quantum communication and quantum cryptography depend very much on how to minimize and control the quantum decoherence. In quantum mechanics the possible physical states ψ_1, ψ_2, ... are represented as vectors in a linear vector space called *Hilbert space*. A linear combination of these wave functions will give a superposition state of the system which can also represent the physical system. These wave functions evolve in time according to the Schrödinger equation in Schrödinger picture. But it is almost impossible to find such superposition states for classical macroscopic systems. In other words, this description of quantum states do not correspond to classical mechanical objects. For example, a quantum mechanical particle can exist at many different positions simultaneously whereas a classical particle can exist only at a particular position at a time.

The next important question to be answered is why the quantum mechanical system prepared in a particular superposition state does not remain stable even for a very small time. *Why are the quantum states degraded almost instantaneously?* The superposition states must remain stable for a fairly longer time for processing quantum information using these states. Quantum information processing and quantum technologies depend entirely on how to generate, maintain and manipulate the superpsotion states.

The quantum state of a quantum particle is rarely completely isolated from its environment. The quantum particle and the environment are bound together as one system. A quantum particle invariably interacts with the environment. When the environment interacts with a quantum state, the quantum state gets entangled with the classical degrees

DOI: 10.1201/9781003172192-8

of freedon. The entanglement affects subsequent measurement of the quantum state as the entangled state becomes a single state. We can say that decoherence describes how this entanglement of the quantum state with the environment influences the results of subsequent measurements of the system. The interaction may be considered like a measurement done on the quantum states by the environment. This enviroment may also be a man-made measuring device. In this sense decoherence can be considered as an observation.

Schrödinger in 1935 found that there exists global states of composite systems that cannot be written as a product of the states of the individual system, This phenomenon is called *entanglement* [1]. Entanglement is purely a quantum phenomenon. As decoherence is an entanglement of a quantum state with classical degrees of freedon, it is a quantum phenomenon. Usually, the many degrees of freedom of the environment are not experimentally controllable. Therefore, the entanglement is usually irreversible for all practical purposes. We cannot reverse the interaction process to get back the initial interference components. Decoherence is a highly efficient process which takes place too fast. But it is not an instantaneous discontinuous process. But new experimental techniques have been found to delay decoherence by decoupling quantum particles from the environment.

We first explain the basic concept of decoherence and how it damps out quantum interference of a superposition state in this chapter. Next, we discuss the master equations which give the dynamical evolution of the quantum system and the environment entangled state. Some of the decoherence models are discussed. A few experimental studies on decoherence are given. Finally, the role played by decoherence in the interpretation of quantum mechanics and also in the transition of quantum state to classical are explained.

8.2 Decoherence and Interference Damping

A double-slit experiment can be used to explain the basic concept of decoherence. This interference experiment when the interference pattern vanishes due to interaction with the environment captures quite well the essence of what is happening in decoherence. The decoherence effect is a mechanism destroying quantum interferences at a macroscopic level. The double-slit experiment is a typical example of quantum interference which demonstrates the dual nature of particles.

In the double-slit experiment, particles like electron, photon etc. behave some times like a particle and some times like a wave. In the experimental set-up, a stream of particles is incident on a double-slit separated by a small distance. The particles are detected on the other side in a detector screen. We will observe an interference pattern on the screen as long as the set-up is totally isolated, in the sense that no attempt is made either by an observer or the environment, to determine which-path was taken by the particles. This is true even if each particle in the beam is incident on the double-slit at a time separation between them. The interference pattern disappears if a detection apparatus tries to determine the path taken by each particle. Therefore, acquiring a particle's path information destroys the interference. It has also been observed that a total determination of the path information destroys the interference pattern totally. A partial determination of the path information reduces the visibility of the interference pattern partially.

In general, it is true that the interference pattern disappears when the observer acquires information about the quantum system. What has really happened is that the information obtained by the observer about the path of the particles has made the interference pattern disappear and we will observe only two peaks on the screen as expected for a classical system.

As decoherence describes the emergence of classcial behaviour from quantum system due to information leakage from the system, the deep relationship between interference and information loss can be understood in the context of decoherence and the entanglement of the quantum system with the environmental degrees of freedom. Decoherence is a statistical concept involving a transition from a pure state to a mixture entangled states. Therefore, the interference terms disappear.

8.3 Interaction of a Detector on the Double-Slit Experiment

Following Maximilian Schlosshauer [2], we consider a double-slit experiment in which we represent the quantum particle as a system S corresponding to the passage of the particle through, say, slit-1 and slit-2 by $|s_1\rangle$ and $|s_2\rangle$, respectively. Consider the environment or the detector of the particles at the slits as the system E. Interaction of E with $|s_1\rangle$ will give the quantum state $|E_1\rangle$ and with $|s_2\rangle$ will give the quantum state $|E_2\rangle$ for the quantum state E. Hence, after the interaction of E at the two slits we will get the final composite state

$$|\psi\rangle = \alpha|s_1\rangle|E_1\rangle + \beta|s_2\rangle|E_2\rangle. \tag{8.1}$$

As $|\psi\rangle$ is not a product state of S, $(a_1|s_1\rangle + a_2|s_2\rangle)$, and E, $(b_1|E_1\rangle + b_2|E_2\rangle)$, it is an entangled state. Therefore, the interaction of the environment state E on S has given an entangled composite state.

The reduced density matrix $\rho_{_S}$ is defined as

$$\rho_{_S} = \mathrm{Tr}_E\left(\rho_{_{SE}}\right) = \mathrm{Tr}_E|\psi\rangle\langle\psi|. \tag{8.2}$$

Tr_E refers to partial trace with respect to E. The statistics of all possible measurements on S are exhaustively encoded in the reduced density matrix $\rho_{_S}$. Finding the density operator $|\psi\rangle\langle\psi|$ and then taking the reduced density operation of the E subsystem and finally finding its trace will give

$$\begin{aligned}\rho_{_S} &= |\alpha|^2|s_1\rangle\langle s_1| + |\beta|^2|s_2\rangle\langle s_2| + \alpha\beta^*|s_1\rangle\langle s_2|\langle E_2|E_1\rangle \\ &\quad +\alpha^*\beta|s_2\rangle\langle s_1|\langle E_1|E_2\rangle.\end{aligned} \tag{8.3}$$

The position probability density $p(x)$ of a particle can be measured as

$$\begin{aligned}p(x) &= \mathrm{Tr}_S\left(\rho_{_S}x\right) \\ &= |\alpha|^2|\psi_1(x)|^2 + |\beta|^2|\psi_2(x)|^2 \\ &\quad +2\mathrm{R.P.}\left[\alpha\beta^*\psi_1(x)\psi_2^*(x)\langle E_2|E_1\rangle\right],\end{aligned} \tag{8.4}$$

where R.P.$[F]$ is the real part of F and $\psi_i(x) = \langle x|s_i\rangle$. The last term in Eq. (8.4) gives the interference to the measurement of position probability at the screen after the beam has gone through the two slits after interacting with the system E. $\langle E_2|E_1\rangle$ is the overlap integral of the basis states of the system E. This overlap integral quantifies the visibility of the interference pattern. If $|E_1\rangle$ and $|E_2\rangle$ are orthogonal then $\langle E_2|E_1\rangle = 0$. The interference term will become zero then.

If the two measurements at the slits are totally independent with no connection between them then $|E_1\rangle$ and $|E_2\rangle$ are perfectly distinguishable. Under this perfect distinguishability

the interference term in Eq. (8.4) will vanish as $\langle E_2|E_1\rangle = 0$. Therefore, we get the position probability on the screen as

$$p(x) \quad = \quad |\alpha|^2|\psi_1(x)|^2 + |\beta|^2|\psi_2(x)|^2. \tag{8.5}$$

Equation (8.5) gives the classically expected distributions on the screen. By measuring Eq. (8.5) on the screen we cannot determine locally the phase relationship between $|s_1\rangle$ and $|s_2\rangle$ as the interference pattern has vanished. The coherence is between the states $|s_1\rangle|E_1\rangle$ and $|s_2\rangle|E_2\rangle$. Only a global measurement acting jointly on S and E can reveal the coherence. As $\langle E_2|E_1\rangle$ can take values from 0 to 1 an interference pattern of reduced visibility is obtained with a probability of $p = 1 - |\langle E_2|E_1\rangle|^2$. Equation (8.4) shows that the reduction of the visibility of the interference increases as $|E_1\rangle$ and $|E_2\rangle$ beccome more distinguishable. What we discussed so far gives the essence of decoherence if we identify S as an arbitrary quantum system interacting with the environment E.

Solved Problem 1:

Show that the state given by Eq. (8.1) is an entangled state for α and β not equal to zero.

For the given $|\psi\rangle$ the determinant of the coefficient of the state is $\begin{vmatrix} \alpha & 0 \\ 0 & \beta \end{vmatrix} = \alpha\beta$. As α and β are not zero the determinant of the coefficient is not zero. That is, $|\psi\rangle$ is an entangled state.

8.4 Decoherence Due to Phase Randomization

The details of decoherence is, in general, quite complicated. John King Gamble and John F. Lindner [3] have given a very simple thought experiment using a phase randomizer in a Stern–Gerlach apparatus to explain how a random environmental interaction leads to the classical result.

Consider a Stern–Gerlach experimental set-up with a source of spin-half neutral silver atoms. The state vector of spin-half state can be given as

$$|\psi\rangle = \alpha|\uparrow\rangle + \beta|\downarrow\rangle. \tag{8.6}$$

The spin-up state is $|\uparrow\rangle = \begin{bmatrix} 1 \\ 0 \end{bmatrix}$ and the spin-down state is $|\downarrow\rangle = \begin{bmatrix} 0 \\ 1 \end{bmatrix}$. Since $|\psi\rangle$ is normalized we have

$$\langle\psi|\psi\rangle = \begin{pmatrix} \alpha^* & \beta^* \end{pmatrix} \begin{pmatrix} \alpha \\ \beta \end{pmatrix} = \alpha\alpha^* + \beta\beta^* = 1. \tag{8.7}$$

The density matrix is

$$\rho = |\psi\rangle\langle\psi| = \begin{pmatrix} \alpha \\ \beta \end{pmatrix} \begin{pmatrix} \alpha^* & \beta^* \end{pmatrix} = \begin{bmatrix} \alpha\alpha^* & \alpha\beta^* \\ \beta\alpha^* & \beta\beta^* \end{bmatrix}. \tag{8.8}$$

We find from Eqs. (8.7) and (8.8)

$$\mathrm{Tr}(\rho) = \alpha\alpha^* + \beta\beta^* = 1. \tag{8.9}$$

Any arbitrary 2×2 matrix can be written as a linear combination of the three Pauli matrices and identity matrix I. Hence, ρ can be written as

$$\rho = r_I I + \frac{1}{2} r_x \sigma_x + \frac{1}{2} r_y \sigma_y + \frac{1}{2} r_z \sigma_z. \tag{8.10}$$

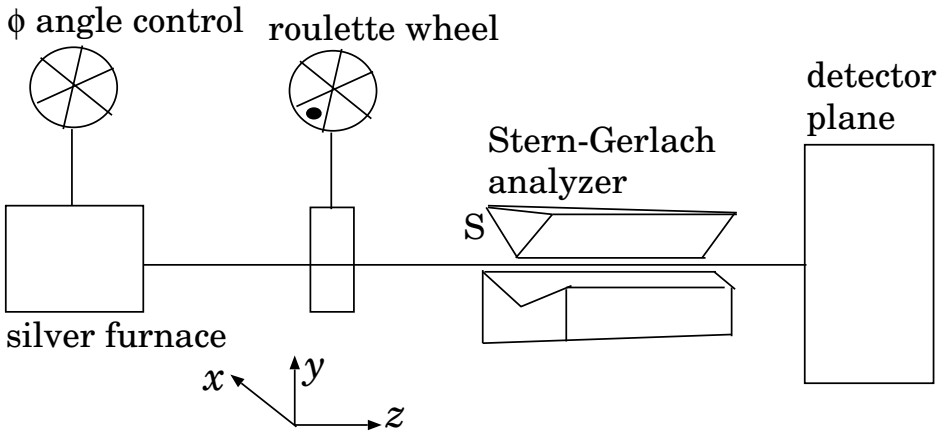

FIGURE 8.1
Schematic set-up of the thought experiment with phase randomizer in a Stern–Gerlach apparatus [3] (Reproduced from J.K. Gample and J.F. Lindner, *Am. J. Phys.* 77:244, 2009 with the permission of the American Association of Physics Teachers.).

As

$$I = \begin{bmatrix} 1 & 0 \\ 0 & 1 \end{bmatrix}, \quad \sigma_x = \begin{bmatrix} 0 & 1 \\ 1 & 0 \end{bmatrix}, \quad \sigma_y = \begin{bmatrix} 0 & -\mathrm{i} \\ \mathrm{i} & 0 \end{bmatrix}, \quad \sigma_z = \begin{bmatrix} 1 & 0 \\ 0 & -1 \end{bmatrix}, \tag{8.11}$$

we obtain

$$\rho = \frac{1}{2} \begin{bmatrix} 2r_I + r_z & r_x - \mathrm{i}r_y \\ r_x + \mathrm{i}r_y & 2r_I - r_z \end{bmatrix} \tag{8.12}$$

and $\mathrm{Tr}(\rho) = 2r_I$. As $\mathrm{Tr}(\rho) = 1$ we get $r_I = 1/2$. ρ is a Hermitian operator, $\rho^\dagger = \rho$. That is, r_x, r_y and r_z are all real. As $\rho^2 = |\psi\rangle\langle\psi|\psi\rangle\langle\psi| = |\psi\rangle\langle\psi| = \rho$ we get $r_x^2 + r_y^2 + r_z^2 = 1$ (see the exercise 2 at the end of this chapter). Therefore, r_x, r_y and r_z can be written as a unit vector $\mathbf{r}$ in spherical polar coordinates with

$$r_x = \sin\theta\cos\phi, \quad r_y = \sin\theta\sin\phi, \quad r_z = \cos\theta. \tag{8.13}$$

Gamble and Lindner considered a silver furnace connected to an angle control device, which polarizes the spin of the out-going copper atom with $x - y$ plane. The angle ϕ is under the control of the user. As $z = 0$ for $x - y$ plane, $\theta = \pi/2$. This atom passes through a Stern–Gerlach analyzer after a random phase ϕ_{R} to the atom's original phase ϕ introduced by a classical roulette wheel. This phase randomizer crudely models the environmental interaction on the spin states of the atoms. The schematic of the thought experiment is given in Fig. 8.1.

Let us first consider the measurement result in the absence of the phase randomizer. As $\theta = \pi/2$, Eq. (8.13) gives

$$r_x = \cos\phi, \quad r_y = \sin\phi, \quad r_z = 0. \tag{8.14}$$

From Eq. (8.12) we get

$$\rho = \frac{1}{2} \begin{bmatrix} 1+0 & \cos\phi - \mathrm{i}\sin\phi \\ \cos\phi + \mathrm{i}\sin\phi & 1-0 \end{bmatrix} = \frac{1}{2} \begin{bmatrix} 1 & \mathrm{e}^{-\mathrm{i}\phi} \\ \mathrm{e}^{\mathrm{i}\phi} & 1 \end{bmatrix}. \tag{8.15}$$

If the magnetic field gradient of the analyzer is along the $+y$-axis then the spin-sorter observer operator is

$$O = y.\mathbf{s} = \frac{\hbar}{2}\sigma_y. \tag{8.16}$$

As the eigenvalue of σ_z is $+1$ or -1, any measurement will give the eigenvalue as $+\hbar/2$ or $-\hbar/2$. The average value of O operator can be found using the relation

$$\langle O\rangle = \mathrm{Tr}(\rho O) = \frac{\hbar}{2}\mathrm{Tr}\left[\begin{pmatrix} 1 & \mathrm{e}^{-\mathrm{i}\phi} \\ \mathrm{e}^{\mathrm{i}\phi} & 1 \end{pmatrix}\begin{pmatrix} 0 & -\mathrm{i} \\ \mathrm{i} & 0 \end{pmatrix}\right] = \frac{\hbar}{2}\sin\phi. \tag{8.17}$$

The detector measures the closeness of the alignment of the silver atoms with the magnetic field gradient. When $\phi = 0$ the spin of the atom points in the x-direction. As the magnetic field is perpendicular to x-direction, half of the measurement of spin will give $\hbar/2$ and another half of the measurement will give $-\hbar/2$. The average value of the magnetic moment will be zero. For $\phi = \pi/2$, the spin points in the field direction y. So, the measurement will give $\hbar/2$ always. For $\phi = 3\pi/2$ the spin direction will be opposite to the field direction giving the magnetic moment $-\hbar/2$. This bechaviour is the characteristic of a coherence quantum superposition and a non-diagonal static operator.

The classical roulette wheel is imagined to add a random phase ϕ_{R} to the original spin angle ϕ of the atom. Therefore, the atom will have a new phase angle. This set-up minimizes the environmental interaction to the pure spin state of the atom. ϕ_{R} will take any random value between 0 to 2π. Therefore, the new phase angle of the atom becomes $\phi' = \phi + \phi_{\mathrm{R}}$. To calculate the expectation value $\langle O\rangle_{\mathrm{R}}$ of the spin observable O with the random phase we must find the new density matrix ρ_{R}. As O is independent of ϕ_{R} we get ρ_{R} by averaging ρ over the angle ϕ' as $\rho_{\mathrm{R}} = \dfrac{1}{2\pi}\displaystyle\int_0^{2\pi} \rho \mathrm{d}\phi'$. Using Eq. (8.15), we obtain

$$\rho_{\mathrm{R}} = \frac{1}{2}\begin{bmatrix} \frac{1}{2\pi}\int_0^{2\pi}\mathrm{d}\phi' & \frac{1}{2\pi}\int_0^{2\pi}\mathrm{e}^{-\mathrm{i}\phi'}\mathrm{d}\phi' \\ \frac{1}{2\pi}\int_0^{2\pi}\mathrm{e}^{\mathrm{i}\phi'}\mathrm{d}\phi' & \frac{1}{2\pi}\int_0^{2\pi}\mathrm{d}\phi' \end{bmatrix} = \frac{1}{2}\begin{bmatrix} 1 & 0 \\ 0 & 1 \end{bmatrix} = \frac{1}{2}I. \tag{8.18}$$

The expectation value of O including the random phase can be found from

$$\langle O\rangle_{\mathrm{R}} = \mathrm{Tr}(\rho_{\mathrm{R}} O) = \mathrm{Tr}\left(\frac{1}{2}I\frac{1}{2}\hbar\sigma_y\right) = \frac{1}{4}\hbar\mathrm{Tr}(\sigma_y) = 0. \tag{8.19}$$

The final measurement with the random phase gives an average value of zero irrespective of the initial ϕ values. Thus, half number of measurements give $\hbar/2$ and another half number of measurements give $-\hbar/2$. This is expected from a classical mixture of spin-up and spin-down atoms.

We find that the inclusion of the random phase (assumed to be an environmental interaction) to the spin state of the atom has changed the density matrix ρ to ρ_{R}. The interaction has effectively destroyed the off-diagonal elements in ρ while leaving the diagonal elements intact. The loss of the off-diagonal elements in ρ has resulted in the loss of the sinusoidal pattern and is a quantum effect. Therefore, we can conclude that the loss of off-diagonal elements in the density matrix is the hallmark of a loss of quantum information due to an environmental interaction and it leads to the emergence of the classical world [4].

8.5 Position Decoherence Due to Environmental Scattering

As an another example for explaining how decoherence theory demonstrates an environmental interaction leading to an entanglement and decaying of the interferance term we provide Lerner model [5] of positional decoherence in a gas of scatterers.

If a state of a particle localized in position X is given by $|\phi_X\rangle$ then it has a classical counterpart. On the other hand, supppose we have a quantum mechanical superposition state $|\phi\rangle = (|\phi_X\rangle + |\phi_Y\rangle)/\sqrt{2}$ in which the particle is appeared to be localized at both X and Y positions simultaneously. In this case $|\phi\rangle$ has no classical counter part. The expectation value of our observable $\langle\phi|A|\phi\rangle$ contains the interference term $\langle\phi_Y|A|\phi_X\rangle$. The measurements thus lead to non-classical nature of $|\phi\rangle$. Lerner has shown how the action of a gas of scatteres on a macroscopic particle via the Schrödinger equation leads to the approximately exponential decay of the interference term $\langle\phi_Y|A|\phi_X\rangle$ using a simplified scattering model.

Let $|\phi_X\rangle$ represent a particle state with a center of mass at X corresponding to the positional wave function $\phi_X(y) = \langle y|\phi_X\rangle$. Let $|\phi\rangle$ represent the state of each of the surrounded gas scatterers with the corresponding position wave function $\phi(x) = \langle x|\phi\rangle$. Consider the scattering to be one-dimensional and the particle is very heavy compared to the gas scatterers. In that case, the scattering can be considered as an elastic reflection at an infinite potential at $x = X$ with the momentum of the scatterer changing from p to $-p$ and a possible translation of $x \to a - x$. As the potential is infinite at $x = X$ the wave function at x must be zero: $\phi(X) - \phi(a - X) = 0$ and $a = 2X$. Hence, the scattering changes

$$\phi_X(y)\phi(x) \xrightarrow{\text{S}} -\phi_X(y)\phi(2X - x). \tag{8.20}$$

We can write the superposition of two orthogonal states centred at two different positions X and Y as

$$\Phi(x, y) = \frac{1}{\sqrt{2}} \left[\phi_X(y) + \phi_Y(y)\right] \phi(x). \tag{8.21}$$

Combining Eqs. (8.20) and (8.21), we obtain the scattered superposition state as

$$\left[\phi_X(y) + \phi_Y(y)\right] \phi(x) \xrightarrow{\text{S}} -\phi_X(y)\phi(2X - x) - \phi_Y(y)\phi(2Y - x). \tag{8.22}$$

The function $\phi(x)$ entangles the scatterer and the particle states and leads to decoherence of the superposition state of the particle. The expectation value of a Hermitian operator A is given by

$$\langle\Phi|A|\Phi\rangle = \frac{1}{2} \left[\langle\phi_X|A|\phi_X\rangle + \langle\phi_Y|A|\phi_Y\rangle + \langle\phi_Y|A|\phi_X\rangle + \langle\phi_X|A|\phi_Y\rangle\right]. \tag{8.23}$$

The terms $r = \langle\phi_Y|A|\phi_X\rangle$ and $r^* = \langle\phi_X|A|\phi_Y\rangle$ are the two interference terms giving the quantum mechanical characteristics of the phase coherence of the superposition state. Absence of these states will lead to classical states. Lerner has shown that the expectation value of this interference term r tends to zero in the presence of scattering when the expectation value does not depend on $|\phi\rangle$. Due to scattering we find from Eq. (8.22)

$$\begin{aligned} r &\xrightarrow{\text{S}} r \int_{-\infty}^{\infty} \phi^*(2Y - x)\phi(2X - x)\mathrm{d}x \\ &\longrightarrow r \int_{-\infty}^{\infty} \phi^*(y)\phi(2X - 2Y + y)\mathrm{d}y. \end{aligned} \tag{8.24}$$

Using the convolution theorem of Fourier transform the above equation becomes (see the exercise 4 at the end of this chapter)

$$r \xrightarrow{\text{S}} r\int_{-\infty}^{\infty} \bar{\phi}^*(p)\mathrm{e}^{2\mathrm{i}(X-Y)p/\hbar}\bar{\phi}(p)\mathrm{d}p, \tag{8.25}$$

where $\bar{\phi}(p)$ is the momentum wave function which is the Fourier transform of $\phi(x)$.

The exponential term $\mathrm{e}^{2\mathrm{i}(X-Y)p/\hbar}$ in Eq. (8.25) can be expanded in a Taylor series. Then

$$\begin{aligned} r &\xrightarrow{\text{S}} r\int_{-\infty}^{\infty} \bar{\phi}^*(p)\left(1+\frac{2\mathrm{i}(X-Y)}{\hbar}p-\frac{2(X-Y)^2}{\hbar^2}p^2+\ldots\right) \\ &\quad \times\bar{\phi}(p)\mathrm{d}p \\ &\xrightarrow{\text{S}} r\left(1+\frac{2\mathrm{i}(X-Y)}{\hbar}\langle p\rangle-\frac{2(X-Y)^2}{\hbar^2}\langle p^2\rangle+\ldots\right), \end{aligned} \tag{8.26}$$

where $\langle p^n\rangle$ is the expectation value of p^n. As the scattering is assumed to be symmetrical on both sides of the particle we have $\langle p\rangle = 0$. If R is the scattering rate then there will be $N = Rt$ collisions in time t. Now, if $(X-Y)^2\langle p^2\rangle/\hbar^2$ is very small then we can approximate Eq. (8.26) as

$$r \xrightarrow{\text{S}} r\left(1-\frac{2(X-Y)^2}{\hbar^2}\langle p^2\rangle\right). \tag{8.27}$$

Then the interference term after time t is

$$\begin{aligned} r(t) &= r(0)\left(1-\frac{2(X-Y)^2}{\hbar^2}\langle p^2\rangle\right)Rt \\ &\approx r(0)\exp\left(-2(X-Y)^2\langle p^2\rangle Rt/\hbar^2\right). \end{aligned} \tag{8.28}$$

If the number of scatterers is large then the number of collisions will be large. In that case the interference of particle state decays exponentially at a rate proportional to the square of the separation, $(X-Y)^2$. So, only the first two terms in Eq. (8.23) will contribute to the expectation value of A. This is what we will get for a classical mixture of particle $|\phi_X\rangle$ and $|\phi_Y\rangle$ with equal weight for both states. As a consequency of decoherence the interference of a particle with itself can be neglected for macroscopic particles.

Solved Problem 2:

Find the density matrix representing the state $\Phi(x,y)$ given by Eq. (8.21). Show that the expectation value of A given by Eq. (8.23) can be given as

$$\langle\Phi|A|\Phi\rangle = \mathrm{Tr}\left[\begin{pmatrix} \langle\phi_X|A|\phi_X\rangle & \langle\phi_X|A|\phi_Y\rangle \\ \langle\phi_Y|A|\phi_X\rangle & \langle\phi_Y|A|\phi_Y\rangle \end{pmatrix}\begin{pmatrix} 1/2 & 1/2 \\ 1/2 & 1/2 \end{pmatrix}\right]. \tag{8.29}$$

Using the $\Phi(x,y)$ given by Eq. (8.21), we obtain

$$\rho = \begin{pmatrix} 1/\sqrt{2} \\ 1/\sqrt{2} \end{pmatrix}\begin{pmatrix} 1/\sqrt{2} & 1/\sqrt{2} \end{pmatrix} = \begin{pmatrix} 1/2 & 1/2 \\ 1/2 & 1/2 \end{pmatrix}. \tag{8.30}$$

Next, we obtain

$$\begin{aligned}
&\mathrm{Tr}\left[\begin{pmatrix} \langle\phi_X|A|\phi_X\rangle & \langle\phi_X|A|\phi_Y\rangle \\ \langle\phi_Y|A|\phi_X\rangle & \langle\phi_Y|A|\phi_Y\rangle \end{pmatrix}\begin{pmatrix} 1/2 & 1/2 \\ 1/2 & 1/2 \end{pmatrix}\right] \\
&= \mathrm{Tr}\begin{bmatrix} \frac{1}{2}\left(\langle\phi_X|A|\phi_X\rangle + \langle\phi_X|A|\phi_Y\rangle\right) & \frac{1}{2}\left(\langle\phi_X|A|\phi_X\rangle + \langle\phi_X|A|\phi_Y\rangle\right) \\ \frac{1}{2}\left(\langle\phi_Y|A|\phi_X\rangle + \langle\phi_Y|A|\phi_Y\rangle\right) & \frac{1}{2}\left(\langle\phi_Y|A|\phi_X\rangle + \langle\phi_Y|A|\phi_Y\rangle\right) \end{bmatrix} \\
&= \frac{1}{2}\left(\langle\phi_X|A|\phi_X\rangle + \langle\phi_Y|A|\phi_Y\rangle + \langle\phi_X|A|\phi_Y\rangle + \langle\phi_Y|A|\phi_X\rangle\right) \\
&= \langle\Phi|A|\Phi\rangle. \qquad (8.31)
\end{aligned}$$

8.6 Master Equations

No quantum mechanical system is closed. Any practical quantum system has an uncontrollable coupling to the environment which influences the time evolution of the system. It is not a simple task to describe the behaviour of open quantum systems theoretically. As a complete description of the environmental degrees of freedom is not feasible, theory of open quantum systems are developed by considering different assumptions about the environments and their interactions. The effective equation of motion which describes the evolution of the quantum system S and the environment E is called the *master equation*.

8.6.1 Liouville–von Neumann Equation

We will first discuss how a closed system evolves with time t. If $\psi(t)$ is a pure state then the time evolution of $\psi(t)$ is given by the Schrödinger equation ($\hbar = 1$)

$$\mathrm{i}\frac{\mathrm{d}}{\mathrm{d}t}|\psi(t)\rangle = H(t)|\psi(t)\rangle. \qquad (8.32)$$

If $|\psi(t_0)\rangle$ is its initial state then

$$|\psi(t)\rangle = U(t,t_0)|\psi(t_0)\rangle, \;\; U(t_0,t_0) = 1. \qquad (8.33)$$

For an isolated system there is no interaction. Hence, the Hamiltonian H will be independent of time. Then we get from Eq. (8.32) $|\psi(t)\rangle = C\mathrm{e}^{-\mathrm{i}Ht}$. For $t = t_0$ we have $|\psi(t_0)\rangle = C\mathrm{e}^{-\mathrm{i}Ht_0}$. Then

$$|\psi(t)\rangle = \mathrm{e}^{-\mathrm{i}H(t-t_0)}|\psi(t_0)\rangle. \qquad (8.34)$$

Comparison of Eq. (8.34) with (8.33) gives

$$U(t,t_0) = \mathrm{e}^{-\mathrm{i}H(t-t_0)}. \qquad (8.35)$$

If the system is an ensemble of states then to find its evolution with time we must find its density matrix

$$\rho(t_0) = \sum_n a_n|\psi_n(t_0)\rangle\langle\psi_n(t_0)|. \qquad (8.36)$$

Then its equation of motion is (see the exercise 7 at the end of this chapter)

$$\frac{\mathrm{d}}{\mathrm{d}t}\rho(t) = -\mathrm{i}\left[H, \rho(t)\right]. \qquad (8.37)$$

This equation is called *Liouville–von Neumann equation*.

We could write the equation of motion for a closed system by Eqs. (8.33) and (8.37) as the states representing a closed systems evolve unitarily. In an open system the interaction of the environment with the quantum state implies that the states representing such systems do not evolve unitarily. The open system cannot be described by the Schrödinger equation as it describes a unitary evolution.

If S represents the quantum system and E the environment then the interaction between these two systems generates a certain correlation between them that is responsible for non-unitary character of the open system. In order to desribe the temporal evolution of an open quantum system first the equation for the unitary temporal evolution of the overall system S and E is written and the environmental coordinates are eliminated by taking a partial trace of the overall density matrix. Then we will get the equation for the reduced density operator which is called a *generalized master equation* [6]. Use of taking partial traces to eliminate environmetnal coordinates and deriving the generalized master equation was developed by many researchers [7]. These works added a second term to the Liouville–von Neumann Eq. (8.37). This term describes the damping or energy dissipation of the open object system.

8.6.2 Markovian Master Equations

Let us consider the quantum state S in the state $|\phi\rangle$ in Hilbert space $\mathcal{H}_S$ spanned by the basis $\{|\phi_j\rangle\}$ and the environment state in state $|E\rangle$ in Hilbert space $\mathcal{H}_E$ with the basis $\{|E_j\rangle\}$. The joint Hilbert space of the system S and the environment E is the tensor product of space $\mathcal{H}_S \otimes \mathcal{H}_E$ and the full Hamiltonian can be written as [8]

$$H = H_S \otimes I_E + I_S \otimes H_E + H_I, \tag{8.38}$$

where I_E and I_S are the unit operators in the Hilbert spaces $\mathcal{H}_E$ and $\mathcal{H}_S$, respectively, and H_I is the Hamiltonian giving the interaction between S and E. H_S and H_E are the Hamiltonains of the quantum system S and the environmental system E, respectively. The system and environment together will evolve according to the Schrödinger equation. Due to the interaction Hamiltonian H_I the initial product terms $|\phi\rangle \otimes |E\rangle$ will evolve into states that cannot be written as product states. $|\phi\rangle \otimes |E\rangle$ will evolve into $|\psi\rangle$ where

$$|\psi\rangle = \sum_j a_j |\phi_j\rangle \otimes |E_j\rangle. \tag{8.39}$$

We get an entangled state due to the environmental interaction H_I with the quantum state S. As the system S and the environment E are now entangled, neither the state nor the environment has pure state. The joint density of the state $\rho_{SE} = |\psi\rangle\langle\psi|$ is constructed. From ρ_{SE} the density of the state ρ_S for the quantum system can be found by taking the partial trace of ρ_{SE} over the environmental degrees of freedom as

$$\rho_S(t) = \mathrm{Tr}\rho_{SE}(t). \tag{8.40}$$

As the composite system evolves according to the Schrödinger equation we can write (taking $t_0 = 0$)

$$|\psi(t)\rangle = U(t)|\psi(0)\rangle, \tag{8.41}$$

where $U(t)$ is the time evoltuion operator for the composite system. Then we get

$$\rho_{SE} = |\psi\rangle\langle\psi| = U(t)|\psi(0)\rangle\langle\psi(0)|U^\dagger = U(t)\rho_{SE}(0)U^\dagger. \tag{8.42}$$

From Eq. (8.40), we obtain

$$\rho_S(t) = \mathrm{Tr}_E \rho_{SE}(t) = \mathrm{Tr}_E \left[U(t) \rho_{SE}(0) U^\dagger \right]. \tag{8.43}$$

The evolution of Eq. (8.41) requires calculating the exact dynamics of the system and environment. The reduced density matrix depends on the entire past history of the full system-environment state. Therefore, solving it is quite difficult without certain assumptions and simplifications of the equation. As we are usually not interested in the dynamics of the environment the calculation of the full composite system-environment state is not needed. To simplify the computation of Eq. (8.43) master equations are based on certain assumptions and simplifications. Consequently, these assumptions lead to an approximate description of the decoherence process. One such approximate master equations are the Markovian master equations

$$\frac{\partial}{\partial t} \rho_S(t) = \mathcal{L} \rho_S(t), \tag{8.44}$$

where the super-operator $\mathcal{L}$ does not depend on time or the initial preparation of the state. Hence, such master equations are local in time and $\mathcal{L}\rho_S(t)$ does not depend on the history of density matrix.

8.6.3 Born–Markov Master Equations

Born–Markov master equations are relatively easy to solve. They are found to be good approximations to many cases of practical interest and their solutions agree well with experimental result. They are based on the following two approximations [2].

1. **The Born Approximation**

   It assumes that the system-environment coupling is very weak and hence there is only a negligible change in ρ_E. The system-environment density operator can be assumed to be $\rho_{SE} \approx \rho_S(t) \otimes \rho_E$ at all times.

2. **The Markov Approximation**

   Denote τ_r as the relaxation time of the open system describing the time on which the environment affects the evolution of the system. τ_c is the time scale for the decay of correlations between the degrees of the environment that are being generated by the interaction with the quantum system. Assume that $\tau_\mathrm{r} \gg \tau_\mathrm{c}$. Therefore, the environment may be considered to be memory-less as it does not retain information over a long time.

In many cases of practical interest H_I in Eq. (8.38) dominates we can write $H \approx H_I$. Let us choose the states $|\phi_i\rangle$ such that the composite system-environment state, starting from the product state $|\phi_i\rangle|E_0\rangle$ at $t = 0$ remains in the product state $|\phi_i\rangle|E(t)\rangle$ for all the time under the interaction H_I. Then it can be proved that H_I takes the tensor product of the form $H_I = S \otimes E$, where S and E are system and environment observables. Then the environment-super selected observables will be those commuting with S [2]. Any H_I can then be written as a diagonal decomposition of the system operators (S_i) and environmental operators (E_i) as

$$H_I = \sum_i S_i \otimes E_i. \tag{8.45}$$

Then the Born–Markov master equation is obtained as [9,10]

$$\frac{\mathrm{d}}{\mathrm{d}t} \rho_S(t) = -\mathrm{i} \left[H_S, \rho_S(t) \right] - \sum_i \left\{ [S_i, B_i \rho_S(t)] + [\rho_S(t) C_i, S_i] \right\}, \tag{8.46}$$

where the system operators B_i and C_i are defined as

$$B_i = \int_0^\infty \mathrm{d}\tau \sum_j C_{ij}(\tau) S_j^{(I)}(-\tau), \quad C_i = \int_0^\infty \mathrm{d}\tau \sum_j C_{ji}(-\tau) S_j^{(I)}(-\tau). \tag{8.47}$$

$S_j^{(I)}(-\tau)$ denotes the system operators S_j in the interaction picture and

$$C_{ij}(\tau) = \langle E_i(\tau) E_j \rangle_{\rho_E} \tag{8.48}$$

gives the environmental self-correction functions which has a rapid decay in Markov approximation. In many situations of interest Born–Markov master equation gets simplified.

8.6.4 Lindblad Master Equation

The Lindblad master equation is a special case of the general Born–Markov master equation that ensures complete positivity [11]. The evolution may not be unitary. But it must take density matrices at $t = 0$ to density matrices at t, but not necessarily pure states to pure states. The general form of Lindblad master equation is given by [12,13]

$$\frac{\mathrm{d}}{\mathrm{d}t}\rho_S(t) = -\mathrm{i}\left[H_S', \rho_S(t)\right] + \frac{1}{2}\sum_{i,j}\gamma_{ij}\left\{\left[S_i, \rho_S(t) S_j^\dagger\right] + \left[S_i \rho_S(t), S_j^\dagger\right]\right\}, \tag{8.49}$$

where H_S' is the renormalization Hamiltonian of the system. The coefficients γ_{ij} are time-independent and they contain information about the physical parameters of the decoherence processes. The matrix $\Gamma = [\gamma_{ij}]$ is positive. So, all its eigenvalues K_μ are ≥ 0. Diagonalizing Γ, the diagonal form of Eq. (8.49) is obtained as [13,14]

$$\begin{aligned}\frac{\mathrm{d}}{\mathrm{d}t}\rho_S(t) &= -\mathrm{i}\left[H_S', \rho_S(t)\right] - \frac{1}{2}\sum_\mu K_\mu \left(\mathcal{L}_\mu^\dagger \mathcal{L}_\mu \rho_S(t) + \rho_S(t)\mathcal{L}_\mu^\dagger \mathcal{L}_\mu \right. \\ &\quad \left. -2\mathcal{L}_\mu \rho_S(t) \mathcal{L}_\mu^\dagger\right),\end{aligned} \tag{8.50}$$

where the Lindbald operators $\mathcal{L}_\mu$ are linear combinations of the system operators S_i with coefficients determined by the diagonalization of Γ. Lindbald operators do not always correspond to physically observables as S_i are not necessarily Hermitian. When $\mathcal{L}_\mu$ correspond to physically observables Eq. (8.50) can be given as

$$\frac{\mathrm{d}}{\mathrm{d}t}\rho_S(t) = -\mathrm{i}\left[H_S', \rho_S(t)\right] - \frac{1}{2}\sum_\mu K_\mu \left[\mathcal{L}_\mu, \left[\mathcal{L}_\mu, \rho_S(t)\right]\right]. \tag{8.51}$$

Lindbald master equation gives a simple way of representing the environmental monitoring of an open quantum system.

Solved Problem 3:

Show that Eq. (8.50) reduces to Eq. (8.51) if $\mathcal{L}_\mu$ operators correspond to physically observables. Show that if $[S_i, \rho_S(t)] = 0$ for all i and t then the eigenstates are not affected by decoherence.

If $\mathcal{L}_\mu$ correspond to observables then $\mathcal{L}_\mu$ must be Hermitian. Thus, $\mathcal{L}_\mu = \mathcal{L}_\mu^\dagger$. Then

$$\begin{aligned}
&\mathcal{L}_\mu^\dagger \mathcal{L}_\mu \rho_S(t) + \rho_S(t)\mathcal{L}_\mu^\dagger \mathcal{L}_\mu - 2\mathcal{L}_\mu \rho_S(t)\mathcal{L}_\mu^\dagger \\
&= \mathcal{L}_\mu \mathcal{L}_\mu \rho_S(t) + \rho_S(t)\mathcal{L}_\mu \mathcal{L}_\mu - 2\mathcal{L}_\mu \rho_S(t)\mathcal{L}_\mu \\
&= (\mathcal{L}_\mu \mathcal{L}_\mu \rho_S(t) - \mathcal{L}_\mu \rho_S(t)\mathcal{L}_\mu) - (\mathcal{L}_\mu \rho_S(t)\mathcal{L}_\mu - \rho_S(t)\mathcal{L}_\mu \mathcal{L}_\mu) \\
&= \mathcal{L}_\mu \left(\mathcal{L}_\mu \rho_S(t) - \rho_S(t)\mathcal{L}_\mu\right) - \left(\mathcal{L}_\mu \rho_S(t) - \rho_S(t)\mathcal{L}_\mu\right)\mathcal{L}_\mu \\
&= \mathcal{L}_\mu \left[\mathcal{L}_\mu, \rho_S(t)\right] - \left[\mathcal{L}_\mu, \rho_S(t)\right]\mathcal{L}_\mu \\
&= \left[\mathcal{L}_\mu, \left[\mathcal{L}_\mu, \rho_S(t)\right]\right]. \qquad (8.52)
\end{aligned}$$

Thus, Eq. (8.50) reduces to Eq. (8.51).

Next, $\mathcal{L}_\mu$ is a linear combination of S_i. As $[S_i, \rho_S(t)] = 0$ for all i and t we get $[\mathcal{L}_\mu, \rho_S] = 0$ for all t. In Eq. (8.51) the decoherence term $[\mathcal{L}_\mu, [\mathcal{L}_\mu, \rho_S(t)]] = 0$. So, the eigenstates of S_i are not affected by decoherence.

8.7 Decoherence Models

We have seen that decoherence of a quantum system arises due to its interaction with environment. Therefore, different decoherence models arise from the ways of representing the quantum systems and the environment. In many situations the physical systems can be represented by a qubit if the state space is discrete and two-dimensional. If the physical system is a particle then it can be described by continuous phase space coordinates. Environments can be modelled as a collection of harmonic oscillators or qubits. At low energies and for weak interactions the environment can be represented by one or two coordinates of the system coupled linearly to an environment of harmonic oscillator [15]. At low temperature environmental interactions arise due to paramagnetic spin, paramagnetic impurities, defects, tunnelling charges and nuclear spins. So, such environments can be represented by qubits. As spin-$\frac{1}{2}$ particle states are represented by qubits we call the models representing the environments by qubits as *spin-environment models*. Generally, there are four imporatant models [2].

8.7.1 Collisional Decoherence Model

In the *collisional decoherence model,* a massive free quantum particle scatters environmental particles. The environmental particles like photons or gas molecules are scattered by the massive quantum particles. Collisional decoherence arises as the scattered particles obtain which-path information about the quantum particle. Joos and Zeh [16] studied first the collisional decoherence models. A more rigorous derivation of the master equation was given in [17]. In these models the quantum particles do not recoil as their masses are considered to be very large compared to the masses of the environmental particles. In situations where the mass of the quantum particle is comparable to the mass of the environmental particle, the no-recoil assumption cannot be considered. For such cases more general models for collisional decoherence have been developed by introducing dissipation terms in master equations [2].

8.7.2 Quantum Brownian Model

Another extensively studied model of decoherence is knwon as *quantum Brownian* model. It considers one-dimensional motion of a particle weakly coupled to a thermal bath of

non-interacting harmonic oscillators. The environmental Hamiltonian is given by

$$H_E = \sum_i \left(\frac{1}{2m_i} p_i^2 + \frac{1}{2} m_i \omega_i^2 q_i^2 \right), \tag{8.53}$$

where q_i, p_i are the canonical position and momentum operators and m_i, ω_i are the mass and natural frequency of the ith oscillator, respectively. The interaction Hamiltonian H_I is chosen as $H_I = x \otimes \sum_i C_i q_i$, where x is the system position and C_i is the coupling of the quantum system with the ith environmental oscillator.

8.7.3 Spin-Boson Models

In the *spin-boson models,* the quantum system is represented by qubits and the environment by collision of harmonic oscillators. This model was a very important model of decoherence studies in the early years of quantum information. This model finds wide applications as many quantum systems can be represented by a two level system. In a simplified spin-boson model the system Hamiltonian is given by

$$H_S = \frac{1}{2} \hbar \omega_0 \sigma_z. \tag{8.54}$$

In the most general case a tunnelling term $\frac{1}{2}\hbar\Delta_0\sigma_x$ will be included. The environmental Hamiltonian is given by Eq. (8.53) and the interaction Hamiltonian is $H_I = \sigma_z \otimes \sum_i C_i q_i$. Then the total Hamiltonian becomes

$$H = \frac{1}{2} \hbar \omega_0 \sigma_z + \sum_i \hbar \omega_i a_i^\dagger a_i + \sigma_z \otimes \sum_i \left(g_i a_i^\dagger + g_i^* a_i \right) \tag{8.55}$$

with $[a_i, a_j^\dagger] = \delta_{ij}$. The zero-point energy part in harmonic oscillator term has been dropped. As H commutes with σ_z there will be no transition between $|0\rangle$ and $|1\rangle$ states of the quantum system. Consequently, no energy is exchanged between the system and environment. Hence, this model describes decoherence without dissipation.

8.7.4 Spin-Spin Model

The fourth important decoherence model is the *spin-spin* model in which the system qubit couples linearly with a collection of the qubits representing the environment. A basic spin-spin model was sutied in [18]. The interaction Hamiltonian with the inclusion of the tunnelling term is

$$H_I = \frac{1}{2} \hbar \Delta_0 \sigma_x + \frac{1}{2} \sigma_z \otimes \sum_{i=1}^{N} g_i \sigma_z^{(i)}. \tag{8.56}$$

The interaction Hamiltonian describes a bilinear coupling between the system and environment spins.

For the master equations, their solutions, decoherence rates and other refinements of these models one may refer to the ref. [2].

8.8 Decoherence Experiments

Though the consequences of decoherence can be experimentally observed, experimental studies of decoherence face many challenges [2]. We have to prepare first a quantum system

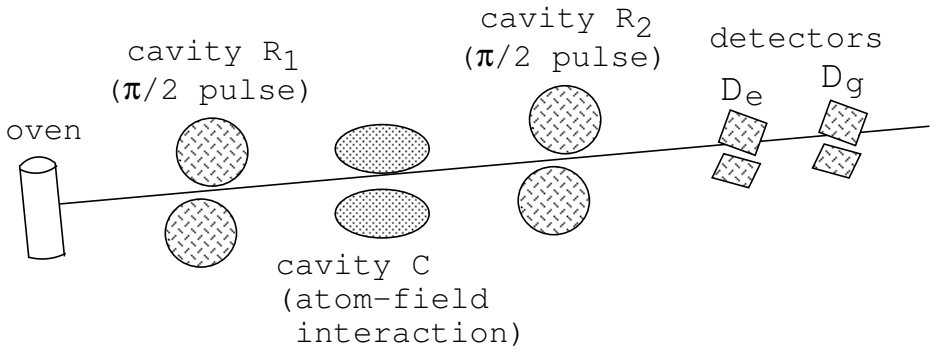

FIGURE 8.2
Schematic illustration of the cavity experiment.

in a superposition of mesoscopically or even macroscopic distinguishgable states. Next, the decoherence time must be sufficiently large so that the gradual action of decoherence can be resolved. Any monitoring of decoherence should not introduce any significant unwanted decoherence. We must be able to control the strength and form of the environmental interaction with the quantum system. Many decoherence experiments have been performed using cavity QED [19], mesoscopic molecules [20], SQUIDs and Cooper-pair boxes [21] and Bose-Einstein condensates [22].

8.8.1 Cavity QED Experiments

In cavity QED type of decoherence experiments an atom interacts with the electromagnetic field inside a cavity producing an atom-field entangled state. A measurement of atomic state then disentangles the atom-field state and produces a superposition of two coherence field states. This superposition state is monitored for decoherence over time.

In an experiment a rubidium atom in upper state $|u\rangle$ and lower state $|g\rangle$ corresponding to two circular Rydberg states was prepared [23]. It was done using a $\pi/2$ pulse in a microwave cavity R_1 at a frequency ν very close to the resonance frequency of the two energy levels. Next, the atom enters a cavity C with long damping time. It contains a radiation field of a few photons represented by the coherent state

$$|\alpha\rangle = \mathrm{e}^{-|\alpha|^2/2} \sum_{n=0}^{\infty} \frac{\alpha^4}{\sqrt{n!}} |n\rangle. \tag{8.57}$$

$|\alpha|^2$ is equal to the mean number $\bar{n}$ of photons. Figure 8.2 gives the schematic illustration of the cavity experiment [23].

The interaction between the atom and field is so tuned that there is no energy transfer between $|g\rangle$ and $|u\rangle$ states but a phase shift of χ is introduced to the coherent state $|\alpha\rangle$ as $|\mathrm{e}^{\mathrm{i}\chi}\alpha\rangle$ if the atom is in $|u\rangle$ state and a phase shift of $-\chi$ is introduced to $|\alpha\rangle$ state as $|\mathrm{e}^{-\mathrm{i}\chi}\alpha\rangle$ if the atom is in $|g\rangle$ state. So, for a superposition state of the atom $(|g\rangle + |u\rangle)/\sqrt{2}$ we get the entangled state as

$$\frac{1}{\sqrt{2}} (|g\rangle + |u\rangle) |\alpha\rangle \rightarrow \frac{1}{\sqrt{2}} \left(|g\rangle |\alpha \mathrm{e}^{-\mathrm{i}\chi}\rangle + |u\rangle |\alpha \mathrm{e}^{\mathrm{i}\chi}\rangle \right). \tag{8.58}$$

Just like R_1 cavity, R_2 cavity applies another $\pi/2$ phase which transforms $|g\rangle$ to $(|g\rangle - |u\rangle)/\sqrt{2}$ and $|e\rangle$ to $(|g\rangle + |u\rangle)/\sqrt{2}$. We then get the combined atom-field state as

$$\begin{aligned} |\psi_{\rm AF}\rangle &= \frac{1}{2}\left(|g\rangle|\alpha e^{-i\chi}\rangle - |u\rangle|\alpha e^{-i\chi}\rangle + |g\rangle|\alpha e^{i\chi}\rangle + |u\rangle|\alpha e^{i\chi}\rangle\right) \\ &= \frac{1}{2}\left(|\alpha e^{-i\chi}\rangle + |\alpha e^{i\chi}\rangle\right)|g\rangle + \frac{1}{2}\left(-|\alpha e^{-i\chi}\rangle + |\alpha e^{i\chi}\rangle\right)|u\rangle. \end{aligned} \tag{8.59}$$

Energy measurement will collapse Eq. (8.59) into either $|u\rangle$ or $|g\rangle$ destroying the entanglement between atom and photon field. If the state $|g\rangle$ ($|u\rangle$) is measured then the field will be in the superposition state $|+\rangle$ ($|-\rangle$)

$$|\pm\rangle = \frac{1}{\sqrt{2}}\left(|\alpha e^{i\chi}\rangle \pm |\alpha e^{-i\chi}\rangle\right). \tag{8.60}$$

For the two coherent states $|\alpha\rangle$ and $|\beta\rangle$ we have $|\langle\alpha|\beta\rangle|^2 = e^{-|\alpha-\beta|^2}$ (refer the solved problem 2 in chapter 4). Then the squarred magnitude of the overlap between $|\alpha e^{i\chi}\rangle$ and $|\alpha e^{-i\chi}\rangle$ is obtained as

$$|\langle\alpha e^{i\chi}|\alpha e^{-i\chi}\rangle|^2 = e^{-2|\alpha|^2(1-\cos 2\chi)} = e^{-4\bar{n}\sin^2\chi}, \quad \bar{n} = |\alpha|^2. \tag{8.61}$$

Equation (8.61) gives the *catness* of the superposition $|\pm\rangle$ and it measures the degree to which the components $|\alpha e^{i\chi}\rangle$ and $|\alpha e^{-i\chi}\rangle$ represent mesoscopically or macroscopic distinguishable states [2]. The overlap depends on χ and $\bar{n}$ and decreases exponentially with $\bar{n}$. It is minimum when $\chi = \pi/2$. In the experiment the phase-shift was found upto $\chi = 0.31\pi$ with $\bar{n} = 10$. This gives overlap $e^{-2|\alpha|^2\sin^2\chi}$ less than 3×10^{-5}.

It has also been observed that the decoherence of the field supeposition $|\pm\rangle$ left behind by sending a second rubidium atom in the cavity C. The second atom will be found in the same state ($|g\rangle$ or $|u\rangle$) provided the superposition has not been decohered. In that case the conditional detection probability P_{uu} or P_{gg} will be one. If the field has started to decohere then P_{uu} or P_{gg} will decrease, reaching the value 1/2 for complete decoherence. By sending the second atom with a time-delay τ the progressive decoherence of a superposition of the two coherence field states as a function of τ was also studied. In an another cavity-QED experiment [24] the field states inside the cavity were reconstructed at different stages of their gradual decoherence.

8.8.2 Matter-Wave Interferometry

Matter-wave interferometry experiments are based on *Talbot effect*, a diffraction effect first noticed by Henry Fox Talbot in 1836. In this effect a plane wave incident on a diffraction grating creates images of the grating at multiples of Talbot length $L_\lambda = d^2/\lambda$ behind the grating. λ is the wave length of the incident wave and d is the grating spacing. Spatial interference fringes have been demonstrated for mesoscopic molecules C_{60}, C_{70} fullerenes and for large molecular clusters [25–27]. As the molecular beams are uncollimated and incoherent the experiment set-up makes use of three gratings with grating spacing of d, placed at distances L_λ one behind the other [28]. The first grating produces transverse coherence of the molecular beam of sufficient quality for the second grating to produce a diffraction pattern on the third grating. The thrid grating can be moved perpendicular to the incident direction of the beam and scan the diffraction pattern. A laser beam ionizes the molecules coming out of the third grating and the ionized molecules are detected by an ion detector. By scanning the third grating the interference of the beam can be studied from the detector output.

Matter-wave interferometry has been used to study the important decoherences, namely, collisional decoherence and thermal decoherence. To study the collisional decoherence a background gas of adjustable pressure was introduced to interact with the molecule of the beam. Scattering of gas molecules by the molecule of the beam creates entanglement. So, the which-way information of the interfering molecular beam is performed by the gas molecule resulting in the reducing of the visibility of the fringes. An increase of the pressure of the gas increases scattering. Therefore, the visibility is found to fall with increase of pressure [29]. To study the thermal decoherence the molecules of the beam are heated using a laser beam. As the photons emitted by the heated molecules carry away which-way information the fringe visibility is reduced. As the heating power of the laser beam is increased the visibility is found to decrease [30].

8.8.3 Decoherence Studies Using SQUIDs

A SQUID consists of a ring of superconducting material in which a thin layer of an insulating barrier is introduced. Such a junction is called *Josephson junction*. Quantum mechanical tunnelling of Cooper pairs through the junction leads to a resistance-free supercurrent around the loop. The two possible direction of the supercurrent can be represented by the two basis states $\{|\circlearrowright\rangle, |\circlearrowleft\rangle\}$. By adjusting an external field the two lowest-lying energy states $|1\rangle$ and $|0\rangle$ can be represented as superposition of $|\circlearrowright\rangle$ and $|\circlearrowleft\rangle$ with equal weight as

$$|0\rangle = \frac{1}{\sqrt{2}}\left(|\circlearrowright\rangle + |\circlearrowleft\rangle\right), \quad |1\rangle = \frac{1}{\sqrt{2}}\left(|\circlearrowleft\rangle - |\circlearrowright\rangle\right). \tag{8.62}$$

The decoherence of these superposition states was measured using Ramsey interferometry [31].

Two consecutive microwave pulses are applied with a delay-time τ during which the system evolves freely. After the second pulse the relative amplitude of the superposition of $|\circlearrowright\rangle$ and $|\circlearrowleft\rangle$ exhibits an oscillatory dependence of τ. Measurement over a range of delay-time gives the occupation probabilities for $|\circlearrowright\rangle$ and $|\circlearrowright\rangle$ states as a function of τ. It is found that the envelope of the oscillation is damped due to decoherence acting on the system during the free evolution interval τ. From the decay envelope we can determine the decoherence time.

A few other systems existing and have potential to be developed for the observation of decoherence are discussed in ref. [2]. They make use of ion traps, quantum dots, mechanical quantum resonantors and Bose-Einstein condensates.

8.9 The Role of Decoherence in the Interpretation of Quantum Mechanics

It is generally claimed by many physicists that decoherence is needed to explain the measurement problem of quantum mechanics and also for explaining the emergence of classical world from quantum mechanics. We will first discuss what is meant by measurement problem in quantum mechanics.

8.9.1 The Measurement Problem of Quantum Mechanics

Schrödinger equation describes the linear, unitary, deterministic evolution of the state function $|\psi\rangle$. $|\psi\rangle$ is a vector in Hilbert space. The Hilbert space is spanned by eigenvectors of

the Hamiltonian operator. For example, for a spin-$\frac{1}{2}$ particle we have a two-dimensional Hilbert space with spin-up $|1\rangle$ and spin-down $|0\rangle$ states spanning the Hilbert space. As the Schrödinger equation is a linear equation a general state of the particle $|\psi\rangle$ is written as a superposition state as $|\psi\rangle = \alpha|1\rangle + \beta|0\rangle$, where $|\alpha|^2 + |\beta|^2 = 1$ and $\langle\psi|\psi\rangle = 1$. For any quantum mechanical system with N eigenfuctions $\{|\phi_i\rangle\}$ of an observable we can write $|\psi\rangle = \sum_i a_i|\phi_i\rangle$.

All observable quantities are represented by self-adjoint operators. In the conventional interpretation of quantum mechanics, the possible outcomes of a measurement of some observables are the eigenvalues of the operators. If $O|\phi_i\rangle = \gamma_i|\phi_i\rangle$ for an operator O then the measurement of O will gives

$$\begin{aligned}\langle\psi|O|\psi\rangle &= \sum_i \sum_j a_j^* a_i \langle\phi_j|O|\phi_i\rangle \\ &= \sum_i \sum_j a_j^* a_i \gamma_i \langle\phi_j|\phi_i\rangle \\ &= \sum_i \sum_j a_j^* a_i \gamma_i \delta_{ij} \\ &= \sum_i |a_i|^2 \gamma_i. \end{aligned} \tag{8.63}$$

Since $|a_i|^2$ gives the probability of getting γ_i we find that the measurement will give any one of the eigenvalues γ_i of the operators with a probability $|a_i|^2$. This is called the *Born probability rule*. According to this rule when a measurement is made the wave function $|\psi\rangle$ is projected to one of its bases vector $|\phi_i\rangle$ corresponding to the actual measurement outcomes γ_i. Before the measurement $|\psi\rangle$ evolves unitarily and deterministically according to the Schrödinger equation. When a measurement is done, it collapses to one of its bases vectors stochastically. This is essentially the measurement problem of quantum mechanics: the question of how to reconcile the linear and deterministic evolution described by the Schrödinger equation with our observation of the occurrence of random measurement outcomes [2].

8.9.2 Explanation of Problematic Differences in the Classical and Quantum Measurements

In the *Schrödinger cat* thought experiment Born interpretation says that the death or survival of the cat happened instantaneously at the moment the box was opened and the measurement was made. But classically the radioactive source would have emitted a particle any time before opening of the box, broken the poison bottle and killed the cat. This explains why there are problematic differences in information that we get from classical measurements and quantum measurements. In short, one can say that the measurement problem arises due to the superposition of wave function in quantum mechanics and no such superposition is observed in classical situations. The superposition in quantum mechanics leads to interference terms which are absent in classical states.

8.9.3 Can the Decoherence Theory Solve the Measurement Problem?

As decoherence suppresses the interference terms it was believed that decoherence can solve the measurement problem of quantum mechanics. But Süssmann [32] explained the formal distinction between decoherence and wave function collapse. Decoherence is a statistical concept involving the transition from a pure state to a mixture state and the disappear-

ance of the interference terms. A collapse refers to transition from a pure state to another pure state. It has been argued [2,9] that decoherence is not tied to any interpretation of quantum mechanics. Decoherence theory relies on reduced density matrix whose formalism and interpretation are based on the collapse postulates and Born's rule. So, decoherence theory cannot solve the measurement problem. However, certain interpretations of quantum mechanics are in need of decoherence for defining their structure.

8.9.4 Emergence of Classical World From Quantum Systems

Next, we will discuss how decoherence can explain emergence of classical world from quantum systems. Generally, the microscopic systems are consiered as quantum systems and macroscopic objects obey classical laws. To distinguish quantum and classical systems based on their size is not correct as there are many macroscopic quantum phenomena like superconductivity, superfluidity, quantum Hall effect, polaritons, nonclassical squeezed states of suitably prepared electromagnetic fields with macroscopic number of photons, Bose-Einstein condensates etc. We can find the correspondence of quantum mechanics to classical mechanics through Hamilton–Jacobi equation, Ehrenfest's principle, the similarity of quantum commutators to Poisson brackets. Still it is quite not clear how does a quantum system described by a vector in Hilbert space goes into a classical system described in phase space. A classical system is specified by giving values to some small set of numbers such as position, momentum, mass, charge, energy etc. Quantum mechanically the system is described by a vector in Hilbert space which will be a superposition of eigenfunctions of an observable. In quantum mechanics superposition of states lead to interference terms. As no such superposition state exists in classical system no interference can be observed for classical particles.

Studies of decoherence in [33,34] consider the emergence of classicality from a quantum world. We have seen that decoherence theory describes interaction between a quantum system and its environment which leads to the superposition of quantum interference. Thus, decoherence is regarded as an indirect measurement process that creates a set of *pointer states* which are eigenstates of the observable of the measuring instrument and they represent the possible positions of the display pointer of the instrument. These pointer states don't show any interference. So, decoherence can be considered to explain how classicality emerges from a quantum world.

8.9.5 Quantum Darwinism

Quantum Darwinism is an idea put forwarded by Wojciech Hubert Zurek [35]. It describes the transition from the quantum to classical world using a quantum process in which only certain states are chosen in the interaction of the quantum system with environment as they survive better than others in a particular environment. We can observe on macroscopic scale only those quantum states which are able to survive interaction with the environment. In quantum Darwinism the quantum system with a vast number of potential superposition states evolves into some final states, pointer states [36] via a selective process performed on the system through continuous interaction with the environment. Pointer states can be observed classically. One of the drawbacks of quantum Darwinism is that it does not answer to the question of what the physical process repsonsible for the transition from quantum to classical possible.

8.10 Concluding Remarks

The wave function $|\psi\rangle$ is written as a superposition of basis states in Hilbert space. The probability density defined as $|\psi|^2$ has interference terms in addition to the classical probability density terms. Therefore, we say that the wave function is in a coherent superposition. Decoherence arises due to the interaction of the quantum system with the environment. Vanishing of interference term due to decoherence leads to classical probabilities. We have given a few examples where the interactions with environments make the interference terms vanishing.

A consequence of decoherence is that a quantum system looses its quantum behaviour due to its interaction with an environment. Interaction leads to transfer of information from the system to the environment. After the interaction coherence of the superposed state is lost. Interaction makes the system and environment entangled joint state which can no longer be separable. Decoherence problems are treated mathematically using master equations which describe the time evolution of reduced density matrix. We have discussed Born-Markov master equations and Lindblad master equations. They are used to study many realistic models of decoherence processess. A few experimental stuides on the action of decoherence in a realistic interaction of quantum system with an environment have been discussed.

A brief account of the role of decoherence in the interpretation of quantum mechanics has been given. Decoherence plays significant roles in explaining the quantum measurement problem and the transition to quantum state to classical state. However, it cannot completely explain them. Study of decoherence phenomenon is very important for the field of quantum information processing. Decoherence has to be minimized to perform quantum computation. Controlled decoherence can do quantum error correction in a quantum communication channel.

8.11 Bibliography

[1] E. Schrödinger, *Naturwissenschaften* 23:807, 1935.

[2] M. Schlosshauer, *Phys. Rep.* 831:1, 2019.

[3] J.K. Gample and J.F. Lindner, *Am. J. Phys.* 77:244, 2009.

[4] W.H. Zurek, *Phys. Today* 44:36, 1991.

[5] L. Lerner, *Am. J. Phys.* 85:870, 2017.

[6] K. Blum, *Density Matrix Theory and Applications*. Plenum, New York, 1981.

[7] F. Haake, *Tra. Mod. Phys.* 66:98, 1973.

[8] R. Omnes, *Phys. Rev. A* 56:3383, 1997.

[9] M. Schlosshauer, *Decoherence and the Quantum-to-Classical Transition*. Springer, Berlin, 2007.

[10] H.P. Breuer and F. Petruccione, *The Theory of Open Quantum Systems*. Oxford University Press, Oxford, 2002.

[11] F. Benatti and R. Floreanini, *Int. J. Mod. Phys. B* 19:3063, 2005.

[12] V. Gorini, A. Kossalowski and E.C.G. Sudarshan, *J. Math. Phys.* 17:821, 1976.

[13] G. Lindblad, *Commun. Math. Phys.* 48:119, 1976.

[14] V. Gorini, A. Frigerio, M. Verri, A. Kossakowski and E.C.G. Sudasrshan, *Rep. Math. Phys.* 13:149, 1978.

[15] A. Caldeira and A. Leggett, *Ann. Phys. New York* 149:374, 1983.

[16] E. Joos and H.D. Zeh, *Z. Phys. B.* 59:223, 1985.

[17] H. Hornberger and J.E. Sipe, *Phys. Rev. A* 68:012105, 2003.

[18] W.H. Zurek, *Phys. Rev. D* 26:1862, 1982.

[19] J.M. Raimond, M. Brune and S. Haroche, *Rev. Mod. Phys.* 73:565, 2001.

[20] M. Arndt, K. Hornberger and A. Zeilinger, *Phys. World* 18:35, 2005.

[21] A.J. Leggett, *J. Phys.: Condens. Matter* 14:R415, 2002.

[22] R. Kaiser, C. Westbrook and F. David (eds.) *Coherent Atomic Matter Waves*. Springer, Berlin, 2001.

[23] M. Brune, E. Hagley, J. Dreyer, X. Maître, A. Maali, C. Wunderlich, J.M. Raimond and S. Haroche, *Phys. Rev. Lett.* 77:4887, 1996.

[24] S. Deleglise, I. Dotsenko, C. Sayrin, J. Bernu, M. Brune and J.M. Raimond, *Nature* 455:510, 2008.

[25] M. Arndt, O. Nairz, J. Vos-Andreae, C. Keller , G. van der Zouw and A. Zeilinger, *Nature* 401:680, 1999.

[26] K. Hornberger, S. Gerlich, P. Haslinger, S. Nimmrichter and M. Arndt *Rev. Mod. Phys.* 84:157, 2012.

[27] S. Gerlich, S. Eibenberger, M. Tomandl, S. Nimmrichter, K. Hornberger, P.J. Fagan, J. Tuxen, M. Mayor and M. Arndt, *Nat. Commun.* 2:263, 2012.

[28] B. Brezger, L. Hackermuller, S. Uttenthaler, J. Petschinka, M. Arndt and A. Zeilinger, *Phys. Rev. Lett.* 88:100404, 2002.

[29] L. Hackermuller, L. Hornberger, B. Brezger, A. Zeilinger and M. Arndt, *Appl. Phys. B* 77:781, 2003.

[30] L. Hackermuller, L. Hornberger, B. Brezger, A. Zeilinger and M. Arndt, *Nature* 427:711, 2004.

[31] I. Chiorescu, Y. Nakamura, C.J.P.M. Harmans and J.E. Mooij, *Science* 21:1869, 2003.

[32] G. Süssmann, *An Analysis of Measurements*. In Observation and Interpretation in the Philosophy of Physics. S. Korner (Ed.). Dover Publications, New York, 1962. pp.131-136.

[33] H.D. Zeb, *Found. Phys.* 1:69, 1970.

[34] W.H. Zurek, *Rev. Mod. Phys.* 75:715, 2003.

[35] W.H. Zurek, *Nature Phys.* 5:543, 2009.

[36] R. Blume-Kohout and W.H. Zurek, *Phys. Rev. A* 73:062310, 2006.

[37] J. Gross, Decoherence: An explanation of quantum measurement, preprint, 2012; https://web.mit.edu/∼jgross/Public/8_06-decoherence-paper.pdf.

8.12 Exercises

8.1 Obtain the reduced density matrix ρ_S given that $\rho_S = \mathrm{Tr}_E\,(\rho_{SE}) = \mathrm{Tr}_E|\psi\rangle\langle\psi|$.

8.2 Prove that $r_x^2 + r_y^2 + r_z^2 = 1$.

8.3 Show that any arbitrary 2×2 matrix can be written as a linear combination of I, σ_x, σ_y and σ_z matrices.

8.4 Show that

$$\int_{-\infty}^{\infty} \phi^*(y)\phi(2X - 2Y + y)\mathrm{d}y = \int_{-\infty}^{\infty} \bar{\phi}^*(p)\mathrm{e}^{2\mathrm{i}(X-Y)p/\hbar}\bar{\phi}(p)\mathrm{d}p,$$

where $\bar{\phi}(p)$ is the momentum wave function which is the Fourier transform of $\phi(x)$.

8.5 Show that $\langle A\rangle = \mathrm{Tr}(\rho A)$.

8.6 Given the pure spin-$\frac{1}{2}$ state of an atom at time $t = 0$ consider an interaction energy of the atom in a magnetic field $= \mu_z B_z = \gamma B_z S_z$, where $S_z = \pm\hbar/2$. Find $|\psi(t)\rangle$ and the correponding $\rho(t)$.

8.7 Prove that the unitary operator $U(t, t_0)$ which transforms $|\psi(0)\rangle$ to $|\psi(t)\rangle$ is given by (with $\hbar = 1$) $U(t, t_0) = \mathrm{e}^{-\mathrm{i}H(t-t_0)}$ if H is independent of time. Hence, obtain the Liouville–von Neumann equation.

8.8 Consider a decoherence model in which the environment monitors the position of a system in one-dimension with $\mathcal{L} = x$ and the free particle Hamiltonian $H'_S = H_S = \frac{1}{2m}p^2$. Obtain the Lindblad master equation. Also, find its form in position representation.

8.9 For the random collision of environmental systems on a quantum particles the master equation can be approximated as

$$\frac{\partial}{\partial t}\rho_S(x, x', t) \approx -2(x - x')^2\frac{\gamma m_S kT}{\hbar^2}\rho_S(x, x', t),$$

where γ is related to the collision rate Γ as $\gamma = \Gamma m_E/m_S$, m_E and m_S are the masses of the environmental and system particles. The wave function for the ground state of harmonic oscillator is given by

$$|\psi(x)\rangle = \left(\frac{m_S\omega}{\pi\hbar}\right)^{1/4}\mathrm{e}^{-m_S\omega x^2/(2\hbar)}.$$

Find $\rho(x, x')$. Obtain the solution of the master equation and show that the off-diagonal terms in the density matrix $\rho_S(x, x', t)$ decays exponentially whereas the diagonal elements do not decay.

8.10 Assume that an environment has N bits or spins with the initial state $\alpha_i|0\rangle + \beta_i|1\rangle$ and each coupled to the measuring instrument by the coupling coefficient g_i. If the time-dependence of the interference term is

$$r(t) = \prod_{i=1}^{N}\left(|\alpha_i|^2\mathrm{e}^{2\mathrm{i}g_i t/\hbar} + |\beta_i|^2\mathrm{e}^{-2\mathrm{i}g_i t/\hbar}\right)$$

determine how quickly $r(t)$ drops-off to zero [37].

9

Quantum Computers

9.1 Introduction

Present day computers perform computations using two-state binary logic. They led to an amazing revolution in data manipulation and processing. The components of a computer are subject to various laws of physics. *What will happen if the components of a computer become very small such that they are subjected to the principles of quantum mechanics?* Alternatively, can a real quantum system be used to build a computer functioning in the quantum mechanical regime? This is one of the major issues in quantum computing. The name *quantum computing* refers to calculations using logic based on the probability amplitude concept.

Classical computers of the present decade are able to answer one question at a time. In contrast a quantum computer will have the ability to carry out more than one problem simultaneously. Essentially, quantum computers manipulate quantum states instead of classical bits. In a quantum computer the eigenstates of, for example, a two-level system are renamed 0 and 1. Now, the two level quantum system becomes a qubit (that is, quantum binary digit) [1–4]. The concept of the quantum computer was introduced first by Paul Anthony Benioff (1980) [5]. Richard Feynman [6,7] contributed to the early development of quantum computation. The first paper on quantum computing was published by David Deutsch [8] in the year 1985.

During the past one decade or so, many quantum algorithms have emerged. Among them the most remarkable successes of quantum computation are Shor's efficient algorithms for integer factorization and the computation of discrete logarithms [9,10]. Peter Williston Shor has shown that quantum computers would solve the problem of finding discrete logarithms (mod N). He predicted that a quantum computer can perform prime factoring in polynomial time: $t \propto k^p$, where p is a constant and k is the number of bits in the number to be factored. For this problem a classical computer is believed to take $e^{ck^{1/3}}$ time, where c is a constant. Shor's breakthrough created an avalanche of research activity in quantum computation and quantum information theory. In addition to Shor's factorization algorithm, Deutsch–(Richard)Jozsa algorithm [8,11] and Lov Kumar Grover's rapid search algorithm [12] are capable of performing certain computational tasks exponentially faster compared to their classical counterparts. In the present chapter, we discuss the basic aspects of quantum computing.

9.2 What is a Quantum Computer?

In a classical information theory 'bit' is an indivisible unit. It takes the values such as yes or no, true or false or simply 0 or 1. A sequence of bits is used to represent classical information.

DOI: 10.1201/9781003172192-9

TABLE 9.1
Examples of two-state quantum systems. Here $|V\rangle$, $|H\rangle$, $|L\rangle$ and $|R\rangle$ represent vertical, horizontal, left-circular and right-circular polarizations, respectively. $|+\rangle$ and $|-\rangle$ denote spin-up and spin-down, respectively. $|E_0\rangle$ and $|E_1\rangle$ represent ground and excited states, respectively.

S.No.	$\|0\rangle$	$\|1\rangle$	Qubit
1.	$\|V\rangle$	$\|H\rangle$	Photon – Linear polarization
2.	$\|L\rangle$	$\|R\rangle$	Photon – Circular polarization
3.	$\|+\rangle$	$\|-\rangle$	Electron, nucleus – Spin
4.	$\|E_0\rangle$	$\|E_1\rangle$	Atoms, quantum dots – Energy levels

In a classical computer, logical gates are employed to evaluate Boolean functions of a set of input bits.

9.2.1 Qubits

Quantum information can be represented by the elementary units called *quantum bits* abbreviated as *qubits* or *qbits*. A qubit is two levels of a quantum system (like the spin of an electron). For example, spin-up, $|\uparrow\rangle$, represents 1 (true) and spin-down, $|\downarrow\rangle$, represents 0 (false). Note that $|\uparrow\rangle$ to $|\downarrow\rangle$ can be achieved by a magnetic field and dissipates no heat. All information can be encoded into a sequence of qubits. In principle, any two-state system can be used as a quantum bit. Some examples are presented in table 9.1.

What is the difference between a classical bit and a qubit? A qubit can be in a state other than $|0\rangle$ and $|1\rangle$. It is possible to form a combination of states called *superposition states* given by $|\psi\rangle = \alpha|0\rangle + \beta|1\rangle$. Denoting $|0\rangle = \begin{bmatrix} 1 \\ 0 \end{bmatrix}$ and $|1\rangle = \begin{bmatrix} 0 \\ 1 \end{bmatrix}$ the quantum state $|\psi\rangle$ is written in vector notation as $\begin{bmatrix} \alpha \\ \beta \end{bmatrix}$. For example, we can represent the spin of an electron in the horizontal direction as the sum of the up and down states. When we measure a qubit, the result will be either 0 with probability $|\alpha|^2$ or 1 with probability $|\beta|^2$. Hence, $|\alpha|^2 + |\beta|^2 = 1$. A classical bit has either 0 state or 1 state whereas a qubit can exist between $|0\rangle$ and $|1\rangle$ until it is observed.

$|\psi_1\rangle \otimes |\psi_2\rangle$ denotes tensor product of $|\psi_1\rangle$ and $|\psi_2\rangle$. If $|\psi_1\rangle = \begin{bmatrix} 1 \\ 2\mathrm{i} \end{bmatrix}$ and $|\psi_2\rangle = \begin{bmatrix} 2 \\ 3 \end{bmatrix}$ then

$$|\psi_1\rangle \otimes |\psi_2\rangle = \begin{bmatrix} 1 \\ 2\mathrm{i} \end{bmatrix} \otimes \begin{bmatrix} 2 \\ 3 \end{bmatrix} = \begin{bmatrix} 1 \times 2 \\ 1 \times 3 \\ 2\mathrm{i} \times 2 \\ 2\mathrm{i} \times 3 \end{bmatrix} = \begin{bmatrix} 2 \\ 3 \\ 4\mathrm{i} \\ 6\mathrm{i} \end{bmatrix}. \tag{9.1}$$

If $|\psi_1\rangle = a|0\rangle + b|1\rangle$ and $|\psi_2\rangle = c|0\rangle + d|1\rangle$ then

$$\begin{aligned} |\psi_1\rangle \otimes |\psi_2\rangle &= |\psi_1\psi_2\rangle \\ &= ac|0\rangle|0\rangle + ad|0\rangle|1\rangle + bc|1\rangle|0\rangle + bd|1\rangle|1\rangle \\ &= ac|00\rangle + ad|01\rangle + bc|10\rangle + bd|11\rangle. \end{aligned} \tag{9.2}$$

Multiple bits have more states. With two classical bits 0 and 1 there are four possible states 00, 01, 10, 11. But a general two qubit system is

$$|\psi\rangle = \alpha_{00}|00\rangle + \alpha_{01}|01\rangle + \alpha_{10}|10\rangle + \alpha_{11}|11\rangle \tag{9.3}$$

with $\sum |\alpha_x|^2 = 1$, where $x = 00, 01, 10, 11$.

As infinite range of values of α and β are possible with $|\alpha|^2 + |\beta|^2 = 1$, in principle a qubit can store an infinite amount of data. But this is misleading because a measurement of the qubit changes its state to yield either 0 or 1. Measurement collapses the state of qubit from the superposition of $|0\rangle$ and $|1\rangle$ to $|0\rangle$ with a probability $|\alpha|^2$ or $|1\rangle$ with probability $|\beta|^2$. So, from a measurement we can obtain only a single bit of information about the qubit's state. Only if infinitely many identical qubits are prepared and then measurements are performed we can determine α and β. As no quantum state can be copied because such an act will lead to the collapse of the superposition state into one of its constituent state, it is impossible to set-up identical states. Hence, in principle, it is impossible to find α and β exactly. The information contained in a qubit is enormous if we do not measure it. That is, nature conceals a great deal of information. This hidden quantum information falls at the center of what makes quantum mechanics a powerful modern emerging tool for information processing.

Solved Problem 1:

Write the Pauli matrices σ_x, σ_y and σ_z in operator form and state their effect on a qubit.

Defining $|0\rangle = \begin{pmatrix} 1 \\ 0 \end{pmatrix}$ and $\langle 0| = \begin{pmatrix} 1 & 0 \end{pmatrix}$ one can find $|0\rangle\langle 0|$ as

$$|0\rangle\langle 0| = \begin{pmatrix} 1 \\ 0 \end{pmatrix} \begin{pmatrix} 1 & 0 \end{pmatrix} = \begin{pmatrix} 1 & 0 \\ 0 & 0 \end{pmatrix}. \tag{9.4}$$

Then

$$\sigma_x = \begin{pmatrix} 0 & 1 \\ 1 & 0 \end{pmatrix} = |0\rangle\langle 1| + |1\rangle\langle 0|, \tag{9.5}$$

$$\sigma_y = \begin{pmatrix} 0 & -\mathrm{i} \\ \mathrm{i} & 0 \end{pmatrix} = -\mathrm{i}|0\rangle\langle 1| + \mathrm{i}|1\rangle\langle 0|, \tag{9.6}$$

$$\sigma_z = \begin{pmatrix} 1 & 0 \\ 0 & -1 \end{pmatrix} = |0\rangle\langle 0| - |1\rangle\langle 1|. \tag{9.7}$$

The action of the Pauli matrices σ_x and σ_z on a qubit is

$$\sigma_x|0\rangle = \begin{pmatrix} 0 & 1 \\ 1 & 0 \end{pmatrix} \begin{pmatrix} 1 \\ 0 \end{pmatrix} = |1\rangle, \quad \sigma_x|1\rangle = |0\rangle, \tag{9.8}$$

$$\sigma_z|0\rangle = |0\rangle, \quad \sigma_z|1\rangle = -|1\rangle. \tag{9.9}$$

We note that σ_x gives rise to bit flip while σ_z causes phase flip. *What is the effect of σ_y?*

9.2.2 Quantum Gates

An elementary quantum logic gate is a unitary transformation. A quantum gate acts on a qubit or pair of qubits. Quantum gates are represented by matrices or operators. Any unitary matrix can specify a valid gate. We can represent them in Dirac notation also. In

quantum computers a unitary transformation is applied to a given initial state of a set of qubits through several quantum gates. The final outcome of a quantum computation is contained in the final state of the qubits.

There are certain major differences between classical and quantum gates.

1. Fan-in[1] is not possible in quantum circuits.
2. In classical circuits wires are joined together to form a single wire. In quantum circuits this irreversible operation is not possible.
3. Fan-out[2] is also not possible. That is, making a number of copies of a bit is not possible.
4. Quantum gates do not permit feedback loops from one part of the circuit to another part.

9.2.3 Quantum Computer

Quantum computation is defined as an arbitrary transformation on a Hilbert space spanned by the complete set of all possible states of bits. The difference between quantum computers and a system of interacting spins is that the computation must be modular, each logical operation considers only a few spins. Essentially, quantum computers will perform computations at the atomic scale.

In a quantum computer, the execution of a program can be thought of as a dynamical process and is governed by the Schrödinger equation. Consequently, a state vector ψ is used to describe the state of the computer. Here ψ is a linear superposition of all the binary states of the bits $x_m \in \{0, 1\}$:

$$\psi(t) = \sum_{x_m \in \{0,1\}} \alpha_x \left| x_1, x_2, \ldots, x_m \right\rangle , \quad \sum_x |\alpha_x|^2 = 1 . \tag{9.10}$$

The time evolution of the state is governed by a unitary operator U on a vector space.

9.3 Why is a Quantum Computer?

Anything a quantum computer can perform can also be done in a classical computer. Then, *why should one think of a quantum computer?* In the following we list some of the difficulties with classical computers and the advantages of quantum computers.

1. A quantum computer is very efficient over a classical computer.

   Example 1:

   Consider a quantum state of a modest number of qubits, for example 100 lines in a Hilbert space of dimensions $2^{100} \sim 10^{30}$. To perform a computation a classical computer has to work with matrices of exponentially large size and this would take a very long time.

[1] A term defining the maximum number of digital inputs allowed by a logic gate.
[2] It defines the maximum number of digital inputs that the output of logic gates can feed.

Example 2:

A single computation acting on say, 300 qubits can achieve the same effect as 2^{300} computations acting simultaneously on classical bits.

Example 3:

To factor a 400 digit number, a powerful workstation would require about 10 years. But a quantum computer could complete the same task in just a few minutes.

2. There are a number of problems for which the underlying process can be speeded-up tremendously through quantum algorithms. Consider a number N of L digits so that $N \approx 10^L$. To determine its factors, in the least case, it is required to divide N by numbers up to $\sqrt{N}$. That is $\sqrt{N} \sim 10^{L/2}$ operations are essential. Hence, the number of operations would increase with L exponentially. The best known classical algorithm requires $s = Ae^{1.9L^{1/3}(\log L)^{2/3}}$ (A is a constant) number of operations for factorizing an L digit number. Therefore, it is not considered an efficient algorithm. To factorize a 130 digit number at the rate of $\sim 10^{12}$ operations per second, a classical computer would require ~ 42 days. It would require ~ 10 years for a 400 digit number. However, a quantum algorithm of Peter Williston Shor requires time $\propto L^3$.
3. Computations cannot be reversible in a classical computer (why can't a computer run backwards?). In quantum theory, reverse time evolution is specified by the unitary operator $U^{-1} = U^\dagger$. A consequence of this is that computations can be reversible in a quantum computer.
4. Calculations in a classical computer lead to dissipation in order to damp out an attempt by the system to make a transition. In contrast, in a quantum computer dissipation cannot be used and further the accuracy of a computation is built-in.
5. In a classical computer errors in the initial data may grow exponentially with the number of steps involved. This is because, the classical dynamics involves the symplectic group that is noncompact. In quantum mechanics, inaccuracies in the initial data do not grow. This is because it uses the compact unitary group.

9.4 Fundamental Properties

In the following we discuss the fundamental properties of quantum systems that are relevant to information processing.

9.4.1 Software, Hardware and CPU [1,13]

Superposition:

A quantum computer can exist in an arbitrary linear combination of classical Boolean states. These states evolve in parallel as per a unitary transformation.

Interference:

Parallel computation paths in the superposition, like a particle's path through an interferometer, can cancel one another or reinforce depending on their relative phase.

Entanglement:

Certain states of a complete quantum system do not form definite states of its parts. For more details see chapter 7.

Nonlocality and uncertainty:

An unknown quantum state cannot be copied (cloned) accurately. It cannot be observed without being disturbed.

A quantum computer has a register with n qubits. A qubit has 0 and 1 classical states so that the register has 2^n classical states. The state of a quantum computer is described by a 2^n-dimensional vector, $\mathbf{x}$, indexed by $i = 000\ldots00, 000\ldots01, 000\ldots10, \ldots, 111\ldots11$ in binary notation. Moreover,

$$||\mathbf{x}||^2 = \sqrt{\sum_j |x_j|^2} = 1 \tag{9.11}$$

and $|x_j|^2$ is the probability that the register is in state j. We call $\mathbf{x}$ the wave function (ψ) of the register.

In a quantum computer, the software is represented by ψ and the hardware by a Hamiltonian. The Hamiltonian describes the dynamics of the central processing unit (CPU). The hardware generates a unitary evolution of $\psi(t)$ representing the state of the software at time t. The software is a finite string of bits with a logical meaning. It includes the inputs (such as programs and data), the output and a scratch pad necessary to store intermediate results. The states, for example, $|\downarrow\rangle$ and $|\uparrow\rangle$ represent a bit with logical values 0 and 1, respectively.

9.4.2 Two-Bit Gates for Universal Computation

In a classical computer logic gates are used to process information. David Deutsch has shown a way to obtain a universal quantum computation. Tommaso Toffoli [14] showed how the AND and XOR gates can be implemented reversibly. Recall that conventional AND and XOR gates are not reversible because a reversible gate must contain the same number of input and output bits. However, XOR can be implemented reversibly with a two-bit gate where one output bit may return the conventional XOR. $\oplus$ is used to denote for the exclusive-or operation. $a_1 \oplus a_2$ (a_1 and a_2 are the binary values of the two input bits) is given by a one output bit, while the second output bit returns the original value of a_1 (or a_2). To implement AND reversibly, a three-bit gate is used, where a_1 and a_2 are passed through unchanged and the third bit is XORed with the AND of the first two, returning $(a_1 \cdot a_2) \oplus a_3$. Because this three-bit gate has both the XOR and the AND functions, it can be considered as a universal reversible gate. This gate is called *Toffoli gate*.

9.4.3 NOT, Z and Hadamard Gates

A simple classical gate is the NOT gate (swap gate) that changes 0 to 1 and 1 to 0. An analogous quantum NOT gate transforms states in a particular basis into states orthogonal to them. The unitary operation U_{NOT} is given by

$$U_{\mathrm{NOT}}|0\rangle = |1\rangle\,, \quad U_{\mathrm{NOT}}|1\rangle = |0\rangle\,. \tag{9.12}$$

TABLE 9.2
The truth table of the quantum NOT gate.

Input	Output
$\|0\rangle$	$\|1\rangle$
$\|1\rangle$	$\|0\rangle$
$\alpha\|0\rangle + \beta\|1\rangle$	$\alpha\|1\rangle + \beta\|0\rangle$

TABLE 9.3
The truth table of the quantum Z gate.

Input	Output	Input	Output	Input	Output
$\|0\rangle$	$\|0\rangle$	$\|1\rangle$	$-\|1\rangle$	$\alpha\|0\rangle + \beta\|1\rangle$	$\alpha\|0\rangle - \beta\|1\rangle$

Unlike the digital gates, the quantum gates are assumed to act on superposition states. The $U_{\rm NOT}$ provides the transformation

$$U_{\rm NOT}(\alpha|0\rangle + \beta|1\rangle) = \alpha|1\rangle + \beta|0\rangle\,. \tag{9.13}$$

Here α and β are the amplitudes of the states. If we represent $|0\rangle$ and $|1\rangle$ in column matrix then the output of the NOT gate is

$$X\begin{pmatrix}\alpha\\ \beta\end{pmatrix} = \begin{pmatrix}0 & 1\\ 1 & 0\end{pmatrix}\begin{pmatrix}\alpha\\ \beta\end{pmatrix} = \begin{pmatrix}\beta\\ \alpha\end{pmatrix}\,. \tag{9.14}$$

The truth table of the quantum NOT gate is given in the table 9.2.

In classical gates, the NOT gate is the only nontrivial single-bit gate. In quantum mechanics there are many nontrivial qubit gates with $|\alpha|^2 + |\beta|^2 = 1$. Examples are the Z gate and Hadamard (H) gate. They are given by

$$Z = \begin{pmatrix}1 & 0\\ 0 & -1\end{pmatrix}, \quad H = \frac{1}{\sqrt{2}}\begin{pmatrix}1 & 1\\ 1 & -1\end{pmatrix}. \tag{9.15}$$

These gates are very useful. The truth table of Z gate and the Hadamard gate are given in tables 9.3 and 9.4, respectively. These gates are represented pictorially as shown in Fig. 9.1. Consider the Hadamard transformation given by

$$H = \frac{1}{\sqrt{2}}\begin{pmatrix}1 & 1\\ 1 & -1\end{pmatrix}, \quad H\begin{pmatrix}1\\ 0\end{pmatrix} = \frac{1}{\sqrt{2}}\begin{pmatrix}1\\ 1\end{pmatrix} = \frac{1}{\sqrt{2}}(|0\rangle + |1\rangle), \tag{9.16a}$$

$$H\begin{pmatrix}0\\ 1\end{pmatrix} = \frac{1}{\sqrt{2}}\begin{pmatrix}1\\ -1\end{pmatrix} = \frac{1}{\sqrt{2}}(|0\rangle - |1\rangle). \tag{9.16b}$$

It acts on a single qubit. Its effect is to rotate the state about the y-axis.

Interestingly, there are infinitely many 2×2 unitary matrices and so infinitely many qubit gates. Remember that the classical NOT gate is the single one-bit. Any single qubit unitary gate can be decomposed as

$$\begin{aligned} U \;=\; & e^{i\alpha}\begin{bmatrix} e^{-i\beta/2} & 0\\ 0 & e^{i\beta/2}\end{bmatrix}\begin{bmatrix} \cos(\gamma/2) & -\sin(\gamma/2)\\ \sin(\gamma/2) & \cos(\gamma/2)\end{bmatrix}\\ & \times\begin{bmatrix} e^{-i\delta/2} & 0\\ 0 & e^{i\delta/2}\end{bmatrix}, \end{aligned} \tag{9.17}$$

where α, β, γ and δ are real numbers. In fact, one can build-up a qubit gate using a finite set of quantum gates called *universal gates*.

TABLE 9.4
The truth table of the Hadamard gate.

Input	Output	Input	Output
$\|0\rangle$	$\frac{1}{\sqrt{2}}(\|0\rangle + \|1\rangle)$	$\|1\rangle$	$\frac{1}{\sqrt{2}}(\|0\rangle - \|1\rangle)$
$\frac{1}{\sqrt{2}}(\|0\rangle + \|1\rangle)$	$\|0\rangle$	$\frac{1}{\sqrt{2}}(\|0\rangle - \|1\rangle)$	$\|1\rangle$
$\alpha\|0\rangle + \beta\|1\rangle$	$\frac{1}{\sqrt{2}}(\alpha+\beta)\|1\rangle$ $+\frac{1}{\sqrt{2}}(\alpha-\beta)\|1\rangle$		

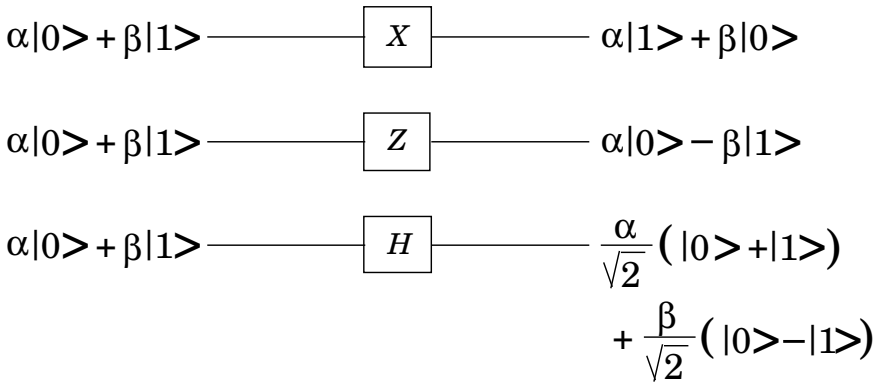

FIGURE 9.1
Qubit logic gates.

Solved Problem 2:

If X, H and Z denote the quantum NOT, Hadamard and Z gates, respectively, show that $HXH = Z$.

We obtain

$$\begin{aligned} HXH &= \frac{1}{\sqrt{2}}\begin{pmatrix} 1 & 1 \\ 1 & -1 \end{pmatrix}\begin{pmatrix} 0 & 1 \\ 1 & 0 \end{pmatrix}\frac{1}{\sqrt{2}}\begin{pmatrix} 1 & 1 \\ 1 & -1 \end{pmatrix} \\ &= \begin{pmatrix} 1 & 0 \\ 0 & -1 \end{pmatrix} \\ &= Z. \end{aligned} \tag{9.18}$$

9.4.4 CNOT (XOR) and Toffoli Gates

CNOT stands for controlled NOT. It is a two qubit gate that modifies the state of one of the qubits depending on the state of the other control qubit. The effect of CNOT on the

TABLE 9.5
The truth table of the quantum CNOT gate.

Control	Target initial	Final
0	0	0
0	1	1
1	0	1
1	1	0

TABLE 9.6
The truth table of Toffoli gate.

Inputs			Outputs		
a	b	c	a'	b'	c'
0	0	0	0	0	0
0	0	1	0	0	1
0	1	0	0	1	0
0	1	1	0	1	1
1	0	0	1	0	0
1	0	1	1	0	1
1	1	0	1	1	1
1	1	1	1	1	0

target state is shown in table 9.5. In this table if we treat the first two columns as the input and third as the output then this table is the truth table of classical XOR gate. In operator form CNOT is

$$CNOT = |00\rangle\langle 00| + |01\rangle\langle 01| + |10\rangle\langle 11| + |11\rangle\langle 10| \,. \tag{9.19}$$

The first qubit is the control and the target is the second qubit. The first two terms in Eq. (9.19) indicates that if the control qubit is in the state $|0\rangle$ then the target state remains the same. The target state is changed when the control state is $|1\rangle$. The last two terms in Eq. (9.19) represent these. Because the state of the second qubit is dependent on the first qubit's state, the two qubits become entangled on passing through the CNOT gate. Combination of the CNOT and the Hadamard gates can be used to realize both quantum superposition and entanglement. We notice that the control and the target qubits are XORed and stored in the target qubit. The matrix representation of the CNOT operation is given by

$$U_{\text{NOT}} \begin{pmatrix} |00\rangle \\ |01\rangle \\ |10\rangle \\ |11\rangle \end{pmatrix} = \begin{pmatrix} 1 & 0 & 0 & 0 \\ 0 & 1 & 0 & 0 \\ 0 & 0 & 0 & 1 \\ 0 & 0 & 1 & 0 \end{pmatrix} \begin{pmatrix} |00\rangle \\ |01\rangle \\ |10\rangle \\ |11\rangle \end{pmatrix} . \tag{9.20}$$

A reversible quantum gate is Toffoli gate. It has three input bits, say a, b and c and three outputs a', b' and c'. The truth table of Toffoli gate is given in table 9.6. a and b are treated as control bits and are unaffected by the target bit c. But c is inverted if both a and b are 1.

Solved Problem 3:

Given $|\psi\rangle = \alpha|0\rangle + \beta|1\rangle$ and an EPR pair $(|00\rangle + |11\rangle)/\sqrt{2}$ find the state of the complete system and the effect of CNOT on it.

We obtain

$$\frac{1}{\sqrt{2}}\left[\alpha|0\rangle\left(|00\rangle + |11\rangle\right) + \beta|1\rangle\left(|00\rangle + |11\rangle\right)\right] = \frac{1}{\sqrt{2}}\begin{pmatrix} u_1 \\ u_2 \end{pmatrix}, \tag{9.21a}$$

where

$$u_1 = \begin{pmatrix} \alpha \\ 0 \\ 0 \\ \alpha \end{pmatrix}, \quad u_2 = \begin{pmatrix} \beta \\ 0 \\ 0 \\ \beta \end{pmatrix}. \tag{9.21b}$$

Performing CNOT we get

$$\frac{1}{\sqrt{2}}\left[\alpha|0\rangle\left(|00\rangle + |11\rangle\right) + \beta|1\rangle\left(|10\rangle + |01\rangle\right)\right] = \frac{1}{\sqrt{2}}\begin{pmatrix} u_1 \\ u_3 \end{pmatrix}, \quad u_3 = \begin{pmatrix} 0 \\ \beta \\ \beta \\ 0 \end{pmatrix}. \tag{9.22}$$

9.4.5 Symbols for Quantum Circuits

The schematic symbols used to denote some unitary operations in quantum circuits are given in Fig. 9.2 with their matrix representations. The connections are represented by the symbols shown in Fig. 9.3. If a gate U acts on an n-qubit, we depict it as in Fig. 9.4.

By a measurement on the n-qubit register of a quantum computer, we mean measuring the observable

$$x = \sum_{i=0}^{2^n-1} i|i\rangle\langle i| \tag{9.23}$$

and it is represented in circuits by the ammeter symbol as in Fig. 9.4. In a measurement we get two quantities, a collapsed state $|k\rangle$ and its probability $|\langle k|U|\psi\rangle|^2$, and hence it is indicated by a double-line in Fig. 9.4.

Solved Problem 4:

Find the output state $|\psi_1\rangle$ of the circuit given in Fig. 9.5 for the input state $|\psi_0\rangle = \alpha|0\rangle + \beta|1\rangle$.

We have

$$Z = \begin{bmatrix} 1 & 0 \\ 0 & -1 \end{bmatrix}, \quad X = \begin{bmatrix} 0 & 1 \\ 1 & 0 \end{bmatrix} \tag{9.24}$$

and

$$|\psi_0\rangle = \alpha|0\rangle + \beta|1\rangle = \alpha\begin{bmatrix} 1 \\ 0 \end{bmatrix} + \beta\begin{bmatrix} 0 \\ 1 \end{bmatrix} = \begin{bmatrix} \alpha \\ \beta \end{bmatrix}. \tag{9.25}$$

Further,

$$Z|\psi_0\rangle = \begin{bmatrix} 1 & 0 \\ 0 & -1 \end{bmatrix}\begin{bmatrix} \alpha \\ \beta \end{bmatrix} = \begin{bmatrix} \alpha \\ -\beta \end{bmatrix} = \alpha|0\rangle - \beta|1\rangle. \tag{9.26}$$

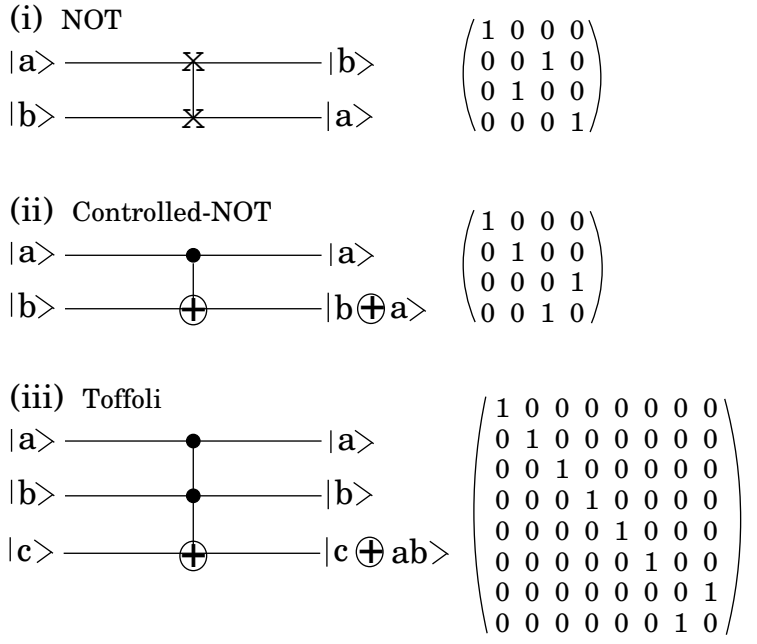

FIGURE 9.2
Circuit symbols and matrix representations of logic gates.

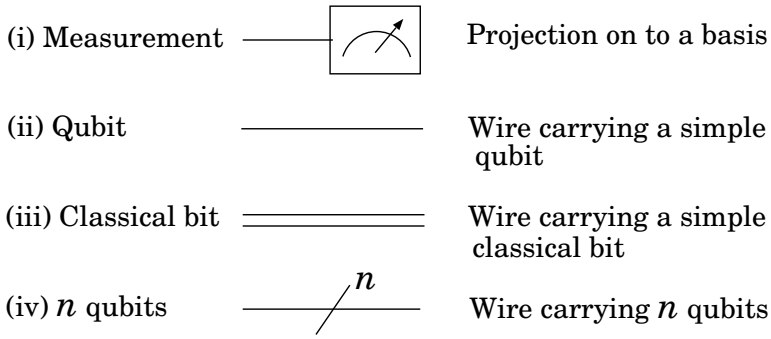

FIGURE 9.3
Symbols for connections in quantum circuits.

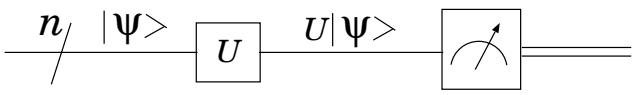

FIGURE 9.4
A quantum circuit.

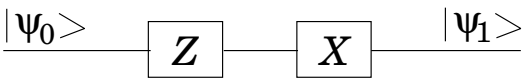

FIGURE 9.5
A quantum circuit with Z and X gates.

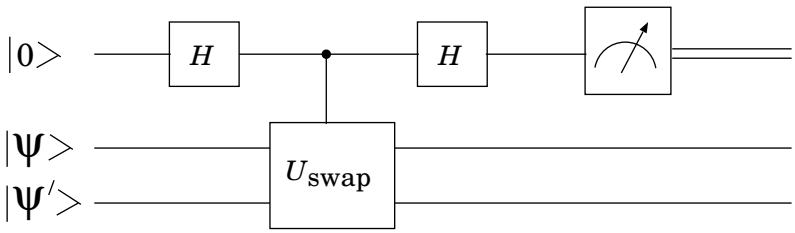

FIGURE 9.6
The quantum circuit for the Fredkin gate.

Then

$$|\psi_1\rangle = XZ|\psi_0\rangle = \begin{bmatrix} 0 & 1 \\ 1 & 0 \end{bmatrix} \begin{bmatrix} \alpha \\ -\beta \end{bmatrix} = \begin{bmatrix} -\beta \\ \alpha \end{bmatrix} = \alpha|1\rangle - \beta|0\rangle \ . \tag{9.27}$$

9.4.6 Some Other Quantum Gates

The *Fredkin gate* also called *controlled swap gate* [15] is designed to compare the two states $|\psi\rangle$ and $|\psi'\rangle$. Figure 9.6 shows the circuit for the Fredkin gate. One can prepare an ancilla qubit $(|0\rangle+|1\rangle)/\sqrt{2}$ and carry out a controlled swap test on $|\psi\rangle$ and $|\psi'\rangle$. For $|\psi\rangle = |\psi'\rangle$, after performing a Hadamard operation the ancilla qubit becomes $|0\rangle$ and is said to pass the swap test. If $\langle\psi|\psi'\rangle \leq \delta$ then the ancilla qubit upon measurement fails the test with probability $(1-\delta^2)/2$ and passes the test with probability $(1+\delta^2)/2$. The matrix representation of the Fredkin gate is given by

$$F \begin{pmatrix} |000\rangle \\ |001\rangle \\ |010\rangle \\ |011\rangle \\ |100\rangle \\ |101\rangle \\ |110\rangle \\ |111\rangle \end{pmatrix} = \begin{pmatrix} 1 & 0 & 0 & 0 & 0 & 0 & 0 & 0 \\ 0 & 1 & 0 & 0 & 0 & 0 & 0 & 0 \\ 0 & 0 & 1 & 0 & 0 & 0 & 0 & 0 \\ 0 & 0 & 0 & 1 & 0 & 0 & 0 & 0 \\ 0 & 0 & 0 & 0 & 1 & 0 & 0 & 0 \\ 0 & 0 & 0 & 0 & 0 & 0 & 1 & 0 \\ 0 & 0 & 0 & 0 & 0 & 1 & 0 & 0 \\ 0 & 0 & 0 & 0 & 0 & 0 & 0 & 1 \end{pmatrix} \begin{pmatrix} |000\rangle \\ |001\rangle \\ |010\rangle \\ |011\rangle \\ |100\rangle \\ |101\rangle \\ |110\rangle \\ |111\rangle \end{pmatrix} . \tag{9.28}$$

This gate can be simulated throught the circuit [16] shown in Fig. 9.7, where $U^2 = X$ with X being the Pauli flip matrix.

The identity gate I represented by the identity matrix $I = \begin{pmatrix} 1 & 0 \\ 0 & 1 \end{pmatrix}$ does not alter the quantum state. The phase-shift gate, for example, maps $|0\rangle \rightarrow |0\rangle$ and $|1\rangle \rightarrow \mathrm{e}^{\mathrm{i}\phi}|1\rangle$. This gates modifies the phase of a quantum state without changing the probability measure. Its

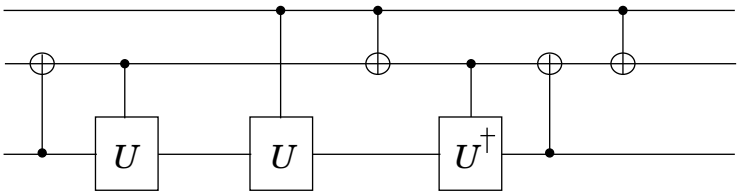

FIGURE 9.7
A quantum circuit of Fredkin gate with five two-qubit gates.

matrix representation is $P(\phi) = \begin{pmatrix} 1 & 0 \\ 0 & \mathrm{e}^{\mathrm{i}\phi} \end{pmatrix}$, where ϕ is the phase shift. A 2-qubit controlled phase-shift gate shifts the phase by ϕ only when it acts on $|11\rangle$. Its matrix representation is

$$CP(\phi) = \begin{pmatrix} 1 & 0 & 0 & 0 \\ 0 & 1 & 0 & 0 \\ 0 & 0 & 1 & 0 \\ 0 & 0 & 0 & \mathrm{e}^{\mathrm{i}\phi} \end{pmatrix} . \tag{9.29}$$

9.4.7 Evaluation of Functions

Let us describe the calculation of functions by quantum computers. Consider a function

$$f : \{0, 1, \ldots, 2^m - 1\} \to \{0, 1, \ldots, 2^n - 1\} \ , \tag{9.30}$$

where m and n are positive integers. A classical computer calculates f by evolving the inputs $0, 1, \ldots, 2^m - 1$ into the outputs $f(0), f(1), \ldots, f(2^m - 1)$. Quantum computers use two registers. Input is stored in the first register and the second is for output. The quantum state of the first register is represented as $|x\rangle$. Output may be represented by $|y\rangle$. The function evaluation is computed by a unitary evolution operator U_f that acts on the two registers, that is,

$$U_f|x\rangle|0\rangle = |x\rangle|f(x)\rangle = |x, f(x)\rangle \ , \tag{9.31}$$

where the output is initially set to 0. The values of $f(0), \ldots, f(2^m - 1)$ found by applying U_f only once to a superposition of all input as

$$|\psi\rangle = U_f \left(\frac{1}{2^{m/2}} \sum_{x=0}^{2^m-1} |x\rangle \right) |0\rangle = \frac{1}{2^{m/2}} \sum_{x=0}^{2^m-1} |x\rangle|f(x)\rangle \, . \tag{9.32}$$

9.5 Quantum Algorithms

One can simulate a classical circuit using a quantum circuit. That is, it is possible to perform classical computations on quantum computers. But the advantage of quantum computing is that powerful functions may be computed by making use of *quantum parallelism*, the fundamental feature of many quantum algorithms. It allows a quantum computer to evaluate $f(x)$ for many different values of x simultaneously. This parallelism is not immediately useful because a measurement would give $f(x)$ for a single value of x only as in the case of a classical computer.

Quantum computation needs something much more than that quantum parallelism to be useful. This is achieved in Deutsch's algorithm [8,17] which combines quantum parallelism

with *interference*. Using Deutsch's algorithm, information about a $f(x)$ can be obtained very quickly compared with a classical computer. Deutsch's algorithm is a simple case of a more general Deutsch–Jozsa algorithm [11]. It suggests that quantum computers may be capable of solving certain problems more efficiently than classical computers.

There are three classes of quantum algorithms that provide an advantage over classical algorithms.

1. There is the class of algorithms based on quantum Fourier transform. Examples are the Deutsch–Jozsa algorithm of finding whether a given function is a constant or not and the Shor's algorithms for factoring and discrete logarithm.
2. The second class is quantum search algorithms. Their principles were discovered by Grover [18]. The goal of a quantum search algorithm is given a search space of size N finding an element of that search space having a known property. A quantum search algorithm achieves this in approximately $\sqrt{N}$ operations whereas a classical computer requires about N operations.
3. Another class of quantum algorithms is quantum simulation, where a quantum computer is explored to simulate a quantum system.

9.5.1 Deutsch's Algorithm

The first and the simplest quantum algorithm is Deutsch's problem. Let $f(x)$ denote one bit functions with $x = 0$ or 1. There are only four possibilities:

$$\begin{array}{llll} f_1(0) = 0, & f_1(1) = 0. & f_2(0) = 0, & f_2(1) = 1. \\ f_3(0) = 1, & f_3(1) = 0. & f_4(0) = 1, & f_4(1) = 1. \end{array} \tag{9.33}$$

Given an unknown f the problem is to determine which one of the above four classes it belongs to. In a classical algorithm we can calculate $f(0)$ and $f(1)$ and then find its class by comparing the values of $f(0)$ and $f(1)$ with Eqs. (9.33). Therefore, we wish to evaluate f at 0 and 1. But a quantum algorithm requires only one evaluation. Deutsch proposed a quantum algorithm for the above problem which is based on the principle that the superposition of quantum states provide the possibility to perform computation on many states simultaneously. The algorithm consists of three steps.

Consider the operation U_A

$$U_A|0\rangle = \frac{1}{\sqrt{2}}\left[|0\rangle + |1\rangle\right] \ , \quad U_A|1\rangle = \frac{1}{\sqrt{2}}\left[|0\rangle - |1\rangle\right] \ . \tag{9.34}$$

Applying n times U_A to an n-bit quantum register in the state $|0\rangle$ we have

$$\begin{aligned} |\psi\rangle &= U_A \otimes U_A \otimes \ldots U_A|000\ldots0\rangle \\ &= \frac{1}{\sqrt{2}}\left(|0\rangle + |1\rangle\right) \otimes \frac{1}{\sqrt{2}}\left(|0\rangle + |1\rangle\right) \otimes \ldots \frac{1}{\sqrt{2}}\left(|0\rangle + |1\rangle\right) \\ &= \frac{1}{2^{n/2}}\left[|00\ldots0\rangle + |00\ldots1\rangle + \ldots + |11\ldots1\rangle\right] \\ &= \frac{1}{2^{n/2}}\sum_{i=0}^{2^n-1}|i\rangle \ . \end{aligned} \tag{9.35}$$

That is, n applications of U_A yields a register state that has 2^n distinct terms. Note that in classical case n elementary operations can only give one state of the register giving one number.

Let us start with two qubits. One bit is set to the state $|0\rangle$ and the other is to the state $|1\rangle$. The total state is $|01\rangle$. In the first step, we apply the gate U_A to each qubit. This gives

$$\frac{1}{\sqrt{2}}\left[\,|0\rangle + |1\rangle\,\right] \otimes \frac{1}{\sqrt{2}}\left[\,|0\rangle - |1\rangle\,\right] = \frac{1}{2}\left[\,|00\rangle - |01\rangle + |10\rangle - |11\rangle\,\right] \ . \tag{9.36}$$

In the second step, compute f on the superposition state given by Eq. (9.36). This is realized by a two-bit gate U_f (Eq. (9.31)) acting on the basis vector

$$|x, y\rangle \to |x, y \oplus f(x)\rangle \ , \quad x, y = 0, 1 \tag{9.37}$$

where $\oplus$ denotes addition mod 2. The last step is to apply U_A again on each qubit.

Let us apply the above algorithm assuming $f = f_1$. The first step yields the superposition state given by Eq. (9.36). This is independent of the function. The second step gives

$$\begin{aligned} |\psi\rangle &= U_f\left(\frac{1}{2}\left[\,|00\rangle - |01\rangle + |10\rangle - |11\rangle\,\right]\right) \\ &= \frac{1}{2}\left[\,|0, 0 \oplus f(0)\rangle - |0, 1 \oplus f(0)\rangle + |1, 0 \oplus f(1)\rangle - |1, 1 \oplus f(1)\rangle\,\right] \\ &= \frac{1}{2}\left[\,|00\rangle - |01\rangle + |10\rangle - |11\rangle\,\right] \ . \end{aligned} \tag{9.38}$$

The final step is the application of U_A on $|\psi\rangle$ given by Eq. (9.38). We obtain

$$\begin{aligned} |\psi\rangle &= \frac{1}{2}\left[\,\frac{1}{\sqrt{2}}\left(|0\rangle + |1\rangle\right)\frac{1}{\sqrt{2}}\left(|0\rangle + |1\rangle\right) - \frac{1}{\sqrt{2}}\left(|0\rangle + |1\rangle\right)\frac{1}{\sqrt{2}}\left(|0\rangle - |1\rangle\right)\right. \\ &\qquad \left. + \frac{1}{\sqrt{2}}\left(|0\rangle - |1\rangle\right)\frac{1}{\sqrt{2}}\left(|0\rangle + |1\rangle\right) - \frac{1}{\sqrt{2}}\left(|0\rangle - |1\rangle\right)\frac{1}{\sqrt{2}}\left(|0\rangle - |1\rangle\right)\right] \\ &= \frac{1}{4}\left[\,|00\rangle + |01\rangle + |10\rangle + |11\rangle - |00\rangle + |01\rangle - |10\rangle + |11\rangle\right. \\ &\qquad \left. + |00\rangle + |01\rangle - |10\rangle - |11\rangle - |00\rangle + |01\rangle + |10\rangle - |11\rangle\right] \\ &= |01\rangle \ . \end{aligned} \tag{9.39}$$

If $f = f_2$ then the second step gives

$$\begin{aligned} |\psi\rangle &= \frac{1}{2}\left[\,|0, 0 \oplus 0\rangle - |0, 1 \oplus 0\rangle + |1, 0 \oplus 1\rangle - |1, 1 \oplus 1\rangle\,\right] \\ &= \frac{1}{2}\left[\,|00\rangle - |01\rangle + |11\rangle - |10\rangle\,\right] \ . \end{aligned} \tag{9.40}$$

Then U_A on $|\psi\rangle$ results in

$$\begin{aligned} |\psi\rangle &= \frac{1}{4}\left[\,|00\rangle + |01\rangle + |10\rangle + |11\rangle - |00\rangle + |01\rangle - |10\rangle + |11\rangle\right. \\ &\qquad \left. + |00\rangle - |01\rangle - |10\rangle + |11\rangle - |00\rangle - |01\rangle + |10\rangle + |11\rangle\,\right] \\ &= |11\rangle \ . \end{aligned} \tag{9.41}$$

In a similar manner for $f = f_3$ and $f = f_4$ we obtain $|\psi\rangle = -|11\rangle$ and $|\psi\rangle = -|01\rangle$, respectively. Therefore, the final state of the two qubits is

$$\begin{array}{rlrl} |01\rangle & \text{if} \quad f = f_1, & |11\rangle & \text{if} \quad f = f_2, \\ -|11\rangle & \text{if} \quad f = f_3, & -|01\rangle & \text{if} \quad f = f_4. \end{array} \tag{9.42}$$

Thus, by comparing the final state of $|\psi\rangle$ with Eq. (9.42) we can identify whether the unknown f is f_1 or f_2 or f_3 or f_4.

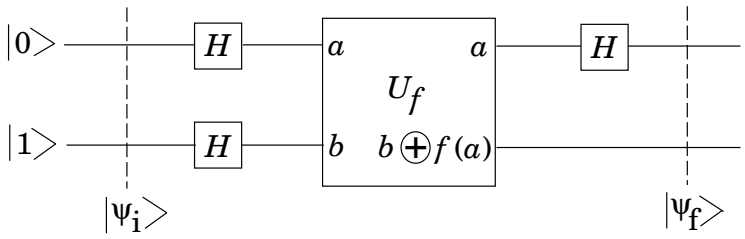

FIGURE 9.8
Quantum circuit to implement Deutsch's algorithm.

The essential features of the above quantum algorithm are:

1. The crucial elements are the superposition and linearity of quantum mechanics. $|\psi\rangle$ in Eq. (9.42) is computed on the superposition states $|00\rangle$, $|01\rangle$, $|10\rangle$ and $|11\rangle$ simultaneously.
2. The final state $|\psi\rangle$ is due to an interference of various parts of the superposition.
3. If it is desired to know whether f is a constant ($f = f_1$ or f_4) or balance ($f = f_2$ or f_3) then it is enough to measure the final state of the first qubit. If the first qubit is $|0\rangle$ then f is a constant. f is balance if the first qubit is $|1\rangle$. Notice that the algorithm does not say whether f is f_1 or f_4 and f_2 or f_3. However, nowhere we learn about either $f(0)$ or $f(1)$. We are able to find out that the f is a constant or not by computing f once. In classical computation we must evaluate f twice before making a decision.

The quantum circuit to implement Deutsch's algorithm is given in Fig. 9.8. The input state is $|\psi_i\rangle = |01\rangle$ and the output is

$$|\psi_f\rangle = \pm|f(0) \oplus f(1)\rangle \left[\frac{|0\rangle - |1\rangle}{\sqrt{2}}\right] . \tag{9.43}$$

So, by measuring the first qubit, we may determine $f(0) \oplus f(1)$ and hence whether $f(x)$ is balance or not. We cannot determine $f(x)$. But determine a global property of $f(x)$, namely, $f(0) \oplus f(1)$ with one evaluation of $f(x)$ only. So, a clever choice of function and final transformation allows efficient determination of useful information about the function. The above is achieved much faster compared to a classical computer.

9.5.2 Grover's Quantum Search Algorithm

In this subsection we explain the quantum search algorithm [12,18,19] and describe some of the exciting ways it can be used.

The kind of search problem that can be solved by a quantum search algorithm is following. Consider a function $f(x)$ with integer arguments 0 to N. Let the value of it be 0 everywhere except for $x = \omega$. The problem is to find ω using few calls to $f(x)$. This is analogous to finding the name of person in a telephone directory with the telephone number given. The data-base we wish to search is of size N. Classically, the probability of the value of a randomly chosen element to be ω is $1/N$. Therefore, to have a $50-50$ chance of getting ω we must call the data-base at least $N/2$ times. But a quantum algorithm can reduce the calls to approximately $\sqrt{N}$.

Lov Kumar Grover, a computer scientist at Lucent Technologies Bell Laboratories proposed a quantum search algorithm. In the following we discuss Grover's algorithm following

mainly the review of Sudarshan [19]. We can model an oracle or a unitary operator $U_\omega(\lambda)$ as a black-box function $f(x)$. It computes $f(x)$ for an input x. It will return 1 if and only if $x = \omega$ and return 0 if $x \neq \omega$. A quantum circuit that has the ability to recognize solutions to the search problem is called a *quantum oracle* which is represented by the unitary operator U_ω.

We begin with the state $|0\,0\rangle$. The two zero's represent two registers of qubits, where all the qubits are set to the 0 state. We can use Hadamard transformation to bring this initial state into superposition of states

$$|\phi\rangle = \frac{1}{\sqrt{N}} \left[\, |00\rangle + |10\rangle + |20\rangle + \ldots + |N-10\rangle \right] . \tag{9.44}$$

In matrix form, the transformation is given by Eq. (9.16). In Grover's algorithm the first register is assumed to be big enough to represent the largest element. In the second register, there is only one qubit. By applying the Hadamard transformations on the individual qubits of the initial state we get

$$|\phi\rangle = \frac{1}{\sqrt{N}} \sum_{i=0}^{N-1} |i\rangle \left(\frac{|1\rangle - |0\rangle}{\sqrt{2}} \right) . \tag{9.45}$$

The number of steps needed for this is $O(\log N)$. The second register is initialized to a state different from $|0\rangle$. The action of the oracle U_ω is

$$U_\omega |i, j\rangle = |i, j \oplus f(i)\rangle . \tag{9.46}$$

$|i\rangle$ is the index register, $|j\rangle$ is the oracle single qubit which is flipped if $f(i) = 1$ and unchanged otherwise. We can find whether i is a solution of the problem by preparing $|i\rangle|0\rangle$, applying the oracle and checking whether the oracle qubit is flipped to $|1\rangle$. We have

$$U_\omega |\phi\rangle = \frac{1}{\sqrt{N}} \left[\sum_{i \neq \omega} |i\rangle \left(\frac{|1\rangle - |0\rangle}{\sqrt{2}} \right) - |\omega\rangle \left(\frac{|1\rangle - |0\rangle}{\sqrt{2}} \right) \right] . \tag{9.47}$$

The action of U_ω on $|\phi\rangle$ is to change the sign of the component in the direction of $|\omega\rangle$. This reflects $|\phi\rangle$ in the Hilbert space of dimension N about the hyperplane orthogonal to $|\omega\rangle$. At this instant the value of ω is unknown to us. We can find the value of ω by consulting the oracle a certain minimum number of times.

Now, we construct another operator U_s which performs a reflection in such a way that the component of $|\phi\rangle$ along $|s\rangle$ is preserved and the signs of the component in the hyperplane perpendicular to $|s\rangle$ is changed. Here one iteration is the unitary transformation $R_{\text{Grov}} = U_s U_\omega$. Let θ be the angle between $|s\rangle$ and $|\omega\rangle$. Then the action of one iteration on $|\phi\rangle$ is to rotate its component along $|s\rangle$ through an angle 2θ that is away from the hyperplane perpendicular to the vector $|\omega\rangle$. Successive iterations with various choices of $|s\rangle$ makes $|\phi\rangle$ close to $|\omega\rangle$ and moreover away from the hyperplane perpendicular to $|\omega\rangle$. The number of queries required to obtain the correct value of $|\omega\rangle$ with large probability when $|\phi\rangle$ is measured after the iterations is $\pi\sqrt{N}/4$. So, Grover's algorithm has a quadratic speed up compared to the best classical algorithm.

9.5.3 Quantum Fourier Transform

The discrete Fourier transform is defined by

$$f_j = \frac{1}{\sqrt{N}} \sum_{k=1}^{N-1} \mathrm{e}^{\mathrm{i}2\pi jk/N} g_k . \tag{9.48}$$

This transforms a set of N numbers $\{g_0, g_1, \ldots, g_{N-1}\}$ (can be complex) into another set of numbers $\{f_0, f_1, \ldots, f_{N-1}\}$. The quantum Fourier transform U_{FT} is defined, on n qubits by its action on basis states $|j\rangle$, where $0 \leq j \leq 2^n - 1$, as

$$U_{\mathrm{FT}}|j\rangle \rightarrow \frac{1}{\sqrt{N}} \sum_{k=0}^{2^n-1} \mathrm{e}^{\mathrm{i}2\pi jk/N}|k\rangle \ . \tag{9.49}$$

It can be easily verified that U_{FT} is a unitary operator: The matrix of the transformation is $M(U_{\mathrm{FT}}) = [M_{jk}] = \mathrm{e}^{\mathrm{i}2\pi jk/N}/\sqrt{N}$. This transformation can be realized as a quantum circuit.

Many of the quantum algorithms are based on quantum Fourier transform (QFT). Shor's fast algorithm for factoring and discrete logarithm are two most interesting examples of algorithms based on the QFT. Classically, the fast Fourier transform takes about $N \log N = n2^n$ steps to Fourier transform $N = 2^n$ numbers. A quantum computer requires only n^2 steps. So, there is an exponential saving of time with a quantum computer compared to a classical computer. But it is to be noted that the set $\{f_j\}$ cannot be measured directly because a measurement would collapse each qubit into $|0\rangle$ or $|1\rangle$. Though quantum computation can be done more efficiently, creating the initial state $\{g_k\}$ and measuring the result are difficult.

A circuit decomposition of the QFT has been developed for hybrid qudits based on generalized Hadamard and controlled-phase gates which would be realized by means of selective rotations in NMR [20]. The hybrid qudit QFT was experimentally implemented on an NMR quantum emulator making use of four qubits to emulate a single qutrit coupled to two qubits. A simplified mathematical construction of the QFT suitable for systems described by Ising type Hamiltonians is reported and is based on one-qubit gates and a free evolution process [21].

9.5.4 Applications of Quantum Search

Let us point out some of the applications of quantum search.

1. An effective search algorithm for hard problems, like constrained optimization, is the so-called randomized algorithm. In it a set of random numbers is used to find a trajectory through some search space. Quantum search is able to speed up randomized algorithms.
2. Quantum search can be applied to determine the statistical properties mean, variance, maxima and minima of functions, etc.
3. With quantum Fourier transform one can count effectively the number of possible solutions of a problem without finding them.
4. Quantum search is useful for experimental physicists to prepare desired superposition states. For example, to create a superposition of indices corresponding to prime numbers we can design an oracle $f(x)$ which returns 1 if x is a prime and 0 otherwise.

9.5.5 Shor's Algorithm

In 1994 Shor [9] developed an efficient quantum algorithm to compute the period of a periodic function. The period finding routine can be used to factorize large numbers in polynomial time. Consider the problem of factorizing a large number N into exactly two large prime numbers [19]. Classically, to find the two prime numbers we have to check all the numbers from 1 to $\sqrt{N}$.

In Shor's algorithm, randomly a number $a < N$, $a^r = 1 \pmod N$ for an even integer value of r is chosen. It can be shown that for most choices of a, N shares a common factor having $a^{r/2} + 1$ or $a^{r/2} - 1$. Once r is found then applying a classical Euclid's algorithm one can easily compute the common factor of N and also $a^{r/2} \pm 1$. Thus, the problem of factorizing N is solved.

Let us choose

$$f_{N,a}(x) = a^x \pmod N, \quad x = 0, 1, 2, \ldots \ . \tag{9.50}$$

Because $a^r = 1 \pmod N$ the period of $f_{N,a}$ is r. Evaluate $f_{N,a}$ on a $|\phi\rangle$ given by

$$|\phi\rangle = \frac{1}{\sqrt{N}} \sum_{i=0}^{N-1} |i0\rangle \ . \tag{9.51}$$

Next, we set-up a unitary oracle $U_{f_{N,a}}$ such that

$$U_{f_{N,a}}|\phi\rangle = \frac{1}{\sqrt{N}} \sum_{i=0}^{N-1} |ia^x (\text{mod } N)\rangle = |\psi\rangle \ . \tag{9.52}$$

The second register has a function with period r. Therefore, if we perform a measurement on it and obtain $|u\rangle$ then the first register will collapse to a linear combination of the values of x. This results in $f(x) = u$. Due to the periodicity of f these values of x form $x_0 + jr$, $j = 0, 2, \ldots, x_{\max}/r$, where $x_{\max}$ is the biggest number contained in the first register. We have $f(x_0) = u$. Suppose $t = x_{\max}/r$ is an integer. The measurement is found to reduce $|\phi\rangle$ to

$$|\phi\rangle = \frac{1}{\sqrt{x_{\max}/r}} \sum_{j=0}^{x_{\max}-1} |x_0 + jr\rangle \, |u\rangle \ . \tag{9.53}$$

Now, to get the value of r apply a quantum Fourier transform on the first register (of the state $|\phi\rangle$). The effect is

$$U_{\text{FT}}|\phi\rangle \to \sum_k \overline{f}(k) \, |k\rangle \, |u\rangle \ , \tag{9.54}$$

where $\overline{f}(k) = 1$ if k is a multiple of $x_{\max}/r$ otherwise 0. The value of k determined by the measurement of the first register will be of the form $k = \lambda x_{\max}/r$. λ and r are unknown. But if λ and r do not have a common factor then $k/x_{\max} = \lambda/r$ can be reduced to an irreducible fraction to read r and λ. On the other hand, if λ and r have a common factor then we conclude that the algorithm fails. In this case we repeat the analysis with another value of a. It is possible to show that the number of steps taken by the algorithm to get the correct answer is $O(\log N)$. This is indeed an exponential speed up compared to the classical case.

9.5.6 Quantum Factorization of Integers

Let us describe the quantum factorization of integers by considering the number $N = 20$. First, choose a number a randomly such that the greatest common divisor of it and N is 1. Consider the periodic function

$$f(x) = a^x \pmod N, \quad x = 0, 1, \ldots \ . \tag{9.55}$$

For $N = 20$, select $a = 9$. Then from Eq. (9.55) we have

$$\begin{aligned} f(0) &= 1 \pmod{20} = 1. \quad f(1) = 9 \pmod{20} = 9. \\ f(2) &= 9^2 \pmod{20} = 81 \pmod{20} = 1. \\ f(3) &= 9^3 \pmod{20} = 729 \pmod{20} = 9. \\ f(4) &= 9^4 \pmod{20} = 6561 \pmod{20} = 1. \end{aligned}$$

From the above, the period T of $f(x)$ is found as $T = 2$. This period can be determined by employing the method described earlier. To find N, calculate $Z = a^{T/2} = 9^1 = 9$. The greatest common divisor of $(Z + 1, N) = (9 + 1, 20) = (10, 20)$ is 10. The greatest common divisor of $(Z - 1, N) = (9 - 1, 20) = (8, 20)$ is 4. 4 and 10 are factors of 20. In this way two factors of a number N can be obtained if the quantum algorithm gives the period T of $f(x)$.

9.6 Testing Quantum Computers Using Grover's Algorithm

Many experimental quantum computers have been developed. But no quantum computer has achieved so far the *quantum supremacy*, which is a crossing point where a quantum computer can simulate a quantum system which cannot be done on a classical super computer. Though publically available quantum processors continue to proliferate, they are all plagued by many errors such as cross-talk, coherent noise drift and decoherence [22]. Consequently, the experimentally available quantum computers suffer from numerous issues that prevent them from running complex algorithms with reasonable accuracy. The physical accuracy of quantum computers has not come closer to reaching the theoretically expected levels. Grover's algorithm has been used to evaluate the accuracy of quantum computers [23]. Tests were conducted using Grover's algorithm and implemented in a variety of different ways on the publically available IBM quantum computers.

We have seen that Gover's algorithm is a quantum search algorithm. This algorithm has been used to find the index of the target element among the list of $N = 2^n$ elements, where n is the number of qubits and N is the size of the list [23]. The procedure of Grover's algorithm to test the IBM quantum computer is given below [23]:

1. Prepare $|0\rangle^{\otimes n}$, where $\otimes$ means tensor multiplication, that is, $|0\rangle^{\otimes n}$ is equivalent to $|0\rangle \otimes |0\rangle \otimes \ldots \otimes |0\rangle$ with n-terms.
2. Apply $H^{\otimes n}$ to create a superposition.
3. Apply the oracle U to mark the target element by negating its sign, that is, $U|x\rangle = -|x\rangle$, where $|x\rangle$ is the target.
4. Apply the Grover's diffusion operator D to amplify the probability amplitude of the target element. D can be written as [3]

$$2|\psi\rangle\langle\psi| - I_N = H^{\otimes n}(2|0\rangle\langle 0| - I_N)H^{\otimes n}. \tag{9.56}$$

   In this expression $|\psi\rangle$ is the uniform superposition of states and I_N is the identity matrix with dimensionality N.
5. Repeat the steps 3 and 4 for about $\sqrt{N}$ times.
6. Perform measurements.

It is found that Grover diffusion can be implemented on a quantum circuit with a phase-shift operator which negates every states except for $|0\rangle$ sandwiched between $H^{\otimes n}$ gates. 2-qubit, 3-qubit and 4-qubit Grover's algorithms have been implemented on the IBM quantum computers[3]. The following five experiments were performed.

1. Identification of the effect of varying the length/complexity of an algorithm.
2. Comparison of the differences between different choices of qubits and finding the significance of using the best qubits in building a quantum circuits.
3. Comparison of the accuracy and speed of each of the IBM quantum devices.
4. Determination of the effect of loading the quantum computer with varying number of executions.
5. Determination of error bar for the results produced by the quantum computers.

The outcomes of the above experiments suggested that there appears to be a long way to go before quantum computers can surpass classical computers in accuracy and speed. Further, the experiments have shown that implementing quantum algorithms can be heavily affected by the qubit choice.

9.7 Features of Quantum Computation

Some of the essential (but not sufficient) features of quantum computers [24] are summarized below:

1. Input, output, program and memory are represented by qubits.
2. A unitary transformation of the computer can represent a computation step.
3. All computations are reversible.
4. Only one-to-one operations are possible and therefore qubits cannot be copied.
5. The values of qubits may depend on the method used to infer them and on the co-measured qubits.
6. A measurement may be performed on any qubit at any stage of computation. However, a qubit cannot be measured by an experiment with a desired accuracy.
7. During a computation, a quantum computer proceeds all paths at once which when managed cleverly may speed up the computation.
8. A subroutine should not leave any qubits over its computed answer. This is because the computational paths with different information cannot interfere.

9.8 Quantum Computation Through NMR

The essential requirement of a quantum computer are two-level isolated quantum systems. The physical systems explored so far to build quantum hardwares range from optical pho-

[3]IBM has set-up *Quantum System One*. Its physical design was tested first time in Milan, Italy. IBM now offers cloud access to its quantum computers to develop and run programs.

tons, cavity quantum electrodynamics, quantum dots, trapped ions to nuclear spins. The basic requirements of a quantum computer are:

1. The quantum states must be sufficiently isolated from the surroundings so that they have very low decoherence.
2. They must be made to evolve as per the unitary transformations performed.
3. It should be possible to prepare the initial state.
4. Suitable measurement technique must be devised for measuring quantum information because a measurement destroys quantum information and replaces it with classical information.

As a candidate for quantum computing, nuclear magnetic resonance (NMR) is attractive because of the spin's long coherence times and also due to the complexity of operations performed on modern spectrometers. Most atomic nuclei have spin and it causes them to act like tiny magnets. These nuclear magnets interact with magnetic fields thereby allowing them to be controlled with high precision. In certain cases, such as in hydrogen, this nuclear spin can assume two values, spin-up and spin-down. This is a two-state quantum system. Therefore, a hydrogen nucleus can be regarded as a qubit. In a molecule, different nuclei can be differentiated by their different resonance frequencies. Consequently, the molecule can act as a quantum computer with each hydrogen providing one qubit. For example, naturally occurring cytosine has five hydrogen atoms in each molecule. It is in fact easy to replace three of them with deuterium, thereby leaving the two hydrogens to serve a two-qubit computer. This system with a conventional NMR spectrometer has been used to demonstrate certain quantum algorithms. Various nonselective pulses, transition and spin-selective pulses, rf gradients, coherence transfer via J-coupling and simultaneous multi-site excitation have been proposed to construct universal quantum gates and implement quantum algorithms for qubit systems. For some details see refs. [13,25–28].

9.9 Why is Making a Quantum Computer Extremely Difficult?

If quantum computers would be so marvelous, *why don't we just build one?* There are several technical problems in setting up a quantum computer. We list some of them:

1. A notable serious problem is decoherence. It is the modification of the quantum state due to interaction with an environment. It can alter the value of a qubit that is uncontrollable.
2. Errors in classical information are discrete. In quantum information they are continuous.
3. To check whether errors have occurred, we must perform a quantum measurement which will affect the state of the system. That is, errors cannot be diagnosed without introducing further errors.
4. To obtain the outcome of a computation, a readout system must carry out a measurement. Any imperfection in the measurement process gives rise to a readout error.
5. A transistor or any conventional computer element cannot be useful to perform quantum computation. The various degrees of freedom of the device (such as the

elastic vibrations of the device, the excitation of its conduction electrons, etc.) interact strongly with one another and also with the state of the device. As a result even approximate unitary evolution is impossible.

9.10 Concluding Remarks

Quantum algorithms for solving both linear and nonlinear differential, equations [29–33], quantum field theories [34] and simulation of sparse Hamiltonian systems [35], chemical dynamics [36] and electronic structure Hamiltonians [37] have been proposed. Quantum computing using coherent photon conversion [38], fullerene based electron spin [39,40], trapped polar molecules [41], Josephson junction arrays [42], scanning tunnelling microscopy [43], antiferromagnetic rings [44], one-dimensional optical lattice [45] and quantum walk [46] have been proposed. Simulation of electronic structure Hamiltonians [47], many-body Fermi systems [48], calculations of molecular properties [49], molecular energies [50] using quantum computers were reported. Implementation of Deutsch's algorithm on an ion-trap quantum computer [51] and experimental realization of it in a one-way quantum computer [52] have been achieved. Magnetic resonance realization of decoherence-free quantum computation [53], performance of adiabatic quantum computation subject to decoherence [54], role of entanglement and correlations in mixed-state quantum computation [55], quantum discord and the power of one qubit [56] enhancement of quantum computation using quantum chaos [57] and geometric phase-shift in quantum computation using superconducting nano circuits [58] were analyzed.

9.11 Bibliography

[1] B. Schumacher, *Phys. Rev. A* 51:2738, 1995.

[2] G.P. Berman, G.D. Doolen, R. Mainieri and V.I. Tsifrinovich, *Introduction to Quantum Computers.* World Scientific, Singapore, 1998.

[3] M. Nielsen and I.L. Chuang, *Quantum Computation and Quantum Information.* Cambridge University Press, Cambridge, 2002.

[4] V. Sahni, *Quantum Computing.* Tata McGraw–Hill, New Delhi, 2007.

[5] P.A. Benioff, *Phys. Rev. Lett.* 48:1581, 1980.

[6] R. Feynman, *Found. Phys.* 16:507, 1986.

[7] R. Feynman, *Int. J. Theor. Phys.* 21:467, 1982.

[8] D. Deutsch, *Proc. Roy. Soc. London A* 400:97, 1985.

[9] P.W. Shor, *Algorithms for quantum computation: Discrete logarithms and factoring*. In Proceedings of 35th Annual Symposium on the Foundations of Computer Science. IEEE Press, 1994.

[10] P.W. Shor, *SIAM J. Comp.* 26:1484, 1997.

[11] D. Deutsch and R. Jozsa, *Proc. Roy. Soc. London A* 439:553, 1992.

[12] L.K. Grover, *A fast quantum mechanical algorithm for database search*. In Proceedings of 28th Annual ACM Symposium on the Theory of Computation. ACM Press, New York, 1996, pp. 212.

[13] C.H. Bennett, *Phys. Today*, October 1995, pp. 24.

[14] T. Toffoli, *Reversible Computing. Technical Report MIT/LCS/TM-151*, 1980.

[15] E. Fredkin and T. Toffoli, *Int. J. Theor. Phys.* 21:219, 1982.

[16] J.A. Smolin and D.P. DiVincenzo, *Phys. Rev. A* 53:2855, 1996.

[17] D. Deutsch, A. Berenco and A. Ekert, *Proc. Roy. Soc. London A* 449:669, 1995.

[18] L.K. Grover, *Phys. Rev. Lett.* 79:325, 1997.

[19] E.C.G. Sudarshan, *Current Science* 84:511, 2003.

[20] S. Dogra, A. Dorai and K. Dorai, *Int. J. Quantum Infor.* 13:1550059, 2015.

[21] S.S. Ivanov, M. Johanning and C. Wunderlich, Simplified implementation of the quantum Fourier transform with Ising-type Hamiltonians: Example with ion traps, *arXiv: 1503.08806v2 [quant-ph]*, 2015.

[22] T. Proctor, K. Rudinger, K. Young, E. Nielsen and R. Blume-Kohout, Measuring the Capabilities of Quantum Computers, *arXiv: 2008.11294v1 [quant-ph]*, 2020.

[23] A. Mandviwalla, K. Ohshiro and B. Ji, *IEEE Int. Conf. Big Data*. Article number 18399305, 2018.

[24] K. Svozil, *J. Univ. Comp. Sci.* 2:311, 1996.

[25] K. Dorai, T.S. Maohesh Arvind and A. Kumar, *Current Science* 79:1447, 2000.

[26] D.P. DiVincenzo, *Phys. Rev. A* 51:1015, 1995.

[27] D.G. Cory, M.D. Price and J.F. Havel, *Physica D* 120:82, 1998.

[28] N.A. Gershenfeld and I.L. Chuang, *Science* 275:350, 1997.

[29] S.K. Leyton and T.J. Osborne, A quantum algorithm to solve nonlinear differential equations, *arXiv: 0812.4423 [quant-ph]*, 2008.

[30] A.W. Harrow, A. Hassidin and S.L. Lloyd, *Phys. Rev. Lett.* 103:150502, 2009.

[31] X.D. Cai, Z.E. Su., M.C. Chen, M. Gu, M.J Zhu, L. Li, N.L. Liu, C.Y. Lu and J.W. Pan, *Phys. Rev. Lett.* 110:230501, 2013.

[32] B.D. Clader, B.C. Jacobs and C.R. Spouse, *Phys. Rev. Lett.* 110:250504, 2013.

[33] D.W. Berry, *J. Phys. A: Math. Theor.* 4:105301, 2014

[34] S.P. Jordan, K.S.M. Lee and J. Preskill, *Science* 336:1130, 2012.

[35] D.W. Berry, G. Ahokas, R. Cleve and B.C. Sanders, *Commun. Math. Phys.* 270:359, 2007.

[36] J. Karsal, S.P. Jordan, P.J. Love, M. Mohseni and A.A. Guzik, *Proc. Natl. Acad. Sci.* 105:18681, 2008.

[37] J.D. Whitfield, J.D. Biamonte and A.A. Guzik, *Mol. Phys.* 109:735, 2011.

[38] N.K. Langford, S. Ramelow, R. Prevedel, W.J. Munro, G.J. Milburn and A. Zeilinger, *Nature* 478:360, 2011.

[39] W. Harneit, *Phys. Rev. A* 65:032322, 2002.

[40] S.C. Benjamin, A. Ardavan, G.A.D. Briggs, D.A. Britz, D. Gunlycke, J. Jefferson, M.A.G. Jones, D.F. Leigh, B.W. Lovett, A.N. Khobystov, S.A. Lyon, J.J.L. Morton, K.Porfyrakis, M.R. Sambrook and A.M. Tyryshkin, *J. Phys.: Condens. Matter* 18:S867, 2006.

[41] D. DeMille, *Phys. Rev. Lett.* 88:067901, 2002.

[42] L.B. Ioffe and M.V. Feigelman, *Phys. Rev. Lett.* 66:224503, 2002.

[43] G.P. Berman, G.W. Brown, M.E. Hawley and V.I. Tsifrinovich, *Phys. Rev. Lett.* 87:097902, 2001.

[44] F. Troiani, A. Ghirri, M. Affronte, S. Carretta, P. Santini, G. Amoretti, S. Piligkos, G. Timco and R.E.P. Winpenny, *Phys. Rev. Lett.* 94:207208, 2005.

[45] J.K. Pachos and P.L. Knight, *Phys. Rev. Lett.* 91:107902, 2003.

[46] A.M. Childs, *Phys. Rev. Lett.* 102:180501, 2009.

[47] J.D. Whitfield, J. Biamonte and A. Aspuru-Guzik, *Mol. Phys.* 109:735, 2011.

[48] D.S. Abrams and S. Lloyd, *Phys. Rev. Lett.* 79:2586, 1997.

[49] B.P. Lanyon, J.D. Whiifield, G.G. Gillett, M.E. Goggin, M.P. Almeida, I. Kassal, J.D. Biamonte, M. Mohseni, B.J. Powell, M. Barbieri, A. Aspuru-Guzik and A.G. White, *Nat. Chemistry* 2:106, 2010.

[50] A. Aspuru-Guzik, A.D. Dutoi, P.J. Love and M. Head-Gordon, *Science* 309:1704, 2005.

[51] S. Gulde, M. Riebe, G.P.T. Lancaster, C. Becher, J. Eschner, H. Haffner, F. Schmidt Kaler, I.L. Chuang and R. Blatt, *Nature* 421:48, 2003.

[52] M.S. Tame, R. Prevedel, M. Paternostro, P. Bohi, M.S. Kim and A. Zeilinger, *Phys. Rev. Lett.* 98:140501, 2007.

[53] J.E. Ollerenshaw, D.A. Lidar and L.E. Kay, *Phys. Rev. Lett.* 91:217904, 2003.

[54] M.S. Sarandy and D.A. Lidar, *Phys. Rev. Lett.* 95:250503, 2005.

[55] A. Datta and G. Vital, *Phys. Rev. A* 75:042310, 2007.

[56] A. Datta, A. Shaji and C.M. Caves, *Phys. Rev. Lett.* 100:050502, 2008.

[57] T. Prosen and M. Znidaric, *J. Phys. A: Math. Gen.* 34:L681, 2001.

[58] S.L. Zhu and Z.D. Wang, *Phys. Rev. A* 66:042322, 2002.

9.12 Exercises

9.1 Assume that a qubit can be expressed as $|\psi\rangle = \cos(\theta/2)\,|0\rangle + \sin(\theta/2)\,\mathrm{e}^{\mathrm{i}\phi}|1\rangle$ with $\theta \in [0, \pi]$ while $\phi \in [0, 2\pi]$. Express the two qubits $|\psi\rangle|\phi\rangle$ in separable form and also find $|\psi\rangle^{\otimes 2}$.

9.2 Obtain the matrix representation of the Hadamard gate.

9.3 Express the Hadamard gate in terms of the Pauli matrices $\sigma_1 = \begin{pmatrix} 0 & 1 \\ 1 & 0 \end{pmatrix}$ and $\sigma_3 = \begin{pmatrix} 1 & 0 \\ 0 & -1 \end{pmatrix}$.

9.4 Determine α, β, γ and δ of the decomposition matrices for the Hadamard gate.

9.5 Find the unitary matrix for the two qubit gate given in Fig. 9.9 and show that it is equivalent to controlled NOT gate.

9.6 If X, H and Z denote the quantum NOT, Hadamard and Z gates, respectively, find HZH.

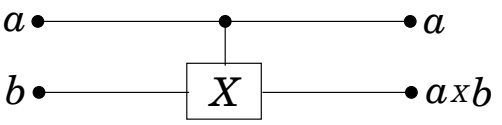

FIGURE 9.9
An equivalent controlled NOT gate.

9.7 Consider the initial state

$$|\psi\rangle = \frac{\lambda}{\sqrt{2}}(|000\rangle + |011) + \frac{\mu}{\sqrt{2}}(|100\rangle + |111\rangle).$$

Find the state after applying a CNOT gate (using the first qubit as the control qubit and the second as the target) followed by Hadamard gate on first qubit.

9.8 Suppose $M_0 = |0\rangle\langle 0| = \begin{pmatrix} 1 \\ 0 \end{pmatrix}\begin{pmatrix} 1 & 0 \end{pmatrix} = \begin{pmatrix} 1 & 0 \\ 0 & 0 \end{pmatrix}$ and $M_2 = |1\rangle\langle 1| = \begin{pmatrix} 0 \\ 1 \end{pmatrix}\begin{pmatrix} 0 & 1 \end{pmatrix} = \begin{pmatrix} 0 & 0 \\ 0 & 1 \end{pmatrix}$ are two measurement operators. If $|\psi\rangle = a|0\rangle + b|1\rangle$ find the probability of measuring $|0\rangle$.

9.9 If $S = \begin{pmatrix} 1 & 0 \\ 0 & \mathrm{i} \end{pmatrix}$ is a quantum phase gate then find $S(\alpha|0\rangle + \beta|1\rangle)$.

9.10 For the quantum phase gate operation S given in the previous exercise form its truth table.

9.11 Form the truth table for the T gate defined as $T = \begin{pmatrix} 1 & 0 \\ 0 & \mathrm{e}^{\mathrm{i}\pi/4} \end{pmatrix}$.

9.12 Consider the two circuits shown in Fig. 9.10. The left-side circuit is the swap gate which exchanges the state of two qubits. Show that the two circuits in Fig. 9.10 are equivalent.

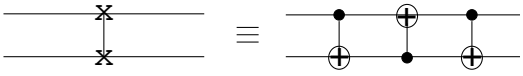

FIGURE 9.10
Two equivalent circuits.

9.13 In the notation $|a\rangle|b\rangle = |ab\rangle$, where a is the control bit and b is the target bit, find the outputs of the quantum circuit shown in Fig. 9.11 for the inputs $|00\rangle$, $|01\rangle$, $|10\rangle$ and $|11\rangle$.

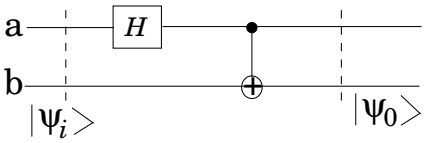

FIGURE 9.11
A quantum circuit with a Hadamard gate.

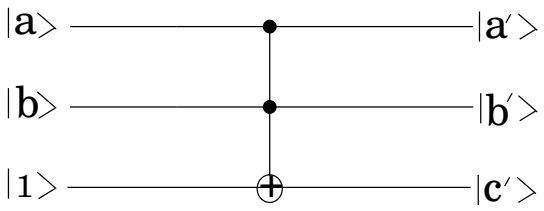

FIGURE 9.12
A Toffoli gate.

9.14 Construct the truth table for the Toffoli gate shown in Fig. 9.12 and show that it stimulates NAND gate.

9.15 Find the output of the circuit given in Fig. 9.13, which can be used to implement the Deutsch's algorithm, for the input $|\psi_i\rangle = |0\rangle\,|1\rangle$.

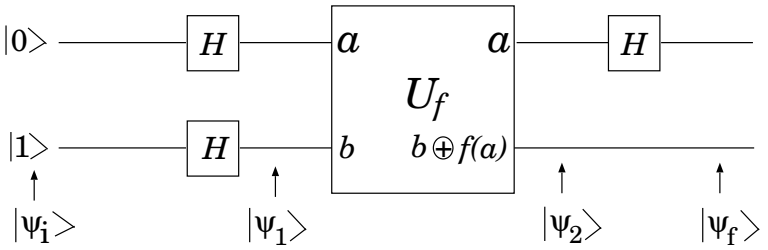

FIGURE 9.13
A quantum circuit of Deutsch's algorithm.

Taylor & Francis
Taylor & Francis Group
http://taylorandfrancis.com

10

Quantum Cryptography

10.1 Introduction

Users of communication channels wish to have their transactions secured. Therefore, it is necessary to develop techniques which can ensure that eavesdroppers cannot intercept the messages transmitted. The technology concerned with the secure communication of data is termed as *cryptography* [1–3]. It is the art of hiding information in the form of a string of bits to an unauthorized party. To achieve this goal, in a classical cryptography system the message bits are combined with random bits of equal length called a *key*. The combined data is known as *cryptogram*. This technique is called *encryption*. A key can be public or private. The public key is to encode plaintext, while the private key is for decoding the previously encoded plaintext or cryptogram. The cryptogram is generally sent through the communication channel. Because of the randomness of the key the encoded message is completely random. Consequently, the message is untraceable to an eavesdropper. The safety of the transmission completely depends on the safety of the key. Therefore, the key should be kept secret by the users.

Classically, the key can be distributed to the users via a trusted courier or in personal meetings. Because of this, for many applications the technique becomes expensive and not practical. Further, the safety could be destroyed by modern technology like faster computers or mathematical advances in algorithms or progress in theoretical computation. Recently, an innovative new technique called *quantum cryptography* [4–8] has been developed where safety does not depend on computing abilities. Quantum cryptography lies at the intersection of information theory and quantum mechanics. The idea of quantum cryptography [9] was first proposed in the 1970s by Stephen Wiesner. After the introduction of three protocols [10] by the computer scientists and physicists Charles H. Bennett and Gilles Brassard in 1984 and their first implementation [11] in 1992, a remarkable interest has propelled quantum theory into computer science and physics.

10.2 Standard Cryptosystems

Cryptosystems come in two major classes depending on whether the key (random string of bits) is shared in public or in secret. The one-time pad system shares a secret key and the other is the public key system [12]. In public key cryptography, messages are exchanged using keys. The keys depend on the underlying difficulty of a mathematical problem. Sender and receiver have a public key and the private key. The former is to encrypt messages. The latter is to decrypt the messages. In the secret key encryption, a key is shared by the users who use it to transform plaintext inputs to an encoded cipher.

DOI: 10.1201/9781003172192-10

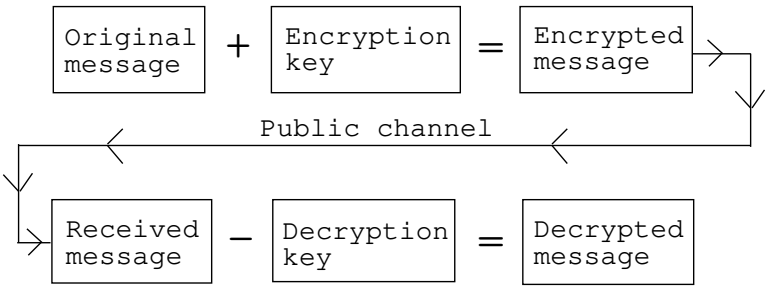

FIGURE 10.1
The Vernam one-time pad system.

10.2.1 One-Time Pad System

The one-time pad system was first proposed by Gilbert Vernam in 1926. It is the only cryptosystem with proven-perfect secrecy. In this scheme a sender is called *Alice* (the conventional name) and a receiver is called *Bob*. Alice encrypts a message using a random key and then adds each bit of the message to the corresponding bit of the key. This text is then sent to the receiver. Bob decrypts the message by subtracting the same key. The above scheme is depicted in (Fig. 10.1). A problem with this scheme is that Alice and Bob should have a common secret key. This key must be as long as the message. They can use the key only once - hence the name *one-time pad*. If the key is utilized more than one encryption then an unauthorized eavesdropper called *Eve* could record all the messages and build-up a picture of the key. Another notable problem is with the exchange of key. The key can be transmitted by a classical channel between Alice and Bob. This procedure is complex, expensive and unsafe. The one-time pad system is used in many applications, for example, e-commerce employs short keys.

10.2.2 Public Key Cryptosystems

The basic idea behind the public key cryptosystems was first proposed by Bailey Whitfield Diffi and Martin E. Hellman [13] in 1977 and implementation was then developed [14,15] by Ronald L. Rivest, Adi Shamir and L. Adlerman in 1978. These systems are based on the so-called *one-way functions*, where it is easy to compute the function $f(x)$ given x but difficult to calculate x from known value of $f(x)$. By difficulty, we mean that the time needed to perform a task grows exponentially with the number of input bits while easy means that the growth is polynomially. For example, the relation between a large number and its primes can be used to generate a public key. In the public key systems, users need not agree on a secret key before sending the message. They work with two keys: public and private. The public key is to lock the message and the private key is to open it. The point is that anyone can have a key to lock the message but only one person has a private key to open it. In this sense the public key cryptosystem can be thought of as a mailbox. Anyone can drop a letter in it but the owner alone can open it with his private key.

For Alice to send a message with a public key cryptosystem, Bob first chooses a private key. He uses this key to find a public key. Alice then uses this public key to encrypt the message. She sends the encrypted message to Bob. He decrypts it using his private key. Public key cryptosystems are convenient and became very popular over the last three decades or so. The security of the internet is partly based on such systems. However, this system suffers

from two problems. First, extracting a private key is very difficult but it is not impossible. The second is that problems that are difficult for a classical computer may become easy for a quantum computer. With the recent progress in the field of quantum computation there are valid reasons to believe that in the near future it will be possible to build these machines.

10.3 Quantum Cryptography–Basic Principle

Classical cryptography systems use mathematical techniques to prevent the eavesdroppers from learning the encrypted messages. In contrast, in quantum cryptography the message is protected by the fundamental laws of physics. Quantum cryptography is based on the uncertainty principle which states that properties with certain pairs of observables are related in such a way that measuring one of the properties sets constraints on the observer in simultaneously measuring the value of the other. Let us assume that we measure the polarization of a photon with a vertical filter. Classically, if the photon passes through, assume that, it is vertically polarized. Therefore, if we keep in front of the photon another filter with an angle θ to the vertical, it cannot pass through. But there is a nonzero probability p_θ for the photon to go through the second filter. p_θ decreases to $0 \to \theta$ reaches $90°$ from $0°$. $p_\theta = \frac{1}{2}$ when $\theta = 45°$. The point is that if the initial polarization is set either vertical or horizontal and if the filter is in the $45°$ (or $135°$) then we cannot determine any details about the initial polarization of the photon.

Suppose a message is encoded using quantum signals (like photons polarized at various angles). One cannot obtain information about the message without perturbations. The perturbations would reveal eavesdropping. If the bits are not changed during transmission we are sure that no eavesdropping took place. Thus, any eavesdropping will be spotted. Eve cannot get information from the qubits transmitted to Bob from Alice without disturbing their state. This is due to the following: (i) By the no-cloning theorem and (ii) disturbance introduced to the signal by Eve's measurement. We prove these statements below.

10.3.1 The No-Cloning Theorem

The no-cloning theorem (for more details see chapter 11) states that it is impossible to produce a copy of an unknown quantum state $|\psi\rangle$. A copying machine will copy $|\psi\rangle$ into a target state. If the target state is a pure state[1] $|\mathrm{p}\rangle$ then the initial state of the machine is

$$|i\rangle = |\psi\rangle|\mathrm{p}\rangle \; . \tag{10.1}$$

After copying, $|\mathrm{p}\rangle$ becomes $|\psi\rangle$. The final state of the machine is

$$|f\rangle = |\psi\rangle|\psi\rangle \; . \tag{10.2}$$

As the copying operation is described by unitary operation U, we have

$$U|i\rangle = |f\rangle \; , \quad U|\psi\rangle|\mathrm{p}\rangle = |\psi\rangle|\psi\rangle \; . \tag{10.3}$$

When we consider another unknown pure state $|\phi\rangle$ then

$$U|\phi\rangle|\mathrm{p}\rangle = |\phi\rangle|\phi\rangle \; . \tag{10.4}$$

[1]It is a state that cannot be represented as a mixture of other states.

Taking the inner product of (10.3) and (10.4) we get

$$\langle \mathrm{p}|\langle\phi|U^\dagger U|\psi\rangle|\mathrm{p}\rangle = \langle\phi|\langle\phi|\psi\rangle|\psi\rangle$$

or

$$\langle\phi|\psi\rangle = (\langle\phi|\psi\rangle)^2 \,. \tag{10.5}$$

Hence, $\langle\phi|\psi\rangle = 1$ or 0. This means $|\psi\rangle = |\phi\rangle$ or $|\psi\rangle$ and $|\phi\rangle$ should be orthogonal. Thus, a cloning machine can only clone states orthogonal to one another. Therefore, a general cloning device is impossible. A cloning machine to clone $|1\rangle$ and $|0\rangle$ is possible. But a device to clone $|1\rangle$ and $(|1\rangle + |0\rangle)/\sqrt{2}$ are not possible.

Solved Problem 1:

Show that any attempt to distinguish two nonorthogonal states will disturb the signal.

Let $|\psi\rangle$ and $|\phi\rangle$ be two nonorthogonal states. Eve tries to obtain information. Let the initial target state of her machine be $|\mathrm{p}\rangle$. Assume that her process does not disturb the states. She obtains

$$|\psi\rangle|\mathrm{p}\rangle \longrightarrow |\psi|u\rangle \,, \quad |\phi\rangle|\mathrm{p}\rangle \longrightarrow |\phi|u'\rangle \,. \tag{10.6}$$

To distinguish $|\psi\rangle$ and $|\phi\rangle$, Eve wants $|u\rangle$ and $|u'\rangle$ to be different. Since the process is described by unitary transformation, the inner product has to be preserved. So,

$$\begin{aligned} & \langle \mathrm{p}|\langle\phi|\psi\rangle|\mathrm{p}\rangle = \langle u'|\langle\phi|\psi\rangle|u\rangle \\ \Longrightarrow \quad & \langle \mathrm{p}|\mathrm{p}\rangle\langle\phi|\psi\rangle = \langle u'|u\rangle\langle\phi|\psi\rangle \\ \Longrightarrow \quad & \langle u'|u\rangle = \langle \mathrm{p}|\mathrm{p}\rangle = 1 \end{aligned} \tag{10.7}$$

which implies $|u\rangle$ and $|u'\rangle$ are identical. Distinguishing between $|\psi\rangle$ and $|\phi\rangle$ would disturb at least one of them. Hence, the sender and receiver can spot the eavesdropping.

10.3.2 Communication Channels

In quantum cryptography, the sender and receiver have two types of communication channels:

1. **A classical public channel**: This can be overheard by anyone. However, message from this channel cannot be altered.
2. **A quantum channel**: In this channel an attempt of eavesdropping will introduce perturbations in the transmission. This ensures the safety of the communication.

The classical channel can be used to exchange information and to transmit the encoded message. The secret key can be transmitted via the quantum channel. Sender and receiver exchange a series of bits via the quantum channel. They use part of the transmitted signal to test for eavesdropping. They compare a randomly chosen part of their data using a public channel. Deviations between their strings imply that an eavesdropper has listened to the transmission and it is thus not a secret. No errors in the series of bits make sure that the key is safe. The logic is

$$\begin{aligned} \text{No disturbance} \quad & \Longrightarrow \quad \text{No measurement} \\ & \Longrightarrow \quad \text{No eavesdropping} \,. \end{aligned}$$

But the intricate problem is that the quantum channels are extremely sensitive devices. Particularly, some errors will be unavoidable because of the imperfections of the channels and detectors. If the information leaked to Eve is not considerably high, then the sender and receiver can make use of modern classical techniques to minimize it to approximately zero by shortening the strings.

Some key features of quantum cryptography are:

1. It allows two parties to prepare and share a random secret key without insisting to meet.
2. It uses the sensitivity of entangled systems to indicate to the two parties whether an enemy has broken their encrypted communication.
3. It also makes use of the principle that a broken measurement on a quantum system perturbs it and turns this fundamental limitation to a great advantage.

10.4 Types of Quantum Cryptography

The first protocol for quantum cryptography was proposed in 1984 by Bennett and Brassard [10]. Some of the basic quantum cryptographic systems [16] are:

1. Four-states protocol,
2. Two-states protocol,
3. $4 + 2$ protocol and
4. Multi-photon and multi-stage protocol.

The first relies on the transmission of single photons polarized randomly along four directions. The second protocol uses two nonorthogonal states. The third is based on the creation of pairs of EPR correlated photons. The fourth protocol is a quantum version of the classical double-lock cryptography. Several variations of four-states protocol have been developed [7,14].

10.4.1 Four-States Protocol [10,11,16]

Let us briefly describe the four-states scheme (BB84) of quantum cryptography. The BB84 protocol forms the basis for most of the practical quantum cryptography.

10.4.1.1 Basic Idea

This system uses polarization of photons to set-up a secret key for Alice and Bob. We know that a photon can travel in any linear direction. When travelling along a linear direction, it will vibrate. The vibration can be in any angle along its line of travel. However, its angle of vibration will always be the same. This vibration is the polarization of the photon. A polarized photon can be detected by a detector with correct polarization. An attempt to eavesdrop the light at another polarization will destroy the stream. With the details of polarizing a light beam, a key can be designed based on the condition of the beam and the particles the other party received.

Each photon can be sent in one of the polarizations: $0°(-)$, $45°(/)$, $90°(|)$ or $135°(\backslash)$.

TABLE 10.1
An example of four-state protocol.

Alice's key:	1	1	0	0	0	0	1	1	1
Alice sends with:	+	×	×	+	×	+	+	×	+
Alice sends to Bob:	|	\	/	−	/	−	|	\	|
Bob measures with:	+	×	+	+	+	+	×	×	+
Bob's results:	|	\	/	−	|	−	/	\	|
Valid data:	|	\		−		−		\	|
Translated to key:	1	1		0		0		1	1

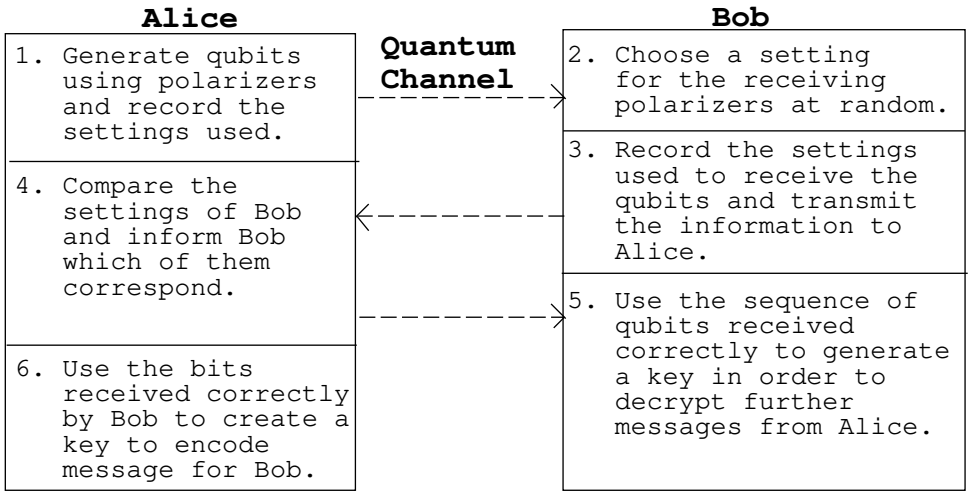

FIGURE 10.2
BB84 protocol.

Alice and Bob have two polarizers. Each one in the $0°/90°(-/|)$ (symbolically represented as '+') basis and one in the $45°/135°$ (//\) (denoted as '×') basis. The photons are assigned a value 0 or 1. 0 for photons type − or / and 1 for photons of type | or \. Alice sends a stream of photons. At the other end Bob measures the photons and determines their state. At this stage Bob has to use a basis polarizer either + or ×. He chooses randomly one of these two polarizers and measures the photon. His choice may or may not be correct. That is, Bob will be wrong in measurements. In order to eliminate false measurements Alice and Bob discuss through a public channel (a telephone or another insecure medium). Alice informs Bob of the polaroid filter she used for the polarization of the photon. But she does not tell how each photon was polarized. Alice will tell Bob whether a photon was sent with diagonal or rectilinear polarizer but not whether the polarization was upper-right/lower-left or upper-left/lower-right. If Alice finds that Bob used the correct polarizer for a particular photon then that photon is retained. The incorrectly measured photons are discarded. They convert the correctly measured series into bit strings of 0 and 1. Table 10.1 gives an example of the above described process with a few photons [17]. Figure 10.2 depicts the BB84 protocol.

Due to the discard of incorrect measurements the newly obtained pad is shorter than the original pad sent by Alice to Bob. Alice and Bob have now developed an unbreakable key making use of the laws of quantum theory. Once the key is set-up they can begin the encryption. If they identify an eavesdropping, they start the process again.

In this protocol the choice of basis is hidden from Eve. Eve cannot know the basis used. If the coherent pulses $|\alpha\rangle$ are used, then the transmission rate $T^{(4)}$ is given by

$$T^{(4)} = \frac{1}{2}\left[1 - |\langle\alpha|0\rangle|^2\right] = \frac{1}{2}\left(1 - \mathrm{e}^{-|\alpha|^2}\right) , \tag{10.8}$$

where 1/2 is because half of the transmissions had to be discarded due to the use of different basis.

Solved Problem 2:

The first two rows in the following show the data transmitted by Alice in the BB84 protocol. The last row specifies the measurement chosen by Bob. Find out the possible result of the measurement.

Alice	Key element	0	0	1	1	0
	Encoding	−	/	\	|	/
	Measurement	+	+	×	×	+

The result is shown below.

Bob	Result	−	−/|	\	\//	−/|
	Key element	0	1	1	1	1

10.4.1.2 Safety of the Four-States System

Suppose Eve intercepts the transmission and transmits a new pulse prepared as per the obtained information. If Eve uses the correct basis then the error introduced is nil whereas the use of wrong basis creates a 50% error rate. On the other hand, Eve gets total message if correct basis is used and none for wrong. Therefore, when Eve eavesdrops on a fraction η of the transmission, the error created is $\eta/4$. The information obtained is $\eta/2$. Hence, we can write the mutual information, shared by sender and Eve and Eve and receiver as

$$I_{\mathrm{SE}}^{(4)} = I_{\mathrm{ER}}^{(4)} = 2Q , \tag{10.9}$$

where Q is error rate. Alice and Bob cannot prevent eavesdropping, but they can detect the eavesdropping. So, whenever they are unsatisfied with the security of the channel they can create the key distribution again.

When noise exists due to eavesdropping, polarization identified by the receiver may not be those of the sender. In order to deal with this possibility the following process is useful.

1. Alice and Bob agree on the perturbation of bit positions in their strings.
2. The strings are divided into blocks of, say, size k.
3. For each block Alice and Bob calculate and announce parities publicly. They discard the last bit of each block.

4. For each block with parities different, Alice and Bob use a binary search and correct the error.
5. To remove undetected errors, steps (1)–(4) are repeated with increasing block sizes.
6. To know whether errors still remain, Alice and Bob repeat a randomized check:
   (a) Alice and Bob agree publicly on a random assortment of, say, half the bit positions in their strings.
   (b) Both compare parities publicly. If the strings differ then the parities will disagree with 1/2 probability.
   (c) If there is a disagreement, Alice and Bob apply a search and eliminate it.
7. If there is no disagreement after k iterations, both conclude that their strings match with low probability error, $1/2^k$.

10.4.2 Two-States Protocol

In the following we consider the protocol of Bennett.

10.4.2.1 Basics of the Scheme

In this protocol [18] the sender uses weak coherent states, with phase encoding 0 or π with respect to strong coherent states. Weak and strong states are denoted as $|\pm\alpha\rangle$ and $|\beta\rangle$, respectively. The expression for the overlap between the two states is

$$|\langle\alpha|-\alpha\rangle| = \cos\delta = \mathrm{e}^{-2|\alpha|^2} \,. \tag{10.10}$$

Sender uses two orthogonal polarizations. $|\pm\alpha\rangle$ and $|\beta\rangle$ have vertical and horizontal polarizations, respectively.

At the receiving end the two states are separated by a polarization beam splitter. $|\beta\rangle$ is rotated to vertical polarization. It is sent through a beam splitter to a detector D_β. A fraction of $|\beta\rangle$, equal to $|\alpha\rangle$ is made to interface with $|\pm\alpha\rangle$ at another beam splitter. The reflected and transmitted beams are sent towards the detectors, say, $\mathrm{D_R}$ and $\mathrm{D_T}$, respectively. Thus, a count in $\mathrm{D_T}$ corresponds to 0 phase while a count in $\mathrm{D_R}$ corresponds to phase π. If no count is recorded in both $\mathrm{D_R}$ and $\mathrm{D_T}$ then the result is regarded as inconclusive. The probability of such a result is worked out as [18]

$$P(?) = \mathrm{e}^{-2|\alpha|^2} \,. \tag{10.11}$$

Then the transmission rate of channel is

$$T^{(2)} = 1 - P(?) = 1 - \mathrm{e}^{-2|\alpha|^2} \,. \tag{10.12}$$

10.4.2.2 Safety of the System

Eve can get a certain amount of information by projecting the signal onto the orthogonal basis $B = (i, j)$ as shown in Fig. 10.3.

This gives probabilistic information only. The error rate introduced by Eve is the probability of wrong prediction. For example, for the input state $|\alpha\rangle$ the probability for getting j is [18]

$$q = P(j/\alpha) = \frac{1-\sin\delta}{2} \,, \tag{10.13}$$

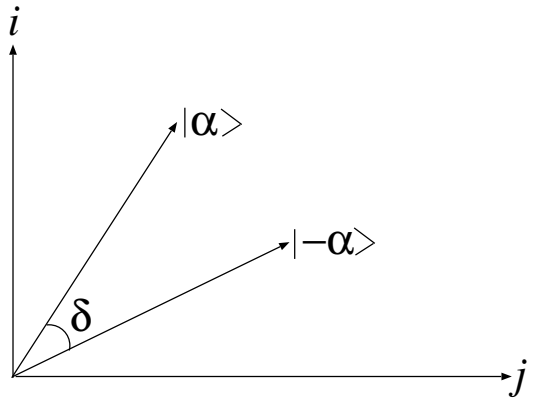

FIGURE 10.3
Representation of two nonorthogonal states.

where δ is defined by Eq. (10.10). The mutual information shared among the sender and eavesdropper is obtained as [18]

$$i_{\mathrm{SE}} = 1 + \left(\frac{1-\sin\delta}{2}\right)\log_2\left(\frac{1-\sin\delta}{2}\right) \tag{10.14a}$$

$$+\left(\frac{1+\sin\delta}{2}\right)\log_2\left(\frac{1+\sin\delta}{2}\right)\,. \tag{10.14b}$$

The error created by Eve is

$$Q = \eta\left(\frac{1-\sin\delta}{2}\right)\,. \tag{10.15}$$

The mutual information is

$$I^{(2)}_{\mathrm{SE}} = \frac{2Q}{1-\sin\delta}\, i_{\mathrm{SE}}(\delta)\,, \quad I^{(2)}_{\mathrm{ER}} = \frac{2Q}{1-\sin\delta}\,. \tag{10.16}$$

10.4.3 $4+2$ Protocol

The idea of this method [19] is that in the four-states method the two states in each basis need not be orthogonal. By choosing nonorthogonal states, we can get the advantage of the two-states protocol: Eve cannot distinguish between the two states in each basis.

The first pair corresponds to 0 and π phase-shifts. The second pair is the phase-shifts $\pi/2$ and $3\pi/2$. The four states are $|\alpha\rangle$, $|-\alpha\rangle$, $|\mathrm{i}\alpha\rangle$ and $|-\mathrm{i}\alpha\rangle$. The detection system is similar to that used in the two-states system with the inclusion of an optional $\pi/2$ phase shifter. Phase-shift will not be used if the observation is in the first basis. Hence, the receiver's detection is able to differentiate between $|\alpha\rangle$ and $|-\alpha\rangle$. $\pi/2$ phase-shift can be used for the second basis. This differentiates between $|\mathrm{i}\alpha\rangle$ and $|-\mathrm{i}\alpha\rangle$.

Eve does not know the basis of the sender. Therefore, Eve is unsure whether the result is relevant. Sender and receiver use a different basis in half of the communication and hence such cases have to be discarded. Now, the transmission rate of the channel is $T^{(4+2)} = (1-P(?))/2$. Using $P(?)$ given by Eq. (10.11), we obtain

$$T^{(4+2)} = (1-\cos\delta)/2. \tag{10.17}$$

The error rate Q in this system is

$$Q = \frac{\eta}{2}\left(1-\frac{\sin\delta}{2}\right)\,. \tag{10.18}$$

The information gained by Eve is

$$I_{\rm SE}^{(4+2)} = \frac{Q}{1-\dfrac{\sin\delta}{2}}\, i_{\rm SE}(\delta)\,, \quad I_{\rm ER}^{(4+2)} = \frac{Q}{1-\dfrac{\sin\delta}{2}}\,. \tag{10.19}$$

Solved Problem 3:

For the $4+2$ states protocol determine $\langle\alpha|-\alpha\rangle$.

As $|\alpha\rangle$ is normalized, it is a unit vector. So, we write

$$\begin{aligned} |\alpha\rangle &= \mathbf{i}\cos\theta + \mathbf{j}\sin\theta \\ |-\alpha\rangle &= \mathbf{i}\cos(\theta+\delta) + \mathbf{j}\sin(\theta+\delta)\,. \end{aligned} \tag{10.20}$$

Therefore,

$$\begin{aligned} \langle\alpha|-\alpha\rangle &= \cos(\theta+\delta)\cos\theta + \sin(\theta+\delta)\sin\theta \\ &= \cos(\theta+\delta-\theta) \\ &= \cos\delta\,. \end{aligned} \tag{10.21}$$

10.4.4 Multi-Photon and Mult-Stage Protocol

Clifford Chan and his collaborators have proposed a multi-photon (MP) QKD [20]. The various steps involved in the MPQKD are the following:

1. The target state X is one of the two orthogonal states $|0\rangle$ and $|1\rangle$ and is to be transferred from Alice to Bob. The qubit can be encoded using the polarization of photons in a coherent state. For example, X can be represented by the polarization angle dented as θ_X. The polarization rotations through angles $\theta_{\rm A}$ and $\theta_{\rm B}$ can represent $U_{\rm A}$ and $U_{\rm B}$, respectively.
2. $U_{\rm A}$ and $U_{\rm B}$ are some secret unitary transformations with the property $U_{\rm A}U_{\rm B} = U_{\rm B}U_{\rm A}$. Alice applies $U_{\rm A}$ on X and then sends it to Bob.
3. Bob randomly chooses to return the recieved signal to Alice after applying $U_{\rm B}$ on it or to retain the received $U_{\rm A}(X)$ for authentication.
4. Alice randomly chooses to send the recieved one after applying $U_{\rm A}^{\dagger}$ on it or to retain $U_{\rm B}U_{\rm A}(X)$.
5. Bob applies $U_{\rm B}^{\dagger}$ on the signal $U_{\rm A}^{\dagger}U_{\rm B}U_{\rm A}(X) = U_{\rm B}(X)$ sent by Alice and get X.
6. Bob, after receiving all the pulses, publicly announces the measured pulses. Then Alice discards the pulses not measured by Bob. If the bit rate of the key is found to be too low then the key is abonded.
7. Bob informs Alice the qubits chosen by him for authentication. Alice discloses Bob the associated transformations and X applied by her for those qubits. The possibility of eavesdropping is tested using these transformations. The pulse retained by Alice can be used for authentication. To find the error rate of the key Alice tells to Bob some part of the exchanged information X. If the error rate and the transformations are found to be below certain thresholds then the rest of the key is accepted.
8. At the end Alice and Bob perform post-processing, that is, privacy amplification and error correction in order to minimize Eve's information.

10.5 Multiparty Quantum Secret Sharing

In the protocols discussed earlier, information is exchanged between two parties. In contrast to this in quantum secret sharing (QSS) the message is split into many shadows so that each shadow alone cannot recover the information, but a specific quantity of shadows can [21–23]. For example, consider a three-party QSS protocol. Alice (boss) splits her secret message into two and transmits one part to Bob and another part to Charlie. Note that each agent alone cannot recover the secret message of Alice. To recover the secret Bob and Charlie have to cooperate. That is, the secret can be locked from being revealed by Eve (a dishonest agent) alone. In this section we briefly outline the multiparty QSS (MQSS) proposed by Hwange et al. [23]. They used the so-called Greenberger–Horne–Zeilinger (GHZ) entangled state. GHZ is a type of quantum superposition states with at least three particles. An example is a three-qubit state: $(|000\rangle + |111\rangle)/\sqrt{2}$. An important property of this GHZ state is that the trace of it over one of the particles is

$$\mathrm{Tr}\left[(|000\rangle + |111\rangle)\,(\langle 000| + \langle 111|)\right] = |00\rangle\langle 00| + |11\rangle\langle 11| \tag{10.22}$$

which is an unentangled mixed state. For three-photon maximally entangled systems there are eight GHZ states:

$$|\psi_1\rangle = \frac{1}{\sqrt{2}}(|000\rangle + |111\rangle), \quad |\psi_2\rangle = \frac{1}{\sqrt{2}}(|000\rangle - |111\rangle), \tag{10.23a}$$

$$|\psi_3\rangle = \frac{1}{\sqrt{2}}(|001\rangle + |110\rangle), \quad |\psi_4\rangle = \frac{1}{\sqrt{2}}(|001\rangle - |110\rangle), \tag{10.23b}$$

$$|\psi_5\rangle = \frac{1}{\sqrt{2}}(|010\rangle + |101\rangle), \quad |\psi_6\rangle = \frac{1}{\sqrt{2}}(|010\rangle - |101\rangle), \tag{10.23c}$$

$$|\psi_7\rangle = \frac{1}{\sqrt{2}}(|011\rangle + |100\rangle), \quad |\psi_8\rangle = \frac{1}{\sqrt{2}}(|011\rangle - |100\rangle)\,, \tag{10.23d}$$

where $|0\rangle$ and $|1\rangle$ are the two eigenstates of the Z-basis $\{|0\rangle, |1\rangle\}$.

10.5.1 Protocol

Suppose Alice wishes to share a secret with her agents Bob and Charlie. They agree that the four unitary operations I, σ_z, σ_x and $\mathrm{i}\sigma_y$ are encoded as 00, 01, 10 and 11, respectively. The protocol essentially consists of six steps [23].

Step 1: Alice first create an ordered sequence GHZ states $|\psi_1\rangle$ and divides them into S_1, S_2 and S_3. They are the set of first, second and third, respectively qubits of all GHZ states. She sends S_1 alone to Bob and nothing to Charlie.

Step 2: After receiving S_1, Bob executes two actions: Making use of, say, the photon number splitter and single photon detectors he finds out whether the received photons are single photons. After confirming that the received photons are indeed single photons, he can carry out any one of the operations $\{I, \sigma_z, \sigma_x, \mathrm{i}\sigma_y\}$ on each photon in S_1 and then randomly add l decoy single photons into S_1. The result is, say, S_1'. Bob sends it to Charlie.

Step 3: In order to check the eavesdropping on S_1', Bob and Charlie use the decoy single photons to perform public discussions. They continue the protocol if no eavesdropping; otherwise, they terminate the communication.

Step 4: Alice performs one of the operations $\{I, \sigma_z, \sigma_x, \mathrm{i}\sigma_y\}$ on each photon in S_2. Then randomly inserts l decoy single photons into S_2 and S_3 thereby forms S_2' and S_3'. She sends both S_2' and S_3' to Charlie.

Step 5: Alice informs the positions of the decoy single photons to Charlie and they use them for checking eavesdropping. The protocol proceeds only if there is no eavesdropping.

Step 6: After the public discussion, Charlie does the GHZ measurement and gets the measurement results, say, MR_{C}. Bob and Charlie work together to get Alice's message using MR_{C} and the unitary operations U_{B}.

The above protocol can be generalized for the case of multiparties: Alice, Bob_1, Bob_2, ..., Bob_m and Charlie. In this case steps 1 and 2 have to be repeated for Bob_1, Bob_2, ..., Bob_m. Finally, photons are sent to Charlie from Bob_m. Then Alice carries out step 4 to encode her message and sends her photons to the final agent Charlie. In step 6, Bob_1, Bob_2, ..., Bob_m and Charlie can cooperate to rebuild Alice's message.

10.5.2 Security Analysis

Let us analyze the intercept-and-resend attack and the entangle-and-measure attack against the above protocol.

1. Intercept-and-resend attack

In step 2, in order to check eavesdropping, Bob randomly inserts l decoy single photons to S_1. Suppose the eavesdropper attempts to measure and resend the sequence assuming to pass the checking process of public discussion. The probability for a random guess on a decoy single photon to overcome the public discussion is 3/4. Hence, the probability that Eve passes the public discussion is $(3/4)^l$. If l is large then the probability that Eve passes the detection is very small. Similar strategy can be made for S_2 and S_3. Hence, S_1, S_2 and S_3 can be securely communicated with the use of decoy single photons.

2. Entangle-and-measure attack

Suppose Bob tries to recover the secret message without cooperating with Charlie and eavesdrop the Charlie's sequence S_2' and S_3'. Bob does not know the positions and states of the decoy photons in S_2' and S_3'. Therefore, he prepares some ancillas (extra), say, $E = \{|E_1\rangle, |E_2\rangle, \ldots, |E_m\rangle\}$ and entangles them with S_2' and S_3' by enacting a unitary operation U in order to overcome the eavesdropping check between Alice and Charlie. But this act of Bob would give rise the following [23]:

$$U \cdot |0\rangle|E_i\rangle = \alpha|0\rangle|e_{00}\rangle + \beta|1\rangle|e_{01}\rangle \,, \tag{10.24a}$$

$$U \cdot |1\rangle|E_i\rangle = \gamma|0\rangle|e_{10}\rangle + \delta|1\rangle|e_{11}\rangle \,, \tag{10.24b}$$

and

$$\begin{aligned} U \cdot |+\rangle|E_i\rangle = \frac{1}{2}\,[\,&|+\rangle(\alpha|e_{00}\rangle + \beta|e_{01}\rangle + \gamma|e_{10}\rangle + \delta|e_{11}\rangle) \\ &+|-\rangle(\alpha|e_{00}\rangle - \beta|e_{01}\rangle + \gamma|e_{10}\rangle - \delta|e_{11}\rangle)]\,, \end{aligned} \tag{10.24c}$$

$$\begin{aligned} U \cdot |-\rangle|E_i\rangle = \frac{1}{2}\,[\,&|+\rangle(\alpha|e_{00}\rangle + \beta|e_{01}\rangle - \gamma|e_{10}\rangle - \delta|e_{11}\rangle) \\ &+|-\rangle(\alpha|e_{00}\rangle - \beta|e_{01}\rangle - \gamma|e_{10}\rangle + \delta|e_{11}\rangle)]\,, \end{aligned} \tag{10.24d}$$

where $UU^\dagger = U^\dagger U = I$, $|E_i\rangle$ is initial state of Bob's ancilla; $|e_{00}\rangle$, $|e_{01}\rangle$, $|e_{10}\rangle$ and $|e_{11}\rangle$ are the four states that can be distinguished by Bob and $|\alpha^2| + |\beta^2| = |\gamma^2| + |\delta^2| = 1$. If the

decoy photons of Alice are $|0\rangle$ or $|1\rangle$ and Bob has chosen $\beta = \gamma = 0$ then he would pass the eavesdropping check. Similarly, he can escape from the check if his choice is

$$\begin{aligned} &\alpha|e_{00}\rangle - \beta|e_{01}\rangle + \gamma|e_{10}\rangle - \delta|e_{11}\rangle \\ &\quad = \alpha|e_{00}\rangle + \beta|e_{01}\rangle - \gamma|e_{10}\rangle - \delta|e_{11}\rangle \\ &\quad = 0 \end{aligned} \tag{10.25}$$

and the decoy photons of Alice are $|+\rangle$ or $|-\rangle$. However, for $\beta = \gamma = 0$, we have $\alpha|e_{00}\rangle - \delta|e_{11}\rangle = 0$ which implies $\alpha|e_{00}\rangle = \delta|e_{11}\rangle$. That is, Bob is unable to differentiate $\delta|e_{11}\rangle$ from $\alpha|e_{00}\rangle$. Thus, he cannot measure these ancillas to get useful information about Charlie's shadow. On the other hand, if Bob wishes to make the ancillas differentiable, $\delta|e_{11}\rangle \neq \alpha|e_{00}\rangle$ then he will disturb the states of the decoy photons and will be detected in the eavesdropping check-up.

10.5.3 A Quantum Relay

To achieve a multiparty networks quantum signals have to be routed via a backbone of quantum nodes. For this quantum repeaters and relays are useful [24–26]. Working of a quantum relay over 1 km of optical fiber was reported [26]. In this relay qubits have been encoded on coherent pulses emitted by a laser. For teleportation entangled photons obtained by means of LED were used.

The experimental set-up consists of four parts: sender, Bell-state measurement (BSM), entangled LED (ELED) and receiver. Sender and receiver are separated by 1.05 km optical fiber. The ELED consists of a layer of indium arsenide quantum dots within a gallium arsenide microcavity. The ELED was driven with pulses of 0.4 V amplitude and 490 ps duration at a repetition rate of 203 MHz. Two strong light emission from individual quantum dots are observed and are designated as B ($\lambda \approx 886$ nm) and X ($\lambda \approx 888$ nm). That is, the entangled photons are divided into two parts, X and B. The X and B photons are sent to the receiver and BSM parts, respectively. At the sender section, from the continuous wave laser diode pulses are produced by an optical intensity modulator. The pulses are rotated by polarization controller (PC1) in order to encode the qubit.

At the BSM section a beam splitter (BS) is used to combine 5% of the laser photons and 95% of the B photons into one output arm. This is then sent through another polarization controller (PC2) and a polarizing beam splitter (PBS). The horizontal (H) and vertical (V) polarized photons are projected onto superconducting single photon detectors (SSPD) D1 and D2. The BSM section performs a Bell-state measurement in the state given by $(|H_{\mathrm{L}}V_{\mathrm{B}}\rangle + |V_{\mathrm{L}}H_{\mathrm{B}}\rangle)/\sqrt{2}$. Here B and L denote the photons from the biexciton and laser, respectively. The input qubits $\cos a|H_{\mathrm{L}}\rangle + \mathrm{e}^{\mathrm{i}b}\sin a|V_{\mathrm{L}}\rangle$ are teleported as $\cos a|V_X\rangle + \mathrm{e}^{\mathrm{i}b}\sin a|H_X\rangle$, where X denotes formerly entangled photon. Correlation measurements can be carried out in $\{H, V\}$ and diagonal $\{D, A\}$ linear polarization bases, where D and A denote the diagonal and anti-diagonal polarizations, respectively. Then one can find Bell's parameter to point out the degree of entanglement. For more details refer [26].

10.6 Applications of Quantum Cryptography

In this section we point out a few promising applications of quantum cryptography [27].

(i) Secure communication

The best application of cryptography [27] is to allow a secure communication. In the near future, quantum cryptography may be used in top-secret applications in the military, for example, as the basis of communication links.

(ii) Protection of private information

The second application is the protection of private information during public discussion [27]. Suppose two businessmen wish to do a joint venture—but are able to do so only if their total available capital is more than, say, 100 million. Both firms want to know if this condition is satisfied, but neither wishes to share the exact amount of capital that he is committing. In classical cryptography, the firms can only execute the deal if they have trusted intermediaries. It has been believed that quantum cryptography would be able to remove these assumptions and provide unconditional security.

(iii) Public key cryptography

Another important nonmilitary application of cryptography is *public key* cryptography. This in its classical version forms the backbone of e-commerce on the internet. Public key cryptosystems are special in that they allow two people, who have not yet met, to communicate securely by looking-up encryption methods in a public directory.

10.7 Implementation and Limitations

How do we achieve quantum cryptography in practice? The best candidates for performing the different quantum states are photons. They are easy to produce and transmit using optical fibers. Over the 20 years the attenuation of light at a wavelength of 1300 km has been reduced from several decibels per metre of fiber to just 0.35 decibels per kilometer. That is, photons can travel about 10 km in a fiber before half of them get absorbed. This is sufficient for quantum cryptography in local networks. Note that amplifiers cannot be used to transmit the photons (*why?*). There are limitations in achieving quantum cryptography in practice. They are given below [27]:

1. The current distance over which photons have been sent securely down optical fibers is at only about 50 Km and is too short.
2. The signals required for cryptography can only be sent via fibers at rates of kilobites per second. This rate is several thousands of times slower than standard single-mode optical fibers.
3. Current quantum cryptography systems are very expensive whereas present software-based encryption method are essentially free.
4. Equipment needed to prepare quantum cryptographic signals is large.

In order to overcome the above technical difficulties considerable developments are necessary before the cost and the data rate of quantum cryptographic devices can compete with conventional ones.

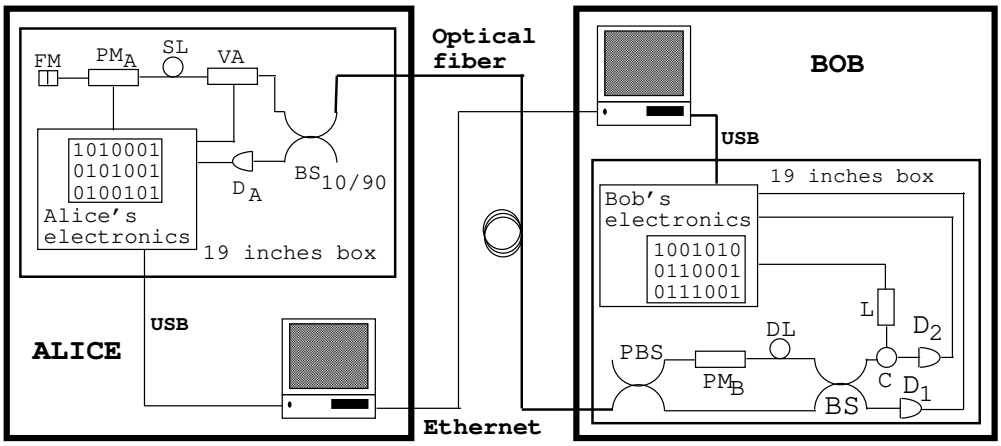

FIGURE 10.4
Schematic of the plug and play prototype quantum key distribution set-up of Stucki et al. [28]. (D. Stucki, N. Gisin, O. Guinnard, G. Ribordy and H. Zbinden, *New J. Phys.* 4:41, 2002. https://doi.org/10.1088/1367-2630/4/1/341. IOP Publishing Ltd and Deutsche Physikalische Gesellschaft. Reproduced by permission of IOP Publishing. CC BY-NC-SA.)

10.8 Fiber-Optical Quantum Key Distribution

A commercially available quantum key distribution (QKD) prototype that allows key exchange about 67 km distance was developed by Stucki et al. [28]. The block diagram of the set-up is shown in Fig. 10.4. We present the features of the system. In Fig. 10.4 BS a PBS are 50 : 50 beam splitter and a polarization beam splitter, respectively. PM_B is a phase modulator and DL is a 50 ns delay time unit. A strong laser pulse (@1550 nm) was emitted at Bob. First it was split into two pulses by the beam splitter BS. They went through a long arm and a short arm, including DL and PM_B, respectively. These two pulses were incident on the input ports of PBS. The optical elements and the fibers were maintained with polarization. In the short arm, the polarization was kept at 90°. The pulses came out from Bob's set-up through the same port of the polarization beam splitter. They travelled to Alice and first reflected on a Faraday mirror. Then they were attenuated and returned back with polarized orthogonally. Next, they followed the other path to Bob and reached at the same time at the 50 : 50 beam splitter and interfered. They were detected either in D_1 or in D_2 after allowing them to pass through the circulator C. In employing the BB84 scheme, the phase-shift of 0 and π and $\pi/2$ or $3\pi/2$ were introduced by Alice on the second pulse with PM_A. Bob used the measurement basis making a 0 or $\pi/2$-shift on the first pulse on its return. With the above, key exchange over different installed cables have been studied. Secure key exchange was successfully realized over 67 km (between Geneva and Lausanne).

10.9 Quantum Cheque Scheme

In 1969 Stephen Wiesner [29] introduced the idea of quantum money. A quantum cheque scheme (QCS) was proposed [30]. In this scheme a bank acts as a centre of key generation

and gives a quantum analogue of the cheque book secretly to its account holders. An account holder can issue cheques and they can be verified by the bank or any of its branches with which the bank accepts to share a classical communication channel. Quantum cheques can be realized through physical devices with the use of quantum memories. Before presenting the QCS, let us present the cryptographic tools needed to realize it.

A. Quantum One Way Functions

We can define a quantum one way function as $\Psi : k \times |0\rangle^{\otimes n} \longrightarrow |\psi_k\rangle$, where $k \in \{0,1\}^*$ and $|\psi_k\rangle$ is a n-qubit quantum state. Further, assume that

1. Ψ is easy to compute, for example, through a polynomial-time algorithm. It is possible to evaluate $\Psi(k, |0\rangle^{\otimes n})$ and get the outputs $|\psi_k\rangle$ and
2. Ψ is difficult to invert, that is, it is difficult to compute k if $|\psi_k\rangle$ is given.

B. Digital Signatures

A digital signature scheme Π is essentially a 6-tuple $(M, \sum, U, G, S, V)$ where

- M is a finite set of valid messages,
- $\sum$ is a finite set of valid signatures,
- U is a finite set of users,
- G is a key generation algorithm which takes a security parameter 1^k and provides the outputs S, V algorithms and the public parameters,
- S is the signing algorithm and is a mapping: $M \times U \to \sum$ and
- V is the verification algorithm and $V : M \times \sum \times U \to \{\text{True, False}\}$.

For all k and $m \in M$ and for users i and j we have $V_j(m, S_i(m), U_i) = \text{True}$. For an adversary it would be impossible to produce a valid signature except with an inappreciable probability. Similarly, the signer would not be able to deny a legitimate signature except with an inappreciable probability.

C. Quantum Cheque

The essential properties of a cheque are:

1. The authenticity of a cheque can be verified by a trusted bank or its branches.
2. After issuing a cheque the issuer must not be able to disapprove it.
3. An adversary will not be able to counterfeit the issued cheque.
4. An adversary will not be able to use a cheque more than once to withdraw money.

A typical QCS consists of the following three stages:

1. G: With a security parameter as an input a cheque book and a key for the user are probabilistically generated.
2. S: A quantum state χ called a *cheque* is produced considering the key of the issuer and the amount to be signed as inputs.
3. V: The validity of the cheque is decided treating the key of the user and the cheque as the inputs.

D. Scheme

For simplicity let us consider the scheme with the parties Alice (customer), Bob (vendor) and the bank. The branches of the bank are assumed to be connected to the main branch of the bank through a securred classical channel. Here by bank we refers to the main branch of the bank. The trusted party is the main branch.

Alice issues a cheque to Bob who then submits it to the bank or to one of its branches to encash. Bank verifies the validity of the cheque. The G, S and V schemes are described in the following.

G: Alice and the bank share a key, say, k, only once using an efficient protocol like BB84 or by any other securred manner. They agree on a secure digital signature scheme $\Pi = (G, S, V)$. Alice submit her public key pk to the bank and also stores secretly her private key sk.

The bank then prepares a string of l, say, GHZ, states as

$$\begin{aligned} |\phi^{(i)}\rangle_{\mathrm{GHZ}} &= \frac{1}{\sqrt{2}}\Big[|0^{(i)}\rangle_{\mathrm{A}_1}|0^{(i)}\rangle_{\mathrm{A}_2}|0^{(i)}\rangle_{\mathrm{B}} \\ &\quad +|1^{(i)}\rangle_{\mathrm{A}_1}|1^{(i)}\rangle_{\mathrm{A}_2}|1^{(i)}\rangle_{\mathrm{B}}\Big], \end{aligned} \tag{10.26}$$

where $1 \leq i \leq l$. The bank has $\left(id,\, pk,\, k,\, s,\, \left\{|\phi^{(i)}\rangle_{\mathrm{B}}\right\}_{i=1:l}\right)$ while Alice has $\left(id,\, pk,\, sk,\, k,\, s\, \left\{|\phi^{(i)}\rangle_{\mathrm{A}_1}, |\phi^{(i)}\rangle_{\mathrm{A}_2}\right\}_{i=1:l}\right)$ and

$$\left\{|\phi^{(i)}\rangle_{\mathrm{GHZ}}\right\}_{i=1:l} \equiv \left\{|\phi^{(1)}\rangle_{\mathrm{GHZ}},\ |\phi^{(2)}\rangle_{\mathrm{GHZ}}, \ldots, |\phi^{(l)}\rangle_{\mathrm{GHZ}}\right\}. \tag{10.27}$$

id is the identity of Alice.

S: Alice, to issue a cheque for an anount M, generates a random number $r \leftarrow U_{\{0,1\}^l}$ and prepares a n-qubit state

$$|\psi_{\mathrm{A}}\rangle = f(k||id||r||M), \tag{10.28}$$

where $f : \{0,1\}^* \times |0\rangle^{\otimes n} \to |\psi\rangle$ is a quantum one way function and $x||y$ denotes concatenation of two bit-strings x and y.

Alice also generates l states $\left\{\left|\psi_{\mathrm{M}}^{(i)}\right\rangle\right\}_{i=1:l}$ for the amount M using $g : \{0,1\}^* \times |0\rangle \to |\psi\rangle$ as

$$\left|\psi_{\mathrm{M}}^{(i)}\right\rangle = g(r||M||i), \quad 1 \leq i \leq l. \tag{10.29}$$

Alice creates a cheque using one of her entangled qubits $|\phi^{(i)}\rangle_{\mathrm{A}_1}$ to encode $\left|\psi_{\mathrm{M}}^{(i)}\right\rangle$. The ith qubit $\left|\psi_{\mathrm{M}}^{(i)}\right\rangle = \alpha_i|0\rangle + \beta_i|1\rangle$ can be encoded with the ith GHZ state. Alice combines $\left|\psi_{\mathrm{M}}^{(i)}\right\rangle$ and one of the $|\phi^{(i)}\rangle_{\mathrm{A}_1}$ and perform a Bell measurement on the above two. The resulting entangled state is

$$\begin{aligned} |\phi^{(i)}\rangle &= \left|\psi_{\mathrm{M}}^{(i)}\right\rangle \otimes |\phi\rangle_{\mathrm{GHZ}} \\ &= \frac{1}{2}\left\{|\Psi^+\rangle_{\mathrm{A}_1}\left(\alpha_i|00\rangle_{\mathrm{A}_2B} + \beta_i|11\rangle_{\mathrm{A}_2B}\right)\right. \\ &\quad +|\Psi^-\rangle_{\mathrm{A}_1}\left(\alpha_i|00\rangle_{\mathrm{A}_2B} - \beta_i|11\rangle_{\mathrm{A}_2B}\right) \\ &\quad +|\Phi^+\rangle_{\mathrm{A}_1}\left(\beta_i|00\rangle_{\mathrm{A}_2B} + \alpha_i|11\rangle_{\mathrm{A}_2B}\right) \\ &\quad \left.+\ |\Phi^-\rangle_{\mathrm{A}_1}\left(\beta_i|00\rangle_{\mathrm{A}_2B} - \alpha_i|11\rangle_{\mathrm{A}_2B}\right)\right\}. \end{aligned} \tag{10.30}$$

In Eq. (10.30) $|\Psi^{\pm}\rangle$ and $|\Phi^{\pm}\rangle$ are the Bell states measured by Alice. When the result of Alice is $|\Psi^{+}\rangle$ or $|\Psi^{-}\rangle$ then the density matrix ρ_{B} of the GHZ particle of the bank is

$$\rho_{\mathrm{B}} = |\alpha_i|^2 |0\rangle_{\mathrm{BB}}\langle 0| + |\beta_i|^2 |1\rangle_{\mathrm{BB}}\langle 1|. \tag{10.31}$$

For the case of $|\Phi^{+}\rangle$ or $|\Phi^{-}\rangle$

$$\rho_{\mathrm{B}} = |\beta_i|^2 |0\rangle_{\mathrm{BB}}\langle 0| + |\alpha_i|^2 |1\rangle_{\mathrm{BB}}\langle 1|. \tag{10.32}$$

Alice then carry out a gate operation depending upon the observed Bell state accordingly as

$$|\Psi^{+}\rangle \to I, \quad |\Psi^{-}\rangle \to \sigma_z, \quad |\Phi^{+}\rangle \to \sigma_x, \quad |\Phi^{-}\rangle \to \sigma_y. \tag{10.33}$$

Alice produces a quantum cheque

$$\chi = \left(id, s, r, \sigma, M, \left\{|\phi^{(i)}\rangle_{A_2}\right\}_{i=1:l}, |\psi_A\rangle\right) \tag{10.34}$$

and passes it to Bob.

V: When the quantum cheque is submitted for encash the validity of (id, s) pair is to be checked with the main branch and to be verified using $V_{pk}(\sigma, s)$. In case (id, s) and σ are invalid then the cheque is to be destroyed otherwise the process is to be continued.

For a valid cheque the main branch makes a measurement on its copy of $|\phi\rangle_{\mathrm{B}}$, gets $|+\rangle$ or $|-\rangle$ and sends the outcomes securely to the relevant branch. The branch in turn to recover $\left|\psi_M^{(i)}\right\rangle$ performs the Pauli matrix on $|\phi^{(i)}\rangle_{\mathrm{A}_2}$: $|+\rangle \to I$, $|-\rangle \to \sigma_z$. $\left\{\left|\psi_M^{(i)}\right\rangle\right\}_{i=1:l}$ is recovered by performing the above l times for each of $\left\{|\phi^{(i)}\rangle_{\mathrm{A}_2}\right\}_{i=1:l}$.

The bank

(a) determines $\left\{\left|\psi_M^{\prime(i)}\right\rangle\right\}_{i=1:l} = \{g(r\|M\|i\}_{i=1:l}$ and executes a swap test on $\left\{\left|\psi_M^{\prime(i)}\right\rangle\right\}$ and $\left\{\left|\psi_M^{(i)}\right\rangle\right\}$ and

(b) determines $|\psi'_{\mathrm{A}}\rangle = f(k\|id\|r\|M)$ and executes a nondestructive swap test on $|\psi_{\mathrm{A}}\rangle$ and $|\psi'_{\mathrm{A}}\rangle$.

If $\langle\psi_{\mathrm{A}}|\psi'_{\mathrm{A}}\rangle \geq \kappa_1$ and $\left\{\left\langle\psi_M^{(i)}\middle|\psi_M^{\prime(i)}\right\rangle \geq \kappa_2\right\}_{i=1:l}$, where κ_1 and κ_2 are the thresholding constants, then the cheque is accepted otherwise the cheque is destroyed and the transaction is terminated.

For a discussion on the security of the quantum cheque scheme with reference to the impossibility of counterfeiting and the impossibility of nonrepudiation by signatory one may refers to the ref. [30].

10.10 Concluding Remarks

Quantum cryptography is the first application of quantum mechanics at the single-quantum level. It is based on a beautiful combination of concepts from information theory and quantum physics. Progress in quantum cryptography is found to be rapid. Several researchers

have proved that it is indeed possible to send messages securely with different protocols in the presence of noise. Information has been sent over a distance of a few kilometers through the open air. Real experiments to transmit quantum signals to satellites have also been proposed. Most of the difficulties mentioned earlier can be overcome. Several groups are actively involved in solving them. In a short time, it is highly feasible that quantum cryptography will be absorbed for top-secret applications. In the past, some classical cryptosystems have been broken. This would be impossible if the quantum cryptography is implemented.

A quantum cryptosystem can be of use to design smart cards authenticate ID and medical IC smart cards, withdrawals, deposits and transfers. The quantum cryptosystem can greatly enhance the security of smart cards and more over it can avoid calculations. In view of this a processor will not be needed and manufacturing cost can be considerably decreased. A quantum cryptosystem can be utilized to develop an information security software system [31–33] which can improve for example e-commerce technology [34,35], national defence and expected to promote development of high technology.

10.11 Bibliography

[1] A.J. Menezes, P.C. van Oorschot and S.A. Vanstone, *Handbook of Applied Cryptography.* CRC Press, New York, 1996.

[2] D.R. Stinson, *Cryptography: Theory and Practice.* Chapman & Hall/CRC Press, New York, 2006.

[3] J. Katz and Y. Lindell, *Introduction to Modern Cryptography.* Chapman & Hall/CRC Press, New York, 2007.

[4] G.V. Assche, *Quantum Cryptography and Secret-Key Distillation.* Cambridge University Press, Cambridge, 2006.

[5] A.V. Sergienko (Ed.), *Quantum Communications and Cryptography.* CRC Press, New York, 2006.

[6] D.J. Bernstein, J. Buchmann and E. Dahmen (Eds.), *Post Quantum Cryptography.* Springer, Berlin, 2009.

[7] N. Gisin, G. Ribordy, W. Tittel and H. Zbinden, *Rev. Mod. Phys.* 74:145, 2002.

[8] W. Tittel, G. Ribordy and N. Gisin, *Phys. World*, March 1998, pp.41.

[9] S. Weisner, *SIGACT News* 15:78, 1983.

[10] C.H. Bennett, G. Brassard, *Quantum cryptography: Public key distribution and coin tossing*. In the Proceedings of IEEE International Conference on Computers Systems and Signal Processing 175:175, 1984.

[11] C.H. Bennett, F. Bessette, G. Brassard, L. Salvail and J. Smolin, *J. Cryptol.* 5:3, 1992.

[12] C.H. Bennett, G. Brassard and A.K. Ekert, *Sci. Am.* 267:50, 1992.

[13] W. Diffie and M.E. Hellman, *IEEE Trans. Inf. Theory* 22:644, 1976.

[14] R.L. Rivest, A. Shamir and L. Adleman, *Commun. ACM* 21:120, 1978.

[15] R.L. Rivest, A. Shamir and L.M. Adleman, *On digital signatures and public key cryptosystems*. In MIT Laboratory for Computer Science, Technical Report, MIT/ LCS/TR- 212, January 1979.

[16] B. Huttner, N. Imoto, N. Gisin and T. Mor, *Phys. Rev. A* 51:1863, 1995.

[17] S. Goldwater, Quantum cryptography and privacy amplification; http://www.ai.sri.com/~goldwate/quantum.

[18] C.H. Bennett, *Phys. Rev. Lett.* 68:3121, 1992.

[19] A.K. Ekert, *Phys. Rev. Lett.* 67:661, 1991.

[20] K.W.C. Chan, M.E. Rifai, P. Verma, S. Kak and Y. Chen, *Multi-photon quantum key distribution based on double-lock encryption*. In 2015 Conference on Lasers and Electro-Optics (CLEO), 2015, pp.1-2, doi: 10.1364/CLEO_QELS.2015.FF1A.3.

[21] G. Gan, *Commun. Theor. Phys.* 52:421, 2009.

[22] S. Ying, W.Q. Yan and Z.F. Chen, *Commun. Theor. Phys.* 54:89, 2010.

[23] T. Hwang, C.C. Hwang and C.M. Li, *Phys. Scr.* 83:045004, 2011.

[24] H.J. Briegel, W. Dur, J.I. Cirac and P. Zoller, *Phys. Rev. Lett.* 81:5932, 1998.

[25] H. de Riedmatten, I. Marcikic, W. Tittel, H. Zbinden, D. Collins and N. Gisin, *Phys. Rev. Lett.* 92:047904, 2004.

[26] C. Varnava, R.M. Stevenson, J. Nilsson, J. Skiba-Szymanska, B. Dzurnak, M. Lucamarini, R.V. Penty, I. Farrer, D.A. Ritchie and A.J. Shields, *NPJ Quant. Infor.* 2:16006, 2016.

[27] Hoi-Kwong Lo, *Phys. World*, June 2000, pp.17-18.

[28] D. Stucki, N. Gisin, O. Guinnard, G. Ribordy and H. Zbinden, *New J. Phys.* 4:41, 2002.

[29] S. Wiesner, *ACM Sigact News* 15:78, 1983.

[30] S.R. Moulick and P.K. Panigrahi, *Quantum Inf. Process* 15:2475, 2016.

[31] A.S.F. Obada, S. Furuichi, H.F. Abdel-Hameed and M. Absel-Afy, *Infor. Sci.* 162:53, 2004.

[32] D. Dimitrovski, J. Pop-Jordanov, N. Pop-Jordanava and E.A. Solovev, *Infor. Sci.* 168:267, 2004.

[33] M. Demirci and Z. Eken, *Infor. Sci.* 177:150, 2007.

[34] C.I. Fan, *Infor. Sci.* 176:263, 2006.

[35] B.B. Anderson, J.V. Hansen, P.B. Lowry and S.L. Summers, *Infor. Sci.* 176:1045, 2006.

10.12 Exercises

10.1 Distinguish quantum cryptanalysis from cryptanalysis.

10.2 Draw a typical block diagram of a quantum cryptosystem.

10.3 List out the negative rules of quantum mechanics on things that cannot be performed. State which one of them is sufficient for quantum cryptography.

10.4 In the two agent (the agents are, say, Bob and Charlie), quantum secret sharing scheme Alice prepared a sequence of pure entangled photon pairs. Each pair is in one of the following states:

$$\begin{aligned} |\phi\rangle_{\mathrm{BC}} &= (\alpha|0\,0\rangle + \beta|1\,1\rangle)_{\mathrm{BC}}\,, \\ |\phi'\rangle_{\mathrm{BC}} &= (\alpha|1\,1\rangle + \beta|0\,0\rangle)_{\mathrm{BC}}\,, \\ |\psi\rangle_{\mathrm{BC}} &= (\alpha|0\,1\rangle + \beta|1\,0\rangle)_{\mathrm{BC}}\,, \\ |\psi'\rangle_{\mathrm{BC}} &= (\alpha|1\,0\rangle + \beta|0\,1\rangle)_{\mathrm{BC}}\,, \quad |\alpha|^2 + |\beta|^2 = 1. \end{aligned}$$

Write the above states for the case of M agents B_1, B_2,...,B_M.

10.5 What do you understand by symmetric encryption and asymmetric encryption? Explain.

10.6 Can an undetectable eavesdropper extract any message from the B92 protocol?

10.7 The photons are assigned a value of 0 for polarizations − and / and 1 for polarizations | and \ in BB84 protocol. Alice sends a set of random bits in a set of random basis as given below.

Alice's random bits	1	0	0	1	0	1	1	0
Alice's random basis	×	+	×	×	×	+	+	+

Eve measures the photon polarization in a random basis and sends the photons of polarization states as shown below.

Eve's random basis	×	+	+	+	×	×	+	+
Polarization measured and sent by Eve	\	−	−	−	/	/	\	−

Bob measures the polarization in a random basis as given below.

Bob's random basis	+	×	×	×	+	×	+	+
Polarization measured	−	\	/	/	|	/	|	−

What is the secret key found after the public discussion of Alice and Bob of the basis and the error introduced in the key due to Eve's measurement?

10.8 For the $4 + 2$ states protocol determine $P(j/\alpha)$.

10.9 An unpolarized light is first passed through a vertical polarization filter and then through another vertically polarized light. Sketch this two set-up and state the outcome.

10.10 An unpolarized light is first passed through a horizontal polarization filter and then through a vertical polarization filter. Sketch this set-up and state the outcome.

Taylor & Francis
Taylor & Francis Group
http://taylorandfrancis.com

11

No-Cloning Theorem and Quantum Cloning Machines

11.1 Introduction

Quantum mechanics is a linear theory. So, a quantum state is a superposition state. In classical information theory the bits 0 and 1 carry information. But in quantum information theory a qubit is a superposition of the two states $|0\rangle$ and $|1\rangle$. A general qubit takes the form $\alpha|0\rangle+\beta|1\rangle$ with $|\alpha|^2+|\beta|^2=1$. Any measurement by an operator on this superposition state will lead to collapse of the quantum state to any of its eigenstate with a probability. Consequently, a quantum state cannot be copied like a classical state. Any arbitrary qubit cannot be duplicated without destroying the original. William Wooters and Wojciech Zurek [1] proved this impossibility by copying a quantum state wave function and it is called *no-cloning theorem*. It leads to a lot of consequences in quantum information processing. Due to this theorem a string of qubits cannot be processed more than one way. But this feature of quantum mechanics helps quantum cryptography as there is no way for someone to perfectly copy the quantum information. No-cloning theorem makes it possible to detect any eavesdropper on a quantum communication channel.

Let U be a quantum operation which duplicates an arbitrary pure state $|\psi\rangle$ as [2]

$$U\left(|\psi\rangle\otimes|R\rangle\otimes|M\rangle\right)=|\psi\rangle\otimes|\psi\rangle\otimes|M(\psi)\rangle. \tag{11.1}$$

$|R\rangle$ is an unknown initial state of the cloning machine and $|M\rangle$ is the initial state of the axiliary state (ancilla). The axiliary state $|M(\psi)\rangle$ is obtained after operation and it depends on $|\psi\rangle$. If there exists such a machine to perform U then any number of copies of $|\psi\rangle$ can be obtained. But no-cloning theorem says that such a machine cannot be built. This limitation arises, not due to the experimental limitations of designing such a machine but due to the inherent properties of quantum states.

This chapter begins by providing proofs of no-cloning and no-broadcasting theorems. Then the features of some of the quantum cloning machines are presented. Next, a tele-cloning scheme that can teleport an unknown 1-qubit to M associates is considered. Finally, certain no-go theorems are defined.

11.2 Proof of No-Cloning Theorem

No-cloning theorem states that no quantum operation exists which can perfectly and deterministically duplicate a pure state. We give here two methods to prove the theorem [2].

DOI: 10.1201/9781003172192-11

Method-1

This was given first by Wooters and Zurek [1] and also by Dennis Geert Bernardus Johan Dieks [3]. It makes use of linearity of quantum mechanics. Let us assume a perfect cloning machine which can copy an arbitrary quantum state $|\psi\rangle$ as

$$|\psi\rangle|\Sigma\rangle|M\rangle \rightarrow |\psi\rangle|\psi\rangle|M(\psi)\rangle \tag{11.2}$$

exists. As given in Eq. (11.1) $|\Sigma\rangle$ is a blank state (onto which one could copy an unknown state) and $|M\rangle$ is the state of the auxiliary system. Such a cloning machine will copy

$$|0\rangle|\Sigma\rangle|M\rangle \rightarrow |0\rangle|0\rangle|M(0)\rangle, \quad |1\rangle|\Sigma\rangle|M\rangle \rightarrow |1\rangle|1\rangle|M(1)\rangle. \tag{11.3}$$

As quantum mechanics admits the superposition state $|\phi\rangle = \alpha|0\rangle + \beta|1\rangle$ this cloning machine will give

$$(\alpha|0\rangle + \beta|1\rangle)|\Sigma\rangle|M\rangle \rightarrow \alpha|00\rangle|M(0)\rangle + \beta|11\rangle|M(1)\rangle. \tag{11.4}$$

But $|\phi\rangle = \alpha|0\rangle + \beta|1\rangle$ is a pure state. Therefore,

$$|\phi\rangle|\Sigma\rangle|M\rangle \xrightarrow{U} \left(\alpha^2|00\rangle + \alpha\beta|01\rangle + \beta\alpha|10\rangle + \beta^2|11\rangle\right)|M(\phi)\rangle, \tag{11.5}$$

where U is the unitary cloning operator. Right-hand-side of Eq. (11.5) is not equal to the right-hand-side of Eq. (11.4). So it can be concluded that our assumption of a cloning machine with operation given by Eq. (11.2) does not exist.

Method-2

This method makes use of the properties of operators to prove the no-cloing theorem. Horace Pak-Hong Yuen [4] proposed first this proof. Suppose the quantum cloner is prepared in a state $|s\rangle$ which does not depend on the unknown state $|\psi\rangle$ to be copied. Let $|0\rangle$ be a known state of a particle onto which the information has to be copied and U be the unitary cloning operator. Denote the state of the quantum copies after $|\psi\rangle$ and $|\overline{\psi}\rangle$ have been cloned as $|s'\rangle$ and $|s''\rangle$, respectively. The cloning process for the two initial states $|\psi\rangle$ and $|\overline{\psi}\rangle$ are written as

$$U(|\psi\rangle|0\rangle|s\rangle) = |\psi\rangle|\psi\rangle|s'\rangle, \tag{11.6}$$

$$U(|\overline{\psi}\rangle|0\rangle|s\rangle) = |\overline{\psi}\rangle|\overline{\psi}\rangle|s''\rangle. \tag{11.7}$$

Equation (11.7) can be rewritten as

$$(\langle s|\langle 0|\langle\overline{\psi}|)U^{-1} = \langle s''|\langle\overline{\psi}|\langle\overline{\psi}|. \tag{11.8}$$

Multiplication of Eq. (11.6) by Eq. (11.8) gives

$$\langle\overline{\psi}|\psi\rangle = \langle\overline{\psi}|\psi\rangle^2\langle s''|s'\rangle. \tag{11.9}$$

Since the magnitude of $\langle\overline{\psi}|\psi\rangle$ and $\langle s''|s'\rangle$ must be ≤ 1 Eq. (11.9) is satisfied only if $|\langle\overline{\psi}|\psi\rangle| = |\langle s''|s'\rangle| = 1$ or zero. Therefore, perfect cloning is possible only if $|\psi\rangle$ and $|\overline{\psi}\rangle$ are either orthogonal or identical. Thus, we conclude that ideal cloning device for arbitrary states does not exist.

The no-cloning theorem is manifested in several versions. In terms of CNOT gate we have the relations [2]

$$CNOT(\sigma_x \otimes I)CNOT = \sigma_x \otimes \sigma_x, \tag{11.10a}$$

$$CNOT(I \otimes \sigma_x)CNOT = I \otimes \sigma_x, \tag{11.10b}$$

$$CNOT(\sigma_z \otimes I)CNOT = \sigma_z \otimes I, \tag{11.10c}$$

$$CNOT(I \otimes \sigma_z)CNOT = \sigma_z \otimes \sigma_z. \tag{11.10d}$$

These relations imply that the bit flip operation can be copied from first qubit to the second qubit and the phase flip operation can be copied backwards. However, they cannot be copied simultaneously.

11.3 No-Broadcasting Theorem

We have seen that no-cloning theorem is applicable only to pure states. It is impossible to clone a mixed state described by the density matrix [5]. As pure states and mixed states exclude each other, none of the proof for these two classes of states can be derivable from one another. We give below the original no-broadcasting theorem for the non-commuting states proposed in [5].

Let AB be a composite quantum system having two parts A and B. A is prepared in one of the states $\{\sigma_i\}$ while B is prepared in the blank state τ. A general broadcasting machine copies a state of the unknown quantum system to be broadcasted to a target system. If $\mathcal{G}$ is the quantum operation performed on the composite system AB as

$$\sigma_k \otimes \tau \longrightarrow \mathcal{G}(\sigma_k \otimes \tau) = \rho_k^{\text{out}} \tag{11.11}$$

and the output state satisfies

$$\text{Tr}_a \rho_k^{\text{out}} = \sigma_k \text{ and } \text{Tr}_b \rho_k^{\text{out}} = \sigma_k \tag{11.12}$$

then we say that $\mathcal{G}$ broadcasts the set of states $\{\sigma_i\}$.

Barnum's theorem [5] states that a set of states $\{\sigma_i\}$ can be broadcasted *if and only if the states* $\{\sigma_i\}$ *commute with each other*. This proof closely follows the proof given in [6], where the property of relative entropy from the fundamental principle of information theory has been used. This theorem has been proved in certain ways [2,5–8]. We give the proof of the theorem given in [2], where the set $\{\sigma_i\}$ is considered to have only two states σ_1 and σ_2.

Let us give the proof for the *if* part first. As σ_1 and σ_2 commute they have simultaneous eigenfunctions. Let $\{|i\rangle\}$ be their simultaneous eigenfunctions. So σ_1 and σ_2 can be expressed in the same orthogonal basis $\{|i\rangle\}$ as

$$\sigma_k = \sum_i \lambda_{k,i} |i\rangle\langle i|, \quad k = 1, 2. \tag{11.13}$$

$\{|i\rangle\}$ is an orthonormal set for the cloning operation $\mathcal{G}$. Therefore, we get

$$\rho_k^{\text{out}} = \mathcal{G}\left(\sigma_k \otimes \tau\right) = \sum_i \lambda_{k,i} |ii\rangle\langle ii|, \quad k = 1, 2. \tag{11.14}$$

Taking the trace for the source state and the target state we have

$$\text{Tr}_a \rho_k^{\text{out}} = \sigma_k \text{ and } \text{Tr}_b \rho_k^{\text{out}} = \sigma_k. \tag{11.15}$$

We find that σ_1 and σ_2 are broadcasted by the broadcasting operator $\mathcal{G}$.

Next, we give the proof for *only if* part of the Barnum's theorem. This proof is based on the concept of relative entropy [9]. The relative entropy of a state ρ_1 with respect to another ρ_2 is defined as

$$S(\rho_1|\rho_2) = \text{Tr}\left[\rho_1 \left(\ln \rho_1 - \ln \rho_2\right)\right]. \tag{11.16}$$

It measures the closeness between ρ_1 and ρ_2. For pair of states which are perfectly distinguishable $S(\rho_1|\rho_2) = \infty$. We consider only the cases where $S < \infty$. With $\rho_1^{\text{in}} = \sigma_1 \otimes \tau$ and $\rho_2^{\text{in}} = \sigma_2 \otimes \tau$, we obtain

$$\begin{aligned} S(\rho_1|\rho_2) &= \text{Tr}\left[\sigma_1 \otimes \tau \left(\ln \sigma_1 \oplus \ln \tau - \ln \sigma_2 \oplus \ln \tau\right)\right] \\ &= \text{Tr}_a\left[\sigma_1 \left(\ln \sigma_1 - \ln \sigma_2\right)\right] \text{Tr}_b \tau \\ &= \text{Tr}_a\left[\sigma_1 \left(\ln \sigma_1 - \ln \sigma_2\right)\right] \\ &= S(\sigma_1|\sigma_2). \end{aligned} \tag{11.17}$$

Equation (11.17) proves that the relative entropy of the two initial states is exclusively given by the relative entropy of the two source systems. As the cloning operation $\mathcal{G}$ is a unitary operation U, on the input state ρ_a^{in} and the ancillary state Σ, we can write

$$\rho_k^{\text{out}} = U\left(\rho_k^{\text{in}} \otimes \Sigma\right) U^\dagger. \tag{11.18}$$

Using Eq. (11.18) we can prove

$$S(\sigma_1|\sigma_2) = S\left(\rho_1^{\text{in}}|\rho_2^{\text{in}}\right) = S\left(\rho_1^{\text{out}}|\rho_2^{\text{out}}\right). \tag{11.19}$$

The relative entropy of the final states of any two broadcasting processes is equal to the relative entropy of the sources prior to copying. We can prove that Eq. (11.19) is violated using the theorem of monotonicity of relative entropy [10]. With ρ_1^b denoting the reduced density matrix of the composite system ρ_1^{ab}, this theorem states

$$S\left(\rho_1^{ab}|\rho_2^{ab}\right) \geq S\left(\rho_1^b|\rho_2^b\right). \tag{11.20}$$

The equality holds if and only if

$$\ln \rho_1^{ab} - \ln \rho_2^{ab} = I^a \otimes \left[\ln \rho_1^b - \ln \rho_2^b\right], \tag{11.21}$$

where I^a denotes the identity operator of the subsystem a. Then

$$S\left(\rho_1^{\text{out}}|\rho_2^{\text{out}}\right) \geq \left(\rho_1^{k,\text{out}}|\rho_2^{k,\text{out}}\right), \quad k = a, b \tag{11.22}$$

and $\rho_i^{k,\text{out}} = \text{Tr}_{a(b)} \rho_i^{\text{out}}$. In this case the equality holds if and only if

$$\begin{aligned} \ln \rho_1^{\text{out}} - \ln \rho_2^{\text{out}} &= \left(\ln \rho_1^{a,\text{out}} - \ln \rho_2^{a,\text{out}}\right) \otimes I^b \\ &= I^a \otimes \left(\ln \rho_1^{b,\text{out}} - \ln \rho_2^{b,\text{out}}\right). \end{aligned} \tag{11.23}$$

This equation under broadcasting becomes

$$\ln \rho_1^{\text{out}} - \ln \rho_2^{\text{out}} = \left(\ln \sigma_1 - \ln \sigma_2\right) \otimes I^b = I^a \otimes \left(\ln \sigma_1 - \ln \sigma_2\right). \tag{11.24}$$

Equation (11.24) will be satisfied only when σ_1 and σ_2 are diagonal or they can be diagonalized in the same eigenfunction space. So, σ_1 and σ_2 must commute. We proved that a realization of a broadcasting machine may be possible only provided all its input states are mutually commuting. For any two non-commuting arbitrary states, the inequality in Eq. (11.20) holds good in contradiction with Eq. (11.19). No-broadcasting is possible as the monotonicity of relative entropy is in conflict with quantum dynamics. No-broadcasting theorem can also be extended to the case of $S(\rho_1|\rho_2) = \infty$ [6].

Solved Problem 1:

Prove that $S\left(\rho_1^{\text{out}}|\rho_2^{\text{out}}\right) = S\left(\rho_1^{\text{in}}|\rho_2^{\text{in}}\right)$.

We obtain

$$\begin{aligned} S\left(\rho_1^{\text{out}}|\rho_2^{\text{out}}\right) &= \text{Tr}\left[\rho_1^{\text{out}}\left(\ln\rho_1^{\text{out}} - \ln\rho_2^{\text{out}}\right)\right] \\ &= \text{Tr}\left[U\left(\rho_1^{\text{in}}\otimes\Sigma\right)U^\dagger\left(\ln\left(U\rho_1^{\text{in}}\otimes\Sigma U^\dagger\right) - \ln\left(U\rho_2^{\text{in}}\otimes\Sigma U^\dagger\right)\right)\right] \\ &= \text{Tr}\left[U\rho_1^{\text{in}}\otimes\Sigma U^\dagger\ln\left(U\rho_1^{\text{in}}\otimes\Sigma U^\dagger\right)\right. \\ &\qquad \left. -U\rho_1^{\text{in}}\otimes\Sigma U^\dagger\ln\left(U\rho_2^{\text{in}}\otimes\Sigma U^\dagger\right)\right] \\ &= \text{Tr}\left[\rho_1^{\text{in}}\otimes\Sigma\ln\left(\rho_1^{\text{in}}\otimes\Sigma\right)U^\dagger U - \rho_1^{\text{in}}\otimes\Sigma\ln\left(\rho_2^{\text{in}}\otimes\Sigma\right)U^\dagger U\right]. \end{aligned}$$

As $U^\dagger U = I$ we get

$$\begin{aligned} S\left(\rho_1^{\text{out}}|\rho_2^{\text{out}}\right) &= \text{Tr}\left[\rho_1^{\text{in}}\otimes\Sigma\left(\ln\left(\rho_1^{\text{in}}\otimes\Sigma\right) - \ln\left(\rho_2^{\text{in}}\otimes\Sigma\right)\right)\right] \\ &= \text{Tr}\left[\rho_1^{\text{in}}\left(\ln\rho_1^{\text{in}} - \ln\rho_2^{\text{in}}\right)\right]\text{Tr}\Sigma \\ &= \text{Tr}\left[\rho_1^{\text{in}}\left(\ln\rho_1^{\text{in}} - \ln\rho_2^{\text{in}}\right)\right] \\ &= S\left(\rho_1^{\text{in}}|\rho_2^{\text{in}}\right). \end{aligned} \tag{11.25}$$

11.4 No-Cloning and No-Superluminar Signalling

According to relativity, no superluminar signalling (faster-than-light) is physically possible. Let a composite system AB is in an entangled state then any action on system B which takes place and is completed at a space-like separation from system A affects this system instantaneously. It has been thought that this instantaneous repsonse of observer A with a space-like separation from B for the action at B can be used for faster-than-light signalling.

A large number of proposals taking advantage of entanglement and the collapse of the wave packet upon measurement appeared in the literature. Those proposals aimed to exploit this possibility for superluminal communication and to prove the incompatability of quantum mechanics with special theory of relativity. In 1982 Nick Herbert [11] proposed an interesting and quite a different way for faster-than-light signalling by using a hypothetical machine which could perform the task of creating many copies of an arbitrary state of quantum system. This suggestion triggered the derivation of no-cloning theorem which proved that the proposal of Herbert was unviable.

Let us outline the idea of the proposal of Herbert [2]. Assume that Alice and Bob separated at an arbitrary distance (even the distance may be space-like) share a pair of entangled qubits in the state $|\psi^-\rangle = (|01\rangle - |10\rangle)/\sqrt{2}$. Alice can measure her qubit using σ_x or σ_z If σ_z is measured in $|\psi^-\rangle$ then there is a probability of 50% for Alice qubit to collapse to the state $|0\rangle$ or $|1\rangle$. So, this measurement by Alice prepares the qubit of Bob in the state $|1\rangle$ if Alice's measurement collapses her state to $|0\rangle$ and in the state $|0\rangle$ if the measurement of Alice collapses her state to $|1\rangle$. Therefore, without knowing the results of the measurement of Alice the density matrix of qubit of Bob is $\frac{1}{2}|0\rangle\langle 0| + \frac{1}{2}|1\rangle\langle 1| = I/2$.

Now, suppose Alice measures σ_x. The qubit of Alice will collapse to one of its eigenvectors $|\phi_{x+}\rangle = (|0\rangle + |1\rangle)/\sqrt{2}$ or $|\phi_{x-}\rangle = (|0\rangle - |1\rangle)/\sqrt{2}$. Then the qubit of Bob is prepared in the state $|\phi_{x-}\rangle$ or $|\phi_{x+}\rangle$, respectively. In this case also the density matrix of qubit of Bob is $\frac{1}{2}|\phi_{x+}\rangle\langle\phi_{x+}| + \frac{1}{2}|\phi_{x-}\rangle\langle\phi_{x-}| = I/2$. So, Bob gets no information about the measurement made by Alice as Bob gets the same density matrix for both σ_z and σ_x measurements of Alice.

Imagine a perfect cloning machine is available to Bob. He can then make arbitrary many copies of his qubit and able to determine the exact state of his qubit, that is, whether an eigenstate of σ_z or σ_x. Using this information Bob can know the type of measurement Alice has done. As no-cloning theorem says that no such copying machine is possible, this type of superluminal signalling scheme cannot be physically realized. Thus, the no-cloning theorem makes quantum mechanics not to contradict the theory of relativity.

11.5 Quantum Cloning Machines

No-cloning theorem forbids a deterministic and perfect cloner for any arbitrary quantum state. This theorem proved that two non-orthogonal states cannot be cloned. It has been shown that two non-commuting mixed states cannot be broadcasted. No-cloning theorem has also been proved for the entangled states. In spite of the no-cloning theorem, it is quite possible to construct a quantum cloning machine (QCM) which copies an unknown state approximately.

As a QCM copies an unknown state approximately, a figure of merit has to be defined and the output of the QCM must be evaluated based on it. The usual figure of merit is called *fidelity*. The process of cloning of pure states to the case of $N \to M$ closing is defined as [12]

$$\left(|\psi\rangle^{\otimes N}\right) \otimes \left(|R\rangle^{\otimes M-N}\right) \otimes \left(|M\rangle\right) \xrightarrow{U} |\psi\rangle, \tag{11.26}$$

where $|\psi\rangle$ is the state of the Hilbert space $\mathcal{H}$ to be copied, $|R\rangle$ is a reference arbitrary state chosen in the same $\mathcal{H}$ and $|M\rangle$ is the ancilla state. For each of the outputs $j = 1, 2, \ldots, M$ of the cloning machine the fidelity F_j is defined as the overlap between ρ_j and the initial state $|\psi\rangle$. That is, F_j is given by [12]

$$F_j = \langle\psi|\rho_j|\psi\rangle, \quad j = 1, 2, \ldots, M, \tag{11.27}$$

where ρ_j is the partial state of clone j in the state $|\psi\rangle$ defined by Eq. (11.26).

QCMs are classified according to the nature of the fidelity F_j. A QCM is called *universal* (UQCM) if it copies equally well for any arbitrary input state and for this the fidelity F_j is independent of $|\psi\rangle$. Nonuniversal QCMs are called *state-dependent*. If all the clones at the output have same fidelity then the QCM is named as *symmetric*. If the fidelities of the clones are the maximal ones allowed by quantum mechanics for a given fidelity of the original state then such a QCM is called *optimal*.

11.5.1 Symmetric UQCM for Qubit

We give two cloning strategies for quantum cloning from one qubit to two qubits [12]. In the first cloning strategy, the qubit is measured in a randomly chosen basis and two copies of the state corresponding to the outcome are produced. If the original state is $|+\mathbf{a}\rangle$ the projector of which is $\frac{1}{2}(1 + \mathbf{a}\cdot\boldsymbol{\sigma})$ then the eigenstates of $\mathbf{b}\cdot\boldsymbol{\sigma}$ are the measurement basis. Two copies of $|\pm\mathbf{b}\rangle$ are produced with the probability $P = \frac{1}{2}(1 \pm \mathbf{a}\cdot\mathbf{b})$. The fidelity for both cases are

$$F_\pm = |\langle\mathbf{a}|\pm\mathbf{b}\rangle|^2 = P_\pm. \tag{11.28}$$

The average fidelity of this case is

$$F_1 = \int_{S_2} \mathrm{d}\mathbf{b}(P_+F_+ + P_-F_-) = \frac{1}{2} + \frac{1}{2}\int_{S_2} \mathrm{d}\mathbf{b}\,(\mathbf{a}\cdot\mathbf{b})^2 = \frac{2}{3}, \tag{11.29}$$

where S_2 is the surface of the Bloch sphere. This cloning is universal as we will get the same fidelity for any arbitrary original state $|+\mathbf{a}\rangle$.

In the second cloning strategy, let the original qubit $|+\mathbf{a}\rangle$ is unperturbed and give a new qubit in a randomly chosen state $|+\mathbf{b}\rangle$. When we detect one particle the original state $|+\mathbf{a}\rangle$ will have a probability $\frac{1}{2}$ with fidelity 1 and the new state will have the probability $\frac{1}{2}$ with the fidelity $F = |\langle+\mathbf{a}|+\mathbf{b}\rangle|^2 = P_+$. We get the average single-copy fidelity for this second strategy as

$$F_2 = \frac{1}{2} + \frac{1}{2}\int_{S_2} \mathrm{d}\mathbf{b}\left(1 + \frac{\mathbf{a}\cdot\mathbf{b}}{2}\right) = \frac{3}{4}. \tag{11.30}$$

The second strategy is also universal. Vladimir Bužek and Mark Hillery [13] proposed an optimal UQCM which outperforms these two cloning strategies.

11.5.2 Bužek–Hillery Optimal Symmetric UQCM

Bužek and Hillery introduced a UQCM which produces two identical copies with quality independent of the input state. It has been shown that this UQCM was optimal [14]. It has the maximum average fidelity between the input and output states. Bužek and Hillery proposed an optimal UQCM by a unitary transformation U on a larger Hilbert space as

$$U|0\rangle_1|0\rangle_2|0\rangle_R = \sqrt{\frac{2}{3}}\,|0\rangle_1|0\rangle_2|0\rangle_R + \sqrt{\frac{1}{6}}\,\left(|0\rangle_1|1\rangle_2 + |1\rangle_1|0\rangle_2\right)|1\rangle_R \tag{11.31}$$

and

$$U|1\rangle_1|0\rangle_2|0\rangle_R = \sqrt{\frac{2}{3}}\,|1\rangle_1|1\rangle_2|1\rangle_R + \sqrt{\frac{1}{6}}\,\left(|0\rangle_1|1\rangle_2 + |1\rangle_1|0\rangle_2\right)|0\rangle_R. \tag{11.32}$$

On the left-hand-side of the Eqs. (11.31) and (11.32) the input state is the first qubit and the second qubit is the blank state. Further, the qubit with the subindex R is the ancillary state of the QCM. In the transformation U of the cloning machine, the original qubit is destroyed. It becomes as one of the output qubit in 1 and the blank state is changed to another copy in party 2. The ancillary state may change or may not change. It will be traced out for the output. As the two outputs are identical it is a symmetric cloning machine. For any arbitrary normalized pure input state $|\psi\rangle = a|0\rangle + b|1\rangle$, U defined by Eqs. (11.31) and (11.32), we can find the density matrix of the output state after tracing out the ancillary state as

$$\begin{aligned}\rho_{\text{out}} \quad = \quad & \frac{2}{3}|\psi\rangle\langle\psi| \otimes |\psi\rangle\langle\psi| + \frac{1}{6}\left(|\psi\rangle|\psi^{\perp}\rangle + |\psi^{\perp}\rangle|\psi\rangle\right) \\ & \times \left(\langle\psi|\langle\psi^{\perp}| + \langle\psi^{\perp}|\langle\psi|\right),\end{aligned} \tag{11.33}$$

where $|\psi^{\perp}\rangle = b^*|0\rangle - a^*|1\rangle$ and is orthogonal to $|\psi\rangle$. If we trace out one of the two states in Eq. (11.33) we will get the single copy density matrix

$$\rho_1 = \rho_2 = \frac{2}{3}|\psi\rangle\langle\psi| + \frac{I}{6}. \tag{11.34}$$

The input state $|\psi\rangle$ can be written as $\cos(\theta/2)|0\rangle + \mathrm{e}^{\mathrm{i}\phi}\sin(\theta/2)|1\rangle$. We measure the quality of the copies by their fidelity

$$F = \int \mathrm{d}\Omega\langle\psi|\rho_{\text{out}}|\psi\rangle, \quad \int \mathrm{d}\Omega = \frac{1}{4\pi}\int_0^{2\pi}\mathrm{d}\phi\int_0^{\pi}\sin\theta\mathrm{d}\theta. \tag{11.35}$$

Substituting Eq. (11.34) in Eq. (11.35) we get the fidelity for Bužek–Hillery copying machine as $F = 5/6$. As the single copy fidelity does not depend on input state the quality of the copies has the state-independent characteristic and hence this cloning machine is universal.

A symmetric universal $N \to M$ QCM for qubits which generalizes Bužek–Hillery QCM was proposed [14] with the transformation for this cloning machine as

$$U|N\psi\rangle|R\rangle = \sum_{j=0}^{M-N} \alpha_j |(M-j)\psi,\, j\psi^{\perp}\rangle|R_j\rangle, \tag{11.36a}$$

where

$$\alpha_j = \sqrt{\frac{N+1}{M+1}}\sqrt{\frac{(M-N)!(M-j)!}{(M-N-j)!M!}} \tag{11.36b}$$

with $|(M-j)\psi,\, j\psi^{\perp}\rangle$ denoting the normalized symmetric state with $M-j$ states $|\psi\rangle$ and j states $|\psi^{\perp}\rangle$. The single copy fidelity for this copying machine is found to be

$$F = \frac{M(N+1)+N}{M(N+2)}\,. \tag{11.37}$$

Equation (11.37) gives the upper bound of $N \to M$ UQCM and hence this UQCM is optimal.

Solved Problem 2:

Trace out the states in Eq. (11.33) and prove Eq. (11.34).

Tracing out one of the states in Eq. (11.33) we get

$$\begin{aligned}
\rho_1 &= \frac{2}{3}|\psi\rangle\langle\psi| + \frac{1}{6}\left[|\psi^{\perp}\rangle\langle\psi^{\perp}| + |\psi\rangle\langle\psi|\right] \\
&= \frac{2}{3}|\psi\rangle\langle\psi| + \frac{1}{6}\left(\begin{bmatrix} a \\ b \end{bmatrix} \otimes \begin{bmatrix} a^* & b^* \end{bmatrix} + \begin{bmatrix} b^* \\ -c^* \end{bmatrix} \otimes \begin{bmatrix} b & -c \end{bmatrix}\right) \\
&= \frac{2}{3}|\psi\rangle\langle\psi| + \frac{1}{6}\left(\begin{bmatrix} |a|^2 & ab^* \\ a^*b & |b|^2 \end{bmatrix} + \begin{bmatrix} |b|^2 & -ab^* \\ -a^*b & |a|^2 \end{bmatrix}\right) \\
&= \frac{2}{3}|\psi\rangle\langle\psi| + \frac{1}{6}\begin{bmatrix} |a|^2+|b|^2 & 0 \\ 0 & |a|^2+|b|^2 \end{bmatrix} \\
&= \frac{2}{3}|\psi\rangle\langle\psi| + \frac{I}{6}.
\end{aligned} \tag{11.38}$$

Next, tracing out the first state, we obtain

$$\rho_2 = \frac{2}{3}|\psi\rangle\langle\psi| + \frac{1}{6}\left[|\psi^{\perp}\rangle\langle\psi^{\perp}| + |\psi\rangle\langle\psi|\right] = \frac{2}{3}|\psi\rangle\langle\psi| + \frac{I}{6}. \tag{11.39}$$

11.5.3 Asymmetric UQCM

In asymmetric UQCM the output clones possibly have different fidelities. For $1 \to 1+1$ cloning the optimum symmmetric UQCM was found [15]. Similar copying machines were also developed [16] with a slightly different formulation but giving the same no-cloning inequality relation between the fidelities F_A and F_B of the two outputs A and B, respectively, as

$$\sqrt{(1-F_A)(1-F_B)} \geq \frac{1}{2} - (1-F_A) - (1-F_B). \tag{11.40}$$

Equation (11.40) was proved to be optimal. If the fidelity of one output is increased, the fidelity of the other output will be decreased. The transformation of the asymmetric UQCM is given as [17]

$$|\psi\rangle_A \left(a|\Phi^+\rangle_{BR} + b|0\rangle_B \frac{1}{\sqrt{2}} (|0\rangle_R + |1\rangle_R) \right) \xrightarrow{U} a|\psi\rangle_A|\Phi^+\rangle_{BR} + b|\psi\rangle_B|\Phi^+\rangle_{AR}, \tag{11.41}$$

where R is an ancillary state and $|\Phi^+\rangle = (|00\rangle + |11\rangle)/\sqrt{2}$ is a Bell state. The parameters a and b are real and for the input state to be normalized they must satisfy the condition $a^2 + ab + b^2 = 1$. The partial states for the two clones are found to be

$$\rho_{A,B} = F_{A,B}|\psi\rangle\langle\psi| + (1 - F_{A,B})\,|\psi^\perp\rangle\langle\psi^\perp|, \tag{11.42}$$

where the fidelities for the two output clones are

$$F_A = 1 - \frac{b^2}{2}, \quad F_B = 1 - \frac{a^2}{2}. \tag{11.43}$$

For $a = b = 1/\sqrt{3}$, we will get the symmetric case of Bužek–Hillery with $F_A = F_B = 5/6$.

11.5.4 Probabilistic Quantum Cloning

All the cloning machines that we have discussed so far can always succeed but the copies cannot be perfect. A probabilistic cloning machine has been proposed [18] which can succeed only with a probability. When it succeeds it will give a perfect copy. This probabilistic quantum cloning is much useful in studying the B92 quantum key distribution protocol which involves only two non-orthogonal states and we can try to clone it with the largest probability. Suppose $S = \{|\psi_0\rangle, |\psi_1\rangle\}$ are the two independent states to be copied. The cloning transformation proposed is

$$U\left(|\psi_0\rangle|\Sigma\rangle|m_p\rangle\right) = \sqrt{\eta_0}\,|\psi_0\rangle|\psi_0\rangle|m_0\rangle + \sqrt{1-\eta_0}\,|\Phi^0_{ABP}\rangle, \tag{11.44a}$$

$$U\left(|\psi_1\rangle|\Sigma\rangle|m_p\rangle\right) = \sqrt{\eta_1}\,|\psi_1\rangle|\psi_1\rangle|m_1\rangle + \sqrt{1-\eta_1}\,|\Phi^1_{ABP}\rangle, \tag{11.44b}$$

where $|m_p\rangle$, $|m_0\rangle$ and $|m_1\rangle$ are ancillary states. The states $|\Phi^0_{ABP}\rangle$ and $|\Phi^1_{ABP}\rangle$ are chosen so that the reduced state of P is orthogonal to $|m_0\rangle$ and $|m_1\rangle$. If the measurements are $|m_0\rangle$ or $|m_1\rangle$ then we know that the states $S = \{|\psi_0\rangle, |\psi_1\rangle\}$ are copied perfectly. Otherwise, the cloning has not succeeded. The probability of success is η_0 for the state $|\psi_0\rangle$ and η_1 for state $|\psi_1\rangle$. For further studies on probabilistic QCM one may refer to the refs. [19–23].

11.5.5 The Pauli Channel

Let us present the QCM called *Pauli channel* [2,16]. Consider an arbitrary quantum pure state $|\psi\rangle = x_0|0\rangle + x_1|1\rangle$, $|x_1|^2 + |x_2|^2 = 1$. A maximally entangled state is given by

$$|\psi^+\rangle = \frac{1}{\sqrt{2}} (|00\rangle + |11\rangle)\,. \tag{11.45}$$

The complete quantum state of three particles can be written as

$$\begin{aligned} |\psi\rangle_A|\psi^+\rangle_{BC} = \frac{1}{2}\big[&|\psi^+\rangle_{AB}|\psi\rangle_C + (I \otimes \sigma_x)\,|\psi^+\rangle_{AB}\sigma_x|\psi\rangle_C \\ &+ (I \otimes \sigma_z)\,|\psi^+\rangle_{AB}\sigma_z|\psi\rangle_C \\ &+ (I \otimes \sigma_x\sigma_z)\,|\psi^+\rangle_{AB}\sigma_x\sigma_z|\psi\rangle_C\big]\,. \end{aligned} \tag{11.46}$$

Let $U_{m,n} = \sigma_x^m \sigma_z^n$, $m, n = 0, 1$ be the unitary transformation. We rewrite (11.46) as

$$|\psi\rangle_A |\psi^+\rangle_{BC} = \frac{1}{2} \sum_{m,n} (I \otimes U_{m,-n} \otimes U_{m,n}) \, |\psi^+\rangle_{AB} |\psi\rangle_C \tag{11.47}$$

and perform the unitary transformation as

$$\begin{aligned} &\sum_{\alpha,\beta} a_{\alpha,\beta} \, (U_{\alpha,\beta} \otimes U_{\alpha,-\beta} \otimes I) \, |\psi\rangle_A |\psi^+\rangle_{BC} \\ &\quad = \frac{1}{2} \sum_{\alpha,\beta,m,n} (U_{\alpha,\beta} \otimes U_{\alpha,-\beta} U_{m,-n} \otimes U_{m,n}) \, |\psi^+\rangle_{AB} |\psi\rangle_C \\ &\quad = \sum_{m,n} b_{m,n} \, (I \otimes U_{m,-n} \otimes U_{m,n}) \, |\psi^+\rangle_{AB} |\psi\rangle_C, \end{aligned} \tag{11.48a}$$

where

$$b_{m,n} = \frac{1}{2} \sum_{\alpha,\beta} (-1)^{\alpha m - \beta m} a_{\alpha,\beta} \, , \quad \sum_{\alpha,\beta} |a_{\alpha,\beta}|^2 = \sum_{m,n} |b_{m,n}|^2 = 1. \tag{11.48b}$$

This is a QCM. The quantum states of A and C are found to be

$$\rho_A = \sum_{\alpha,\beta} |a_{\alpha,\beta}|^2 U_{\alpha,\beta} |\psi\rangle\langle\psi| U_{\alpha,\beta}^\dagger, \tag{11.49a}$$

$$\rho_C = \sum_{m,n} |b_{m,n}|^2 U_{m,n} |\psi\rangle\langle\psi| U_{m,n}^\dagger. \tag{11.49b}$$

After cloning ρ_A is the original quantum state and ρ_C is the copy.

Solved Problem 3:

Suppose in the Pauli channel we have $b_{0,0} = 1$, $b_{0,1} = b_{1,0} = b_{1,1} = 0$. What are the quantum states of A and C? What do you conclude from the obtained result?

We can choose

$$a_{0,0} = a_{0,1} = a_{1,0} = a_{1,1} = \frac{1}{2}. \tag{11.50}$$

Then from

$$\rho_{\mathrm{A}} = \sum_{\alpha,\beta} |a_{\alpha,\beta}|^2 U_{\alpha,\beta} |\psi\rangle\langle\psi| U_{\alpha,\beta}^\dagger, \tag{11.51}$$

$$\rho_{\mathrm{C}} = \sum_{m,n} |b_{m,n}|^2 U_{m,n} |\psi\rangle\langle\psi| U_{m,n}^\dagger \tag{11.52}$$

we obtain

$$\rho_{\mathrm{A}} = \frac{1}{2} I, \quad \rho_{\mathrm{C}} = |\psi\rangle\langle\psi|. \tag{11.53}$$

That is, the original quantum state in A ($|\psi\rangle$) is destroyed.

11.6 Quantum Telecloning

A telecloning scheme combines cloning with teleportation. In teleportation an arbitrary state describing a quantum system is transmitted from a recipient (Alice) to another (Bob). In telecloning Alice holds an unknown state which she wishes to teleclone to M associates, Bob, Claire, etc. A quantum telecloning system for two-level system in which one input is sent to M-receivers has been proposed [24]. The case of distribution of N identical inputs among M receivers is reported [18]. The two-level system scheme is extended for the d-level case [25]. In this section we give Murao quantum cloning scheme [24] for teleporting an unknown 1-qubit $|\phi\rangle_X$ to M associates.

Teleportation has been discussed more elaborately in chapter 15. Here we give the basic protocol of teleportation in which an unknown state $|\phi\rangle_X$ of a quantum system X is to be faithfully transmitted between Alice and Bob who are spatially separated. In an 1-qubit system Alice and Bob share a maximally entangled state of two qubits A and B, such as $|\Phi^+\rangle = (|00\rangle_{AB} + |11\rangle_{AB})/\sqrt{2}$. After this Alice does a joint measurement of the 2-qubit $X \otimes A$ in the Bell states

$$|\Phi^{\pm}\rangle = \frac{1}{\sqrt{2}}(|00\rangle \pm |11\rangle), \quad |\Psi^{\pm}\rangle = \frac{1}{\sqrt{2}}(|01\rangle \pm |10\rangle). \tag{11.54}$$

After performing this measurement Alice sends a two-bit message to Bob informing him of her measurement result. At the receiving end Bob rotates his qubit by the unitary operators I, σ_z, σ_x or σ_y according to whether Alice's result was $|\Phi^+\rangle$, $|\Phi^-\rangle$, $|\Psi^+\rangle$ or $|\Psi^-\rangle$, respectively. Then regardless of the measurement result the final state of the qubit of Bob will be equal to the original state $|\phi\rangle_X$. Telecloning scheme makes use of the property of this insensitivity to the measurment results.

Next, we have to incorporate a optimal UQC (OUQC) into the telecloning system. We have already discussed Bužek–Hillery OUQC for producing two copies with the optimal fidelity of 5/6. A $N - M$ UQCM in which the copying machine performs unitary transformations that transform N input systems which are identically prepared in state $|\phi_{\text{in}}\rangle$ onto M output system ($M \geq N$) has been proposed [14]. Each of the M output state is a mixed state with the reduced density operator

$$\rho_{\text{out}} = F|\phi_{\text{in}}\rangle\langle\phi_{\text{in}}| + (1 - F)|\phi_{\text{in}}^{\perp}\rangle\langle\phi_{\text{in}}^{\perp}|, \tag{11.55}$$

where $\langle\phi_{\text{in}}|\phi_{\text{in}}^{\perp}\rangle = 0$, that is, $|\phi_{\text{in}}^{\perp}\rangle$ is orthogonal to $|\phi_{\text{in}}\rangle$. The fidelity factor is given by Eq. (11.37).

In telecloning only one original qubit is sent and hence $N = 1$. If $|\phi_{\text{in}}\rangle = a|0\rangle + b|1\rangle$ then the cloning transformation is given with $M - N$ blank qubits prepared in some fixed state $|00\ldots0\rangle_B$ and an ancilla system containing at least $M - N + 1$ levels in some fixed state $|00\ldots0\rangle_A$ as

$$U_{1M}\left(|\phi_{\text{in}}\rangle \otimes |00\ldots0\rangle_A|00\ldots0\rangle_B\right) = a|\phi_0\rangle_{AC} + b|\phi_1\rangle_{AC}, \tag{11.56}$$

where

$$
\begin{aligned}
|\phi_0\rangle_{AC} &= U_{1M}|0\rangle|00\ldots0\rangle_A|00\ldots0\rangle_B \\
&= \sum_{j=0}^{M-1} \alpha_j |A_j\rangle_A \otimes |\,\{0, M-j\}, \{1, j\}\rangle_C, \qquad (11.57) \\
|\phi_1\rangle_{AC} &= U_{1M}|1\rangle|00\ldots0\rangle_A|00\ldots0\rangle_B \\
&= \sum_{j=0}^{M-1} \alpha_j |A_{M-1-j}\rangle_A \otimes |\,\{0, j\}, \{1, M-j\}\rangle, \qquad (11.58) \\
\alpha_j &= \sqrt{\frac{2(M-j)}{M(M+1)}}\,. \qquad (11.59)
\end{aligned}
$$

In the above equations C denotes the M qubits holding the copies, $|A_j\rangle_A$ are M orthonormal states of the ancilla. $|\,\{0, M-j\}, \{1, j\}\rangle$ represents the symmetric and normalized state of M qubits. Out of these M qubits $(M-j)$ of them are in the $|0\rangle$ state while j are in the state $|1\rangle$. The ancilla qubits can be represented as the symmetrical states of $(M-1)$ qubits as

$$
|A_j\rangle_A = |\,\{0, M-1-j\}, \{j, 1\}\rangle_A. \qquad (11.60)
$$

Then states $|\phi_0\rangle$ and $|\phi_1\rangle$ become $(2M-1)$ qubits obeying the following symmetries:

$$
\begin{aligned}
\sigma_z \otimes \ldots \otimes \sigma_z |\phi_0\rangle &= |\phi_0\rangle, \quad \sigma_z \otimes \ldots \otimes \sigma_z |\phi_1\rangle = -|\phi_1\rangle, \qquad (11.61a) \\
\sigma_x \otimes \ldots \otimes \sigma_x |\phi_0\rangle &= |\phi_1\rangle, \quad \sigma_x \otimes \ldots \otimes \sigma_x |\phi_1\rangle = |\phi_0\rangle. \qquad (11.61b)
\end{aligned}
$$

We find that $|\phi_0\rangle$ and $|\phi_1\rangle$ transform under simultaneous action of Pauli operators on all $(2M-1)$ qubits like $|0\rangle$ and $|1\rangle$ transform under the corresponding single Pauli operator.

In the telecloning scheme proposed in [24] Alice has an unknown 1-qubit state $|\phi\rangle_X$ and she has to teleclone it to M associates Bob, Claire etc. All of them must share a multiparticle entangled state $|\psi_{\rm TC}\rangle$ as a starting resource. This entangled state is needed for each of the M associates to get an optimal copy given by Eq. (11.55) after performing local rotations with Pauli operators once Alice performs a local measurement and informs its results to them. A $|\psi_{\rm TC}\rangle$ having these properties is

$$
|\psi_{\rm TC}\rangle = \frac{1}{\sqrt{2}} \left(|0\rangle_P \otimes |\phi_0\rangle_{AC} + |1\rangle_P \otimes |\phi_1\rangle_{AC}\right). \qquad (11.62)
$$

It is a $2M$-qubit state. $|\phi_0\rangle_{AC}$ and $|\phi_1\rangle_{AC}$ are given in Eqs. (11.57) and (11.58), respectively. C denotes the M qubits holding the copies with each copy is held by one of the M associates. A represents $M-1$ qubit ancilla assumed to be on Alice's side. A single qubit held by Alice is denoted by P and is called *port qubit*. We will get a $(2M+1)$ qubit state if we take the tensor product of $|\psi_{\rm TC}\rangle$ with the unknown state $|\phi\rangle_X = a|0\rangle_X + b|1\rangle_X$. We can rewrite in the Bell basis of qubits X and P as

$$
\begin{aligned}
|\psi\rangle_{XPAC} = \frac{1}{\sqrt{2}} \big[& |\Phi^+\rangle_{XP} \left(a|\phi_0\rangle_{AC} + b|\phi_1\rangle_{AC}\right) \\
& + |\Phi^-\rangle_{XP} \left(a|\phi_0\rangle_{AC} - b|\phi_1\rangle_{AC}\right) \\
& + |\Psi^+\rangle_{XP} \left(b|\phi_0\rangle_{AC} + a|\phi_1\rangle_{AC}\right) \\
& + |\Psi^-\rangle_{XP} \left(b|\phi_0\rangle_{AC} - a|\phi_1\rangle_{AC}\right) \big]. \qquad (11.63)
\end{aligned}
$$

Now, telecloning can be accomplished by performing local rotation operations with the

Pauli spin operators at the receiving end. When Alice performs a Bell measurement of qubit X and P she will get one of the four results $|\Phi^{\pm}\rangle$, $|\Psi^{\pm}\rangle$. Assume that $|\Phi^{+}\rangle_{XP}$ is the result of her measurement then AC is projected into the state given by Eq. (11.56) (optimal cloning state). This achieves our task. In case other Bell states are obtained by Alice measurements then the associates can still recover the correct state of AC by making use of the Pauli matrix operations of Eqs. (11.61). For $|\Phi^{-}\rangle_{XP}$, σ_z operation on the $2M-1$ qubits in AC must be performed. Like-wise, for $|\psi^{+}\rangle_{XP}$ or $|\Psi^{-}\rangle_{XP}$, σ_x and $\sigma_x\sigma_z$ operations must be performed, respectively, to recover the correct state. We find that given the telecloning state Eq. (11.62) and using only local operations and classical communication of the measuremed result by Alice we are able to optimally transform information from one to several qubits.

Solved Problem 4:

Show that the Pauli operators give similar transformations like Eqs. (11.61) on the states $|0\rangle$ and $|1\rangle$.

We obtain

$$\sigma_z|0\rangle = \begin{bmatrix} 1 & 0 \\ 0 & -1 \end{bmatrix}\begin{bmatrix} 1 \\ 0 \end{bmatrix} = \begin{bmatrix} 1 \\ 0 \end{bmatrix} = |0\rangle, \tag{11.64a}$$

$$\sigma_z|1\rangle = \begin{bmatrix} 1 & 0 \\ 0 & -1 \end{bmatrix}\begin{bmatrix} 0 \\ 1 \end{bmatrix} = \begin{bmatrix} 0 \\ -1 \end{bmatrix} = -|1\rangle, \tag{11.64b}$$

$$\sigma_x|0\rangle = \begin{bmatrix} 0 & 1 \\ 1 & 0 \end{bmatrix}\begin{bmatrix} 1 \\ 0 \end{bmatrix} = |1\rangle, \quad \sigma_x|1\rangle = \begin{bmatrix} 0 & 1 \\ 1 & 0 \end{bmatrix}\begin{bmatrix} 0 \\ 1 \end{bmatrix} = |0\rangle. \tag{11.64c}$$

11.7 Other No-Go Theorems

Apart from no-cloning there are a few other impossibilities in quantum information. The impossibility theorems are consequences of linearity and unitarity properties of quantum theory. We briefly point out the various no-go theorems.

1. No-Hiding Theorem

As per the *no-hiding theorem* [26] if information is found to be missing in one system, for example due to the interaction of the system with the environment, then it is residing somewhere else in the universe. This means it is not possible to hide the missing information in the correlations between a system and its environment. This theorem addressing about information loss has been proven experimentally [27] on a 3-qubit NMR quantum information processor. The no-hiding theorem is found to have applications in black hole evaporation, quantum teleportation and private quantum channels.

2. No-Deletion Theorem

A given finite number of copies of an unknown quanta state can be partly estimated [28,29] and teleported. But, similar to cloning, deletion of an unknown state from several copies is also not allowed. This is known as *no-deletion principle* [30]. Note that if cloning and deletion of an unknown state are possible then we can transmit signals faster than light using two pairs of EPR states.

3. No-Splitting Theorem

Another impossibility theorem is the no-splitting problem [31]. It has been proven that quantum information of an unknown qubit cannot be split into two complementary qubits in a product state. This implies that the information contained in one qubit is inseparable.

4. No-Partial Erase Theorem

According to the *no-erase theorem* it is impossible to erase quantum information partially [31]. Here partial erasure refers to reduction of the dimension of the parameter space for the quantum state representing the quantum information, such as a qubit. Suppose a qubit contains information about, say, azimuthal angle and polar angle: $|\Omega\rangle = \cos(\theta/2)|0\rangle + e^{i\phi}\sin(\theta/2)|1\rangle$, with $\Omega = (\theta, \phi)$, $\theta \in [0, \pi]$ and $\phi \in [0, 2\pi]$. Here the states $|0\rangle$ and $|1\rangle$ are the logical zero and one states. Each pure state can be a point on the Poincaré sphere with θ and ϕ being the polar and azimuthal angles, respectively. It is impossible to erase, for example, polar angle information keeping the information about the azimuthal angle. In the above, complete erasure would result in mapping of all qubit states into a fixed qubit state $|\Omega_0\rangle = |\Sigma\rangle$ whatever the values of θ and ϕ.

11.8 Concluding Remarks

No-cloning theorem makes it impossible to clone a quantum state perfectly. But a lot of attention has been paid to the possibility of producing copies close to the original state. The first approximate cloning protocol was proposed for $1 \to 2$ symmetric cloning of a completely unknown qubit state with the optimal fidelity of $5/6$. It was later generalized to $N - M$ cloning of an arbitrary state. Asymmetric cloning machines with the output clones having different fidelities were investigated. Many other cloning machines such as state-dependent cloning, phase-covariant QCMs, probabilistic QCMs have been studied. In [2] a detailed account of various cloning machines and their applications has been presented. QCMs have been realized by various schemes experimentally. They have been implemented experimentally in NMR system, in a single photon with different degrees of freedom and also in optical system. Apart from using QCMs in quantum teleportation they can be used in metrology. Optical cloning machines can be used as radiometer to measure the amount of radiated power. Of course the most important application of QCM is on state estimation and eavesdropping of quantum cryptography.

11.9 Bibliography

[1] W.K. Wooters and W.H. Zurek, *Nature* 299:802, 1992.

[2] H. Fan, Y.N. Wang, L. Jing, J.D. Yue, H.D. Shi, Y.L. Zhang and L.Z. Mu, *Phys. Rep.* 544:241, 2014.

[3] D. Dieks, *Phys. Lett. A* 92:271, 1982.

[4] H.P. Yuen, *Phys. Lett. A* 113:405, 1986.

[5] H. Barnum, C.M. Caves, C.A. Fuchs, R. Jozsa and B. Schumacher, *Phys. Rev. Lett.* 76:2818, 1996.

[6] A. Kalev and I. Hen, *Phys. Rev. Lett.* 100:210502, 2008.
[7] H. Barnum, J. Barrett, M. Leifer and A. Wilce, *Phys. Rev. Lett.* 99:240501, 2007.
[8] G. Lindblad, *Lett. Math. Phys.* 47:189, 1999.
[9] H. Umegaki, *Kodai Math. Sem. Rep.* 14:59, 1962.
[10] G. Lindblad, *Commun. Math. Phys.* 40:147, 1975.
[11] N. Herbert, *Found. Phys.* 12:1171, 1982.
[12] V. Scarani, S. Iblisdir, N. Gisin and A. Acín, *Rev. Mod. Phys.* 77:1225, 2005.
[13] V. Bužek and M. Hillery, *Phys. Rev. A* 54:1844, 1996.
[14] N. Gisin and S. Massar, *Phys. Rev. Lett.* 79:2153, 1997.
[15] C.S. Niu and R.B. Griffiths, *Phys. Rev. A* 58:4377, 1998.
[16] N.J. Cerf, *Phys. Rev. Lett.* 84:4497, 2000.
[17] V. Buzek, S.L. Braunstein, M. Hillery and D. Bruß, *Phys. Rev. A* 56:3446, 1997.
[18] W. Dur and J.I. Cirac, *J. Mod. Opt.* 47:247, 2000.
[19] L.M. Duan and G.C. Guo, *Phys. Rev. Lett.* 80:4999, 1998.
[20] L. Hardy and D.D. Song, *Phys. Lett. A* 259:331, 1999.
[21] A.K. Pati, *Phys. Rev. Lett.* 83:2849, 1999.
[22] C.W. Zhang, Z.Y. Wang, C.F. Li and G.C. Guo, *Phys. Rev. A* 61:062310, 2000.
[23] K. Azuma, J. Shimamura, M. Koashi and N. Imoto, *Phys. Rev. A* 72:032335, 2005.
[24] M. Murao, M.B. Plenio, S. Plenio, S. Popescu, V. Vedral and P.L. Knight, *Phys. Rev. A* 57:4075, 1998.
[25] M. Murao, M.B. Plenio and V. Vedral, *Phys. Rev. A* 61:032311, 2000.
[26] S.L. Braunstein and A.K. Pati, *Phys. Rev. Lett.* 98:080502, 2007.
[27] J.R. Samal, A.K. Pati and A. Kumar, *Phys. Rev. Lett.* 106:080401, 2011.
[28] R. Derka, V. Buzek and A. Ekert, *Phys. Rev. Lett.* 80:1571, 1998.
[29] A.K. Pati and S.L. Braunstein, *Nature* 404:164, 2000.
[30] D.L. Zhou, B. Zheng and L. You, *Phys. Lett. A* 352:41, 2006.
[31] A.K. Pati and B.C. Sanders, *Phys. Lett. A* 359:31, 2006.

11.10 Exercises

11.1 If $|\phi\rangle = \alpha|0\rangle + \beta|1\rangle$ show that the unitary transformation defined by $|\psi\rangle|\Sigma\rangle|M\rangle \rightarrow |\psi\rangle|\psi\rangle|M(\psi)\rangle$ gives $|\phi\rangle|\Sigma\rangle|M\rangle \xrightarrow{U} \left(\alpha^2|00\rangle + \alpha\beta|01\rangle + \beta\alpha|10\rangle + \beta^2|11\rangle\right)|M(\phi)\rangle$.

11.2 Prove $CNOT(\sigma_x \otimes I)CNOT = \sigma_x \otimes \sigma_x$ and $CNOT(\sigma_z \otimes I)\ CNOT = \sigma_z \otimes I$.

11.3 Show that σ_1 and σ_2 given by $\sigma_k = \sum_i \lambda_{k,i}|i\rangle\langle i|$, $k = 1, 2$ commute.

11.4 Show that $S(\rho_1(t)|\rho_2(t)) = S(\rho_1(0)|\rho_2(0))$.

11.5 Prove that $\frac{1}{2}|0\rangle\langle 0| + \frac{1}{2}|1\rangle\langle 1| = I/2$.

11.6 Show that $\frac{1}{2}|\phi_{x+}\rangle\langle\phi_{x+}| + \frac{1}{2}|\phi_{x-}\rangle\langle\phi_{x-}| = I/2$.

11.7 Let $|\alpha\rangle$ and $|\beta\rangle$ be the eigenvectors of an operator O. Consider a unitary operation U which copies the normalized state $|\phi\rangle = a|\alpha\rangle + b|\beta\rangle$ into the state $|\alpha\rangle$ as $U|\phi\rangle|\alpha\rangle = |\phi\rangle|\phi\rangle$. Show that $U(a|\alpha\rangle + b|\beta\rangle)|\alpha\rangle = a^2|\alpha\rangle|\alpha\rangle + ba|\beta\rangle|\alpha\rangle + ab|\alpha\rangle|\beta\rangle + b^2|\beta\rangle|\beta\rangle$. Take the inner product with $\langle\alpha|\langle\alpha|$ on both sides of the above equation to get $a\langle\alpha\alpha|U|\alpha\alpha\rangle + b\langle\alpha\alpha|U|\beta\alpha\rangle = a^2$. Find the matrix elements for the cases $a = 1$, $b = 0$; $a = 0$, $b = 1$; and $a = b = 1/\sqrt{2}$ to satisfy the normalization condition $|a|^2 + |b|^2 = 1$. Show that no such unitary copying operation U can exist.

11.8 Show that $F = 5/6$ for $\rho_1 = \dfrac{2}{3}|\psi\rangle\langle\psi| + \dfrac{I}{6}$.

11.9 Prove that $\rho_1 = \rho_2 = \frac{1}{2}(1 + \frac{2}{3}\mathbf{n}\cdot\boldsymbol{\sigma})$, where $\mathbf{n} = (\langle\sigma_x\rangle, \langle\sigma_y\rangle, \langle\sigma_z\rangle)$.

11.10 Show that for a d-dimensional system (d is prime) the set of maximally entangled states $\{|\psi_j\rangle\}_{j=0}^{N-1}$ given by $|\psi_j\rangle = (U_j \otimes I)|\Phi^+\rangle$, $U_j = \sum_{j=1}^{N-1} \omega^{jk}|k\rangle\langle k|$ can be locally copied.

12

Quantum Tomography

12.1 Introduction

The complete information about a state of a physical system is obtained by all possible measurements on the system. One can do any number of measurements on a classical system and determine the state of the system. For example, measurements of position and momentum of an oscillating pendulum can be used to find the complete trajectory of the pendulum. This is possible as our measurements do not affect the classical system in any way. But in quantum mechanics there are inherent limitations due to Heisenberg uncertainty principle and also due to no-cloning theorem. Our measurements on any quantum state alters the state and hence repeated measurements cannot be done on any initial quantum state. Measurements on a perfect copy of the initial state cannot also be possible as the no-cloning theorem forbids creation of a perfect copy of any quantum state.

Consider an ensemble of a number of identical copies of an unknown state $|\psi\rangle$. The ensemble can be written as the direct product of copies of the unknown state as

$$|\psi\rangle^{\otimes n} = \otimes^n |\psi\rangle = |\psi\rangle \otimes |\psi\rangle \otimes \ldots \otimes |\psi\rangle \text{ (up to } n \text{ terms)}. \tag{12.1}$$

As the individual copies in the direct product are independent, performing several different measurements on many copies of the state, one can get fairly a good idea about the state $|\psi\rangle$. If we could construct such an ensemble of identical state then we can solve the problem of characterizing an unknown state $|\psi\rangle$. Unfortunately, it is impossible to copy a given state and construct an ensemble $|\psi\rangle^{\otimes n}$ due to no-cloning theorem and hence this process of determining the unknown state is impossible.

Suppose that we can prepare a quantum system repeatedly in the same state. Assume that each one of the prepared quantum system is a mixed state described by the density matrix ρ. *Quantum tomography* aims to determine the state of the system by determining its density matrix ρ by means of a series of measurements done on fairly a large number of identically prepared copies of the same system. The term tomography originates from the Greek word *tomos* meaning *part* and *graphein* meaning *to write*. As the classical tomography aims at reconstructing three-dimensional images via a series of two-dimensional projections along various dimensions, it is possible to determine the unknown quantum state of a system if many identical copies are available in the same state by performing different measurements in each copy.

Ugo Fano [1] in 1957 first addressed the problem of finding the procedure to determine the state of a system from multiple copies by defining a sufficient set of observables called *quorum* for a complete determination of ρ. A *quorum of observables* refers to a complete set of noncommuting observables whose measurements on the ensemble of identical states are used in quantum tomography to estimate the ensemble averages of all operators of a quantum system including its density matrix ρ. *Quantum tomography* can be described as an inverse statistical problem in which the unknown parameters and the data are given by the results of measurements performed on identical quantum states.

DOI: 10.1201/9781003172192-12

Fano stated first the problem of quantum state determination through repeated measurements on identically prepared systems. He recognized the need for more than two noncommuting observables to achieve that purpose. But we can say that the proposal by Vogel and Risken [2] led to the birth of quantum tomography.

Wolfgang Ernst Pauli problem [3] asks the question whether measurements of probability densities of position and momentum of a particle determine its quantum state wave function ψ. But it has been proved that the knowledge of position and momentum distributions alone does not single out one specific state. One can easily determine the expectation values of operators in a given pure or mixed state of a quantum state. But the inverse problem of determining the quantum state of an ensemble of identically prepared individual system by performing measurements is a nontrivial task. We need a generator which generates particles in the same state any number of times to create an ensemble of the same state ψ. For example, we may have a laser generating photons in a given state. As a complete set of observables (quorum) was needed for a complete determination of the density matrix and as it was difficult to device concretely measurables apart from position, momentum and energy the problem of determining the quantum state remained as mere speculation for many years. Experimentally determining the quantum state was realized only through the pioneering experiments by Raymer's group [4] in the domain of quantum optics.

This chapter provides the relevant theory and techniques of quantum tomography. To start with, first a counter example for negative answer to the Pauli problem and the reason for it are given. Quantum tomography set out the density matrix of quantum states. The determination of density matrix from Wigner function is considered. Then the optical homodyne tomography technique of reconstruction of Wigner function is outlined. Next, the single and multiqubits tomography are discussed. Details of quantum states can be explored through quantum process tomography. A few of such methods are presented.

12.2 Pauli Problem

We associate wave functions or vectors in a Hilbert space for pure quantum states and density matrices represent mixed quantum states. These wave functions give probability distributions of position and momentum using which one can find the expectation values of observables. Pauli [3] posed the inverse problem whether it was possible to reconstruct uniquely the quantum state from the knowledge of the probability distributions of position and momentum. It was found that the answer to Pauli's problem is negative.

12.2.1 Answer to the Pauli Problem

The negative answer to the original Pauli problem may be given by counter examples as shown in Hans Reichenbach's book [5]. For example, consider the two squeezed states [6,7] in the position representation ($\hbar = 1$) given by

$$\psi_1(q) = N\mathrm{e}^{-\alpha q^2 + \mathrm{i}\beta q}, \quad \psi_2(q) = N\mathrm{e}^{-\alpha^* q^2 + \mathrm{i}\beta q} \tag{12.2}$$

with $\mathrm{Re}\,\alpha \geq 0$ and β real. Normalization of the two ψ's gives $N = ((\alpha + \alpha^*)/\pi)^{1/4}$ (see the exercise 2 at the end of this chapter). Finding the momentum wave functions for the coordinate wave functions given by Eq. (12.2), we obtain (see the exercise 3 at the end of

this chapter)

$$\phi_1(p) = \frac{N}{\sqrt{2\alpha}} \mathrm{e}^{-(\beta-p)^2/(4\alpha)}, \quad \phi_2(p) = \frac{N}{\sqrt{2\alpha^*}} \mathrm{e}^{-(\beta-p)^2/(4\alpha^*)}. \tag{12.3}$$

From Eqs. (12.2) and (12.3) we find, respectively, the probability densities in coordinate and momentum representations as

$$|\psi_1(q)|^2 = |\psi_2(q)|^2 = |N|^2 \mathrm{e}^{-(\alpha+\alpha^*)q^2}, \tag{12.4a}$$

$$|\phi_1(p)|^2 = |\phi_2(p)|^2 = \frac{|N|^2}{2|\alpha|} \mathrm{e}^{-(\beta-p)^2(\alpha+\alpha^*)/(4\alpha\alpha^*)}. \tag{12.4b}$$

The two states given by Eq. (12.2) have the same probability densities in both coordinate and momentum representations given, respectively, by Eqs. (12.4a) and (12.4b). If $\psi_1(q)$ and $\psi_2(q)$ are same then the *fidelity* $\mathcal{F} = |\langle\psi_1|\psi_2\rangle|^2$ must be one. The fidelity $\mathcal{F}$ for the ψ_1 and ψ_2 given by Eq. (12.2) is found to be (see the exercise 4 at the end of this chapter)

$$\mathcal{F} = \frac{\alpha + \alpha^*}{2\sqrt{\alpha\alpha^*}}. \tag{12.5}$$

Since $\mathcal{F} \neq 1$ we conclude that the two states are different even though they have same probability densities in coordinate and momentum representations. It establishes that the answer to Pauli's problem is negative. Coordinate and momentum probability densities don't determine uniquely a quantum state.

12.2.2 Reason For Negative Answer To Pauli Problem

To find the reason why the knowledge of the two marginal probability distributions of position and momentum is not sufficient to determine an unique quantum state, we follow the procedure given by Ibort et al. [7].

Consider the family of dimensionless observables depending on two real parameters μ and ν as

$$X(\mu, \nu) = \mu Q + \nu P. \tag{12.6}$$

Q and P generate Weyl-Heisenberg algebra $[Q, P] = \mathrm{i}\hbar I$ if Planck constant $\hbar$ is restored. The spectrum $X(\mu, \nu)$ is the real line parametrized by X for the corresponding improper eigenvectors $|X_{\mu\nu}\rangle$. In the position representation

$$X(\mu, \nu) = -\mathrm{i}\hbar\nu \frac{\mathrm{d}}{\mathrm{d}q} + \mu q. \tag{12.7}$$

The improper eigenfuctions for the operator given in Eq. (12.7) are found to be (see the exercise 5 at the end of this chapter)

$$\phi_{X_{\mu\nu}}(q) = \langle q|X_{\mu\nu}\rangle = \frac{1}{\sqrt{2\pi\hbar|\nu|}} \mathrm{e}^{-\mathrm{i}\mu q^2/(2\hbar\nu) + \mathrm{i}Xq/(h\nu)}. \tag{12.8}$$

The operator in Eq. (12.6) can be given in momentum representation as

$$X(\mu, \nu) = \nu p - \mathrm{i}\hbar\mu \frac{\mathrm{d}}{\mathrm{d}p}. \tag{12.9}$$

Similar to the eigenfunctions given by Eq. (12.8) the eigenfuctions in momentum representation can be found as

$$\tilde{\phi}_{X_{\mu\nu}}(p) = \frac{1}{\sqrt{2\pi\hbar|\mu|}} \mathrm{e}^{\mathrm{i}\nu p^2/(2\hbar\mu) - \mathrm{i}Xp/(\hbar\mu)}. \tag{12.10}$$

For the case of the operators $X(\mu,\nu)$ the symplectic tomogram of a normalized pure state ψ is defined as

$$\begin{aligned} T_\psi(X,\mu,\nu) &= |\langle X_{\mu\nu}|\psi\rangle|^2 \\ &= \frac{1}{2\pi\hbar|\nu|}\left|\int \psi(q)\mathrm{e}^{i\mu q^2/(2\hbar\nu)-\mathrm{i}Xq/(\hbar\nu)}\mathrm{d}q\right|^2, \quad \nu\neq 0 \\ &= \frac{1}{2\pi\hbar|\mu|}\left|\int \tilde{\psi}(p)\mathrm{e}^{-i\nu p^2/(2\hbar\mu)+\mathrm{i}Xp/(\hbar\mu)}\mathrm{d}p\right|^2, \quad \mu\neq 0. \end{aligned} \tag{12.11}$$

In the above equation $\tilde{\psi}(p)$ is the momentum representation of $\psi(q)$ given by the Fourier transform

$$\tilde{\psi}(p) = \frac{1}{\sqrt{2\pi\hbar}}\int \psi(q)\mathrm{e}^{-\mathrm{i}pq/\hbar}\mathrm{d}q. \tag{12.12}$$

Physically $T_\psi(X,\mu,\nu)\mathrm{d}X$ represents the marginal probability of a measure between X and $X+\mathrm{d}X$ in the given state $|\psi\rangle$ of the observable $X(\mu,\nu)$ with fixed μ and ν. If ψ is normalized then the total marginal probability is

$$\int T_\psi(X,\mu,\nu)\mathrm{d}X = 1. \tag{12.13}$$

The density matrix $\rho(q,q') = \psi(q)\psi^*(q')$ is given by the reconstruction formula [8]

$$\begin{aligned} \rho(q,q') &= \frac{1}{2\pi}\int T_\psi(X,\mu,(q-q')/\hbar)\,\mathrm{e}^{\mathrm{i}[X-\mu(q+q')/2]}\mathrm{d}X\mathrm{d}\mu \\ &= \frac{1}{(2\pi)^2}\int T_\psi(X,\mu,\nu)\mathrm{e}^{\mathrm{i}p(q-q')/\hbar} \\ &\qquad \times \mathrm{e}^{\mathrm{i}(X-\mu q-\nu p)}\mathrm{d}X\mathrm{d}\mu\mathrm{d}\nu\mathrm{d}p\,. \end{aligned} \tag{12.14}$$

From Eq. (12.11) we find that $T_\psi(X,1,0)$ gives the marginal probability distribution of position and $T_\psi(X,0,1)$ gives the marginal probability distribution of momentum. We find from Eq. (12.14), the density matrix cannot be found using just $T_\psi(X,1,0)$ and $T_\psi(X,0,1)$. So, the answer to the Pauli problem is negative. This is due to the fact that the reconstruction of density matrix needs details of several different marginal probability distributions with respect to several different observables of the family $X(\mu,\nu)$. A minimal set of such observables is termed as a *quorum*.

12.3 Recovery of Density Matrix from Wigner Function

Quantum state tomography, for short, quantum tomography can be defined as a method for estimating the ensemble averages of all operators of a quantum system including its density matrix. This estimation is done from a set of measurements of a complete set of noncommuting observables (quorum). So, the tomographic probability representation is equivalent to the conventional Schrödinger, Heisenberg and Feynman path integral representations of quantum mechanics. Ideally speaking, the quantum state is perfectly recovered through quantum tomography only in the limit of infinite number of measurements. But practically only finite number of measurements can be done resulting in an appropriate state with a

statistical error. Also, increase in the dimension of the Hilbert space requires enormous measurements resulting in high statistical errors which make it almost impossible to estimate the density matrix of the quantum state.

In classical tomography a picture of a hidden object is buidup using various observations from different angles. The foundation of tomography rests on the problem formulated and solved by Johannes Radon [9]. Suppose we have a function $f(x, y)$ satisfying some regularity conditions. If we integrate $f(x, y)$ along all possible lines in the $x - y$ plane and get $F(l)$, where l denotes a line. Radon found the solution to reconstruct the initial function $f(x, y)$ out of $F(l)$. The tomographic reconstruction techniques used in medical imaging follow this Radon mathematical techniques. If x and y are taken as phase space variables then the function f can be thought as the Wigner function (refer chapter 6). Then the function on lines F becomes the measured probability distribution. The Radon transformation of the probability distribution gives the Wigner function. The density matrix can be then recovered from the Wigner functions.

We have discussed the original Wigner function introduced by Wigner [10] in chapter 6. Quantum tomography aims to reconstruct the density matrix of quantum states. Wigner function is found to play the role of a quasi-probability distribution (QPD) as it can also have negative values. It can be used to find quantum mechanical expectation values in the form of averages over phase space complex plane.

Field operators are given in terms of ordered products of annihilation and creation operators. We have the annihilation operator a and creation operator $a^\dagger$. Conventionally, the product $(a^\dagger)^n a^m$ is called *normally ordered* (a appears right of $a^\dagger$) and the product $a^m(a^\dagger)^n$ is called *anti-normally ordered* (a appears left of $a^\dagger$). If the products appear symmetrically in the expansion we say that it is *symmetrically ordered*.

We follow the general theory of quantum tomography given by Chen et al [11] and discuss below how the density matrix is recovered from Wigner function. One can evaluate the expectations of symmetrically ordered product of the field operators using the original Wigner function. To evaluate a generalized order expectation values, a generalized s-order Wigner function $W(\alpha, \alpha^*)$ is defined as [12–13]

$$W_s(\alpha, \alpha^*) = \frac{1}{\pi^2} \int_{\mathrm{C}} \mathrm{d}^2\lambda \mathrm{e}^{\alpha\lambda^* - \alpha^*\lambda + (s/2)|\lambda|^2} \mathrm{Tr}[D(\lambda)\rho], \tag{12.15}$$

where $D(\lambda)$ is the displacement operator $\mathrm{e}^{\lambda a^\dagger - \lambda^* a}$ [14,15] and ρ is the density operator. α^* is the complex conjugate of α and the integral is performed in the complex plane C with measure $\mathrm{d}^2\lambda = \mathrm{d}\,\mathrm{Re}\lambda\,\mathrm{Im}\lambda$. The s-ordered expectation values of the field operators are evaluated through the relation

$$\mathrm{Tr}\left[: (a^\dagger)^n a^m :_s \rho\right] = \int_{\mathrm{C}} \mathrm{d}^2\alpha W_s(\alpha, \alpha^*)\alpha^{*n}\alpha^m. \tag{12.16}$$

$s = -1, 0, 1$ corresponds, respectively, to anti-normal, symmetrical and normal ordering. The generalized Wigner function $W(\alpha, \alpha^*)$ for the three cases are given by the following symbols and names:

$\frac{1}{\pi}Q(\alpha, \alpha^*)$ for $s = -1$, *Q function*,

$W(\alpha, \alpha^*)$ for $s = 0$, *usual Wigner function*,

$P(\alpha, \alpha^*)$ for $s = 1$, *P function*.

With $|\alpha\rangle = D(\alpha)|0\rangle$ and $|0\rangle$ is the vacuum state of the field the density matrix can be evaluated from the normal and anti-normal ordering from the relations

$$Q(\alpha,\alpha^*)=\langle\alpha|\rho|\alpha\rangle,\quad \rho=\int_{\mathrm{C}}\mathrm{d}^2\alpha P(\alpha,\alpha^*)|\alpha\rangle\langle\alpha|\,. \tag{12.17}$$

The usual Wigner function gives the probability distribution of the quadrature of the field as

$$\int_{-\infty}^{\infty}\mathrm{d}\,\mathrm{Im}\alpha W\left(\alpha\mathrm{e}^{\mathrm{i}\phi},\alpha^*\mathrm{e}^{-\mathrm{i}\phi}\right)\,{}_\phi\langle\mathrm{Re}\alpha|\rho|\mathrm{Re}\alpha\rangle_\phi, \tag{12.18}$$

where $|x\rangle_\phi$ represents the eigenstate of the field quadrature

$$X_\phi=\frac{1}{2}\left(a^\dagger\mathrm{e}^{\mathrm{i}\phi}+a\mathrm{e}^{-\mathrm{i}\phi}\right) \tag{12.19}$$

with real eigenvalues x. Through Eqs. (12.17) and (12.18) we can recover the density matrix ρ.

Solved Problem 1:

Express the displacement operator $D(\alpha)=\mathrm{e}^{\alpha a^\dagger-\alpha^* a}$ in (i) normally ordered form and (ii) anti-normally ordered form.

Case (i)

Using the identity

$$\mathrm{e}^A\mathrm{e}^B=\mathrm{e}^{A+B}\mathrm{e}^{[A,B]/2} \tag{12.20}$$

with $A=\alpha a^\dagger$ and $B=-\alpha^* a$ we write

$$\begin{aligned}\mathrm{e}^{\alpha a^\dagger}\mathrm{e}^{-\alpha^* a} &= \mathrm{e}^{\alpha a^\dagger-\alpha^* a}\mathrm{e}^{[\alpha a^\dagger,-\alpha^* a]/2}\\ &= \mathrm{e}^{\alpha a^\dagger-\alpha^* a}\mathrm{e}^{|\alpha|^2(-a^\dagger a+aa^\dagger)/2}\\ &= \mathrm{e}^{\alpha a^\dagger-\alpha^* a}\mathrm{e}^{|\alpha|^2[a,a^\dagger]/2}\end{aligned} \tag{12.21}$$

As $[a,a^\dagger]=1$, we obtain

$$\begin{aligned}\mathrm{e}^{\alpha a^\dagger}\mathrm{e}^{-\alpha^* a} &= \mathrm{e}^{\alpha a^\dagger-\alpha^* a}\mathrm{e}^{|\alpha|/2}\\ &= D(\alpha)\mathrm{e}^{|\alpha|/2}.\end{aligned} \tag{12.22}$$

That is,

$$D(\alpha)=\mathrm{e}^{-|\alpha|/2}\mathrm{e}^{\alpha a^\dagger}\mathrm{e}^{-\alpha^* a}. \tag{12.23}$$

Case (ii)

With $A=-\alpha^* a$ and $B=\alpha a^\dagger$ the identity given by Eq. (12.20) becomes

$$\begin{aligned}\mathrm{e}^{-\alpha^* a}\mathrm{e}^{\alpha a^\dagger} &= \mathrm{e}^{-\alpha^* a+\alpha a^\dagger}\mathrm{e}^{[-\alpha^* a,\alpha a^\dagger]/2}\\ &= \mathrm{e}^{-\alpha^* a+\alpha a^\dagger}\mathrm{e}^{|\alpha|^2(-aa^\dagger+a^\dagger a)/2}\\ &= \mathrm{e}^{-\alpha^* a+\alpha a^\dagger}\mathrm{e}^{-|\alpha|^2/2}\\ &= D(\alpha)\mathrm{e}^{-|\alpha|^2/2}.\end{aligned} \tag{12.24}$$

That is, $D(\alpha)=\mathrm{e}^{|\alpha|^2/2}\mathrm{e}^{-\alpha* a}\mathrm{e}^{\alpha a^\dagger}$.

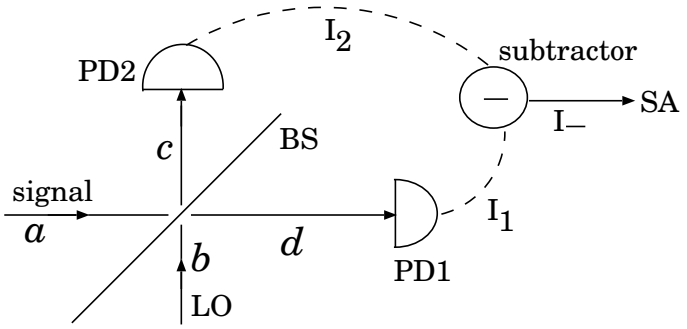

FIGURE 12.1
Schematic of homodyne detector. For details see the text. (Reproduced with permission from Z. Chen, Q. Wu and C. Zhang, *J. Electromag. Anal. Appl.* 2:333, 2010. Copyright 2010, Scientific Research Publishing.)

12.4 Optical Homodyne Tomography

We have seen in the previous section that there is a one to one correspondance between the Wigner function and the density matrix of a quantum state. So, quantum state reconstruction (QSR) can be done by reconstruction of QPDs.

The concept of tomography was introduced by Bertrand and Bertrand [13]. They pointed out a way to reconstruct Wigner functions from marginals. The pioneering paper of Vosel and Risken [2] inspired many works of QSR in quantum optics. They discussed a method to reconstruct QSR from the measured quadrature amplitude distribution of optical homodyne measurements. The first experiments of QSR were reported in the refs. [4,16,17] by Smithey et al. In their experiments they used the balanced homodyne detection in which a pulsed signal field was superposed in a 50 : 50 beam spliter with a local pulsed coherent state field. They determined Wigner functions of a vacuum and a quadrature squeezed state. This new technique was called *Optical Homodyne Tomography (OHT)*. Later OHT was performed for a continuous wave light field [18,19]. So, in OHT, the probability distributions of the quadrature amplitudes are measured. Next, the Wigner distribution is obtained by tomographic inversion of the set of measured probability distributions. Then density operator ρ is obtained from the Wigner function. ρ will give the expectation value of any observable O as $\langle O\rangle = \mathrm{Tr}(\rho O)$.

The probability distributions of the quadrature amplitudes X_ϕ given by Eq. (12.19) can be measured for different phase ϕ using a *balanced homodyne detector*. The schematic of homodyne detector is shown in Fig. 12.1 [11]. The signal and a local oscillator (LO) wave are mixed at a 50 : 50 beam splitter (BS). The LO is excited by a laser in a coherent state $|z\rangle$. By controlling the path length of the LO beams the relative phase ϕ between signal and LO wave can be varied. X_ϕ at various paths can be measured by tuning ϕ. PD1 and PD2 are high efficient matched photo detectors measuring the two output beams from BS. a, b, c and d are the annihilation operators of the corresponding four ports. Since the number operators are $c^\dagger c$ and $d^\dagger d$ the difference current measured by the spectrum analyser (SA) is given by

$$I_- = I_1 - I_2 = \eta(d^\dagger d - c^\dagger c), \tag{12.25}$$

where $\eta = 2|z|$ is the rescaling factor. For a 50 : 50 beam splitter

$$c = \frac{1}{\sqrt{2}}(a - b), \quad d = \frac{1}{\sqrt{2}}(a + b). \tag{12.26}$$

From Eqs. (12.25) and (12.26) we get

$$I_- = \eta(b^\dagger a + a^\dagger b). \tag{12.27}$$

In homodyne detection the LO wave is made very large so that it can be treated as a classical wave. So, b can be replaced by a complex number $b = Ae^{i\phi}$. Substituting this in Eq. (12.27) we find

$$I_- = \eta A(ae^{-i\phi} + a^\dagger e^{i\phi}) = 2\eta A X_\phi, \quad X_\phi = \frac{1}{2}(ae^{-i\phi} + a^\dagger e^{i\phi}). \tag{12.28}$$

Hence, Eq. (12.28) proves that measurement of the difference current I_- is equivalent to measurement of quadrature amplitude X_ϕ. By changing ϕ we can measure any quadrature we want.

If one wants to preserve the complete information and to extract the density matrix or the Wigner function of any arbitrary state of the signal then it is essential to measure all the quadrature amplitude distributions $w(X, \phi)$. Here X is the quadrature amplitude value. Vogel and Risken [2] pointed out that the s-parametrized Wigner function can be reconstructed from the measure marginals $w(X, \phi)$ as

$$\begin{aligned} W(\alpha_r, \alpha_i; s) \quad = \quad & \frac{1}{4\pi^2} \int_{-\infty}^{\infty} \int_{-\infty}^{\infty} \int_0^{\pi} w(X, \phi) \\ & \times \exp[s\eta^2/8 + i\eta(X - \alpha_r \cos\phi - \alpha_i \sin\phi)] \\ & \times |\eta| dX d\eta d\phi. \end{aligned} \tag{12.29}$$

Here η is an integrating factor, α_r and α_i are the real and imaginary parts of α.

The first experiment and reconstruction of the Wigner functions of a vacuum state and a quadrature squeezed state are reported in [16,17]. As Eq. (12.29) is similar to the classical tomographic inversion from the projections of two-dimensional objects it is called an *inverse Radon transform*. Hence, this method is called as *optical homodyne tomography*.

12.5 Qubit Quantum Tomography

We need to understand the representation of quantum states before analysing them. Generally, specific parametrization of states simplifies the reconstruction of unknown states. We discuss this in this section [20].

12.5.1 Density Matrix in Qubit Representation

We can represent any single qubit as

$$|\psi\rangle = \alpha|0\rangle + \beta|1\rangle, \tag{12.30}$$

where α and β are complex constants. If $|\psi\rangle$ is normalized then $|\alpha|^2 + |\beta|^2 = 1$. As we have already discussed, quantum tomography requires an ensemble of such pure states. We can

represent a mixed pure state by a density matrix ρ as

$$\begin{aligned}\rho &= \sum_i p_i|\psi_i\rangle\langle\psi_i| \\ &= \begin{array}{c} \\ |0\rangle \\ |1\rangle \end{array} \begin{array}{c} \begin{array}{cc} \langle 0| & \langle 1| \end{array} \\ \begin{pmatrix} A & C\mathrm{e}^{\mathrm{i}\phi} \\ C\mathrm{e}^{-\mathrm{i}\phi} & B \end{pmatrix} \end{array}, \end{aligned} \tag{12.31}$$

where p_i is the probabilistic weighting factor for the state $|\psi_i\rangle$ in the mixed state. Thus, $\sum_i p_i = 1$. A, B and C are real constants. For the ensemble of pure states $\mathrm{Tr}(\rho) = A+B = 1$ and $C \leq \sqrt{AB}$.

As ρ is Hermitian it can be diagonalized with eigenvalues $\{E_1, E_2\}$ corresponding to mutually orthogonal eigenvectors $\{|\psi\rangle, |\psi^{\perp}\rangle\}$. So, in this orthonormal eigenvector basis ρ is diagonlized. That is,

$$\rho = \begin{array}{c} \\ |\psi\rangle \\ |\psi^{\perp}\rangle \end{array} \begin{array}{c} \begin{array}{cc} \langle\psi| & \langle\psi^{\perp}| \end{array} \\ \begin{pmatrix} E_1 & 0 \\ 0 & E_2 \end{pmatrix} \end{array} = E_1|\psi\rangle\langle\psi| + E_2|\psi^{\perp}\rangle\langle\psi^{\perp}|. \tag{12.32}$$

For a polarized single photon we can take the two orthogonal states as the horizontal $|H\rangle = |0\rangle$ and vertical $|V\rangle = |1\rangle$ polarized states. The other pure polarization states diagonal $|D\rangle$, antidiagonal $|A\rangle$, right-circular $|R\rangle$ and left-circular $|L\rangle$ polarization sates can be constructed from coherent superposition of $|H\rangle$ and $|V\rangle$ states as

$$|D\rangle = \frac{1}{\sqrt{2}}(|H\rangle + |V\rangle), \quad |A\rangle = \frac{1}{\sqrt{2}}(|H\rangle - |V\rangle), \tag{12.33a}$$

$$|R\rangle = \frac{1}{\sqrt{2}}(|H\rangle + \mathrm{i}|V\rangle), \quad |L\rangle = \frac{1}{\sqrt{2}}(|H\rangle - \mathrm{i}|V\rangle). \tag{12.33b}$$

Suppose we have a photon source which emits in each second a single photon wave packet. However, they are altered between vertical, horizontaland diagonal polarizations. Assume that the timing information is ignored when the polarization is measured. In this case the state density matrix can be given by

$$\rho = \frac{1}{3}\left(|H\rangle\langle H| + |V\rangle\langle V| + |D\rangle\langle D|\right). \tag{12.34}$$

Since $|H\rangle = \begin{bmatrix} 1 \\ 0 \end{bmatrix}$, $|V\rangle = \begin{bmatrix} 0 \\ 1 \end{bmatrix}$ and $|D\rangle = \frac{1}{\sqrt{2}}\begin{bmatrix} 1 \\ 1 \end{bmatrix}$ in the $|0\rangle$ and $|1\rangle$ basis the density matrix ρ can be found in the basis $|0\rangle$ and $|1\rangle$ as

$$\rho = \frac{1}{3}\left[\begin{bmatrix} 1 & 0 \\ 0 & 0 \end{bmatrix} + \begin{bmatrix} 0 & 0 \\ 0 & 1 \end{bmatrix} + \frac{1}{2}\begin{bmatrix} 1 & 1 \\ 1 & 1 \end{bmatrix}\right] = \frac{1}{6}\begin{bmatrix} 3 & 1 \\ 1 & 3 \end{bmatrix}. \tag{12.35}$$

Diagonalizing the matrix ρ given above we get the eigenvalues as 2/3 and 1/3 (see the exercise 10 at the end of present chapter) corresponding to the orthogonal eigenvectors $|D\rangle$ and $|A\rangle$. So, ρ can be written in the $|D\rangle$ and $|A\rangle$ basis as

$$\rho = \begin{array}{c} \\ |D\rangle \\ |A\rangle \end{array} \begin{array}{c} \begin{array}{cc} \langle D| & \langle A| \end{array} \\ \begin{pmatrix} 2/3 & 0 \\ 0 & 1/3 \end{pmatrix} \end{array} = \frac{2}{3}|D\rangle\langle D| + \frac{1}{3}|A\rangle\langle A|. \tag{12.36}$$

12.5.2 Stokes Parameters and Density Matrix

Polarized light wave is described by the commonly used Stokes parameters introduced by George Gabriel Stokes in 1852. The same parameters can be used for qubits. Any single qubit density matrix ρ can be given uniquely as

$$\rho = \frac{1}{2}\sum_{i=0}^{3} S_i \sigma_i, \tag{12.37}$$

where S_i is the Stokes parameters given by $S_i = \mathrm{Tr}(\sigma_i \rho)$ and

$$\sigma_0 = \begin{pmatrix} 1 & 0 \\ 0 & 1 \end{pmatrix}, \quad \sigma_1 = \begin{pmatrix} 0 & 1 \\ 1 & 0 \end{pmatrix}, \tag{12.38a}$$

$$\sigma_2 = \begin{pmatrix} 0 & -\mathrm{i} \\ \mathrm{i} & 0 \end{pmatrix}, \quad \sigma_3 = \begin{pmatrix} 1 & 0 \\ 0 & -1 \end{pmatrix}. \tag{12.38b}$$

Due to normalization $S_0 = 1$. For pure and mixed states $\sum_{i=1}^{3} S_i^2$ become 0 and < 1, respectively. The outcome of a specific pair of projective measurements will give the Stokes parameters as

$$S_0 = P_{|0\rangle} + P_{|1\rangle}, \quad S_1 = P_{\frac{1}{\sqrt{2}}(|0\rangle+|1\rangle)} - P_{\frac{1}{\sqrt{2}}(|0\rangle-|1\rangle)}, \tag{12.39a}$$

$$S_2 = P_{\frac{1}{\sqrt{2}}(|0\rangle+\mathrm{i}|1\rangle)} - P_{\frac{1}{\sqrt{2}}(|0\rangle-\mathrm{i}|1\rangle)}, \quad S_3 = P_{|0\rangle} - P_{|1\rangle}. \tag{12.39b}$$

In Eqs. (12.39) $P_{|\phi\rangle}$ gives the probability to measure $|\phi\rangle$. For the single qubit state

$$P_{|\psi\rangle} + P_{|\psi^{\perp}\rangle} = 1, \quad P_{|\psi\rangle} - P_{|\psi^{\perp}\rangle} = 2P_{|\psi\rangle} - 1. \tag{12.40}$$

If we define

$$|\phi\rangle_1 = \frac{1}{\sqrt{2}}(|0\rangle + |1\rangle), \quad |\phi\rangle_2 = \frac{1}{\sqrt{2}}(|0\rangle + \mathrm{i}|1\rangle), \quad |\phi\rangle_3 = |0\rangle \tag{12.41}$$

then their orthogonal vectors are given by

$$|\phi^{\perp}\rangle_1 = \frac{1}{\sqrt{2}}(|0\rangle - |1\rangle), \quad |\phi^{\perp}\rangle_2 = \frac{1}{\sqrt{2}}(|0\rangle - \mathrm{i}|1\rangle), \quad |\phi^{\perp}\rangle_3 = |1\rangle. \tag{12.42}$$

Using Eqs. (12.40) we find from Eqs. (12.39) and Eqs. (12.41) the projective measurement of the three states given by Eq. (12.41) will give the three Stokes parameters S_1, S_2 and S_3. As $S_0 = 1$ these four Stokes parameters can be used to find the density matrix ρ using Eq. (12.37).

For the photon case

$$|H\rangle = |0\rangle, \tag{12.43a}$$

$$|D\rangle = \frac{1}{\sqrt{2}}(|H\rangle + |V\rangle) = \frac{1}{\sqrt{2}}(|0\rangle + |1\rangle), \tag{12.43b}$$

$$|R\rangle = \frac{1}{\sqrt{2}}(|H\rangle + \mathrm{i}|V\rangle) = \frac{1}{\sqrt{2}}(|0\rangle + \mathrm{i}|1\rangle). \tag{12.43c}$$

Comparing Eqs. (12.41) and (12.43) we find that S_1 corresponds to the measurement of diagonal, S_2 corresponds to the measurement of right-circular and S_3 corresponds to the measurement of horizontal polarizations of the photon. We have seen the representation of

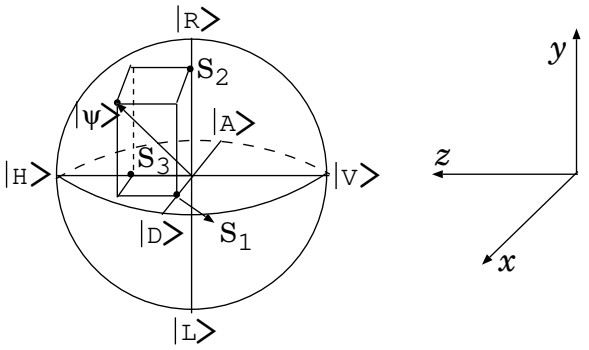

FIGURE 12.2
The three Stokes parameters define the state $|\psi\rangle$ in the Bloch sphere.

polarization states in Poincaré sphere (Bloch sphere) in sec. 5.9. The three Stokes parameters represent the given state $|\psi\rangle$ as a point in the sphere as shown in Fig. 12.2. So, the projective measurements of the three states $|D\rangle$, $|R\rangle$ and $|H\rangle$ of the photon state leads to the determination of the density matrix of the state of input photon.

Solved Problem 2:

The polarization measurements of a single photon state in qubit tomography experiment gives the Stokes parameters as $S_{|D\rangle} = -0.0463$, $S_{|R\rangle} = -0.0127$ and $S_{|H\rangle} = 0.3103$. Find the density matrix of the photon state.

For the single photon case measurements of $|\psi_1\rangle = |D\rangle$ gives S_1, $|\psi_2\rangle = |R\rangle$ gives S_2 and $|\psi_3\rangle = |H\rangle$ gives S_3. Also, $S_0 = 1$ always. We obtain $\rho = \frac{1}{2}\sum_{i=0}^{3} S_i\sigma_i$ as

$$\begin{aligned}
\rho &= \frac{1}{2}\left[S_0\sigma_0 + S_1\sigma_1 + S_2\sigma_2 + S_3\sigma_3\right] \\
&= \frac{1}{2}\left[\begin{bmatrix} 1 & 0 \\ 0 & 1 \end{bmatrix} - 0.0463\begin{bmatrix} 0 & 1 \\ 1 & 0 \end{bmatrix} - 0.0127\begin{bmatrix} 0 & -\mathrm{i} \\ \mathrm{i} & 0 \end{bmatrix}\right. \\
&\quad \left. +0.3103\begin{bmatrix} 1 & 0 \\ 0 & -1 \end{bmatrix}\right] \\
&= \begin{bmatrix} 0.65515 & -0.02315 + 0.00635\mathrm{i} \\ -0.02315 - 0.00635\mathrm{i} & 0.34485 \end{bmatrix}. \qquad (12.44)
\end{aligned}$$

12.6 Experimental Measure of Polarization of a Photonic Qubit

The experimental set-up [21] to analyse the polarization of a photonic qubit is shown in Fig. 12.3. The source beam passes through a quarter-wave plate (QWP), a half-wave plate (HWP) and the polarizing beam spliter (PBS). The PBS transmits the horizontally polarized light and reflects the vertically polarized light. The two output beams from PBS are

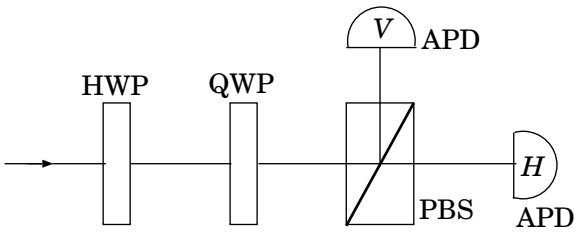

FIGURE 12.3
Experimental set-up for measuring polarization of a photon in an arbitrary base.

TABLE 12.1
The angles of the wave plates for the three directions x, y and z [21].

Measurement directions	HWP	QWP
$x(\sigma_1)$	22.5°	0°
$y(\sigma_2)$	0°	45°
$z(\sigma_3)$	0°	0°

fed into two separate avalanche photo diodes (APD). We have seen in the previous section that measurements of polarization along the three mutually perpendicular directions will give the three Stokes parameters S_1, S_2 and S_3. Measurements of S_1, S_2 and S_3 will give the density matrix of the input state of the source. Projective measurement on different direction can be done by different rotations of HWP and QWP.

The state vector is rotated by 180° around an axis by the HWP which is 2α times rotation of the crystal in the plane perpendicular to the incident light. If 0° position is defined as the direction in which horizontal polarized light stays horizontal (z-direction in Bloch sphere) then for an α-degree rotation the operator of the HWP is given by

$$\mathrm{HWP}(\alpha) = \begin{pmatrix} \cos 2\alpha & \sin 2\alpha \\ \sin 2\alpha & -\cos 2\alpha \end{pmatrix} = \sin 2\alpha \boldsymbol{\sigma}_1 + \cos 2\alpha \boldsymbol{\sigma}_3. \tag{12.45}$$

The operator for the QWP which rotates the state vector by 45° around an axis as in the case of HWP is given by

$$\begin{aligned} \mathrm{QWP}(\alpha) &= \begin{pmatrix} \cos^2\alpha - \mathrm{i}\sin^2\alpha & (1+\mathrm{i})\sin\alpha\cos\alpha \\ (1+\mathrm{i})\sin\alpha\cos\alpha & -\mathrm{i}\cos^2\alpha + \sin^2\alpha \end{pmatrix} \\ &= \frac{1}{2}\left[(1-\mathrm{i})(\mathbb{1} + \sin 2\alpha\boldsymbol{\sigma}_1) + (1+\mathrm{i})\cos 2\alpha\boldsymbol{\sigma}_3\right]. \end{aligned} \tag{12.46}$$

As S_1, S_2 and S_3 can be found from the projective measurements on the three standard directions x, y and z (refer Fig. 12.2) the angles for the three directions are given in table 12.1.

Single photons are recorded as clicks in the APD in either the horizontal or vertical channels. Recorded number of events can be transformed to represent the probability $P_{|\psi\rangle}$ by normalizing with the total number of events during the measurements as

$$P_{|\psi\rangle} \approx \frac{N(|\psi\rangle)}{N_{\mathrm{total}}}. \tag{12.47}$$

Only for $N_{\text{total}} \to \infty$ the equality will hold good. Having measured these values for the three directions of polarizations the parameters S_1, S_2 and S_3 can be estimated. Then Eq. (12.37) can be used to find the density matrix ρ. Instead of the three orthogonal axes represented by the Pauli matrices another independent three directions (not necessarily orthogonal) can also be chosen. From those measurements also the three Stokes parameters can be estimated.

12.7 Multiqubit Tomography

The idea used for the single qubit tomography can be extended to multiqubit tomography also. Let us outline it in this section [21].

The density of state for N-qubit state is given by [21–23]

$$\rho = \frac{1}{2^N} \sum_{i_1,i_2,\ldots,i_N=0}^{3} T_{i_1,i_2,\ldots,i_N} \sigma_{i_1} \otimes \sigma_{i_2} \otimes \ldots \otimes \sigma_{i_N}, \tag{12.48}$$

where the bases are coded as $i = 0 \Rightarrow \sigma_0 = \mathbb{1}$, $\sigma_1 = \sigma_x$, $\sigma_2 = \sigma_y$ and $\sigma_3 = \sigma_z$. The tensor, T, components are the measured values of the polarizations in certain bases combinations. The tensor products of the Pauli's matrices give the choice of basis. As for the case of single qubit the measurements are done on the three orthogonal directions (x, y, z). For example, in a two-qubit the term $\sigma_x \otimes \sigma_y = (\sigma_x \otimes \mathbb{1})(\mathbb{1} \otimes \sigma_y)$ corresponds to a measurement along the x-axis on qubit 1 and y-axis on qubit 2. This measurement will give the matrix element T_{XY}, where the measurement directions are coded in the order and label of the subindex. Then the Stokes parameters are normalized for the single qubit case taking $S_0 = 1$. For the N-qubit the normalization is done by taking $T_{11\ldots1} = 1$. So, the remaining $2^N \times 2^N - 1$ tensor components have to be determined by polarization measurements.

If we use PBSs for measurements then it will give an *overestimate of measurements*. For example, for two-qubit the tensor components T_{ZY} and T_{1Y} can be estimated using same measurements. We write

$$\begin{aligned} T_{ZY} &= T_Z \otimes T_Y \\ &= S_3 \otimes S_2 \\ &= \left(P_{|H\rangle} - P_{|V\rangle}\right) \otimes \left(P_{|R\rangle} - P_{|L\rangle}\right) \\ &= P_{|HR\rangle} - P_{|HL\rangle} - P_{|VR\rangle} + P_{|VL\rangle} \end{aligned} \tag{12.49}$$

and $T_{1Y} = T_1 \otimes T_Y = S_0 \otimes S_2$ becomes

$$\begin{aligned} T_{1Y} &= \left(P_{|H\rangle} + P_{|V\rangle}\right) \otimes \left(P_{|R\rangle} - P_{|L\rangle}\right) \\ &= P_{|HR\rangle} - P_{|HL\rangle} + P_{|VR\rangle} - P_{|VL\rangle}. \end{aligned} \tag{12.50}$$

Here $P_{|HR\rangle}$ refers to the probability to measure the state $|H\rangle$ in qubit 1 and $|R\rangle$ in qubit 2. We find from Eqs. (12.49) and (12.50), same four probability values will give two tensor components T_{1Y} and T_{ZY}. So, in a measurement set-up using PBSs only $3^N - 1$ unique settings are needed for measurements of the complete T tensor if the correlations in the outputs of the PBS are recorded. Figure 12.4 gives the schematic experimental set-up for a two-qubit quantum tomography [21].

A two-photon state is detected only when a photon is detected in arm-1 and arm-2 simultaneously. As multiqubit entangled states produced by most sources have low count

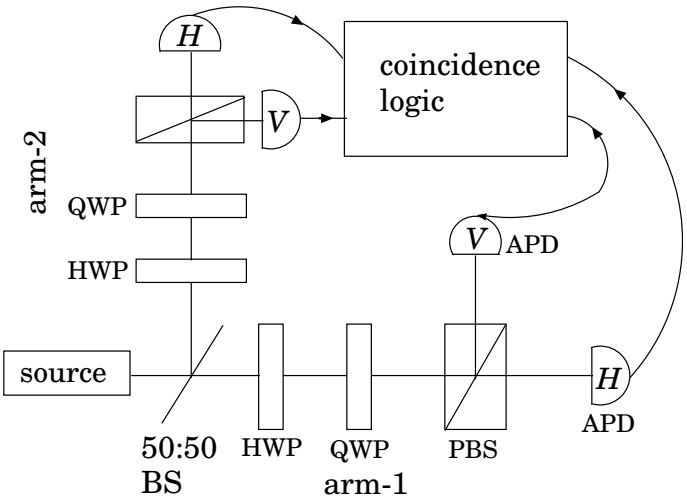

FIGURE 12.4
Schematics of two-qubit tomography set-up.

rate the time needed for measurements of $3^N - 1$ probability measurements increases exponentially with N. The combination of exponential increase of time and exponential decrease in brightness restrict the N values to be less than 6 in a practical experiment.

12.8 Quantum Process Tomography

Characterization of quantum dynamical systems is very important for quantum control and quantum information processing. The state of the system can be determined using quantum state tomography. It is equally important to identify an unknown quantum process acting on a quantum system. Any open quantum system suffers due to the noisy process known as *decoherence*. The characterization of such systems is a key issue in quantum information science. *Quantum process tomography* (QPT) aims to give full information on the dynamics of a quantum state. QPT can be used to improve the design and control of quantum hardware. For example, the characterization of single- and two-qubit controlled NOT gates are very important as they are the building blocks of a quantum computers. As QPT can give information about the noise sources affecting quantum information processor it can help in designing good error correcting strategies.

QPT methods can be classified as direct methods or indirect methods. Direct methods need the use of quantum state tomography. In indirect methods first the information about the quantum process of a system is mapped onto the state of some probe quantum systems. Secondly, the process is reconstructed using quatum state tomography on the output states. Indirect methods need application of an inversion on the final output data. Standard quantum process tomography (SQPT) [24–27] and ancilla-assisted process tomography (AAPT) [28–31] belong to indirect methods. In direct methods, experimental outcome will give directly information about the process without the need for quantum state tomography [27,32–36]. An extensive review of all these methods was presented in [27]. In this review

the required physical resources that arise in preparation and quantum measurements are analyzed and the complexity analysis of different QPT schemes is also presented.

12.8.1 Quantum Dynamical Maps

Let us briefly introduce the concept of quantum dynamical maps [27]. The dynamics (evolution) of an open quantum system can be described by a completely-positive linear map as

$$\mathcal{E}(\rho) = \sum_i A_i \rho A_i^\dagger. \tag{12.51}$$

This provides the transformation from an input state ρ_{in} to an output state ρ_{out}. The output ρ_{out} is given by the *Kraus operator-sum representation* [37]. We can write $\rho_{\text{out}} = \mathcal{E}(\rho_{\text{in}}) = \sum_i A_i \rho_{\text{in}} A_i^\dagger$. The physical process acting on the quantum system ρ is described by the channel (quantum operation) $\mathcal{E}$. $\mathcal{E}$ maps ρ_{in} to ρ_{out}. $\{A_i\}$ is a set of mappings (called Kraus operators) from the input Hilbert space to the output Hilbert space with $\sum_i A_i A_i^\dagger \leq I$ which gaurantees that $\text{Tr}\mathcal{E}(\rho) \leq 1$ [37]. Instead A_i we can choose a set of fixed Hermitian basis operators $\{E_i\}_{i=0}^{d-1}$ which satisfy the orthogonality condition $\text{Tr}\left(E_i^\dagger E_j\right) = d\delta_{ij}$. For example, for multiqubit systems E_i's can be tensor products of identity and Pauli matrices.

If A_i are decomposed as $A_i = \sum_m a_{im} E_m$ then Eq. (12.51) becomes

$$\mathcal{E}(\rho) = \sum_{m=0,\, n=0}^{d^2-1} \chi_{mn} E_m \rho E_n^\dagger, \tag{12.52}$$

where the matrix $\chi = \sum_{i,j} a_{mi} a_{nj}^*$ includes all information about the map $\mathcal{E}$ with respect to the $\{E_i\}$ basis. Measurements of the observables E_i will lead to determination of the d^4 independent matrix elements of χ.

12.8.2 Standard Quantum Process Tomography

In SQPT d^2 linearly independent inputs $\{\rho_k\}_{k=0}^{d^2-1}$ are prepared and the output states $\mathcal{E}(\rho_k)$ are measured using quantum state tomography [27]. If $\{|m\rangle\}_{m=0}^{d-1}$ is an orthonormal basis of Hilbert space $\mathcal{H}$ then $\{\rho(k)\}_{k=0}^{d^2-1}$ can be chosen as the linearly independent basis set of operators, where $\rho_k = |m\rangle\langle n|$. The output state of the channel $\mathcal{E}$ acting on one of these inputs $\mathcal{E}(|m\rangle\langle n|)$ can be found by preparing the input states

$$|m\rangle,\ \ |n\rangle,\ \ |+\rangle = \frac{1}{\sqrt{2}}(|m\rangle + |n\rangle),\ \ |-\rangle = \frac{1}{\sqrt{2}}(|m\rangle + \mathrm{i}|n\rangle)$$

and then forming the linear combination of the outputs $\mathcal{E}(|m\rangle\langle m|)$, $\mathcal{E}(|n\rangle\langle n|)$, $\mathcal{E}(|+\rangle\langle +|)$ and $\mathcal{E}(|-\rangle\langle -|)$. We write

$$\begin{aligned} \mathcal{E}(|m\rangle\langle n|) \;\; = \;\; & \mathcal{E}(|+\rangle\langle +|) + \mathrm{i}\mathcal{E}(|-\rangle\langle -|) \\ & - \frac{(1+\mathrm{i})}{2}\left[\mathcal{E}(|m\rangle\langle m|) + \mathcal{E}(|n\rangle\langle n|)\right]. \end{aligned} \tag{12.53}$$

So, measurements of $\mathcal{E}(|+\rangle\langle +|)$, $\mathcal{E}(|-\rangle\langle -|)$, $\mathcal{E}(|m\rangle\langle m|)$ and $\mathcal{E}(|n\rangle\langle n|)$ will be sufficient to determine $\mathcal{E}(|m\rangle\langle n|)$.

As every $\mathcal{E}(\rho_k)$ can be expressed as a linear combination of the basis state we get $\mathcal{E}(\rho_k) = \sum_l \lambda_{kl}\rho_l$. Since λ_{kl} are expectation values obtained by measurements of the fixed basis operator E_k, we obtain $\lambda_{kl} = \text{Tr}\left[E_k \mathcal{E}(\rho_l)\right]$. If we combine this relation with the

relation $E_n\rho_k E_n^\dagger = \sum_l B_{mn,lk}\rho_l$ we get $\sum_{m,n} B_{mn,lk}\chi_{mn} = \lambda_{kl}$. This equation can be given in matrix form as $\mathbf{B}\boldsymbol{\chi} = \boldsymbol{\lambda}$. The $(d^4 \times d^4)$-dimensional matrix $\mathbf{B}$ is determined from the choice of bases $\{\rho_k\}$ and $\{E_m\}$ and the d^4-dimensional vector $\boldsymbol{\lambda}$ is determined from the state tomography experiments. Inversion of $\mathbf{B}\boldsymbol{\chi} = \boldsymbol{\lambda}$ will give $\boldsymbol{\chi}$. In general $\mathbf{B}\boldsymbol{\chi} = \boldsymbol{\lambda}$ does not give a unique $\boldsymbol{\chi}$.

An ensemble of states (ρ_j) are prepared and each of them goes through the process given by the map $\mathcal{E}$ and then measurements of E_m are performed at the output [27]. Therefore, for SQPT d^2 linearly independent inputs $\{\rho_j\}$ have to be prepared. Each input ρ_j is subjected to the quantum process $\mathcal{E}$ followed by QST on the corresponding outputs. For each ρ_j the expectation values of the d^2 fixed basis operations $\{E_k\}$ have to be measured in the output state $\mathcal{E}(\rho_j)$. So, one has to perform d^4 measurements. All these measurements have to be done on an ensemble of identically prepared quantum systems corresponding to a given experimental setting.

12.8.3 Ancilla-Assisted Quantum Process Tomography

In SQPT an ensemble of a number of different quantum states is prepared then each one of them is subjected to the same quantum process to be characterized and then QST is performed on the outputs. Ancilla-assisted quantum process tomography (AAQPT) is an alternative technique to SQPT. In AAQPT an extra *ancilla* qubit is introduced. It involves preparation and tomography of only a single two-qubit quantum state rather than four one-qubit state.

According to *Choi-Jamiolkowski isomorphism* [38,39] a correspondence exists between the positive quantum maps $(\mathcal{E})$ and quantum state $\rho_\mathcal{E}$ as

$$\rho_\mathcal{E} = (\mathcal{E} \otimes I)(|\phi^+\rangle\langle\phi^+|), \quad |\phi^+\rangle = \sum_{i=1}^{d} \frac{1}{\sqrt{d}}|i\rangle \otimes |i\rangle, \tag{12.54}$$

where $|\phi^+\rangle$ is the maximally entangled state of the system and an ancilla with the same size. Actually the one-to-one map between $\mathcal{E}$ and $\rho_\mathcal{E}$ has made the quantum process to be equivalent to a quantum state in a large Hilbert space $\mathcal{H}_{\text{AB}}$ of the principal system A and the ancilla system B. That is, AAQPT reduces the problem of QPT to QST.

12.8.4 Direct Characterization of Quantum Dynamics

SQPT and AAQPT uses mapping of the dynamics onto a state. One may like to avoid mapping and perform a direct measurement of quantum dynamics thereby avoid any state tomography. Such direct methods are referred as *direct characterization of quantum dynamics* [36,40] and include the estimation of general functions of a quantum state [41], detection of quantum entanglement [33,42], reconstruction of quantum states or dynamics from incomplete measurements [43,44], measurement of nonlinear properties of bipartite quantum states [34], estimation of the average fidelity of a quantum gate or process [45–47], universal source coding and data compression [48] a few to mention.

Direct characterization of quantum dynamics (DCQD) differs in many ways from SQPT and AAQPT. AAQPT it does not require inversion of a full $d^2 \times d^2$ matrix as in AAQPT [36,40]. In DCQD certain entangled states are used as inputs and simple error-detecting measurements on the joint system-ancilla Hilbert space are performed. A combination of these input states and measurements give rise to direct encoding of the elements of the quantum map into results. Therefore, there is no need for QST of the output states. The measured probability distributions are directly related to the elements χ thus avoiding the

need for a complete inversion as in the indirect methods. So, in DCQD the χ matrix elements of the linear quantum maps become experimentally observable directly.

12.9 Conclusion

Knowledge of state preparation, state evolution and measurements are essential in all quantum technologies such as quantum computers. QST and QPT are used to characterize the quantum state and quantum evolution. Diagnosing errors and improving designs of quantum gates and architectures need a full characterization of a quantum process using QPT. As QPT dpends on measurement outcomes which may contain errors due to noise and imperfection of the measuring devices the resulting process may not be physical. Such nonphysicallity may be corrected using maximum likelihood estimation or through Bayesian interference technique [49]. More information on SQPT, AAQPT and DCQD can be obtained from the ref. [27].

Though QST and QPT are powerful techniques they do not take advantage of any prior information available to the experimentalists. Bayesian estimation is a class of techniques that allow one to include prior information related to the experiment. Bayesian tomography is gaining importance due to many recent developments. Though QST was implemented in optical system first, it has been demonstrated in many different experimental platforms like atomic ions, atomic spins of neutral atoms, orbital angular momentum modes of light and superconducting qubits. Similarly, QPT has been used in many different processes such as entangling gates with trapped atomic ions and optical systems, the motion of atoms in optical lattice and three qubits in NMR.

The major difficulty in using tomography is the presence of the sources of noise and dechoherence in any experimental set-up. Due to the errors introduced by noise, the estimates are not always accurrate. Also, as the order of the qubits increases the system becomes too large and highly expensive. To overcome these difficulties many new technologies are being developed.

12.10 Bibliography

[1] U. Fano, *Rev. Mod. Phys.* 29:74, 1957.

[2] K. Vogel and H. Risken, *Phys. Rev. A* 40:2847, 1989.

[3] W. Pauli, *Die allgemeinen Prinzipien der Wellenmechanik*. In Handbuch der Physik, vol 24, part 1, H. Geiger and K. Scheel (Eds.), pp. 83-272, Springer, Berlin, 1933. Reprinted in S. Flugge (Ed.), Encyclopedia of Physics, vol. V, part 1, Springer, Berlin, 1958, pp. 1-168.

[4] D.T. Smithey, M. Beck and M.G. Raymer, *Phys. Rev. Lett.* 70:1244, 1993.

[5] Reichenbach, *Philosophic Foundations of Quantum Mechanics*. University of California Press, Berkeley and Los Angeles, 1944.

[6] V.I. Man'ko, G. Marmo, A. Simoni, A. Stern and F. Ventriglia, *Phys. Lett. A* 343:251, 2005.

[7] A. Ibort, V.I. Man'ko, G. Marmo, A. Simoni, A. Stern and F. Ventriglia, *Phys. Scr.* 79:065013, 2009.

[8] S. Mancini, V.I. Man'ko and P. Tombesi, *Found. Phys.* 27:801, 1997.

[9] J. Radon, *Ber. Verh. Sachs. Akad.* 69:262, 1917.

[10] E. Wigner, *Phys. Rev.* 40:749, 1932.

[11] Z. Chen, Q. Wu and C. Zhang, *J. Electromag. Anal. Appl.* 2:333, 2010.

[12] K.E. Cahill and R.J. Glauber, *Phys. Rev.* 177:1857, 1969.

[13] J. Bertrand and P. Bertrand, *Found. Phys.* 17:397, 1987.

[14] V. Potocek and S.M. Barnett, *Phys. Scr.* 90:065208, 2015.

[15] S.M. Barnett and P.M. Radmore, *Methods in Theoretical Quantum Optics*. Oxford University Press, New York, 1997.

[16] D.T. Smithey, M. Beck, J. Cooper, M.G. Raymer and A. Faridani, *Phys. Scr.* T48:35, 1993.

[17] D.T. Smithey, M. Beck, J. Cooper and M.G. Raymer, *Phys. Rev. A* 48:3159, 1993.

[18] V. Leonhart and H. Paul, *Prog. Quantum Electron.* 19:89, 1995.

[19] G. Breitenbach, S. Schiller and J. Mlynek, *Nature* 387:471, 1997.

[20] J.B. Altepeter, D.F.V. James and P.G. Kwiat, *Qubit Quantum State Tomography*. In Quantum State Estimation (Lecture Notes in Physics, Vol. 649), Springer, Berlin, 2004, pp. 113-145.

[21] A. Niggebaum, *Quantum State Tomography of the 6 Qubit Photonic Symmetric Dicke State*. Master Thesis, Ludwig-Maximillians-University, Munich, 2011.

[22] M.G.A. Paris and J. Rehacek, *Quantum State Estimation*. Springer, Berlin, 2004.

[23] D.F.V. James, P.G. Kwiat, W.J. Munro and A.G. White, *On the Measurement of Qubits*. In Asymptotic Theory of Quantum Statistical Inference – Selected Papers, M. Hayashi (Ed.), pp. 509-538, World Scientific, Singapore, 2005.

[24] G.M. D'Ariano, M.G.A. Paris and M.F. Sacchi, *Advances in Imaging and Electron Physics* 128:205, 2003.

[25] G.M. D'Ariano and P. Lo Presti, *Characterization of Quantum Devices*. In Quantum State Estimation (Lecture Notes in Physics, Vol. 649), Springer, Berlin, 2004, pp. 297-332.

[26] L.M. Artiles, R.D. Gill and M.I. Gut, *J. R. Statist. Soc. B* 67:109, 2005.

[27] M. Mohseni, A.T. Rezakhani and D.A. Lidar, *Phys. Rev. A* 77:032322, 2008.

[28] G.M. D'Ariano and P. Lo Presti, *Phys. Rev. Lett.* 86:4195, 2001.

[29] J.B. Altepeter, D. Branning, E. Jeffrey, T.C. Wei, P.G. Kwiat, R.T. Thew, J.L. O'Brien, M.A. Nielsen and A.G. White, *Phys. Rev. Lett.* 90:193601, 2003.

[30] G.M. D'Ariano and P. Lo Presti, *Phys. Rev. Lett.* 91:047902, 2003.

[31] A. Shukla, K. Rama Koteswara Rao and T.S. Mahesh, *Phys. Rev. A* 87:062317, 2013.

[32] A.K. Ekert, C.M.Alves, D.K.L. Oi, M. Horodecki, P. Horodecki and L.C. Kwek, *Phys. Rev. Lett.* 88:217901, 2002.

[33] P. Horodecki and A. Ekert, *Phys. Rev. Lett.* 89:127902, 2002.

[34] F.A. Bovino, G. Castagnoli, A. Ekert, P. Horodecki, C.M. Alves and A.V. Sergienko, *Phys. Rev. Lett.* 95:240407, 2005.

[35] J. Emerson, Y.S. Weinstein, M. Saraceno, S. Lloyd and D.G. Cory, *Science* 302:2098, 2003.

[36] M. Mohseni and D.A. Lidar, *Phys. Rev. Lett.* 97: 17050, 2006.

[37] M.A. Nielsen and I.L. Chuang, *Quantum Computation and Quantum Information*. Cambridge University Press, Cambridge, 2000.

[38] A. Jamiolkowski, *Rep. Math. Phys.* 3:275, 1972.

[39] M.D. Choi, *Linear Algebra Appl.* 10:285, 1975.

[40] M. Mohseni and D.A. Lidar, *Phys. Rev. A* 75:062331, 2007.

[41] A.K. Ekert, C.M. Alves, D.K.L. Oi, M. Horodecki, P. Horodecki and L.C. Kwek, *Phys. Rev. Lett.* 88:217901, 2002.

[42] Y. Turek, *J. Phys. Commun.* 4:075007, 2020.

[43] V. Buzek, G. Drobny, R. Derka, G. Adam and H. Wiedemann, *Chaos, Solitons & Fractals* 10:981, 1999.

[44] M. Ziman, M. Plesch and V. Buzek, *Eur. Phys. J. D* 32:215, 2005.

[45] J. Emerson, Y.S. Weinstein, M. Saraceno, S. Lloyd and D.G. Cory, *Science* 302:2098, 2003.

[46] J. Emerson, R. Alicki and K. Zyczkowski, *J. Opt. B: Quantum Semiclassical Opt.* 7:S347, 2005.

[47] H.F. Hofmann, *Phys. Rev. Lett.* 94:160504, 2005.

[48] C.H. Bennett, A.W. Harrow and S. Lloyd, *Phys. Rev. A* 73:032336, 2006.

[49] D.F.V. James, P.G. Kwiat, W.J. Munro and A.G. White, *Phys. Rev. A* 64:052312, 2001.

12.11 Exercises

12.1 Assume that the initial state of a copying device is $|0\rangle$ and copying of the two basis states $|0\rangle$ and $|1\rangle$ requires the controlled-NOT operation $|0\rangle|0\rangle \to |0\rangle|0\rangle$ and $|1\rangle|0\rangle \to |1\rangle|1\rangle$. Show that this cloning operation cannot be done on a general state $|\psi\rangle = \alpha|0\rangle + \beta|1\rangle$.

12.2 Normalize $\psi_1(q) = N_1 \mathrm{e}^{-\alpha q^2 + \mathrm{i}\beta q}$ and $\psi_2(q) = N_2 \mathrm{e}^{-\alpha^* q^2 + \mathrm{i}\beta q}$ with $\mathrm{Re}\,\alpha \geq 0$ and β real.

12.3 Determine the momentum wave functions of $\psi_1(q)$ and $\psi_2(q)$ given by Eq. (12.2).

12.4 Show that for the wave functions $\psi_1(q)$ and $\psi_2(q)$ given by Eq. (12.2) the fidelity $\mathcal{F}$ is given by Eq. (12.5).

12.5 Determine the eigenfunction of the operator $-\mathrm{i}\hbar\nu \frac{\mathrm{d}}{\mathrm{d}q} + \mu q$.

12.6 Convert the normally ordered product $a^\dagger a^2$ into anti-normally ordered product and anti-normally ordered product $a^2 a^\dagger$ into normally ordered product.

12.7 Assuming $\frac{1}{\pi^2}\int_{\mathrm{C}} \mathrm{d}^2\alpha\, \mathrm{e}^{\alpha\lambda^*-\alpha^*\lambda} = \delta^2(\lambda)$, where $\delta^2(\lambda)$ is the two-dimensional delta function show that the s-ordered Wigner function $W_s(\alpha,\alpha^*)$ is normalized.

12.8 Prove that the average of the normally ordered products of creation and annihilation operators is $\langle [a^\dagger]^n a^k\rangle = \int_{\mathrm{C}} P(\alpha)\alpha^k[\alpha^*]^n \mathrm{d}^2\alpha$.

12.9 Given the quadrature operator $\chi_\phi = a\mathrm{e}^{-\mathrm{i}\phi}+a^\dagger \mathrm{e}^{\mathrm{i}\phi}$ prove that the expectation value of the χ_ϕ in coherent state $|\alpha\rangle = \mathrm{e}^{-|\alpha|^2/2}\sum_{n=0}^{\infty}\frac{\alpha^n}{\sqrt{n!}}|n\rangle$ is $2\mathrm{Re}\left[\alpha \mathrm{e}^{-\mathrm{i}\phi}\right]$. Show that the uncertainty of the expectation of the quadrature is $\Delta^2(\chi_\phi) = \langle\chi_\phi^2\rangle - \langle\chi_\phi\rangle^2 = 1$.

12.10 Diagonalize the density matrix $\rho = \frac{1}{6}\begin{pmatrix} 3 & 1 \\ 1 & 3 \end{pmatrix}$ and find the eigenvectors.

12.11 Show that the Stokes parameters are given by $S_i = \mathrm{Tr}(\sigma_i\rho)$.

12.12 Find the Stokes parameters for the input state $|D\rangle = \frac{1}{\sqrt{2}}(|H\rangle + |V\rangle)$.

12.13 Obtain the Stokes parameters for the input state $|A\rangle = \frac{1}{\sqrt{2}}(|H\rangle - |V\rangle)$.

12.14 Determine the density matrix and then the Stokes parameters for the input state $|R\rangle = \frac{1}{\sqrt{2}}(|H\rangle + \mathrm{i}|V\rangle)$.

12.15 Find the Stokes parameters for the input state with $\rho = \begin{pmatrix} \frac{5}{8} & -\frac{1}{2\sqrt{2}}\mathrm{i} \\ \frac{1}{2\sqrt{2}}\mathrm{i} & \frac{3}{8} \end{pmatrix}$.

13

Quantum Simulation

13.1 Introduction

The laws governing the behaviour of microscopic quantum systems are given by quantum mechanics. Though the basic laws of low-energy physics is well known at microscopic level, many fundamental questions remain open about the collective dynamics of the macroscopic scale. When a system as in condensed matter physics has a large number of constituents or degrees of freedom, it cannot be treated exactly by quantum mechanics. The collective behaviour of a macroscopic system can drastically change from that of its microscopic constituents. For example, in phase transition of the bulk materials the elementary interaction at the microscopic level remains same, eventhough dramatic changes are observed in macroscopic level. A few such examples for these dramatic changes occurring at some critical temperatures are: magnetic phase transition at Curie temperature, superfuid transition in helium, superconducting transition in electronic metal-insulator transition in electronic systems. Though these phenomena appear only in very large scale macroscopic systems, they arise mainly due to the mutual interactions of their elementary constituents. In many situations, local two-body interactions are sufficient to explain the dramatic changes taking place at the macroscopic bulk materials. It has been found that the well established classical laws of physics fail to explain both the microscopic behaviour of the fundamental constituents of the bulk material and also the dynamical behaviour of macroscopic physical systems made of several interacting fundamental constituents.

Quantum mechanics is the most complete and successful theory we have currently to describe the dynamics of the elementary constituents of a macroscopic system. A variety of methods and simulation tools like quantum Monte-Carlo molecular dynamics, tensor networks have been developed in the past to solve some of the theoretical models formulated in quantum mechanical terms and correctly describe a large variety of quantum phenomena [1]. These methods make use of mathematical modelling in which the informations we know about a system of interest are mapped on a certain set of variables and equations. The resulting mathematical identities, to be solved either exactly or numerically, can be called as a *simulator*.

A quantum simulator can be used to study the behaviour of the concerned real system. The accuracy with which this simulation predicts the behaviour of the real system depends on the validity of the initial mathematical model chosen and the available computational power. It has been found that even the modern classical supercomputers currently available are not able to solve most of these simulation models. So, quantum simulators have long been proposed as a possible replacement of these classical simulation models.

In the present chapter, first we point out the limitations in simulating quantum systems in classical computers. We give a general scheme of quantum simulation. We present the features of analog and digital quantum simulators. Then we discuss the basic theory of quantum simulation of Schrödinger equation. Next, we describe the various stages of quantum simulation using quantum computers and relevant quantum circuits.

DOI: 10.1201/9781003172192-13

13.2 Limitations of Classical Computers in Simulating Quantum Systems

Simulations of many quantum models using classical computers have been done over many decades in the past. The most successful methods are the quantum Monte Carlo algorithms. These classical stochastic methods generally work well only when the functions being integrated do not change sign so that sampling of these functions at a relatively small points give good approximations to the integrals of these functions. But for some quantum systems like fermionic and frustrated systems sign problems arise in numerical evaluation of integrals due to the problem of sampling of nonpositive semi-definite weight functions. This leads to exponential growth of statistical errors in the results with increase of number of particles. Other classical methods such as mean-field and dynamical mean-field theory, tensor network theory, density functional theory, many-body perturbation theories or Green's function based methods have their own limitations which restrict their applicability to large quantum systems.

In a general quantum simulation problem we are interested to find the wave function $\psi(t)$ at time t given its value at $t = 0$. Using $\psi(t)$, we can compute the values of some physical quantities of the system. The time evolution of $\psi(t)$ is given by the Schrödinger equation

$$\mathrm{i}\hbar\frac{\mathrm{d}}{\mathrm{d}t}|\psi\rangle = H|\psi\rangle. \tag{13.1}$$

For time-independent Hamiltonian H the solution of the above equation is

$$|\psi(t)\rangle = \mathrm{e}^{-\mathrm{i}Ht/\hbar}|\psi(0)\rangle. \tag{13.2}$$

For numerical computation of $|\psi(t)\rangle$ we have to discretize the problem so that it can be encoded in the computer memory.

Unlike a classical state, a quantum state represented by a wave function $|\psi\rangle$ is a superposition of all the configuration of the system. Classically, a spin-1/2 particle can be represented as a spin-up state 1 and a spin-down state 0. But quantum mechanically, the spin state of the particle is a superposition state $c_1|0\rangle + c_2|1\rangle$, where c_1 and c_2 are the expansion coefficients for the two configurations $|0\rangle$ and $|1\rangle$ states. For a two particle system, there are four configurations $|00\rangle$, $|01\rangle$, $|10\rangle$ and $|11\rangle$. So the state of the system is a vector in a 4-dimensional Hilbert space

$$|\psi\rangle = c_1|00\rangle + c_2|01\rangle + c_3|10\rangle + c_4|11\rangle. \tag{13.3}$$

There are $2^2 = 4$ coefficients needed to describe the quantum state. For a system of N spin-1/2 particles the memory needed to store the state will be 2^N. In a classical computer with a memory of 10^{12}, one can store the state of N particles, where $N = \log\left(10^{12}\right)/\log 2 \approx 40$. So it is possible to do quantum simulation on a classical computer with a memory capacity of 10^{12} for a quantum system with just 40 spin-1/2 particles. Moreover, to calculate the time evolution given by Eq. (13.2) requires the exponentiation of a $2^{40} \times 2^{40}$ matrix with nearly 10^{24} entries. So it is practically impossible to use classical computers to perform quantum simulation for systems with large number of particles.

It has been found that simulating quantum mechanical system is a very challenging problem in classical computers due to the difficulty of storing the quantum state of a large physical system. Quantum state is described by a number of parameters that grows exponentially with the number of particles or degrees of freedom of the system. Moreover,

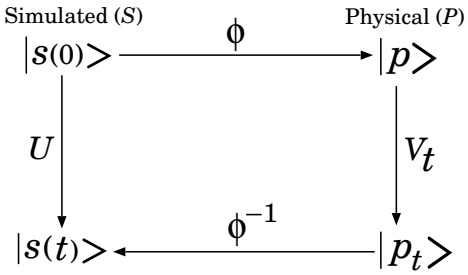

FIGURE 13.1
A scheme for quantum simulation with $U = \mathrm{e}^{-\mathrm{i}Ht/\hbar}$.

stimulating the temporal evolution of the quantum system requires a number of operations which also increases exponentially with system size. All these limitations of classical computer in simulating quantum systems make it quite inefficient even for small quantum systems and not suitable to handle large systems.

13.3 Quantum Simulators

In 1982 Feynman [2] conjectured that quantum computers would be able to simulate a quantum system more efficiently than classical computers as they work based on the principle of quantum mechanics. It was felt that one can avoid the experimental scaling associated with the simulation of increasingly large quantum systems on conventional computers using quantum computers. After Feynman introduced the concept of quantum simulators, Seth Lloyd [3] showed that a variety of quantum systems including quantum computers can be programmed to simulate the behaviour of arbitrary quantum systems whose dynamics are determined by local interactions. Lloyd proved that quantum simulation can be performed with arbitrary precision in a computer time that grows at most polynomially proveded the interaction is limited to only a few other neighbours.

A quantum simulator can be defined as a process in which the dynamics of a quantum system is mapped onto the dynamics of a controllable quantum system. That is, a quantum simulator is a controllable quantum system used to simulate or emulate other quantum systems of interest.

A general scheme [4] for quantum simulation of a quantum system (S) is given in Fig. 13.1. Quantum simulator aims to simulate the quantum system of interest $|s(t)\rangle$ from the initial state $|s(0)\rangle$ using the physical system (P). The invertible map ϕ determines a correspondence between all the operators and states of S and P. The propagator of the quantum system U maps to $V_t = \phi U \phi^{-1}$ of the experimental controllable quantum system P. To simulate the quantum system S one needs methods for controlling precisely the dynamics of the experimental quantum system (P) so that it mimics the dynamics of the system S. A series of operations performed by the experimenter to move the experimental quantum system P towards the quantum system of interest S by altering the Hamiltonian by each operation to get H as closely as possible.

Quantum simulation works by evolving the system forward locally over samll discrete times slices [3]. It is possible to find local Hamiltonians H_1, H_2, ..., H_n such that

$H = \sum_{i=1}^{l} H_i$, where the H_i operators are all local and operating in a small dimensions m_i with limited variables k. One can write [3] (with $\hbar = 1$)

$$\mathrm{e}^{-\mathrm{i}Ht} = \left(\mathrm{e}^{-\mathrm{i}H_1 t/n}\mathrm{e}^{-\mathrm{i}H_2 t/n}\ldots\mathrm{e}^{-\mathrm{i}H_l t/n}\right)^n + \sum_{i>j}[H_i, H_j]\,\frac{t^2}{2n} + \sum_{k=3}^{\infty} E(k). \tag{13.4}$$

In this equation $E(k)$ are bounded by $||E(k)|| \leq n||Ht/n||_{\mathrm{m}}^k/k!$, where $||A||_{\mathrm{m}}$ refers to maximum of the expectation value of the operator A. In quantum simulation $\mathrm{e}^{-\mathrm{i}Ht}$ is approximated as

$$\mathrm{e}^{-\mathrm{i}Ht} \approx \left(\mathrm{e}^{-\mathrm{i}H_1 t/n}\cdot\mathrm{e}^{-\mathrm{i}H_2 t/n}\ldots\mathrm{e}^{-\mathrm{i}H_l t/n}\right)^n \tag{13.5}$$

with an error less that $||n\left(\mathrm{e}^{-\mathrm{i}Ht} - 1 - \mathrm{i}Ht/n\right)||_m$. The error can be made as small as possible by taking n sufficiently large. So it is quite possible to simulate to any desired accuracy ϵ by taking sufficiently large n.

It has been proved that for any local Hamiltonian H_i acting on a local Hilbert space of only m_i dimensions, the number of operations needed to simulate $\mathrm{e}^{-\mathrm{i}H_i t/n}$ is found to be nearly equal to m_i^2 only [3]. So, the evolution of $\mathrm{e}^{-\mathrm{i}Ht}$ given by Eq. (13.5) needs only a total operations of nearly equal to $n\sum_{i=1}^{l} m_i^2$. If m is the maximum of m_i then the number of operations to simulate $\mathrm{e}^{-\mathrm{i}Ht}$ will be $\leq nlm^2$. Therefore, as long as l is a polynomial functions of N (the number of variables of the system) the number of computations increases only polynomially. Hence, decomposing the total Hamiltonian H into a series of local Hamiltonians H_i as given by Eq. (13.5) makes the number of computation to increase as polynomials instead of exponential growth with the increase of the system size. In a quantum simulator we are able to break our original problem of evaluating $\mathrm{e}^{-\mathrm{i}Ht}$ into smaller pieces $\mathrm{e}^{-\mathrm{i}H_i t/n}$ which can be implemented with limited number of operations on the experimental system or with a limited number of quantum gates in a quantum computer. The maximum number of operations for a given error ϵ increases only polynomially with the increase of system size as long as the Hamiltonians H_i are having only nearest neighbour interactions.

We can use quantum simulators to solve scientific problems that are not solvable by other methods. Quantum simulation will be considered successful only if the initial state preparation, the implementation of the time evolution and the measurements of observables are realized using only polynomial resources. The measurements from the simulators are more important as they only give useful informations about the quantum system. Generally, all these procedures to be used in a quantum simulators are not easy tasks. Quantum simulators are classified into two types: (i) *analog* quantum simulators [5–14] and (ii) *digital* quantum simulators [3,12,15–24]. We present these in the next two sections.

13.4 Analog Quantum Simulators

In an analog quantum simulator the physical properties of a targeted model are reproduced on a physical set-up under externally controlled conditions. The evolution of the quantum system is simulated onto the controlled evolution of the quantum simulator. One quantum system will mimic the evolution of another quantum system. In analog quantum simulator the Hamiltonian H_{sys} is mapped on the Hamiltonian H_{sim} of the simulator. So the qunatum

system to be simulated and the controllable simulator system must be fairly similar. Consequently, any analog quantum simulator can only be used for a limited class of quantum systems.

Designing an analog quantum simulator for a specific problem is relatively simple. For example, the study of many-body problems in condensed matter physics could be achieved using analog quantum system consisting of an arrays of qubits realized with atoms in optical lattices, atoms in arrays of cavities, arrays of trapped ions, superconducting circuits and quantum dots. The controls of the quantum simulators are done using laser pulses, radio frequency pulses and electric and magnetic fields.

Now, we give an example of mapping between a quantum system and the corresponding simulator [11,12]. For a spin-1/2 relativistic particle in $(1+1)$ dimension the Dirac equation is

$$\mathrm{i}\hbar\frac{\partial\psi}{\partial t} = H_{\mathrm{sys}}\psi = \left(cp_x\sigma_x + mc^2\sigma_z\right)\psi. \tag{13.6}$$

The H_{I} of a single ion interacting with a bichromatic light field with η as Lamb–Dicke parameter, Δ as the spatial size of the ground state wave function and $\overline{\Omega}$ as the parameter controllable by the intensity of the bichromatic light field is given by

$$H_{\mathrm{sim}} = 2\eta\Delta\overline{\Omega}\sigma_x p_x + \hbar\Omega\sigma_z. \tag{13.7}$$

Comparing Eq. (13.6) with Eq. (13.7) we find them similar if $c = 2\eta\Delta\overline{\Omega}$ and $mc^2 = \hbar\Omega$. Analog quantum simulation of the one-dimensional Dirac equation using a simple trapped ion was performed [22]. In the simulation, the position of the particle was measured as a function of time and Zitterbewegung was studied for different initial superposition of positive and energy spinor states. Further, the cross-section from relativistic to nonrelativistic dynamics was also analyzed. Interestingly, control of the trapped ion experimental parameters of the simulator was successfully realized in the simulation study. A more detailed discussion on the Hamiltonians of several quantum simulators and those of the systems to be simulated has been presented in ref. [12].

Experimental platforms based on neutral atoms, trapped ions, photons and superconducting circuits have been used to perform analog quantum simulations of different types. In [13] many experimental analog simulations done using small quantum structures like a single ion to simulate the Dirac quation, a system of two and three trapped ions to simulate two and three quantum spins, respectively, have been presented. Ion trap techniques were used to simulate nonequilibrium dynamics of quasiparticles. Superconducting flux qubit interaction with the electromagnetic field is found to be analogous to that of a dipole atom-field interaction. This interaction was used to simulate a variety of quantum optical effects. Superconducting quantum circuits are used to simulate a number of fundamental effects like Casimir effect, Unruh effect and Dicke superradiance. Larger structures are needed to simulate many-body physics. Optical lattices are used for many analog simulations like Zak phase.

13.5 Digital Quantum Simulators

Unlike in analog quantum simulators, in digital quantum simulators the time evolution of $|\psi(t)\rangle$ from the initial state $|\psi(0)\rangle$ for a system with Hamiltonian H by the unitary transofrmation $U = \mathrm{e}^{-\mathrm{i}Ht}$ $(\hbar = 1)$ is constructed by quantum circuits with quantum gates. Qubits are used to encode state of the quantum system, the unitary transformation U

is translated in terms of elementary quantum gates and then they are implemented in a circuit-based quantum computer. Computing the time evolution operator $U(t)$ is equivalent to the task of implementing a unitary matrix and any unitary transformation can be done in a quantum computer using a universal set of quantum gates [19].

As discussed in sec. 13.3 the quantum computer can calculate $U(t)$ effectively with polynomial time and memory resources if $H = \sum_l H_l$, where H_l are all having only local interactions like nearest neighbours or second-to-nearest neighbours interactions in a lattice. From Eq. (13.4) we can write the total Hamiltonian as

$$U(t) = \prod_l U_l(t), \quad U_l(t) = \mathrm{e}^{-\mathrm{i}H_l t}. \tag{13.8}$$

$U(t)$ can be implemented on a universal computer by decomposing the circuit implementation of the single $U_l(t)$ unitaries. Use of the Suzuki–Trotter (ST) decomposition gives

$$U(t) = \exp\left(-\mathrm{i}\sum_l H_l t\right) = \left(\prod_l \mathrm{e}^{-\mathrm{i}H_l t/n}\right)^n + O\left(\frac{t^2}{n}\right). \tag{13.9}$$

So, $U(t)$ can be approximated by repeating n times the sequence of gates corresponding to the product of local times $U_l(t)$ for time slices t/n. It is thus possible for systems with $H = \sum_l H_l$ to break the problem into smaller pieces of $\mathrm{e}^{-\mathrm{i}H_l t/n}$. Each of the unitary transformation $\mathrm{e}^{-\mathrm{i}H_l t/n}$ can now be implemented using only a limited set of elementary quantum gates. The last term in Eq. (13.9) gives the error which can be minimized to a desired value by increasing n.

Solved Problem 1:

Show that the error term $O(t^2/n)$ vanishes in ST decomposition if all the operators commute among themselves.

We have $H = \sum_{l=1}^{k} H_l$ and as all the Hamiltonians commute among themselves $[H_i, H_j] = 0$ we write

$$U = \mathrm{e}^{-\mathrm{i}Ht} = \mathrm{e}^{-\mathrm{i}\sum_l H_l t} = \mathrm{e}^{-\mathrm{i}H_1 t} \cdot \mathrm{e}^{-\mathrm{i}H_2 t} \cdot \ldots \cdot \mathrm{e}^{-\mathrm{i}H_k t}. \tag{13.10}$$

Consider $\mathrm{e}^{-\mathrm{i}H_1 t} \cdot \mathrm{e}^{-\mathrm{i}H_2 t}$. We obtain

$$\begin{aligned}
\mathrm{e}^{-\mathrm{i}H_1 t} \cdot \mathrm{e}^{-\mathrm{i}H_2 t} &= \left[I - \mathrm{i}H_1 t - \frac{1}{2}H_1^2 t^2 + \frac{\mathrm{i}}{6}H_1^3 t^3 - \ldots\right] \\
&\quad \times \left[I - \mathrm{i}H_2 t - \frac{1}{2}H_2^2 t^2 + \frac{\mathrm{i}}{6}H_2^3 t^3 - \ldots\right] \\
&= I - \mathrm{i}(H_1 + H_2)t - \frac{1}{2}\left(H_1^2 + H_1 H_2 + H_2 H_1 + H_2^2\right) t^2 \\
&\quad + \frac{\mathrm{i}}{6}\left(H_1^3 + H_2^3 + H_1^2 H_2 + H_2^2 H_1 + H_1 H_2 H_1\right. \\
&\quad \left. + H_2 H_1^2 + H_1 H_2^2 + H_2 H_1 H_2\right) - \ldots.
\end{aligned} \tag{13.11}$$

As $H_1 H_2 = H_2 H_1$ the above equation becomes

$$\begin{aligned}
\mathrm{e}^{-\mathrm{i}H_1 t} \cdot \mathrm{e}^{-\mathrm{i}H_2 t} &= I - \mathrm{i}(H_1 + H_2)t - \frac{1}{2}\left(H_1^2 + 2H_1 H_2 + H_2^2\right) t^2 \\
&\quad + \frac{\mathrm{i}}{6}\left(H_1^3 + H_2^3 + 3H_1 H_2^2 + 3H_1^2 H_2\right) t^3 - \ldots \\
&= \mathrm{e}^{-\mathrm{i}(H_1 + H_2)t}.
\end{aligned} \tag{13.12}$$

As H_3 commutes with $H_1 + H_2$ we get

$$\mathrm{e}^{-\mathrm{i}H_1 t} \cdot \mathrm{e}^{-\mathrm{i}H_2 t} \cdot \mathrm{e}^{-\mathrm{i}H_3 t} = \mathrm{e}^{-\mathrm{i}(H_1+H_2+H_3)t}. \tag{13.13}$$

Extending this procedure, we obtain

$$\mathrm{e}^{-\mathrm{i}H_1 t} \cdot \mathrm{e}^{-\mathrm{i}H_2 t} \cdot \mathrm{e}^{-\mathrm{i}H_k t} = \mathrm{e}^{-\mathrm{i}(\sum_l H_l)t} = \prod_{l=1}^{k} \mathrm{e}^{-\mathrm{i}H_l t} = \prod_l \left(\mathrm{e}^{-\mathrm{i}H_l t/n}\right)^n. \tag{13.14}$$

Thus, the error term $O(t^2/n)$ vanishes if all H_i's commute among themselves.

13.6 Theory of Quantum Simulation of the Schrödinger Equation

We give the outline of the theory of quantum simulation of one-dimensional Schrödinger equation [25,26] in this section.

A quantum register of size n stores a collection of n qubits and the wave function is a vector in 2^n-dimensional complex Hilbert space with 2^n basis functions $|k\rangle = |k_{n-1}\rangle \ldots |k_0\rangle$, where $|k_j\rangle$, gives the state of the qubit. $k_0, \ldots, k_{n-1}$ will give the binary bits $\{1, 0\}$. In a n-bit quantum computer the wave function can be written as a linear combination of the basis functions as

$$|\psi\rangle = \sum_{k=0}^{n-1} C_k |k\rangle, \quad \sum_{k=0}^{n-1} |C_k|^2 = 1. \tag{13.15}$$

The one-dimensional Schrödinger equation is

$$\mathrm{i}\hbar \frac{\mathrm{d}}{\mathrm{d}t}\psi(x,t) = H\psi, \quad H = H_0 + V(x), \quad H_0 = -\frac{\hbar^2}{2m}\frac{\mathrm{d}^2}{\mathrm{d}x^2}. \tag{13.16}$$

To solve Eq. (13.16) we discretize the continuous variables x and t. If the motion takes place between $-d$ and d then $-d \le x \le d$. We can devide this region into 2^n intervals of length $\Delta x = 2d/2^n$ and represent these intervals in n-qubit quantum register. Then we can write the wave function (13.15) approximately as

$$\sum_{k=0}^{2^n-1} C_k(t)|k\rangle = \frac{1}{N}\sum_{k=0}^{2^n-1} \psi(x_k, t)|k\rangle, \quad x_k = -d + \left(k + \frac{1}{2}\right)\Delta x. \tag{13.17}$$

The normalising factor is $N = \sqrt{\sum_{k=0}^{2^n-1} |\psi(x_k,t)|^2}$. If Δx is small then Eq. (13.17) will give good approximation. Equation (13.16) can be integrated over a time step δt as

$$\psi(x, t+\delta t) = \mathrm{e}^{-\mathrm{i}(H_0+V(x))\delta t/\hbar}\psi(x,t). \tag{13.18}$$

The unitary transformation $U = \mathrm{e}^{-\mathrm{i}(H_o+V(x))\delta t/\hbar}$ gives the evolution of the wave function over a time interval δt. Using ST decomposition and Fourier transform (F) the total evolution during δt can be approximated as

$$U \approx \mathrm{e}^{-\mathrm{i}V\delta t/(2\hbar)} F^{-1} \mathrm{e}^{-\mathrm{i}(p^2/(2m))\delta t/\hbar} F \mathrm{e}^{-\mathrm{i}V\delta t/(2\hbar)}. \tag{13.19}$$

Application of $U_V = \mathrm{e}^{-\mathrm{i}V\delta t/(2\hbar)}$, F, $\mathrm{e}^{-\mathrm{i}(p^2/(2m))\delta t/\hbar}$ and F^{-1} provides the evolution of ψ over a single time-step δt. In a quantum computer each of these unitary operations can be implemented using universal quantum gates.

13.7 Quantum Simulators Using Quantum Computers

We now discuss the basics of using quantum computers as universal quantum simulators. We essentially follow the treatment in [1].

A digital quantum computer can be used to simulate the dynamics of any quantum system with a Hamiltonian model that can be suitably encoded on a given quantum register and implemented using a sequence of a quantum gate opedrations. The time evolution of a quantum system described by the Hamiltonian H is given by the unitary operation $U(t) = \mathrm{e}^{-\mathrm{i}Ht}$ ($\hbar = 1$). Its implementation in a quantum computer is equivalent to evaluate a unitary matrix. As a quantum computer can evaluate any unitary transformation with a set of universal quantum gates, it can be used to simulate any quantum system. Of course, for a practical possibility of application of this simulation H must be a sum of local terms as discussed earlier. Digital quantum simulators invlove three sequential steps:

1. initial state $|\psi(0)\rangle$ preparation,
2. unitary evolution U and
3. final measurement of $|\psi(t)\rangle$.

13.7.1 Initial State Preparation

In order to extract useful results from a quantum simulator it is important to start with the right initial state. These initial states will be often complex or unknown. So significant research has taken place in providing efficient methods for preparing the initial states. There are efficient methods to prepare an unknown ground state when a simple property defining it is specified [27]. If an explicit description about the initial state required is given then Grover's search algorithm based methods are available to construct the initial state directly [28,29]. A method for generating a antisymmetric state from an unsymmetrized many-particle state of fermions $|00\ldots0\rangle$ was developed [15]. An adiabatic evolution method [30] has been proposed for preparing the ground state of a desired Hamiltonian H from the ground state of another Hamiltonian H_0 for which it is easy to prepare the ground state. A state-preparation algorithm was introduced which incorporates quantum simulation [31]. Still preparing a well-defined initial state either in a pure state or a mixed state remains one of the major challenges of quantum simulators.

13.7.2 Unitary Evolution

We have to implement the evolution of the unitary operator $U = \mathrm{e}^{-\mathrm{i}Ht}$ on a universal quantum computer which is qubit-based, obeying the algebra of Pauli matrices and operating with a universal set of quantum gates as discussed in chapter 9. Then U can be implemented in such a quantum digital device by following a few simple steps [1].

1. First, a model Hamiltonian of interest $\mathcal{H}$ which contains all the dynamical informations necessary to describe and characterize the physical quantum system must be defined.
2. In the second step, the target Hamiltonian $\mathcal{H}$ is mapped and represented by the Hamiltonian H using the qubit Pauli algebra as $\mathcal{H} \to H(\{\sigma_\alpha\})$. This mapping is quite straight-forward for spin-1/2 systems as they obey Pauli algebra. But it is

also possible to map many other physical system Hamiltonians in terms of Pauli matrices.

3. As the third step, the Hamiltonian is found as a sum of local Hamiltonians H_l, $H = \sum_l H_l$. Then we get

$$U = \mathrm{e}^{-\mathrm{i}Ht} = \prod_l \mathrm{e}^{-\mathrm{i}H_l t} \tag{13.20}$$

if all the H_l's commute with each other with no error. Otherwise, U is approximated as

$$U \approx \left(\prod_l \mathrm{e}^{-\mathrm{i}H_l t/n} \right)^n \tag{13.21}$$

with an error which decreases with increase of n.

4. As the fourth step, each local unitary operator $\mathrm{e}^{-\mathrm{i}H_l t}$ or $\mathrm{e}^{-\mathrm{i}H_l t/n}$ are implemented using a sequence of quantum gates. Each of the factors in ST decomposition given by Eq. (13.21) is sequently encoded in a quantum circuit.

13.7.3 Final Measurement

After obtaining $|\psi(t)\rangle = U|\psi(0)\rangle$, final measurement has to be performed to extract the desired information. One cannot use quantum state tomography as it will require resources that grow exponentially with the size of the system. So in the final measurements only direct estimation of certain physical quantities such as correlation functions or eigenvalues of operators are done instead of quantum state tomography. When an observable of interest O is mapped onto a combination of the Pauli spin matrices the expectation value $\langle O \rangle = \langle \psi(t)|O|\psi(t)\rangle$ can be reconstructed using appropriate unitary operations U_m and measurements in the computational basis. As generally the eigenstates of O is different from the computational basis U_m is needed.

We discuss the quantum circuits for measurement of the dynamical correlation functions and the spectrum of the Hermitian operators in the next section.

13.8 Quantum Circuits

All the stages of quantum simulation depend on the translation of unitary operators into elementary quantum gates. As any unitary operation can be written in terms of universal quantum gates, in principle, quantum simulation can be done for any system. As the unitary operation has to be efficiently simulated with polynomial resources there are Hamiltonians which cannot be simulated with polynomial resources. Also, finding an efficient decomposition in terms of universal gates is generally a difficult problem. Moreover, any unitary operation obtained by the decomposition into single and two-qubit gates is generally an approximation of the desired unitary operation.

13.8.1 Spin Hamiltonians

The mathematical properties of qubits on which a quantum computer works are those of spin-1/2 systems. So, it works obeying the algebraic properties of Pauli matrices. Hence,

any target Hamiltonian $\mathcal{H}$ must be mapped into an equivalent Hamiltonian H, of Pauli matrices to be simulated on a qubit-based architecture. For spin-based Hamiltonians of Heisenberg models, the target Hamiltonian will be given directly only in terms of Pauli matrices. Effective mapping for a variety of systems with $s > 1/2$, fermionic and fermionic-bosonic systems and lattice models related to gauge theories are possible. The most general form of H for a N-qubit digital quantum simulation is given by [1]

$$H = \sum_{\substack{i=1 \\ \alpha = x,y,z}}^{N} h^{(1)}_{\alpha,i}\sigma^{(i)}_{\alpha} + \sum_{\substack{i,j=1 \\ \alpha,\beta = x,y,z}}^{N} h^{(2)}_{\alpha,\beta,ij}\sigma^{(i)}_{\alpha}\sigma^{(j)}_{\beta}. \tag{13.22}$$

Hamiltonian given by Eq. (13.22) contains both signle and two-spin terms. For a large number of many body systems the Hamiltonian can be reduced into the form given by Eq. (13.22).

13.8.2 Quantum Circuits for Evolution Operator U

On a quantum computer based on N spin-1/2 systems a register of N qubits can be used to encode and perform the quantum simulation by identifying each qubit with a single spin-1/2 element [1]. Single qubit gate operations can be done using selected control pulses on the single qubits. The most appropriate single qubit operator is

$$U(\theta,\phi,\lambda) = \begin{pmatrix} \cos(\theta/2) & -\mathrm{e}^{\mathrm{i}\lambda}\sin(\theta/2) \\ \mathrm{e}^{\mathrm{i}\phi}\sin(\theta/2) & \mathrm{e}^{\mathrm{i}(\lambda+\phi)}\cos(\theta/2) \end{pmatrix} \tag{13.23}$$

which can be obtained using single qubit quantum gates such as Hadamard gate H and the phase gate $\Phi(\delta)$ given by

$$\mathrm{H} = \frac{1}{\sqrt{2}}\begin{pmatrix} 1 & 1 \\ 1 & -1 \end{pmatrix}, \quad \Phi(\delta) = \begin{pmatrix} 1 & 0 \\ 0 & \mathrm{e}^{\mathrm{i}\delta} \end{pmatrix}. \tag{13.24}$$

U can be given in terms of these two gates as

$$U(\theta,\phi,\lambda) = \mathrm{e}^{-\mathrm{i}\theta/2}\Phi(\pi/2+\phi)\mathrm{H}\Phi(\theta)\mathrm{H}\Phi(-\pi/2+\lambda). \tag{13.25}$$

Choosing particular parameters in $U(\theta,\phi,\lambda)$ we can implement the rotations around the coordinate axes by means of the operation (apart from global phase factors)

$$R_{\alpha}(\theta) = \mathrm{e}^{-\mathrm{i}(\theta/2)\sigma_{\alpha}}, \quad \alpha = x,y,z. \tag{13.26}$$

Solved Problem 2:

Prove that

$$R_x(\theta) = U(\theta,-\pi/2,\pi/2), \quad R_y(\theta) = U(\theta,0,0), \quad R_z(\lambda) = U(0,0,\lambda) \tag{13.27}$$

apart from a global phase factor.

We write $R_{\alpha}(\theta)$ as

$$\begin{aligned} R_{\alpha}(\theta) &= \mathrm{e}^{-\mathrm{i}(\theta/2)\sigma_{\alpha}} \\ &= I - \frac{\mathrm{i}\theta}{2}\sigma_{\alpha} - \frac{1}{2!}\frac{\theta^2}{2^2}\sigma_{\alpha}^2 - \frac{\mathrm{i}}{3!}\frac{\theta^3}{2^3}\sigma_{\alpha}^3 + \frac{1}{4!}\frac{\theta^4}{2^4}\sigma_{\alpha}^4 + \ldots . \end{aligned} \tag{13.28}$$

As $\sigma_x^2 = \sigma_\alpha^2 = \ldots = I$ and $\sigma_\alpha^3 = \sigma_\alpha^5 \ldots = \sigma_\alpha$ we get

$$\begin{aligned} R_\alpha(\theta) &= I - \frac{1}{2!}\frac{\theta^2}{2^2} I + \frac{1}{4!}\frac{\theta^4}{2^4} I - \ldots - \frac{\mathrm{i}\theta}{2}\sigma_\alpha - \frac{\mathrm{i}}{3!}\frac{\theta^3}{2^3}\sigma_\alpha + \ldots \\ &= \cos(\theta/2) I - \mathrm{i}\sin(\theta/2)\sigma_\alpha. \end{aligned} \tag{13.29}$$

Then

$$\begin{aligned} R_x(\theta) &= \cos(\theta/2) I - \mathrm{i}\sin(\theta/2)\sigma_x \\ &= \cos(\theta/2) \begin{pmatrix} 1 & 0 \\ 0 & 1 \end{pmatrix} - \mathrm{i}\sin(\theta/2) \begin{pmatrix} 0 & 1 \\ 1 & 0 \end{pmatrix} \\ &= \begin{pmatrix} \cos(\theta/2) & -\mathrm{i}\sin(\theta/2) \\ -\mathrm{i}\sin(\theta/2) & \cos(\theta/2) \end{pmatrix}. \end{aligned} \tag{13.30}$$

Comparison of Eq. (13.30) with the U given by Eq. (13.23) gives $\mathrm{e}^{\mathrm{i}(\lambda+\phi)} = 1$, $\mathrm{e}^{\mathrm{i}\lambda} = \mathrm{i}$ and $\mathrm{e}^{\mathrm{i}\phi} = -\mathrm{i}$. From these we find $\phi = -\pi/2$ and $\lambda = \pi/2$. That is, $R_x(\theta) = U(\theta, -\pi/2, \pi/2)$. Similarly, we can prove that $R_y(\theta) = U(\theta, 0, 0)$.

For R_z Eq. (13.29) gives

$$\begin{aligned} R_z(\lambda) &= \cos(\lambda/2) I - \mathrm{i}\sin(\lambda/2)\sigma_z \\ &= \cos(\lambda/2) \begin{pmatrix} 1 & 0 \\ 0 & 1 \end{pmatrix} - \mathrm{i}\sin(\lambda/2) \begin{pmatrix} 1 & 1 \\ 0 & -1 \end{pmatrix} \\ &= \mathrm{e}^{-\mathrm{i}\lambda/2} \begin{pmatrix} 1 & 0 \\ 0 & \mathrm{e}^{\mathrm{i}\lambda} \end{pmatrix}. \end{aligned} \tag{13.31}$$

When $\theta = 0$ and $\phi = 0$ Eq. (13.23) gives

$$U(0, 0, \lambda) = \begin{pmatrix} 1 & 0 \\ 0 & \mathrm{e}^{\mathrm{i}\lambda} \end{pmatrix}. \tag{13.32}$$

That is, $U(0, 0, \lambda) = R_z(\lambda)$ apart from a global phase factor $\mathrm{e}^{-\mathrm{i}\lambda/2}$.

In any platform where single qubit rotation about the coordinate axes can be implemented it is possible to implement $U(\theta, \phi, \lambda)$ as

$$U(\theta, \phi, \lambda) = R_z(\phi) R_y(\theta) R_z(\lambda). \tag{13.33}$$

The first term in Eq. (13.22) represents a magnetic field applied along the direction of the vector $\mathbf{h} = \mathbf{i}h_x^{(i)} + \mathbf{j}h_y^{(i)} + \mathbf{k}h_z^{(i)}$. Then $U_1^{(i)}(t) = \mathrm{e}^{-\mathrm{i}H_1^{(i)}t}$ gives a precession of the $\mathbf{h}$-axis. It can be expressed in the $U(\theta, \phi, \lambda)$ form and implemented in a quantum circuit using Hadamard and phase gates.

The two spin interaction terms appearing on the second term in Eq. (13.22) can be implemented in quantum simulation protocols using single- and two-qubits gates. The evolution operator of a typical two-spin interaction is

$$U_{\alpha,\beta}^{(i,j)}(t) = \mathrm{e}^{-\mathrm{i}H_{\alpha,\beta}^{(i,j)}t} = \mathrm{e}^{-\mathrm{i}\delta\sigma_\alpha^{(i)} \otimes \sigma_\beta^{(j)}}, \tag{13.34}$$

where δ is a dimensionless phase factor. They are found to occur in several spin models. For example, in the Heisenberg model

$$H = J \sum_{\langle i,j \rangle} \left(\sigma_x^{(i)} \sigma_x^{(j)} + \sigma_y^{(i)} \sigma_y^{(j)} + \sigma_z^{(i)} \sigma_z^{(j)} \right) \tag{13.35}$$

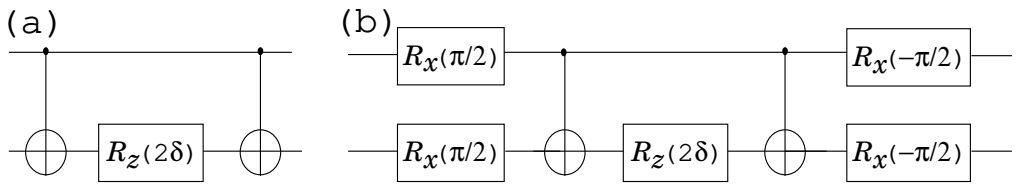

FIGURE 13.2
Quantum circuit realization of the unitary operations (a) $e^{-i\delta\sigma_z\otimes\sigma_z}$ and (b) $e^{-i\delta\sigma_y\otimes\sigma_y}$.

and in the XYZ model

$$H = \sum_{\langle i,j\rangle} \left(J_{xx}\sigma_x^{(i)}\sigma_x^{(j)} + J_{yy}\sigma_y^{(i)}\sigma_y^{(j)} + J_{zz}\sigma_z^{(i)}\sigma_z^{(j)} \right), \tag{13.36}$$

where $\langle i, j\rangle$ denote nearest neighbours spin pairs. For these spin models direct implementation of these Hamiltonians are possible as they have been already expressed in terms of spin operators.

Depending upon the platforms on which quantum computers work the decompositions of the evolution operators $U_{\alpha,\beta}^{(i,j)}(t)$ are done using different sets of quantum gates. A universal set $S_1 = \{R_\alpha(\theta), CNOT\}$ having single bit rotations and two-qubit $CNOT$ entangling gate are commonly used for many platforms [32–34]. For example, the unitary operation $ZZ(\delta) = e^{-i\delta\sigma_z\otimes\sigma_z}$ can be realized in a quantum circuit [1]. The circuit is given in Fig. 13.2a. As $R_x(\pi/2)\sigma_z R_x(-\pi/2) = -\sigma_y$ the quantum circuit [1] implementing $e^{-i\delta\sigma_y\otimes\sigma_y}$ is as given in Fig. 13.2b. These gate sequences can be combined to simulate the spin models mentioned above.

There are other universal sets to implement different unitary evolutions in other platforms. In S_2 universal set the $CNOT$ in S_1 is replaced by a parametric $XX+YY$ interaction [35–38]

$$U_{xy}(\delta) = e^{-i\delta(\sigma_x\otimes\sigma_x+\sigma_y\otimes\sigma_y)}. \tag{13.37}$$

Another universal set of quantum gates are $S_3 = \{R_\alpha(\theta), C\Phi(\delta)\}$, where the controlled phase gate has

$$C\Phi(\delta) = \begin{bmatrix} 1 & 0 & 0 & 0 \\ 0 & 1 & 0 & 0 \\ 0 & 0 & 1 & 0 \\ 0 & 0 & 0 & e^{i\delta} \end{bmatrix}. \tag{13.38}$$

For further details on quantum circuits for U one may refer to the ref. [1].

Solved Problem 3:

Determine $R_x(\pi/2)\sigma_z R_x(-\pi/2)$.

From $R_x(\theta)$ given by Eq. (13.30) $R_x(\pi/2)$ and $R_x(-\pi/2)$ are obtained as

$$R_x(\pi/2) = \frac{1}{\sqrt{2}} \begin{pmatrix} 1 & -i \\ -i & 1 \end{pmatrix}, \quad R_x(-\pi/2) = \frac{1}{\sqrt{2}} \begin{pmatrix} 1 & i \\ i & 1 \end{pmatrix}. \tag{13.39}$$

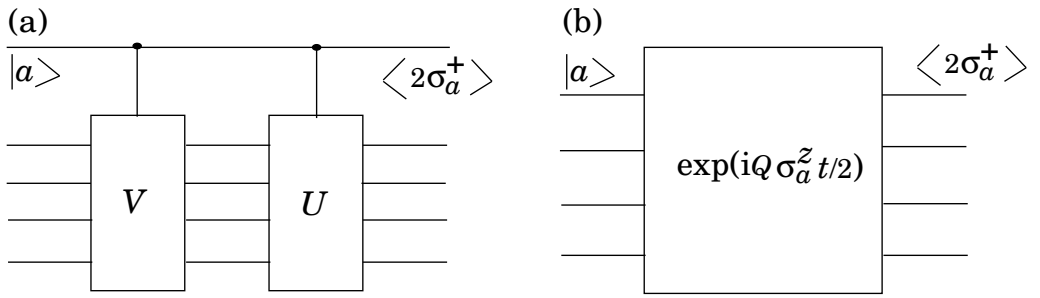

FIGURE 13.3
Quantum circuits for the measurement of (a) $\langle U^\dagger V\rangle$ and (b) the spectrum of a Hermitian Q [22]. (Reproduced with permission from R. Somma, G. Ortiz, J.E. Gubernatis, E. Knill and R. Laflamme, *Phys. Rev. A* 65:042323, 2002. Copyright 2002, American Physical Society.)

Then

$$\begin{aligned} R_x(\pi/2)\sigma_z R_x(-\pi/2) &= \frac{1}{2}\begin{pmatrix} 1 & -\mathrm{i} \\ -\mathrm{i} & 1 \end{pmatrix}\begin{pmatrix} 1 & 0 \\ 0 & -1 \end{pmatrix}\begin{pmatrix} 1 & \mathrm{i} \\ \mathrm{i} & 1 \end{pmatrix} \\ &= \frac{1}{2}\begin{pmatrix} 0 & 2\mathrm{i} \\ -2\mathrm{i} & 0 \end{pmatrix} \\ &= -\sigma_y. \end{aligned} \tag{13.40}$$

Similarly we can find that $R_y(\pi/2)\sigma_z R_y(-\pi/2) = \sigma_x$.

13.9 Quantum Circuits for Final Measurements

The unitary evolution U gives the wave function $|\psi(t)\rangle$. One must perform final measurements on $|\psi(t)\rangle$ to extract the desired information about the simulated quantum system. As discussed earlier correlation functions and eigenvalues are extracted. If U and V are unitary operators then $\langle U^\dagger V\rangle$ refers to the correlation of these two quantities. Figure 13.3a gives the quantum circuit for the measurement of the quantity $\langle U^\dagger V\rangle$. One ancilla qubit a is initially in the state $|+\rangle = (|0\rangle + |1\rangle)/\sqrt{2}$. This can be done by applying the Hadamard gate to the state $|0\rangle$. Next, two controlled unitary evolutions are done using $C-V$ and $C-U$ gates. The first operation on $C-V$ evolves the system to $\widetilde{V}$ if the ancilla a is in the state $|1\rangle$. So we get $\widetilde{V} = |0\rangle\langle 0|\otimes I + |1\rangle\langle 1|\otimes V$. The second operation evolves the system to $\widetilde{U}$ if the ancilla is in the state $|0\rangle$ giving $\widetilde{U} = |0\rangle\langle 0|\otimes U + |1\rangle\langle 1|\otimes I$. Then the measurement of the expectation value of $2\sigma_+^a$ $(= \sigma_x^a + \sigma_y^a)$ on the ancilla will give the correlation function $\langle U^\dagger V\rangle$.

Figure 13.3b gives the quantum circuit for measuring the spectrum of Hermitian operator Q. The ancilla qubit $|a\rangle$ is in the state $|+\rangle = (|0\rangle + |1\rangle)/\sqrt{2}$. The eigenvalues of Q operator are obtained by analysing the time dependence of $\langle 2\sigma_+^a\rangle$.

13.10 Concluding Remarks

The problem of simulating quantum dynamics will be the most natural application of quantum computers. As long as the initial state preparation, the implementation of the time evolution and final measurement are realized with polynomial resources the quantum simulators can solve many difficult problems. We have discussed analog quantum simulators with many examples. If a similar controllable quantum system can be found for mapping the real quantum system to it, then one can do analog quantum simulation. Compared to the digital quantum device an analog quantum simulation is relatively easy. Finding a mapping in an analog quantum simulator is sometimes simpler than obtaining the most efficient quantum decomposition for a given Hamiltonian in digital quantum simulators. Also, unlike in digital quantum simulator physical quantities can be measured directly in analog quantum simulators. Analog quantum simulation can be implemented on a quantum system even if it is not a potential quantum computer. Consequently, analog quantum simulators are implemented experimentally even though developing universal quantum computers is only at an early stage. A number of platforms used for quantum simulations and their applications in various fields are discussed more elaborately in the review [12].

In digital quantum simulations the general purpose quantum computers can be programmed to solve the exact time evolution of an arbitrary Hamiltonian model. For a physical model which can be mapped onto an effective local Hamiltonian obeying the algebra of Pauli matrices digital quantum simulator can be implemented in a qubit-based quantum computer through a quantum circuit model. The final measurements on such a quantum simulating circuits will give a number of observables such as spectra and correlation functions. The ref. [1] has elaborately discussed the theory of using quantum computers as universal quantum simulators. They have also discussed in detail the decomposition of evolution operators in terms of elementary quantum gates and simulate them in quantum circuits. It has also reviewed recent experimental results on two leading quantum technologies, namely, trapped ions and superconducting quantum circuits.

Quantum simulation of the Klein paradox with trapped ions [39], systems in chemistry [40,41], many-body system [42], quantum simulations with ultracold quantum gases [43] and Rydberg atoms [44], photonic technology for quantum simulations [45], NMR as quantum simulators [46–48], certifying the correct functioning of quantum simulators [49] and dynamical structure factors of quantum simulators [50] have been analyzed.

13.11 Bibliography

[1] F. Tacchino, A. Chiesa, S. Carretta and D. Gerace, *Adv. Quant. Tech.* 3:1900052, 2020.

[2] R.P. Feynman, *Int. J. Theor. Phys.* 21:467, 1982.

[3] S. Llyod, *Science* 273:1073, 1996.

[4] S. Somaroo, C.H. Tseng, T.F. Havel, R. Laflamme and D.G. Cory, *Phys. Rev. Lett.* 82:5381, 1999.

[5] E. Manousakis, *J. Low. Temp. Phys.* 126:1501, 2002.

[6] U.R. Fischer and R. Schutzhold, *Phys. Rev. A* 70:063615, 2004.

[7] D. Porras and J.I. Cirac, *Phys. Rev. Lett.* 92:207901, 2004.

[8] A. Smirnov, S. Savel'ev, L. Mourokh and F. Nori, *Europhys. Lett.* 80:67008, 2007.

[9] A. Zagoskin, S. Savel'ev and F. Nori, *Phys. Rev. Lett.* 98:120503, 2007.

[10] I. Buluta and F. Nori, *Science* 326:8, 2009.

[11] R. Gerritsma, G. Kirchmair, F. Zahringer, E. Solano, R. Blatt and C.F. Roos, *Nature* 463:68, 2010.

[12] I.M. Georgescu, S. Ashhab and F. Nori, *Rev. Mod. Phys.* 86:153, 2014.

[13] A. Zagoskin, *Rev. Phys.* 3:1, 2018.

[14] R. Shaffer, E. Megidish, J. Broz, W.T. Chen and H. Haffner, *NPJ Quant. Infor.* 7:46, 2021.

[15] D. Abrams and S. Lloyd, *Phys. Rev. Lett.* 79:2586, 1997.

[16] D.A. Lidar and O. Biham, *Phys. Rev. E* 56:3661, 1997.

[17] C. Zalka *Proc. R. Soc. A* 454:313, 1998.

[18] B.M. Terharl and D.P. DiVincenzo *Phys. Rev. A* 61:022301, 2000.

[19] M.A. Nielson and I.L. Chuang, *Quantum Computation and Quantum Information*. Cambridge University Press, Cambridge, 2000.

[20] G. Ortiz, J.E. Gubernatis, E. Knill and R. Laflamme, *Phys. Rev. A* 64:022319, 2001.

[21] A. Marzouli and M. Rasetti, *Phys. Lett. A* 306:79, 2002.

[22] R. Somma, G. Ortiz, J.E. Gubernatis, E. Knill and R. Laflamme *Phys. Rev. A* 65:042323, 2002.

[23] F. Verstraete, J.I. Cirac and J.I. Latorre *Phys. Rev. A* 79:032316, 2009.

[24] S. Raeisi, N. Wiebe and B.C. Sanders, *New J. Phys.* 14:103017, 2012.

[25] G. Benenti and G. Strini, *Am. J. Phys.* 76:657, 2008.

[26] R. Shankar, S.S. Hegde and T.S. Mahesh, *Phys. Lett. A* 378:10, 2014.

[27] K.L. Brown, W.J. Munro and V.M. Kendon, *Entropy* 12:2268, 2010.

[28] A.N. Soklakov and R. Schack, *Opt. Spect.* 99:211, 2005.

[29] D. Poulin and P. Wocjan, *Phys. Rev. Lett.* 102:130503, 2009.

[30] D. Aharonov and A. Ta-Shma, *Adiabatic quantum state generation and statistical zero knowledge*. In the Proceedings of the Thirty-Fifth Annual ACM Symposium on Theory of Computing. Association for Computing Machinery, New York, 2003. pp.20-29.

[31] H. Wang, S. Ashhab and F. Nori, *Phys. Rev. A* 79:042335, 2009.

[32] C. Rigetti and M. Devoret, *Phys. Rev. B* 81:134507, 2010.

[33] J.M. Chow, A.D. Corcoles, J.M. Gambetta, C. Rigetti, B.R. Johnson, J.A. Smolin, J.R. Rozen, G.A. Keefe, M.B. Rothwell, M.B. Ketchen and M. Steffen, *Phys. Rev. Lett.* 107:080502, 2011.

[34] S. Sheldon, E. Magesan, J.M. Chow and J.M. Gambetta, *Phys. Rev. A* 93:060302, 2016.

[35] U. Las Heras, A. Mezzacapo, L. Lamata, S. Filipp, A. Wallraff and E. Solano, *Phys. Rev. Lett.* 112:200501, 2014.

[36] Y. Salathe, M. Mondal, M. Oppliger, J. Heinsoo, P. Kurpiers, A. Potocnik, A. Mezzacapo, U. Las Heras, L. Lamata, E. Solano, S. Filipp and A. Wallraff, *Phys. Rev. X* 5:021027, 2015.

[37] D.C. McKay, S. Filipp, A. Mezzacapo, E. Magesan, J.M. Chow and J.M. Gambetta, *Phys. Rev. Appl.* 6:064007, 2016.

[38] F. Tacchino, A. Chiesa, M.D. LaHaye, S. Carretta and D. Gerace, *Phys. Rev. B* 97:214302, 2018.

[39] R. Gerritsma, B.P. Lanyon, G. Kirchmair, F. Zahringer, C. Hempel, J. Casanova, J.J. Garcia-Ripoll, R. Solano, R. Blatt and C.F. Roos, *Phys. Rev. Lett.* 106:060503, 2011.

[40] I. Kassal, J.D. Whitfield, A. Perdomo-Ortiz, M.H. Yung and A. Aspuru-Guzik, *Annual Rev. Phys. Chem.* 62:185, 2011.

[41] D. Turkpence and A. Geneten, *J. Quant. Infor. Sci.* 3:78, 2013.

[42] T.S. Cubitt, A. Montanaro and S. Piddock, *PNAS* 115:9497, 2018.

[43] I. Bloch, J. Dalibard and S. Nascimbene, *Nat. Phys.* 8:267, 2012.

[44] H. Weimer, M. Muller, I. Lesanovsky, P. Zoller and H.P. Buchler, *Nat. Phys.* 6:382, 2010.

[45] A. Aspuru-Guzik and P. Walther, *Nat. Phys.* 8:285, 2012.

[46] C.H. Tseng, S. Somaroo, Y. Sharf, E. Knill, R. Laflamme, T.F. Havel and D.G. Cory, *Phys. Rev. A* 61:012302, 1999.

[47] G.A. Alverez and D. Suter, *Phys. Rev. Lett.* 104:230403, 2010.

[48] D. Lu, N. Xu, R. Xu, H. Chen, J. Gong, X. Peng and J. Du, *Phys. Rev. Lett.* 107:020501, 2011.

[49] D. Hangleiter, M. Kliesch, M. Schwarz and J. Eisert, *Quantum Sci. Technol.* 2:015004, 2017.

[50] M.L. Baez, M. Goihl, J. Haferkamp, J. Bermejo-Vega, M. Gluza and J. Eisert, *PNAS* 117:26123, 2020.

13.12 Exercises

13.1 Show that in a general scheme of quantum simulation the propagator U of a quantum system S maps to $V_t = \phi U \phi^{-1}$ of an experimental controllable system P.

13.2 A classical supercomputer has memory of 200 TB. Find the maximum number of spin states that can be represented in this supercomputer for single precision.

13.3 Show that the Dirac equation in $(1 + 1)$ dimension for a spin-1/2 particle is $\mathrm{i}\hbar\partial\psi/\partial t = (cp_x\sigma_x + mc^2\sigma_z)\psi$.

13.4 Show that $U = \mathrm{e}^{-\mathrm{i}[H_0+V]\delta t/\hbar}$ is equal to $\mathrm{e}^{-\mathrm{i}V\delta t/(2\hbar)}F^{-1}\mathrm{e}^{-\mathrm{i}(p^2/2m)\delta t/\hbar}F\mathrm{e}^{-\mathrm{i}V\delta t/(2\hbar)}$ using ST decomposition.

13.5 Show that $\langle\sigma_x(t)\rangle$ can be measured by performing $U_\mathrm{m} = [H]$, the Hadamard gate, on the σ_z computation basis.

13.6 Show that $U(\theta, \phi, \lambda)$ is unitary.

13.7 Prove that $U(\theta, \phi, \lambda) = \mathrm{e}^{-\mathrm{i}\theta/2}\Phi(\pi/2 + \phi)\mathrm{H}\Phi(\theta)\mathrm{H}\Phi(-\pi/2 + \lambda)$.

13.8 Show that $U(\theta, \phi, \lambda) = R_z(\phi)R_y(\theta)R_z(\lambda)$ apart from a phase factor.

13.9 Show that the ancilla qubit $|+\rangle$ can be prepared by applying Hadamard gate to the state $|0\rangle$.

13.10 The molecular Hamiltonian of ethylene $2p - \pi$ electrons is given by $H = \begin{bmatrix} -1.2627 & 0.1529 \\ 0.1529 & -0.8198 \end{bmatrix}$. Express H in terms of I, σ_x, σ_y and σ_z [41].

Taylor & Francis
Taylor & Francis Group
http://taylorandfrancis.com

14

Quantum Error Correction

14.1 Introduction

Quantum computers hold the promise to be advantageous to the classical computers for certain class of problems like factorization of prime numbers and in search algorithms. But quantum states are highly fragile. The advantages of quantum computers will disappear if noise, losses and decoherence are not kept below a certain threshold. In any information processor errors will occur. Error-correcting codes to rectify unknown errors in qubits are an important ingredient for large scale quantum information processing. Without error correction the presence of noise during both storage and entangling operations will diminish the gain of quantum information processing. Realization of long distance quantum cryptography requires quantum error correction (QEC) of the errors introduced by noise on communication channels.

A variety of physical systems are being explored for use as qubits. For quantum information processing qubits using photons, trapped ions, superconducting circuits and spins in semiconductors have been considered. But none of these platforms used for computation or quantum signal processing can be sufficiently isolated from environment. So, errors during quantum computation due to these external noise are inevitable.

Once Shor's algorithm [1] demonstrated that the utilization of a quantum computer could lead to algorithms far more efficient than used in classical computers, the next question raised was whether a large scale controllable quantum system could be practically built. Many believed that as the quantum states were extremely fragile, it was quite unrealistic to maintain large and multi-qubit coherent quantum states for a long enough time to complete any quantum algorithm. Only the development of QEC protocols convinced the general community that quantum computation is indeed a possibility.

The present chapter starts with presenting common sources of errors in QEC. The obstacles in introducing the classical error correction codes into quantum case is listed. Digitization of continuum of quantum errors which is helpful to correct quantum errors is described. Next, redundant encoding of quantum information and detection of errors through projective measurement are considered. The stabilizer formalism helpful for setting QEC codes is introduced. Then the surface code, an efficient QEC model is considered. Finally, some practical diffuculties in the applications of QEC codes are pointed out.

14.2 Sources of Errors in Quantum Information Processing

We essentially follow [2] to discuss different sources of quantum errors, their causes and effects. In [2] various quantum errors and their effects on quantum computations have been

DOI: 10.1201/9781003172192-14

explained with simple algorithms. Consider a simple algorithm of a single qubit initialized in the $|0\rangle$ state through N identity operations. If there were no error introduced in these N-identity operations then the final state will be just $|0\rangle$:

$$|\psi\rangle_{\text{final}} = \prod \sigma_I |0\rangle = |0\rangle\,. \tag{14.1}$$

The probability of measurement of $|0\rangle$ in such a error free state will be just unity. We will discuss how do various quantum errors affect the measurement probability of $|0\rangle$ state in this simple algorithm.

14.2.1 Coherent Quantum Error

Coherent quantum errors arise due to the errors associated with system controls and/or characterization where imprecise operation on the qubit introduces inaccurate Hamiltonian dynamics. This type of errors do not produce mixed states from pure states and are called *coherent quantum errors*. In the simple algorithm that we considered, we have N times σ_I operations sequentially performed on the initial state $|0\rangle$. Suppose the incorrect characterization of the control dynamics, instead of σ_I, leads to a different identity gate and results in a small rotation about the x-axis of the Bloch sphere. In this case the final state is given by (see the exercise 1 at the end of this chapter)

$$|\psi\rangle_{\text{final}} = \prod^{N} \mathrm{e}^{\mathrm{i}\epsilon\sigma_x}|0\rangle = \cos(N\epsilon)|0\rangle + \mathrm{i}\sin(N\epsilon)|1\rangle\,. \tag{14.2}$$

This equation gives the probability of measurement of $|0\rangle$ as $P(0) = \cos^2(N\epsilon)$ and the probability of measurement of $|1\rangle$ as $P(1) = \sin^2(N\epsilon)$. For small $N\epsilon$

$$P(0) = \cos(N\epsilon) = 1 - \sin^2(N\epsilon) \approx 1 - (N\epsilon)^2, \quad P(1) \approx (N\epsilon)^2\,. \tag{14.3}$$

As the number of quantum operations increase even a small coherent error ϵ will lead to wrong results.

14.2.2 Decoherence

We have discussed decoherence in chapter 8. The interaction of environment with the quantum systems leads to decoherence of quantum systems. For simplicity, assume that the environment has two orthonormal basis states $|e_0\rangle$ and $|e_1\rangle$ satisfying the relations $\langle e_i|e_j\rangle = \delta_{ij}$ and $|e_0\rangle\langle e_0| + |e_1\rangle\langle e_1| = I$.

Assume that the environment couples to the qubit such that when the qubit is in the $|1\rangle$ state the effect is flipping the environment state while the qubit is in the $|0\rangle$ state there is no effect on the environmental state. Instead of N identity operations (σ_I), perform two Hadamard operations (H) separated by a wait stage governed by σ_I on the initial state $|0\rangle$. In this case

$$|\psi\rangle_{\text{final}} = H\sigma_I H|0\rangle = |0\rangle. \tag{14.4}$$

Suppose the environment state $|E\rangle$ starts with the pure state $|E\rangle = |e_0\rangle$ and the coupling to the system is such that we have

$$H\sigma_I H|0\rangle|E\rangle = \frac{1}{2}(|0\rangle + |1\rangle)|e_0\rangle + \frac{1}{2}(|0\rangle - |1\rangle)|e_1\rangle\,. \tag{14.5}$$

Assume that the environment interacts with the system only on the wait state σ_I. As the decoherence due to environmental interaction transforms pure states into mixed states, it is convenient to treat the state $H\sigma_I H|0\rangle|E\rangle$ by density matrix representation as

$$\begin{aligned}\rho_{\rm f} &= \left[\frac{1}{2}\left(|0\rangle+|1\rangle\right)|e_0\rangle+\frac{1}{2}\left(|0\rangle-|1\rangle\right)|e_1\rangle\right] \\ &\quad\times\left[\frac{1}{2}\left(\langle 0|+\langle 1|\right)\langle e_0|+\frac{1}{2}\left(\langle 0|-\langle 1|\right)\langle e_1|\right] \\ &= \frac{1}{4}\left(|0\rangle\langle 0|+|0\rangle\langle 1|+|1\rangle\langle 0|+|1\rangle\langle 1|\right)|e_0\rangle\langle e_0| \\ &\quad+\frac{1}{4}\left(|0\rangle\langle 0|-|0\rangle\langle 1|-|1\rangle\langle 0|+|1\rangle\langle 1|\right)|e_1\rangle\langle e_1| \\ &\quad+\frac{1}{4}\left(|0\rangle\langle 0|-|0\rangle\langle 1|+|1\rangle\langle 0|-|1\rangle\langle 1|\right)|e_0\rangle\langle e_1| \\ &\quad+\frac{1}{4}\left(|0\rangle\langle 0|+|0\rangle\langle 1|-|1\rangle\langle 0|-|1\rangle\langle 1|\right)|e_1\rangle\langle e_0|\,. \end{aligned} \tag{14.6}$$

We are not going to perform the measurement of environmental degrees of freedom. Therefore, we consider

$$\begin{aligned}{\rm Tr}_E(\rho_{\rm f}) &= \frac{1}{4}\left(|0\rangle\langle 0|+|0\rangle\langle 1|+|1\rangle\langle 0|+|1\rangle\langle 1|\right) \\ &\quad+\frac{1}{4}\left(|0\rangle\langle 0|-|0\rangle\langle 1|-|1\rangle\langle 0|+|1\rangle\langle 1|\right) \\ &= \frac{1}{2}\left(|0\rangle\langle 0|+|1\rangle\langle 1|\right)\,. \end{aligned} \tag{14.7}$$

Now, we find that the interaction of the environment on the wait state of $H\sigma_I H|0\rangle$ leads to Eq. (14.7) with measurement probability of $|0\rangle$ state to be 1/2 and that of the state $|1\rangle$ also to be 1/2. So, the environment decoherence has produced a complete mixture of the qubit state $|0\rangle$ and $|1\rangle$ with equal probability just like in a classical system. The coupling of the environment has removed the coherence between the $|0\rangle$ and $|1\rangle$ states. The second H transform which has to rotate $(|0\rangle+|1\rangle)/\sqrt{2}$ to $|0\rangle$ has become ineffective.

Solved Problem 1:

Prove Eq. (14.5).

As $H=\frac{1}{\sqrt{2}}\begin{bmatrix}1 & 1\\ 1 & -1\end{bmatrix}$, we obtain

$$H|0\rangle=\frac{1}{\sqrt{2}}\begin{bmatrix}1 & 1\\ 1 & -1\end{bmatrix}\begin{bmatrix}1\\ 0\end{bmatrix}=\frac{1}{\sqrt{2}}\begin{bmatrix}1\\ 1\end{bmatrix}=\frac{1}{\sqrt{2}}\left[|0\rangle+|1\rangle\right]. \tag{14.8}$$

Next,

$$\begin{aligned}H|e_0\rangle H|0\rangle &= \frac{1}{\sqrt{2}}H|e_0\rangle(|0\rangle+|1\rangle) \\ &= \frac{1}{\sqrt{2}}H(|0\rangle|e_0\rangle+|1\rangle|e_1\rangle) \\ &= \frac{1}{2}\begin{bmatrix}1 & 1\\ 1 & -1\end{bmatrix}(|0\rangle|e_0\rangle+|1\rangle|e_1\rangle) \\ &= \frac{1}{2}\begin{bmatrix}1 & 1\\ 1 & -1\end{bmatrix}\begin{bmatrix}1\\ 0\end{bmatrix}|e_0\rangle+\frac{1}{2}\begin{bmatrix}1 & 1\\ 1 & -1\end{bmatrix}\begin{bmatrix}0\\ 1\end{bmatrix}|e_1\rangle \\ &= \frac{1}{2}(|0\rangle+|1\rangle)|e_0\rangle+\frac{1}{2}(|0\rangle-|1\rangle)|e_1\rangle\,. \end{aligned} \tag{14.9}$$

14.2.3 Loss, Leakage, Measurement and Initialization Errors

The errors due to qubit loss, qubit leakage, errors in qubit initialization and measurements can also be modelled in the same way as environmental decoherence.

If P_{M} is the probability of measurement error then the measurement projection on a qubit can be given as

$$A = (1 - P_{\mathrm{M}})\,|0\rangle\langle 0| + P_{\mathrm{M}}|1\rangle\langle 1|\,. \tag{14.10}$$

Therefore, for a pure state $\rho = |0\rangle\langle 0|$ the probability of measuring a $|0\rangle$ state is given by

$$P|0\rangle = \mathrm{Tr}(A\rho) \;= (1 - P_{\mathrm{M}})\;. \tag{14.11}$$

Then $1 - P_{\mathrm{M}}$ is the probability for measuring the correct result.

Qubit loss can also be modelled as the environmental coupling. A loss of qubit means it is acutally coupled to the environment. In this case as in Eq. (14.7) $A = \frac{1}{2}(|0\rangle\langle 0| + |1\rangle\langle 1|)$. Comparing it with Eq. (14.10) we find the measurement error probability as $P_{\mathrm{M}} = 1/2$.

We can model the error in the initialization of the qubit using the decoherence model or coherent symmetric error model depending on the physical mechanisms involved in the initialization. In the decoherence model if P_{I} is the initialization error probability, then the initial state is given by the mixture density of state

$$\rho_{\mathrm{I}} = (1 - P_{\mathrm{I}})\,|0\rangle\langle 0| + P_{\mathrm{I}}|1\rangle\langle 1|\,. \tag{14.12}$$

In the case of coherent symmetric error model with a coherent unitary operation, the initial state can be assumed as pure, but have an undesired state, say, $|\psi\rangle_{\mathrm{I}} = \alpha|0\rangle + \beta|1\rangle$, where $|\alpha|^2 + |\beta|^2 = 1$ and $|\beta|^2 \ll 1$.

Qubit leakage errors occur as any two level qubit operation can couple other nearby quantum levels. For example, an operation $U|0\rangle$ may contain an additional state $|2\rangle$ as

$$U|0\rangle = \alpha|0\rangle + \beta|1\rangle + \gamma|2\rangle\,. \tag{14.13}$$

As the computer works with a qubit structure with two level systems, the introduction of the third level error in a two level algorithm will induce unwanted dynamics. Leakage is one of the most problematic errors to correct using QEC.

14.3 Difficulties of Using Classical Error Correction Techniques to QEC

We have discussed many different quantum errors that may arise in quantum machine in the previous section. Compared to a classical digital machine quantum machines are more susceptible to making errors. In classical information technologies the binary values 0 and 1 are used to encode in which data is represented as sequences of these two bits. The basic principle involved in classical error correction is to increase the number of bits more than is required for a given amount of information. A set of instructions specifying this excess coding is known as *error correction codes* [3,4].

Let us give an example of error correction code [5]. Consider the three-bit repetition code in which each bit value is duplicated as $0 \to 000$ and $1 \to 111$. A three-bit encoder changes the binary alphabet $\mathcal{B}\{0, 1\}$ into a code alphabet $C_3 = \{000, 111\}$. Assume that it is desired to communicate a single-bit message 0 to a recipient at an another location. In

three-bit coding the word 000 will be sent. Suppose this codeword underwent a flip error during communication. The received codeword can be 001 or 010 or 100. By deciding the majority of the bits the recipient can decide the actual original codeword as 000. If the code 000 is subjected to more than one error like 011, 101, 110 and 111 then the recipient will decide incorrectly, by majority of the bits, the codeword as 111. Theory of classical error correction is very well developed that any classical error can be satisfactorily corrected.

Unfortunately, the classical methods of error correction cannot be applied to QEC. In classical information the bits are either in 0 state or in 1 state. Consequently, the only error possible is the flip-flop of the bits. But in quantum information we consider a superposition of the two states $|0\rangle$ and $|1\rangle$ as the qubit. So, a general quantum qubit is represented by

$$|\psi\rangle = \alpha|0\rangle + \beta|1\rangle, \quad |\alpha|^2 + |\beta|^2 = 1. \tag{14.14}$$

The qubit given by Eq. (14.14) can vary continuously, unlike the classical bits 0 and 1, as long as $|\alpha|^2 + |\beta|^2 = 1$. Consequently, a qubit is subject to an infinite number of errors.

In a geometrical representation $|\psi\rangle$ given by Eq. (14.14) can be written as

$$|\psi\rangle = \cos(\theta/2)|0\rangle + \mathrm{e}^{\mathrm{i}\phi}\sin(\theta/2)|1\rangle, \quad |\cos(\theta/2)|^2 + |\sin(\theta/2)|^2 = 1\,. \tag{14.15}$$

In this case a qubit state can represent a point on a Bloch sphere and is specified by θ and ϕ. Any qubit error represented by a unitary operator $U(\delta\theta, \delta\phi)$ can rotate the state given by Eq. (14.15) in the Bloch sphere to a new state as

$$U(\delta\theta, \delta\phi)|\psi\rangle = \cos((\theta + \delta\theta)/2)|0\rangle + \mathrm{e}^{\mathrm{i}(\phi+\delta\phi)}\sin((\theta + \delta\theta)/2)|1\rangle\,. \tag{14.16}$$

As $\delta\theta$ and $\delta\phi$ can vary continuously, a qubit is subjectable to a continuum of errors. However, one can digitize the quantum errors. Then the ability to correct a finite set of errors is enough to correct any error [6]. As a result of digitization of quantum errors we get two fundamental error types:

1. Flip-flop error (Pauli X-type error): $\sigma_x|1\rangle = |0\rangle$ and $\sigma_x|0\rangle = |1\rangle$.
2. Phase-flip error (Pauli Z-type error): $\sigma_z|0\rangle = |0\rangle$ and $\sigma_z|1\rangle = -|1\rangle$.

The phase-flip error has no classical analogue. Even though the digitization of quantum errors may be useful to apply the classical coding theory to QEC to some extent, a straightforward translation of classical codes to quantum codes is not possible.

There are three main obstacles [5] to introduce classical error correction codes into quantum realm. They are enumerated in the following.

1. A difficulty arises due to the continuous nature of quantum errors as discussed earlier. As all quantum operations are continuous, it can be implemented only with a certain precision. A small error can accumulate over many operations and may add up to a large uncontrollable error.
2. In classical error correction, information is encoded in a redundant way to protect against errors as expalined earlier. That technique cannot be used in QEC due to the no-cloning theorem (refer chapter 11). As it is impossible to copy an unknown quantum system, information cannot be stored in a redundant way as is being done in classical information processing.
3. Another obstacle arises due to the measurement problem of quantum mechanics. In order to correct an error we have to acquire some information about the nature and type of error. Hence, we have to perform a measurement on the system. But any quantum mechanical measurement collapses the quantum system and

hence might destroy the information that we have encoded in the quantum state. Extracting information about the error through the measurement of the quantum system is not possible. Hence, in general the well developed classical error correction techniques cannot be applied to QEC technique directly.

14.4 Digitization of Quantum Errors

We have seen that a general error can be described by a unitary operator as given by Eq. (14.16). Varying of $\delta\theta$ and $\delta\phi$ lead to a continuum of quantum errors. Digitization of quantum errors makes it possible to correct any quantum error using the ability to correct a finite set of errors [5,6]. This is possible as the coherent noise processes are described by matrices which can be expanded in terms of the set of three Pauli matrices and the identity matrix given by

$$\mathbb{1} = \begin{pmatrix} 1 & 0 \\ 0 & 1 \end{pmatrix}, \quad X = \begin{pmatrix} 0 & 1 \\ 1 & 0 \end{pmatrix}, \quad Y = \begin{pmatrix} 0 & -\mathrm{i} \\ \mathrm{i} & 0 \end{pmatrix}, \quad Z = \begin{pmatrix} 1 & 0 \\ 0 & -1 \end{pmatrix}.$$

As the single-qubit coherent process described by the unitary operator $U(\delta\theta, \delta\phi)$ is a 2×2 matrix and as $\mathbb{1}$, X, Y and Z are linearly independent the 2×2 matrix $U(\delta\theta, \delta\phi)$ can be expanded as a linear combination of the four matrices. Hence, Eq. (14.16) can be expanded as

$$U(\delta\theta, \delta\theta)|\psi\rangle = \alpha_I \mathbb{1}|\psi\rangle + \alpha_X X|\psi\rangle + \alpha_Y Y|\psi\rangle + \alpha_Z Z|\psi\rangle\,. \tag{14.17}$$

QEC process involves performing projective measurements that cause the superposition given by Eq. (14.15) to collapse to a subset of its terms. Consequently, a QEC code with the ability to correct errors described by the X and Z Pauli matrices will be able to correct any coherent errors. So, only the X-type of errors (bit-flips) and Z-type of errors (phase-flips) are the two fundamental error types to be accounted by quantum correction codes.

14.5 QEC Mechanisms Using Quantum Redundancy

The simplest possible error correction code in the classical information theory is the repetition code in which each bit is replaced by three of its copies: $0 \to 000$ and $1 \to 111$. If any one of the bits in this code is fliped by taking a majority decision then we can correctly decode the information. If two or three bits flip then we cannot correctly decode the information. But this idea of classical error correction cannot be extended to QEC as there is no way to copy quantum information. Moreover, as we have discussed earlier, in addition to the bit-flip errors, there are phase-flip errors and combinations of both errors. It is not possible to do measurement for taking a majority decision without causing disturbance to the quantum codes. These problems were solved by Shor [7].

14.5.1 The Two-Qubit Error Correction Code

Shor proposed that redundancy can be added in quantum codes by expanding the Hilbert space in which the qubits are encoded. To explain how it is done consider an example of

a two-qubit code designed to detect a single-bit flip error [5]. $|\psi\rangle = \alpha|0\rangle + \beta|1\rangle$ is encoded using CNOT gate to get $|\psi\rangle_{\mathrm{L}}$, where L stands for logical. The action is

$$|\psi\rangle = \alpha|0\rangle + \beta|1\rangle \xrightarrow{\text{two-qubit encoder}} |\psi\rangle_{\mathrm{L}}\,, \tag{14.18}$$

where

$$|\psi\rangle_{\mathrm{L}} = \alpha|00\rangle + \beta|11\rangle = \alpha|0\rangle_{\mathrm{L}} + \beta|1\rangle_{\mathrm{L}}\,. \tag{14.19}$$

After encoding we get the logical codewords $|0\rangle_{\mathrm{L}} = |00\rangle$ and $|1\rangle_{\mathrm{L}} = |11\rangle$. $|\psi\rangle_{\mathrm{L}}$ is not a cloning of $|\psi\rangle$.

As the encoding operation has distributed the quantum information in the initial state $|\psi\rangle$ across the two-party logical state $|\psi\rangle_{\mathrm{L}}$, we can use this redundancy for error detection. $|\psi\rangle = \alpha|0\rangle + \beta|1\rangle$ is a vector in a two-dimensional Hilbert space $\mathcal{H}_2$, spanned by the kets $|0\rangle$ and $|1\rangle$. Encoding has made the logical qubit to occupy a four-dimensional Hilbert space $\mathcal{H}_4$ spanned by the kets $|00\rangle$, $|01\rangle$, $|10\rangle$ and $|11\rangle$. The logical qubit $|\psi\rangle_{\mathrm{L}}$ is defined in a two-dimensional subspace of $\mathcal{H}_4$ spanned by $|00\rangle$ and $|11\rangle$. Let us call this space as the *code space* $\mathcal{C}$.

Suppose a bit-flip flop is introduced to the encoded $|\psi\rangle_{\mathrm{L}}$ so that $X_1|\psi\rangle_{\mathrm{L}} = \alpha|10\rangle + \beta|01\rangle$, where X_1 is a bit-flip error acting on the first qubit. Now, we get a new subspace of $\mathcal{H}_4$ spanned by $|01\rangle$ and $|10\rangle$. Let us call $\mathcal{F}$ as error subspace. If no error occurs then the logical state $|\psi\rangle_{\mathrm{L}}$ occupies $\mathcal{C}$-code space and a single qubit flip-flop error makes it to occupy the error subspace $\mathcal{F}$. The subspace of $\mathcal{C}$ and $\mathcal{F}$ are mutually orthogonal. Therefore, it is now possible to do a projective measurement without compromising the uncoded quantum information to know whether the logical qubit is in $\mathcal{C}$ or $\mathcal{F}$ subspace. This type of measurements are called *stabilizer measurements*. For example, a stabilizer operator Z_1Z_2 can be used for the projective measurement in this case to differentiate $\mathcal{C}$ and $\mathcal{F}$ subspaces as

$$\begin{aligned}
Z_1Z_2|\psi\rangle_{\mathrm{L}} &= Z_1Z_2\left(\alpha|00\rangle + \beta|11\rangle\right) \\
&= \begin{pmatrix} 1 & 0 \\ 0 & -1 \end{pmatrix}\begin{pmatrix} 1 & 0 \\ 0 & -1 \end{pmatrix}\left(\alpha\begin{pmatrix} 1 & 1 \\ 0 & 0 \end{pmatrix} + \beta\begin{pmatrix} 0 & 0 \\ 1 & 1 \end{pmatrix}\right) \\
&= \alpha\begin{pmatrix} 1 & 1 \\ 0 & 0 \end{pmatrix} + \beta\begin{pmatrix} 0 & 0 \\ 1 & 1 \end{pmatrix} \\
&= \alpha|00\rangle + \beta|11\rangle \\
&= (+1)|\psi\rangle_{\mathrm{L}}\,.
\end{aligned} \tag{14.20}$$

The Z_1Z_2 operator projects the error state $X_1|\psi\rangle_{\mathrm{L}}$ and $X_2|\psi\rangle_{\mathrm{L}}$ into the (-1) eigenspace. The measurement of Z_1Z_2 has not changed α and β the coefficients of $|\psi\rangle$ [8]. Hence, the projective measurement Z_1Z_2 has not disturbed the quantum information.

A three stage quantum circuit can be set-up for the implementation of the two-qubit code [5]. Stage I uses a CNOT gate to entangle $|\psi\rangle$ to get the logical code $|\psi\rangle_{\mathrm{L}}$ with a redundancy qubit. In the second stage, the logical qubit $|\psi\rangle_{\mathrm{L}}$ may be subject to a bit-flip error E. In the third stage, an ancilla qubit $|0\rangle_{\mathrm{A}}$ is introduced to perform the measurement of the Z_1Z_2 stabilizer. This stage contains the ancilla qubit measurement. The coutcome of the ancilla qubit measurement is referred as a *syndrome* which gives information whether the logical state has been subject to error or not. This stage is the syndrome extraction stage where the state $E|\psi\rangle_{\mathrm{L}}$ is transformed as

$$\begin{aligned}
E|\psi\rangle_{\mathrm{L}}|0\rangle_{\mathrm{A}} \xrightarrow{\text{syndrome extraction}} & \frac{1}{2}\left(\mathbb{1}_1\mathbb{1}_2 + Z_1Z_2\right)E|\psi\rangle_{\mathrm{L}}|0\rangle_{\mathrm{A}} \\
& + \frac{1}{2}\left(\mathbb{1}_1\mathbb{1}_2 - Z_1Z_2\right)E|\psi\rangle_{\mathrm{L}}|1\rangle_{\mathrm{A}}\,.
\end{aligned} \tag{14.21}$$

In Eq. (14.21) E is an error from the set $\{\mathbb{1}, X_1, X_2, X_1X_2\}$. If $E = X_1$ or X_2 then $E|\psi\rangle_{\rm L}$ will be in the $\mathcal{F}$ subspace. In this case the first term in right-side of Eq. (14.21) becomes zero. Hence, the ancilla qubit is determined as 1. The ancilla is measured as 0 if $E = \{\mathbb{1}, X_1X_2\}$. The syndrome bit S corresponding to the outcomes of a stabilizer measurement for the errors $\mathbb{1}_1\mathbb{1}_2$ and X_1X_2 is 0 while for the errors $X_1\mathbb{1}_2$ and $\mathbb{1}_1X_2$ is 1.

Solved Problem 2:

Show that in the syndrome extraction given by Eq. (14.21), for $E = \{\mathbb{1}, X_1X_2\}$ ancilla is measured as 0 and for $\{X_1, X_2\}$ ancilla is measured as 1.

We have $Z|1\rangle = -|1\rangle$, $Z|0\rangle = |0\rangle$ and Z_1 operates on the first ket, Z_2 operates on the second ket. Also, $X|1\rangle = |0\rangle$ and $X|0\rangle = |1\rangle$.

For $E = \mathbb{1}$ we find

$$\begin{aligned} E|\psi\rangle_{\rm L} &= \mathbb{1}|\psi\rangle_{\rm L} = |\psi\rangle_{\rm L}, && (14.22a)\\ \mathbb{1}_1\mathbb{1}_2|\psi\rangle_{\rm L} &= |\psi\rangle_{\rm L}, && (14.22b)\\ Z_1Z_2|\psi\rangle_{\rm L} &= (+1)|\psi\rangle_{\rm L}. && (14.22c) \end{aligned}$$

So, the second term in Eq. (14.21) is $\frac{1}{2}\left(\mathbb{1}_1\mathbb{1}_2|\psi\rangle_{\rm L} - Z_1Z_2|\psi\rangle_{\rm L}\right)|1\rangle_{\rm A} = 0$. Hence, for $E = \mathbb{1}$ we get only the first term in Eq. (14.21). Then the ancilla qubit is just $|0\rangle$.

For $E = X_1X_2$ as $X_1|\psi\rangle_{\rm L} = \alpha|10\rangle + \beta|01\rangle$ we get

$$\begin{aligned} E|\psi\rangle_{\rm L} &= X_1X_2\left(\alpha|00\rangle + \beta|11\rangle\right)\\ &= \alpha|11\rangle + \beta|00\rangle, && (14.23a)\\ \mathbb{1}_1\mathbb{1}_2E|\psi\rangle_{\rm L} &= \alpha|11\rangle + \beta|00\rangle, && (14.23b)\\ Z_1Z_2E|\psi\rangle_{\rm L} &= Z_1\left(Z_2\left(\alpha|11\rangle + \beta|00\rangle\right)\right)\\ &= Z_1\left(-\alpha|11\rangle + \beta|00\rangle\right)\\ &= \alpha|11\rangle + \beta|00\rangle. && (14.23c) \end{aligned}$$

Then $\mathbb{1}_1\mathbb{1}_2E|\psi\rangle_{\rm L} - Z_1Z_2E|\psi\rangle_{\rm L} = 0$. So, $E = X_1X_2$ error also gives the ancilla qubit in $|0\rangle$ state.

Next, for $E = X_1$

$$\begin{aligned} E|\psi\rangle_{\rm L} &= X_1|\psi\rangle_{\rm L} = \alpha|10\rangle + \beta|01\rangle, && (14.24a)\\ \mathbb{1}_1\mathbb{1}_2E|\psi\rangle_{\rm L} &= \alpha|10\rangle + \beta|01\rangle, && (14.24b)\\ Z_1Z_2E|\psi\rangle_{\rm L} &= Z_1\left(Z_2\left(\alpha|10\rangle + \beta|01\rangle\right)\right)\\ &= Z_1\left(\alpha|10\rangle - \beta|01\rangle\right)\\ &= -\alpha|10\rangle - \beta|01\rangle\,. && (14.24c) \end{aligned}$$

The first term in Eq. (14.21) becomes $\left(\mathbb{1}_1\mathbb{1}_2 + Z_1Z_2\right)X_1|\psi\rangle_{\rm L} = 0$. The ancilla gives the state $|1\rangle$. So, it is measured as 1. Similarly, $\left(\mathbb{1}_1\mathbb{1}_2 + Z_1Z_2\right)X_2|\psi\rangle_{\rm L} = 0$. Again, for $E = X_2$ the ancilla will be measured as 1.

14.5.2 The Three-Qubit Error Correction Code

What do we get from the syndrome created in the two-qubit code? It simply informs the presence of an error. It does not provide sufficient message to identify the bit where the error has occurred. It is necessary to develop an error correction code to identify and localize

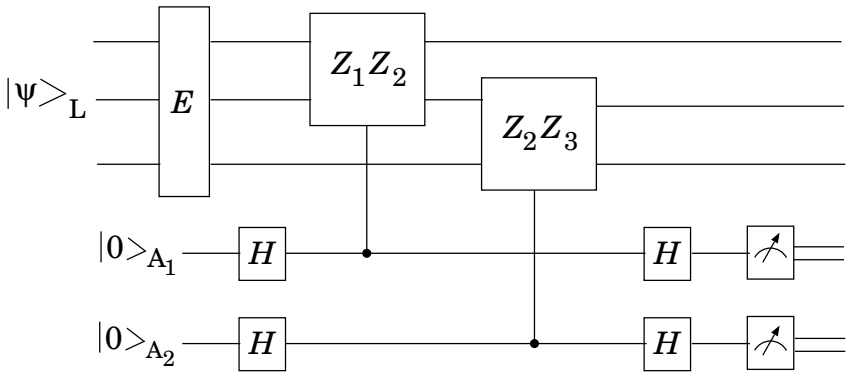

FIGURE 14.1
The circuit diagram for syndrome extraction for three-qubit code [5].

the errors. For this purpose multiple stabilizer measurements can be done. A three-bit code will give a basic introduction to both detect and localize the errors.

The three-qubit code encodes a single logical qubit into three logical qubits. The encoding operation distributes the quantum information across an entangled three-party state. The two logical basis states are defined as $|0\rangle_{\rm L} = |000\rangle$ and $|1\rangle_{\rm L} = |111\rangle$. The arbitrary single qubit state $|\psi\rangle = \alpha|0\rangle + \beta|1\rangle$ is mapped to

$$\alpha|0\rangle + \beta|1\rangle \longrightarrow \alpha|0\rangle_{\rm L} + \beta|1\rangle_{\rm L} \longrightarrow \alpha|000\rangle + \beta|111\rangle = |\psi\rangle_{\rm L}\,. \tag{14.25}$$

$|\psi\rangle$ can be encoded to get $|\psi\rangle_{\rm L}$ using two initialized ancilla qubits via CNOT gates.

The dimension of the Hilbert space occupied by $|\psi\rangle_{\rm L}$ is eight. This Hilbert space $\mathcal{H}_8$ is spanned by the basis $\{|000\rangle, |001\rangle, |010\rangle, |011\rangle, |100\rangle, |101\rangle, |110\rangle, \ |111\rangle\}$. $\mathcal{H}_8$ can be partitioned into four subspaces as given below:

$$\begin{aligned} \mathcal{C} &= \text{span}\,\{|000\rangle, |111\rangle\}\,, \quad \mathcal{F}_1 = \text{span}\,\{|100\rangle, |011\rangle\}\,, \\ \mathcal{F}_2 &= \text{span}\,\{|010\rangle, |101\rangle\}\,, \quad \mathcal{F}_3 = \text{span}\,\{|001\rangle, |110\rangle\}\,, \end{aligned}$$

where $\mathcal{C}$ is the logical code space and $\mathcal{F}_1$, $\mathcal{F}_2$ and $\mathcal{F}_3$ are logical error spaces. Any error E_1 rotates $\mathcal{C}$ into any of the three error space. The four subspaces can be distinguished by carrying out two stabilizer measurements Z_1Z_2 and Z_2Z_3. This can be done using the circuit shown in Fig. 14.1. Table 14.1 gives the syndrome $\mathcal{S}$ for all the bit-errors. We find from this table that each single-qubit error gives a unique two-bit syndrome $\mathcal{S} = s_1s_2$. It will help us to choose a suitable recovery operation.

14.5.3 Quantum Code Distance

The minimum size of the undetectable error is called a *quantum code distance* d [5]. This is also a logical Pauli operation that transforms one codeword to another. For example, in the three qubit code, we find that Pauli-X operator $\overline{X} = X_1X_2X_3$ transforms $\overline{X}|0\rangle_{\rm L} = |1\rangle_{\rm L}$ and $\overline{X}|1\rangle_{\rm L} = |0\rangle_{\rm L}$. $d = 3$ if the qubits in the three-qubit code are exposed to only X-errors. For phase-flip errors the Pauli Z-operator $\overline{Z} = Z_1Z_2Z_3$ will determine d. To find d for the

TABLE 14.1
The syndrome table for all the flip-flop errors [5].

Error	Syndrome	Error	Syndrome
$\mathbb{1}_1\mathbb{1}_2\mathbb{1}_3$	00	$X_1X_2\mathbb{1}_3$	01
$X_1\mathbb{1}_2\mathbb{1}_3$	10	$\mathbb{1}_1X_2X_3$	10
$\mathbb{1}_1X_2\mathbb{1}_3$	11	$X_1\mathbb{1}_2X_3$	11
$\mathbb{1}_1\mathbb{1}_2X_3$	01	$X_1X_2X_3$	00

Z-error instead of $|0\rangle$ and $|1\rangle$ we consider the basis $\{|+\rangle, |-\rangle\}$ where

$$|+\rangle = \frac{1}{\sqrt{2}}\left(|0\rangle + |1\rangle\right), \quad |-\rangle = \frac{1}{\sqrt{2}}\left(|0\rangle - |1\rangle\right). \tag{14.26}$$

Encoding in the basis $|+\rangle$ and $|-\rangle$ we get the logical states

$$|+\rangle_{\mathrm{L}} = \frac{1}{\sqrt{2}}\left(|000\rangle + |111\rangle\right) \text{ and } |-\rangle_{\mathrm{L}} = \frac{1}{\sqrt{2}}\left(|000\rangle - |111\rangle\right). \tag{14.27}$$

As $\overline{Z} = Z_1$ will transform $Z|+\rangle_{\mathrm{L}} = |-\rangle_{\mathrm{L}}$ the code cannot detect the presence of a single qubit phase-flip error. Consequently, the three qubit code has $d = 1$ if we consider both X- and Z-errors.

14.6 QEC with Stabilizer Codes

We have seen that for the three-qubit code if an X-error occurs then it can be detected via a sequence of two stabilizer measurements Z_1Z_2 and Z_2Z_3. First, we describe the generalization of this scheme to create $[[n, k, d]]$ stabilizer codes, where n is the total number of qubits, k is the number of logical qubits and d is the code distance [5].

14.6.1 Creation of Stabilizer Codes

Figure 14.2 depicts the basic quantum circuit for an $[[n, k, d]]$ stabilizer code. For the ith stabilizer P_i the mapping of the logical states by the syndrome extracting circuit is done as

$$\begin{aligned} E|\psi\rangle_{\mathrm{L}}|0\rangle_{\mathrm{A}_i} \xrightarrow{\text{syndrome extraction}} & \frac{1}{2}\left(\mathbb{1}^{\otimes n} + P_i\right) E|\psi\rangle_{\mathrm{L}}|0\rangle_{\mathrm{A}_i} \\ & + \frac{1}{2}\left(\mathbb{1}^{\otimes n} - P_i\right) E|\psi\rangle_{\mathrm{L}}|1\rangle_{\mathrm{A}_i}. \end{aligned} \tag{14.28}$$

When P_i commutes with E then the measurement of ancilla qubit A_i returns 0 while in the case of anticommuting 1 is returned. Therefore, a good code can be constructed if a stabilizer anticommuting with error E can be found. An m-bit syndrome can be obtained by combining the outcomes of m stabilizer measurements. These syndromes can be utilized to get the best recovery operator to reinstate the logical state to the codespace.

The code stabilizers must possess the following properties [5].

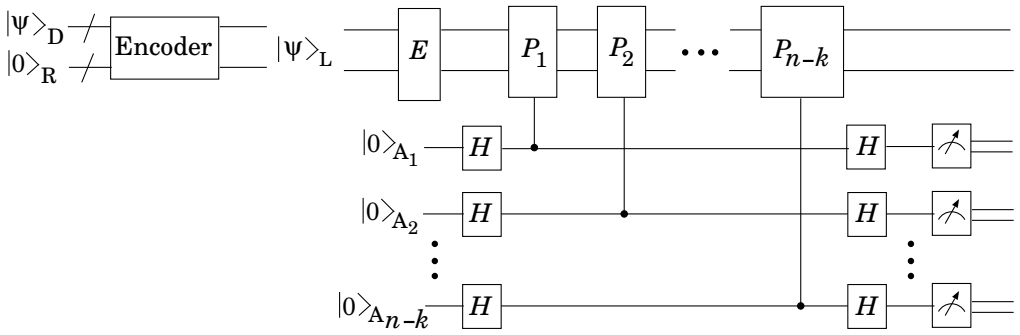

FIGURE 14.2
A schematic of the quantum circuit for an $[[n, k, d]]$ stabilizer code [5].

1. P_i should belong to the Pauli group $\mathcal{G}_n$ over n-qubits. $\mathcal{G}_n$ is formed by the elements from the direct product of the single-qubit Pauli group $\mathcal{G}_1 = \{\pm\mathbb{1}, \pm i\mathbb{1}, \pm X, \pm iX, \pm Y, \pm iY, \pm Z, \pm iZ\}$.
2. For all possible values of the logical states $P_i|\psi\rangle_{\mathrm{L}} = (+1)$, that is, the stabilizers must stabilize the logical states of the codes.
3. $[P_i, P_j] = 0$ for all i and j, that is, the stabilizers must commute with each other.

The $n - k$ stabilizers needed for syndrome extraction must be a minimal set of the stabilizer group. An $[[n, k, d]]$ stabilizer code has $2k$ logical operators $\overline{\mathcal{L}}_i$ which allows logical states to be modified without having to decode and then encode. Any $\overline{\mathcal{L}}_i P_j$ is also a logical operator as $\mathbb{1}_i P_j|\psi\rangle_{\mathrm{L}} = \overline{\mathcal{L}}_i|\psi\rangle_{\mathrm{L}}$.

14.6.2 An Error Correction Scheme

Let us denote the number of correctable errors as t. It is given by $t = (d-1)/2$. t is ≥ 1 for $d \geq 3$. Therefore, the stabilizer codes with $d \geq 3$ are essentially error correction codes. For these codes recovery operations have to be applied. The use of stabilizer codes to describe QEC codes is highly useful. It allows for easy synthesis of correction circuits and also shows how logical operations can be performed directly on encoded data.

For a single cycle of an $[[n, k, d]]$ stabilizer code an error correction scheme is the following [5]. The encoded $|\psi\rangle_{\mathrm{L}}$ goes through the error process E. Next, making use of the syndrome extraction method the code stabilizers are measured. Then the measured results are copied to a register of $m = n - k$ ancilla qubits $|A\rangle^{\otimes m}$. The m-bit syndrome S are found from the reading of the ancilla qubits. Then decoding process is performed. A decoding circuit processes the syndrome to identify the best unitary operation $\mathcal{R}$ in order to send $|\psi\rangle_{\mathrm{L}}$ to the codespace. The decoding process is considered as success if

$$\mathcal{R}E|\psi\rangle_{\mathrm{L}} = (+1)|\psi\rangle_{\mathrm{L}}\,. \tag{14.29}$$

Any $\mathcal{R}E$ which is an element of the code stabilizer with $\mathcal{R}E = P \in \mathcal{S}$ will satisfy Eq. (14.29). Note that $\mathcal{R}$ is not unique because one can set-up degenerate codes with mapping of multiple errors to the same syndrome.

14.6.3 The Shor Nine-Qubit Code

The first QEC code was developed by Shor [7]. It is a nine-qubit error correcting code and is an example of a code with $d = 3$ and $k = 1$. The code is thus denoted as $[[9, 1, 3]]$. It can be used to correct a logical qubit from one bit flip-flop (X-error) or one discrete phase-flip (Z)-error or one of each on any of the nine qubits. So, it can correct any linear combination of errors on a single qubit. Shor code can be constructed by a method known as *code concatenation* [5].

In the code concatenation, the output of one code is embedded into the input of another. Two codes are concatenated in the Shor nine-qubit codes. They are the three-qubit code for phase-flip and the three-qubit code for the bit-flip [9]. The three-qubit codes for bit-flip and phase flip are defined as

$$\begin{aligned} \mathcal{C}_{3\mathrm{b}} &= \mathrm{span}\left\{|0\rangle_{3\mathrm{b}} = |000\rangle,\, |1\rangle_{3\mathrm{b}} = |111\rangle\right\}, \\ &\quad \mathcal{S}_{3\mathrm{b}} = \langle Z_1Z_2, Z_2Z_3\rangle, \end{aligned} \tag{14.30}$$

$$\begin{aligned} \mathcal{C}_{3\mathrm{p}} &= \mathrm{span}\left\{|0\rangle_{3\mathrm{p}} = |++\!+\rangle,\, |1\rangle_{3\mathrm{p}} = |--\!-\rangle\right\}, \\ &\quad \mathcal{S}_{3\mathrm{p}} = \langle X_1X_2, X_2X_3\rangle, \end{aligned} \tag{14.31}$$

respectively. To get the Shor code the bit-flip code is embedded into codewords of phase-flip codes as

$$|0\rangle_{3\mathrm{p}} = |++\!+\rangle \xrightarrow{\text{concatenation}} |0\rangle_9 = |+\rangle_{3\mathrm{b}}|+\rangle_{3\mathrm{b}}|+\rangle_{3\mathrm{b}} \tag{14.32}$$

and

$$|1\rangle_{3\mathrm{p}} = |--\!-\rangle \xrightarrow{\text{concatenation}} |1\rangle_9 = |-\rangle_{3\mathrm{b}}|-\rangle_{3\mathrm{b}}|-\rangle_{3\mathrm{b}}\,, \tag{14.33}$$

where

$$|\pm\rangle_{3\mathrm{b}} = \frac{1}{\sqrt{2}}\left(|000\rangle \pm |111\rangle\right)\,. \tag{14.34}$$

Then for the Shor code $[[9, 1, 3]]$, in computational basis, the codes space $\mathcal{C}_{[[9,1,3]]}$ and the corresponding stabilizers $\mathcal{S}_{[[9,1,3]]}$ are given by

$$\mathcal{C}_{[[9,1,3]]} = \mathrm{span}\begin{cases} |0\rangle_9 = \dfrac{1}{\sqrt{8}}\left(|000\rangle + |111\rangle\right) \otimes \left(|000\rangle + |111\rangle\right) \\ \qquad\qquad \otimes \left(|000\rangle + |111\rangle\right) \\ |1\rangle_9 = \dfrac{1}{\sqrt{8}}\left(|000\rangle - |111\rangle\right) \otimes \left(|000\rangle - |111\rangle\right) \\ \qquad\qquad \otimes \left(|000\rangle - |111\rangle\right) \end{cases} \tag{14.35}$$

and

$$\begin{aligned} \mathcal{S}_{[[9,1,3]]} = \langle &Z_1Z_2,\, Z_2Z_3,\, Z_4Z_5,\, Z_5Z_6,\, Z_7Z_8,\, Z_8Z_9, \\ &X_1X_2X_3X_4X_5X_6,\, X_4X_5X_6X_7X_8X_9\rangle\,. \end{aligned} \tag{14.36}$$

In $\mathcal{S}_{[[9,1,3]]}$ the terms $Z_1Z_2, \ldots, Z_8Z_9$ are the stabilizers for the bit-flip codes and are in the three blocks of codes. The stabilizers $X_1X_2X_3X_4X_5X_6$ and $X_4X_5X_6X_7X_8X_9$ are for the phase-flip codes. The encoded Shor's nine bit code is

$$|\psi\rangle_{\mathrm{L}} = \alpha|0\rangle_9 + \beta|1\rangle_9\,. \tag{14.37}$$

The syndrome for all the single-qubit errors on the Shor's nine-qubit code can be easily set-up. From this table one can observe that unique syndromes result from the X-errors. But same syndrome is produced by the Z-errors occurring in the same block of the codes. Even though we have the degeneracy in the code syndromes, it does not affect the code distance. So, this nine-qubit code is able to correct all single-qubit errors and $d = 3$.

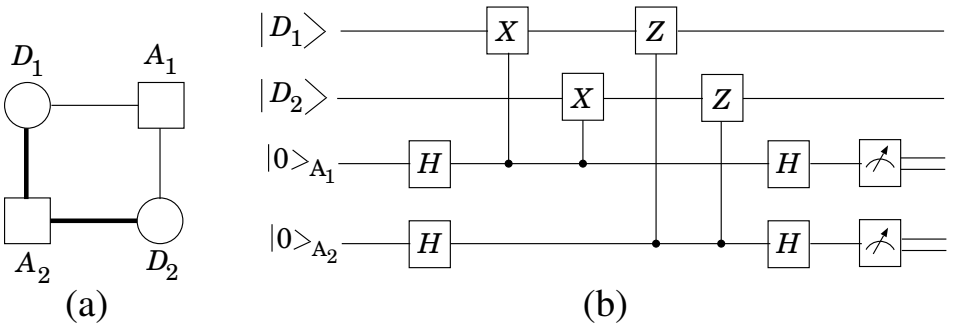

FIGURE 14.3
(a) Pictorial represenation of the surface code four-cycle. (b) Quantum circuit for the surface code four-cycle [5].

14.7 The Surface Code

Finding the commuting sets of stabilizers for identifying errors without altering the encoded information to create QEC is very difficult. Special code construction models are necessary to determine such stabilizers. One such efficient error correction model is the surface code [10–14]. It is defined over a two-dimensional lattice of qubits. It can be implemented on architectures that only allow for the coupling of nearest neighbour qubits. It also has the highest fault-tolerent thresholds of any QEC scheme. Moreover, the surface code can correct problematic error channels such as qubit loss and leakage. We give below the outline of constructing the surface code [10–12]. It is one of the efficient QEC codes among a variety of topological codes [15] in which code structure is defined on a lattice and scaling of the code to correct more errors is conceptually straight-forward.

Surface codes are given in a pictorial representation of the code qubits instead of quantum circuits [5,16]. Figure 14.3a shows a surface code four-cycle which is the fundamental building block of other surface codes. The open circles D_1 and D_2 represent the code (data) qubits and the squares A_1 and A_2 represent ancilla qubits. The edges with thin lines represent controlled X gates. The thick line edges represent controlled Z operation. They are controlled by ancilla qubits and action on data qubits. A_1 (A_2) connects to D_1 and D_2 via the thin (thick) edges and hence the stabilizer measured is $X_{D_1}X_{D_2}$ ($Z_{D_1}Z_{D_2}$). Figure 14.3b gives the same surface codes four-cycle in circuit notation.

In the four-cycle surface code, the total number of qubits and the number of stabilizers both are 2, that is, $n = m = 2$. Thus, the number of logical qubits it codes is $k = n - m = 2 - 2 = 0$. This indicates that the four-cycle is not a useful code. However, multiple four-cycles can be used to form square lattices for realizing quantum detection and correction codes. As an example, we discuss the five-qubit surface code $[[5, 1, 2]]$ formed by tiling four four-cycles in square lattice [17].

In the pictorial representation of the surface code $[[5, 1, 2]]$, there are five data qubits (D_1, D_2, D_3, D_4, D_5) and four ancilla qubits (A_1, A_2, A_3, $A4$). D_3 is at the centre and the other D's are at the four corners. A_1 and A_4 are at the top and the bottom, respectiverly. A_2 and A_3 are at the left-side and the right-side, respectively, of the lattice. The ancilla qubit A_1 connects the data qubits D_1, D_2 and D_3 via thin lines. A_4 connects D_3, D_4 and D_5 via thin lines. The ancilla qubit A_2 (A_3) connects the data qubits D_1 (D_2), D_4 (D_5)

and D_3 via thick lines. By looking at how each ancilla qubit connects the data qubits the stabilizers of the code corresponding to $A_1 - A_4$ is [5]

$$\begin{aligned} \mathcal{S}_{[[5,1,2]]} &= \langle X_{D_1} X_{D_2} X_{D_3},\ Z_{D_1} Z_{D_3} Z_{D_4},\ Z_{D_2} Z_{D_3} Z_{D_5}, \\ &\quad X_{D_3} X_{D_4} X_{D_5} \rangle. \end{aligned} \tag{14.38}$$

As $n = 5$ and $m = 4$ this code encodes $n - m = 1$ logical qubit.

Next, consider two examples of errors on $[[5, 2, 1]]$ and their detection. Suppose there is a Z_{D_1}-error on the qubit D_1. Z_{D_1} anticommutes with the stabilizer $X_{D_1} X_{D_2} X_{D_3}$. The result is triggering of 1 syndrome measurement in A_1. In the pictorial form, this can be depicted by representing A_1 by a filled square. In the second example, say, X_{D_5} error is in D_5. X_{D_5} anticommutes with $Z_{D_2} Z_{D_3} Z_{D_5}$ and thereby triggers a 1 syndrome measurement in A_3. Filled square is now used to represent A_3.

As described above the surface code is considered as a square lattice with two types of boundaries, namely, thin line and thick line. The thin (thick) lines of horizontal (vertical) boundaries are associated with the X-type (Z-type) stabilizer measurements. Chains of Pauli operators along the edges of these boundaries give the logical operators of the surface code. Let the Pauli operator $\overline{X} = X_{D_1} X_{D_4}$ acts along the vertical boundary along which Z-type stabilizers are measured. Next, say, the Pauli operator $\overline{Z} = Z_{D_1} Z_{D_2}$ acts along the horizontal boundary along which X-type stabilizers are measured. Both $\overline{X} = X_{D_1} X_{D_4}$ and $\overline{Z} = Z_{D_1} Z_{D_2}$ commute with all the stabilizers in $[[5, 1, 2]]$ given by Eq. (14.38). Moreover, $\overline{X}$ and $\overline{Z}$ are anticommuting with themselves (see the solved problem 3). The Pauli-X and Pauli-Z logical operators for each encoded qubits are pairs of operators. They anticommute with one another and commute with all code stabilizers. Thus, we have found suitable logical operators of the $[[5, 1, 2]]$ surface code as $\overline{X}$ and $\overline{Z}$. As the minimum weight of the logical operation is 2 the five-qubit surface code $[[5, 1, 2]]$ is a detection code with $d = 2$.

Solved Problem 3:

Show that $\overline{X} = X_{D_1} X_{D_4}$ and $\overline{Z} = Z_{D_1} Z_{D_2}$ anticommute and they commute with $X_{D_1} X_{D_2} X_{D_3}$ and $Z_{D_1} Z_{D_3} Z_{D_4}$

X and Z operating on different bits commute. Using this result, we obtain

$$\begin{aligned} \overline{X}\,\overline{Z} + \overline{Z}\,\overline{X} &= X_{D_1} X_{D_4} Z_{D_1} Z_{D_2} + Z_{D_1} Z_{D_2} X_{D_1} X_{D_4} \\ &= X_{D_1} Z_{D_1} X_{D_4} Z_{D_2} + Z_{D_1} X_{D_1} Z_{D_2} X_{D_4} \\ &= X_{D_1} Z_{D_1} X_{D_4} Z_{D_2} + Z_{D_1} X_{D_1} X_{D_4} Z_{D_2}\,. \end{aligned} \tag{14.39}$$

As

$$XZ = \begin{bmatrix} 0 & 1 \\ 1 & 0 \end{bmatrix} \begin{bmatrix} 1 & 0 \\ 0 & -1 \end{bmatrix} = \begin{bmatrix} 0 & -1 \\ 1 & 0 \end{bmatrix}, \tag{14.40a}$$

$$ZX = \begin{bmatrix} 1 & 0 \\ 0 & -1 \end{bmatrix} \begin{bmatrix} 0 & 1 \\ 1 & 0 \end{bmatrix} = \begin{bmatrix} 0 & 1 \\ -1 & 0 \end{bmatrix} = -XZ\,. \tag{14.40b}$$

Therefore, $X_{D_1} Z_{D_1} = -Z_{D_1} X_{D_1}$. Using this result in Eq. (14.39) we get

$$\overline{X}\,\overline{Z} + \overline{Z}\,\overline{X} = X_{D_1} Z_{D_1} X_{D_4} Z_{D_2} - X_{D_1} Z_{D_1} X_{D_4} Z_{D_2} = 0\,. \tag{14.41}$$

That is, $\overline{X}$ and $\overline{Z}$ anticommute.

Next, consider $[\overline{X}, X_{D_1}X_{D_2}X_{D_3}]$. As X's operating on different qubit commut and $X_{D_1}^2 = I$, we obtain

$$\begin{aligned}
\left[\overline{X}, X_{D_1}X_{D_2}X_{D_3}\right] &= X_{D_1}X_{D_4}X_{D_1}X_{D_2}X_{D_3} - X_{D_1}X_{D_2}X_{D_3}X_{D_1}X_{D_4} \\
&= X_{D_1}^2 X_{D_4}X_{D_2}X_{D_3} - X_{D_1}^2 X_{D_2}X_{D_3}X_{D_4} \\
&= X_{D_4}X_{D_2}X_{D_3} - X_{D_2}X_{D_3}X_{D_4} \\
&= X_{D_2}X_{D_3}X_{D_4} - X_{D_2}X_{D_3}X_{D_4} \\
&= 0\,. \qquad (14.42)
\end{aligned}$$

Similarly, we can prove

$$\begin{aligned}
\left[\overline{X}, Z_{D_1}Z_{D_3}Z_{D_4}\right] &= 0, \quad \left[\overline{Z}, X_{D_1}X_{D_2}X_{D_3}\right] = 0, \\
\left[\overline{Z}, Z_{D_1}Z_{D_3}Z_{D_4}\right] &= 0\,. \qquad (14.43)
\end{aligned}$$

14.8 Practical Issues in the Implementation of QEC Codes

We have discussed the procedure to correct the quantum errors by assuming that errors do not occur on ancilla qubits. We have not taken into consideration that systematic errors may be introduced by the quantum gates themselves. In the hardware implementation of QEC codes practical difficulties occur. It is thus imperative that any error correction procedure and logical operations need to be designed such that these errors are also get corrected. In this section let us point out certain practical issues in the implementation of QEC codes [2,5].

14.8.1 Fault Tolerance

If a QEC code is capable of accounting errors occurring at anywhere in a quantum circuit then it is called a *fault tolerant* [18,19]. In the fault tolerant quantum correction code, the quantum circuits involved in gate operations and error correction schemes should not lead to errors to propagate. To avoid the propagation of errors quantum circuits need to be modified. There are certain techniques proposed for this purpose [18–27].

Consider the quantum circuits given in Fig. 14.4. The circuit in Fig. 14.4a is a CNOT circuit with out an error for the transformation $|110\rangle|010\rangle \rightarrow |110\rangle|101\rangle$. In Fig. 14.4b, a single X-error is assumed to occur on the top most qubit. This single error will cascade and propagate to four qubits. Figure 14.4c presents a modified quantum circuit for the transformation $|110\rangle|010\rangle \rightarrow |110\rangle|101\rangle$. In this circuit, the same X-error propagates to only two of the six qubits. If we consider the each three single logical qubit as a single block then the circuit of Fig. 14.4c introduces only a single error in each block.

A standard definition of a fault tolerant circuit element is that [2] *a single error will cause at most one error in the output for each logical qubit block*. Of course, the above definition is valid only for a single error correcting code. If a code corrects $t = [(d-1)/2]$ errors then the requirement for fault tolerance is that any error less than or equal to t should not lead to errors greater than t in the output for each logical qubit. For modifying a QEC circuit for fault tolerance we may need additional ancilla qubits. In general, a fault tolerant modified circuit will always have increased overhead compared to the original circuit.

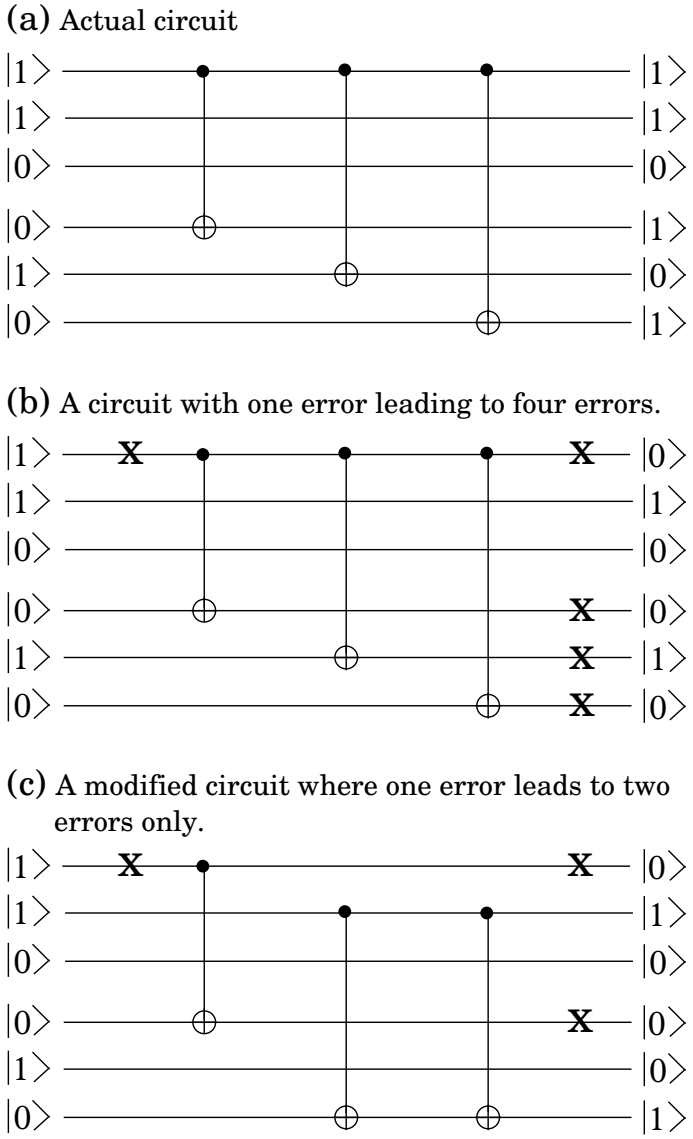

FIGURE 14.4
(a) A CNOT circuit for the transformation $|110\rangle|010\rangle \rightarrow |110\rangle|101\rangle$. (b) The result for the case of a single X-error. (c) A modified equivalent circuit where one error propagates to two errors only.

14.8.2 Threshold Theorem

The ability to perform dynamical error correction depends on a threshold of a code given by the threshold theorem [2,28]. We explain the importance of the code threshold where a quantum code is utilized to correct only a single error, using a model that assumes uncorrelated errors on individual qubits.

Let us assume the probability per gate operation for each physical qubit to encounter

either an X or Z or both errors independently. Further, a cycle of error correction is done after each elementary gate operation consistent with the rules of fault tolerance. This ensures that this error will only propagate to at most one error in each block. Then a cycle of error correction will remove the error. Therefore, the occurrence of two or more errors alone makes the logical step fail. With p as the failure probability of un-encoded qubits per step, the failure rate p_{L}^1 of each logical gate operation of a 1st level logical qubit is cp^2 [2]. Here c is the maximum of the number of 2-error combinations. Suppose in all the levels of operations same gate operations and same error correction schemes are employed. We write

$$p_{\mathrm{L}}^2 = c\left(p_{\mathrm{L}}^1\right)^2 = c^3p^4 = \frac{(cp)^{2^2}}{c}, \tag{14.44}$$

$$p_{\mathrm{L}}^3 = c\left(p_{\mathrm{L}}^2\right)^2 = c\left(c^3p^4\right)^2 = c^7p^8 = \frac{(cp)^{2^3}}{c}. \tag{14.45}$$

Then after k iterations the logical failure rate can be written as

$$p_{\mathrm{L}}^k = c\left(p_{\mathrm{L}}^{k-1}\right)^2 = \frac{c^{2^2}}{c}\left(\left(p_{\mathrm{L}}^{k-2}\right)^2\right)^2 = \ldots = \frac{(cp)^{2^k}}{c}. \tag{14.46}$$

If $cp < 1$ then p_{L}^k can be made as small as possible by increasing the number of iterations k. Note that $cp < 1$ defines the threshold. Thus, any large quantum circuit can be successfully implemented provided $p_{\mathrm{th}} < 1/c$. Of course, more resources will be needed. The computation of threshold is an extremely important in designing quantum architecture [28–35].

14.8.3 Finding Efficient Decoding Algorithms From Code Syndromes

A decoder must find out the most appropriate recovery operation $\mathcal{R}$ to recover the encoded information to the codespace from the measurement of the stabilizers which produce the syndrome $\mathcal{S}$, An $[[n, k, d]]$ code gives an $m = n - k$-bit syndrome. Therefore, there are 2^m possible syndromes for each code. Making use of the syndrome tables it is possible to find the best $\mathcal{R}$-operator for small code examples discussed in this chapter. When the code size increases it is impractical to find a decoding strategy. In the case of the surface code $[[41, 1, 5]]$, the number of possible syndromes is $2^m = 2^{40} \approx 10^{12}$. That is, the look-up table of syndrome will have the size $\approx 10^{12}$. Many other interference techniques have been developed and used to find the mostly likely error that can happen for a given syndrome. But so far an universal decoder is not achieved.

14.8.4 Fault Tolerant Computation

As any quantum information processing need computations to be performed by logical gates, these gates may also be faulty. Therefore, the gate operations must be done without introducing errors uncontrollable and also following the guidelines of fault tolerance. A universal quantum computer performs an unitary operation U leading to $U|\psi\rangle = |\psi'\rangle$, that is, U evolves a qubit register from one state to another. Any unitary operation can be effectively performed with a set of elementary gates. A prime challenge in establishing a universal encoded gate set is to determine the schemes by which the gate operations can be performed following the rules of fault tolerance. For many codes, a subset of universal gates performing fault tolerantly can be identified. This is achieved with logical operators having a property known as *transversality*. This property ensures that error will not spread in the quantum circuit uncontrollably. But no-go theorem prohibits any such implementation of a full universal gate [36]. Other methods are available but they all require more number of additional qubits [37–40].

14.9 Concluding Remarks

Efficient quantum algorithms make use of large scale quantum interference which is sensitive to imprecision in the computer and to unwanted coupling between the quantum states and environment. Large scale quantum computation and information processing is practically impossible unless efficient error correction methods are used. This chapter has discussed the stabilizer formalism, basic idea on circuit synthesis and fault tolerant circuit construction. The usefulness of stabilizers in investigating the properties of error correction codes is explained. It is possible to correct and suppress any quantum error at least in principle if certain threshold conditions on the qubits are satisfied. Unfortunately, any effective QEC protocols need large number of qubits and thereby increasing the expenses associated with the quantum computing.

We have given the basics of the surface code which is the most used QEC scheme. But there are certain drawbacks with the surface code. Alternatives to the surface code have been proposed but they have low thresholds. When developing a large scale quantum computer the actual quantum code and the error correction procedure must be effectively incorporated. There are many challenges to be overcome in building a circuit model of quantum computer. Methods for realization and control of qubits have to be improved very much. Theoretically finding better ways to achieve fault tolerant error correction is a major challenge.

Some notable advancements in the field of QEC include theory of QEC for general noise [41], new codes and their bounds [42], analog QEC routines [43], effects of multiple-particle interference [44] and mixed state entanglement [45], geometries of QEC codes [46,47], experimental demonstration of QEC [48–55], optimization of QEC [56,57] and applications to communication [58 metrology [59] and quantum memories [60].

14.10 Bibliography

[1] P.W. Shor, *Algorithms for quantum computation: Discrete logarithms and factoring*. In the Proceedings of 35th Annual Symposium on the Foundations of Computer Science. IEEE Press, Los Alamos, 1994.

[2] S.J. Devitt, W.J. Munro and K. Nemoto, *Rep. Prog. Phys.* 76:076001, 2013.

[3] R.W. Hamming, *Bell System Technical Journal* 29:147, 1950.

[4] D.J. MacKay, *Information Theory, Inference, and Learning Algorithms*. Cambridge University Press, Cambridge, 2003.

[5] J. Roffe, *Contem. Phys.* 60:226, 2019.

[6] E. Knill and R. Laflamme, *Phys. Rev. A* 55:900, 1997.

[7] P.W. Shor, *Phys. Rev. A* 52:R2493, 1995.

[8] D. Gottesman, An Introduction to quantum error correction and fault-tolerant quantum computation. *arXiv:0904.2557v1*, 2009.

[9] B.M. Terhal, *Rev. Mod. Phys.* 87:307, 2015.

[10] S.B. Bravyi and A.Y. Kitaev, Quantum codes on a lattice with boundary. *arXiv.9811052*, 1998.

[11] M.H. Freedman and D.A. Meyer, *Found. Comput. Math.* 1:325, 2001.

[12] S.B. Bravyi and A.Y. Kitaev, *Quantum Comp. Comput.* 2:43, 2001.

[13] A.G. Fowler, M. Mariantoni, J.M. Martinis and A.N. Cleland, *Phys. Rev. A* 86:032324, 2012.

[14] S. Bravyi, M. Englbrecht, R. Konig and N. Peard, *NPJ Quant. Inf.* 4:55, 2018.

[15] A. Kitaev, *Annals Phys.* 303:2, 2003.

[16] A.G. Fowler, M. Mariantoni, J.M. Martinis and A.N. Cleland, *Phys. Rev. A* 86:032324, 2012.

[17] C. Horsman, A. Fowler, S. Devitt and R. Van Meter, *New J. Phys.* 14:123011, 2012.

[18] D. Gottesman, *Phys. Rev. A* 57:127, 1998.

[19] D. Gottesman, *Quantum Info. Comput.* 14:1338, 2014.

[20] P.W. Shor, *Fault-tolerant quantum computation*. In Proceedings of 37th Conference on Foundations of Computer Science, 1996, 55-65, doi: 10.1109/SFCS.1996.548464.

[21] A.M. Steane, *Phys. Rev. Lett.* 78:2252, 1997.

[22] A.M. Steane, *Nature* 399:124, 1999.

[23] D. Gottesman, *J. Mod. Opt.* 47:333, 2000.

[24] B.M. Terhal and G. Burkard, *Phys. Rev. A* 71:012336, 2005.

[25] D. Aharonov, A. Kitaev and J. Preskill, *Phys. Rev. Lett.* 96:050504, 2006.

[26] D.P. DiVincenzo and P. Aliferis, *Phys. Rev. Lett.* 98:020501, 2007.

[27] H.K. Ng and J. Preskill, *Phys. Rev. A* 79:032318, 2009.

[28] D. Aharonov and M. Ben-Or, *Fault-tolerant quantum computation with constant error.* In Proceedings of 29th Annual ACM Symposium on Theory of Computing, page 46, 1997.

[29] A.Y. Kitaev, *Russ. Math. Serv.* 52:1191, 1997.

[30] D. Gottesman, *Stabilizer codes and quantum error correction* arXiv.9705052, 1997.

[31] T. Metodiev, A. Cross, D. Thaker, K. Brown, D. Copsey, F.T. Chong and I.L. Chuang, *Preliminary results on simulating a scalable fault-tolerant ion trap system for quantum computation*. In the 3rd Workshop on Non-Silicon Computing (NSC-3), 2004.

[32] S. Balensiefer, L. Kregor-Stick and M. Oskin, *SIGARCH Comput. Archit. News* 33:186, 2005.

[33] T. Szkopek, P.O. Boykin, H. Fan, V.P. Roychowdhury, E. Yablonovitch, G. Simms, M. Gyure and B. Fong, *IEEE Trans. Nano.* 5:42, 2006.

[34] K.M. Svore, D.P. DiVincenzo and B.M. Terhal, *Quant. Inf. Comp.* 7:297, 2007.

[35] A. Stephens, A.G. Fowler and L.C.L. Hollenberg, *Quant. Inf. Comp.* 8:330, 2008.

[36] B. Eastin and E. Knill, *Phys. Rev. Lett.* 102:110502, 2009.

[37] S. Bravyi and A. Kitaev, *Phys. Rev. A* 71:022316, 2004.

[38] A.J. Landahl and C. Ryan-Anderson, Quantum computing by color-code lattice surgery. *arXiv:1407.5103*, 8 July 2014.

[39] T.J. Yoder, Universal fault-tolerant quantum computation with Bacon-Shor codes. *arXiv:1705.01686*, 4 May 2017.

[40] M. Vasmer and D.E. Browne, *Phys. Rev. A* 100:012312, 2019.

[41] E. Knill, R. Laflamme and L. Viola, *Phys. Rev. Lett.* 84:2525, 2000.

[42] A.R. Calderbank, E.M. Rains, P.M. Shor and N.J.A. Sloane, *IEEE Trans. Inf. Theory* 44:1369, 1998.

[43] S. Lioyd and J.J.E. Slotine, *Phys. Rev. Lett.* 80:4088, 1998.

[44] A. Steane, *Proc. Roy. Soc. A* 452:2551, 1996.

[45] C.H. Bennett, D.P. DiVincenzo, J.A. Smolin and W.K. Wootters, *Phys. Rev. A* 54:3824, 1996.

[46] A.R. Calderbank, E.M. Rains, P.W. Shor and N.J.A. Sloane, *Phys. Rev. Lett.* 78:405, 1997.

[47] S. Ball, A. Centelles and F. Huber, Quantum error-correcting codes and their geometries. *arXiv.2007.05992v1*, 2000.

[48] J. Chiaverini, D. Leibfried, T. Schaetz, M.D. Barett, R.B. Blakestad, J. Britton, W.M. Itano, J.D. Jost, E. Knill, C. Langer, R. Ozeri and D.J. Wineland, *Nature* 432:602, 2004.

[49] D.J. Cory, M.D. Price, W. Maas, E. Knill, R. Laflamme, W.H. Zuerek, T.F. Havel and S.S. Somaroo, *Phys. Rev. Lett.* 81:2152, 1998.

[50] C.Y. Lu, W.B. Gao, J. Zhang, X.Q. Zhou, T. Yang and J.W. Pan, *Proc. Natl. Acad. Sci. USA* 105:11050, 2008

[51] M.D. Reed, L.D. Carlo, S.E. Nigg, L. Sun, L. Frunzio, S.M. Girvin and R.J. Schoelkopf, *Nature* 482:382, 2012.

[52] B.A. Bell, D.A. Herrera-Marti, M.S. Tame, D. Markham, W.J. Wadsworth and J.G. Rarity, *Nat. Commun.* 5:3658, 2014.

[53] A.D. Corecoles, E. Magesan, S.J. Srinivasan, A.W. Cross, M. Steffen, J.M. Gambetta and J.M. Chow, *Nat. Commun.* 6:6979, 2015.

[54] D. Riste, S. Poletto, M.Z. Huang, A. Bruno, V. Vesterinen, O.P. Saira and L. Dicarlo, *Nat. Commun.* 6:6983, 2015.

[55] R. Chao and B.W. Reichardt, *Phys. Rev. Lett.* 121:050502, 2018.

[56] H.P. Nautrup, N. Delfosse, V. Dunjko, H.J. Briegel and N. Friis, *Quantum* 3:215, 2019.

[57] M. Reimpell and R.F. Werner, *Phys. Rev. Lett.* 94:080501, 2005.

[58] A. Ekert and C. Macchiavello, *Phys. Rev. Lett.* 77:2585, 1996.

[59] D. Layden, S. Zhou, D. Cappellaro and L. Jiang, *Phys. Rev. Lett.* 122:040502, 2019.

[60] B.M. Terhal, *Rev. Mod. Phys.* 87:307, 2015.

14.11 Exercises

14.1 Show that $\prod^N \mathrm{e}^{\mathrm{i}\epsilon\sigma_x}|0\rangle = \cos(N\epsilon)|0\rangle + \mathrm{i}\sin(N\epsilon)|1\rangle$.

14.2 Find the value of $H\sigma_I H$.

14.3 Show that phase-flip error can be changed into bit-flip error and vice-versa using Hadamard transformation.

14.4 Obtain the value of $\mathrm{Tr}(A\rho)$, where $A = (1 - P_{\mathrm{M}})|0\rangle\langle 0| + P_{\mathrm{M}}|1\rangle\langle 1|$ and $\rho = |0\rangle\langle 0|$.

14.5 Assuming the probability of a bit-flip is ϵ and independent of each other in the three bit repetition code, find the probability of not correctly decoding the information. Show that as long as $\epsilon < 1/2$, the probability of correctly decoding is more than the probability of wrong decoding.

14.6 Show that $|\psi\rangle_{\mathrm{L}}$ is not a cloning of $|\psi\rangle = \alpha|0\rangle + \beta|1\rangle$.

14.7 Draw a three stage quantum circuit for the complete implementation of the two-qubit code.

14.8 Sketch the circuit using CNOT gate for encoding $|\psi\rangle = \alpha|0\rangle + \beta|1\rangle$ to get $|\psi\rangle_{\mathrm{L}}$.

14.9 Give the quantum circuit to encode $|\psi\rangle = \alpha|0\rangle + \beta|1\rangle$ with $|\psi\rangle_{\mathrm{L}} = \alpha|000\rangle + \beta|111\rangle$ using two ancilla qubits and two CNOT gates.

14.10 If P_i and P_j are stabilizers then find whether $P_i P_j$ is also a stabilizer.

14.11 Schematically represent the general error correction procedure for a single cycle of an $[[n, k, d]]$ stabilizer code.

14.12 Set up the syndrome table for the case of single-qubit X- and Z-errors on the Shor nine-bit code.

14.13 Find the values of $[Z_1, Z_2]$, $[Z_2, Z_3]$ and $[Z_1Z_2, Z_2Z_3]$ with $|\psi\rangle_{\mathrm{L}} = \alpha|000\rangle + \beta|111\rangle$.

14.14 Give the group multiplication table for the group $\zeta_1 = \{\pm I, \pm \mathrm{i}I, \pm X, \pm \mathrm{i}X, \pm Y, \pm \mathrm{i}Y, \pm Z, \pm \mathrm{i}Z\}$.

14.15 Show that the three-bit code stabilizer $\mathcal{S} = \{Z_1Z_2, Z_2Z_3, Z_1Z_3\}$ is not a minimal set.

14.16 Give the circuit to encode a single qubit $|\psi\rangle = \alpha|0\rangle + \beta|1\rangle$ into Shor's nine qubit.

14.17 Show that in Shor's code any one flip-flop error in any of the bit can be detected by taking a majority decision on the bits and any one of the phase-flip error can be detected by taking a majority decision on the signs.

14.18 In the case of Shor's none-bit code with single-qubit errors in Z_1 and Z_2 the syndrome is 00000010 and hence the nine-bit code is degenerate. Show that this degeneracy does not reduce the code distance.

14.19 Consider the transformation $|111\rangle|000\rangle \rightarrow |111\rangle|111\rangle$. (a) Construct an actual CNOT circuit. (b) Construct a CNOT circuit where a single X-error leads to four errors so that the resulting transformation is $|011\rangle|000\rangle$. (c) Modify the circuit so that the transformation will become $|011\rangle|011\rangle$.

14.20 For the $[[4, 2, 2]]$ detection code sketch the circuit for the code state $|\psi_1\psi_2\rangle_{\mathrm{L}}$, (b) Sketch the syndrome extraction stage circuit and (c) the codes space $\mathcal{C}_{[[4,2,2]]}$ and the stabilizers $\mathcal{S}_{[[4,2,2]]}$.

Taylor & Francis
Taylor & Francis Group
http://taylorandfrancis.com

15

Some Other Advanced Topics

15.1 Introduction

In the earlier chapters, we presented basic features of certain advanced topics including supersymmetric quantum mechanics, coherent and squeezed states, Berry's phase, quantum entanglement, quantum decoherence, quantum computers, quantum cryptography and quantum cloning. There are several other topics which also received considerable interest and have a wide range of applications. In the present chapter, we consider some of them. Particularly, we give a very brief introduction to the following fascinating topics:

1. Quantum gravity.
2. Quantum cosmology.
3. Quantum Zeno effect.
4. Quantum teleportation.
5. Quantum games.
6. Quantum pseudo-telepathy games.
7. Quantum steering.
8. Quantum diffusion.
9. Quantum chaos.

There are several other interesting and important topics like quantum Hall effect, quantum dots, quantum annealing, quantum brain dynamics, quantum consciousness etc. These are not covered in this book.

15.2 Quantum Theory of Gravity

Quantum physics deals with the behaviour of microscopic objects whereas the general relativity deals with much larger bodies. Both theories have limitations in their abilities to describe the universe. At present we do not have a full theory because such a theory must be based on a single framework but such a theory is lacking. In the present forms, quantum theory and relativity cannot make predictions about certain kinds of physical phenomena. These phenomena are found to occur at extremely small distances of the order of Planck length or at very high energies – some 20 orders of magnitude far from the scales of particle accelerators.

Planck units are measurement units defined in terms of five universal constants namely, the gravitational constant ($G = 6.673 \times 10^{-11}\,\mathrm{m^3 kg^{-1} s^{-2}}$), reduced Planck constant ($\hbar = 1.055 \times 10^{-34}\,\mathrm{Js}$), speed of light ($c = 10^8\,\mathrm{m/s}$), Coulomb constant

DOI: 10.1201/9781003172192-15

$(1/(4\pi\epsilon_0) = 9 \times 10^9\,\mathrm{Nm^2C^{-2}})$ and Boltzmann's constant $(k_\mathrm{B} = 1.4 \times 10^{-23}\,\mathrm{J\Delta K^{-1}})$. In these units, Planck length $\sqrt{\hbar G/c^3} = 1.616 \times 10^{-35}\,\mathrm{m}$, Planck mass $\sqrt{\hbar c/G} = 1.2209 \times 10^{19}\,\mathrm{GeV}/c^2 = 2.17644 \times 10^{-8}\,\mathrm{kg}$, Planck time $\sqrt{\hbar G/c^5} = 5.39124 \times 10^{-44}\,\mathrm{s}$, Planck charge $\sqrt{4\pi\epsilon_0\hbar c} = 1.8755 \times 10^{-18}\,\mathrm{C}$, Planck energy $\sqrt{c^5\hbar/G} \sim 10^{19}\,\mathrm{GeV}$ and Planck temperature $\sqrt{\hbar c^5/(Gk_\mathrm{B}^2)} = 1.416785 \times 10^{32}\,\mathrm{K}$. A theory of quantum gravity is essential to describe the situations at these Planck's scales. For example, understanding the universe where it was at a time less than one Planck time $(\sim 10^{-44}\,\mathrm{s})$ old needs a theory of quantum gravity. At Planck temperature $(\sim 10^{32}\,\mathrm{K})$ all the forces of nature may be unified. At energies of the order of Planck energy the gravitational interactions are strong enough and we cannot neglect them. The theory we are looking for must unify Einstein's theory of gravity, relativity and also the quantum theory and hence is called a *quantum theory of gravity*.

Because the problems in quantum gravity are so big and very fundamental, there is generally more than one place to begin. Some of the starting points are the following:

1. Modification of quantum theory by taking account of the gravitational force.
2. Modification of quantum theory by incorporating the principles of relativity.
3. Stating the general relativity in quantum mechanical description.

There are groups of people focusing with different starting points. We now have various approaches to quantum gravity, with different names such as string theory, loop quantum gravity, twistor theory, random geometry, toposes and so on. In this section we present some basic ideas and the features of quantum gravity.

15.2.1 Three Approaches of Quantum Gravity [1]

In the following we give a compact summary of fundamental ideas of the approaches of semiclassical gravity, loop quantum gravity and string theory.

1. Semiclassical Gravity

The coupling of quantum theory and classical gravity, called *semiclassical gravity*,was proposed by Jesper Moller Grimstrup and Leon Rosenfeld in which the Einstein field equations are written as

$$G_{\mu\nu} = 8\pi G \langle\psi|T_{\mu\nu}|\psi\rangle\,. \tag{15.1}$$

Here $T_{\mu\nu}$ is an operator. The energy-valued tensor of matter $T_{\mu\nu}$ is replaced by an expectation value. This model gives rise to a nonlinear Schrödinger equation. So, the principle of superposition here fails and further it violates the basics of quantum mechanics. Therefore, to couple a quantum system to classical gravity, we need to modify either the general relativity or quantum mechanics.

In the semiclassical approach, matter is dealt with quantum mechanically and space-time is treated as per the general theory of relativity. Certain intriguing predictions are made by this approach. For example, a particle detector accelerated, say, with the acceleration g in a vacuum will behave as if it was kept in a thermal bath at temperature $hg/(2\pi c)$. According to this, a black hole appears as a hot thermodynamic system with a temperature inversely proportional to its mass and entropy.

2. Loop Quantum Gravity

In this theory, the effects of quantum gravity are not treated as excitations of a classical geometry. It predicts that measures like areas and volumes are discrete. These quantities are represented by operators and possess discrete spectra. This theory succeeds in problems

where string theory fails and vice-versa. In this sense, the loop quantum gravity is thought of as a complementary to string theory.

3. String Theory

String theory is formulated as a theory of everything with gravity and the other fundamental interactions. In this theory, gravitons are regarded as particles travelling in a fixed non-dynamical space-time. These particles scatter and interact weakly with each other. Further, they are the excitations of one-dimensional curves known as *strings* instead of point-like objects. All the other particles and forces in nature are thought of as arising from the excitations of the strings. Thus, particles such as electrons, quarks, photons correspond to modes of vibration of the string. The strings possess a characteristic length scale. Experiments at energies below Planck energy cannot resolve distances which are as small as Planck length. Thus, at such energies, strings can be approximated by point-like particles.

Five consistent string theories are known. Four of them have only closed strings forming closed loops. Of these four, two are based on unoriented strings: One has an open string and the other a closed string. Two other theories are formulated with oriented closed strings differing in internal symmetry. One of these is called *type-II string theory* and other as *heterotic string theory*. It is indeed remarkable that the spectra of the classical solutions of all the string theories have exactly one massless spin graviton. In physical theories, the number of dimensions is generally a free parameter and usually fixed to three. But string theory predicts 9 spatial dimensions. This is the only theory known so far that unifies the quantum theory and general relativity. It was realized that every string theory describes a limit of an underlying general theory called *M-theory* defined in 11 dimensions of space.

15.2.2 Pictures of the Physical World [1]

Combining the predictions of different approaches of quantum gravity we will be able to describe the physical world. This picture may not be correct, but provides a certain kind of complete picture that experimentalists may realize if they probe Planck scale. Some of the main features are the following:

1. Space, time and all physical quantities are regarded as relations between things in the world. The theory knows nothing of points in space or events in time. It knows only details of relations between things that occur.
2. The fundamental of the world is information instead of fields.
3. Quantities such as area, volume and electric charge are discrete.
4. The basic excitations are not thought of as point-like but are one or more dimensional.
5. Observable quantities are only connected with information flowing across the boundaries between the observer and the system. The theory does not predict the events happening in space-time but provides information reached by an observer.
6. There is a restriction on the quantum of information flowing across any surface in space. There will not be more bits of information than the surface area, measured in units of Planck area – $G\hbar/c^3 \approx 10^{-70}\,\mathrm{m}^2$. In other words, only one bit of information can flow across every $10^{-70}\,\mathrm{m}^2$.
7. The value of electric charge, masses of particles, etc. may vary with time.
8. Distinctions between different particles and forces are because of symmetry breaking.

TABLE 15.1
Upper limits of certain physical quantities estimated by the theory of quantum gravity.

Physical quantities	Upper limit
Cosmic ray particle energies	10^{28} eV
Elastic modulus	10^{112} dyne/cm
Density	$c^5/(G^2\hbar)$
Electric/magnetic fields strength	$c^{7/2}/(G\sqrt{\hbar}\,)$
Temperature	$\sqrt{\hbar c^5/G}\,/k_{\rm B} \sim 10^{32}$ degree
Surface tension	10^{80} dyne/cm^2

15.2.3 Implications of Quantum Gravity

There are many different approaches for quantizing gravity. A fully acceptable theory is yet to emerge. However, many implications of quantum gravity found to exist for a range of phenomena in our every day physics. Some of them are listed below [2]:

1. It has been estimated that in sun, 10^9 W of thermal gravitational radiation could be generated because of Coulomb collisions in the plasma core. The number of gravitons, $N_{\rm g}$, emitted in an explosion of energy E is $N_{\rm g} = GE^2/(\hbar c^5)$. For a 100 megaton nuclear explosion, the above predicts a dimensionless strain of 10^{-31}.
2. The life-time of a 3d-1s transition in hydrogen with the emission of graviton is

$$\frac{Gm_{\rm e}^2\omega_{\rm hyd}\alpha^4}{\hbar c} \sim 10^{35}\,{\rm s}\,, \tag{15.2}$$

   where $m_{\rm e}$ is the mass of the electron, $\omega_{\rm hyd}$ is the frequency of the 3d-1s transition and α is the fine structure constant.
3. For a gravitating body with mass m, the minimum radius into which it may collapse in a comoving frame is

$$R_{\rm min} = \left(\frac{G^3\hbar m^2}{c^7}\right)^{1/4}. \tag{15.3}$$

4. Table 15.1 gives upper limits of certain physical quantities.
5. A possible smallest time interval is $\sqrt{\hbar G/c^5} \sim 10^{-43}$ s.
6. The highest power generated or emitted by a physical system is

$$P_{\rm max} \sim \frac{c^5}{G} \sim 3 \times 10^{59}\,{\rm ergs}. \tag{15.4}$$

   That is, a universal bound on the rate of information processing is

$$f = \sqrt{P_{\rm max}/\hbar} \sim 10^{44}\,{\rm bits/s}. \tag{15.5}$$

7. It is possible to have photons with energies $\sim 10^{20}$ eV or larger.
8. Photons with a few TeV energy will be able to travel freely through the background of microwave or infrared photons.

9. String theory implies a modification of the Heisenberg's uncertainty principle. The uncertainties in the position and momentum of a string are $\Delta x \approx \sqrt{\hbar/T}$ and $\Delta p_x \approx \sqrt{\hbar T}$, where T is the string tension.
10. The energy eigenvalues of a hydrogen atom are

$$E_n = B\left[-\frac{1}{n^2} + 4\left(\frac{l_s}{a_0}\right)^2\right]\frac{\left(4n - 3\left(l + \frac{1}{2}\right)\right)}{n^4\left(l + \frac{1}{2}\right)}, \tag{15.6}$$

where l_s is the minimal length scale and a_0 is Bohr radius.

So far there is no experimental evidence for quantized gravity. If the gravitational field is not quantized then violation of the uncertainty principle will result [3].

15.2.4 Tests Proposed to Detect Quantum Gravity

The characteristic energy scale for quantum gravity is Planck energy $\sim 10^{19}$ GeV. This is so far out of the range of experiment. Hence, direct tests appear impossible. However, certain tests have been proposed.

1. Quantum gravity may lead to violation of the equivalence principle. This may be detectable in precision tests in atomic and neutron interferometry.
2. It may lead to violations of CPT invariance, for example, with the formation of virtual black holes. Present experimental techniques are greatly improving and thus such effects may be observable.
3. Quantum gravity may distort the dispersion relations over long distances for light and neutrinos. This leads to a frequency-dependent speed of light. This effect can be testable with the observations of gamma ray bursts.
4. Quantum fluctuations may be noticeable in the geometry of space with the help of a sensitive interferometer suitable for gravitational wave detection.
5. It has been suggested that the use of lasers to accelerate electrons may open the possibility to indirectly observe Unruh radiation (a black-body radiation observed by an accelerated observer) which is the counterpart of Hawking radiation for the case of an accelerating particle in flat space-time.
6. Another test is from condensed matter analogs of black holes which emit Hawking radiation phonons from sonic horizons, regions where the fluid flow attains the speed of sound.

Though these experiments open the possibility of detecting quantum gravitational effects, at present it is not at all certain that they are feasible. For more discussions on quantum gravity one may refer to refs. [4–8].

15.3 Quantum Cosmology

Both classical cosmology and quantum cosmology aim to provide answer to the fundamental question – *Where did it all come from?* Quantum cosmology is considered an application of quantum mechanics to the universe as a whole. If the universe is considered as a quantum

system then it must be described by a quantum state vector which contains all the possible information one can obtain about the universe. As we usually associate quantum mechanical wave functions to micro-systems it may seen as a paradox to associate wave function to the whole universe. But when the evolution of the universe is tracked backwards we reach a point near Planck scale, where the classical description of the universe has to be replaced by the quantum description.

15.3.1 Classical Cosmology

The classical cosmology theory is mainly based on the cosmological principle and the expansion of the universe. As the universe appears to be isotropic and homogeneous the cosmological principle says that there is no special location in the universe. As the distant galaxies are observed to be red-shifted, the universe is expanding as given by Hubble law which states that the recessional velocity is proportional to the distance of the galaxy.

Howard P. Robertson [9] and Arthur Geoffrey Walker [10] derived first independently the metric of the space-time for all isotropic homogeneous uniformly expanding model of the universe. It is given as

$$\mathrm{d}s^2 = \mathrm{d}t^2 - Q^2(t)\left[\frac{\mathrm{d}r^2}{1-kr^2} + r^2\mathrm{d}\theta^2 + r^2\sin^2\theta\mathrm{d}\phi^2\right] \tag{15.7}$$

in terms of the comoving coordinates (t, r, θ, ϕ). In fact, it is the only space-time metric which gives homogeneity and isotropy of co-moving universe. Here $Q(t)$ is the expansion factor. The curvature factor k denoting the spatial curvature of the three-space takes one of the possible three values -1, 0 or $+1$. The universe is negatively curved, flat or positively curved as $k = -1$, $k = 0$ or $k = +1$.

The metric and the curvature is determined by solving the Einstein field equations relating the geometry of space-time to the distribution of mass energy. These equations are ten coupled, nonlinear and partial differential equations. It was Alexander Alexandrovich Friedmann [11] who obtained the solutions of Einstein field equations for the line element Eq. (15.7). Einstein equations are given in tensor form as

$$G_{\mu\nu} = 8\pi G T_{\mu\nu}. \tag{15.8}$$

The Einstein tensor $G_{\mu\nu}$ is a function of the metric and its first and second space-time derivatives. $T_{\mu\nu}$ is the stress-energy tensor which represents the matter and energy distribution. G is the gravitational constant. The expanding, homogeneous and isotropic universe is described by the *Friedmann–Robertson–Walker* (FRW) line element Eq. (15.7).

In FRW universe the stress-energy tensor is taken to be that of a perfect fluid with its density $\rho(Q)$ and pressure $P(Q)$. Then the ten nonlinear equations given by Eq. (15.8) reduce to two independent equations

$$\dot{Q}^2 = \frac{8\pi G\rho}{3}Q^2 - k, \tag{15.9}$$

$$\ddot{Q} = -\frac{4\pi G}{3}(\rho + 3P)Q, \tag{15.10}$$

where natural units such as $\hbar = c = 1$ are assumed. Differentiating Eq. (15.9) with respect to t and then substituting Eq. (15.10) for $\ddot{Q}$ we obtain the continuity equation

$$\frac{\mathrm{d}\rho}{\mathrm{d}Q} = -\frac{3}{Q}(\rho + P). \tag{15.11}$$

Equations (15.9) and (15.11) are considered as the dynamical equations of big-bang cosmology [12]. To determine $Q(t)$, $\rho(Q)$ and $P(Q)$ we have only the two Eqs. (15.9) and (15.11). The third equation is given by the *matter equation of state* $P = P(\rho)$.

If we consider the configuration of the universe consisting of electromagnetic radiation and a pressureless dust then their matter equation of state may be written as

$$P(\rho) = \frac{\gamma}{3}\rho, \tag{15.12}$$

where $\gamma = 1$ for radiation and $\gamma = 0$ for dust. The solution of Eq. (15.11) after substituting Eq. (15.12) for P is

$$\rho(Q) = \rho(Q_\mathrm{i})\,(Q_\mathrm{i}/Q)^{\gamma+3}\,, \tag{15.13}$$

where Q_i is value of Q at an arbitrary reference time t_i. Next, substituting Eqs. (15.12) and (15.13) in Eqs. (15.9) and (15.10), we obtain

$$\dot{Q}^2 = \frac{C_1}{Q^{\gamma+1}} - k, \quad C_1 = \frac{8\pi G}{3}\rho(Q_\mathrm{i})Q_\mathrm{i}^{\gamma+3}, \tag{15.14a}$$

$$\ddot{Q} = -\frac{C_2}{Q^{\gamma+2}}, \quad C_2 = \frac{4\pi G}{3}(1+\gamma)\rho(Q_\mathrm{i})Q_\mathrm{i}^{\gamma+3}. \tag{15.14b}$$

Equations (15.14) give the time evolution of FRW universe. We consider the solution of Eqs. (15.14) in sec. 15.3.3. Before that now we draw some useful information from Eqs. (15.14) [12]. As Q is the scale factor Eq. (15.14b) gives the deceleration of the universal expansion and is independent of the value of k. For $k = -1$ $\dot{Q}$ is always greater than zero. Hence, for the negatively curved universe ($k = -1$) the universe expands forever. For the flat universe ($k = 0$) we have $\dot{Q} \to 0$ only when $Q \to \infty$. So, the universe expands eternally. For the spherically closed universe ($k = 1$) $\dot{Q}$ will become zero at one stage and the universe will start collapsing.

15.3.2 Big-Bang Model

Friedmann showed in 1922 that the equations of general relativity allow an expanding solution that starts from a singularity. George Antonovich Gamow and his collaborators Ralph Asher Alpher and Robert Herman proposed the Big-Bang model of the universe to account for the abundances of the elements. They proposed that the early universe was once very hot and dense so as to allow for the nucleosynthetic processing of hydrogen. There after it has expanded and cooled to its present state [13,14].

The observation of 3 K background radiation and the relative abundance of elements as predicted by the Big-Bang model confirmed that this model is the most suitable model to describe our universe.

Though the Big-Bang theory described the early universe fairly well, it could not explain two important facts of the present universe. It was not able to explain the homogeneous and isotropic nature of the universe over astronomically large distances and also it could not explain how the structures like the galaxies, stars and planets were formed. Also, the standard Big-Bang theory leads to the horizon and flatness problems [15].

15.3.3 Theory of Cosmic Inflation

To overcome the problems faced by the classical Big-Bang theory Alexei Alexandrovich Starobinsky [16], Alan Harvey Guth [17] and Andrei Dmitriyevich Linde [18,19] developed a theory of cosmic inflation. Inflation, defined as a period of accelerating expansion in

the early universe, is now considered as a reasonable explanation for many cosmological problems. Cosmic inflation is based on the hypothesis that the early universe underwent an extremely rapid expansion. It explains successfully how quantum mechanical fluctuations of the vacuum starting about 10^{-36} seconds after the Big-Bang could have given rise to the large-scale structure of the universe we observe today. The simplest possible inflationary cosmological model is based on the concept of the spontaneous birth from nothing of an empty closed universe via quantum tunnelling [17,20].

Now, consider Eq. (15.14a). As $k = 1$ for a closed universe and the equation of state for vacuum is $P = -\rho_{\text{vac}}$ the Einstein Eq. (15.9) with the cosmological term $\Lambda = 8\pi G\rho_{\text{vac}}$ gives

$$\dot{Q}^2 + \left(1 - (\Lambda/3)Q^2\right) = 0. \tag{15.15}$$

If $\rho(Q)$ is constant or slowly varying then the universe expands exponentially as given by the solution of Eq. (15.15)

$$Q(t) = Q_0 \cosh\left(t/Q_0\right), \quad Q_0 = \sqrt{3/\Lambda}\,. \tag{15.16}$$

This is the Guth's inflationary epoch in which the universe expands rapidly when the universe is about 10^{-34} sec for a period of 10^{-30} sec. In that short duration the universe expands by a factor of roughly 10^{50} [12].

Inflation in the early universe is now accepted as addressing many cosmological problems. For inflation to occur initially the universe must contain some matter in highly excited state. Inflation theory does not explain why the matter was in such an excited state. Two theories trying to address the pre-inflationary initial conditions are: (i) the chaotic inflation theory proposed by Linde [18,19] and (ii) quantum cosmology. According to chaotic inflation the universe starts-off in a completely random state. Due to the random nature of the state there may be regions of matter more energetic than other and hence inflation could produce the present universe.

The possibility of the creation of the universe from nothing, where nothing means the absence of classical space and time, led to two important proposals for such boundary conditions. The first is the *no-boundary* proposal of James Burkett Hartle and Stephen William Hawking path integral method [21] and the second is the tunnelling proposal advocated by Alexander Vilenkin [22] using canonical quantization method.

15.3.4 Wheeler-De Witt Equation

Quantum cosmology depends on the calculation of the quantum state of the universe as a whole. Such a quantum state must be represented by a wave function. Using this wave function one hopes to make predictions about the outcome of comological observations. Using a combination of path integral and canonical methods an equation analogous to the Schrödinger equation called the *Wheeler-De Witt (WD) equation* was derived [23,24].

We consider the action of interacting gravitational and scalar fields

$$S = \int \left[\left(\frac{\mathcal{R}}{16\pi G}\right) + \frac{1}{2}\left(\partial_\mu \phi\right)^2 - V(\phi)\sqrt{-g}\right] \mathrm{d}^4 x, \tag{15.17}$$

where the metric and scalar field ϕ are considered to be homogeneous and isotropic and $Q(t)$ is the scale factor. Due to these constraints we have only two degrees of freedom $Q(t)$ and $\phi(t)$. For the nonzero tunnelling probability of the formation of the universe the universe

must be closed ($k = 1$). Hence, for FRW universe Eq. (15.7) gives the metric tensor

$$g_{\mu\nu} = \begin{bmatrix} 1 & 0 & 0 & 0 \\ 0 & -\dfrac{Q^2}{1-r^2} & 0 & 0 \\ 0 & 0 & -Q^2 r^2 & 0 \\ 0 & 0 & 0 & -Q^2 r^2 \sin^2\theta \end{bmatrix}. \tag{15.18}$$

Therefore, we get

$$\det g_{\mu\nu} = \sqrt{-g} = \frac{Q^3 r^2 \sin\theta}{\sqrt{1-r^2}}. \tag{15.19}$$

The Ricci scalar $\mathcal{R}$ is given by

$$\mathcal{R} = 6\left(1 + \dot{Q}^2 + Q\ddot{Q}\right)/Q^2. \tag{15.20}$$

Using $\mathrm{d}^4x = \mathrm{d}r\mathrm{d}\theta\mathrm{d}\phi\mathrm{d}t$ we can write Eq. (15.17) as

$$S = \int L(Q, \dot{Q}, \phi, \dot{\phi})\mathrm{d}t, \tag{15.21}$$

where the Lagrangian L is given by

$$L = \frac{3\pi}{4G}\left(1 - \dot{Q}^2\right)Q + \pi^2 Q^3\dot{\phi}^2 - 2\pi^2 Q^3 V(\phi). \tag{15.22}$$

The generalized momenta are

$$P_Q = \frac{\partial L}{\partial \dot{Q}}, \quad P_\phi = \frac{\partial L}{\partial \dot{\phi}}. \tag{15.23}$$

Then the Hamiltonian H from L is obtained as

$$\begin{aligned} H &= P_Q\dot{Q} + P_\phi\dot{\phi} - L \\ &= -\frac{G}{3\pi Q}P_Q^2 + \frac{1}{4\pi^2 Q^3}P_\phi^2 - \frac{3\pi}{4G}Q\left[1 - \frac{8\pi G}{3}Q^2 V(\phi)\right]. \end{aligned} \tag{15.24}$$

So, we get the WD equation $H\psi = 0$, where H is the Hamiltonian operator and ψ is the wave function of the universe. We may write [25]

$$P_Q^2 = \frac{1}{Q^p}\frac{\partial}{\partial Q}\left[Q^p\frac{\partial}{\partial Q}\right] = \frac{\partial^2}{\partial Q^2} + \frac{p}{Q}\frac{\partial}{\partial Q}, \tag{15.25a}$$

$$P_\phi^2 = \frac{1}{\phi^q}\frac{\partial}{\partial \phi}\left[\phi^q\frac{\partial}{\partial \phi}\right] = \frac{\partial^2}{\partial \phi^2} + \frac{q}{\phi}\frac{\partial}{\partial \phi}, \tag{15.25b}$$

where p and q are two arbitrary positive integers. For the choice $p = 1$ and $q = 0$

$$P_Q^2 = \frac{\partial^2}{\partial Q^2} + \frac{1}{Q}\frac{\partial}{\partial Q}, \quad P_\phi^2 = \frac{\partial^2}{\partial \phi^2}. \tag{15.26}$$

In the above we have the ambiquity, namely, the factor ordering of the quantum operators. For the choice $p = 0$ and $q = 0$

$$P_Q^2 = \frac{\partial^2}{\partial Q^2}, \quad P_\phi^2 = \frac{\partial^2}{\partial \phi^2}. \tag{15.27}$$

Then the WD equation $H\psi = 0$ becomes

$$\left[\frac{\partial^2}{\partial Q^2} - \frac{1}{Q^2}\frac{\partial^2}{\partial \tilde{\phi}^2} - U(Q,\phi)\right]\psi(Q,\phi) = 0, \tag{15.28}$$

where $\tilde{\phi}^2 = 4\pi G\phi^2/3$ and U is the super potential given by

$$U(Q,\phi) = \left(\frac{3\pi}{2G}\right)^2 Q^2\left(1 - \frac{8\pi G}{3}Q^2V(\phi)\right). \tag{15.29}$$

As the wave function is a function of two variables Q and ϕ with $0 \leq Q < \infty$, $-\infty < \phi < \infty$ the superspace is reduced to a two-dimensional manifold called *mini-superspace*.

The two regions $U(Q,\phi) > 0$ and $U(Q,\phi) < 0$ are called *Euclidean* and *Lorentzian* regions, respectivley. The boundary between the two regions ($U(Q,\phi) = 0$) is given by

$$Q_{\mathrm{B}}^2 = \frac{3}{8\pi GV(\phi)}. \tag{15.30}$$

The Euclidean region behaves like a classically forbidden region with its wave function being exponential and the Lorentzian region behaves like the classically allowed region with its wave function being oscillatory. So, the quantum mechanical tunnelling occurs from the line $Q = 0$ (nothing – no classical space-time) through the classically forbidden region into the classically allowed region. The region $Q \geq Q_{\mathrm{B}}$ is the classically allowed region of the FRW metric universe. Hence, $Q = 0$ is separated from the classically allowed region by a potential barrier. Then using the semi-classical WKB approximation the tunnelling probability of the creation of our universe can be obtained as

$$P \approx \mathrm{e}^{-2\int_0^{Q_{\mathrm{B}}}[U(Q,\phi)]^{1/2}\mathrm{d}Q}. \tag{15.31}$$

The WD equation can be solved only for very simple models.

Solved Problem 1:

If

$$S = \frac{3\pi}{4G}\int\left[-\dot{Q}^2Q + Q\left(1 - \frac{Q^2}{Q_{\mathrm{B}}^2}\right)\right]\mathrm{d}t \tag{15.32}$$

for a closed FRW universe find the WD equation and hence the probability of formation of the universe.

As $S = \int L\mathrm{d}t$ we have

$$L = \frac{3\pi}{4G}\left[-\dot{Q}^2Q + Q\left(1 - \frac{Q^2}{Q_{\mathrm{B}}^2}\right)\right]. \tag{15.33}$$

Then

$$P_Q = \frac{\partial L}{\partial \dot{Q}} = -\frac{3\pi}{2G}\dot{Q}Q. \tag{15.34}$$

That is,

$$\dot{Q} = -\frac{2G}{3\pi Q}P_Q. \tag{15.35}$$

The Hamiltonian is

$$H(Q,P_Q)=P_Q\dot{Q}-L=P_Q\dot{Q}-\frac{3\pi}{4G}\left[-\dot{Q}^2Q+Q\left(1-\frac{Q^2}{Q_{\rm B}^2}\right)\right]. \tag{15.36}$$

Substitution of (15.35) in (15.36) gives

$$H(Q,P_Q)=P_Q^2+\left(\frac{3\pi}{2G}\right)^2Q^2\left(1-\frac{Q^2}{Q_{\rm B}^2}\right). \tag{15.37}$$

Then using Eqs. (15.26) the WD equation $H\psi=0$ becomes

$$\left[\frac{\partial^2}{\partial Q^2}-\left(\frac{3\pi}{2G}\right)^2Q^2\left(1-\frac{Q^2}{Q_{\rm B}^2}\right)\right]\psi=0. \tag{15.38}$$

We find the potential as

$$U(Q)=\left(\frac{3\pi}{2G}\right)^2Q^2\left(1-\frac{Q^2}{Q_{\rm B}^2}\right). \tag{15.39}$$

Using this U in Eq. (15.31), we obtain

$$P\approx {\rm e}^{-\frac{3\pi}{G}\int_0^{Q_{\rm B}}Q\left(1-\frac{Q^2}{Q_{\rm B}^2}\right)^{1/2}{\rm d}Q}\approx {\rm e}^{-\pi Q_{\rm B}^2/G}. \tag{15.40}$$

15.3.5 Conceptual Problems in Quantum Cosmology

Quantum cosmology is more speculative as we do not have a fully self-consistent theory of quantum gravity. Quantum cosmology gives the wave function of the universe which cannot be interpretted physically. ψ depends only on metric variable Q and the scalar potential ϕ. It is independent of time. Therefore, time itself has to be defined interms of Q and ϕ. No such definition for time has been found yet. The second serious problem is that the probability defined using ψ is not positive definite as in the case of Klein–Gordon equation. These problems are overcome only by the semiclassical approximations. Otherwise time and probability cannot be defined and consequently no measurement can be done at all. So, an observational test of quantum cosmology has to be developed to understand the complete picture of the universe. The review article [26] can be referred for more information on conceptual problems in quantum gravity and quantum cosmology.

15.4 Quantum Zeno Effect

The effect of a measurement on a quantum state is usually described by the projection postulate of von Neumann and Gerhart Lüders. According to this, depending on the result of a measurement, the wave function of the system is projected onto the eigenspaces of the observable. This is also called *collapse of the wave function* in a measurement. Before a measurement, the wave function is a superposition of all states − an arbitrary quantum state. At the time of measurement it collapses into a particular state. Baidyanaith Misra and Ennackal Chandy George Sudarshan raised the question: *What would happen if we observe the system all the time?* With some reasonable assumptions, they have investigated the

influence of rapidly repeating measurements at times Δt apart on a system [27]. They found a slow down of time development of the system in the limit $\Delta t \to 0$, called the *quantum Zeno paradox* as it is reminiscent of Zeno's *arrow paradox*. The quantum Zeno effect refers to a freezing of a quantum state. Even a system with high energy and highly unstable will remain in the same initial state, as long as it is observed, like an unmoved rabbit when a bright light is shined on its eyes.

Zeno of Elea (490 BC–425 BC) was a pre-Socretic Greek philosopher of southern Italy. He formulated many paradoxes to show that *all is one*. His most famous paradoxes are Achilles (the legendary Greek warrior) and the tortoise and the arrow paradox. In a race, the quickest runner cannot overtake the slowest, because the pursuer must first reach the point whence the pursued started (ahead), so that the slower must always have a lead. If a tortoise will be allowed to start from a point ahead of Achilles then the tortoise when running will not be overtaken by Achilles. To overtake the tortoise, Achilles first must reach the point from which the tortoise started. Then by that time the tortoise will have moved a distance. That is, the tortoise must always be some distance ahead of Achilles. The arrow paradox is that if everything when it occupies an equal space is at rest, and if that which is in locomotion is always occupying such a space at any time, the flying arrow is thus motionless. Consider an arrow in motion. Suppose we divide the time into a number of indivisible instants. Then at any given instant if we see the arrow it has an exact position. It is thus not moving. Therefore, if we continuously observe the arrow then it is at rest all the time.

15.4.1 Theoretical Consideration

Consider a quantum system Q with its states belonging to the Hilbert space $\mathcal{H}$. The evolution of it is described by the unitary operator $U(t) = \mathrm{e}^{-\mathrm{i}Ht/\hbar}$, where H is the Hamiltonian. Let E be a projection operator such that $E\mathcal{H}E = \mathcal{H}_E$, where $\mathcal{H}_E$ is the subspace spanned by its eigenstates. The initial density matrix $\rho(0)$ of Q belongs to $\mathcal{H}_E$. For an undisturbed evolution at time T

$$\rho(T) = U(T)\rho(0)U^\dagger(T)\,. \tag{15.41}$$

The probability $P(T)$ for Q to be in $\mathcal{H}_E$ at T is

$$P(T) = \mathrm{Tr}\left[U(T)\rho(0)U^\dagger(T)E\right]\,. \tag{15.42}$$

$P(T)$ is called *survival probability* and is < 1.

By definition

$$\rho(0) = E\rho(0)E\,, \quad \mathrm{Tr}[\rho(0)E] = 1\,. \tag{15.43}$$

When a measurement is made at t then $\rho(t)$ becomes

$$\rho(t) = EU(t)\rho(0)U^\dagger(t)E\,. \tag{15.44}$$

Now,

$$P(T) = \mathrm{Tr}\left[U(t)\rho(0)U^\dagger(t)E\right]\,. \tag{15.45}$$

Suppose we carry out a series of observations at $t_n = nT/N$, $n = 1, 2, \ldots, N$. After N measurements the state of Q is given by

$$\rho^{(N)}(T) = V_N(T)\rho(0)V_N^\dagger(T)\,, \quad V_N(T) = [EU(T/N)E]^N \tag{15.46}$$

and

$$P^{(N)}(T) = \mathrm{Tr}\left[V_N(T)\rho(0)V_N^\dagger(T)\right]\,. \tag{15.47}$$

Define

$$\nu(T) = \lim_{N\to\infty} V_N(T)\,. \tag{15.48}$$

Then in the limit of $N \to \infty$ (continuous observation)

$$\dot{\rho}_f(T) = \nu(T)\rho(0)\nu^\dagger(T) \tag{15.49}$$

and

$$P_f(T) = \lim_{N\to\infty} P^{(N)}(T) = \mathrm{Tr}\left[\nu(T)\rho(0)\nu^\dagger(T)\right]\,. \tag{15.50}$$

Misra and Sudarshan assumed that $\lim_{t\to 0}\nu(t) = E$ and proved that $\nu(T)$ exists for all real T and $\nu^\dagger(T) = \nu(-T)$ so that $\nu^\dagger\nu = E$. Then by Eq. (15.43)

$$\rho_f(T) = \mathrm{Tr}\left[\rho(0)\nu^\dagger\nu\right] = \mathrm{Tr}\left[\rho(0)E\right] = 1\,. \tag{15.51}$$

The significant implication is that if the system is continuously observed then it will never undergo a transition to $\mathcal{H} - \mathcal{H}_E$. In other words, continuous observation of a time-independent projection operator prevents a change of state. Thus, an unstable quantum state that is observed continuously is never found to decay or a *watched pot never boils* [28] or a *watched clock does not move*. This is the *quantum Zeno paradox*. By repeating the same measurement considerably large number of times in a finite time the system can be arrested in its initial state. The paradoxial point[1] is that the system is found to have its decay influenced by the presence of a measuring device. The Zeno paradox differs from the two other famous paradoxes: the Schrödinger cat and the EPR. Those two are paradoxes of interpretation. The Zeno paradox is a prediction and can be tested.

15.4.2 Quantum Zeno Effect in a Neutron Spin System

Consider the evolution of the neutron spin subjected to a magnetic field [30]. The interaction of a neutron with a static field B is given by $H = \mu B\sigma_1$, where μ is the magnetic moment of the neutron and σ_i, $i = 1, 2, 3$ are the Pauli matrices. Denote the spin states of neutron along the z-axis as $|\uparrow\rangle$ and $|\downarrow\rangle$. Assume the initial state of neutron as $\rho(0) = \rho_{\uparrow\uparrow} = |\uparrow\rangle\langle\uparrow|$. $\rho^{(N)}$ is then obtained as [30]

$$\rho^{(N)}(T) = \left[\cos^2\left(\frac{\pi}{2N}\right)\right]^N \rho_{\uparrow\uparrow}\,. \tag{15.52}$$

Further,

$$P_\uparrow^{(N)}(T) = \left[\cos^2\left(\frac{\pi}{2N}\right)\right]^N\,. \tag{15.53}$$

This is the survival probability − the probability that neutron spin is in $|\uparrow\rangle$ state at every measurement time t_n. We note that $P_\uparrow^{(N)}(T) > P_\uparrow^{(N-1)}(T)$ for $N \geq 2$. As N increases the evolution is slowed down. In the limit $N \to \infty$

$$P_f(T) = \lim_{N\to\infty} P_\uparrow^{(N)}(T) = 1\,. \tag{15.54}$$

The significant effect of frequent observations is to *freeze* the system in its initial state, by delaying (for $N \geq 2$) and hindering (for $N \to \infty$) transitions to other states. *What is the essence of the quantum Zeno effect?* The essential point is that when the number

[1] In the words of John Gribbin [29]: *If, as quantum theory suggests, the world only exists because it is being observed, then it is also true that the world only changes because it is not being observed all the time.*

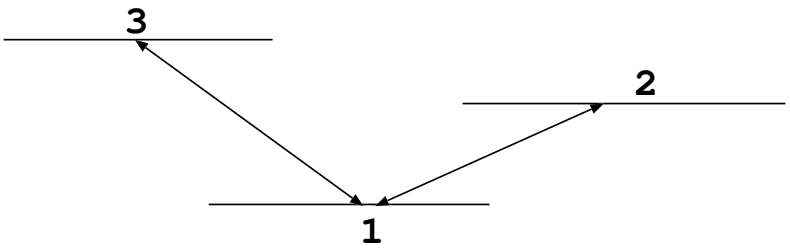

FIGURE 15.1
Energy level diagram for Cook's proposal.

of measurements is *finite* the decay rate is slowed and we have the *quantum Zeno effect*. When the number of measurements becomes *infinite* the transition is completely frozen and the result is the *quantum Zeno paradox*. The quantum Zeno effect was shown theoretically about three decades ago. However, interest on it was renewed by the idea of Cook [31] and its subsequent experimental verification.

15.4.3 Experimental Verification

Richard J. Cook [31] proposed an experiment on a trapped ion to test the quantum Zeno effect on induced transitions. Suppose the ion has three levels as shown in Fig. 15.1. Level-1 is the ground state. Level-2 is an excited metastable state. Cook's suggestion was to drive $1 \to 2$ transition with a π-pulse (a square-pulse of duration $T = \pi/\Omega$) while simultaneously applying a sequence of short measurement pulses. Suppose the ion is in level-1 at time $t = 0$. The π-pulse is applied at $t = nT/N = n\pi/(N\Omega)$, where $n = 1, 2, \ldots, N$.

In the rotating wave approximation the evolution equations for the density matrix ρ_{ij}, $i, j = 1, 2$ are given by

$$\dot{\rho}_{11} = \frac{1}{2}\mathrm{i}\Omega\left(\rho_{21} - \rho_{12}\right), \quad \dot{\rho}_{12} = \frac{1}{2}\mathrm{i}\Omega\left(\rho_{22} - \rho_{11}\right), \tag{15.55a}$$

$$\dot{\rho}_{22} = \frac{1}{2}\mathrm{i}\Omega\left(\rho_{12} - \rho_{21}\right). \tag{15.55b}$$

Define

$$R_1 = \rho_{12} + \rho_{21}, \quad R_2 = \mathrm{i}\left(\rho_{12} - \rho_{21}\right), \quad R_3 = \rho_{22} - \rho_{11} = P_2 - P_1 \tag{15.56}$$

with $P_1 + P_2 = 1$. In terms of $\mathbf{R} = (R_1, R_2, R_3)$ and $\Omega = (\Omega, 0, 0)$ Eqs. (15.55) become $\dot{\mathbf{R}} = \Omega \times \mathbf{R}$. At $t = 0$ we have $\mathbf{R} = (0, 0, -1)$. The applied pulse induces transition from level 1 to 3. Subsequently, a spontaneous emission of a photon happens. The measurement pulse projects the system into level-1 or level-2. The measurement kills the terms ρ_{12} and ρ_{21} and leave ρ_{11} and ρ_{22} as such. Now, $\mathbf{R}$ becomes

$$\mathbf{R} = \left[0, \sin\left(\frac{\pi}{N}\right), -\cos\left(\frac{\pi}{N}\right)\right]. \tag{15.57}$$

Setting $R_2 = 0$ gives $\mathbf{R} = [0, 0, -\cos(\pi/N)]$. At $t = \pi/(N\Omega)$, $\mathbf{R}$ is the same at $t = 0$, however, the magnitude of it is reduced by a factor of $\cos(\pi/N)$. After the first measurement, $\mathbf{R}^{(1)}$ is given by

$$\mathbf{R}^{(1)} = -\cos\left(\frac{\pi}{N}\right) = P_2^{(1)} - P_1^{(1)}, \tag{15.58}$$

where $P_j^{(1)}$ is the occupation probability of level-j $(j = 1, 2)$ at time $t = \pi/(N\Omega)$ [32]. We have

$$P_2^{(1)} = \frac{1}{2}\left(1 + R_3^{(1)}\right) = \sin^2\left(\frac{\pi}{2N}\right), P_1^{(1)} = 1 - P_2^{(1)} = \cos^2\left(\frac{\pi}{2N}\right). \tag{15.59}$$

The survival probability, namely, the probability of finding the system in level-1 both in the first and second measurements is given by

$$P_1^{(1,2)} = \cos^2\left(\frac{\pi}{2N}\right)\cos^2\left(\frac{\pi}{2N}\right) = \cos^4\left(\frac{\pi}{2N}\right). \tag{15.60}$$

The survival probability after N measurements is

$$P_1^{(N)}(T) = \cos^{2N}\left(\frac{\pi}{2N}\right), \quad P_2^{(N)}(T) = 1 - P_1^{(N)}(T). \tag{15.61}$$

Cook considered a slight variance of the quantum Zeno effect of Misra and Sudarshan with

$$\dot{P}_1 = \frac{\Omega\pi}{2N}(P_2 - P_1), \quad \dot{P}_2 = \frac{\Omega\pi}{2N}(P_1 - P_2). \tag{15.62}$$

From this set of equations we have [31]

$$P_2(T) = \frac{1}{2}\left[1 - \mathrm{e}^{-\pi^2/(2N)}\right]. \tag{15.63}$$

$P_2(T)$ is the occupation probability of level-2 with the transitions $1 \to 2 \to 1$ and so on. Note that P_2 given by Eq. (15.63) is not the one given by Eq. (15.61).

Itano and his coworkers [33] did an experiment with $^9Be^+$, similar to the one proposed by Cook [31]. The time development was given by a π-pulse tuned to the $1 - 2$ transition frequency. A π-pulse (a radio frequency (RF) pulse) transformed the initial state $|1\rangle$ into $|2\rangle$ at the end of the pulse, provided there was no measurement. The population of lower level was measured nonselectively and also without recording the results in rapid succession by the fluorescence induced by very short pulses of laser which coupled level-1 with the level-3. The population at time T was measured by a final pulse and recorded. The experimental result was found to be in good agreement with prediction of the quantum Zeno effect. The P_2 calculated for $N = 1, 2, 4, 8, 16, 32$ are $0.995, 0.5, 0.335, 0.194, 0.103, 0.013$, respectively. These values are in agreement with (15.63).

15.4.4 Further Development on Zeno Effect

The quantum Zeno effect has been shown theoretically for two states wave functions like spin particles [34], right- and left-isomers [35], two-state model of the localized Born–Oppenheimer states [36], multi-level system [37], a system of particles with spin-1/2 interacting with a magnetic field [38], quantum version of an inverted pendulum [39], neutron spin [40], Raman scattering [40] and models of trapped ions [41]. Experimental verification of quantum Zeno effect has been done with the system of $^{172}Yb^+$ ion [42] and $^{171}Yb^+$ ion [43], in an optical pumping [44], systems with forced Rabi oscillations between discrete atomic levels [33] and spontaneously decaying systems [45]. Stochastic quantum Zeno [46] and quantum Zeno effect in the strong measurement regime of circuit quantum electrodynamics [47] were reported. It was predicted that there are regimes in which repeated measurements can accelerate transitions [48–53] and this phenomenon was found experimentally [45] as well. This effect is known as *anti-Zeno effect* or *anti-Zeno paradox* or *inverse Zeno effect*.

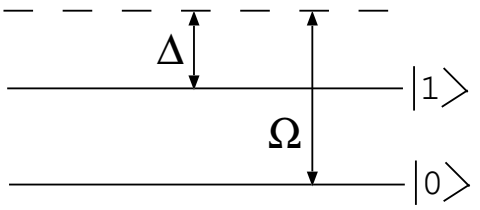

FIGURE 15.2
A two-level system.

Specifically, the quantum Zeno and anti-Zeno paradoxes arise due to infinitely frequent measurements of time-independent and time-dependent projection operators, respectively. It is shown that the transition from coherent to incoherent fluorescence energy transfer can be regarded as a demonstration of quantum Zeno or anti-Zeno effect [54].

Some applications of quantum Zeno effect are suggested, Numerical simulation of a new method of quantum Zeno tomography in which a Mach–Zehnder interferometer is adopted to measure transmissivity of gray samples was considered [55]. In contrast to standard tomography, considerable reduction of false reproduced points is demonstrated. A possible construction of photon-phonon interferometer is suggested, where interference between an optical mode in a cavity and one-dimensional vibration phonon mode of an ion trapped in the same cavity takes place [56]. Its inner degrees of freedom are removed with the application of Zeno effect by freezing the ion in its initial state. The effect has explained the suppression of the conversion decay of an isomer of uranium-235 in the lattice of silver [57].

The occurrence of quantum Zeno effect does not depend on whether information is taken from the measurements or not. Therefore, decoherence processes, such as optical pumping and coupling to stochastic external fields can result in the quantum Zeno effect. This also points out that there exists a classical counterpart. Quantum Zeno effect has been found in wave or oscillatory systems [58] and optical fibers [59]. The quantum Zeno effect is found to vanish at all orders in $\hbar$, when $\hbar \to 0$. This implies that it is a quantum phenomenon without a classical analog [60].

Quantum Zeno effect is important in understanding quantum theory of measurement and is in fact a vital tool in quantum computing. Due to decoherence, storing a quantum state for a long time is impossible. Quantum Zeno effect may be utilized to store a quantum state as long as we wish. For a detailed discussion on mathematical and physical aspects of Zeno dynamics one may refer to ref. [61].

15.4.5 Anti-Zeno Effect

Alfred Luis demonstrated the anti-Zeno effect in a two-level system (Fig. 15.2) with the Hamiltonian [62]

$$H = \hbar\Delta|0\rangle\langle 0| + \frac{\hbar\Omega}{2}\left(|0\rangle\langle 1| + |1\rangle\langle 0|\right). \tag{15.64}$$

Here Δ is the detuning and Ω is the coupling constant of the term stimulating the level transitions (refer Fig. 15.2). H given by Eq. (15.64) can represent a two-level atomic system subjected to a classical monochromatic electromagnetic wave with frequency ω. If ω_0 is the resonant frequency of the atom then $\Delta = \omega - \omega_0$.

Assume that the state of the system at $t = 0$ is $|1\rangle$. Then $P(t)$, the probability for the system to be in the state $|1\rangle$ is

$$P(t) = 1 - \frac{\Omega^2}{\Omega^2 + \Delta^2} \sin\left(\sqrt{\Omega^2 + \Delta^2}\, t/2\right). \tag{15.65}$$

Because $P(t)$ is rapidly oscillating we consider the time average of $P(t)$ over a time interval T with $\sqrt{\Omega^2 + \Delta^2}\, T \gg 1$ and denote it as $\bar{P}$. We obtain

$$\bar{P} = \frac{1}{T} \int_{t-(T/2)}^{t+(T/2)} P(t')\mathrm{d}t' = 1 - \frac{1}{2} \frac{\Omega^2}{\Omega^2 + \Delta^2}. \tag{15.66}$$

When $\Delta \gg \Omega$ we have $\bar{P} \approx 1$ and the system is always close to $|1\rangle$.

Suppose measurement is performed at $t = n\tau$. *What is the probability* $p(n)$ *for observing the system in the initial state* ($|1\rangle$) *in all the first* n *measurements?* It is given by $p(n) = (P(\tau))^n$. For $\sqrt{\Omega^2 + \Delta^2}\, \tau \ll 1$

$$p(n) \approx \mathrm{e}^{-n\Omega^2\tau^2/4} = \mathrm{e}^{-\Omega^2 t\tau/4}. \tag{15.67}$$

$p(n)$ is independent of Δ. In the limit of $\tau \to 0$, we have $p(n) \approx 1$ and it refers to the Zeno effect and is the case for $t \ll 1/(\Omega^2\tau)$. If the observations are made with finite τ during a period of time exceeding the short-time condition, that is the long-time regime $t \gg 1/(\Omega^2\tau)$ then $p(n) \approx 0$ and $|1\rangle \to |0\rangle$ will occur with certainty. This is the *anti-Zeno effect*.

15.5 Quantum Teleportation

Classically, transport of an object is to transport all the particles of it. An object to be teleported can be characterized by its properties. These properties can be determined by measurement in classical physics. Scanned information is useful for reconstructing the object and notably the original parts of the object are not needed. But a fundamental question is *what is the case if an object is a quantum state? What does happen to the quantum properties of the system, that are not measurable with desired accuracy due to Heisenberg's uncertainty principle?*

Reconstructing the quantum state of a system on another system of the same type at a distant place is termed as *quantum teleportation*. The point is that the quantum state of the system to be teleported is unknown and in fact we cannot find it. Therefore, quantum teleportation is the transmission and reconstruction of an unknown quantum state of a system over arbitrary distances. Essentially, in quantum teleportation the system is not to be teleported but only its state is to be teleported to another system of same kind. In quantum teleportation the original state is destroyed and an exact copy of the quantum state is produced. In the case of fax copy, the original is preserved and only a partial copy is made. The quantum teleportation was first discussed by Yakir Aharonov and David Z. Albert using the method of nonlocal measurements [63].

15.5.1 A Three Stage Scheme

Charles H. Bennett and his co-workers [64] have pointed out that the quantum state of a particle can be transferred to another particle provided one does not get any information about the state during the course of transportation. The above can be realized by using entanglement. The scheme of Bennett et al consists of essentially three stages:

1. An EPR source of entangled particles is prepared. Sender and receiver share each particle from a pair emitted by the source.
2. Sender performs a Bell-operator measurement on his EPR and the teleportation-target particles.
3. Sender transmits the result of the measurement to the receiver through a classical channel. Then the receiver performs a suitable unitary operation on the EPR particle.

Let us describe the above three stages scheme in detail. Suppose Alice (sender) has two two-level particles, say, particle-1 and particle-2. A two-level quantum system is a *qubit*. Bob (receiver) who is at a distant location has a particle, say, particle-3. The two states of a particle are labelled as $|0\rangle$ and $|1\rangle$. The superposition state is $|\psi\rangle = a|0\rangle + b|1\rangle$, $|a|^2 + |b|^2 = 1$. Alice wants Bob, to have the particle-3 with the state of the particle-1. Since properties of quantum systems cannot be fully obtained by measurements Alice is unable to provide required information of the particle-1 to Bob by carrying out the measurements on it.

The joint state of particles 2 and 3 is, for example,

$$|\psi\rangle_{\mathrm{AB}} = \frac{1}{\sqrt{2}}\Big(|0\rangle_{\mathrm{A}}|0\rangle_{\mathrm{B}} + |1\rangle_{\mathrm{A}}|1\rangle_{\mathrm{B}}\Big)\,. \tag{15.68}$$

This state is *entangled* because it is not possible to write it as a product of the individual states, like $|00\rangle$. $|\psi\rangle_{\mathrm{AB}}$ gives no information about the individual particles but points out that the particles 2 and 3 are in same states. *What is the feature of the above entangled state?* A measurement on, say, particle-2 gives the state of the particle-3 and vice-versa.

Suppose the state of the particle-1 is labelled as $|\phi\rangle = a|0\rangle + b|1\rangle$ with the unknown a and b: $|\phi\rangle$ is to be teleported to Bob. Now, the total state of the three particles is

$$|\phi\rangle_{\mathrm{AB}} := |\phi\rangle|\psi\rangle_{\mathrm{AB}} = \frac{1}{\sqrt{2}}\left(a|0\rangle + b|1\rangle\right)\left(|00\rangle + |11\rangle\right)\,. \tag{15.69}$$

Write the above state as

$$\begin{aligned} |\phi\rangle_{\mathrm{AB}} &= \frac{1}{\sqrt{2}}\left[a|000\rangle + a|011\rangle + b|100\rangle + b|111\rangle\right] \\ &= \frac{1}{2}\left[|\phi^+\rangle(a|0\rangle + b|1\rangle) + |\phi^-\rangle(a|0\rangle - b|1\rangle)\right. \\ &\qquad \left. + |\psi^+\rangle\left(a|1\rangle + b|0\rangle\right) + |\psi^-\rangle\left(a|1\rangle - b|0\rangle\right)\right], \end{aligned} \tag{15.70a}$$

where

$$|\phi^+\rangle = \frac{1}{\sqrt{2}}\left[|00\rangle + |11\rangle\right], \quad |\phi^-\rangle = \frac{1}{\sqrt{2}}\left[|00\rangle - |11\rangle\right], \tag{15.70b}$$

$$|\psi^+\rangle = \frac{1}{\sqrt{2}}\left[|01\rangle + |10\rangle\right], \quad |\psi^-\rangle = \frac{1}{\sqrt{2}}\left[|01\rangle - |10\rangle\right]\,. \tag{15.70c}$$

$|\phi^+\rangle$, $|\phi^-\rangle$, $|\psi^+\rangle$ and $|\psi^-\rangle$ form an orthonormal basis for Alice's two particles. This basis is called the *Bell basis*. In the above $|01\rangle$ indicates that particle-1 is in the state $|0\rangle$ while the particle-2 is in $|1\rangle$. Similar meaning for $|00\rangle$, $|10\rangle$ and $|11\rangle$. The protocol then proceeds as follows:

1. Alice will carry out projection measurements on her particles. She will get any one of the four Bell states randomly with equal probability.

2. Suppose the state got by Alice is $|\psi^+\rangle$. Then in the state $|\phi\rangle_{AB}$ the three particles collapse into the state
$$|\phi\rangle_{AB} = |\psi^+\rangle\,[a|1\rangle + b|0\rangle]\ , \tag{15.71}$$
where $a|1\rangle + b|0\rangle$ represents the state of the particle-3 (of Bob). Now, Alice wants to convey this result to Bob by a classical channel, for example, over the phone. She informs the difference in the state of the particles 2 and 3.
3. *What does Bob do now?* The state $|\psi^+\rangle$ indicates that (refer to Eq. (15.70c)) the states of the particles 1 and 2 are orthogonal (opposite). But the states of particles 2 and 3 are prepared as in Eq. (15.68) which means their states are the same. The state of the particle-2 is hence opposite to 1 but the same as 3. This is true only if particles 1 and 3 are orthogonal. The states of them are thus opposite. Since the state of particle-1 is $|\phi\rangle = a|0\rangle + b|1\rangle$ the state of particle-3 is $a|1\rangle + b|0\rangle$. Therefore, Bob has to do the NOT operation that changes the state of particle-3 into $a|0\rangle + b|1\rangle$. This completes the protocol.

   What has to be done if Alice got some other Bell state instead of $|\psi^+\rangle$*?*

15.5.2 Features of the Three Stage Scheme

Some of the features of the above teleportation scheme are summarized as follows:

1. During the Bell-state measurement particle-1 is set entangled with particle-2. Hence, particle-1 lost its identity. The state $|\phi\rangle$ on Alice's side during teleportation is destroyed.
2. Alice need not know the location of Bob.
3. The initial state of particle-1 is unknown to anyone and even undefined at the time of measurement.
4. The measurements of Alice and the operations of Bob are local.
5. Bob's operations are independent of the state of the particle-1 state.
6. The classical communication used is local.
7. The measurement does not provide information of the particles involved. Thus, no damage to the no-cloning theorem of Wooters and Zuerk [65].
8. According to the theory of relativity, information transfer faster than light is not possible. Quantum teleportation does not take place faster than light, because the communication channel used is classical.

Motivated by the proposal of Bennett and his coworkers various groups have initiated investigation on experimental quantum teleportation. Bouwmeester et al [66] reported the first experimental quantum teleportation. They used pairs of polarization entangled photons produced through pulsed down-conversion. Two photon interferometric method is employed to transfer the state of one photon onto another. Furasawa et al [67] demonstrated teleportation using the protocol in ref. [68] with squeezed state entanglement. The experiment of Boschi et al [69] involved a quantum optical implementation.

The teleportation schemes could be used to set up links between quantum computers. Research on quantum teleportation also opens new types of experiments and investigation on the fundamentals of quantum mechanics. It can be used to transmit information desirably in a noisy environment. Quantum teleportation can be used to construct quantum gates. As the particle is not sent, a quantum teleportation is a novel scheme of secure transfer of information. For more details on teleportation one may refer to refs. [63–71].

Solved Problem 2:

To teleport an EPR pair, we require a maximally entanglement of three particles. Find out the useful initial states.

The wave function of an entangled pair can be

$$|\psi_{12}\rangle = \alpha|00\rangle + \beta|11\rangle, \tag{15.72}$$

where $|\alpha|^2 + |\beta|^2 = 1$ or $|\psi_{\text{EPR}}\rangle = \alpha|01\rangle + \beta|10\rangle$. The possible maximally entangled states are

$$\begin{aligned} &\frac{1}{\sqrt{2}}(|000\rangle \pm |111\rangle), \quad \frac{1}{\sqrt{2}}(|001\rangle \pm |110\rangle), \\ &\frac{1}{\sqrt{2}}(|010\rangle \pm |101\rangle), \quad \frac{1}{\sqrt{2}}(|100\rangle \pm |011\rangle). \end{aligned} \tag{15.73}$$

We can choose a triplet in the form of GHZ

$$|\psi_{\text{GHZ}}\rangle = \frac{1}{\sqrt{2}}(|000\rangle \pm |111\rangle). \tag{15.74}$$

Then the initial state is $|\psi\rangle = |\psi_{\text{EPR}}\rangle \otimes |\psi_{\text{GHZ}}\rangle$.

15.6 Quantum Games

Game theory is referred to as the study of decision making in conflict situation. It has applications in military warfare, anthropology, social psychology, economics, politics, business and philosophy [72–75]. Interest has been paid on extending classical game theory to the quantum domain to study the problems of quantum computation, information and communication. Quantum game theory began with the seminal work of David A. Meyer (1999). It deals with classical games in the realm of quantum mechanics. Considerable progress has been made in this area. Several protocols have been proposed and certain classical games have been extended to the quantum case. The interesting point is that quantum superposition and entanglement between the states of the players ensure the players to outperform the classical moves through quantum mechanical strategies.

15.6.1 Classical Game

In classical game theory, a game essentially consists of

1. a set of players,
2. a set of strategies dictating the actions of players and
3. a payoff function specifying the reward for a set of strategy choices. The payoff to a player is a numerical value.

In a game theory the goal of a player is to optimize his payoff. In a game, a dominant strategy is that the player has to do at least as well as any other competing strategy. The *Nash equilibrium* is the most important among the possible equilibria [74,76]. It is the combination of strategies with which none of the players can improve his/her payoff by a unilateral change of strategy. A *Pareto optimal* outcome is that from which no player is able to obtain a higher profit without reducing the utility of another.

15.6.2 Quantum Game

A quantum system manipulated by players, where the usefulness of the possible moves are defined, can be thought of as a quantum game [76–78]. A two player game $\Gamma = (\mathcal{H}, P, P_{\rm A}, P_{\rm B})$ is specified by

1. the Hilbert space $\mathcal{H}$ of the system,
2. the initial state $P \in \mathcal{P}(\mathcal{H})$, with $\mathcal{P}(\mathcal{H})$ being the state space,
3. $P = P_{\rm A} \otimes P_{\rm B}$ describing the players, say Alice (A) and Bob (B) and
4. initial strategies $P_{\rm A}$ and $P_{\rm B}$.

$P_{\rm A}$ and $P_{\rm B}$ specify the payoff or utility for the players. Quantum tactics $S_{\rm A}$ and $S_{\rm B}$ are linear quantum operations mapping the state space on itself and are positive trace-preserving. A change of strategy of the players is represented by a linear map. Schematically, we have

$$P \xrightarrow{S_{\rm A}, S_{\rm B}} \sigma \Rightarrow (P_{\rm A}, P_{\rm B})\,. \tag{15.75}$$

The generalization of the above for the N players is straight-forward. A most notable feature of quantum game theory is that effects not possible in the classical case can occur due to quantum entanglement and interference. Quantum game theory differs from classical game theory by using superposed initial states, quantum entanglement of initial states and superposition of strategies to be used in the initial states. Quantum game approach has been applied to typical classical games such as coin tossing [76,79], the prisoners' dilemma [80–84], the Monty Hall problem [85,86], the battle of the sexes [87,88], rock-scissors-paper [89] and others [90–92].

15.6.3 Parrondo's Games

Juan Manuel Rodríguez Parrondo has discovered an apparent and fascinating paradox called *Parrondo paradox* in game theory. In it, two games when played individually are losing can be combined to yield a winning game [93–96]. That is, Parrondo paradox results when a losing game is played by disturbing the winning feedback by a second losing game so that the first losing game becomes a winning.

15.6.3.1 Classical Games

Classical Parrondo's games cast in the form of gambling games by utilizing a set of biased coins. However, here we first illustrate the paradox with a deterministic game [97] and then that of Parrondo. Suppose the current capital of a player is M (even) dollars.

Game A:

The player wins 1 dollar if M is even, otherwise loses 3 dollars.

Game B:

The player wins 1 dollar if M is odd, otherwise loses 3 dollars.

Playing only the game A or B repeatedly leads to a steady loss of 1 dollar per play. *What will happen if these two games are played alternately?* Playing ABAB... gives a steady win of 1 dollar per play: a combination of two losing games results in a winning game. So, Parrondo's paradox seems to be conveying that playing the sequence $(\mathrm{AB})^m$ is better than $\mathrm{A}^m\mathrm{B}^m$. *What is the outcome of the game if we replace the loss of* 3 *dollars by the loss of* 1 *dollar and the sequence* ABAB... *is followed?*

The original games of Parrondo is capital-dependent (CD) requiring feedback loops [96].

TABLE 15.2
The choice of the coin to be tossed at nth game.

Game_{n-2}	Game_{n-1}	Coin chosen
Loss	Loss	2
Loss	Win	3
Win	Loss	3
Win	Win	4

Parrondo, Gregory P. Harmer and Derek Abbott [95] proposed a capital-independent but history-dependent (HD) game with feed-forward loops. The construction of the games is the following.

Game A:

It involves tossing a weighted coin 1 with probability $p_{\text{w}} = 0.5 - \epsilon$, $0 < \epsilon \ll 1$ for winning and $p_{\text{l}} = 1 - p_{\text{w}}$ for losing.

Game B:

CD and HD types of games differ. There are two biased coins (coins 2 and 3) in the CD game and $p_{2\text{w}} = 0.1 - \epsilon$ and $p_{3\text{w}} = 0.75 - \epsilon$. Coin 2 or 3 is tossed depending on the capital M at the instant and hence the name CD game. Coin 2 is tossed if M is a multiple of 3, otherwise coin 3. Note that, on the average, coin 3 will be played more frequently than coin 2. However, coin 2 outweighs coin 3 because of its poor winning probability. As a result, game B is overall a losing game.

In an HD game 3 coins are used. One of them is tossed based on the outcome of the previous game. This is illustrated in table 15.2. *What are the probabilities of the three coins?* Evidently, coin 3 is tossed more often than the other coins, and hence this is a losing game.

In the Parrondo's games, both A and B are losing games for small positive values of ϵ. However, simulation of the games have predicted that switching between the losing games, e.g., playing two times A, two times B, two times A, and so on result in winning. That is, a player can play the two losing games A and B in such an order to realize a winning expectation. For detailed results see refs. [95–98]. Promising application areas for Parrondo's paradox are in biogenesis spin systems, stochastic signal processing, economics and sociological modelling [98].

15.6.3.2 Quantum Version of Parrondo's Games

We present the quantum version of the HD Parrondo's games formulated by Flitney, Ng and Abbott [99] A quantum version CD Parrondo's games is reported in ref.[100]. In classical gambling games there is a random element. It is replaced by a superposition of all the possible results in quantum games. We can realize new behaviour by this. The coin tossing game can be quantized by an $SU(2)$ operation on a qubit. A physical system may be a collection of polarized photons with $|0\rangle$ and $|1\rangle$ representing horizontal and vertical polarizations, respectively.

An arbitrary $SU(2)$ operation on a qubit is expressed as

$$\begin{aligned} \widehat{A}(\theta,\gamma,\delta) &= \widehat{P}(\gamma)\widehat{R}(\theta)\widehat{P}(\delta) \\ &= \begin{pmatrix} \mathrm{e}^{-\mathrm{i}(\gamma+\delta)/2}\cos\theta & -\mathrm{e}^{-\mathrm{i}(\gamma-\delta)/2}\sin\theta \\ \mathrm{e}^{\mathrm{i}(\gamma-\delta)/2}\sin\theta & \mathrm{e}^{\mathrm{i}(\gamma+\delta)/2}\cos\theta \end{pmatrix}, \end{aligned} \tag{15.76}$$

where $\theta \in [-\pi, \pi]$ and $\gamma,\ \delta \in [0, 2\pi]$. This is the quantum analogue of the game A−a single toss of a biased coin. Game B consists of four $SU(2)$ operations, each of the form of Eq. (15.76):

$$\widehat{B} = \begin{pmatrix} A(\phi_1, \alpha_1, \beta_1) & 0 & 0 & 0 \\ 0 & A(\phi_2, \alpha_2, \beta_2) & 0 & 0 \\ 0 & 0 & A(\phi_3, \alpha_3, \beta_3) & 0 \\ 0 & 0 & 0 & A(\phi_4, \alpha_4, \beta_4) \end{pmatrix}. \tag{15.77}$$

This acts on the state $|\psi(t-2)\rangle \otimes |\psi(t-1)\rangle \otimes |i\rangle$, where $|\psi(t-1)\rangle$ and $|\psi(t-2)\rangle$ represent the results of the two previous games. $|i\rangle$ is the qubit's initial state. We write $\widehat{B}|q_1 q_2 q_3\rangle = |q_1 q_2 b\rangle$, where $q_i \in \{0, 1\}$ and b is the output of the game B. The result of n successive games of B is found by

$$|\psi_f\rangle = \left(\widehat{I}^{n-1} \otimes \widehat{B}\right)\left(\widehat{I}^{n-2} \otimes \widehat{B} \otimes \widehat{I}\right) \ldots \left(\widehat{B} \otimes \widehat{I}^{n-1}\right)|\psi_i\rangle\,, \tag{15.78}$$

where $|\psi_i\rangle$ is the initial state of $n+2$ qubits.

Suppose a player plays AAB n times. Then

$$\begin{aligned} |\psi_f\rangle &= \left\{\widehat{I}^{3n-3} \otimes \left[\widehat{B}\left(\widehat{A} \otimes \widehat{A} \otimes \widehat{I}\right)\right]\right\} \\ &\quad \times \left\{\widehat{I}^{3n-6} \otimes \left[\widehat{B}\left(\widehat{A} \otimes \widehat{A} \otimes \widehat{I}\right)\right] \otimes \widehat{I}^3\right\} \\ &\quad \ldots \left\{\left[\widehat{B}\left(\widehat{A} \otimes \widehat{A} \otimes \widehat{I}\right)\right]\widehat{I}^{3n-3}\right\}|\psi_i\rangle \\ &= \widehat{G}^n|\psi_i\rangle\,, \end{aligned} \tag{15.79}$$

where $\widehat{G}^n = \widehat{B}\left(\widehat{A} \otimes \widehat{A} \otimes \widehat{I}\right)$ and $|\psi_i\rangle$ is an initial state of $3n$ qubits.

The classical game can be reproduced by $|\psi_i\rangle = |00\ldots0\rangle$. Suppose $|\psi_i\rangle$ is the entangled state

$$|\psi_i\rangle = \frac{1}{\sqrt{2}}\left(|00\ldots0\rangle + |11\ldots1\rangle\right). \tag{15.80}$$

In this case interference effects enhance or reduce the success of the player. The addition of nonzero phases in the operators $\widehat{A}$ and $\widehat{B}$ alter this interference. Let the payoff for a $|1\rangle$ state be 1 and for a $|0\rangle$ state be -1. Since quantum mechanics is a probabilistic theory $\langle\text{payoff}\rangle$ is important and is given by

$$\langle\text{payoff}\rangle = \langle\$\rangle = \sum_{j=0}^{n}\left[(2j-n)\sum_{j'}|\langle\psi_j^{j'}|\psi_f\rangle|^2\right]. \tag{15.81}$$

In Eq. (15.81) the second summation is over all basis states $\langle\psi_j^{j'}|$ with $n-j$ zero's and j ones.

For the sequence AAB with $|\psi_i\rangle = (|000\rangle + |111\rangle)/\sqrt{2}$ we have

$$\begin{aligned} \langle\$_{\text{AAB}}\rangle &= \frac{1}{2}\cos 2\theta\,(\cos 2\phi_4 - \cos 2\phi_1) \\ &\quad + \frac{1}{4}\sin^2 2\theta\,[\cos(2\delta+\beta_1)\sin 2\phi_1 \\ &\quad - \cos(2\delta+\beta_2)\sin 2\phi_2 - \cos(2\delta+\beta_3)\sin 2\phi_3 \\ &\quad + \cos(2\delta+\beta_4)\sin 2\phi_4]\,. \end{aligned} \tag{15.82}$$

The maximum payoff is for $\beta_1 = \beta_4 = -2\delta$ and $\beta_2 = \beta_3 = \pi - 2\delta$. The result is minimum for $\beta_1 = \beta_4 = \pi - 2\delta$ and $\beta_2 = \beta_3 = -2\delta$. Observe that the values of ϕ_i's are irrelevant. $\langle\$_{\text{AAB}}\rangle$ varies between $-0.812 + 0.03\epsilon$ and $0.812 + 0.24\epsilon$. The classical payoff is $1/60 - 28\epsilon/15$. The classical and quantum payoffs for the sequence AAB...AAB are $1/60 - 28\epsilon/15$ and $2\epsilon/15$, respectively. For more results see ref. [99].

TABLE 15.3
Payoff for the PD. The first and second entries in the parenthesis denote the payoffs of Alice and Bob, respectively. (Reproduced with permission from J. Eisert, M. Wilkens and M. Lewenstein, *Phys. Rev. Lett.* 83:3077, 1999. Copyright 1999, American Physical Society.)

	Bob:C	Bob:D
Alice:C	$(3, 3)$	$(0, 5)$
Alice:D	$(5, 0)$	$(1, 1)$

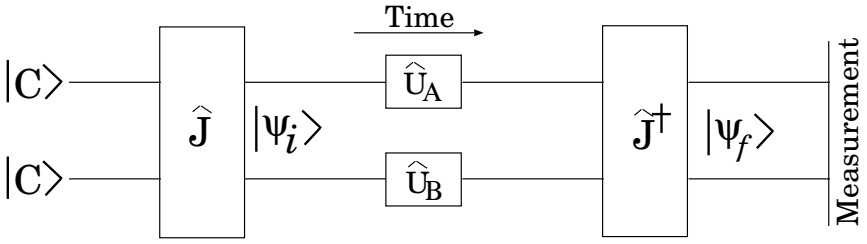

FIGURE 15.3
The set-up for the two player PD quantum game showing the flow of information. (Reproduced with permission from J. Eisert, M. Wilkens and M. Lewenstein, *Phys. Rev. Lett.* 83:3077, 1999. Copyright 1999, American Physical Society.)

15.6.4 Prisoners' Dilemma

The prisoners' dilemma (PD) is an another famous classical game extended into quantum domain [80]. The Parrondo's games are played by a single player whereas PD game is played by two players. It is a nonzero sum game. The two players are not in opposition to each other. They may benefit from mutual cooperation.

15.6.4.1 A Classical Game

In the classical version of the PD game, the two players, say, Alice and Bob, decide independently to choose defect (strategy D) or cooperate (strategy C). Depending on their own decision they receive a certain payoff as in table 15.3.

There exists a dominant strategy, that of always defecting, because it gives a better payoff when if the other player cooperates (5 instead of 3) or if the other player defects (1 instead of 3). If both players have a dominant strategy then this combination is the Nash equilibrium. The Nash equilibrium outcome {D,D} is not a good one for the players. However, since both the players would receive a payoff of 3 if they cooperate, the Pareto optimal results. Here no player will be able to improve his/her payoff by unilaterally changing own strategy. *This is the dilemma.*

15.6.4.2 A Quantum PD Game

Does a quantum version of the PD game have a different solution? A quantum model of the PD is proposed by Eisert et al [80]. In this model the two players escape the dilemma by carrying out quantum strategies. The quantum version is depicted in Fig. 15.3. To get nonclassical results entanglement between the players' moves is created. Initial state of the

qubits is $|\psi_i\rangle = |\mathrm{C}\rangle|\mathrm{C}\rangle = |\mathrm{CC}\rangle$. The final state is

$$|\psi_f\rangle = \widehat{J}^{\dagger}\left(\widehat{U}_{\mathrm{A}} \otimes \widehat{U}_{\mathrm{B}}\right)\widehat{J}|\psi_i\rangle\,, \tag{15.83}$$

where $\widehat{J}$ is an operator entangling the qubits of the players. Strategic moves are associated with $\widehat{U}_{\mathrm{A}}$ (Alice) and $\widehat{U}_{\mathrm{B}}$ (Bob). A disentangling gate $\widehat{J}^{\dagger}$ is used for a measurement on the final state. The expectation value of payoff of Alice is

$$\begin{aligned}\langle \$_{\mathrm{A}}\rangle \;=\; & P_{\mathrm{CC}}|\langle\psi_f|\mathrm{CC}\rangle|^2 + P_{\mathrm{CD}}|\langle\psi_f|\mathrm{CD}\rangle|^2 \\ & + P_{\mathrm{DC}}|\langle\psi_f|\mathrm{DC}\rangle|^2 + P_{\mathrm{DD}}|\langle\psi_f|\mathrm{DD}\rangle|^2\,,\end{aligned} \tag{15.84}$$

where P_{ij}, $i, j \in \{\mathrm{C}, \mathrm{D}\}$ is the payoff for Alice with the game outcome ij. Interchanging i and j in P_{ij} in Eq. (15.84) gives the payoff of Bob. We note that expected payoff of Alice depends on $\widehat{U}_{\mathrm{A}}$ and also on Bob's choice $\widehat{U}_{\mathrm{B}}$. If the players play with classical strategies the quantum game gives nothing surprise. However, if they utilize quantum strategies the entanglement opens the opportunity for their moves to interact in ways which have no classical analogue.

Suppose we have quantum strategies of the form

$$\widehat{U}(\theta, \phi) = \begin{pmatrix} \mathrm{e}^{\mathrm{i}\phi}\cos(\theta/2) & \mathrm{i}\sin(\theta/2) \\ \mathrm{i}\sin(\theta/2) & \mathrm{e}^{-\mathrm{i}\phi}\cos(\theta/2) \end{pmatrix}, \tag{15.85}$$

where $\theta \in [0, \pi]$, $\phi \in [0, \pi/2]$ and consider the entangling operator in the form

$$\widehat{J} = \exp\left(\mathrm{i}\gamma\widehat{D} \otimes \widehat{D}/2\right), \quad \gamma \in [0, \pi/2]\,. \tag{15.86}$$

The strategy that *always cooperate* is $\widehat{C} = \widehat{U}(0) = \widehat{I}$ and *always defect* strategy is $\widehat{D} = \widehat{U}(\pi) = \widehat{F}$. Against a classical Alice playing with $\widehat{U}(\theta)$, a quantum Bob can play Eisert's *miracle* move [80]

$$\widehat{M} = \widehat{U}(\pi/2, \pi/2) = \frac{\mathrm{i}}{\sqrt{2}}\begin{pmatrix} 1 & 1 \\ 1 & -1 \end{pmatrix} \tag{15.87}$$

that gives $\langle \$_{\mathrm{B}}\rangle = 3 + 2\sin\theta$ for Bob and only $\langle \$_{\mathrm{A}}\rangle = (1 - \sin\theta)/2$. The dilemma is removed. It has been demonstrated that there was a new Nash equilibrium producing a payoff of 3 to both the players and is Pareto optimal. In ref.[101] a quantum PD with Eisert et al's scheme was achieved on a two qubit NMR computer with various degrees of entanglement from a classical to a maximally entangled quantum game. Good agreement between theory and experiment was obtained.

Solved Problem 3:

In the quantum version of prisoners' dilemma game what is the state of the game after passing the state $|CC\rangle$ through the gate $\hat{J}$? What are the explicit expressions of both players' payoff?

We obtain

$$|\psi_i\rangle = \hat{J}|CC\rangle = \cos(\gamma/2)|CC\rangle + \mathrm{i}\sin(\gamma/2)|DD\rangle. \tag{15.88}$$

For the case of payoff in table 9.3, we obtain

$$\$_{\mathrm{A}} \;=\; 3P_{\mathrm{CC}} + 1P_{\mathrm{DD}} + 0P_{\mathrm{CD}} + 5P_{\mathrm{DC}}, \tag{15.89a}$$

$$\$_{\mathrm{B}} \;=\; 3P_{\mathrm{CC}} + 1P_{\mathrm{DD}} + 5P_{\mathrm{CD}} + 0P_{\mathrm{DC}}. \tag{15.89b}$$

The behaviour of prior entanglement shared among the two spatially separated partner can be extended to the relativistic set-up in noninertial frames [102–104]. Quantum Parrondo's games

15.6.5 Why are Quantum Games Interesting? What are the Possible Uses of Quantum Games?

There are several reasons for interest on quantum games [80]. Some of them are listed below.

1. Classical game theory has applications in various fields. Because it is based on probabilities, there is a fundamental interest in generalizing the theory to quantum probabilities.
2. Most of the applications of game theory in science have been in biology, in particular the competition and cooperation between species in individual animals. We believe that survival games are played on the molecular level, where quantum mechanics is the ruler.
3. Whenever a player conveys his/her decision to the other player he/she communicates information. Thus, there exists a link between game theory and quantum communication.
4. Eavesdropping in quantum communication and quantum cloning can be conceived in a strategic game between two or more players.
5. Quantum mechanics may be useful to certain specially designed games such as PQ penny flip [76] and may assure fairness in remote gambling.
6. Quantum games provide a deeper insight into quantum complexity particularly in the design of quantum algorithms.

15.7 Quantum Pseudo-Telepathy Games

The main criticism of Einstein on quantum mechanics was that it is not local and not realistic. According to his conviction, a measurement at some location A could not have any effect at some other location B in a time faster than that required by light to travel from A to B. Also, he felt that any measurement of a system must only be real elements of reality that were already present in the system being measured. But the presence of quantum entanglement and Heisenberg uncertainty relations make quantum mechanics nonlocal and contradict Einstein realism. Bell's theorem [105] and subsequent experiments done [106–108] concluded that physical world is not local realistic. The theoretical and experiment study of pseudo-telepathy provides a convinsing demonstration that the physical world cannot be local realistic. Quantum pseudo-telepathy games [109–117] are considered as a form of quantum games. When a game has no winning strategies for classical players but if the sharing of entanglement gives a winning strategy certainly then it is a *quantum pseudo-telepathy class of game*.

1. Magic Square Game

Consider the so-called magic square game. A magic square consists of 3×3 array of cells as shown in Fig. 15.4a. Each cell can be assigned a value either 1 or -1. The product of the numbers in each row is to be 1 while the product of numbers in each column is to be -1. In the magic square shown in Fig. 15.4b, the product of the numbers in the filled rows and columns satisfy the above conditions. What about the third row and column? Assigning either 1 or -1 does not satisfy the requirement on the product. The conclusion is the magic square does not exist.

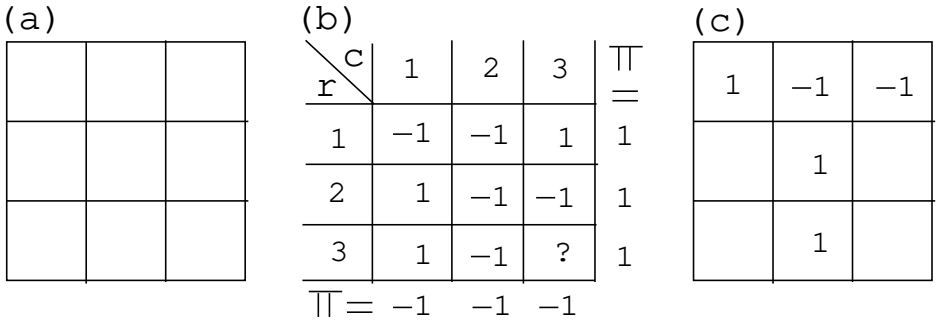

FIGURE 15.4
(a) A square with 3×3 array of cells. (b) A magic square filled (except one cell) with ± 1. (c) An example of a magic square with first row filled by Alice and the second column filled by Bob.

Suppose the magic square game is played by two players Alice and Bob. Neither Alice nor Bob has details of row or column the other has filled and nor they are aware of the values the other has assigned. If Alice and Bob enter the same number in the cell common to their row and column and the product of the numbers in row (column) becomes 1 (-1) then the game is said to be won. Xavier and Yolande each generate a random integer number from the set $\{1, 2, 3\}$. Xavier (Yolande) informs the number to Alice (Bob). If the number generated by Xavier is 1 then Alice has to fillup the first row with ± 1 so that the product of the numbers in the first row is 1. Similarly, if the number generated by Yolande is 2 then Bob has to fillup the second column with the numbers ± 1 so that the product the numbers in the column 2 has to be -1. Further, they should assign same number to the intersecting cell. An example is shown in Fig. 15.4c.

2. Classical Strategy of the Magic Square Game

In the classical strategy, the success rate is not higher than 8/9 [116]. There is no classical strategy that leads to winning with probability 1. To prove this [118] assume that a classical strategy of 100% success exists. Denote m_{rc} as the number in the cell designated as rc, where r and c represent the row and column, respectively. For 100% success we require for the rows

$$m_{11}m_{12}m_{13} = 1, \quad m_{21}m_{22}m_{23} = 1, \quad m_{31}m_{32}m_{33} = 1 \tag{15.90a}$$

and for the three columns

$$m_{11}m_{21}m_{31} = -1, \quad m_{12}m_{22}m_{32} = -1, \quad m_{13}m_{23}m_{33} = -1\,. \tag{15.90b}$$

From Eqs. (15.90) we write

$$m_{11}m_{12}m_{13}m_{21}m_{22}m_{23}m_{31}m_{32}m_{33} = \prod_r \prod_c m_{rc} = 1\,, \tag{15.91a}$$

$$m_{11}m_{21}m_{31}m_{12}m_{22}m_{32}m_{13}m_{23}m_{33} = \prod_c \prod_r m_{rc} = -1\,. \tag{15.91b}$$

The left-side terms in Eqs. (15.91) are the same. That is,

$$1 = \prod_r \prod_c m_{rc} = \prod_c \prod_r m_{rc} = -1 \tag{15.92}$$

which is not possible. This completes the proof.

r \ c	1	2	3
1	$\sigma_x \otimes \sigma_x$	$\sigma_x \otimes I$	$I \otimes \sigma_x$
2	$\sigma_y \otimes \sigma_y$	$-\sigma_x \otimes \sigma_z$	$-\sigma_z \otimes \sigma_x$
3	$\sigma_z \otimes \sigma_z$	$I \otimes \sigma_z$	$\sigma_z \otimes I$

FIGURE 15.5
An example of a quantum strategy for the magic square game. For details see the text.

3. Quantum Strategy of the Magic Square Game

The magic square game can become certainly winning [119,120] if Alice and Bob share an entangled quantum state. From Eqs. (15.91) we observe that if m_{rc} commute with each other, so that the order of occurrence of m_{rc} can be rearranged, then solution does not exist [118]. Therefore, we look for solutions of Eqs. (15.90) those are noncommutative. In other words, it is desired to determine operators m_{rc} satisfying (15.90). As the numbers in the cells are real numbers ± 1 the operators m_{rc} have to be Hermitian and their eigenvalues are ± 1. In each row the operators have to commute with each other and similarly in each column. Consequently, the associated observables can be jointly measured.

A possible observables in the cells of the magic square game are presented in Fig. 15.5, where σ_x, σ_y and σ_z are Pauli spin operators and I is the identity operator. The operators in each row are mutually commuting with others and their product becomes I. Similarly, the operators in each column are mutually commuting and their product is $-I$. Further, the operators have eigenvalues $+1$ and -1. These satisfy the rules of the game. As the operators satisfy Eqs. (15.91) the product of the outputs of Alice becomes $+1$ and that of Bob becomes -1. Next, we need to check the compatibility condition. That is, both Alice and Bob should obtain identical output for the cell common to them. For this purpose Alice and Bob share the product of the two maximally entangled two-qubit Bell states given by

$$|\psi\rangle_{\mathrm{AB}} = \frac{1}{\sqrt{2}}\left[\,|00\rangle_{\mathrm{A_1B_1}} + |11\rangle_{\mathrm{A_1B_1}}\right] \otimes \frac{1}{\sqrt{2}}\left[\,|00\rangle_{\mathrm{A_2B_2}} + |11\rangle_{\mathrm{A_2B_2}}\right]. \tag{15.93}$$

Based on the row and column are assigned to Alice and Bob, respectively, they perform measurements on their quantum systems as per the observables specified in the cells in Fig. 15.5. The outcomes of the measurements supply the values which Alice and Bob have to assign in their respective row and column with certainly winning.

The topic of pseudo-telepathy games received great interest for several reasons [116]. Classical impossibility and the possibility of the quantum version of these games are easy to understand. They are capable of providing loophole-free description that the physical world is not local realistic. Certain other popular pseudo-telepathy games are colouring games [109,112,121], parity games [108,114,116,122–124], Deutsch–Joszsa games [125–127] and matching games [116].

Solved Problem 4:

Show that every observables in the magic square of Fig. 15.5 has eigenvalues $+1$ and -1 with equal probability.

As an example, we consider the observable $-\sigma_x \otimes \sigma_z$. It is given by

$$-\sigma_x \otimes \sigma_z = \begin{bmatrix} 0 & 1 \\ 1 & 0 \end{bmatrix} \otimes \begin{bmatrix} 1 & 0 \\ 0 & -1 \end{bmatrix} = \begin{bmatrix} 0 & 0 & -1 & 0 \\ 0 & 0 & 0 & 1 \\ -1 & 0 & 0 & 0 \\ 0 & 1 & 0 & 0 \end{bmatrix} . \tag{15.94}$$

The characteristic equation is

$$|A - \lambda I| = \begin{vmatrix} -\lambda & 0 & -1 & 0 \\ 0 & -\lambda & 0 & 1 \\ -1 & 0 & -\lambda & 0 \\ 0 & 1 & 0 & -\lambda \end{vmatrix} = 0 . \tag{15.95}$$

Expanding the determinant we get

$$\begin{aligned} 0 &= -\lambda \begin{vmatrix} -\lambda & 0 & 1 \\ 0 & -\lambda & 0 \\ 1 & 0 & -\lambda \end{vmatrix} - \begin{vmatrix} 0 & -\lambda & 1 \\ -1 & 0 & 0 \\ 0 & 1 & -\lambda \end{vmatrix} \\ &= \lambda^2 \begin{vmatrix} -\lambda & 0 \\ 0 & -\lambda \end{vmatrix} - \lambda \begin{vmatrix} 0 & -\lambda \\ 1 & 0 \end{vmatrix} - \lambda \begin{vmatrix} -1 & 0 \\ 0 & -\lambda \end{vmatrix} - \begin{vmatrix} -1 & 0 \\ 0 & 1 \end{vmatrix} \\ &= \lambda^4 - \lambda^2 - \lambda^2 + 1 \\ &= \left(\lambda^2 - 1\right)^2 . \end{aligned} \tag{15.96}$$

That is, $\lambda = \pm 1$. So, the eigenvalues of $-\sigma_x \otimes \sigma_z$ are $+1$, $+1$, -1 and -1. Therefore, $+1$ and -1 occur with equal probability $1/2$. Similarly, all the observables can be proved to have the eigenvalues as ± 1 with equal probability.

4. Magic Square Game With Entries 0 and 1

There is another version of magic square game where the entries are 0 and 1. The rule here is that the sum of the entries in row must be even while the sum of the entries in each column must be odd [116]. Such a square does not exist. In the classical case for 100% success the requirement is

$$\text{even} = \sum_r \sum_c m_{rc} = \sum_c \sum_r m_{rc} = \text{odd} . \tag{15.97}$$

The quantum winning strategy for this version of the magic square is presented in [116]. The entangled state to be shared by Alice and Bob is

$$|\psi\rangle = \frac{1}{2} \left[|0011\rangle - |0110\rangle - |1001\rangle + |1100\rangle \right] . \tag{15.98}$$

The first two qubits are for Alice while the last two qubits are for Bob. The unitary transformation that Alice has to apply for the cases of rows 1, 2 and 3 are

$$A_1 = \frac{1}{\sqrt{2}}\begin{bmatrix} \mathrm{i} & 0 & 0 & 1 \\ 0 & -\mathrm{i} & 1 & 0 \\ 0 & \mathrm{i} & 1 & 0 \\ 1 & 0 & 0 & \mathrm{i} \end{bmatrix}, \quad A_2 = \frac{1}{2}\begin{bmatrix} \mathrm{i} & 1 & 1 & \mathrm{i} \\ -\mathrm{i} & 1 & -1 & \mathrm{i} \\ \mathrm{i} & 1 & -1 & -\mathrm{i} \\ -\mathrm{i} & 1 & 1 & -\mathrm{i} \end{bmatrix}, \tag{15.99a}$$

$$A_3 = \frac{1}{2}\begin{bmatrix} -1 & -1 & -1 & 1 \\ 1 & 1 & -1 & 1 \\ 1 & -1 & 1 & 1 \\ 1 & -1 & -1 & -1 \end{bmatrix}. \tag{15.99b}$$

For Bob the unitary transformations for the columns 1, 2 and 3 are

$$B_1 = \frac{1}{2}\begin{bmatrix} \mathrm{i} & -\mathrm{i} & 1 & 1 \\ -\mathrm{i} & -\mathrm{i} & 1 & -1 \\ 1 & 1 & -\mathrm{i} & \mathrm{i} \\ -\mathrm{i} & \mathrm{i} & 1 & 1 \end{bmatrix}, \quad B_2 = \frac{1}{2}\begin{bmatrix} -1 & \mathrm{i} & 1 & \mathrm{i} \\ 1 & \mathrm{i} & 1 & -\mathrm{i} \\ 1 & -\mathrm{i} & 1 & \mathrm{i} \\ -1 & -\mathrm{i} & 1 & -\mathrm{i} \end{bmatrix}, \tag{15.99c}$$

$$B_3 = \frac{1}{\sqrt{2}}\begin{bmatrix} 1 & 0 & 0 & 1 \\ -1 & 0 & 0 & 1 \\ 0 & 1 & 1 & 0 \\ 0 & 1 & -1 & 0 \end{bmatrix}. \tag{15.99d}$$

It is easy to verify that A_i's and B_i's are unitary, that is, $A_i^\dagger A_i = I$ and $B_i^\dagger B_i = I$, $i = 1, 2, 3$. In the computational basis Alice and Bob measure their qubits. The measurement gives two bits for Alice and another two bits for Bob. These are the first two entries for them. Alice and Bob identify their third entry applying the conditions that the sum of the entries in the row must be even and the sum of the entries in the column must be odd, respectively.

Let us illustrate the quantum strategy with an example. Suppose Alice and Bob have to fillup the third row and third column, respectively. The state given by Eq. (15.98) evolves to $(A_3 \otimes B_3)|\psi\rangle$:

$$\begin{aligned}(A_3 \otimes B_3)|\psi\rangle &= \frac{1}{2}A_3|00\rangle \otimes B_3|11\rangle - \frac{1}{2}A_3|01\rangle \otimes B_3|10\rangle \\ &\quad -\frac{1}{2}A_3|01\rangle \otimes B_3|10\rangle + \frac{1}{2}A_3|11\rangle \otimes B_3|00\rangle. \end{aligned} \tag{15.100}$$

We find

$$|00\rangle = |0\rangle|0\rangle \begin{bmatrix} 1 \\ 0 \end{bmatrix} \otimes \begin{bmatrix} 1 \\ 0 \end{bmatrix} = \begin{bmatrix} 1 \\ 0 \\ 0 \\ 0 \end{bmatrix}, \tag{15.101a}$$

$$|01\rangle = \begin{bmatrix} 0 \\ 1 \\ 0 \\ 0 \end{bmatrix}, \quad |10\rangle = \begin{bmatrix} 0 \\ 0 \\ 1 \\ 0 \end{bmatrix}, \quad |11\rangle = \begin{bmatrix} 0 \\ 0 \\ 0 \\ 1 \end{bmatrix}. \tag{15.101b}$$

Next,

$$A_3|00\rangle = \frac{1}{2}\begin{bmatrix} -1 & -1 & -1 & 1 \\ 1 & 1 & -1 & 1 \\ 1 & -1 & 1 & 1 \\ 1 & -1 & -1 & -1 \end{bmatrix}\begin{bmatrix} 1 \\ 0 \\ 0 \\ 0 \end{bmatrix} = \frac{1}{2}\begin{bmatrix} -1 \\ 1 \\ 1 \\ 1 \end{bmatrix}. \tag{15.102}$$

Using Eqs. (15.101) we rewrite Es. (15.103) as

$$A_3|00\rangle = \frac{1}{2}\left(-|00\rangle + |01\rangle + |10\rangle + |11\rangle\right) . \tag{15.103a}$$

Similarly, we obtain

$$A_3|01\rangle = \frac{1}{2}\left(-|00\rangle + |01\rangle - |10\rangle - |11\rangle\right) , \tag{15.103b}$$

$$A_3|10\rangle = \frac{1}{2}\left(-|00\rangle - |01\rangle + |10\rangle - |11\rangle\right) , \tag{15.103c}$$

$$A_3|11\rangle = \frac{1}{2}\left(|00\rangle + |01\rangle + |10\rangle - |11\rangle\right) \tag{15.103d}$$

and

$$B_3|00\rangle = \frac{1}{\sqrt{2}}\left(|00\rangle - |01\rangle\right), \quad B_3|01\rangle = \frac{1}{\sqrt{2}}\left(|10\rangle + |11\rangle\right), \tag{15.104a}$$

$$B_3|10\rangle = \frac{1}{\sqrt{2}}\left(|10\rangle - |11\rangle\right), \quad B_3|11\rangle = \frac{1}{\sqrt{2}}\left(|00\rangle + |01\rangle\right). \tag{15.104b}$$

Then we find

$$\begin{aligned} A_3|00\rangle \otimes B_3|11\rangle &= \frac{1}{2}\left(-|00\rangle + |01\rangle + |10\rangle + |11\rangle\right) \otimes \frac{1}{\sqrt{2}}\left(|00\rangle + |01\rangle\right) \\ &= \frac{1}{2\sqrt{2}}\left(-|0000\rangle + |0100\rangle + |1000\rangle + |1100\rangle\right. \\ &\quad \left. -|0001\rangle + |0101\rangle + |1001\rangle + |1101\rangle\right), \end{aligned} \tag{15.105a}$$

$$\begin{aligned} A_3|01\rangle \otimes B_3|10\rangle &= \frac{1}{2\sqrt{2}}\left(-|0010\rangle + |0110\rangle - |1010\rangle - |1110\rangle\right. \\ &\quad \left. +|0011\rangle - |0111\rangle + |1011\rangle + |1111\rangle\right), \end{aligned} \tag{15.105b}$$

$$\begin{aligned} A_3|10\rangle \otimes B_3|01\rangle &= \frac{1}{2\sqrt{2}}\left(-|0010\rangle - |0110\rangle + |1010\rangle - |1110\rangle\right. \\ &\quad \left. -|0011\rangle - |0111\rangle + |1011\rangle - |1111\rangle\right), \end{aligned} \tag{15.105c}$$

$$\begin{aligned} A_3|11\rangle \otimes B_3|00\rangle &= \frac{1}{2\sqrt{2}}\left(|0000\rangle + |0100\rangle + |1000\rangle - |1100\rangle\right. \\ &\quad \left. -|0001\rangle - |0101\rangle - |1001\rangle + |1101\rangle\right). \end{aligned} \tag{15.105d}$$

Using Eqs. (15.105) the state given by Eq. (15.100) becomes

$$\begin{aligned} (A_3 \otimes B_3)|\psi\rangle &= \frac{1}{2\sqrt{2}}\left(|0100\rangle + |1000\rangle + |1101\rangle + |0010\rangle\right. \\ &\quad \left. +|1110\rangle + |0111\rangle - |0001\rangle - |1011\rangle\right). \end{aligned} \tag{15.106}$$

Any measurement will collapse the wave function in one of its eigenstates. Therefore, measurement by Alice will give any one of the four states (first two bits) 00, 01, 10 and 11. Similarly, measurement by Bob will give third and fourth bits. Suppose due to the measurement the wave function becomes $|1000\rangle$. Alice gets the bits 10 and Bob's bits are 00. The requirement is that the Bob must choose a third bit such a way that the sum of the bits of Alice must be even and Bob must choose his bit such a way that sum of his three bits must be odd. So, Alice has to add 1 to get 101. Bob choose 1 and make his bits 001. The magic square after Alice and Bobl filled their respective ro and column is as in Fig. 15.6. As the third entry of the third row is the same as the third entry of the third column, Xavier and

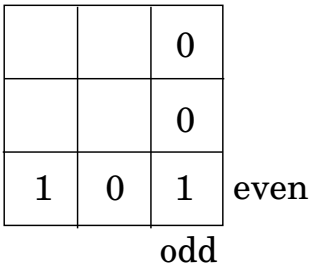

FIGURE 15.6
A magic square filled by Alice and Bob following a quantum strategy.

Yolande will accept that Alice and Bob have won the game. Consideran another example in which Alice gets 00 and Bob gets 10. By adding 0 Alice make her bits into 000 while Bob also adds 0 to make his bits 100 and they win. They can win for any measurements by choosing appropriate third bit. It can be proved that this quantum strategy wins for all the other eight possible questions for $A_1 \otimes B_1$, $A_1 \otimes B_2$, $A_1 \otimes B_3$, $A_2 \otimes B_1$, $A_2 \otimes B_2$, $A_2 \otimes B_3$, $A_3 \otimes B_1$ and $A_3 \otimes B_2$.

15.8 Quantum Steering

In 1935 Schrödinger [128,129] introduced the concept of steering when responding to the Einstein–Podolsky–Rosen (EPR) paradox [130]. *Quantum steering* is a phenomenon wherein, for example, Alice sharing an entangled state of a system with Bob (at a remote place) can *steer* the state of the system of Bob by performing a measurement on her system [131].

Consider a system consisting of two identical particles. Assume that the overall spin of the system is zero and the spin of each particle is $\hbar/2$. In an experiment the system is made to split into two particles and the total angular momentum is conserved. Each particle moves in opposite directions. Due to the conservation of total angular momentum if the spin of the particle-1 is in some direction then the spin of the particle-2 must be in the opposite direction. The axis of rotation cannot be defined with certainty. Performing measurement on a particle gives the particle a specific axis of rotation. But before the measurement the particle cannot be said to spin about a well defined axis. Suppose in a spin measurement each particle is found to posses z-component of its spin. Denote ϕ^1_+ (ϕ^1_-) as the wave function of particle-1 with spin-up (spin-down). Similarly, define $\phi^2_\pm$.

Without knowing the actual state of the particles we know that either particle-1 has spin-up and the particle-2 has spin-down or versa. The superposition of product state given by

$$\psi_{1,2} = \frac{1}{\sqrt{2}} \left(\phi^1_+ \phi^2_- - \phi^1_- \phi^2_+ \right) \tag{15.107}$$

constitute entangled states. In $\psi_{1,2}$ the minus sign is because the total spin is zero. The above ψ describes both particles together, even if they are far apart. A measurement on one particle would collapse $\psi_{1,2}$ to a definite state of the particles 1 and 2. Alice by measurement on particle-1 steer the state on the particle-2. That is, quantum steering is a form of

entanglement and a form of correlation realized in quantum mechanics. The locality principle implies that the actual situation of particle-2 is independent of the measurement done on the particle-1 which is spatially separated. In the above, the principle of locality is violated.

Let ρ be an entangled state shared by Alice and Bob. They perform local measurements on ρ. Denote the choice of the measurements as x and y with a and b being their corresponding outputs. Positive-operator-valued mesures (POVMs) $\{M_{a|x}\}$ and $\{M_{b|y}\}$ can be used to describe the measurements with $M_{a|x}$, $M_{a|y} \geq 0$, $\sum_a M_{a|x} = \mathbb{1}$ and $\sum_a M_{b|y} = \mathbb{1}$ [132]. The probability distribution $p(ab|xy)$ is $\mathrm{Tr}\left(\rho M_{a|x} \otimes M_{b|y}\right)$. If p admits a decomposition of the form

$$p(ab|xy) = \int \mathrm{d}\lambda \pi(\lambda) p_{\mathrm{A}}(a|x,\lambda) p_{\mathrm{B}}(b|y,\lambda) \tag{15.108}$$

then p is said to be *Bell local*. In Eq. (15.108) λ is some variable or hidden variable with probability density $\pi(\lambda)$ and p_{A} and p_{B} are local probability functions. When Eq. (15.108) is satisfied then ρ is said to be local or admitting a local hidden variable (LHV) model. ρ is nonlocal and said to be violating a Bell inequality if the decomposition of p given by Eq. (15.108) is not possible.

Suppose Bob not trusted Alice and wants to check whether ρ is entangled or not. Bob asks Alice to carry out measurement x on particle-1. The result is a. The measurement by Alice led to steering of the state of the particle-2 of Bob and so

$$\sigma(a|x) = \mathrm{Tr}_{\mathrm{A}}\left(M_{a|x} \otimes \mathbb{1}\rho\right) , \tag{15.109}$$

where Tr_{A} represents the partial trace over particle-1. Bob has to now check whether $\sigma_{a|x}$ admit or not the decomposition form

$$\sigma_{a|x} = \int \mathrm{d}\lambda \pi(\lambda) p_{\mathrm{A}}(a|x,\lambda) \sigma_\lambda , \tag{15.110}$$

where σ_λ are some quantum states. The state ρ is steerable if $\{\sigma_{a|x}\}$ does not admit a decomposition (15.110) and a local hidden state model. Any state violating a Bell inequality can be made use for steering. ρ is unsteerable when for all the measurements if the decomposition form (15.110) exists. Steering can be detected in this way. The following statements have been proved [131–133]:

1. Any steerable state is entangled.
2. There are entangled states that cannot be steerable.
3. There are steerable states that do not violate any Bell inequality.
4. There are entangled states which are one-way steerable but not two-way steerable.

For methods of constructing states for the above cases and for explicit examples one may refer to the ref. [132]. Methods to detect steerable state, quantifying them and their properties [131] and experimental demonstration of steering [134–138] have been reported.

15.9 Quantum Diffusion

Spreading of a wave packet in a dissipative environment at zero temperature is termed as *quantum diffusion*. This phenomenon is theoretically described by means of models of quantum state diffusion [139], quantum Brownian motion [140], quantum drift-motion [141],

etc. It is a fundamental phenomenon associated with the atomic migration in crystalline solids, where the quantum mechanical tunnelling plays a key role.

Consider a quantum particle of mass m moving in a vacuum [142]. We write the wave function in the polar form as $\psi(r,t) = \sqrt{\rho}\mathrm{e}^{\mathrm{i}S(r,t)/\hbar}$, where $\rho(r,t)$ is the probability density to find the quantum particle at a point r at time t and S is the phase of the wave function. Substituting ψ in the Schrödinger equation

$$\mathrm{i}\hbar\frac{\partial\psi}{\partial t} = -\frac{\hbar^2}{2m}\nabla^2\psi + U\psi \tag{15.111}$$

and equating the real and imaginary parts separately to zero, we obtain

$$m\frac{\partial V}{\partial t} + mV\cdot\nabla V = -\nabla U - \nabla\cdot P_{\mathrm{Q}}/\rho\,, \tag{15.112a}$$

$$\frac{\partial\rho t}{\partial t} + \nabla\cdot(\rho V) = 0\,, \tag{15.112b}$$

where the velocity $V = \nabla S/m$ represents the flow in the probability space and $P_{\mathrm{Q}} = -(\hbar^2/4m)\rho\nabla\otimes\nabla\ln\rho$ is the quantum pressure tensor [142]. When the quantum particle moves in a dissipative medium it will experience a friction force, say, proportional to velocity of the particle. In this case, Eq. (15.112a) becomes

$$m\frac{\partial V}{\partial t} + mV\cdot\nabla V + dV = -\nabla(U+Q)\,, \tag{15.113}$$

where d is the friction constant and

$$Q = -\hbar^2\nabla^2\rho/2m\sqrt{\rho}\,. \tag{15.114}$$

Thus, Eq. (15.112b) describes the probability spreading in a dissipative environment, that is, quantum diffusion.

15.9.1 Free Particle

For a free particle of unit mass the Gaussian wave packet is given by

$$\psi = \left(\frac{1}{\sqrt{2\pi}\,\sigma}\right)^{3/2}\mathrm{e}^{-r^2/4\sigma^2}\,, \tag{15.115}$$

where $\sigma^2(t)$ is the dispersion of the wave packet. For the ψ given by Eq. (15.115) from (15.112b), we obtain $V = r\dfrac{\mathrm{d}}{\mathrm{d}t}\ln\sigma$. Then Eq. (15.112a) gives

$$\frac{\mathrm{d}^2\sigma}{\mathrm{d}t^2} + d\frac{\mathrm{d}\sigma}{\mathrm{d}t} = \frac{\hbar^2}{4\sigma^3}\,. \tag{15.116}$$

The above equation describes the evolution of σ. Introducing the change of variables $\xi^2 = 2d\sigma^2/\hbar$ and $\tau = dt$ Eq. (15.116) becomes

$$\xi'' + \xi' - \frac{1}{\xi^3} = 0\,, \quad {}' = \frac{\mathrm{d}}{\mathrm{d}\tau}\,. \tag{15.117}$$

Appropriate initial condition for (15.117) is $\xi(\tau=0) = \xi_0 = \sqrt{2d/\hbar}$ and $\xi'(\tau=0) = \xi_0' = 0$. For $\tau \gg 1$, one can approximate Eq. (15.117) as $\xi' = 1/\xi^3$. Its solution is $\xi^4 = \xi_0^4 + 4\tau$ giving $\sigma^2 = \sqrt{\sigma_0^4 + \hbar^2 t/d}$. For large τ, $\sigma^2 = \hbar\sqrt{t/d}$, a subdiffusive law. Figure 15.7 shows

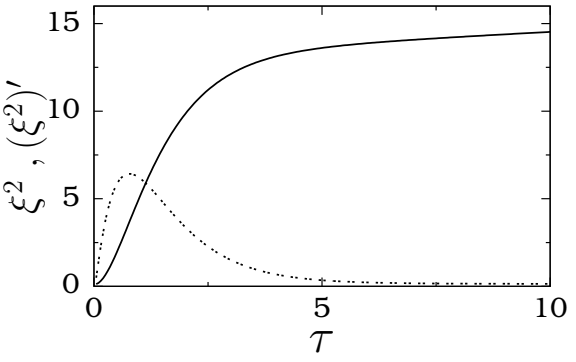

FIGURE 15.7
Variation of dispersion ξ^2 (solid curve) and its rate of change (dashed curve) with time τ where $\xi_0 = \sqrt{0.1}$ and $\xi_0' = 0$.

the plot of ξ^2 and $\mathrm{d}\xi^2/\mathrm{d}\tau$ obtained by numerically solving Eq. (15.117) with $\xi_0^2 = 0.1$ and $\xi_0' = 0$. The dispersion increases with time and then for large time it increases according to $\xi^2 = 2\sqrt{\tau}$. The maximum of $\mathrm{d}\xi^2/\mathrm{d}\tau$ is called *quantum diffusion constant* because for $\mathrm{d}^2\xi^2/\mathrm{d}\tau^2$, ξ^2 increases linearly with τ.

Numerically computed quantum diffusion constant is found to decrease with an increase in the initial dispersion ξ_0^2. The quantum diffusion constant is obtained as [142]

$$D_{\mathrm{Q}} = \frac{1}{2}\left(\frac{\partial}{\partial t}\sigma^2\right)_{\max} = \frac{\hbar^2}{16md\sigma_0^2}\,. \tag{15.118}$$

We note that the classical Einstein diffusion constant is $D = k_{\mathrm{B}}T/d$. The point is that D_{Q} is not a universal constant and depends on the initial wave packet. This result explains the large spread of quantum surface diffusion coefficient measured at low temperatures [143].

15.9.2 Linear Harmonic Oscillator

For the Guassian wave packet of linear harmonic oscillator with the potential $U = m\omega^2 r^2/2$ we have [144–146]

$$\xi'' + \xi' + \alpha^2\xi = \frac{1}{\xi^3}\,, \quad \alpha = m\omega/d\,. \tag{15.119}$$

Figure 15.8 depicts the dispersion ξ^2 versus time τ. In the limit $\tau \to \infty$, $\xi^2 \to 1$. Due to the friction force the energy drops to the ground state level.

For a discussion on quantum diffusion in a periodic potential system one may refer to ref. [142]. A general theory of quantum diffusion is developed to describe diffusion dynamics in biased semiconductors and semiconductor superlattices [147]. The mechanism responsible for quantum diffusion in the quasiperiodic kicked rotor is studied by Lignier et al.[148]. They reported experimental results on the diffusion constant on the atomic version of the system and proposed a theoretical approach to account for the observed results. Anomalous diffusions of wave packets in quasiperiodic systems has received a considerable interest [149]. Quantum diffusion in the generalized Harper equation is reported in ref. [150]. Transport property of diffusion in a finite translationaly invariant quantum subsystem is analyzed [151].

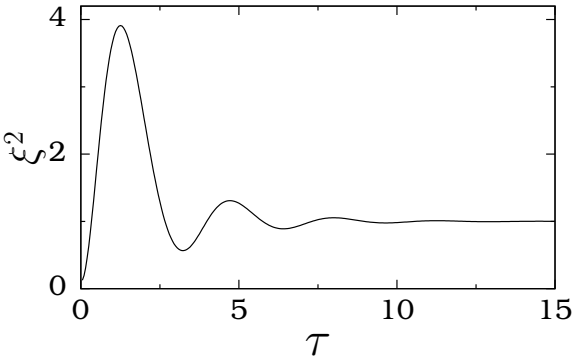

FIGURE 15.8
Variation of dispersion ξ^2 with time τ where $\xi_0 = \sqrt{0.1}$, $\xi_0' = 0$ and $\alpha = 1$.

15.10 Quantum Chaos

In classical physics, dynamical systems are broadly classified into two classes: linear and nonlinear. When the force acting on a system is directly proportional to displacement then it is said to be a *linear force* otherwise a *nonlinear force*. The systems driven by linear forces are termed as *linear systems*. The force acting on a linear harmonic oscillator is $F = -kx \propto x$ and is thus a linear system. For an anharmonic oscillator and the pendulum system the force is essentially nonlinear. Linear systems are described by linear differential equations while the nonlinear systems are described by nonlinear differential equations. *How do we define nonlinear differential equations?* In a differential equation if each of the terms, after rationalization, has a total degree either 1 or 0 in the dependent variables and their derivatives then it is a linear differential equation. Even if one of the terms has a degree different from 0 or 1 in the dependent variables (and their derivatives) then it is *nonlinear*. The presence of independent variables does not affect the linearity and nonlinearity nature. The classical equation of motion of linear harmonic oscillator is linear while those of an anharmonic oscillator and the pendulum system are nonlinear. The Schrödinger equation is linear.

Linear systems display smooth and regular behaviour. In contrast, certain nonlinear systems are capable of exhibiting smooth and regular as well as complicated irregular behaviour depending upon the various factors. A type of irregular dynamics exhibited by nonlinear systems with phase space dimension greater than two is the *chaotic motion*. It is a nonperiodic and bounded motion with high sensitive dependence on initial conditions. In a chaotic system two trajectories starting from two nearby initial conditions diverge exponentially until they become completely uncorrelated so that the future state becomes unpredictable. For a detailed discussion on classical chaos one may refer to refs. [152–154]. For microscopic systems one may ask: *What are the features of a quantum system whose classical counterpart exhibits chaotic motion?* In other words, *what are the quantum manifestations of classical chaos?*

It has been argued that anything that erratically 'wiggles' and 'jiggles' in quantum mechanics should be termed as *quantum chaos*. Berry defined quantum chaos as the study of semiclassical, but nonclassical, behaviour characteristic of systems whose classical motion exhibits chaos [155]. The problem of characterizing chaos in quantum mechanics naturally divides into two classes [156]:

1. Static properties (eigenvalues and eigenfunctions) and
2. Dynamical properties (time evolution of localized initial states and observables).

For bounded quantum systems the energy eigenvalue spectrum is discrete. Consequently, the dependence of the stationary state wave function on time is always almost periodic. Therefore, stationary state wave function cannot display sensitive dependence on initial conditions. Because the wave function itself is well behaved, it is hard to imagine the sensitivity in the expectation values of observables [157]. On the other hand, for nonstationary problems, for example, for periodic time-dependent Hamiltonians, the existence of the time evolution operator and the Floquet's theorems assert that the wave function to be quasiperiodic and thus sensitivity to initial state is precluded [157]. Therefore, we are compelled to look at the signatures of chaos in the eigenvalues and eigenvectors.

15.10.1 Signatures of Quantum Chaos

From many calculations it has been realized that a very fruitful approach to characterize quantum chaos is the analysis of statistical properties of energy level sequences. Specifically, the distribution ($P(s)$) of energy level spacing is the most significant characteristic of quantum chaos. The Hermitian matrix representation of a Hamiltonian can be parametrized in terms of its energies and the associated states. One can go from probability distribution over matrix elements to a distribution over energies in Hilbert space. Assume that the energy eigenvalues E_i are arranged in increasing order. Then the level spacing between the successive energy levels E_i and E_{i+1} is $E_{i+1} - E_i$. We can find the level spacing distribution $P(s)$ over a set of random Hermitian matrices.

For classically integrable systems it has been proven that in the semiclassical limit, successive energy levels arrive randomly, resulting in a Poisson distribution for $P(s)$. For general irregular systems (that is, nonintegrable) it has been conjectured [158] that spectral fluctuations are reproduced by appropriate random matrix ensembles like Gaussian orthogonal ensemble (GOE), Gaussian unitary ensemble (GUE) and Gaussian symplectic ensemble (GSE) depending upon the underlying time-reversal symmetry and nature of the spin of the system involved. The remarkable result is that in the case of systems with many symmetries, $P(s)$ reaches a maximum when s approaches zero and it becomes a minimum for the case of few symmetries. That is, quantized regular systems display *level clustering* while quantized chaotic systems show *level repulsion*. Consider the Hamiltonian of the form $H = H_0 + \lambda V$, where λ is the strength of the perturbation. As λ varies, the energy levels change but cannot cross each other unless there is a symmetry in the Hamiltonian. That is, due to lack of symmetries of chaotic systems, energy levels avoid approaching at a short distance from one another.

For a classically integrable system, due to the presence of many symmetries, one can write the Hamiltonian in a block-diagonal form with one block per invariant subspace. This is because two states $|i\rangle$ and $|j\rangle$ cannot have finite matrix elements $\langle i|H|j\rangle$ if H satisfies certain symmetries. These blocks are statistically independent. The point is that within a block, the energy levels are correlated. Levels belonging to different blocks cannot be identified in the spectrum of the entire Hamiltonian. As a result, the energy spacing distribution becomes a Poissonian, a characteristic of uncorrelated random variable.

For intermediate systems the phase space of a classical system consists of infinitely many distinct regions filled with regular or irregular orbits. Assuming that the quantum spectrum is generated by statistically independent superposition of Poisson and Wigner distributions, Berry and Robnik [159] found semiclassical formula for $P(s)$ that interpolates between the two limiting distributions. For a time-dependent periodic Hamiltonians, a continuous transition between Poisson to circular orthogonal ensemble statistics is observed when the

corresponding classical system changes from regular to chaotic behaviour [160–162]. As far as eigenfunctions are concerned, for integrable systems, regular nodal patterns and strongly correlated wave functions are noticed. In contrast to this, for nonintegrable systems irregular nodal pattern and negligible correlation between wave functions have been found [163].

15.10.2 Random Matrix Theory and Level Statistics

When the classical system is chaotic (nonintegrable) then its corresponding quantum version follows the so-called random matrix theory results. Therefore, we point out the salient features and some important results of random matrix theory relevant for the study of quantum chaos. We mainly follow the ref. [164]. In nuclear physics often finding an appropriate Hamiltonian is very difficult. Wigner suggested to study ensembles of Hamiltonians. The ensembles are usually defined in a matrix space where all the Hamiltonian members of the ensemble have the same symmetry properties like translational and rotational invariance or time reversal or nontime reversal invariance. For the eigenvalues of these ensemble of matrices we can analyze (i) nearest neighbor spacing distribution (NNSD) and (ii) Δ_3-statistics. NNSD is the probability $P(s)$ for finding a separation s of neighboring levels in the eigenvalue spectrum. For a given subsequence $[\alpha, \alpha + L]$ of the spectrum, $\Delta_3(\alpha, L)$ measures the least-squares deviation of the spectral staircase function from the best straight-line fitting it [165]:

$$\Delta_3(\alpha, L) = \frac{1}{L} \min \int_0^{\alpha+L} [N(\epsilon) - A(\epsilon) - B]^2 \, \mathrm{d}\epsilon \,. \tag{15.120}$$

When the energy eigenvalues ϵ_i are discrete then

$$\begin{aligned} \Delta_3(\alpha, L) \quad = \quad & \frac{n^2}{16} - \frac{1}{L^2} \left[\sum_{i=1}^{n} \hat{\epsilon}_i \right]^2 + \frac{3n}{L^2} \left[\sum_{i=1}^{n} \hat{\epsilon}_i^2 \right]^2 \\ & - \frac{3}{L^4} \left[\sum_{i=1}^{n} \hat{\epsilon}_i^2 \right]^2 + \frac{1}{L} \left[\sum_{i=1}^{n} (n + 1 - 2i) \hat{\epsilon}_i \right] \end{aligned} \tag{15.121}$$

where $\hat{\epsilon}_i = \epsilon_i - (\alpha + \dfrac{L}{2})$. The NNSD and Δ_3-statistics are known analytically for certain special types of random matrices [166,167]. Some of them are given below.

15.10.2.1 Gaussian Orthogonal Ensemble (GOE)

GOE consists of real symmetric matrices with their elements obeying Gaussian distribution. Classically, chaotic spinless or integral spin systems with time reversal symmetry systems follow the GOE statistics. For GOE [165,168]

$$P(s) \approx \frac{\pi}{2} s \mathrm{e}^{-\pi s^2/4} \tag{15.122}$$

and

$$\Delta_3(L) = \begin{cases} \dfrac{L}{15} \quad \text{for} \quad L \ll 1 \\ \\ \ln\left(\dfrac{L}{\pi^2}\right) - 0.00695 \quad \text{for} \quad L \gg 1. \end{cases} \tag{15.123}$$

15.10.2.2 Gaussian Unitary Ensemble (GUE)

GUE consists of complex Hermitian matrices whose elements are Gaussian distributed in order to make the statistics of the ensemble invariant under unitary transformations.

Usually, GUE is displayed by classically chaotic systems without time reversal symmetry. For GUE [165,168]

$$P(s) \approx \frac{32s^2}{\pi^2} e^{-4s^2/\pi}, \quad \Delta_3(L) \approx \begin{cases} \dfrac{L}{15} \ \text{ for } \ L \ll 1 \\ \\ \ln\left(\dfrac{L}{2\pi^2}\right) + 0.05902 \ \text{ for } \ L \gg 1. \end{cases} \tag{15.124}$$

15.10.2.3 Gaussian Symplectic Ensemble (GSE)

GSE consists of quaternion real Hermitian matrices with Gaussian distributed elements which make the ensemble invariant under symplectic transformations. Usually, classically chaotic systems with half-integer spin and with time reversal symmetry follows GSE statistics. For GSE [165,168]

$$P(s) \approx \frac{2^{18}s^4}{3^6\pi^3} e^{-64s^2/(9\pi)} \tag{15.125}$$

and

$$\Delta_3(L) \approx \begin{cases} \dfrac{L}{15} \ \text{ for } \ L \ll 1 \\ \\ \ln\left(\dfrac{L}{4\pi^2}\right) + 0.07832 \ \text{ for } \ L \gg 1. \end{cases} \tag{15.126}$$

In addition to the above mentioned random matrix universality classes there are few other universality classes useful for the study of quantum chaos. Some of them are the following.

15.10.2.4 Poisson Statistics

For a classical system exhibiting regular and integrable dynamics the short range properties, such as NNSD, of the corresponding energy level spectrum of the quantum mechanical system tend to resemble that of Poisson spectrum. This is because the integrable or near integrable properties translate into a number of independent conserved operator quantities and each energy level can be characterized by the associated quantum numbers. Superposing terms arising from independent contributions from the various quantum numbers generate a spectrum that closely resembles a spectrum of random numbers. The NNSD for Poisson spectrum is [155] $P(s) = e^{-s}$ while $\Delta_3(L) = L/15$. Note that Poisson statistics are identified with clustering of levels so that there is a large probability for small spacing while random matrix ensemble statistics are associated with level repulsion.

15.10.2.5 Intermediate Statistics

Many of the classical conservative systems are neither purely regular nor purely chaotic, but show mixed behaviour. For the corresponding quantum mechanics systems the spectral statistics will interpolate between those of the Poisson and the appropriate random matrix universality classes. In this case

$$P(s) = (1+q)\alpha s^q e^{-\alpha s^{q+1}}, \quad \alpha = \Gamma\left[\left(\frac{q+2}{q+1}\right)^{q+1}\right] \tag{15.127}$$

and q represents the chaotic fraction of the classical phase space volume. The above distribution is known as a *Brody distribution*. It become Poisson distribution for $q = 0$ and GOE for $q = 1$. Generally, near-integrable systems show this kind of statistic.

15.10.3 Hydrogen Atom in a Generalized van der Waals Potential

In the following we discuss the features of quantum chaos in the hydrogen atom in a generalized van der Waals potential [164,169]. The Hamiltonian of this system is

$$H = \frac{1}{2}\mathbf{p}^2 - \frac{1}{r} + \gamma\left[r^2 + \left(\beta^2 - 1\right)z^2\right], \tag{15.128}$$

where γ and β have different meanings under different physical situations. For example, $\gamma = B/(2.35\times10^5\ \mathrm{T})$ (the magnetic field parameter) and $\beta = 0$ correspond to the quadratic Zeeman effect problem and $\gamma = -1/(16d^3)$, where d represents the distance from the atom to a metal surface and $\beta = \sqrt{2}$, the system corresponds to the instantaneous van der Waals interaction existing between the atom and nearby metal surface. Further, the Hamiltonian (15.128) has a very close analogy with the Paul-trap Hamiltonian realized in precision atomic spectroscopy for ion confinement.

The time-independent Schrödinger equation of the problem is

$$\left\{\frac{1}{2}r\mathbf{P}^2 - 1 + \gamma r\left[r^2 + \left(\beta^2 - 1\right)z^2\right] - rE\right\}\psi = 0\,, \tag{15.129}$$

where $\mathbf{P} = -\mathrm{i}\nabla$. For convenience introduce a scaling parameter b so that (15.129) becomes

$$\left\{\frac{1}{2b}r\mathbf{P}^2 - 1 + \gamma b^3 r\left[r^2 + \left(\beta^2 - 1\right)z^2\right] - Ebr\right\}\psi = 0\,. \tag{15.130}$$

It is possible to solve the eigenvalue Eq. (15.130) in many ways. A useful scheme is the Crawford algorithm [170]. Ganesan and Lakshmanan [164,169] investigated the quantum manifestation of chaos in the system with the Hamiltonian (15.128). They noticed that in the classical system as the parameter β increases for arbitrary γ, there is a remarkable

$$chaos \rightarrow order \rightarrow chaos \rightarrow order \rightarrow chaos \rightarrow order \rightarrow chaos \tag{15.131}$$

type of transition. Further, the system is found to be exactly integrable at $\beta = 1/2$, 1 and 2. In the quantum case as the parameter increases the level statistics has shown

$$GOE \rightarrow Poisson \rightarrow Brody \rightarrow Poisson \rightarrow Brody \rightarrow Poisson \rightarrow GOE \tag{15.132}$$

type of transitions [164,169]. Table 15.4 summarizes classical and quantum results [169].

15.11 Concluding Remarks

Advanced research topics in quantum mechanics arise on the fundamental levels, quantum analogue of newly observed classical phenomena, application of quantum theoretical treatment and ideas to other branches of science and on the technological side. Deeper study of basic quantum mechanical systems leads to the concepts like quantum revivals [171,172] and quantum carpets [173–175]. Certain classical nonlinear systems display novel phenomena such as stochastic resonance [176], vibrational resonance [177], auto-resonance [178,179], ghost resonance [180,181], synchronization [182], amplitude death [183] to mention a few. Quantum version of stochastic resonance is realized in certain quantum systems [184,185]. The quantum analogue of other nonlinear dynamics has to be explored.

TABLE 15.4
Comparison of classical and quantum results of Hamiltonian (15.128). (Reproduced with permission from K. Ganesan and M. Lakshmanan, *Phys. Rev. A* 48:964, 1993. Copyright 1993, American Physical Society.)

β	Classical results	Quantum results
1/4	Completely chaotic (nonintegrable)	GOE statistics
1/2	Integrable	Poisson statistics
$\sqrt{0.4}$	Small-scale chaos (near-integrable)	Intermediate statistics
1	Integrable	Poisson statistics
1.5	Small-scale chaos (near-integrable)	Intermediate statistics
2	Integrable	Poisson statistics
3	Completely chaotic (nonintegrable)	GOE statistics

Until recently, biology and quantum mechanics were thought of as independent branches of science. Interestingly experimental data have opened the possible realization of quantum superposition, quantum entanglement and quantum coherence during certain biological processes and systems [186–188]. It has been proposed that the so-called Fenna–Mathews–Olson (FMO)
pigment protein complex executes a kind of quantum search algorithm which is seen to be considerably more efficient than a classical random hopping mechanism [186]. Quantum mechanical description is needed for describing cellular biochemical reactions, energy metabolism in eukaryotes interaction of light and biological photo-receptors, etc. These opened a new branch called quantum biophysics or quantum biology.

Quantum technology is occuping certain technologies such as image processing, metrology, lithography, sensing, batteries and internet. In the next concluding chapter, we bring out the underlying basics and the developments in them.

15.12 Bibliography

[1] L. Smolin, *Phys. World*, December 1999, pp.79.

[2] C. Sivaram, *Current Science* 79:413, 2000.

[3] K. Eppley and E. Hannah, *Found. Phys.* 7:51, 1977.

[4] J.H. Schwarz, *Current Science* 81:1547, 2001.

[5] A. Sen, *Current Science* 81:1561, 2001.

[6] I. Antoniads, *Current Science* 81:1609, 2001.

[7] R.P. Woodard, *Rep. Prog. Phys.* 72:122501, 2009.

[8] C. Rovelli, *Quantum Gravity.* Cambridge University Press, Cambridge, 2004.

[9] H.P. Robertson, *Astrophys. J.* 82:248, 1935.

[10] A.G. Walker, *Proc. Lond. Math. Soc.* 42:90, 1936.

[11] A. Friedmann, *Z. Phys.* 10:377, 1922.

[12] D. Atkatz, *Am. J. Phys.* 62:619, 1994.

[13] G. Gamow, *Phys. Rev.* 70:572, 1946.

[14] R.A. Alpher, H. Bethe and G. Gamow, *Phys. Rev.* 73:803, 1948.

[15] J.V. Narlikar, *Resonance* 1:6, 1996.

[16] A.A. Starobinsky, *Phys. Lett. B* 91:99, 1980.

[17] A.H. Guth, *Phys. Rev. D* 23:347, 1981.

[18] A.D. Linde, *Phys. Lett. B* 108:389, 1982.

[19] A.D. Linde, *Phys. Lett. B* 129:177, 1983.

[20] D. Atkatz and H. Pagels, *Phys. Rev. D* 25:2065, 1982.

[21] J.B. Hartle and S.W. Hawking, *Phys. Rev. D* 25:2065, 1982.

[22] A. Vilenkin, *Phys. Lett. B* 117:25, 1982.

[23] B.S. De Witt, *Phys. Rev.* 160:1113, 1967.

[24] J.A. Wheeler, *Superspace and the nature of quantum geometrodynamics*. In Battelle Rencontres – 1967 Lectures in Mathematics and Physics. Eds.: C.M. DeWitt and J.A. Wheeler. Benjamin Inc, New York, 1968.

[25] M. Cavaglia, Functional change of variables in the Wheeler–De Witt equation, *arXiv:gr-qc/9304045v1*, 30 April 1993.

[26] C. Kiefer, *ISRN Math. Phys.*, Article ID: 509316, 2013.

[27] B. Misra and E.C.G. Sudarshan, *J. Math. Phys.* 18:756, 1977.

[28] A.M. Wolsky, *Found. Phys.* 6:367, 1976.

[29] J. Gribbin, *Schrödinger's Kittens And The Search For Reality*. Orion Publishing Co., London, 2003.

[30] K. Machida, H. Nakazato, S. Pascazio, H. Rauch and S. Yu, *Phys. Rev. A* 60:3448, 1999.

[31] R.J. Cook, *Phys. Scr.* 21:49, 1988.

[32] H. Nakazato, M. Namiki, S. Pascazio and H. Rauch, *Phys. Lett. A* 217:203, 1996.

[33] W.H. Itano, D.J. Heinzen, J.J. Bollinger and D.J. Wineland, *Phys. Rev. A* 41:2295, 1990.

[34] Y. Aharonov and M. Vardi, *Phys. Rev. D* 21:2235, 1980.

[35] R.A. Harris and L. Stodolsky, *J. Chem. Phys.* 74:2145, 1981.

[36] M. Bixon, *Chem. Phys.* 70:199, 1982.

[37] D. Bar, *Physica A* 280:374, 2000.

[38] D. Bar, *Physica A* 267:434, 1999.

[39] P. Facchi, H. Nakazato, S. Pascazio, J. Perina and J. Rehacek, *Phys. Lett. A* 279:117, 2001.

[40] K. Thun, J. Perina and J. Krepelka, *Phys. Lett. A* 299:19, 2002.

[41] B. Militello, A. Messina and A. Napoli, *Phys. Lett. A* 286:369, 2001.

[42] C. Balzer, R. Huesmann, N. Neuhauser and P.E. Toschek, *Opt. Commun.* 180:115, 2000.

[43] C. Balzer, R. Huesmann, N. Neuhauser and P.E. Toschek, *Opt. Commun.* 211:1235, 2002.

[44] K. Molhave and M. Drewsen, *Phys. Lett. A* 268:45, 2000.

[45] M.C. Fisher, B.G. Medlna and M.G. Ralzen, *Phys. Rev. Lett.* 87:040402, 2001.

[46] S. Gherardini, S. Gupta, F. Saverio Cataliotti, A. Smerzi, F. Caruso and S. Ruffo, *New J. Phys.* 18:013048, 2016.

[47] D.H. Slichter, C. Muller, R. Vijay, S.J. Weber, A. Blais and I. Siddiqi, *New J. Phys.* 18:053031, 2016.

[48] G. Bernardini, L. Maiani and M. Testa, *Phys. Rev. Lett.* 71:2687, 1993.

[49] P. Facchi and S. Pascazio, *Phys. Lett. A* 241:139, 1998.

[50] P. Facchi and S. Pascazio, *Phys. Rev. A* 62:023804, 2000.

[51] P. Facchi, H. Nakazato and S. Pascazio, *Phys. Rev. Lett.* 86:2699, 2001.

[52] S.M. Roy, *Pramana J. Phys.* 56:169, 2001.

[53] A.P. Balachandran and S.M. Roy, *Phys. Rev. Lett.* 84:4019, 2000.

[54] S.K. Sekatsii, *Phys. Lett. A* 317:1, 2003.

[55] P. Facchi, Z. Hradil, G. Krenn, S. Pascazio and J. Rehacek, *Phys. Rev. A* 66:012110, 2002.

[56] A. Luis, *J. Opt. B.* 3:238, 2001.

[57] A.D. Panov, *Annals Phys.* 249:1, 1996.

[58] M. Kitano, *Opt. Commun.* 141:39, 1997.

[59] K. Yamane, M. Ito and M. Kitano, *Opt. Commun.* 192:299, 2001.

[60] P. Facchi, S. Graffi and M. Ligabo, *J. Phys. A: Math. Theor.* 43:032001, 2010.

[61] P. Facchi and S. Pascazio, *J. Phys. A: Math. Theor.* 41:493001, 2008.

[62] A. Luis, *Phys. Rev. A* 67:062113, 2003.

[63] O.Y. Aharonov and D.Z. Albert, *Phys. Rev. D* 24:359, 1981.

[64] C.H. Bennett, G. Brassard, C. Crepeau, R. Jozsa, A. Peres and W.K. Wooters, *Phys. Rev. Lett.* 70:1895, 1993.

[65] W.K. Wooters and W.H. Zurek, *Nature* 299:802, 1992.

[66] D. Bouwmeester, J.W. Pan, K. Mattle, M. Eibl, H. Weinfurter and A. Zeilinger, *Nature* 390:575, 1997.

[67] A. Furasawa, J.L. Sorensen, S.L. Braunstein, C.A. Fuchs, H.J. Kimble and E.S. Polzik, *Science* 282:706, 1998.

[68] S.L. Braunstein and H.J. Kimble, *Phys. Rev. Lett.* 80:869, 1998.

[69] D. Boschi, S. Branca, F. de Martini, L. Hardy and S. Popescu, *Phys. Rev. Lett.* 80:1121, 1998.

[70] L. Vaidman, *Phys. Rev. A* 49:1473, 1994.

[71] T. Sudbery, *Nature* 390:551, 1997.

[72] K.C. Binmore, *Fun and Games: A Text on Game Theory.* Heath, Lexington, 1992.

[73] K. Sigmund, *Games of Life: Explorations in Ecology, Evolution and Behaviour.* Penguin, London, 1995.

[74] E. Rasmusen, *Games and Information.* Blackwell, Oxford, 1995.

[75] R.B. Myerson, *Game Theory: An Analysis of Conflict.* MIT Press, Cambridge, 1991.

[76] D. Meyer, *Phys. Rev. Lett.* 82:1052, 1999.

[77] A.P. Flitney and D. Abbott, *Fluct. Noise Lett.* 02:R175, 2002.

[78] J. Sladkowski, *Physica A* 324:234, 2003.

[79] J. Ng and D. Abbott, *Introduction to quantum games and a quantum Parrondo game*. In Annals of the International Society on Dynamic Games. A. Nowac (Ed.), Birkhauser, Boston, 2003.

[80] J. Eisert, M. Wilkens and M. Lewenstein, *Phys. Rev. Lett.* 83:3077, 1999; 87:069802, 2001.

[81] S.C. Benjamin and P.M. Hayden, *Phys. Rev. Lett.* 87:069801, 2001.

[82] H. Li, X. Xu, M. Shi, J. Wu, X. Zhou and R. Han, *Phys. Rev. Lett.* 88:137902, 2002.

[83] A. Iqbal and A.H. Tour, *Phys. Lett. A* 280:249, 2001.

[84] C.F. Lee and N.F. Johnson, *Phys. World*, October, 2002, pp.25

[85] C.F. Li, Y.S. Zhang, Y.F. Huang and G.C. Guo, *Phys. Lett. A* 280:257, 2001.

[86] A.P. Flitney and D. Abbott, *Phys. Rev. A* 65:062318, 2002.

[87] L. Marinatto and T. Weber, *Phys. Lett. A* 272:291, 2000; 277:183, 2000.

[88] J. Du, X. Xu, H. Li, X. Zhou and R. Han, Nash equilibrium in the quantum battle of sexes game. *arXiv:quant-ph/0010050*, 28 November 2001.

[89] A. Iqbal and A.H. Toor, *Phys. Rev. A* 65:022036, 2002.

[90] N.F. Johnson, *Phys. Rev. A* 63:020302, 2001.

[91] S.C. Benjamin and P.M. Hayden, *Phys. Rev. A* 64:030301, 2001.

[92] A. Iqbal and A.H. Tour, *Phys. Rev. A* 65:052328, 2002; *Phys. Lett. A* 286:245, 2001; 294:261, 2002.

[93] G.P. Harmer, D. Abbott, P.G. Taylor and J.M.R. Parrondo, *Parrondo's paradoxical games and the discrete Brownian ratchet*. In the Proceedings of the Second International Conference on Unsolved Problems of Noise and Fluctuations. Am. Inst. Phys., 1999.

[94] P.V.E. McClintock, *Nature* 401:23, 1999.

[95] J.M.R. Parrondo, G.P. Harmer and D. Abbott, *Phys. Rev. Lett.* 85:5226, 2000.

[96] G.P. Harmer and D. Abbott, *Nature* 402:864, 1999.

[97] S.B. Ekhad and D. Zeilberger, Remarks on the Parrondo's Paradox, preprint; http://www.math.rutgers.edu/∼zeilberg/mamarim/mamarimPS/parrondo.ps.

[98] G.P. Harmer, D. Abbott, P.G. Taylor and J.M.R. Parrondo, *Chaos* 11:705, 2001.

[99] A.P. Flitney, J. Ng and D. Abbott, *Physica A* 314:35, 2002.

[100] A.P. Flitney and D. Abbott, *Physica A* 324:152, 2003.

[101] J.F. Du, J.H. Wu, M.J. Shi, L. Han, X.Y. Zhou, B.J. Ye, H.M. Weng and R.D. Han, *Chin. Phys. Lett.* 17:64, 2000.

[102] S. Khan and M. Khalid Khan, *J. Phys. A: Math. Theor.* 44:355302, 2011.

[103] Q. Pan and J. Jing, *Phys. Rev. A* 77:024302, 2008.

[104] P.M. Alsing, I. Fuentes-Schuller, R.B. Mann and T.E. Tessier, *Phys. Rev. A* 74:032326, 2006.

[105] J.S. Bell, *Physics* 1:195, 1964.

[106] J.J. Freedman and J.S. Clauser, *Phys. Rev. Lett.* 28:938, 1972.

[107] A. Aspect, J. Dalibard and G. Roger, *Phys. Rev. Lett.* 49:1804, 1982.

[108] D.M. Greenberger, M.A. Horne, A. Shimony and A. Zeilinger, *Am. J. Phys.* 58:1131, 1990.

[109] P.K. Aravind, *Found. Phys. Lett.* 15:397, 2002.

[110] V. Galliard and S. Wolf, *Pseudo-telepathy, entanglement and graph colouring*. In Proceedings of IEEE International Symposium on Information Theory, 2002.

[111] V. Galliard, A. Tapp and S. Wolf, *The impossibility of pseudo-telepathy without entanglement*. In Proceedings of IEEE International Symposium on Information Theory, 2002.

[112] P.K. Aravind, *Am. J. Phys.* 72:1303, 2004.

[113] R. Renner and S. Wolf, *Quantum pseudo-telepathy and the Kochen–Specker theore*. In Proceedings of IEEE International Symposium on Information Theory, 2004.

[114] G. Brassard, A. Broadbent and A. Tapp, *Quantum Inf. Comp.* 5:538, 2005.

[115] G. Brassard, A. Methot and A. Tapp, *Quantum Inf. Comp.* 5:275, 2005.

[116] G. Brassard, A. Broadbent and A. Tapp, *Found. Phys.* 35:1877, 2005.

[117] F. Ozaydin, *Laser Phys.* 30:025203, 2020.

[118] M. Christandl and R. Renner, *Advanced topics in quantum information theory solutions I*; https://edu.itp.phys.ethz.ch/fs13/atqit/sol01.pdf.

[119] N.D. Mermin, *Phys. Rev. Lett.* 65:3373, 1990.

[120] A. Peres, *Phys. Lett. A* 151:107, 1990.

[121] V. Galliard, A. Tapp and S. Wolf, *Theor. Comp. Sci.* 486:20, 2013.

[122] D.M. Greenberger, M.A. Horne and A. Zeilinger, *Going beyond Bell's theorem*. In Bell's Theorem, Quantum Theory and Conceptions of the Universe. M. Kafatos (Ed.), Kluwer, Academic, Dordrecht, 1989, pp.69-92.

[123] N.D. Mermin, *Phys. Rev. Lett.* 65:1838, 1990.

[124] H. Buhrman, P. Hoyer, S. Massar and H. Rohrig, *Phys. Rev. Lett.* 91:047903, 2003.

[125] D. Deutsch and R. Josza, *Proc. R. Soc. London Ser. A* 439:553, 1992.

[126] G. Brassard, R. Cleve and A. Tapp, *Phys. Rev. Lett.* 83:1874, 1999.

[127] J. Bub, *Phil. Sci.* 75:458, 2008.

[128] E. Schrödinger, *Math. Proc. Camb. Phil. Soc.* 31:555, 1935.

[129] E. Schrödinger, *Math. Proc. Camb. Phil. Soc.* 32:446, 1936.

[130] A. Einstein, B. Podolsky and N. Rosen, *Phys. Rev.* 47:777, 1935.

[131] R. Uola, A.C.S. Costa, H. Chau Nguyen and O. Gruhne, *Rev. Mod. Phys.* 92:015001, 2020.

[132] M.T. Quintino, T. Vertesi, D. Cavalcanti, R. Augusiak, M. Demianowicz, A. Acin and N. Brunner, *Phys. Rev. A* 92:032107, 2015.

[133] H.M. Wiseman, S.J. Jones and A.C. Doherty, *Phys. Rev. Lett.* 98:140402, 2007.

[134] W.P. Bowen, R. Schnabel, P.K. Lam and T.C. Ralph, *Phys. Rev. Lett.* 90:043601, 2003.

[135] S.P. Walborn, A. Salles, R.M. Gomes, F. Toscano and P.H. Souto Ribeiro, *Phys. Rev. Lett.* 106:30402, 2011.

[136] B. Wittmann, S. Ramelow, F. Steinlechner, N.K. Langford, N. Brunner, H.M. Wiseman, R. Ursin and A. Zeilinger, *New J. Phys.* 14:053030, 2012.

[137] M. Piani and J. Watrous, *Phys. Rev. Lett.* 114:060404, 2015.

[138] M.M. Weston, S. Slussarenko, H.M. Chrzanowski, S. Wollmann, L.K. Shalm, V.B. Verma, M.S. Aliman, S.W. Nam and G.J. Pryde, *Sci. Adv.* 4:e1701230, 2018.

[139] I.C. Percival, *Quantum State Diffusion.* Cambridge University Press, Cambridge, 1998.

[140] J. Ankerhold, *Quantum Tunnelling in Complex Systems.* Springer, Berlin, 2007.

[141] A. Jungel, *Transport Equations for Semiconductors.* Springer, Berlin, 2009.

[142] R. Tsekov, *Phys. Scr.* 83:035004, 2011.

[143] D. Drakova and G. Doyen, *J. Surf. Sci. Nanotechnol.* 8:6, 2010.

[144] H. Dekker, *Phys. Rep.* 80:1, 1981.

[145] R. Tsekov and G.N. Vayssilov, *Chem. Phys. Lett.* 195:423, 1992.

[146] A.B. Nassar, J.M.F. Bassalo, P.T.S. Alencar, L.S.G. Cancela and M. Cattani, *Phys. Rev. E* 56:1230, 1997.

[147] V.V. Bryksin and P. Kleinert, *J. Phys. Condens. Matter* 15:1415, 2003.

[148] H. Lignier, J.C. Garreau, P. Szriftgiser and D. Delande, *Europhys. Lett.* 69:327, 2005.

[149] H.Q. Yuan, U. Grimm, P. Repetowicz and M. Schreiber, *Phys. Rev. B* 62:15569, 2000 and references therein.

[150] G.S. Jeon, B.J. Kim, S.W. Yi and M.Y. Choi, *J. Phys. A: Math. Gen.* 31:1353, 1998.

[151] M. Esposito and P. Gaspard, *J. Stat. Phys.* 121:463, 2005.

[152] M. Lakshmanan and S. Rajasekar, *Nonlinear Dynamics: Integrability, Chaos and Pattern.* Springer, Berlin, 2003.

[153] H.G. Schuster and W. Just, *Deterministic Chaos: An Introduction.* Wiley VCH, Weinheim, 2005.

[154] G.M. Zaslavsky, *The Physics of Chaos in Hamiltonian Systems.* Imperial College Press, London, 2007.

[155] M.V. Berry, *Proc. R. Soc. Lond. A* 413:183, 1987.

[156] B. Eckhardt, *Phys. Rep.* 163:205, 1988.

[157] J.V. Jose, *Quantum manifestations of classical chaos: Statistics of Spectra*. In New Directions in Chaos, Volume-II, Hao Bai Lin (Ed.). World Scientific, Singapore, 1988.

[158] O. Bohigas, M.J. Giannoni and C. Schmit, *Phys. Rev. Lett.* 52:1, 1984.

[159] M.V. Berry and M. Robnik, *J. Phys. A: Math. Gen.* 17:2413, 1984.

[160] R.V. Jensen, *Phys. Rev. Lett.* 49:1365, 1982.

[161] R.V. Jensen, *Phys. Rev. A* 30:386, 1984.

[162] J.V. Jose and R. Cordery, *Phys. Rev. Lett.* 56:290, 1986.

[163] M. Shapiro and G. Goelman, *Phys. Rev. Lett.* 53:1714, 1984.

[164] K. Ganesan, *Classical and Quantum Chaos of the Hydrogen Atom in a Generalized van der Waals Potential.* Ph.D. Thesis, Bharathidasan University, Tiruchirapalli, 1993.

[165] F.J. Dyson and M.L. Mehta, *J. Math. Phys.* 4:701, 1963.

[166] M.L. Mehta, *Random Matrices and the Statistical Theory of Energy Levels.* Academic Press, London, 1967.

[167] M. Carmeli, *Statistical Theory and Random Matrices.* Marcel Dekker Inc., New York, 1983.

[168] C.E. Porter, *Statistical Theories of Spectra: Fluctuations.* Academic Press, New York, 1965.

[169] K. Ganesan and M. Lakshmanan, *Phys. Rev. A* 48:964, 1993.

[170] C.R. Crawford, *Commun. ACM* 16:41, 1973.

[171] R.W. Robinett, *Phys. Rep.* 392:1, 2004.

[172] T. García, N.A. Cordero and E. Romera, *Phys. Rev. B* 89:075416, 2014.

[173] A.E. Kaplan, I. Marzoli, W.E. Lamb and W.P. Schleich, *Phys. Rev. A* 61:032101, 2000.

[174] M. Berry, I. Marzoli and W. Schleich, *Phys. World*, June 2001, pp.39.

[175] P. Kazemi, S. Chaturvedi, I. Marzoli, R.F. O'Connell and W.P. Schleich, *New J. Phys.* 15:013052, 2013.

[176] M.D. McDonnell, N.G. Stocks, C.E.M. Pearce and D. Abbott, *Stochastic Resonance.* Cambridge University Press, Cambridge, 2008.

[177] P.S. Landa and P.V.E. McClintock, *J. Phys. A: Math. Gen.* 33:L433, 2000.

[178] B. Meerson and L. Friedland, *Phys. Rev. A* 41:5233, 1990.

[179] J. Fajans and L. Friedland, *Am. J. Phys.* 69:1096, 2001.

[180] D.R. Chialvo, O. Calvo, D.L. Gonzalez, O. Piro and G.V. Savino, *Phys. Rev. E* 65:050902(R), 2002.

[181] G. Van der Sande, G. Verschaffelt, J. Danckaert and C.R. Mirrasso, *Phys. Rev. E* 72:016113, 2005.

[182] A. Pikovsky, M. Rosenblum and J. Kurths, *Synchronization - A Universal Concept in Nonlinear Science.* Cambridge University Press, Cambridge, 2001.

[183] G. Saxena, A. Prasad and R. Ramaswamy, *Phys. Rep.* 521:205, 2012.

[184] R. Lofstedt and S.N. Coppersmith, *Phys. Rev. Lett.* 72:1947, 1994.

[185] A. Buchleitner and R.N. Mantegna, *Phys. Rev. Lett.* 80:3932, 1998.

[186] G.S. Engel, T.R. Calhoun, E.L. Read, T.K. Ahn, T. Mancal, Y.C. Cheng, R.E. Blankenship and G.R. Fleming, *Nature* 446:782, 2007.

[187] G. Panitchayangkoon, D.V. Voronine, D. Abramavicius, J.R. Caram, N.H.C. Lewis, S. Mukamel and G.S. Engel, *PNAS* 108:20908, 2011.

[188] N. Lambert, Y.N. Chen, Y.C. Cheng, C.M. Li, G.Y. Chen and F. Nori, *Nature Phys.* 9:10, 2013.

15.13 Exercises

15.1 Obtain the Hamiltonian (15.24) from the Lagrangian (15.22).

15.2 Assume a quantum system with a decay rate proportional to t^m for short times. Evaluate the probability of survival to time t_0. Now imagine a measurement of survival is made at $t = t_0/2$. Evaluate the probability of survival at $t = t_0$ after the measurement. Compare the two probabilities to show that the probability of decay at time t_0 is reduced by a factor 2^{m-1} due to measurements at $t_0/2$ for $m > 1$. Hence, establish quantum Zeno effect.

15.3 In quantum teleportation, find out the operations that Bob has to perform if Alice finds (i) $|\phi^+\rangle$, (ii) $|\phi^-\rangle$ and (iii) $|\psi^-\rangle$.

15.4 For the prisoners' dilemma game set out possible payoffs for zero-sum game, that is $\langle \$_A \rangle + \langle \$_B \rangle = 0$. Formulate a quantum game circuit for the same and calculate the probabilities of A and B to win.

15.5 One Sunday evening a husband and wife wanted to watch a cricket (C) match on a television and a movie (M) in a theatre, respectively. They also are happier to stay together rather than far apart. The payoff table is as given below. Assume that $\alpha > \beta > \gamma$. Analyze the classical version of this game, specifically, obtain and analyze the Nash equilibria.

	Husband:M	Husband:C
Wife:M	(α, β)	(γ, γ)
Wife:C	(γ, γ)	(β, α)

15.6 For the quantum version of the husband and wife game obtain the payoffs of the players for the factorizable quantum states (unentangled).

15.7 Analyze the partial erasure of two nonorthogonal qubit states $|\Omega\rangle = |\theta, \phi\rangle = \cos(\theta/2)|0\rangle + e^{i\phi} \sin(\theta/2)|1\rangle$ and $|\Omega'\rangle = |\theta', \phi'\rangle$ by removing the azimuthal angle information. What is the result if $\phi = \phi' + 2n\pi$ where n is an integer?

15.8 A quantum deleting machine involves two initially identical qubits in some state $|\psi\rangle$ and an ancilla in some initial state $|A\rangle$. A quantum deleting operation on an input $|\psi\rangle|\psi\rangle$ is defined by $|\psi\rangle|\psi\rangle|A\rangle \rightarrow |\psi\rangle|\Sigma\rangle|A_\psi\rangle$, where a copy of $|\psi\rangle$ is replaced by some standard state of a qubit $|\Sigma\rangle$ and $|A_\psi$ is the final state of the ancilla. What does the deleting machine yield for the input state $|\psi\rangle = \alpha|\mathrm{H}\rangle + \beta|\mathrm{V}\rangle$, where H and V refers to horizontal and vertically polarized photons? Express the output state in density matrix form after the deleting operation.

15.9 Show that in the example of quantum strategy of the magic square game depicted in Fig. 15.5 the product of the observables in (a) each row is I and (b) each column is $-I$ and (c) the observables in each row and column mutually commute with each other.

15.10 Consider the magic square game with boxes to be filled with 0 or 1 with the sum of the numbers in the row has to be even and the sum of the numbers in the column has to be odd. The intersection box should be filled with same number. Consider the case that Alice and Bob have to fill the row 2 and the column 3, respectively, and share the entangled state $|\psi\rangle = \frac{1}{2}(|0011\rangle - |0110\rangle - |1001\rangle + |1100\rangle)$. Determine the evolved state. Take a case Alice and Bob obtain after measurement and explain how they choose the bits to win.

16

Quantum Technologies

16.1 Introduction

In contrast to conventional technology understandable by classical mechanics, quantum technology relies on the principles of quantum physics. *What is the need for quantum technology?* There are mainly two good reasons for developing quantum engineering:

1. In the last fifty years or so, the size of the components of a computer has halved every eighteen months, providing the technological boom for modern society. As the computer components are decreasing in size, they approach atomic dimensions more closely. Then quantum mechanics imposes a fundamental limit, beyond which development of traditional technology is not feasible. To accomplish this, we specifically need new and novel devices utilizing the laws of quantum mechanics.
2. The quantum devices promise to offer a vastly improved performance over that achieved in a classical frame work.

Quantum technologies are expected to revolutionize our society in a similar way the semiconductor electronics did in the second half of the twentieth century. But the task of developing quantum technologies is an enormous challenge not only to physicists but also for engineers and computer scientists.

What is the aim of quantum technology? Quantum technology aims to invent useful devices and processes that are based on quantum principles such as quantization, uncertainty principle, quantum superposition, tunnelling, entanglement and decoherence. The development of fundametal concepts in quantum mechanics is considered as *first quantum revolution*. The evolution of quantum technology is thought of as *second quantum revolution* [1]. This revolution applies the features of quantum mechanics to change the quantum face of the world.

Fundamental discoveries in the field of quantum information have the potential for a dramatic impact on many technological fields. For example, quantum imaging is a newly born branch of quantum optics. It investigates the ultimate performance limits of optical imaging permitted by the principles of quantum mechanics. Recent developments in quantum optics and information science have opened the possibility of entirely new schemes of obtaining optical images with unexpected sensitivity and resolution. Quantum imaging addresses the problem of image formation, processing and detection with sensitivity and resolution beyond the limits of classical imaging.

According to classical physics, a beam of light has at least a minimum level of unavoidable noise, known as the *shot-noise*. Such a noise consists of natural random fluctuations which will have influences in all the properties of the light. Quantum imaging utilizes the latest achievements in quantum optics that allows to cut-off the distribution of quantum fluctuations in the transverse area of light beams and to minimize these quantum fluctuations below the shot-noise limit. This reduction of spatial quantum fluctuations provides new avenues for greatly enhancing the performance in recording, storage and read-out of

DOI: 10.1201/9781003172192-16

optical images over the limits set by the shot-noise. Quantum imaging has found potential applications in microscopy, wave front correlation, image processing, optical data storage and optical measurements.

Considerable advancements have been realized in the following quantum technologies:

1. Ghost imaging.
2. Detection of weak amplitude objects.
3. Entangled two-photon microscopy.
4. Detection of small displacements.
5. Quantum lithography.
6. Quantum metrology.
7. Quantum teleportation of optical images.
8. Quantum sensors.
9. Quantum batteries.
10. Quantum internet.

In this last chapter we present the underlying basic ideas and the salient features of the above fascinating quantum technologies. To start with, first we briefly describe the quantum entangled photons utilized in many quantum technologies.

16.2 Quantum Entangled Photons

Entangled photons are key elements in quantum engineering. Historically, high quality polarization-entangled states have been achieved through the nonlinear process of the so-called spontaneous parametric down-conversion (SPDC). The first SPDC source of photon pairs was given by Burnham and Weinberg in 1970 [2]. The entanglement of two-particle system is with respect to a certain observable. For quantum entangled photons, three of such observables are distinguished. They are polarization, energy or time and momentum or space. The corresponding types of entanglement are called polarization, time and spatial entanglement of photons, respectively. Note that the entanglement of photons is simultaneous in the three mentioned observables. Polarization-entangled photons are usually realized in two ways: type-I and type-II. In type-I, two photons of similar polarization states are entangled. In type-II, crossed polarization states of two photons are entangled.

Type-I entanglement sources have advantages due to their relatively high brightness, stability and ease-of-entanglement. Sources based on type-II are dominant for ultrafast entanglement generation and are limited by small solid angles over which entanglement persists or require interferometric configurations.

In the SPDC process, a pump photon of frequency ω_p is annihilated thereby producing a signal and idler photon at frequency ω_s and ω_i, respectively. The term parametric in SPDC indicates that the down-conversion medium is unchanged in the process. Thus, a series of conservation laws have to be satisfied by the pump, signal and idler photons. The relevant conversion laws are:

$$\omega_p = \omega_s + \omega_i\,, \quad \mathbf{k}_p = \mathbf{k}_s + \mathbf{k}_i\,. \tag{16.1}$$

The first and the second equations in Eqs. (16.1) are referred to as the frequency matching condition and phase matching condition, respectively. The wave vectors in Eqs. (16.1) are expressed as

$$\mathbf{k}_j = \frac{n_j(\omega_j)\omega_j}{c}\mathbf{s}_j \ , \tag{16.2}$$

where $n_j(\omega_j)$ is the dispersive refractive index of the material dependent on frequency ω_j, $\mathbf{s}_j$ is the unit vector pointing in the $\mathbf{k}_j$ direction and c is the speed of light. So, the second equation in (16.1) becomes

$$n_p(\omega_p)\omega_p\mathbf{s}_p = n_s(\omega_s)\omega_s\mathbf{s}_s + n_i(\omega_i)\omega_i\mathbf{s}_i \ . \tag{16.3}$$

We note that the refractive index n for most dielectric materials decreases with increasing frequency. Therefore, both frequency and phase matching conditions cannot be satisfied simultaneously in an isotropic medium. But this is achievable in a birefringent medium like β-barium-borate (BBO), where there are two different refractive indices n_o and n_e for the ordinarily (o) and extraordinarily (e) polarized light, respectively.

An e-polarized pump is used in a type-II down-conversion. The condition (16.3) with an e-polarized pump is written in terms of n_o and n_e as

$$n_e(\omega_p)\omega_p\mathbf{s}_p = n_e(\omega_e)\omega_e\mathbf{s}_e + n_o(\omega_o)\omega_o\mathbf{s}_o \ . \tag{16.4}$$

Observe that the down-conversion results in photon pairs with each consisting of an o-polarized photon and an e-polarized photon. These are emitted from the down-conversion process in two different cones from the crystal.

Let $|\mathrm{H}\rangle$ and $|\mathrm{V}\rangle$ be the horizontal and vertical polarization states of a photon, respectively. Then for polarization-entangled photon pairs, we require two decay paths given by the combinations $|\mathrm{H}\rangle_1|\mathrm{V}\rangle_2$ and $|\mathrm{V}\rangle_1|\mathrm{H}\rangle_2$. This situation is realized at the two intersections of the e and o-emission cones. The entangled wave function describing the polarization-entangled photon state is given by

$$|\psi\rangle = \frac{1}{\sqrt{2}}\left(|\mathrm{H}_o\rangle_1|\mathrm{V}_e\rangle_2 + \mathrm{e}^{\mathrm{i}\delta}|\mathrm{V}_e\rangle_1|\mathrm{H}_o\rangle_2\right) \ . \tag{16.5}$$

Actually, the photon pairs at the intersection of the o and e-emission cones are not in a pure polarization-entangled state given by (16.5). The refractive indices n_o and n_e of the birefringent crystal give rise to the difference in the velocity of the o and e waves in the crystal. This results in a relative delay between the arrival time of the o and e-polarized photon in each pair and is dependent on the site of the crystal where they are created. Hence, when the photon pairs from all the creation sites are included, we get a mixed state resulting in a lower polarization entanglement quality. We can minimize this problem using a very thin crystal or using a combination of half-wave plate and compensation crystals [3]. Also, the pair is obtained in such a way that the energy or time and momentum or space of neither one is determinate. Hence, the state of a signal-idler photon pair of SPDC is considered a typical entangled state described by the wave function [4]

$$|\psi\rangle = \sum_{s,i}\delta(\omega_s + \omega_i - \omega_p)\delta(\mathbf{k}_s + \mathbf{k}_i - \mathbf{k}_p)a_s^\dagger(\omega(\mathbf{k}_s))a_i^\dagger(\omega(\mathbf{k}_i))|0\rangle \ , \tag{16.6}$$

where $a_s^\dagger$ and $a_i^\dagger$ are the creation operators.

16.3 Ghost Imaging

In the classical imaging, when a picture of an object is taken the camera captures photons bounced-off the object of the image. Ghost imaging is the phenomenon in which images are created by photons that never touched the object during their life time [5]. Ghost imaging measures the correlation between two light beams, where only one beam probes the object. Further, in ghost imaging, the entanglement of two or more different particles are used to record images of unseen objects.

Some of the important definitions of ghost imaging [6]:

1. Ghost imaging is a visual image of an object obtained through light but without allowing light to incident on the object.
2. Ghost imaging is a peculiar effect, where an image is obtained with light patterns which do not emanate from the target.
3. It is a fascinating technique where the object and the image of the target are in separate light paths.
4. It is similar to obtaining a flash photo of an object with an ordinary camera. In an ordinary camera, the image is formed by the photons coming from the flash, reflected by the object and focused with the lens on a photo film. But in ghost imaging, the image is not constructed from the light that fell on the object and reflected back.

Pittman and his coworkers [7] demonstrated the working principle of ghost imaging experimentally making use of entangled photon pairs as the light source. A simplified schematic of the experiment is shown in Fig. 16.1. The nonlinear optical crystal-β-barium borate (BBO) splits each photon into two entangled photons (of orthogonal polarization), referred to as the signal and idler photon. The polarizing beam splitter sends the signal photon up towards the object under consideration and the idler towards the CCD (charge coupled device) camera that will image it. The object is an absorbing screen with a pattern to be imaged.

The signal photon either hits the screen and is absorbed or it passes through an aperture and detected by a bucket detector which only indicates whether or not a photon hit but does not provide information about the location where it hit. The bucket detector cannot produce any image of the object. The CCD camera detects the position of the idler photon. The information from the CCD camera and the bucket detector are allowed to pass through a coincidence circuit. This circuit would record the data from the CCD camera only if photons hit both the detectors simultaneously. An image of the object is built-up once a sufficient number of photons have been accumulated in a computer. Notice that an image has been recorded by the CCD camera though the photons hit the CCD have not come from the object.

As the two photons are quantum entangled, they are linked to one another though they may be separated by a distance. The position where the two photons hit their respective targets are correlated. Ghost imaging that uses the quantum entangled photons is called *type-I* ghost imaging. It has been demonstrated experimentally [8] that quantum entanglement is not required to get ghost imaging. It has been proved that even classically correlated photons can give rise to ghost imaging which is called the *type-II thermal ghost imaging*.

Quantum ghost imaging with entangled swapped photons [9], quantum states of light [10], atoms [11], biphotons [12] and security test based on quantum entanglement [13] have been reported. Quantum ghost imaging has potential applications in remote sensing, satellite

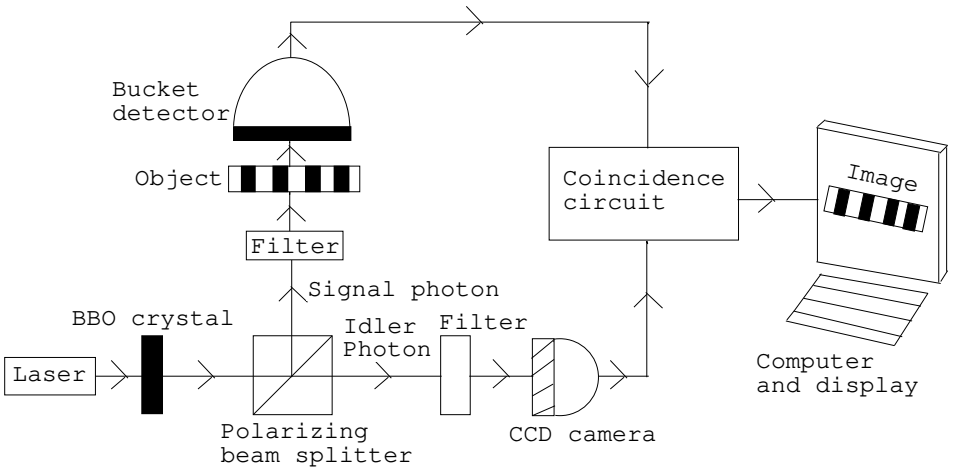

FIGURE 16.1
A schematic experimental set-up for ghost imaging using two photon quantum entanglement.

missions, millitary, high quality X-ray images, superresolution microscopy a few to mention. Various real applications of quantum imaging have been explored [14–17]. An experimental and theoretical investigation of storing quantum imaging in both space and time was analyzed [18].

Solved Problem 1:

Find the transformation matrix for a lossless beam splitter.

Let E_1 and E_2 be the electric fields at port 1 and port 2, respectively. If E_3 and E_4 are, respectively, the fields at the two input ports then we write

$$E_1 = TE_3 + RE_4, \quad E_2 = RE_3 + TE_4 \,, \tag{16.7}$$

where T and R are complex transmission and reflection coefficients, respectively. We write

$$\begin{bmatrix} E_1 \\ E_2 \end{bmatrix} = \begin{bmatrix} T & R \\ R & T \end{bmatrix} \begin{bmatrix} E_3 \\ E_4 \end{bmatrix} = [B] \begin{bmatrix} E_3 \\ E_4 \end{bmatrix} \,. \tag{16.8}$$

The transformation matrix $[B] = \begin{bmatrix} T & R \\ R & T \end{bmatrix}$ is unitary as the beam splitter is lossless. That is,

$$[B] = [B]^\dagger = I \rightarrow \begin{bmatrix} T & R \\ R & T \end{bmatrix} \begin{bmatrix} T^* & R^* \\ R^* & T^* \end{bmatrix} = \begin{bmatrix} 1 & 0 \\ 0 & 1 \end{bmatrix} \,. \tag{16.9}$$

16.4 Detection of Weak Amplitude Object

Let us consider the case of a weak amplitude object located, say, in the signal branch of the SPDC far field. Both signal and idler are noisy with respect to fluctuations of intensity as

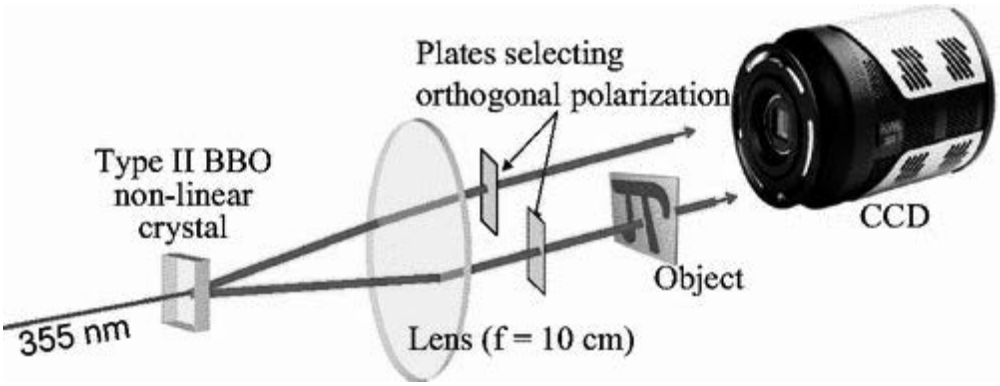

FIGURE 16.2
A typical experimental set-up for weak amplitude detection. (Reproduced with permission from G. Brida, M. Genovese, A. Media and I.R. Berchera, *Phys. Rev. A* 83:033811, 2011. Copyright 2011, American Physical Society.)

their photon number statistics are thermal. Therefore, in the high gain regime, the signal-to-noise ratio (SNR) characterizing the detection of a weak object in the signal field can be quite low. But, fluctuations in the intensity difference between signal and idler are small because of the spatial quantum correlation. Hence, if the object is detected using the signal-idler intensity difference, the SNR becomes much better. It has been shown that when the absorption is weak enough, the SNR value can be enhanced beyond the standard quantum limit [19]. Further, by making use of the strong correlation in noise of entangled modes of light produced by SPDC, the image of a weak absorbing object hidden in the noise in one part, can be recovered by subtracting the spatial noise measured in the other part [20]. This is termed as *sub-shot-noise quantum imaging* (SSNQI).

The above imaging experiment is conceptually similar to the ghost imaging experiment. Let us denote N_i and N_s as the photon numbers of an idler and signal, respectively. Then $N_\mathrm{i}(\mathbf{X})$ and $N_\mathrm{s}(-\mathbf{X})$, at $\mathbf{X}$ and $-\mathbf{X}$ in the far field are correlated because of conservation of the transverse components of the momentum. For the case of $\lambda_\mathrm{s} = \lambda_\mathrm{i}$ (degeneracy wavelength), the correlation degree is characterized by the noise reduction factor (NRF) [21]

$$\sigma = \frac{\langle \delta^2(N_\mathrm{i} - N_\mathrm{s})\rangle}{N_\mathrm{i} + N_\mathrm{s}} = \frac{\langle \delta^2 N_\mathrm{s}\rangle + \langle \delta^2 N_\mathrm{i}\rangle - 2\langle \delta N_\mathrm{s}, \delta N_\mathrm{i}\rangle}{N_\mathrm{i} + N_\mathrm{s}}\,. \tag{16.10}$$

σ is normalized with respect to the shot-noise limit ($N_\mathrm{i} + N_\mathrm{s}$). For SPDC, due to the correlation in $N_\mathrm{i}(\mathbf{X})$ and $N_\mathrm{s}(-\mathbf{X})$ in Eq. (16.10), σ becomes $\sigma = 1 - \eta$ where the balanced losses are assumed as $\eta_\mathrm{i} = \eta_\mathrm{s} = \eta$. Therefore, in an ideal case ($\eta = 1$), σ approaches zero. *What is the result for classically correlated beams?* For the subtraction of two classical beams we have $\sigma_\mathrm{CL} \geq 1$. The lowest limit $\sigma_\mathrm{CL} = 1$ is reached for coherent beams or classically correlated beams.

In a typical experimental set-up [21] shown in Fig. 16.2, a UV laser beam pumps a type-II BBO crystal producing SPDC. After removing the pump beam the correlated signal beam is allowed to cross a weakly absorbing object and is then directed to a CCD array. The other idler beam is directly sent to another area of the CCD camera.

The experiment measures the intensity pattern in signal branch (where the object has been placed) and then subtracts the correlated noise pattern measured in the idler branch. The number of photons detected in the presence of the object in the signal region is $N'_\mathrm{s}(\mathbf{X}) = [1 - \alpha(\mathbf{X})]\langle N_\mathrm{s}\rangle$, where $\alpha(\mathbf{X})$ is the absorption in the position $\mathbf{X}$. Therefore, in the SSNQI

scheme the absorption is found as [21]

$$\alpha(\mathbf{X}) = \frac{\langle N_{\mathrm{i}}(-\mathbf{X}) - N_{\mathrm{s}}'(\mathbf{X})\rangle}{\langle N_{\mathrm{i}}\rangle} \,. \tag{16.11}$$

Then the ratio between the SNR in quantum and in the differential classical imaging (DCL), with a coherent beam split by a 50% beam splitter, is found to be

$$R_{\mathrm{DCI}} = \frac{SNR_{\mathrm{SSNQI}}}{SNR_{\mathrm{DCI}}} = \sqrt{\frac{2-\alpha}{\alpha^2 E_n + 2\sigma(1-\alpha) + \alpha}} \,. \tag{16.12}$$

The noise that exceeds the standard quantum limit is given by

$$E_n = \frac{\langle \delta^2 N_{\mathrm{i}}\rangle - \langle N_{\mathrm{i}}\rangle}{\langle N_{\mathrm{i}}\rangle} \tag{16.13}$$

of the SPDC. Equation (16.12) shows that when the excess noise is very weak ($\alpha^2 E_n \ll 1$) then SSNQI gives an advantage with respect to a classical differential imaging for a weakly absorbing object ($\alpha \to 0$) once $\sigma < 1$. Brida et al [22] first realized experimentally SSNQI.

Realization of sub-shot noise wide field microscope [23], improving the resolution sensitivity trade-off [24], a model of twin-beam experiments for sub-shot noise imaging [25], processing of information through high-dimensional spatial states of phtons with sub-shot noise levels [26], use of squeezed light for sub-shot noise imaging [27,28] and enhancement of detection [29], displacement measurement [30] and biological measurement [31] below the standard quantum limit were investigated.

16.5 Entangled Two-Photon Microscopy

Microscopy based on classical sources of light are considerably noisy because of the photons arriving randomly in time and position. In recent years there has been a lively interest in entangled-photon microscopy. The two-photon laser scanning fluorescence microscopy (TPLSM) is found to be more efficient. This technique uses a highly focused optical beam in order to localize the region from which fluorescence is observed. For classical light the rate of simultaneous absorption of n photons is proportional to ϕ^n, where ϕ is the optical photon flux density. So, in TPLSM, the rate of two-photon absorption is proportional to ϕ^2. This is a quadratic behaviour and is a result of the accidental arrival of pairs of photons emitted by a classical light source. Therefore, TPLSM needs the utility of high photon flux density sources (such as femtosecond pulsed lasers), to make sure that two photons have a significantly considerable probability of reaching simultaneously and resulting in an absorption.

Entangled photon microscopy (EPM) using quantum photon pairs as source was proposed [32]. In EPM, the entangled photons' arrival times are correlated. As a result the two-photon absorption rate is substantially enhanced. This process depends linearly, on the photon flux density [33]. Consequently, lower values of the photon flux density are also used in EPM. It has been realized that correlated two-photon absorption dominates over random two-photon absorption in the case of small values of photon-flux density (below a critical photon flux density ϕ_{c}). If ϕ_{c} is sufficiently large, EPM has a number of features rendering it superior to TPLSM. A typical experimental set-up for EPM is shown in Fig. 16.3.

EPM offers several advantages over TPLSM. Some of them are listed below:

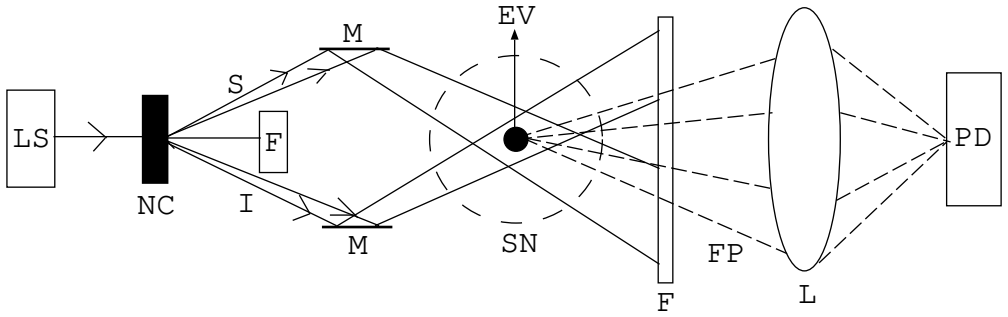

FIGURE 16.3
A typical experimental set-up for EPM where LS – laser source, NC – nonlinear crystal, S – signal, I – idler, F – filter, M – mirror, SN – specimen, EV – entangled volume, FP – fluorescence photons, L – lens and PD – photo detector. (Reproduced with permission from M.C. Teich and B.E.A. Saleh, *Ceskoslovensky Cosopis pro fygiku* 47:3, 1997.)

1. EPM operates at reduced levels of light compared to TPLSM, minimizes undesirable photo-toxicity and photo-bleaching.
2. By appropriate optical components the two excitation beams can be directed to cross one another with a variable relative path length delay. This permits us to select the position in the specimen at which the entangled photons arrive simultaneously. Moreover, they can be arranged to intersect the specimen in various configurations, including multiple locations.
3. It gives increased resolution and localization in both the axial and lateral directions.
4. EPM causes the resolution and localization to be independent of laser power fluctuations. The influence of misalignment errors are reduced in EPM relative to TPLSM.
5. The low light level needed for EPM opens the possibility of using continuous wave rather than pulsed sources of light.
6. The frequency spectrum of the summed energy of the entangled photon pair is narrow. Thus, with EPM we can effectively investigate the materials with narrow two-photon absorption spectra.

Applications of two-photon microscopy for brain imaging [34], bioimaging [35], clinical research [36,37], Raman excitation [38], detecting optically forbidden transition [39], semiconductor devices [40] are possible.

16.6 Detection of Small Displacements

Measurement of the position of a laser spot accurately is necessary in certain fields. The measurement of displacement of a light beam is often done as shown in Fig. 16.4 [41]. A split detector is used to measure the intensities of the two parts of the image plane. If the intensity difference is gradually displaced, a curve such as that shown in Fig. 16.4 is

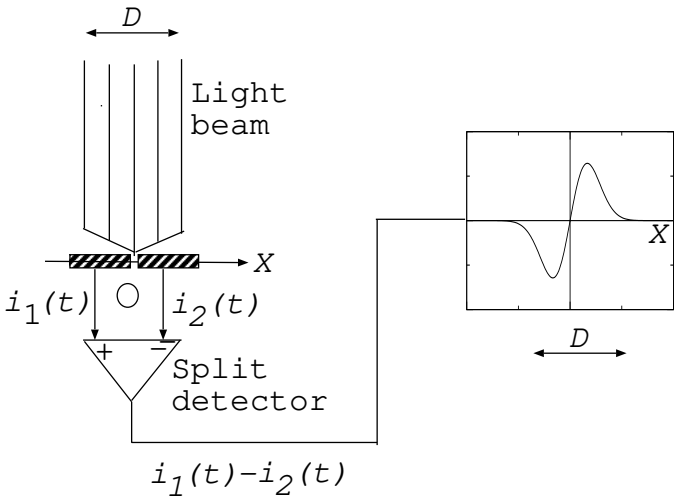

FIGURE 16.4
Measurement of displacement of a light beam (L.A. Lugiato, A. Gatti and E. Brambilla, *J. Opt. B: Quantum Semiclass. Opt.* 4:S176, 2002. https://doi.org/10.1088/1464-4266/4/3/372. IOP Publishing Ltd and Deutsche Physikalische Gesellschaft. Reproduced by permission of IOP Publishing. CC BY-NC-SA.).

obtained. Close to the point of exact balance, it is noticed that the difference between these intensities gives a signal which is proportional to the beam displacement D. The limitation in the precision in the measurement of the displacement is set by noise. For a classical, shot-noise limited laser source, the smallest measurable displacement (denoted as D_{SQL}) is worked out as [8]

$$D_{\mathrm{SQL}} = \frac{\sqrt{N}}{2I(0)} \,. \tag{16.14}$$

For a TEM_{00} Gaussian beam with radius ω_0, D_{SQL} becomes

$$D_{\mathrm{SQL}} = \sqrt{\frac{\pi}{8}} \frac{\omega_0}{\sqrt{N}} \,. \tag{16.15}$$

$\omega_0 = \lambda$ for a maximum focusing of the Gaussian beam. In this case $D_{\mathrm{SQL}} \approx \lambda/\sqrt{N}$. It is simply the absolute minimum displacement of a system measurable with the use of classical beam. Equation (16.15) suggests that a more powerful laser or a longer measurement time would provide enhanced measurement precision. But in many applications it is not practical to use a very powerful laser.

A single spatial mode, even squeezed, is not useful to reduce the noise in a displacement measurement below the shot-noise limit. This is because it lacks spatial correlation [42]. As the signal and idler beams in SPDC are correlated (both temporally and spatially), it has been proposed that these two beams could be useful in the two half parts of the image plane in the split detector. Now, the number of photons in the two paths is the same. As a result the fluctuations in the intensity difference are quite small. Hence, we can surpass the measurement limit in Eq. (16.15).

Small transverse displacement of a light beam beyond the standard quantum limit has been measured [43]. A strong spatially correlated light source was obtained. This can be

achieved, for example, by mixing a vacuum squeezed beam and a coherent beam falling in two specific orthogonal spatial modes. The position of this light beam can be measured using a beam split detector with an increased precision compared to the standard quantum limit. Further, a quantum laser pointer, a light beam the direction of which is measured with a precision higher than that possible with a usual laser beam, was achieved experimentally [44].

16.7 Quantum Lithography

The semiconductor industry exploits optical lithography to etch patterns on silicon wafer for making integrated circuits. So, the reduction in the size of the electronic components consequently depends on the minimum resolution of the light set forth. For classical light, the minimum resolution is given by *Rayleigh criterion*. It states that the minimal resolvable size occurs at a spacing corresponding to the distance between a peak and the adjacent through in an interference pattern. This criterion renders a limit for the resolution to be half the wavelength of the light used. We can reduce the size of the components making use of shorter wavelength. But use of high energy photons may cause damage to the object under investigation. Moreover, efficient mirrors and lenses for such short wavelengths are not easily available. So, it is impractical to consider the classical optical lithography for wavelengths shorter than about 100 nm.

Even using a classical light source we can double the resolution with two-photon absorption [45]. Quantum lithography which utilizes interference between groups of N-entangled photons has been proposed to overcome the diffraction limit by a factor N [46]. We give below the theory of quantum interferometric optical lithography proposed by Boto et al [46].

Figure 16.5 shows the interferometric lithographic set-up. Photons entering the ports A and B are made to strike the symmetric, lossless beam splitter (BS). Next, they are reflected by two mirrors (M). The photon amplitude in the upper path acquires a phase-shift ϕ at the phase-shifter (PS). Finally, the two branches interfere on the substrate S. In a typical classical interferometric lithography, when two coherent laser lights intersect at an angle 2θ then the normalized exposure dose at the substrate corresponding to the grazing angle $\theta = \pi/2$ is found to be $1 + 2\cos kx$, where $k = 2\pi/\lambda$ and $\phi = kx$. The Rayleigh criterion requires that $\phi_{\min} = \pi/2$. This gives $x_{\min} = \lambda/2$. This is the best resolution that is realizable using uncorrelated classical light.

In Yablonvich and Vrijen scheme [45], the classical two-photon are absorbed. So, two-photon the absorption probability scales quadratically with intensity. In this case the classical two-photon exposure dosage is

$$\Delta^{\mathrm{c}}_{2\gamma} = \frac{1}{2}(1 + \cos 2\phi)^2 = \frac{3}{4} + \cos 2\phi + \frac{1}{4}\cos 4\phi\,. \tag{16.16}$$

Note that if $\cos 2\phi$ in the above equation is eliminated then the $\cos 4\phi$ term gives $x_{\min,2\gamma} = \lambda/4$, a factor of 2 improvement.

In the theory of Boto et al. [46], the two input ports A and B are identified by the two annihilation operators a and b, respectively. These operators obey the photon commutation rules $\{a, a^\dagger\} = \{b, b^\dagger\} = 1$ and $\{a, b\} = 0$. On the screen S, the output electric field operator for the upper branch (C) is found to be c while that for the lower branch (D) is d. The transformation matrices for BS, M and PS are

$$B = \frac{1}{\sqrt{2}}\begin{pmatrix} -1 & \mathrm{i} \\ \mathrm{i} & -1 \end{pmatrix}, \quad R = \begin{pmatrix} -1 & 0 \\ 0 & -1 \end{pmatrix}, \quad P = \begin{pmatrix} \mathrm{e}^{\mathrm{i}\phi} & 0 \\ 0 & 1 \end{pmatrix}, \tag{16.17}$$

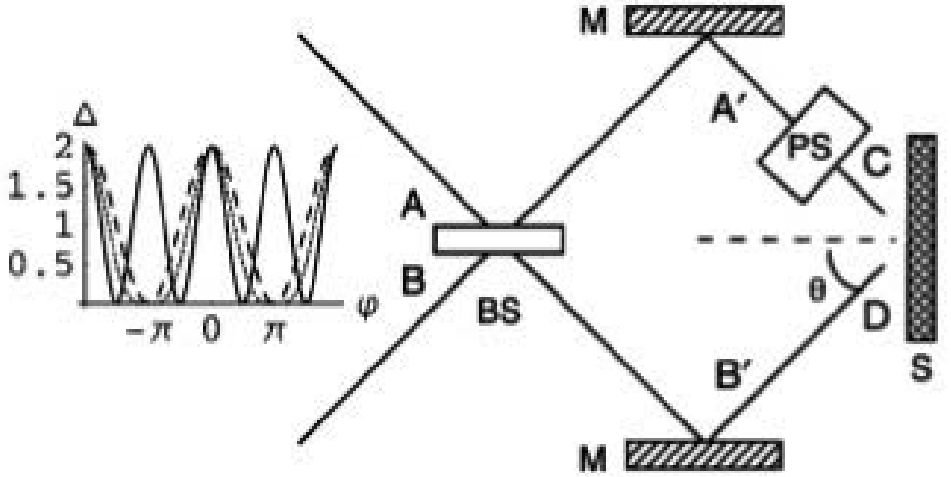

FIGURE 16.5
Interferometric lithography set-up. (Reproduced with permission from A.N. Boto, P. Kok, D.S. Abrams, S.L. Braunstein, C.P. Williams and J.P. Dowling, *Phys. Rev. Lett.* 85:2733, 2000. Copyright 2000, American Physical Society.)

respectively. Then $\begin{bmatrix} a \\ b \end{bmatrix}$ and $\begin{bmatrix} c \\ d \end{bmatrix}$ are related as

$$\begin{bmatrix} c \\ d \end{bmatrix} = PRB \begin{bmatrix} a \\ b \end{bmatrix} . \tag{16.18}$$

So, the total, scaled, electric field annihilation operator e is

$$c = (a - \mathrm{i}b)\,\mathrm{e}^{\mathrm{i}\phi}/\sqrt{2}, \quad d = (-\mathrm{i}a + b)/\sqrt{2}, \tag{16.19a}$$

$$e = c + d = \frac{1}{\sqrt{2}}\left(-\mathrm{i} + \mathrm{e}^{\mathrm{i}\phi}\right) a + \frac{1}{\sqrt{2}}\left(1 - \mathrm{i}\mathrm{e}^{\mathrm{i}\phi}\right) b\,. \tag{16.19b}$$

At the screen S, the N-photon absorption rate is proportional to the expectation value of $\delta_N = (e^\dagger)^N (e)^N / N!$. Then a two-photon exposure dosage $\Delta_{2\gamma}$ will be proportional to the expectation value of $(e^\dagger)^2 (e)^2 / 2!$.

For classical uncorrelated light, the input state is $|\psi_I\rangle = |1\rangle_A |0\rangle_B$ because the photons are incident one at a time on A. So, the classical deposition rate is given by

$$\Delta_{1\gamma}(\phi) = \langle\psi_I|\delta_1|\psi_I\rangle = 1 - \sin 2\phi = 1 + \cos(2\phi + \pi/2). \tag{16.20}$$

This is the usual classical result, apart from an unimportant phase factor. The classical two-photon deposition rate is then given by Eq. (16.16) dropping the phase factor. This gives $x_{\min} = \lambda/4$. This minimum value is achievable using a nonclassical product state $|\psi_{II}\rangle = |1\rangle_A |1\rangle_B$. This state is the output of a SPDC event. The deposition rate for this state is $\Delta^q_{2\gamma} = \langle\psi_{II}|\delta_2|\psi_{II}\rangle = 1 + \cos 4\phi$, where the $\cos 2\phi$ term does not appear as in the case of the classical two-photon absorption technique. Consequently, the quantum lithographic pattern gives the same $x_{\min} = \lambda/4$ with a narrower feature compared to the classical pattern.

The improvement has arisen because of quantum entanglement of the two photons. The input state $|\psi_{II}\rangle = |1\rangle_A |1\rangle_B$, after BS but before PS at the points A′ and B′ becomes the entangled state

$$|\psi_{\mathrm{E}}\rangle = \frac{1}{\sqrt{2}}\left(|2\rangle_{A'}|0\rangle_{B'} + |0\rangle_{A'}|2\rangle_{B'}\right) \tag{16.21}$$

as a result of interference effects upon passaging through BS. However, notice that the entanglement is between photon number and path. It is not possible to state whether both photons followed the lower path or the upper path. These two photons appeared as a single quantum mechanical object called a *diphoton*. The amplitude corresponding to the indistinguishable two paths would interfere after the diphoton passed the upper path thereby acquiring twice the phase-shift as with a single-photon process. So, at C and D the entangled state becomes

$$|\psi_{\rm E}(\phi)\rangle = \frac{1}{\sqrt{2}}\left(\mathrm{e}^{\mathrm{i}2\phi}|2\rangle_C|0\rangle_D + |0\rangle_C|2\rangle_D\right) . \tag{16.22}$$

This is the origin of the doubling of the resolution in the deposition rate $\Delta^q_{2\gamma}$.

For an entangled number state of the form $\left(|N\rangle_{A'}|0\rangle_{B'} + |0\rangle_{A'}|N\rangle_{B'}\right)/\sqrt{2}$ ($N00N$-state[1]), a phase of $N\phi$ has to be added at PS in the upper branch resulting in

$$|\psi_{\rm E}(N,\phi)\rangle = \frac{1}{\sqrt{2}}\left(\mathrm{e}^{\mathrm{i}N\phi}|N\rangle_C|0\rangle_D + |0\rangle_C|N\rangle_D\right) . \tag{16.23}$$

If the substrate is N-photon absorbing then the deposition function is given by [46]

$$\Delta^q_{N\gamma}(\phi) = \langle\psi_{\rm E}(N,\phi)|\delta_N|\psi_{\rm E}(N,\phi)\rangle = 1 + \cos 2N\phi . \tag{16.24}$$

It is with a resolution of $\lambda/(2N)$, N-times smaller than the classical value.

Though theoretically, quantum lithography is found to be more efficient than the classical one, the practical implementation of quantum lithography has to overcome several problems. Two significant experimental challenges are:

1. Producing efficient intense source of photons in $N00N$ state and
2. finding a sensitive N-photon lithographic recording medium.

For more discussions on quantum lithography one may refer to refs. [47–57].

16.8 Quantum Metrology

Metrology is the science of measurement and estimation of parameters of a system. Quantum metrology [58] takes into account (i) the quantum character of the systems and (ii) processes involved in the estimation of parameters. It also deals with the physical limits to measurements. Essentially, the use of quantum correlations leads to high precision phase measurements even with a lower particle flux than would be needed by classical systems. A typical measurement consists of three parts: the preparation of a probe, its interaction with the measuring system and the probe read-out. All measurements have statistical errors and are due to insufficient control of the probes or of the measured systems. Errors may occur as a consequence of fundamental constraint like the Heisenberg uncertainty relations. They can be reduced by repeating the measurement, say N-times, and then averaging the outcomes. This process may be repeated either with N-series of probes over time or with N-multiple probe systems simultaneously.

The error in a parameter estimation may be quantified by means of the statistical average of the square of the difference between the estimated and the true value of the parameter.

[1] A $N00N$ state is a many body entangled state given by $|\psi_{\rm E}(N,\phi)\rangle = \frac{1}{\sqrt{2}}[|N\rangle|0\rangle + \mathrm{e}^{\mathrm{i}N\phi}|0\rangle|N\rangle]$, where $|0\rangle|N\rangle$ represents 0 particle in one mode and N particle in another mode and the phase factor is ϕ.

The Cramér–Rao limit [59] provides a lower bound to this error and is inversely proportional to $\sqrt{N}$, where N is the number of repetitions of the measurement process. This is the case of classical measurement techniques. This limit is called the *standard quantum limit* (SQL). Using quantum mechanical strategies such as entanglement among the various probing devices used, we are able to get still lower bound, the so-called *Heisenberg bound*. This bound varies as $1/N$, an improvement of $\sqrt{N}$ times the classical accuracy.

In a single parameter estimation, Cramér–Rao bound is stated in terms of a quantity known as *Fisher information* [60]. Larger Fisher information results in a more accurate determination of the parameter. The quantum of information to be extracted from experiments about the exact value of a parameter is given by the Fisher information. This Fisher information depends on various factors including properties of the probe, the parameter-dependent process and the measurement on the probe considered to investigate the process. An important aim of metrology is to determine the Fisher information to identify the ways to maximize it and also to find protocols for better estimation. The ultimate estimation is realized by maximizing the *quantum Fisher information*.

The phase difference between interfering two light beams is a significant parameter which requires high precision. Optical phase measurement is useful to measure distance, position displacement, acceleration and optical path length. High precision optical phase measurements have several notable applications, such as microscopy, defining time-standards, measuring magnetic fields, material properties, gravity-wave detection and medical and biological sensing. The method of using non-classical states of light (the squeezed states) in order to enhance optical interferometers' sensitivity below the shot-noise limit has been proposed [61].

In quantum metrology, $N00N$ states are the enabling technology in quantum measurement schemes. In optics a $N00N$ state with N-entangled photons get a phase at a rate N-times of that acquired by the classical light, as discussed in the previous section. This leads to greatly improved phase sensitivity and is useful for attaining the Heisenberg limit. We show below that $N00N$ states lead to this limit.

We have seen in the previous section that the classical state $|\psi_I\rangle = |1\rangle_{\rm A}|0\rangle_{\rm B}$ becomes the state $|\psi(\phi)\rangle = (|0\rangle + {\rm e}^{{\rm i}\phi}|1\rangle)/\sqrt{2}$ in the interferometric set-up given in Fig. 16.5 at the screen. If the phase estimating operator is $A = |0\rangle\langle 1| + |1\rangle\langle 0|$ then $\langle A\rangle$ is $\langle\psi(\phi)|A|\psi(\phi)\rangle = \cos\phi$. When we repeat the experiment N times we get

$$_N\left\langle \psi(\phi)\right| \ldots {}_1\left\langle \psi(\phi)\right| \bigoplus_{k=1}^{N} A^k \left|\psi(\phi)\right\rangle_1 \ldots \left|\psi(\phi)\right\rangle_N = N\cos\phi\,. \tag{16.25}$$

Since $A^2 = 1$, the variance of A (denoted as $(\Delta A)^2$), is computed to be [62]

$$(\Delta A)^2 = N(1-\cos^2\phi) = N\sin^2\phi\,. \tag{16.26}$$

Then according to the estimation theory, the uncertainty in ϕ is [62]

$$\Delta\phi = \frac{\Delta A}{|{\rm d}\langle A\rangle/{\rm d}\phi|} = \frac{1}{\sqrt{N}}\,. \tag{16.27}$$

This is the standard uncertainty in ϕ after N trials. The point is that the uncertainty associated with the classical measurement of phase is inversely proportional to the square-root of the number of trials. This is called the *shot-noise limit*.

Quantum entanglement can considerably enhance the sensitivity of this scheme by a factor $\sqrt{N}$. For the nm-classical input state $|1\rangle|1\rangle$ in Fig. 16.5, at the screen we obtain $|\psi_{\rm E}(N,\phi)\rangle = |N,0\rangle + {\rm e}^{{\rm i}N\phi}|0,N\rangle$ (the $N00N$ state). For the phase estimation operator $A_N = |0,N\rangle\langle N,0| + |N,0\rangle\langle 0,N|$, we find $\langle\psi_{\rm E}(N,\phi)|A_N|\psi_{\rm E}(N,\phi)\rangle = \cos N\phi$. Notice that

$A_N^2 = 1$, $(\Delta A_N)^2 = 1 - \cos^2 N\phi = \sin^2 N\phi$. Using the same estimation, we arrive at the phase uncertainty for the $N00N$ state as

$$\Delta\phi_{\rm H} = \frac{\Delta A_N}{|{\rm d}\langle A_N\rangle/{\rm d}\phi|} = \frac{1}{N}\ . \tag{16.28}$$

We obtain the *Heisenberg limit* to the minimal detectable phase with notable improvement of $\sqrt{N}$ compared with the classical shot-noise limit.

An optical phase measurement has been shown [63] with an entangled four-photon interference visibility higher than the threshold to beat the standard quantum limit. $N00N$ states based on nuclear spin [64] and atomic spin waves [65] have been shown to achieve improved measurement sensitivity. Recent theoretical work has pointed out that interaction among particles is a very good resource for quantum metrology, scaling beyond the Heisenberg limit [66] and this was proved experimentally [67]. We know that any real system cannot be totally isolated from the environment. This leads to decoherence, which mitigates quantum effects, thereby setting limitations on the use of quantum strategies. The work reported [68] provides a general framework for quantum metrology in the presence of noise.

For various advances and the applications made on quantum metrology one may refer to the refs. [61,69–73]. Quantum metrology with multiparameter estimation [74], atomic ensembles [75], quantum error correction [76], non-Markovian environments [77], entanglement against noise [78], entangled coherent states [79,80], compatability features [81], sensitivity beyond Heisenberg limit [82] and scanning probe atom interferometer [83] have been analyzed.

Solved Problem 2:

Polarization beam splitter (PBS) is a device that transmits one polarization of light and reflects the other polarization orthogonal to the transmitted one. Let $|H\rangle$ and $|V\rangle$ represent the horizontal polarization state and vertical polarization state, respectively. Show that if we represent the states $|D\rangle$ and $|A\rangle$ for light polarized along 45° and −45°, respectively, and single photon of each of these states is supplied to the two input ports of a PBS then in the output port a 2002 state in the V/H basis is produced.

The annihilation operators have the transformation due to PBS as

$$a_{\rm D} = \frac{1}{\sqrt{2}}(a_{\rm H} + a_{\rm V}), \quad a_{\rm A} = \frac{1}{\sqrt{2}}(a_{\rm H} - a_{\rm V}), \tag{16.29}$$

$$a_{\rm D}^\dagger = \frac{1}{\sqrt{2}}(a_{\rm H}^\dagger + a_{\rm V}^\dagger), \quad a_{\rm A}^\dagger = \frac{1}{\sqrt{2}}(a_{\rm H}^\dagger - a_{\rm V}^\dagger). \tag{16.30}$$

Since the input state is $|1\rangle_{\rm D}|1\rangle_{\rm A}$, we write it as $a_{\rm D}^\dagger a_{\rm A}^\dagger|0\rangle|0\rangle$. Using Eq. (16.30), we get the output state as

$$\begin{aligned} |\psi\rangle_{\rm HV} &= \frac{1}{\sqrt{2}}(a_{\rm H}^\dagger + a_{\rm V}^\dagger)\frac{1}{\sqrt{2}}(a_{\rm H}^\dagger - a_{\rm V}^\dagger)|0\rangle|0\rangle \\ &= \frac{1}{2}a_{\rm H}^{\dagger^2}|0\rangle|0\rangle - \frac{1}{2}a_{\rm V}^{\dagger^2}|0\rangle|0\rangle \\ &= \frac{\sqrt{2}}{2}|2\rangle_{\rm H}|0\rangle_{\rm V} - \frac{\sqrt{2}}{2}|0\rangle_{\rm H}|2\rangle_{\rm V} \\ &= \frac{1}{\sqrt{2}}(|2\rangle_{\rm H}|0\rangle_{\rm V} - |0\rangle_{\rm H}|2\rangle_{\rm V}) \end{aligned} \tag{16.31}$$

which is a 2002 state.

16.9 Quantum Teleportation of Optical Images

Sokolov and his coworkers [84] proposed a continuous variable teleportation scheme to teleport the quantum state of spatially multimode electromagnetic fields. This method allows the reconstruction of an image with preserving its quantum correlation. It generalizes the proposal in the refs.[85,86]. Solokov et al established the possibility of achieving parallel teleportation of two-dimensional optical images by taking into account a spatially multimode field. The crucial part of the scheme is a pair of EPR light beams. As a consequence of the multimode nature of entanglement the scheme can be used for parallel teleportation of N elements of input wave front with the preservation of their space and time correlations.

The EPR beams are obtained by interference mixing at a $50:50$ beam splitter of two multimode broadband squeezed beams, generated by two degenerate optical parametric amplifiers (OPA). It is possible to generate them by a single broadband OPA, degenerate in frequency, with type-II phase matching.

Let $E_1(\rho,t)$ and $E_2(\rho,t)$ be the two EPR beam fields and $A_{\rm in}(\rho,t)$ is the input image field. To detect the components of the input field, it is mixed with the EPR beam $E_1(\rho,t)$ at a $50:50$ beam splitter. By this we get the input fields of two balanced homodyne detectors D_x and D_y:

$$B_{x,y}(\rho,t)=\frac{1}{\sqrt{2}}\left[\pm A_{\rm in}(\rho,t)+E_1(\rho,t)\right] \tag{16.32}$$

with $+(-)$ sign corresponding to $x(y)$. These fields are mixed with two oscillator fields with amplitudes B_0 and $-{\rm i}B_0$, where B_0 is real, at two symmetric beam splitters. Suppose the pixels of the CCD matrices are smaller than the coherence area of the EPR beam. In this case the photo-currents collected from the pixels D_x and D_y at the points ρ are given by

$$I_x=B_0\left[B_x(\rho,t)+B_x^{\dagger}(\rho,t)\right]\ ,\quad I_y=-{\rm i}B_0\left[B_y(\rho,t)-B_y^{\dagger}(\rho,t)\right]. \tag{16.33}$$

These currents are sent from Alice to Bob through two multichannel classical communication lines. Bob uses them for local modulation of an external coherent wave phase matched with the EPR fields. In the modulated beam, the field component proportional to $I_x-{\rm i}I_y$ is created. The teleported field $A_{\rm out}(\rho,t)$ is got by interference mixing at a mirror with high reflectivity of the field with the second EPR beam $E_2(\rho,t)$. The teleported field $A_{\rm out}(\rho,t)$ becomes

$$A_{\rm out}(\rho,t)=A_{\rm in}(\rho,t)+F(\rho,t)\ , \tag{16.34}$$

where $F(\rho,t)=\widetilde{E}_2(\rho,t)+\widetilde{E}_1^{\dagger}(\rho,t)$ is the noise field added by the teleportation process.

In the ideal case of perfect entanglement of the EPR beams, $E_2(\rho,t)$ and $E_1^{\dagger}(\rho,t)$ are perfectly anticorrelated and thereby cancel their quantum fluctuations. This corresponds to the perfect *point-to-point* in space and instantaneous in time teleportation of the quantum state of the input fields (as $A_{\rm out}(\rho,t)$ equals $A_{\rm in}(\rho,t)$). As this process appears like holography, it is called as *quantum holographic teleportation*. In a new version of quantum holographic teleportation [87] quantum entanglement between the light fields of different frequencies is used. It permits the wavelength conversion between the original and the teleported images.

16.10 Quantum Sensors

Quantum sensors employ quantum probes to estimate parameters. A quantum sensor makes use of a quantum system, quantum properties or quantum phenomena to perform a mea-

surement of a physical quantity. It can estimate a parameter with precision beyond what is possible by classical resources [88]. Quantum sensors are being used for sensing and estimating various physical quantities ranging from magnetic and electric fields, time, frequency, rotations, phonon density, gravity, voltage, displacement, refractive index, temperature and pressure. As quantum systems have strong sensitivity to external disturbances quantum sensors are expected to have high sensitivity.

1. Definition

Quantum sensing is defined by any one of the following [89]:

1. Use of a quantum object such as the quantized energy levels to measure a physical quantity.
2. Use of quantum coherence (wave-like spatial and temporal superposition states) to measure a physical quantity.
3. Use of quantum entanglement to get sensitivity and precision of a measurement beyond that can be achieved by classical sensors.

2. Attributes

For a quantum system to function as a quantum sensor, it must have the following four attributes [89]:

1. The quantum system must have discrete resolvable energy levels. For example, it can be a two-level system with upper energy level $|1\rangle$ and lower energy level $|0\rangle$ with the energy difference $E = \hbar\omega_0$. Changes in the transition frequency ω_0 or the transition rate Γ can be sensed by a quantum probe.
2. It should be possible to initialize the quantum system to a known state and to read-out its state.
3. An external time-dependent field must be able to coherently manipulate the quantum system.
4. The quantum system should interact with a relevant physical quantity $V(t)$ such as an electric field and magnetic field. The interaction is quantified by the parameter $\gamma = \partial^q E/\partial V^q$ which gives the change of energy with respect to change of $V(t)$.

3. Characteristics

Certain physical characteristics can be defined and used for applicability and experimental realization of quantum sensors. One characteristic is the type of external parameter(s) for which the quantum system responds to. For example, a trapped ion quantum system responds to external electric field whereas a spin-based system is sensitive to external magnetic field. Sensor's intrinsic sensitivity is the second characteristic. The sensitivity of a quantum sensor is decided by two conflicting factors. Though a strong response to an external signal will increase the sensitivity, the unwanted noise will also affect the sensitivity of that system more. The sensitivity is proportional to $1/(\gamma\sqrt{T_X})$ [89], where T_X is the decoherence time. Large γ and longer decoherence time will optimize the sensitivity.

4. Examples

An exhaustive list of the most important experimental implementations of quantum sensors exists [89]. A Rydberg atom is an excited atom having one or more electrons with very

high principal quantum number n. Such atoms are suitable for sensing electric fields. The loosely confined electrons found in a highly excited state are coupled by electric dipole transitions. These transitions are strong and the states undergo strong Stark shifts [90,91]. Laser excitation and spectroscopy are useful for preparation and read-out of states. Rydberg atoms are utilized as single-photon sensors in a cryogenic cavity for microwave photons [92–95]. Rydberg states are also used to detect weak electric fields [96,97] and microwave.

Beams of neutrons have been used for the measurement of Berry's phase by introducing spin rotations by means of magnetic fields along the parts of the neutron trajectory [98]. Spin polarization of slow beams of thermal neutrons are possible by employing Bragg reflection on an appropriate magnetic crystal. Using spin sensitive Bragg analyzer the spin read-out is realizable. Sensing gravity on small length scale by ultracold neutrons is feasible. This experimental sensing process considers the reflection of the matter waves associated with slow neturons by suitable materials and trapping of the neutrons over a bulk surface by the earth's gravity [99]. Certain properties of materials can be explored by the measurement of small (1 neV) energy loss of neutrons in inelastic scattering process.

Sensing qubits by alkali atoms, magnetic/electric fields by atomic vapors, cold atomic clouds, trapped ions, NMR ensemble, SQUIDs and single electron transistors, phase-drift of a local oscillator by atomic clocks, materials characterization and measuring small fields ($\sim$ 100 fT) of electric currents in the brain and signal processing by SQUIDs have been reported. Optomechanical sensors are applied to measure minute forces ($12\,\mathrm{zN}/\sqrt{\mathrm{Hz}}$), mass ($2\,\mathrm{yg}/\sqrt{\mathrm{Hz}}$), acceleration ($100\,\mathrm{ng}/\sqrt{\mathrm{Hz}}$) and voltage ($5\,\mathrm{pV}\sqrt{\mathrm{Hz}}$).

5. Sensing Protocol

The quantum sensing protocol consists of the following three elementary steps [89]:

1. The initialization of the quantum sensors.
2. The interaction with the signal of interest.
3. The read-out of the final state.

Phase estimation [100] and parameter estimation [101] techniques are then used to reconstruct the physical quantity from a series of measurements. An intereference measurement using pump-probe spectroscopy is generally done.

The generic Hamiltonian to describe the quantum sensors is assumed as

$$H(t) = H_0 + H_V(t) + H_c(t)\,, \tag{16.35}$$

where H_0 is the internal Hamiltonian, $H_V(t)$ is the Hamiltonian for the signal $V(t)$ and H_c is the control Hamiltonian which is chosen for manipulating and tuning the sensor in a controlled way. The aim of the sensor is to measure $V(t)$ from the effect it has on the qubit due to its Hamiltonian H_V under the control of H_c. The internal Hamiltonian may be a static one with two energy eigenvalues E_0 and E_1 with eigenstates $|0\rangle$ and $|1\rangle$. So, H_0 can be given as

$$H_0 = E_0|0\rangle\langle 0| + E_1|1\rangle\langle 1|\,. \tag{16.36}$$

The signal Hamiltonian $H_V(t)$ acts as a small perturbation to H_0 and it can be separated into two parts, namely, parallel and transverse components as

$$H_V(t) = H_{V_\parallel}(t) + H_{V_\perp}(t)\,, \tag{16.37}$$

where $H_{V_\parallel}(t)$ is the parallel and $H_{V_\perp}(t)$ is the transverse components. If γ is the coupling constant then the two components can be given as

$$H_{V_\parallel}(t) = \frac{1}{2}\gamma V_\parallel \left(|1\rangle\langle 1| - |0\rangle\langle 0|\right), \tag{16.38a}$$

$$H_{V_\perp}(t) = \frac{1}{2}\gamma \left(V_\perp(t)|1\rangle\langle 0| + V_\perp^\dagger(t)|0\rangle\langle 1|\right). \tag{16.38b}$$

The parallel and transverse components of $V(t)$ have different effects on the sensors as $H_{V_\parallel}(t)$ commutes with H_0 and $H_{V_\perp}(t)$ does not commute with H_0.

Solved Problem 3:

Show that the signal Hamiltonian $H_V(t) = (\gamma/2)\mathbf{V}(t)\cdot\boldsymbol{\sigma}$, for the two signal functions $V_\parallel(t)$ and $V_\perp(t)$ defined by Eqs. (16.38) gives $V_\parallel = V_z(t)$ and $V_\perp = V_x + \mathrm{i}V_y$ if the qubit quantization axis is taken as the z-axis, apart from a phase factor.

We write $H_V = (\gamma/2)\left(V_x\sigma_x + V_y\sigma_y + V_z\sigma_z\right)$, $H_{V_\parallel} = (\gamma/2)V_z\sigma_z$ and $H_{V_\perp} = (\gamma/2)\left(V_x\sigma_x + V_y\sigma_y\right)$. Then Eq. (16.38a) gives $V_z\sigma_z = V_\parallel\left(|1\rangle\langle 1| - |0\rangle\langle 0|\right)$. As

$$\begin{aligned} |1\rangle\langle 1| - |0\rangle\langle 0| &= \begin{bmatrix} 0 \\ 1 \end{bmatrix} \otimes \begin{bmatrix} 0 & 1 \end{bmatrix} - \begin{bmatrix} 1 \\ 0 \end{bmatrix} \otimes \begin{bmatrix} 1 & 0 \end{bmatrix} \\ &= \begin{bmatrix} 0 & 0 \\ 0 & 1 \end{bmatrix} - \begin{bmatrix} 1 & 0 \\ 0 & 0 \end{bmatrix} \\ &= \begin{bmatrix} -1 & 0 \\ 0 & 1 \end{bmatrix} \\ &= -\sigma_z \end{aligned} \tag{16.39}$$

from $V_z\sigma_z = V_\parallel\left(|1\rangle\langle 1| - |0\rangle\langle 0|\right)$ we get $V_\parallel = V_z$ apart from a phase factor.

Next, from Eq. (16.38b) we obtain

$$V_x\sigma_x + V_y\sigma_y = V_\perp(t)|1\rangle\langle 0| + V_\perp^\dagger(t)|0\rangle\langle 1|. \tag{16.40}$$

Then

$$\begin{aligned} V_x\sigma_x + V_y\sigma_y &= V_x \begin{pmatrix} 0 & 1 \\ 1 & 0 \end{pmatrix} + V_y \begin{pmatrix} 0 & -\mathrm{i} \\ \mathrm{i} & 0 \end{pmatrix} \\ &= \begin{pmatrix} 0 & V_x - \mathrm{i}V_y \\ V_x + \mathrm{i}V_y & 0 \end{pmatrix} \end{aligned} \tag{16.41}$$

and

$$\begin{aligned} V_\perp(t)|1\rangle\langle 0| + V_\perp^\dagger(t)|0\rangle\langle 1| &= V_\perp \begin{bmatrix} 0 \\ 1 \end{bmatrix} \begin{bmatrix} 1 & 0 \end{bmatrix} + V_\perp^\dagger \begin{bmatrix} 1 \\ 0 \end{bmatrix} \begin{bmatrix} 0 & 1 \end{bmatrix} \\ &= V_\perp \begin{bmatrix} 0 & 0 \\ 1 & 0 \end{bmatrix} + V_\perp^\dagger \begin{bmatrix} 0 & 1 \\ 0 & 0 \end{bmatrix} \\ &= \begin{bmatrix} 0 & V_\perp^\dagger \\ V_\perp & 0 \end{bmatrix}. \end{aligned} \tag{16.42}$$

From Eqs. (16.40)-(16.42) we find $V_\perp = V_x + \mathrm{i}V_y$.

A typical quantum sensing process contains the following steps [89]. First, the quantum sensor is initialized to a basis state, say, $|0\rangle$. Then the transformation $|\psi_0\rangle = U_\mathrm{a}|0\rangle$ is applied

to get the desire initial sensing state $|\psi_0\rangle$ using a set of control pulses represented by U_a. After that the $|\psi_0\rangle$ evolves for a time duration t under the Hamiltonian H and we get the final sensing state

$$|\psi(t)\rangle = U_H(0,t)|\psi_0\rangle = C_0|\psi_0\rangle + C_1|\psi_1\rangle\,, \tag{16.43}$$

where $|\psi_0\rangle$ and $|\psi_1\rangle$ are orthogonal. Next, $|\psi(t)\rangle$ is transformed into the read-out state $|\alpha\rangle$ by the transformation U_b:

$$|\alpha\rangle = U_\mathrm{b}|\psi(t)\rangle = C_0'|0'\rangle + C_1'|1'\rangle\,. \tag{16.44}$$

If the initial basis $\{|0\rangle, |1\rangle\}$ is the same as the read-out basis $\{|0'\rangle, |1'\rangle\}$ then $U_\mathrm{b} = U_\mathrm{a}^\dagger$. Under this condition $C_0' = C_0$ and $C_1' = C_1$. The final state of the quantum sensor is read-out. The projective read out process yields an answer 1 with a probability p' and an answer 0 with probability $1 - p'$. Here $p' = |C_1'|^2 \propto p$. Note that $p = 1 - |C_0|^2 = |C_1|^2$ is the measurable transition probability. The measurement apparatus detects 0 and 1 as a voltage, current, photon counts or polarization. This whole process is repeated many times to get more accurate estimate of p. p is measured as a function of time or as a function of a parameter of the control Hamiltonian. Then using the data $\{p_i\}$ the desired signal V is inferred.

As an example of this quantum sensing protocol, let us consider the measurement of the static energy splitting ω_0 using Ramsey interferometry measurement [89,102,103]. After the quantum sensor is initialized into $|0\rangle$ a $\pi/2$ pulse transforms it into

$$|\psi_0\rangle = |+\rangle = \frac{1}{\sqrt{2}}\left(|0\rangle + |1\rangle\right)\,. \tag{16.45}$$

It evolves under H_0 during a time t and

$$|\psi(t)\rangle = \frac{1}{\sqrt{2}}\left(|0\rangle + \mathrm{e}^{-\mathrm{i}\omega_0 t}|1\rangle\right)\,. \tag{16.46}$$

Applying again a $\pi/2$ pulse $|\psi(t)\rangle$ is transformed into the measurable state

$$|\alpha\rangle = \frac{1}{2}\left(1 + \mathrm{e}^{-\mathrm{i}\omega_0 t}\right)|0\rangle + \frac{1}{2}\left(1 - \mathrm{e}^{-\mathrm{i}\omega_0 t}\right)|1\rangle\,. \tag{16.47}$$

The final read-out state gives the transition probability

$$p = 1 - |\langle 0|\alpha\rangle|^2 = \frac{1}{2}\left(1 - \cos\omega_0 t\right)\,. \tag{16.48}$$

Measurement of p as a function of t gives the frequency. In this way, Ramsey measurement can be used to measure the energy splitting ω_0.

Many advanced sensing techniques like adaptive methods to enhance the dynamic range of sensors, techniques using multiple qubits, entangled enhanced sensing and quantum correction schemes have been discussed in [89]. Multiparameter estimation [104], evaluating resources for precesion measurement [105], layer thickness measurement using terahertz photons [106], sensing with a single electron spin [107], enhancement of nuclear spin imaging [108] and nano sensors prepared with implanted nitrogen-vacancy centers [109] have been reported.

Quantum sensing is an exciting new development which is linking various efforts in science and technology thereby developing new applications in metrology. Applications of quantum sensing continue to expand as new types and more sophisticated advanced sensor implementations are more and more available. Quantum sensing become an important resource for quantum technologies as it can help to understand decoherence which affects all quantum devices.

16.11 Quantum Batteries

It is well known that collective quantum phenomena offer many advantages compared to classical systems in areas such as computations, secure communication and metrology. It has been found that quantum batteries can have more advantages than the classical batteries [110–115]. Robert Alicki and Mark Fannes suggested that the entangling operations lead to increased work extraction from an energy storage device called *quantum battery* [112]. A battery is a physical system where energy is stored. Quantum batteries are quantum mechanical systems for storing energy, where quantum effects can be used to obtain more efficient and faster charging and discharging compared to classical analog systems. In a quantum battery energy is stored in the energy levels and coherence.

1. Hamiltonian and Density Matrix

Let us consider the wave functions of the battery to be chosen in a d-dimensional Hilbert space $\mathcal{H}$. The basis of $\mathcal{H}$ is chosen as the eigenvectors of the Hamiltonian H of the system. H is assumed as [112]

$$H = \sum_{j=1}^{d} \epsilon_j |j\rangle\langle j| \,, \quad \epsilon_{j+1} > \epsilon_j \,. \tag{16.49}$$

The internal Hamiltonian H is expressed with increasing energy levels ϵ_j and are assumed to be nondegenerate. A simple quantum battery can be considered as a spin-1/2 system to which a uniform magnetic field is applied. Its internal Hamiltonian has a higher energy level ϵ for the eigenvector $|1\rangle$ and $-\epsilon$ for the eigenvector $|-1\rangle$. We can think of $|1\rangle$ state as a charged battery and $|-1\rangle$ state as the empty battery. No work can be deposited into $|1\rangle$ state and no work can be extracted from $|-1\rangle$ state.

If the initial state of the battery is described by a density matrix ρ then the internal energy of the battery is given by $\mathrm{Tr}(\rho H)$. Charging a battery is to change the battery state ρ to a more energetic state ρ' such that $\mathrm{Tr}\,[(\rho' - \rho)H] \geq 0$. Usuage of the battery will take it to a lower energy state ρ'' such that $\mathrm{Tr}\,[(\rho'' - \rho)H] \leq 0$. Both charging and discharging processes are done by unitary processes. This is achieved by using time-dependent fields $V(t)$ which act for the duration $0 \leq t \leq \tau$. $V(t) = 0$ for $t > \tau$.

Let us consider that the field $V(t)$ is used to extract energy from the battery. At time $t = 0$, $\rho = \rho(0)$. To find $\rho(t)$ we consider the Liouville–von Neumann equation ($\hbar = 1$)

$$\dot{\rho}(t) = -\mathrm{i}\,[H + V(t),\, \rho(t)] \,. \tag{16.50}$$

A solution of Eq. (16.50) is written as

$$\rho(t) = U(t)\rho U^{\dagger}(t), \quad \rho = \rho(0), \tag{16.51}$$

where U is the time-ordered unitary transformation on the Hilbert space $\mathcal{H}$ of the battery. During the charging process no heat will be generated since the evolution is unitary.

With $\mathcal{T}$ being the time-ordering operator U is given as the exponential of the generator $H + V(t)$ as [112]

$$U(\tau) = \mathcal{T}\left\{\exp\left[-\mathrm{i}\int_0^{\tau} \mathrm{d}s\,(H + V(s))\right]\right\} \,. \tag{16.52}$$

2. Ergotropy – Maximal Extractable Work

We find the work W extracted after time τ by the above procedure as

$$W = \mathrm{Tr}\,[\rho H] - \mathrm{Tr}\,[\rho(\tau)H] = \mathrm{Tr}\,[\rho H] - \mathrm{Tr}\left[U(\tau)\rho U^{\dagger}(\tau)H\right] \,. \tag{16.53}$$

The average charging power is $P = W/\tau$. We can get the maximum amount of work by optimizing W over all unitary operations. Therefore, the maximal amount of extractable work $W_{\max}$ is defined as

$$W_{\max} = \mathrm{Tr}\left[\rho H\right] - \min \mathrm{Tr}\left[U(\tau)\rho U^{\dagger}(\tau) H\right] . \tag{16.54}$$

The minimum in Eq. (16.54) is found by taking all unitary transformations of the Hiolbert space $\mathcal{H}$. $W_{\max}$ is known as *ergotropy* [112,116].

An energy state σ is called a *passive state* if no work can be extracted from it [112,117,118]. Then for such a σ, for all the unitary transformations U

$$\mathrm{Tr}(\sigma H) \leq \mathrm{Tr}(U\sigma U^{\dagger} H) . \tag{16.55}$$

Equivalently, σ is passive *if and only if* [112]

$$\sigma = \sum_{j=1}^{d} s_j |j\rangle\langle j| , \quad s_{j+1} \leq s_j . \tag{16.56}$$

So, σ is passive if and only if it commutes with H and further its eigenvalues s_j are not increasing with energy. For a given state ρ there exists a unique passive state σ_ρ which can be obtained by a unitary transformation U_ρ as

$$\sigma_\rho = U_\rho \rho U_\rho^{\dagger} = \sum_{j=1}^{d} \lambda_j |j\rangle\langle j| , \quad \lambda_{j+1} \leq \lambda_j , \tag{16.57}$$

where λ_j are the eigenvalues of ρ. Using Eqs. (16.49) and (16.57) we find the minimal energy as $\sum_{j=1}^{d} \lambda_j \epsilon_j$ and the maximum amount of extractable work as

$$W_{\max} = \mathrm{Tr}(\rho H) - \mathrm{Tr}(\sigma_\rho H) . \tag{16.58}$$

3. Lower Bound On $W_{\max}$

A lower bound to $W_{\max}$ can be obtained by considering the Gibbs state $\omega_{\bar{\beta}}$ (an equilibrium probability distribution which does not vary while a system evolves with time) which has the same entropy as ρ. Here β is inverse temperature and $\bar{\beta}$ is a suitably chosen β. $\omega_{\bar{\beta}}$ is given by

$$\omega_{\bar{\beta}} = \frac{1}{Z} \mathrm{e}^{-\beta H} , \tag{16.59}$$

where Z is a partition function. Then the von Neumann entropy $S(\rho)$ of a density matrix is $S(\rho) = -\mathrm{Tr}(\rho \ln \rho)$. There exists a unique value of $\beta = \bar{\beta}$ such that $S(\rho) = S(\omega_{\bar{\beta}})$. Then using the variational principle of statistical mechanics one can prove that

$$\mathrm{Tr}(\rho H) - \frac{1}{\bar{\beta}} S(\rho) \geq \mathrm{Tr}(\omega_{\bar{\beta}} H) - \frac{1}{\bar{\beta}} S(\omega_{\bar{\beta}}) . \tag{16.60}$$

As $S(\rho) = S(\omega_{\bar{\beta}})$ for $\beta = \bar{\beta}$ the above equation gives $\mathrm{Tr}(\rho H) \geq \mathrm{Tr}(\omega_{\bar{\beta}} H)$. Equation (16.58) gives $\mathrm{Tr}(\rho H) > \mathrm{Tr}(\sigma_\rho H)$. Therefore,

$$\mathrm{Tr}(\rho H) \geq \mathrm{Tr}(\sigma_\rho H) \geq \mathrm{Tr}(\omega_{\bar{\beta}} H) . \tag{16.61}$$

Then from Eqs.(16.58) and (16.61) the bound for $W_{\max}$ is

$$W_{\max} \leq \mathrm{Tr}(\rho H) - \mathrm{Tr}(\omega_{\bar{\beta}} H)\,. \tag{16.62}$$

Generally, the Gibbs state $\omega_{\bar{\beta}}$ and the passive state σ_ρ (or ρ) have different eigenvalues and hence they are different.

4. Ensemble of Batteries

As the product of two independent copies of a passive state is not still passive generally, it is possible to enhance $W_{\max}$ by using several copies of a system. Using entangling of many batteries one can, in general, extract more work per battery from several independent copies of a battery [112]. Consider an ensemble consisting of n identical d-dimensional batteries. The Hamiltonian of this new battery is written as $H^{(n)} = \sum_{l=1}^{n} H_l$. For a single battery the bound on $W_{\max}$ is given by Eq. (16.62). For the case of the ensemble of n batteries the $W_{\max}$ per battery is [112]

$$\begin{aligned} W_{\max}^{(n)} &= \frac{1}{n}\left\{\mathrm{Tr}\left[(\otimes^n \rho)\, H^{(n)}\right] - \mathrm{Tr}\left[\sigma_{\otimes^n \rho} H^{(n)}\right]\right\} \\ &\leq \mathrm{Tr}\left(\rho H^{(1)}\right) - \mathrm{Tr}\left(\omega_{\bar{\beta}} H^{(1)}\right)\,. \end{aligned} \tag{16.63}$$

Solved Problem 4:

A five-level system with internal Hamiltonian $H = L_z \sum_{l=1}^{5}(l-3)|l\rangle\langle l|$ in state $\rho = 0.1|1\rangle\langle 1| + 0.2|2\rangle\langle 2| + 0.3|4\rangle\langle 4| + 0.4|5\rangle\langle 5|$ has an associated passive state $\sigma_\rho = 0.4|1\rangle\langle 1| + 0.3|2\rangle\langle 2| + 0.2|3\rangle\langle 3| + 0.1|4\rangle\langle 4|$. Find the ergotropy $W_{\max}$ and show that σ_ρ can be obtained by the unitary transformation $U = |1\rangle\langle 5| + |2\rangle\langle 4| + |5\rangle\langle 3| + |3\rangle\langle 2| + |4\rangle\langle 1|$ of ρ.

$W_{\max}$ is given by Eq. (16.58). The given Hamiltonian is

$$H = L_z\,[-2|1\rangle\langle 1| - 1|2\rangle\langle 2| + 1|4\rangle\langle 4| + 2|5\rangle\langle 5|\,]\,. \tag{16.64}$$

Using the given ρ and the orthogonality relations $\langle i|j\rangle = \delta_{ij}$, we obtain

$$\begin{aligned} \mathrm{Tr}(\rho H) &= L_z \mathrm{Tr}\,[\,(\,0.1|1\rangle\langle 1| + 0.2|2\rangle\langle 2| + 0.3|4\rangle\langle 4| + 0.4|5\rangle\langle 5|\,) \\ &\qquad \times (\,-2|1\rangle\langle 1| - 1|2\rangle\langle 2| + 1|4\rangle\langle 4| + 2|5\rangle\langle 5|\,)\,] \\ &= L_z \mathrm{Tr}\,[-0.2|1\rangle\langle 1| - 0.2|2\rangle\langle 2| + 0.3|4\rangle\langle 4| + 0.8|5\rangle\langle 5|\,] \\ &= L_z(-0.2 - 0.2 + 0.3 + 0.8) \\ &= 0.7 L_z\,. \end{aligned} \tag{16.65}$$

Next,

$$\begin{aligned} \mathrm{Tr}(\sigma_\rho H) &= L_z \mathrm{Tr}\,[\,(\,0.4|1\rangle\langle 1| + 0.3|2\rangle\langle 2| + 0.2|3\rangle\langle 3| + 0.1|4\rangle\langle 4|\,) \\ &\qquad \times (\,-2|1\rangle\langle 1| - 1|2\rangle\langle 2| + 1|4\rangle\langle 4| + 2|5\rangle\langle 5|\,)] \\ &= L_z \mathrm{Tr}\,[-0.8|1\rangle\langle 1| - 0.3|2\rangle\langle 2| + 0.1|4\rangle\langle 4|\,] \\ &= -L_z\,. \end{aligned} \tag{16.66}$$

Thus, $W_{\max} = \mathrm{Tr}(\rho H) - \mathrm{Tr}(\sigma_\rho H) = 1.7 L_z$.

For the given U the $U^\dagger$ is

$$U^\dagger = |5\rangle\langle 1| + |4\rangle\langle 2| + |3\rangle\langle 5| + |2\rangle\langle 3| + |1\rangle\langle 4|\,. \tag{16.67}$$

Then

$$\rho U^\dagger = 0.1|1\rangle\langle 4| + 0.2|2\rangle\langle 3| + 0.3|4\rangle\langle 2| + 0.4|5\rangle\langle 1| \tag{16.68}$$

and then

$$U\rho U^\dagger = 0.4|1\rangle\langle 1| + 0.3|2\rangle\langle 2| + 0.2|3\rangle\langle 3| + 0.1|4\rangle\langle 4| = \sigma_\rho\,. \tag{16.69}$$

The process of charging and discharging the identical batteries (cells) in an ensemble could introduce quantum correlation among them. The question is whether these correlations offer any quantum advantages to outperform a classical battery. A battery is characterized by capacity, power and variance. Capacity refers to the amount of energy a battery can store and deliver. Power signifies how fast a battery can be charged or discharged. Variance in the stored energy determines to which extent the stored energy can be deterministically accessed. For a battery composed of many noninteracting identical quantum cells, correlations play no role as the capacity is additive. On the other hand, intercell correlations offer certain quantum advantages to power as it is not additive [119].

Theory for random quantum batteries [120], adiabatic protocol for stable charged state [121], open quantum batteries protocol [122–124] and models of quantum batteries [125–127] are developed. Role of correlations [128] and numerical analysis of energy flow [129] in quantum batteries and comparison of quantum batteries with classical versions [130] have been reported.

Many new quantum devices for applications in quantum information processing such as quantum gates are being developed. So, developing strategies to store energy to be consumed by quantum devices has made quantum batteries a significant field of research. Many different models of quantum batteries have been theoretically proposed. Still developing quantum batteries for practical applications faces many technological challenges, for example, the small and sensitive systems like quantum batteries would interact with the surrounding environment which could dissipate the energy stored.

16.12 Quantum Internet

A long range quantum communication network is one of the most promising applications of quantum technologies. We have seen in sec. 16.9 how an original qubit can be sent by Alice to Bob by a process called quantum teleportation making use of entanglement of two quantum particles. The number of qubits that can be embedded and interconnected in a quantum device dictates the computational power of that device. But currently available quantum computing devices operate only with a few tens of qubits. The number of qubits are to be increased significantly in order to have quantum supremacy over classical computers. The problem of scaling up the number of qubits can be solved by interconnecting multiple low qubit devices through a quantum communication network called *quantum internet* [131–138]. This network with nodes and quantum links is capable of permitting the parties to do efficient quantum communications.

1. Essential Quantum Hardware Elements

There are three essential quantum hardware elements with a quantum internet [136]:

(i) Quantum Channel

It is a physical connection for supporting the qubit transmission. The standard optical fibers presently used for telecommunication or communication via satellites or combination of both can be considered as a channel.

(ii) Quantum Repeaters

These are intermediate nodes in a quantum channel for achieving long distance quantum communication. During the transmission of a photon via a quantum channel absorption and dephasing lead to loss of quantum of information over distance takes place. To overcome this loss, quantum repeaters need to be used at regular distances in the quantum channel. The nodes share entangled connections formulating entangled links.

(iii) Quantum Processors

The end nodes need to have quantum processors to prepare and measure single qubits for the purpose of large-scale quantum computers. The end nodes can serve as quantum repeaters also.

2. Long Distance Communication

Quantum internet design is governed by strange quantum phenomena and laws like no-cloning, measurement collapse, entanglement and teleporting which don't have classical analogue. So, the classical internet design cannot be used for design of quantum internet. For the same reasons, a quantum internet cannot be interconnected to the conventional classical internet network. Long distance quantum communication is affected by losses and dephasing errors. To succesfully transmit quantum information between nodes over long distances, quantum error correction have to be done at repeat stations (nodes) spaced at regular intervals. A way to send quantum information is to use the technique of teleportation using quantum entanglement.

3. Quantum Resources

In the classical internet of multiple network for, say, Alice to communicate with Bob an internet protocol finds an appropriate path or a channel through which the data has to flow across the multiple networks from Alice to Bob. In a similar way, for achieving quantum communication between Alice and Bob the resources will be provided by the quantum internet protocol. A resource can be, for example, a secret key for the unconditional secure communication. In the case of quantum teleportation, the resource can be quantum entanglement.

4. Quantum Repeaters

As photon has weak interaction with environment and can be easily controlled with standard optical components, it is considered as the most suitable candidate for generating entanglement between remote qubits. The photons transport the qubit from a physical quantum device at the receiver. Direct transmission of quantum information using photon through a fibre or open space suffers absorption and dephasing limiting the distance to which the information can be sent to a few hundred kilometers. But entanglement swapping at each intermediate repeater station allows a long distance quantum communication. The repeaters have to be entangle in pairs or clusterly to broadcast to all the nodes. Intensive research, both theoretical and experimental is being done to realize quantum repeaters. Many of the

building blocks of a quantum repeaters have been experimentally demonstrated [135]. In the laboratory, the linking of thousands of nodes clusterly has been achieved [139].

A quantum internet can share quantum states among remote nodes and increase the number of qubits of the interconnected quantum commuting devices. An isolated 10-qubit device represents 2^{10} states. When two such isolated devices are interconnected with a quantum internet then the resulting cluster can represent upto 2^{18} states [137]. In this distributed quantum computing scenario data centres can be interconnected for providing the specialized quantum equipment and any user can have access to the quantum computing power through cloud. At present IBM offers facilities to researchers to develop and analyse quantum algorithm design through a cloud access of isolated quantum devices of 5, 16 and 20 qubits.

5. Quantum Memories

Quantum networks need memories to store quantum information ideally for hours. This is necessary for both the end users and the quantum repeaters. The repeaters store the quantum states in their memory for the purpose of selection of a path and path recovery. The information should be isolated from unwanted interactions with the environment. As storage of photon is difficult, photonic states are transferred to physical changes like atomic excitations with high read-write fidelity. Interfaces between photon with quantum states of trapped ions, ultracold atomic gases, crystalline-solid spin ensembles, superconducting interference devices and solid state qubits are highly promising quantum memories.

6. Applications

Quantum internet is capable of supporting functionalities such as secure communication, blind computing, exponential increase of quantum computer power and advanced quantum sensing techniques. These functionalities of quantum internet have the potential to change markets and industries such as commerce, inteliigence and military affairs [140]. The best known application of a quantum internet is quantum key distribution. It enables two remote nodes to establish a secured encryption key. Quantum internet will help to access remote quantum computers, secure identification, two-party cryptographic tasks and more accurate clock synchronization.

Realization of a quantum internet with its possible applications is technically possible. Important building blocks of quantum internet and experimental small-scale networks have already been demonstrated. Quantum cryptographic networks have been practically realized and tested in several countries [140]. A simulator called SimulaQron is introduced for developing quantum internet software [141]. Various stages of development and advancement towards a successful quantum internet is discussed in [136]. While a full-scale quantum computer is technically challenging, developing quantum internet has become a realistic possibility.

16.13 Concluding Remarks

In the last two decades, quantum science and engineering has created several extremely valuable tools operating exclusively under the laws of quantum mechanics and offering practical optical measurement and characterization techniques that have great advantages over existing technologies. In addition to various applications discussed in this chapter, quantum technology has potential for applications in fields like remote sensing, artificial photo synthesis, medical science to photographing tissue layers, infra-red photography, etc. In many

equipments when generating power a considerable amount of heat energy is produced, for example, by their motors. Such heat energy can be turned to useful. It is noteworthy to mention that using quantum interference it is possible to make a molecular thermoelectric material capable of converting heat energy into electric energy without pollution. Quantum technology may revolutionize the computer and communication fields. But there are still number of challenges to be solved in quantum technologies before they come into use in practical applications.

A great deal of effort has to be put in to develop quantum sensors to exploit the improved resolution and sensitivity obtained due to quantum entanglement. A major hurdle is the inability to generate a large number of entangled photons. Because of the low-illumination of an entangled beam, the sensors may take a long time to record the data and it may become undesirable for many applications. New materials to record N-photon absorption have to be found. The decoherence due to environment limits the capability of quantum technology in many situations. New technologies have to be developed to overcome the problem of noise in quantum systems. Though many quantum technologies have been successful in laboratories, it may take still more time to bring them to practical applications.

16.14 Bibliography

[1] J.P. Dowling and G.J. Milburn, *Phil. Trans. Roy. Soc. A* 361:1655, 2003.

[2] D.C. Burnham and D.L. Weinberg, *Phys. Rev. Lett.* 25:84, 1970.

[3] P.G. Kwiat, K. Mattle, H. Weinfurter and A. Zeilinger, *Phys. Rev. Lett.* 75:4337, 1995.

[4] M.H. Rubin, D.N. Klyshko and Y.H. Shih, *Phys. Rev. A* 50:5122, 1994.

[5] M.J. Padgett and R.W. Boyd, *Phil. Trans. R. Soc. A* 375:20160233, 2016.

[6] D.B. Ion, M.L. Ion and L. Rusu, *Opt. Commun.* 283:1026, 2010.

[7] T.B. Pittman, Y.H. Shih, D.V. Strekalov and A. Sergienko, *Phys. Rev. A* 52:3429, 1995.

[8] R.S. Bennink, S.J. Bentley and R.W. Boyd, *Phys. Rev. Lett.* 89:113601, 2002.

[9] N. Bornman, M. Agnew, F. Zhu, A. Valles, A. Forbes and J. Leach, *NPJ Quan. Inf.* 5:63, 2019.

[10] P.A. Moreau, E. Toninelli, T.Gregory and M.J. Padgett, *Nat. Rev. Phys.* 1:367, 2019.

[11] R.I. Khakimov, B.M. Henson, D.K. Shin, S.S. Hodgman, R.G. Dall, K.G.H. Baldwin and A.G. Truscott, *Nature* 540:100, 2016.

[12] A. Vega, S. Saravi, T. Pertsch and F. Setzpfandt, *Appl. Phys. Lett.* 117:094003, 2020.

[13] X. Yao, X. Liu, L. You, Z. AWang, X. Feng, F. Liu, K. Cui, Y. Huang and W. Zhang, *Phys. Rev. A* 98:063816, 2018.

[14] M. Genovese, *J. Opt.* 18:073002, 2016.

[15] D. Walter, C. Pitsch, G. Paunescu and P. Lutzmann, *Proc. SPIE11134, Quantum Communications and Quantum Imaging XVII* 111340W1, 2019.

[16] M.G. Basset, F. Setzpfandt, F. Steinlechner, E. Beckert, T. Pertsch and M. Grafe, *Laser & Photonics Rev.* 13:1900097, 2019.

[17] W. Li, Z. Tong, K. Xiao, Z. Liu, Q. Gao, J. Sun, S. Liu, S. Han and Z. Wang, *Optica* 6:1515, 2019.

[18] R.E. Meyers and K.S. Deacon, *Entropy* 17:1508, 2015.

[19] E. Brambilla, L. Caspani, O. Jedrkiewicz, L.A. Lugiato and A. Gatti, *Phys. Rev. A* 77:053807, 2008.

[20] G. Brida, L. Caspani, A. Gatti, M. Genovese, A. Medal, and I. Ruo Berchera, *Phys. Rev. Lett.* 102:213602, 2009.

[21] G. Brida, M. Genovese, A. Medal and I.R. Berchera, *Phys. Rev. A* 83:033811, 2011.

[22] G. Brida, M. Genovese and I. Ruo Berchera, *Nat. Photonics* 4:227, 2010.

[23] N. Samantaray, I. Ruo-Berchera, A. Meda and M. Genovese, *Light Science & Appl.* 6:e17005.2017.

[24] I. Ruo-Berchera, A. Meda, E. Losero, A. Avella, N. Samantaray and M. Genovese, *Appl. Phys. Lett.* 116:214001, 2020.

[25] J.D. Meuller, W. Samantary and J.C.F. Mathews, *Appl. Phys. Lett.* 117:03400, 2020.

[26] O.S. Magana-Loaiza and R.W. Boyd, *Rep. Prog. Phys.* 82:124401, 2019.

[27] R.W. Spiers, N.R. Brewer, M.C. Wu and P.D. Lett, *OSA Technical Digest* article number JW3A.59, 2018.

[28] R.W. Speirs, N.R. Brewer, M.C. Wu and P.D. Lett, *OSA Technical Digest* article number JTu2A.37, 2019.

[29] E. Toninelli, P.A. Moreau, T. Gregory, A. Mihalyi, M. Edgar, N. Radwell and M. Padgett, *Optica* 6:347, 2019.

[30] D. Mason, J. Chen, M. Rossi, Y. Tsaturyan and A. Schliesser, *Nat. Phys.* 15:745, 2019.

[31] M.A. Taylor, J. Janousek, V. Daria, J. Knittel, B. Hage, H.A. Bachor and W.P. Bowen, *Nat. Photonics* 7:229, 2013.

[32] M.C. Teich and B.E.A. Saleh, *Ceskoslovensky Cosopis pro fysiku* 47:3, 1997.

[33] H. Fei, B. Jost, S. Popescu, B. Saleh and M. Teich, *Phys. Rev. Lett.* 78:1679, 1997.

[34] W. Zong, R. Wu, M. Li, Y. Hu, Y. Li, J. Li, H. Rong, H. Wu, Y. Xu, Y. Lu, H. Jia, M. Fan, Z. Zhou, Y. Zhang, A. Wang, L. Chen and H. Cheng, *Nat. Methods* 14:713, 2017.

[35] X. Lou, Z. Zhao and B.Z. Tang, *Small* 12:6430, 2016.

[36] J. Bender, C. Simonsson, M. Smedh, S. Engstrom and M.B. Ericson, *J. Control Release* 129:163, 2008.

[37] B.G. Wang, K. Konig and K.J. Hallhuber, *J. Micros.* 238:1, 2010.

[38] A. Svidzinsky, G. Agarwal, A. Classen, A.V. Sokolov, A. Zheltikov, M. Suhail Zubairy and M.O. Scully, *Phys. Rev. Res.* 3:043029, 2021.

[39] H. Oka, *J. Chem. Phys.* 152:044106, 2020.

[40] A. Hayat, A. Nevet, P. Ginzburg and M. Orenstein, *Semicond. Sci. Technol.* 26:083001, 2011).

[41] L.A. Lugiato, A. Gatti and E. Brambilla, *J. Opt. B: Quantum Semiclass. Opt.* 4:S176, 2002.

[42] C. Fabre, J.B. Fouet and A. Matre, *Opt. Lett.* 25:76, 1999.

[43] N. Treps, U. Andersen, B. Buchler, P.K. Lam, A. Maitre, H.A. Bachor and C. Fabre, *Phys. Rev. Lett.* 88:203601, 2002.

[44] N. Treps, N. Grosse, W.P. Bowen, C. Fabre, H.A. Bachor and P.K. Lam, *Science* 301:940, 2003.

[45] E. Yablonovich and R.B. Vrijen, *Opt. Eng.* 38:334, 1999.

[46] A.N. Boto, P. Kok, D.S. Abrams, S.L. Braunstein, C.P. Williams and J.P. Dowling, *Phys. Rev. Lett.* 85:2733, 2000.

[47] M. D'Angelo, M.V. Chekhova and Y. Shih, *Phys. Rev. Lett.* 87:013602, 2001.

[48] G. Bjork, L.L. Sanchez-Soto and J. Soderholm, *Phys. Rev. Lett.* 86:4516, 2001.

[49] O. Steuernagel, *J. Opt. B: Quantum Semiclass. Opt.* 6:S606, 2004.

[50] Y. Shih, *Eur. Phys. J. D* 22:485, 2003.

[51] A. Pe'er, B. Dayan, M. Vucelja, Y. Silberberg and A.A. Friesem, *Opt. Exp.* 12:6600, 2004.

[52] N.H. Peeters, J.J. Renema and M.P. van Exter, *Phys. Rev. A* 79:043817, 2009.

[53] C. Kothe, G. Bjork, S. Inoue and M. Bourennane, *New J. Phys.* 13:043028, 2011.

[54] R.W. Boyd, H.J. Chang, H. Shin and C. O'Sullivan-Hale, *Progress in quantum lithography*. In Proc. SPIE 5893, Quantum Communications and Quantum Imaging III, 58930G, 2005; https://doi.org/10.1117/12.617683.

[55] S. Kyang Lee and H.W. Lee, *J. Phys. Soc. Japan* 77:124001, 2008.

[56] P.R. Hemmer, A. Muthukrishnan, M.O. Scully and M.S. Zubairy, *Phys. Rev. Lett.* 96:163603, 2006.

[57] R.W. Boyd and J.P. Dowling, *Quantum Inf. Process* 11:891, 2012.

[58] V. Giovannetti, S. Lloyd and L. Maccone, *Phys. Rev. Lett.* 96:010401, 2006.

[59] N. Gershenfeld, *The Nature of Mathematical Modeling.* Cambridge University Press, New York, 1999.

[60] B.R. Frieden, *Physics From Fisher Information: A Unification.* Cambridge University Press, Cambridge, 1998.

[61] V. Giovannetti, S. Lloyd and L. Maccone, *Nat. Photonics* 5:222, 2011 and references therein.

[62] L.D. Didomenico, H. Lee, P. Kok and J.P. Dowling, *Quantum interferometric sensors*. In Quantum Sensing and Nanophotonic Devices. (Eds.) M. Razeghi and G.J. Brown, Proc. SPIE 5359, SPIE Bellingham, 2004 pp.169.

[63] 4 015001 T. Nagata, R. Okamoto, J.L. O'Brien, K. Sasaki and S. Takeuchi, *Science* 316:726, 2007.

[64] J.A. Jones, S.D. Karlen, J. Fitzsimons, A. Ardavan and S.C. Benjamin, *Science* 324:1166, 2009.

[65] Y.A. Chen, X.H. Bao, Z.S. Yuan, S. Chen, B. Zhao and J.W. Pan, *Phys. Rev. Lett.* 104:043601, 2010.

[66] S. Boixo, A. Datta, M.J. Davis, S.T. Flammia, A. Shaji and C.M. Caves, *Phys. Rev. Lett.* 101:040403, 2008.

[67] M. Napolitano, M. Koschorreck, B. Dubost, N. Behbood, R.J. Sewell and M.W. - Mitchell, *Nature* 471:486, 2011.

[68] B.M. Escher, *Nat. Phys.* 7:406, 2011.

[69] H. Katori, *Nat. Photonics* 5:203, 2011.

[70] G. Toth and I. Apellaniz, *J. Phys. A: Math. Theor.* 47:424006, 2014.

[71] M.A Taylor and W.P. Bowena, *Phys. Rep.* 615:1, 2016.

[72] D.S. Simon, G. Jaeger and A.V. Sergienko, *Quantum Metrology, Imaging, and Communication*. Springer, Cham, Switzerland, 2017.

[73] E. Polino, M. Valeri, N. Spagnolo and F. Sciarrino, *AVS Quantum Sci.* 2:024703, 2020.

[74] M. Szczykulska, T. Baumgratz and A. Datta, *Adv. Phys.:X* 1:621, 2016.

[75] L. Pezze, A. Smerzi, M.K. Oberthaler, R. Schmied and P. Treutlein, *Rev. Mod. Phys.* 90:035005, 2018.

[76] W. Dur, M. Skotiniotis, F. Froewis and B. Kraus, *Phys. Rev. Lett.* 112:080801, 2014.

[77] A.W. Chin, S.F. Huelga and M.B. Plenio, *Phys. Rev. Lett.* 109:233601, 2012.

[78] R. Demkowicz-Dobrzanski and L. Maccone, *Phys. Rev. Lett.* 113:250801, 2014.

[79] J. Joo, W.J. Munro and T.P. Spiller, *Phys. Rev. Lett.* 107:083601, 2011.

[80] K. Berrada, S. Abdel Khalek and C.H. Raymond Ooi, *Phys. Rev. A* 86:033823, 2012.

[81] S. Ragy, M. Jarzyna and R. Demkowicz-Dobrzanski, *Phys. Rev. A* 94:052108, 2016.

[82] M. Zwierz, C. A. Perez-Delgado and P. Kok, *Phys. Rev. Lett.* 105:180402, 2010.

[83] C.F. Ockeloen, R. Schmied, M.F. Riedel and P. Treutlein, *Phys. Rev. Lett.* 111:143001, 2013.

[84] I. Sokolov, M. Kolobov, A. Gatti and L. Lugiato, *Opt. Commun.* 193:175, 2001.

[85] L. Vaidman, *Phys. Rev. A* 49:1473, 1994.

[86] S.L. Braunstein and H.J. Kimple, *Phys. Rev. Lett.* 80:869, 1998.

[87] L.V. Magdenko, I.V. Sokolov and M.I. Kolobov, *Opt. Spect.* 103:62, 2007.

[88] V. Giovannetti and S. Lloyd, *Science* 306:1330, 2004.

[89] C.L. Degen, F. Reinhard and P. Cappellaro, *Rev. Mod. Phys.* 89:035002, 2017.

[90] P.P. Herrmann, J. Hoffnagle, N. Schlumpf, V.L. Telegdi and A. Weis, *J. Phys. B* 19:1271, 1986.

[91] A. Osterwalder and F. Merkt, *Phys. Rev. Lett.* 82:1831, 1999.

[92] G. Nogues, A. Rauschenbeutel, S. Osnaghi, M. Brune, J.M. Raimond and S. Harosche, *Nature* 400:239, 1999.

[93] S.Gleyzes, S. Kuhr, C. Guerlin, J. Bernu, S. DelEglise, U. Busk Hoff, M. Brune, J.M. Raimond and S. Haroche, *Nature* 446:297, 2007.

[94] S. Haroche, *Rev. Mod. Phys.* 85:1083, 2013.

[95] A. Facon, E.K. Dietsche, D. Grosso, S. Harosche, J.M. Raimond, M. Brune and S. Gleyzes, *Nature* 535:262, 2016.

[96] J.A. Sedlacek, A. Schwettmann, H. Kbler, R. Lw, T. Pfau and J.P. Shaffer, *Nat. Phys.* 8:819, 2012.

[97] H. Fan, S. Kumar, J. Sedlacek, H. Kbler, S. Karimkashi and J.P. Shaffer, *J. Phys. B* 48:202001, 2015.

[98] T. Bitter and D. Dubbers, *Phys. Rev. Lett.* 58:251, 1987.

[99] V.V. Nesvizhevsky, H.G. Borner, A.K. Petukhov, H. Abele, S. Baeβler, F.J. Rueβ, T. Stoferle, A. Westphal, A.M. Gagarski, G.A. Petrov and A.V. Strelkov, *Nature* 415:297, 2002.

[100] P.W. Shor, *Algorithms for quantum computation: discrete logarithms and factoring*. In the Proceedings of 35th Annual Symposium on Foundations of Computer Science, 1994, pp. 124-134, doi: 10.1109/SFCS.1994.365700.

[101] S.L. Braunstein and C.M. Caves, *Phys. Rev. Lett.* 72:3439, 1994.

[102] H. Lee, P. Kok and J.P. Dowling, *J. Mod. Opt.* 49:2325, 2002.

[103] J.M. Taylor, P. Cappellaro, L. Childress, L. Jiang, D. Budker, P.R. Hemmer, A. Yacoby, R. Walsworth and M.D. Lukin, *Nat. Phys.* 4:810, 2008.

[104] T.J. Proctor, P.A. Knott and J.A. Dunningham, *Phys. Rev. Lett.* 120:080501, 2018.

[105] N.T. Peter, B.J. Smith, A. Datta, L. Zhang, U. Dorner and I.A. Walmsley, *Phys. Rev. Lett.* 107:113603, 2011.

[106] M. Kutas, B. Haase, P. Bickert, F. Riexinger, D. Molter and G. von Freymann, *Sci. Adv.* 6:eaaz8065, 2020.

[107] C. Bonato, M.S. Blok, H.T. Dinani, D.W. Berry, M.L. Markham, D.J. Twitchen and R. Hanson, *Nat. Nanotech.* 11:247, 2016.

[108] A. Ajoy, U. Bissbort, M.D. Lukin, R.L. Walasworth and P. Cappellaro, *Phys. Rev. Lett.* 5:011001, 2015.

[109] Y. Wu, F. Jelezko, M.B. Plenio and T. Weil, *Angew. Chem. Int. Ed.* 55:6586, 2016.

[110] A.W. Hubler and V. Gintautas *Complexity* 14:7, 2008.

[111] A.W. Hubler and O. Osuagwu, *Complexity* 15:48, 2010.

[112] R. Alicki and M. Fannes, *Phys. Rev. E* 87:042123, 2013.

[113] F.C. Binder, S. Vinjanampathy, K. Modi and J. Goold, *New J. Phys.* 17:075015, 2015.

[114] F. Campaioli, F.A. Pollock, F.C. Binder, L. Celeri, J. Goold, S. Vinjanampathy and K. Modi, *Phys. Rev. Lett.* 118:150601, 2017.

[115] F. Campaioli, F.A. Pollock and S. Vinjanampathy, *Quantum Batteries*. In Thermodynamics in the Quantum Regime. F. Binder, L.A. Crrea, C. Gogolin, J. Anders and G. Adesso (Eds.). Springer, New York, 2018, pages 207-225.

[116] A.E. Allahverdyan, R. Balian and T.M. Nieuwenhuizen, *Europhys. Lett.* 67:565, 2004.

[117] W. Pusz and S.L. Woronowicz, *Commun. Math. Phys.* 58:273, 1977.

[118] A. Lenard, *J. Stat. Phys.* 19:575, 1978.

[119] S. Julia-Farre, T. Salamon, A. Riera, M.N. Bera and M. Lewenstein, *Phys. Rev. Res.* 2:023113, 2020.

[120] F. Caravelli, G. Coulter-De Wit, L.P. García-Pintos and A. Hamma, *Phys. Rev. Res.* 2:023095, 2020.

[121] A.C. Santos, B. Cakmak, S. Campbell and N.T. Zinner, *Phys. Rev. E* 100:032107, 2019.

[122] J.Q. Quach and W.J. Munro, *Phys. Rev. Appl.* 14:024092, 2020.

[123] D. Farina, G.M. Andolina, A. Mari, M. Polini and V. Giovannetti, *Phys. Rev. B* 99:035421, 2019.

[124] S. Gherardini, F. Campaioli, F. Caruso and F.C. Binder, *Phys. Rev. Res.* 2:013095, 2020.

[125] G.M. Andolina, D. Farina, A. Mari, V. Pellegrini, V. Giovannetti and M. Polini, *Phys. Rev. B* 98:205423, 2018.

[126] D. Ferraro, M. Campisi, G.M. Andolina, V. Pellegrini and M. Polini, *Phys. Rev. Lett.* 120:117702, 2018.

[127] T.P. Le, J. Levinsen, K. Modi, M.M. Parish and F.A. Pollock, *Phys. Rev. A* 97:022106, 2018.

[128] G.M. Andolina, M. Keck, A. Mari, M. Campisi, V. Giovannetti and M. Polini, *Phys. Rev. Lett.* 122:047702, 2019.

[129] D. Rossini, G.M. Andolina and M. Polini, *Phys. Rev. B* 100:115142, 2019.

[130] G.M. Andolina, M. Keck, A. Mari, V. Giovannetti and M. Polini, *Phys. Rev. B* 99:205437, 2019.

[131] S. Lloyd, J.H. Shapiro, P. Kumar, M. Shahriar and H.P. Yuen, *ACM SIGCOMM Comp. Comm. Rev.* 34:9, 2004.

[132] H.J. Kimble, *Nature* 453:1023, 2008.

[133] S. Muralidharan, J. Kim, N. Lutkenhaus, M.D. Lukin and I. Jiang, *Phys. Rev. Lett.* 112:250501, 2014.

[134] K. Azuma, A. Mizutani and H.R. Lo, *Nat. Commun.* 7:13523, 2016

[135] W. Dur, R. Lamprecht and S. Heusler, *Eur. J. Phys.* 38:043001, 2017.

[136] S. Wehner, D. Elkouss and R. Hanson, *Science* 362:303, 2018.

[137] M. Caleffi, A. Sara Cacciapuoti and G. Bianchi, *Quantum internet: from communication to distributed computing*. In Proceedings of the 5th ACM International Conference on Nanoscale Computing and Communication, 2018.

[138] M. Caleffi, D. Chandra, D. Cuomo, S. Hassanpour and A. Sara Cacciapuoti, *Computer* 53:67, 2020.

[139] S. Yokoyama, R. Ukai, S.C. Armstrong, C. Sornphiphatphong, T. Kaji, S. Suzuki, J. Yoshikawa, H. Yonezawa, N.C. Menicucci and A. Furusawa, *Nat. Photonics* 7:982, 2013.

[140] A. Sara Cacciapuoti, *IEEE Trans. Commun.* 68:3808, 2020.

[141] A. Dahlberg and S. Wehner, *Quantum Sci. Tech.* 4:015001, 2018.

16.15 Exercises

16.1 Obtain the transformation matrix for a 50 : 50 lossless beam splitter.

16.2 Refer to the interferometric lithography set-up shown in Fig. 16.5. For the input state $|1\rangle_{\rm A}|1\rangle_{\rm B}$ obtain the entangled state $|\psi_{\rm E}(\phi)\rangle$ at C and D.

16.3 For the set-up shown in Fig. 16.5 show that $\langle N_{\rm C}N_{\rm D}\rangle = 0$ in the entangled state $|\psi_{\rm E}(\phi)\rangle = \frac{1}{\sqrt{2}}\left[{\rm e}^{2{\rm i}\phi}|2\rangle_{\rm C}|0\rangle_{\rm D} + |0\rangle_{\rm C}|2\rangle_{\rm D}\right]$, where $N_{\rm C}$ and $N_{\rm D}$ are the number operators in port C and port D.

16.4 Consider the previous exercise. What is the significance of $\langle N_{\rm C}N_{\rm D}\rangle = 0$?

16.5 Let $|H\rangle$ and $|V\rangle$ represent the horizontal polarization state and vertical polarization statem respectively. Show that a 2002 N00N state in the same V/H basis is produced if the two inputs to the polarization beam splitter (PSB) are single photon of the left circularly polarized light in the state $|L\rangle$ and right circularly polarized light in the state $|R\rangle$.

16.6 For any type of polarization (i), we can write $a_i = {\rm C_V}a_{\rm V} + {\rm C_H}a_{\rm H}$, where ${\rm C_V C_V^*} + {\rm C_H C_H^*} = 1$. Determine the average number of photons having any type polarization i in the $N00N$ state

$$|\psi_{\rm E}(N)\rangle = \frac{1}{\sqrt{2}}[|N\rangle_{\rm V}|0\rangle_{\rm H} + |0\rangle_{\rm V}|N\rangle_{\rm H}],$$

where V and H represent the vertical and horizontal polarization modes, respectively.

16.7 Prove the relation $\langle\psi_{\rm E}(N,\phi)|A_N|\psi_{\rm E}(N,\phi)\rangle = \cos N\phi$.

16.8 Determine the $N00N$ state obtained by operating the operator

$$\frac{1}{\sqrt{12}}(a_{\rm C}^\dagger + a_{\rm D}^\dagger)(a_{\rm C}^\dagger + {\rm e}^{{\rm i}\chi}a_{\rm D}^\dagger)(a_{\rm C}^\dagger + {\rm e}^{2{\rm i}\chi}a_{\rm D}^\dagger)$$

with $\chi = 2\pi/3$ on the vacuum state $|0\rangle$.

16.9 Find the matrix for the phase estimating operator $A = |0\rangle\langle 1| + |1\rangle\langle 0|$. Show that $A^2 = I$.

16.10 Show that $H_0 = E_0|0\rangle\langle 0| + E_1|1\rangle\langle 1|$ commutes with $H_{V_\parallel} = \frac{1}{2}\gamma V_\parallel\,(|1\rangle\langle 1| - |0\rangle\langle 0|)$.

16.11 Show that $H_0 = E_0|0\rangle\langle 0| + E_1|1\rangle\langle 1|$ does not commute with $H_{V_\perp} = \frac{1}{2}\gamma\left(V_\perp(t)|1\rangle\langle 0| + V_\perp^\dagger(t)|0\rangle\langle 1|\right)$.

16.12 Draw a flow-chart describing the various steps involved in a quantum sensing process.

16.13 Prove that the transition probability in the Ramsey interferometry measurement given by $p = 1 - |\langle 0|\alpha\rangle|^2$ is $\frac{1}{2}(1 - \cos\omega_0 t)$.

16.14 Show that the passive state given by $\sigma = \sum_{j=1}^d s_j|j\rangle\langle j|,\ s_{j+1} \le s_j$ commutes with $H = \sum_{j=1}^d \epsilon_j|j\rangle\langle j|,\ \epsilon_{j+1} \le \epsilon_j$.

16.15 For an ensemble of n identical quantum batteries show that $\lim_{n\to\infty} W_{\rm max}^{(n)} = {\rm Tr}\left(\rho H^{(1)}\right) - {\rm Tr}\left(\omega_{\bar\beta}H^{(1)}\right)$ [112].

Solutions to Selected Exercises

1.2 $\ddot{\psi} - \psi_{xx} + m^2\psi = 0,\ \mathcal{H} = \frac{1}{2}\dot{\psi}^2 + \frac{1}{2}m^2\psi^2 + \frac{1}{2}\left(\frac{\partial\psi}{\partial x}\right)^2.$

1.4 $\Box^2\phi - m^2\phi = 0\ , \quad \Box^2 = \nabla^2 - \frac{1}{c^2}\frac{\partial^2}{\partial t^2}.$

1.6 $\mathrm{i}\hbar\frac{\mathrm{d}\psi}{\mathrm{d}t} = -\frac{\hbar^2}{2m}\nabla^2\psi + V\psi.$

1.8 $\pi = \frac{1}{\sqrt{2}}(\pi_1 - \mathrm{i}\pi_2), \quad \overline{\pi} = \frac{1}{\mathrm{i}\sqrt{2}}(\pi_1 + \mathrm{i}\pi_2).$

1.10 $|n_1 n_2 \cdots\rangle = \frac{1}{\sqrt{n_1! n_2! \cdots}}(a_1^\dagger)^{n_1}(a_2^\dagger)^{n_2}\cdots|000\cdots\rangle.$

1.12 $\left[\pi,\ \int(\nabla'\psi')^2\,\mathrm{d}^3x'\right] = 2\mathrm{i}\hbar\nabla^2\psi$ and $\left[\pi,\ \int m^2\psi'^2\,\mathrm{d}^3x'\right] = -2\mathrm{i}\hbar m^2\psi.$

1.14 $\mathbf{a}_{\mathbf{k}\lambda}(t) = \mathbf{a}_{\mathbf{k}\lambda}(0)\mathrm{e}^{-\mathrm{i}\omega\mathbf{k}t}.$

1.16 $\mathcal{H} = \psi^\dagger\mathrm{i}\partial_0\psi,\ \mathrm{i}\partial_0 = -\mathrm{i}\alpha\cdot\nabla + m\beta.$

1.18 $H = \frac{1}{8\pi}\int\left(\mathbf{E}^2 + \mathbf{H}_B^2\right)\,\mathrm{d}^3x.$

1.20 $\frac{\partial}{\partial t}\nabla\cdot\mathbf{E} = 0$ and $\frac{\partial}{\partial t}\nabla\cdot\mathbf{H}_B = 0.$

2.2 $S(x_{\mathrm{CM}}(t)) = \frac{m\omega}{2\sin\omega T}\left[(x_i^2 + x_f^2)\cos\omega T - 2x_i x_f\right].$

2.4 $Z(t_f, t_i) = \int_{x(t_f)=x(t_i)}\hat{\mathcal{D}}x(t)\,\mathrm{e}^{\mathrm{i}S[x(t)]/\hbar}.$

2.6 $K(\phi_f, t; \phi_i, 0) = \sum_{l=-\infty}^{\infty} C_l\mathrm{e}^{\mathrm{i}l(\phi_f-\phi_i)},\ C_l = \frac{1}{2\pi}\mathrm{e}^{-\mathrm{i}\hbar l^2 t/(2mR^2)}.$

2.8 $H(x, p_x, t) = \frac{p_x^2}{2m(t)} + \frac{1}{2}m(t)\omega_0^2 x^2.$

2.10 $\ddot{x} + \Lambda\dot{x}^2 = g.$

3.2 $H_2 = -\frac{1}{2}\frac{\mathrm{d}^2}{\mathrm{d}x^2} + \frac{v^2}{2} - \frac{1}{2}v'.$

3.4 $A^+H_2 - H_1A^+ = 0$ and $A^-H_1 - H_2A^- = 0.$

3.6 The ground state energy level is nondegenerate.

3.8 $A^-\phi_0^{(1)} = 0.$

3.10 $\{Q^-, Q^+\} = \begin{pmatrix} A^+A^- & 0 \\ 0 & A^-A^+ \end{pmatrix}$, $\{Q^+, Q^+\} = 0$ and $\{Q^-, Q^-\} = 0.$

3.12 $\{Q^-, Q^+\} = \frac{1}{2}\left(\pi_x^2 + \pi_y^2 - eB\sigma_z\right) = H_{\mathrm{s}}.$

3.14 $\phi_0^{(1)} = N\mathrm{e}^{-\omega x^2/2}$, $E_0^{(1)} = \omega/2$ and $\phi_0^{(2)} = N\mathrm{e}^{-\omega x^2/2}$, $E_0^{(2)} = 3\omega/2.$

3.16 $V_2 = -\left(\lambda_1 - Q_1 + \frac{1}{2}\right)\operatorname{sech}^2 x$ and

$$E_n^{(2)} = -\frac{1}{2}\left[Q_1 - 1 + \left(n + \frac{1}{2}\right)\right]^2, \quad n = 0, 1, \ldots, N < Q_1 - \frac{1}{2}.$$

3.18 $V_2 = -\dfrac{1}{r} + \dfrac{l(l+1)(l+2)}{2r^2}$.

4.2 a and $a^\dagger$ are not Hermitian.

4.4 The ground state is a coherent state.

4.6 $|\alpha\rangle = \mathrm{e}^{-|\alpha|^2/2}\,\mathrm{e}^{\alpha a^\dagger}|0\rangle$.

4.8 (a) $\langle\alpha|\alpha\rangle = 1$. (b) I. (c) $\big||\alpha\rangle - |\alpha'\rangle\big|^2 = 2\,(1 - \text{R.P.}\langle\alpha|\alpha'\rangle)$.
(d) $\langle n\rangle = |\alpha|^2$.

4.12 $\big|\,|\alpha(x,t)\rangle\,\big|^2 = \dfrac{1}{\sqrt{\pi}}\mathrm{e}^{-[x-\sqrt{2}\,|\alpha(0)|\,\cos(t-\theta)]^2}$.

4.14 $\langle x\rangle = \langle\alpha|x|\alpha\rangle = \sqrt{2}\,|\alpha(0)|\,\cos t$. $\quad\langle x^2\rangle = \langle\alpha|x|\alpha\rangle^2 + \frac{1}{2}$.
$\langle p_x\rangle = \langle\alpha|p_x|\alpha\rangle = -\sqrt{2}\,\sin t$. $\quad\langle p_x^2\rangle = \langle\alpha|p_x|\alpha\rangle^2 + \frac{1}{2}$.

4.18 $\langle x\rangle = -\sqrt{2}\,\beta(\mu-\nu)\cos t$. $\quad\langle p_x\rangle = -\sqrt{2}\,\beta(\mu-\nu)\sin t$.
$\langle x^2\rangle = \big(\beta^2(\mu-\nu)^2 - \mu\nu\big)\cos 2t + \beta^2(\mu-\nu)^2 + \frac{1}{2}(\mu^2+\nu^2)$.
$\langle p_x^2\rangle = \cos 2t\,\left[\mu\nu - \beta^2(\mu-\nu)^2\right] + \frac{1}{2}(\mu^2+\nu^2) + \beta^2(\mu-\nu)^2$.

5.2 $U^\dagger(t) = \mathrm{e}^{-(\mathrm{i}/\hbar)\int_0^t H(t')\,\mathrm{d}t'}$.

5.4 For $\rho \le R$, $\mathbf{B} = B\mathbf{k}$ and for $\rho \ge R$, $\mathbf{B} = 0$.

6.2 $R(\theta/2) = \begin{pmatrix} \cos(\theta/2) & -\sin(\theta/2) & 0 \\ \sin(\theta/2) & \cos(\theta/2) & 0 \\ 0 & 0 & 1 \end{pmatrix}$.

6.4 $N_2 = -\mathrm{i}\partial/\partial p$.

6.6 $\overline{W} = \dfrac{1}{\pi}\psi^*(x+s,t)\psi(x-s,t)$.

6.8 $W = \dfrac{1}{\pi}\Big[|A|^2\mathrm{e}^{-(p_x-p_A)^2}\mathrm{e}^{-x^2} + |B|^2\mathrm{e}^{-(p_x-p_B)^2}\mathrm{e}^{-x^2}$
$+2\mathrm{e}^{-(p_x-\overline{p})^2}\mathrm{e}^{-x^2}\mathrm{Re}\left(AB^*\mathrm{e}^{\mathrm{i}(p_A-p_B)x}\right)\Big]$, $\overline{p} = (p_1+p_2)/2$.

6.10 $W = \dfrac{2}{\pi}\left(x^2 + p_x^2 - \dfrac{1}{2}\right)\mathrm{e}^{-(x^2+p_x^2)}$.

7.4 For both the particles A and B all the probabilities are equal to 1/2.

7.10 For θ values satisfying $|\sin 2\theta| = 1$ we get product states.

7.14 $W^{(\alpha)} = |00\rangle\dfrac{1+\cos\alpha}{2}\langle 00| + |11\rangle\dfrac{1-\cos\alpha}{2}|11\rangle$
$+|\psi_+\rangle\dfrac{\sin\alpha}{2}\langle\psi_+| - |\psi_-\rangle\dfrac{\sin\alpha}{2}|\psi_-\rangle$,
where $|\psi_\pm\rangle = \frac{1}{\sqrt{2}}\,(|01\rangle + |10\rangle)$.

8.6 $|\psi(t)\rangle = a|\uparrow\rangle + b|\downarrow\rangle$, $\quad a = \dfrac{1}{\sqrt{2}}\mathrm{e}^{-\mathrm{i}\beta/2}$, $\quad b = \dfrac{1}{\sqrt{2}}\mathrm{e}^{\mathrm{i}\beta/2}$, $\quad \beta = \gamma B_z t$.

8.8 $\dfrac{\mathrm{d}}{\mathrm{d}t}\rho_{_S}(t) = -\dfrac{\mathrm{i}}{2m}\left[p^2, \rho_{_S}(t)\right] - \dfrac{1}{2}K\left[x, [x, \rho_{_S}(t)]\right]$.
In the position representation
$\dfrac{\partial}{\partial t}\rho_{_S}(x,x',t) = -\dfrac{\mathrm{i}}{2m}\left(\dfrac{\partial^2}{\partial x'^2} - \dfrac{\partial^2}{\partial x^2}\right)\rho_{_S}(x,x',t) - \dfrac{1}{2}K(x-x')^2\rho_{_S}(x,x',t)$.

9.2 $\dfrac{1}{\sqrt{2}}\begin{pmatrix} 1 & 1 \\ 1 & -1 \end{pmatrix}$.

9.4 $\alpha = -\pi/2$, $\beta = \pi$, $\gamma = 3\pi/2$ and $\delta = -\pi/2$.

9.6 $HZH = X$.

9.8 $P(0) = |a|^2$.

10.4 The states for the case of M agents are

$$\begin{aligned}
|\phi\rangle_{\mathrm{B_1B_2\cdots B}_M} &= (\alpha|0\,0\,\cdots\,0\rangle + \beta|1\,1\,\cdots\,1\rangle)_{\mathrm{B_1B_2\cdots B}_M}\,, \\
|\phi'\rangle_{\mathrm{B_1B_2\cdots B}_M} &= (\alpha|1\,1\,\cdots\,1\rangle + \beta|0\,0\,\cdots\,0\rangle)_{\mathrm{B_1B_2\cdots B}_M}\,, \\
|\psi\rangle_{\mathrm{B_1B_2\cdots B}_M} &= (\alpha|0\,0\,\cdots\,1\rangle + \beta|1\,1\,\cdots\,0\rangle)_{\mathrm{B_1B_2\cdots B}_M}\,, \\
|\psi'\rangle_{\mathrm{B_1B_2\cdots B}_M} &= (\alpha|1\,1\,\cdots\,0\rangle + \beta|0\,0\,\cdots\,1\rangle)_{\mathrm{B_1B_2\cdots B}_M}\,.
\end{aligned}$$

10.6 Cannot extract any message.

10.8 $P(j/\alpha) = (1 - \sin\delta)/2$.

12.2 $N_1 = N_2 = \left(\dfrac{\alpha + \alpha^*}{\pi}\right)^{1/4}$.

12.10 The eigenvalues are $\lambda_1 = 2/3$ and $\lambda_2 = 1/3$. For $\lambda_1 = 2/3$ the normalized eigenvector is $\dfrac{1}{\sqrt{2}}\begin{bmatrix} 1 \\ 1 \end{bmatrix}$. For $\lambda_1 = 1/3$ the normalized eigenvector is $\dfrac{1}{\sqrt{2}}\begin{bmatrix} 1 \\ -1 \end{bmatrix}$.

12.12 $S_0 = S_1 = 1$ and $S_2 = S_3 = 0$.

12.14 $\rho = \dfrac{1}{2}\begin{bmatrix} 1 & -\mathrm{i} \\ \mathrm{i} & 1 \end{bmatrix}$. $S_0 = S_2 = 1$ and $S_1 = S_3 = 0$.

13.2 50 spin-1/2 particles can be represented in that supercomputer.

13.10 $H = -1.0413I + 0.1529\sigma_x - 0.2215\sigma_z$.

14.2 $H\sigma_I H = I$.

14.4 $\mathrm{Tr}(A\rho) = 1 - P_{\mathrm{M}}$ and $\rho = \begin{bmatrix} 1 & 0 \\ 0 & 0 \end{bmatrix}$.

14.10 P_iP_j is also a stabilizer.

15.4 $P_{\mathrm{A}} = 1 - \left(|a|^2 - 2|a|^2|c|^2 + |c|^2\right), \quad P_{\mathrm{B}} = 1 - P_{\mathrm{A}}$.

15.8 $|\psi\rangle|\psi\rangle|A\rangle \to |\psi\rangle|\Sigma\rangle|A_\psi\rangle$ is not uncopying but swaps onto a two-dimensional subspace of the ancilla.

16.2 $|\psi_{\mathrm{E}}(\phi)\rangle = \dfrac{1}{\sqrt{2}}\left[\mathrm{e}^{2\mathrm{i}\phi}|2\rangle_{\mathrm{C}}|0\rangle_{\mathrm{D}} + |0\rangle_{\mathrm{C}}|2\rangle_{\mathrm{D}}\right]$.

16.4 It signifies that photons cannot be simultaneously measured at ports C and D. The two photons travel as a diphoton in any of the port.

16.6 $N/2$.

16.8 $\dfrac{1}{\sqrt{2}}[\,|3\rangle_{\mathrm{C}}|0\rangle_{\mathrm{D}} + |0\rangle_{\mathrm{C}}|3\rangle_{\mathrm{D}}]$.

Taylor & Francis
Taylor & Francis Group
http://taylorandfrancis.com

Index

Aharonov–Bohm effect, 120

Barnum's theorem, 253
Bell
  basis, 344
  state, 156
Berry's
  curvature, 109
  phase, 105, 107
    classical analogue, 110
    properties, 108
  vector potential, 107
bipartite states
  mixed states
    condition for entangled, 161
  pure states, 159
    condition for entangled, 160
    condition for separable, 160
Born probability rule, 196
bosonic oscillator, 57
Brody distribution, 365

chaotic motion, 362
CHSH
  -type witness, 165
  inequality, 165
  operator, 164
code
  space, 311
  concatenation, 316
coherent state, 75, 78
  generalized, 84
  its minimum uncertainty product, 79
  nonlinear, 94, 96
  of harmonic oscillator, 80
  of position-dependent mass systems, 89
  spin, 86
  time evolution, 83
complex superpotentials, 68
cryptosystems
  four-states protocol, 233
  one-time pad system, 230
  public key system, 230

d'Alembert equation, 15
decoherence
  cavity experiment, 193
  models
    collisional decoherence, 191
    quantum Brownian, 191
    spin-boson, 192
    spin-environment, 191
density matrix
  for N-qubit state, 279
  reconstruction formula, 270
Deutsch's algorithm, 214
displacement operator, 271
dynamical phase, 105

Einstein equations, 332
entangled state(s), 154
  bound, 169
  nonlocal, 152
entanglement, 151
  distillation, 168
    protocal, 168
  hyper, 166
  measure, 167
    concurrence, 170
    cost, 169
    distillable, 168
    formation, 169
    negativity, 171
  witnesses, 163, 164
    decomposable, 164
    optimal, 164
environmental Hamiltonian, 192
Ermakov equation, 68
error
  box, 144
  correction codes, 308
Euler–Lagrange equation, 5

f-oscillators, 94
fault tolerant, 319
fermionic oscillator, 57
Feynman's kernel, 34, 37

fidelity, 256, 269
  of Bužek–Hillery copying machine, 257
field, 2
  equations, 2, 5
  theory, 2
  variable, 2
Fisher information, 387
force
  linear, 362
  nonlinear, 362
free particle
  supersymmetric partners, 70
Friedmann–Robertson–Walker equation, 332

gauge transformation, 120
Gaussian
  integrals, 42
  orthogonal ensemble, 364
  symplectic ensemble, 365
  unitary ensemble, 364
  wave packet, 84
geometric phase, 105, 107
ghost imaging, 378
  type-I, 378
  type-II, 378
GHZ state, 165, 239
gravitons, 329

Hamiltonian density, 6
Hannay angle, 110
Heisenberg limit, 388
homodyne detector, 273

identity operator, 154

Klein–Gordon equation, 20

Lagrangian density, 3
linear harmonic oscillator
  coherent state, 80
  supersymmetric partners, 63, 64
  Wigner function, 138
Liouville–von Neumann equation, 188

magic square game, 352
master equations, 187, 188
  Born–Markov, 189
  generalized, 188
  Lindblad equation, 190
  Liouville–von Neumann, 188
  Markovian, 189
minimum uncertainty state, 77, 79
mixed states, 152
  condition for
    k-separable, 166
    entangled, 161

N00N-state, 386
no-
  broadcast theorem, 253
  cloning theorem, 231, 251
  deletion principle, 263
  hiding theorem, 263
  partial erase theorem, 264
  splitting problem, 264
Noether theorem, 5
nonlinear
  differential equation, 362
  force, 362

operator(s)
  annihilation, 10
  creation, 10
  deformed, 94
  number, 9
  squeeze, 89

paradox
  anti-Zeno, 341, 343
  Parrondo, 347
  Zeno, 338, 339
Pareto optimal, 346
Parrondo
  games
    classical, 347
    quantum, 348
  paradox, 347
partial trace, 157
path integral, 37
Pauli
  channel, 259
  problem, 268
Peres criterion, 162
phase space distribution function, 131, 135
Planck
  area, 329
  charge, 328
  constant, 327
  energy, 328
  length, 328
  mass, 328
  temperature, 328

time, 328
pointer states, 197
Poisson statistics, 365
prisoners' dilemma, 350
classical version, 350
quantum version, 350
propagator, 34, 41
pure state, 152, 153
condition for
k-separable, 166
entangled, 159
separable, 159
single qubit, 274

q-deformed oscillator, 95
quantization
first, 8
second, 8
quantum
algorithm
Deutsch's, 214
factorization, 219
Grover's, 216
batteries, 394
ergotropy, 395
extractable work, 394
Hamiltonian, 394
passive state, 395
carpets, 142
channel, 232
chaos, 362
cloning machine
of Bužek and Hillery, 257
optimal, 256
symmetric, 256
universal, 256
code distance, 313
computation, 201, 204
computer
universal, 321
cosmology, 331
cryptography
$4+2$ protocol, 237
four-states protocol, 233
multiparty, 239
two-states protocol, 236
diffusion, 359
errors
coherent, 306
decoherence, 306
qubit loss, 308
Fourier transform, 218
game, 347
internet, 397
channel, 398
processors, 398
repeaters, 398
logic gates, 203
C-swap, 212
CNOT, 208
Fredkin, 212
Hadamard, 207
identity, 212
NOT, 206
phase-shift, 212
Toffoli, 206
universal, 207
Z, 207
oracle, 217
pseudo-telepathy game, 352
sensing, 390
sensors, 389
simulation scheme, 289
simulator, 287, 289
analog, 290
digital, 291
steering, 358
teleportation, 343
tomography, 267, 270
Zeno effect, 338
qubits, 202
quorum, 267, 270
of observables, 267, 270

Rayleigh criterion, 384

Sagnac effect, 125, 126
Schrödinger equation, 34, 288
separable states, 153, 154, 159
Peres criterion, 162
three-qubit state, 165
Shor code, 316
shot-noise, 375
limit, 387
squeezed state, 75, 89, 90
cat, 93
entangled, 93
minimum uncertainty product, 91
uncertainty product, 91
stabilizer measurements, 311
Stokes parameters, 276
string theory, 329

sum-over-histories, 33
superparticles, 51
supersymmetric
    commutation, 55
    Hamiltonian, 52
        of linear harmonic oscillator, 63, 64
    partner potentials, 55
        of linear harmonic oscillator, 63, 64
        shape invariant, 71
    partner potentials
        of free particle, 70
        of linear harmonic oscillator, 71
    potential, 52
surface code, 317
survival probability, 338
swap operator, 163
syndrome, 311

Talbot effect, 194
telecloning, 261
Toffoli gate, 206
tomography, 267

von Neumann entropy, 167

wave packet spread, 144
Weyl-Heisenberg algebra, 269
Wigner
    distribution function, 135
    distribution function, 131
        s-order, 271
    state, 162

Zak phase, 111
Zeno paradox, 339